NASA Conference Publication 2118

Large Space Systems Technology - 1979

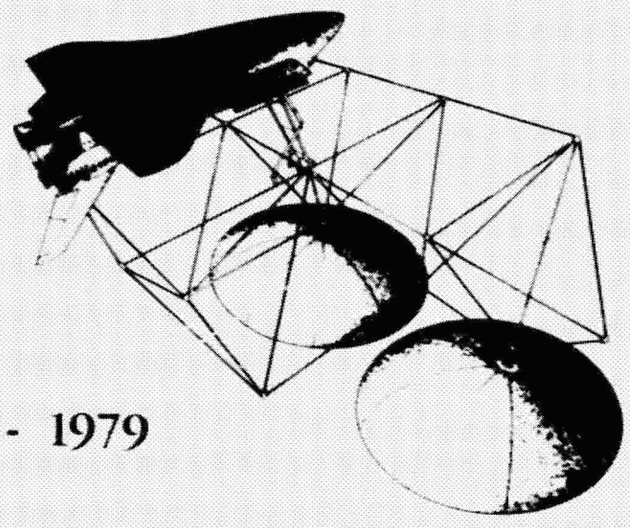

(NASA-CP-2118) LARGE SPACE SYSTEMS TECHNOLOGY, 1979 (NASA) 487 p HC A21/MF A01 CSCL 22B

N80-19145 THRU N80-19172 Unclas G3/15 12940

First Annual Program Technical Review
held at NASA Langley Research Center
Hampton, Virginia
November 7-8, 1979

RECEIVED NASA ST; FACILITY ACCESS DEPT.

NASA

PREFACE

This publication is a compilation of the papers presented at the First Annual Large Space Systems Technology (LSST) Program Technical Review conducted at the Langley Research Center on November 7-8, 1979. The Review provided personnel of government, university, and industry with an opportunity to exchange information, to assess the present status of technology developments on the LSST Program, and to plan the development of new technology for large space systems.

The papers describe items of technology or developmental efforts that were accomplished during Fiscal Year 1979 in support of the LSST Program and were prepared by those in government, university, and industry who performed the work. These papers were divided into three major areas of interest: (1) technology pertinent to large antenna systems, (2) technology related to large space platform systems, and (3) activities that support both antenna and platform systems.

This compilation provides the participants and their organizations with the papers presented at the Review in a referenceable format. Also, users of large space systems technology can follow the development progress with this document and subsequent ones. The LSST Program Office, Langley Research Center, which hosted the Review, will utilize this information as an aid in its measurement of performance and in planning future tasks. The historical background of the LSST Program is given in the introduction to NASA CP-2035, 1978, which covered a NASA/industry seminar that provided ideas and plans to the Program Office for its initial year of operation.

This publication was expedited and enhanced through the efforts of Earl H. Arrowood, Documentation Manager of the LSST Program Office, and the staff of the Scientific and Technical Information Programs Division, Langley Research Center.

The use of trade names or manufacturers' names in this publication does not constitute endorsement, either expressed or implied, by the National Aeronautics and Space Administration. The requirement that all dimensional quantities be expressed in the International System of Units (SI) has been waived. A table of conversion factors from U.S. Customary Units to SI Units is included on page viii.

PRECEDING PAGE BLANK NOT FILMED

CONTENTS

PREFACE iii

CONVERSION FACTORS FOR UNITS viii

LARGE ANTENNA SYSTEMS TECHNOLOGY

1. ANTENNA TECHNOLOGY DEVELOPMENT AT JPL - SUMMARY 1
   R. E. Freeland

2. OFFSET WRAP RIB CONCEPT AND DEVELOPMENT 5
   A. A. Woods, Jr.

3. ADVANCED SUNFLOWER ANTENNA CONCEPT DEVELOPMENT 33
   J. S. Archer

4. CONSTRUCTION ALIGNMENT SENSOR FEASIBILITY DEMONSTRATIONS (LASER MEASUREMENT) 59
   R. H. Anderson

5. JPL SELF PULSED LASER SURFACE MEASUREMENT SYSTEM DEVELOPMENT 77
   Martin Berdahl

6. FY 79 - LSST ANTENNA TECHNOLOGY DEVELOPMENT 95
   Thomas G. Campbell

7. DEVELOPMENT OF THE MAYPOLE (HOOP/COLUMN) DEPLOYABLE REFLECTOR CONCEPT FOR LARGE SPACE SYSTEMS APPLICATIONS 115
   D. C. Montgomery and L. D. Sikes

8. SURFACE ACCURACY MEASUREMENT SENSOR FOR DEPLOYABLE REFLECTOR ANTENNAS (SAMS DRA) 157
   Robert S. Neiswander

9. DEVELOPMENT OF ELECTROMAGNETIC ANALYSIS METHODS FOR LARGE APERTURE ANTENNAS 173
   C. R. Cockrell, L. D. Staton, and P. K. Agrawal

10. ELECTROSTATIC FORMING 187
    J. W. Goslee

11. SURFACE MEASURING TECHNIQUE 193
    Robert B. Spiers, Jr.

PRECEDING PAGE BLANK NOT FILMED

SPACE PLATFORM SYSTEMS TECHNOLOGY

12. STRUCTURAL CONCEPTS FOR LARGE SPACECRAFT 199
H. G. Bush, W. L. Heard, Jr., and J. E. Walz

13. ERECTABLE/DEPLOYABLE CONCEPTS FOR LARGE SPACE SYSTEM TECHNOLOGY . . . 217
W. E. Agan

14. SPACE FABRICATION: GRAPHITE COMPOSITE TRUSS WELDING AND CAP FORMING SUBSYSTEMS 247
L. M. Jenkins and D. L. Browning

15. STRUCTURAL ASSEMBLY IN SPACE 263
Jack W. Stokes and Edwin C. Pruett

16. SPACE CONSTRUCTION AND UTILITY DISTRIBUTION 287
K. A. Bloom

17. A HIGH RESOLUTION SOIL MOISTURE RADIOMETER 303
L. R. Dod

SUPPORTING ACTIVITIES

18. LARGE SPACE SYSTEM CONTROL TECHNOLOGY - OVERVIEW 313
Gary Parker

19. LARGE SPACE SYSTEM CONTROL TECHNOLOGY - STATUS AND ACCOMPLISHMENTS 323
G. Rodriguez

20. LARGE SPACE SYSTEM CONTROL TECHNOLOGY - MODEL ORDER REDUCTION STUDY 343
R. E. Skelton

21. LaRC CONTROLS ACTIVITY FOR LSST 359
R. C. Montgomery

22. INTERACTIVE ANALYSIS PROGRAM ACTIVITY 383
J. P. Young, H. P. Frisch, G. K. Jones, and W. J. Walker

23. JPL ANALYTICAL PERFORMANCE PREDICTION CAPABILITY 409
R. Chen

24. LARGE SPACE SYSTEMS TECHNOLOGY ELECTRONICS - DATA AND POWER DISTRIBUTION 423
W. G. Dunbar

25. SOLID-STATE SWITCH MODELING 443
Wilford D. Raburn

26. FY 79 - DEVELOPMENT OF FIBER OPTICS CONNECTOR TECHNOLOGY FOR LARGE SPACE SYSTEMS 453
Thomas G. Campbell

27. FLEXIBLE MATERIALS TECHNOLOGY 467
W. H. Steurer

28. ADVANCED MATERIALS FOR SPACE 485
Darrel R. Tenney, Wayne S. Slemp, Edward R. Long, Jr., and George F. Sykes

CONVERSION FACTORS FOR UNITS

To convert from U.S. Customary Unit	To SI Unit	Multiply by
Btu/hr-ft-^{o}F (thermal conductivity)	W/m-K	1.729 577
Fahrenheit (^{o}F) (temperature)	kelvin (K)	$t_K = (t_{o_F} + 459.67)/1.8$
	Celsius (^{o}C)	$t_{o_C} = (t_{o_F} - 32)/1.8$
foot (ft)	meter (m)	3.048×10^{-1}
inch (in.)	meter (m)	2.54×10^{-2}
kip/inch^2 (ksi)	pascal (Pa)	$6.894\ 757 \times 10^{6}$
pound force (lb)	newton (N)	4.448 222
pound mass (lb)	kilogram (kg)	$4.535\ 924 \times 10^{-1}$

ANTENNA TECHNOLOGY DEVELOPMENT AT JPL - SUMMARY

R. E. Freeland
Jet Propulsion Laboratory

LSST 1st ANNUAL TECHNICAL REVIEW

November 7-8, 1979

Objectives

To determine the applicability of the axisymmetric wrap-rib reflector technology for offset feed configurations for antennas up to 100 meters in diameter for operation up to 11 GHZ to establish technologies requiring development.

To estimate the potential mechanical performance of the Advanced Sunflower Precision Deployable Antenna Concept for antennas up to 30 meters in diameter for operation up to 100 GHZ and above along with the identification of critical technologies to formulate a rational development program.

The verification of in-flight antenna surface precision for design validation and/or automated figure control will require the capability for remote measurement. The FY'79 objective is to identify, evaluate and demonstrate concepts for the specific antennas under development.

The applicability of specific concepts for potential missions is usually first evaluated analytically. A simplified and cost effective analytical capability, intended for such a first assessment of the specific concepts under development, is required. The FY'79 objective is to develop technical approaches for such a development.

- TO DETERMINE THE APPLICABILITY OF THE WRAP-RIB DEPLOYABLE ANTENNA CONCEPT FOR OFFSET FEED CONFIGURATIONS.

- TO DETERMINE THE LIMITS OF POTENTIAL PERFORMANCE FOR THE ADVANCED SUNFLOWER PRECISION DEPLOYABLE ANTENNA CONCEPT.

- IDENTIFY, EVALUATE AND DEVELOP SURFACE MEASUREMENT SYSTEMS FOR THE ANTENNAS UNDER DEVELOPMENT.

- TO DEVELOP TECHNICAL APPROACH FOR A SIMPLIFIED ANALYSIS CAPABILITY FOR THE PREDICTION OF ANTENNA MECHANICAL PERFORMANCE.

Accomplishments

Development of the optimum configuration for the offset feed reflector structure by LMSC extensively exploited the axisymmetric technology. Feed structure functional requirements were based on potential reflector capability. The technology development plan considers analysis, design, manufacturing, assembly ground testing and facility requirements.

Development of the Advanced Sunflower Precision Deployable Antenna Concept by TRW indicates the largest diameter for basic concept is 12.5 meters for operation up to 100 GHZ. Advanced configurations show diameters up to 26 meters for operation up to 60 GHZ. Critical technologies were developed for both configurations.

Several surface measurement systems were evaluated analytically. Hardware conceptual demonstrations were accomplished for the LMSC structural alignment and JPL self-pulsed systems. The LMSC system demonstration measurement resolution of 0.20 mm. with a CO_2 and Helium-Neon laser. The JPL system demonstrated an unambiguous measurement with a resolution of 0.15 mm.

Technical approaches, that will be implemented during FY'80, have been developed for the analytical prediction of reflector surface precision. This capability will cover thermal distortion and structural/control interaction for specific concepts. The approaches are intended for simplified or first cut characterizations of potential performance.

- COMPLETED OPTIMIZATION OF OFFSET WRAP RIB REFLECTOR STRUCTURE, DEVELOPED REQUIREMENTS AND CANDIDATES FOR FEED STRUCTURE ALONG WITH TECHNOLOGY DEVELOPMENT PLAN.

- DETERMINED SIZE AND RF FREQUENCY LIMITS FOR BASELINE CONFIGURATION, DEVELOPED ADVANCED CONCEPTS FOR LARGE SIZE PRECISION DEPLOYABLE ANTENNAS ALONG WITH CRITICAL TECHNOLOGY IDENTIFICATION.

- SEVERAL SURFACE MEASUREMENT SYSTEM CONCEPTS WERE EVALUATED INCLUDING THE LMSC STRUCTURAL ALIGNMENT AND JPL SELF-PULSED SYSTEMS WHICH WERE EVALUATED WITH HARDWARE SYSTEMS.

- DEVELOPED BASIC TECHNICAL APPROACH FOR SIMPLIFIED ANALYTICAL PREDICTION OF ANTENNA MECHANICAL PERFORMANCE.

D1

N80-19146

OFFSET WRAP RIB CONCEPT AND DEVELOPMENT

A. A. Woods, Jr.
Lockheed Missiles & Space Company, Inc.
Space Systems Division
Sunnyvale, California

LSST 1st Annual Technical Review

November 7-8, 1979

INTENTIONALLY BLANK

BACKGROUND AND STUDY OBJECTIVES

A ten month contract for "Study of Wrap Rib Antenna Design" was undertaken by Lockheed Missiles and Space Company, Inc. in January 1979. This contract was originated by Jet Propulsion Laboratory in direct support of the Large Space Structures Technology Program.

The objectives of the contract are summarized in Figure 1. LMSC was to perform a study of the Wrap Rib Antenna Design and determine the applicability of the design for offset feed configurations for antennas up to 300 meters in diameter. In addition, a technical approach was to be developed and costed which would provide a high degree of confidence for the space flight application of a large Wrap Rib Antenna.

- CHARACTERIZE OFFSET AND SYMMETRIC WRAP RIB REFLECTORS
- IDENTIFY AND QUANTIFY CRITICAL DEVELOPMENT TECHNOLOGIES
- IDENTIFY ROM COST AND SCHEDULES FOR DEVELOPMENT
- DEVELOP A TECHNOLOGY PLAN FOR LOW RISK DEMONSTRATION

Figure 1.- Study objectives.

STUDY TASKS

The specific technical tasks performed in support of this contract were to (a) define the wrap rib antenna design for both symmetric and offset configurations in terms of surface quality, cost, weight and mechanical complexity, (b) develop a supporting deployable feed support structure and characterize it in terms of performance impact, cost, weight and mechanical complexity, and (c) develop a technical approach for implementation consisting of a combination of analysis and component test, model testing, and possibly space flight hardware demonstrations.

These tasks are summarized in Figure 2.

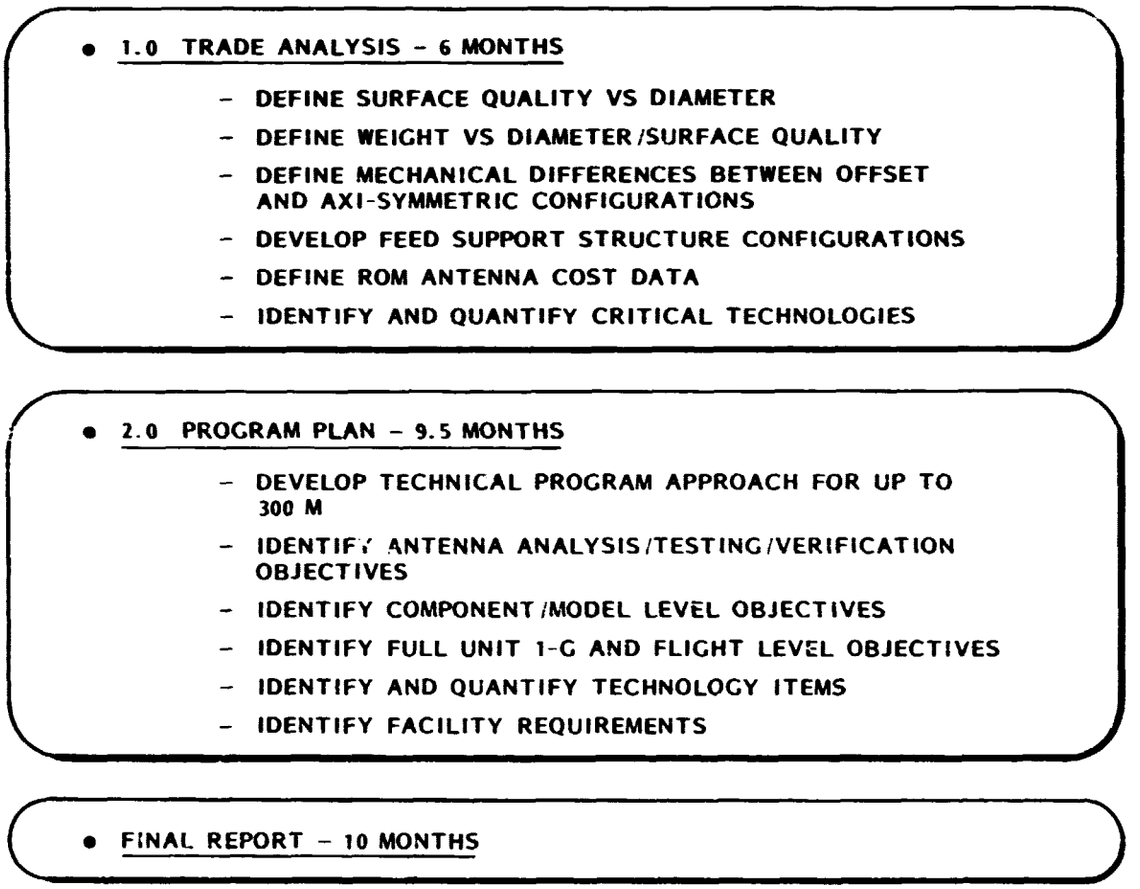

Figure 2.- Study tasks/schedule.

ANTENNA GEOMETRY

To date the large antenna systems are most commonly constructed as symmetric reflector systems. This geometry is shown in the left of Figure 3. Concerns with efficiency and side lobe levels have recently placed emphasis on the offset feed configuration shown in the right of the figure.

Geometrically an offset reflector is described by a parabolid where the geometric centerline is not coincident with the parabolic axis of symmetry. In order to gain the electrical advantages of reduced blockage, the parabolic axis and, therefore, the focal point must in fact be located external to the section aperture. This section can most easily be visualized by forming a large paraboloid of diameter D and then passing a cylinder, with a parallel axis of symmetry, through the paraboloid. If the cylinder has a diameter (d) less than D/2 and its radius is common with the radius of the parabola, the section of the paraboloid bounded by the cylinder is representative of the desired offset reflector surface. Further, if D/2-d is larger than the radius of the feed and the feed support structure is attached external to the radius of the offset section, there is no blockage of the electrical field of view.

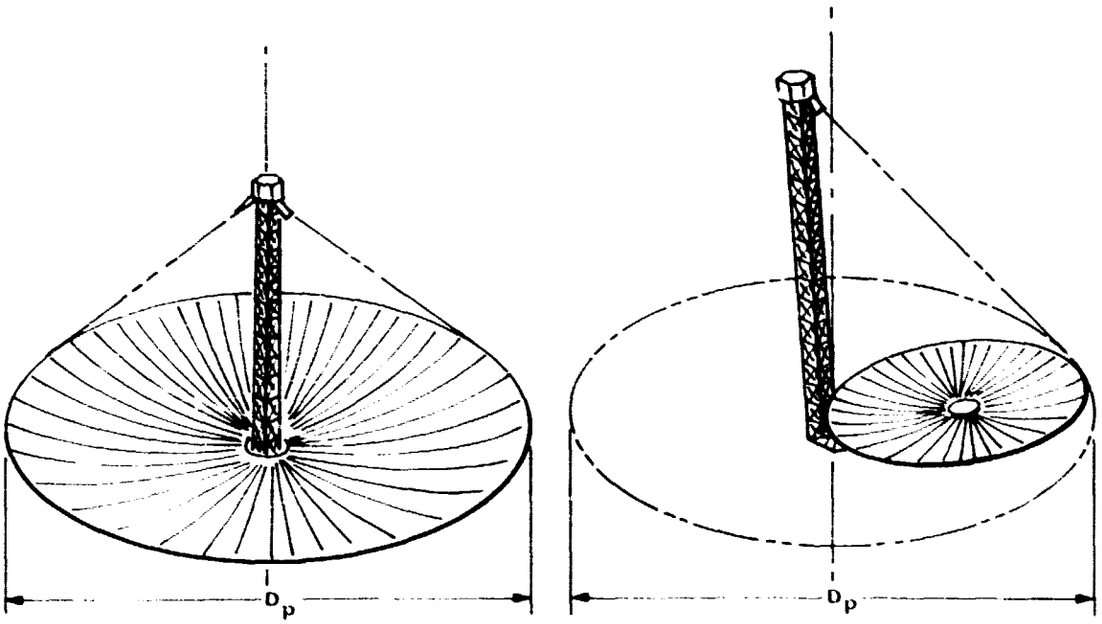

Figure 3.- Symmetric and offset antenna configuration comparison.

ASCENT AND DEPLOYMENT CONFIGURATIONS

Figure 4 presents an overview of the ascent sequence through the operational state of the vehicle. The STS stack shows an IUS attached to a vehicle from which the stowed feed support tower and reflector are attached. After achieving the desired operational orbit the deployment sequence begins with the tower extending, separating the vehicle from the reflector. The final event is the reflector deployment which occurs after the feed support tower has been completely deployed. The operational vehicle configuration was chosen to place the feeds, electronics and electrical power system components together for maximum efficiency since for the offset configuration this package does not block the antenna aperture.

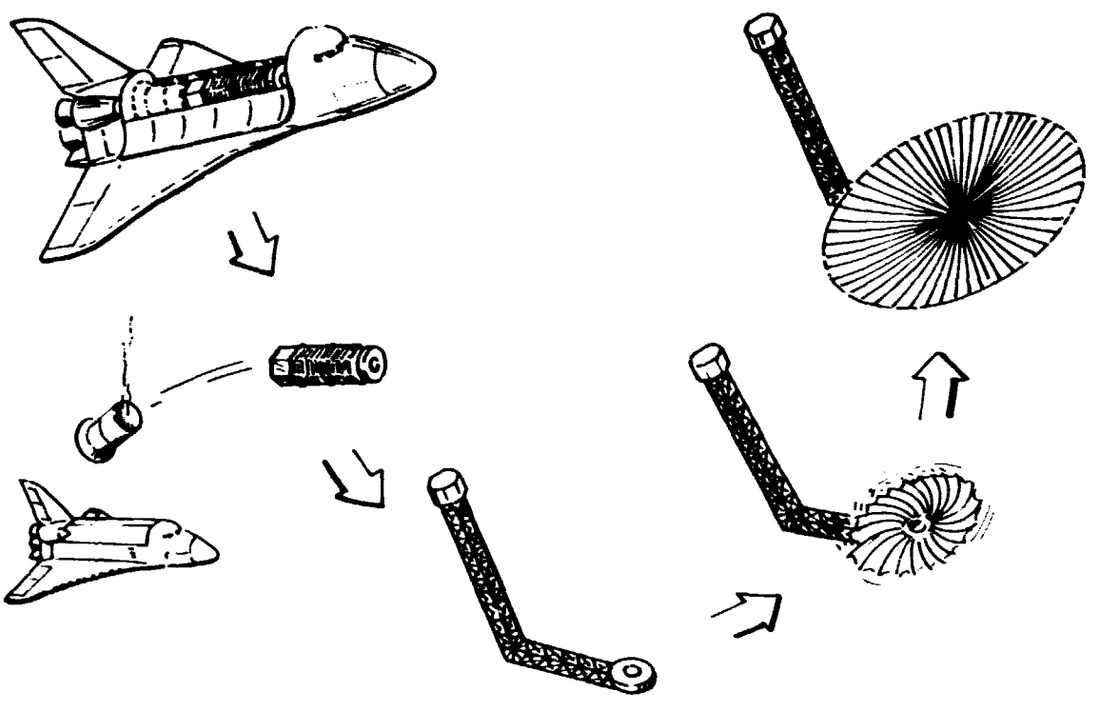

Figure 4.- Ascent configuration and deployment sequence.

WRAP RIB REFLECTOR DESIGN

The wrap-rib parabolic reflector is based on an approximation to a paraboloid of revolution. The wrap-rib antenna is comprised of radially emmanating gores between the ribs which take the form of parabolic cylinders. The parabolic cylinders more closely approximate a true paraboloid of revolution as the number of gores is increased. The point of diminishing returns for this reflector in terms of antenna performance is a function of both the radio frequency wavelength of interest and the reflector diameter. Figure 5 illustrates the physical appearance of the resulting reflector.

The gores are fabricated from a flexible membrane material which is usually a knitted or woven fabric of electrically conductive material. The gores are sewn to parabolically curved cantilevered ribs terminated at the central hub structure in a hinge fitting. For launch the antenna must be folded into a package size which will fit into the shuttle transportation system. For stowage the ribs are rotated on the hinge pin, then elastically buckled and wrapped around the hub. Once in space, the reflector is deployed by a deployment restraint mechanism which simply controls the rate of energy release and therefore the deployment rate.

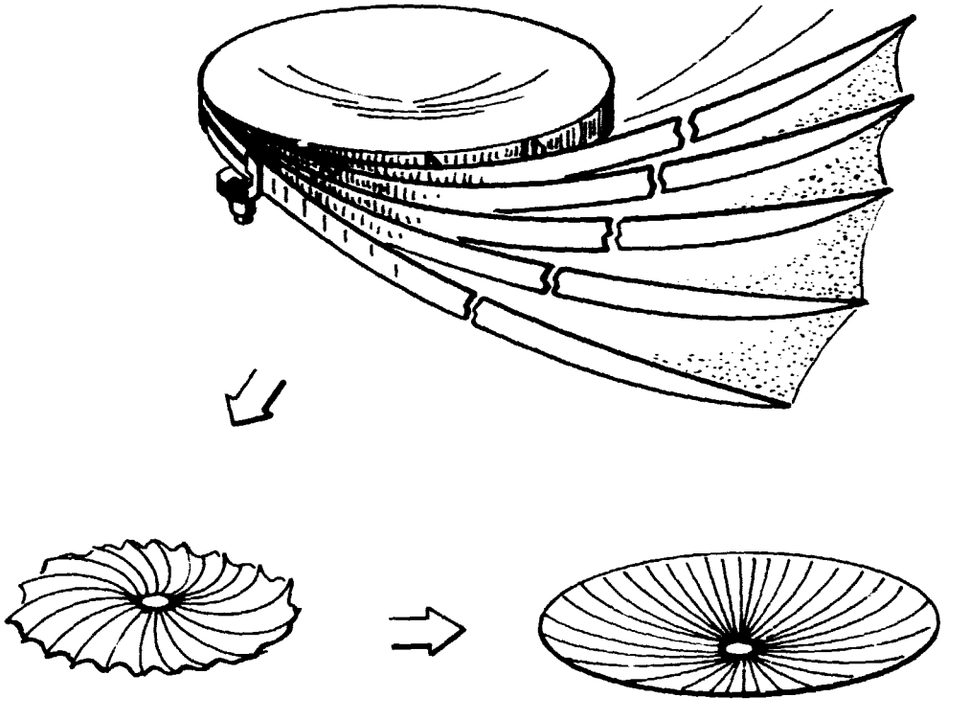

Figure 5.- Wrap rib reflector overview.

REDEPLOYABLE MAST

The key elements in the Redeployable Mast are the three lenticular shaped longitudinal members which can support an appreciable load when erect, but which can be folded upon themselves through the application of lateral and axial forces. For resisting torsional and lateral shear forces, wire tension cables are provided. The battens are necessary for supporting section hinges and for resisting the lateral, destablilizing cable reactions.

Figure 6 shows the overall mast system and emphasizes the stowage and deployment systems. The inner system performs the actual, section-by-section deployment and retraction of the mast through the use of three syncronous motor, sprocket, chain and development cog systems. It also serves as the bottom mast section until that section, itself, is fully erect. The guide rails in which these devices operate, are also provided with ramp cams which actuate the strikers for collapsing the lenticulars during retraction. The outer base system acts as the stowage bay for both the mast sections and the inner base system which must be extended during mast extension or retraction, but to minimize stowed length is retracted into the outer base system during full stowage. A chain drive system is also provided for the latter purpose.

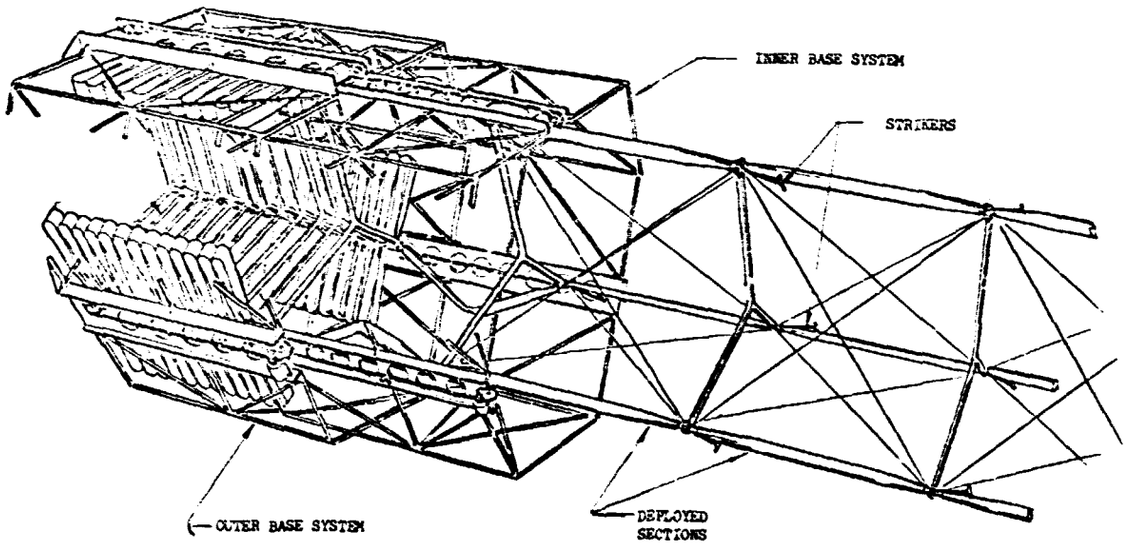

Figure 6.- Redeployable mast.

STUDY APPROACH

The approach taken to develop the parametric design and performance data focussed on the construction of a computer aided reflector and mast design packages. The reflector design package was constructed to accept basic material and structural element characteristics and develop design solutions which satisfied these inputs and the mission constraints of weight, stowed diameter and antenna system geometry. The developed designs were then analyzed to determine the extent of orbital and assembly surface errors, deployment integrity, and development costs.

Having defined the reflector size and operational frequency, a mast design could be developed with a design constraint that the pointing error be held to less then 0.05 beam widths. The mast design package approach was similar to the reflector package.

This developed program is overviewed in Figure 7.

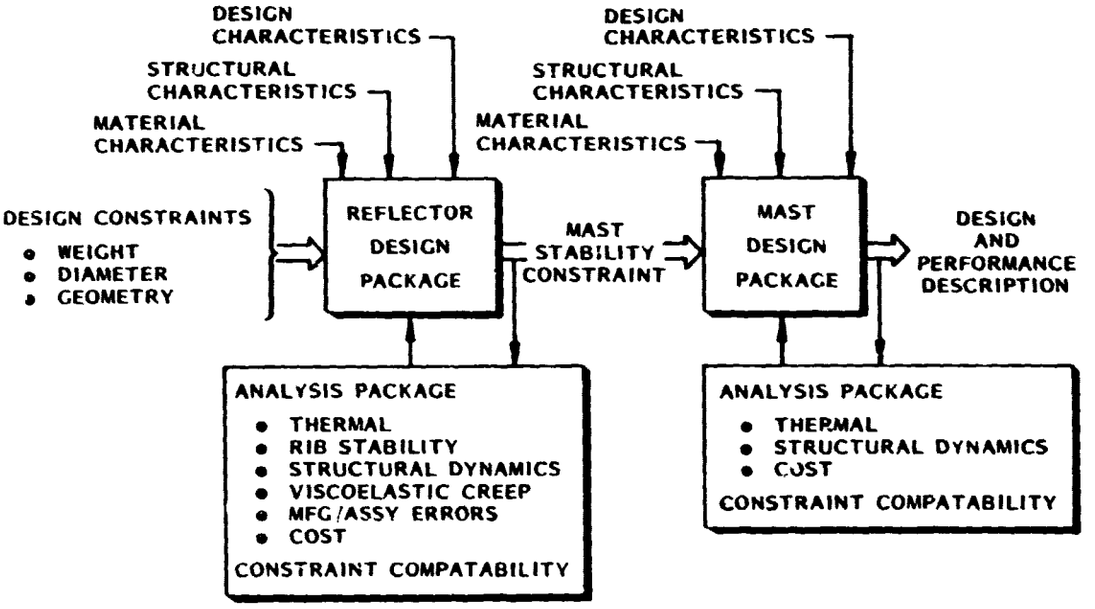

Figure 7.- Modeling approach.

COMPUTER PROGRAM OVERVIEW

The computer program assembled for this study of necessity provided more capability than a simple parametric study tool. In fact it is required to generate a complete preliminary design and performance analysis. This resulted in a flow chart and data output which, although meaningful, requires extensive discussion to make the reviewer comfortable. The final study report will contain this information, and for this overview Figure 8 was selected to introduce the operation.

This figure contains a flow chart developed from study case input data, computer programs, and output data. There are thirty-six input values, two of which describe mission constraints (weight and stowed diameter). The remaining variables are design and material characteristics. The main computer program develops the required compatible antenna designs and directly outputs a summary of the key output parameters while writing all of the detailed information to a file. Any or all of the design cases can be recovered in a readable form at a time selected by the user. This detailed information contains complete element design descriptions, weight breakdown and performance budget and can be used as a baseline preliminary design.

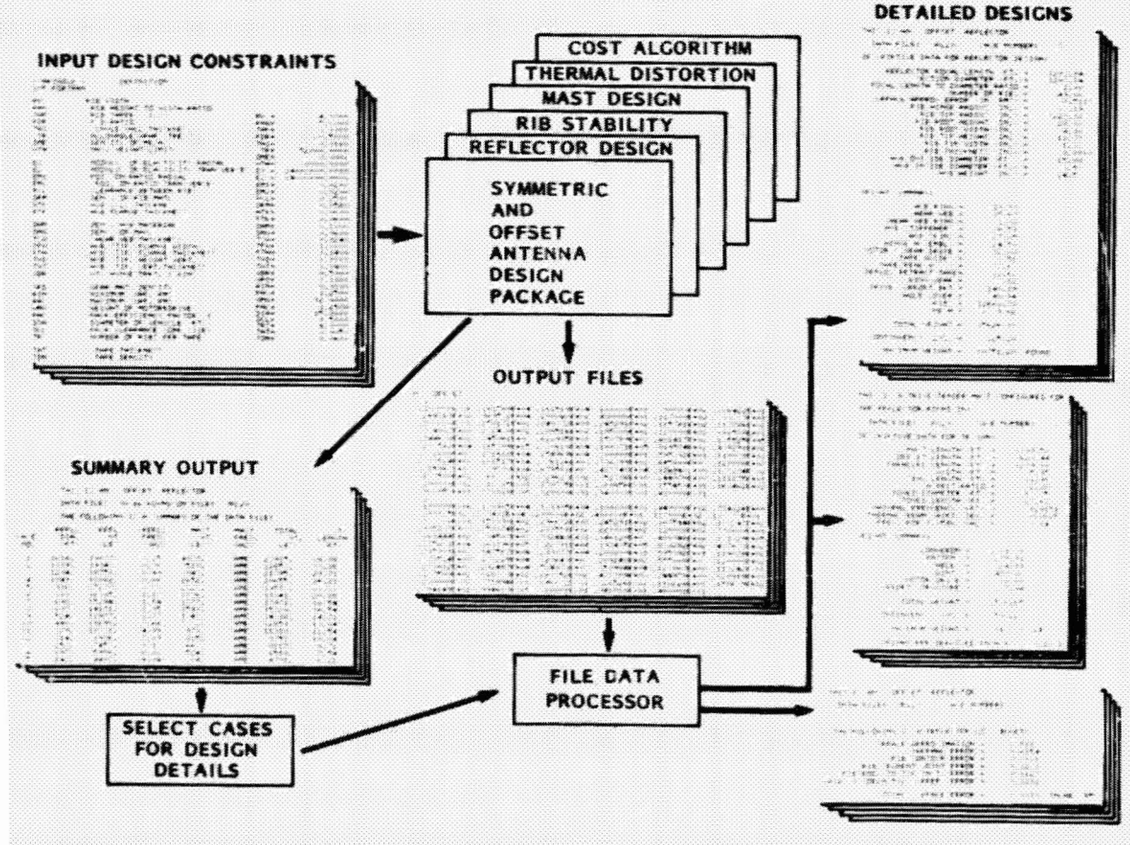

Figure 8.- Antenna optimization package overview.

ORIGINAL PAGE IS
OF POOR QUALITY

Figure 9 illustrates the effect that limiting the antenna weight has on the resulting system capability. With allowable antenna weights greater than approximately 4500 Kg (≈ 10,000 lb.), the maximum aperture diameter at a given operating frequency is limited by the STS diameter. As the weight limit is reduced, a corresponding reduction in the maximum aperture at a frequency can also be anticipated. The performance advantage the offset antenna configuration has over the symmetric system is also evident in that for any aperture diameter, the offset system will operate at a higher frequency, and at any frequency a larger offset reflector is possible than for the symmetric case.

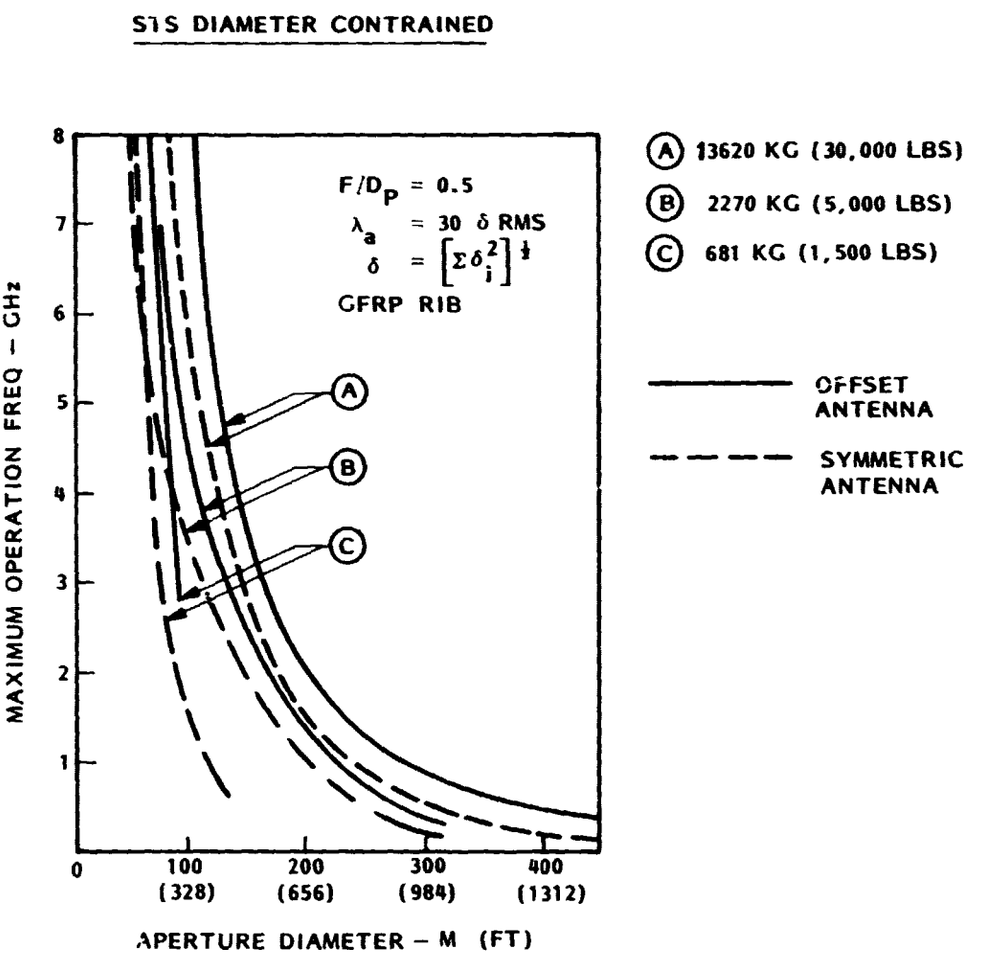

Figure 9.- Antenna aperture limits.

The analysis performed included calculations of the resulting system stowed length. As could be anticipated, the offset system exhibits a longer package than the symmetric counterpart as shown in Figure 10. This is due to the additional feed support tower length required.

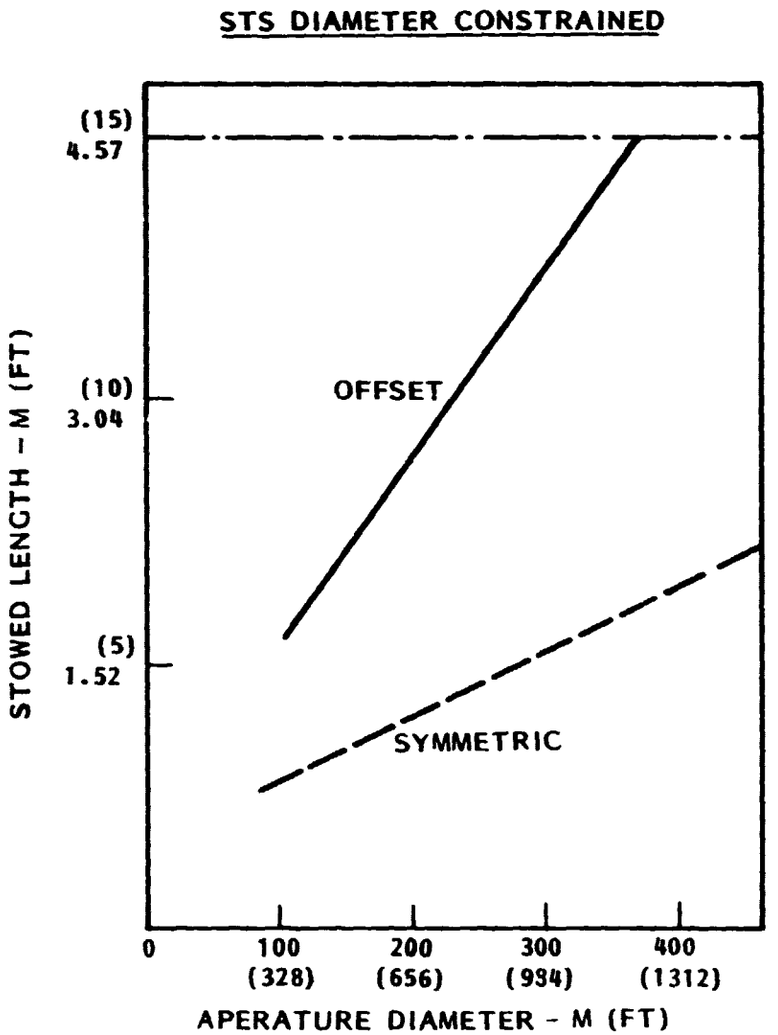

Figure 10.- Stowed diameter characteristics.

Using essentially no bounds on the allowable antenna weight (≈ 5000 Kg), the maximum reflector aperture is limited by the STS diameter and, as will be shown later, the allowable surface figure. The STS diameter limit causes the number of ribs to reduce as the aperture diameter increases. These results shown in Figure 11 indicate an increased surface error and a corresponding reduction in operating frequency.

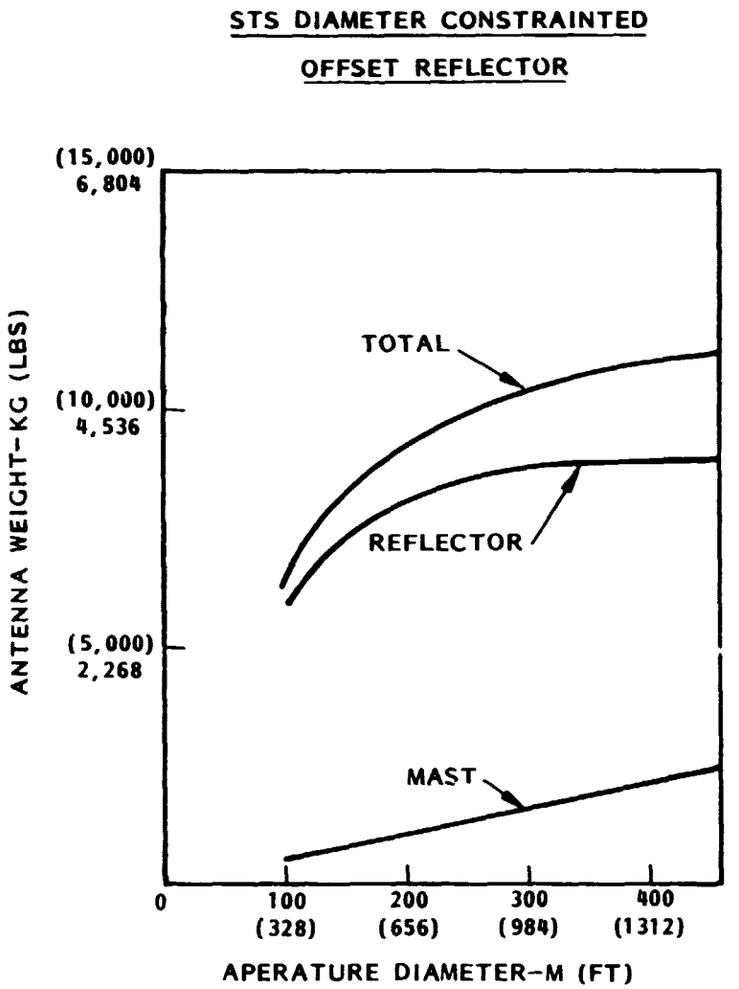

Figure 11.- Antenna weight characteristics.

The surface figure of a graphite epoxy reflector structure is a function of six seperate causes; rib segment fabrication, rib assembly, reflector assembly, viscoelastic creep, thermal distortion, and designed surface approximation.

The total effect of these errors was taken as the root-sum-squared (RSS) of the individual error components.

The surface approximation and the thermal distortion are the dominant error contributors for the cases performed. It is interesting to note from Figure 12 that, for the smaller (less than 300 meters) symmetric apertures and correspondingly higher frequencies, the thermal distortion is the larger of the two while at larger apertures and lower frequencies, the surface approximation dominates. This is due to the limiting effect of the STS diameter constraint which takes over at about that point.

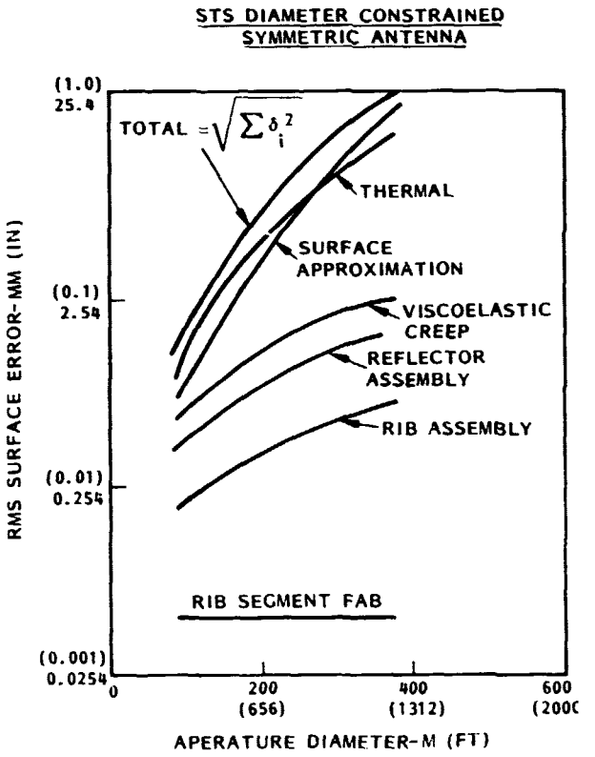

Figure 12.- Surface figure characteristics.

The longer f/D ratio for the offset antenna causes the surface approximation errors to be less than for the symmetric system. As a result, the thermal distortion error for the offset reflector, Figure 13, is the dominant factor thoughout the area of interest.

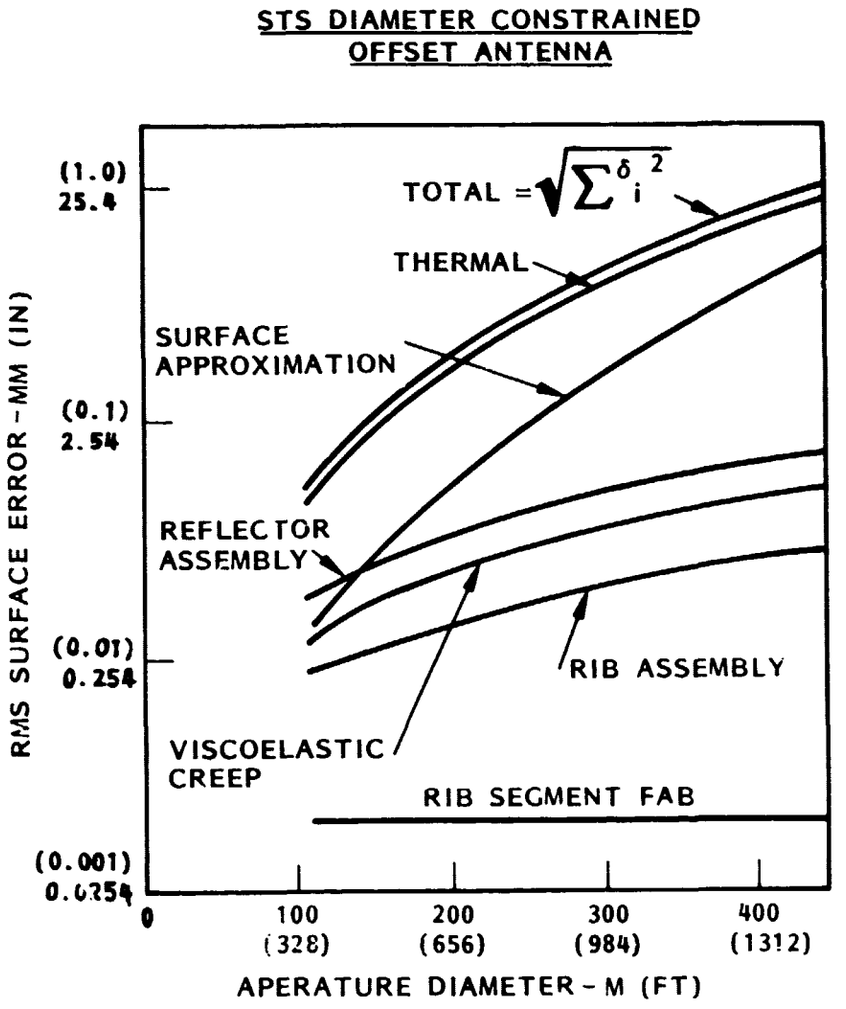

Figure 13.- Surface figure characteristics.

When the weight limit of 2300 Kg is applied, the surface approximation error for the symmetric case was found to become dominant at a much smaller aperture. This occurs due to the decrease in the number of ribs that must occur at a given diameter in order to meet the weight constraint. The effect can be seen by comparing Figures 12 and 14.

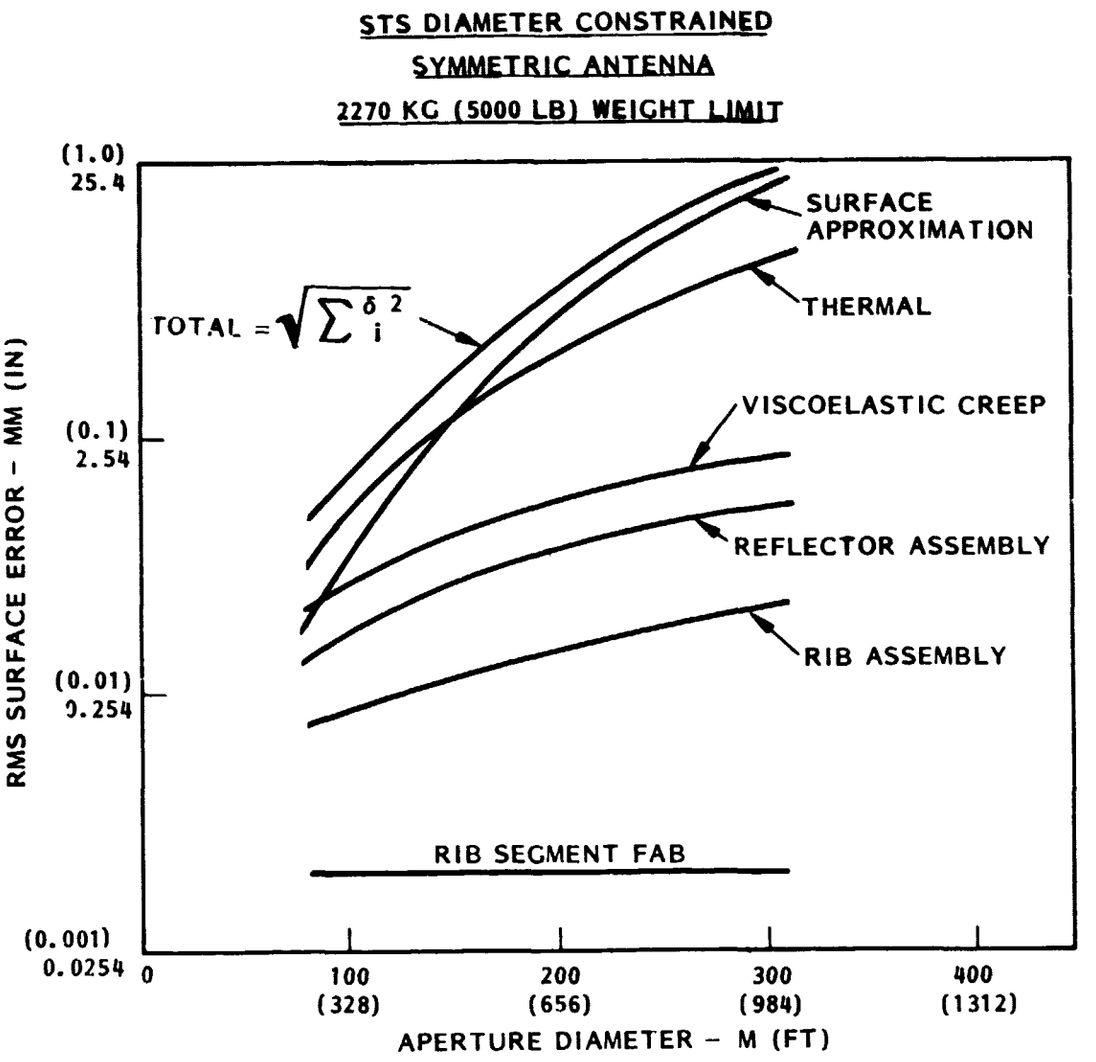

Figure 14.- Synchronous P/L surface characteristics.

When the 2300 Kg weight constraint is applied to the offset antenna, the surface approximation error more closely matches the thermal distortion contribution. Comparison of Figures 13 and 15 illustrate this effect.

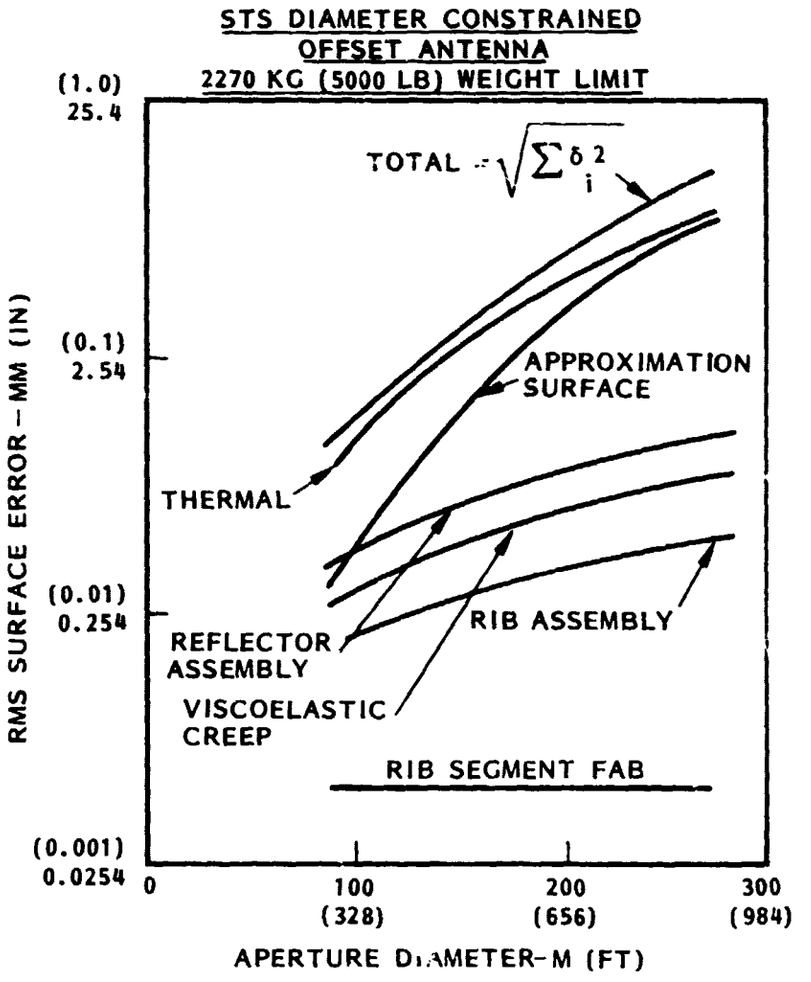

Figure 15.- Synchronous P/L surface characteristics.

Limiting the allowable reflector weight to 680 Kg results in a surface figure that is almost totally driven by the surface approximation contribution and in fact, the thermal errors become comparable to those associated with material properties and fabrication capabilities. This, shown in Figure 16, is due to the greatly reduced aperture associated with the lighter system.

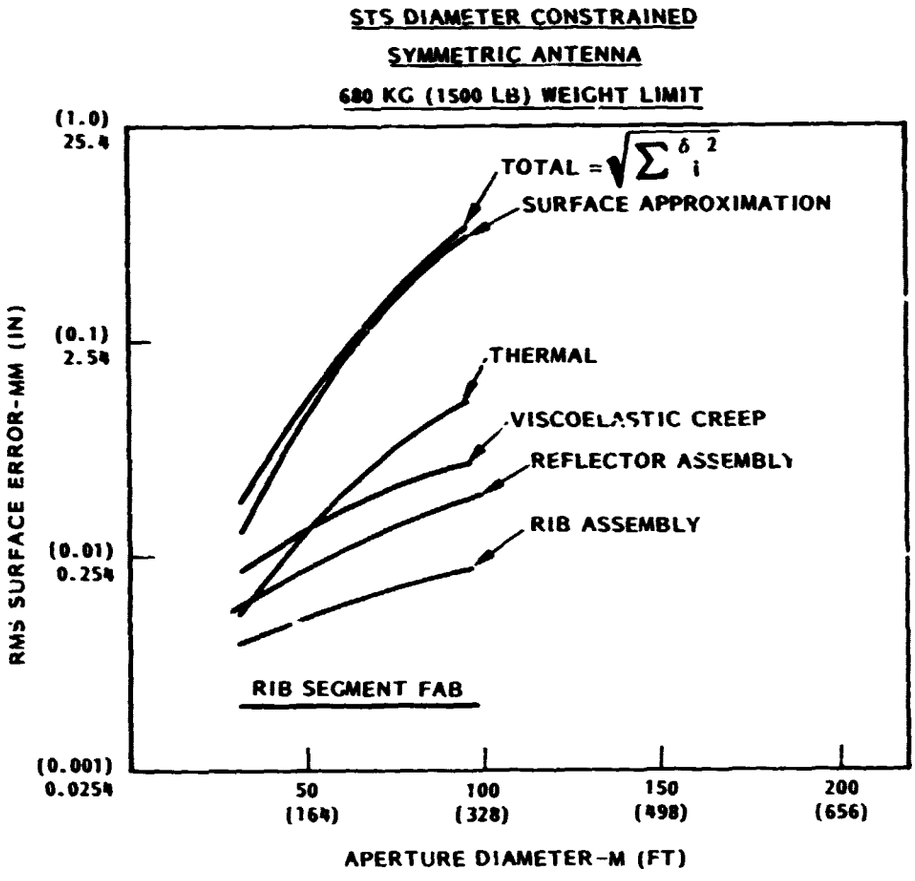

Figure 16.- Synchronous component surface characteristics.

Applying the 680 Kg limit to the offset reflector, Figure 17, has the same effect on the error distribution as for the symmetric antenna. The effect of the higher f/D ratio can be readily seen in comparing this and the previous chart.

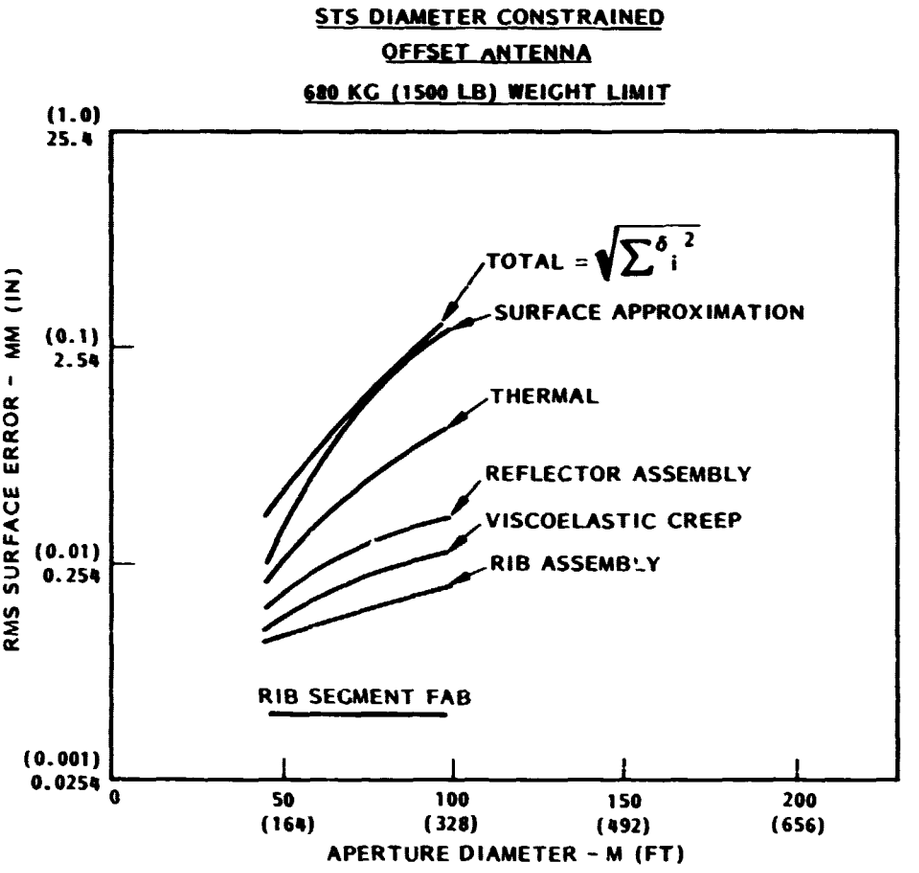

Figure 17.- Synchronous component surface characteristics.

The relationship the f/D ratio has on the frequency and aperture are illustrated in Figure 18. A given offset reflector with a parent f/D ratio of 0.25 will not perform at the same frequency as the same reflector configured with an f/D ratio of 0.50. Conversely, at a given frequency, a larger aperture can be made to work at an f/D ratio of 0.50 than at 0.25. This effect is present up to an f/D ratio of approximately 0.75. Beyond that, the curvature effect is not discernable.

The reason for this effect is due to the segmented reflector geometry. As the reflector curvature becomes less (higher f/D and flatter reflector) the effect of the flat panel approximation becomes less significant. In the limit, with an f/D of infinity, the reflector would be a flat plate and the segmented reflector would exactly approximate the surface.

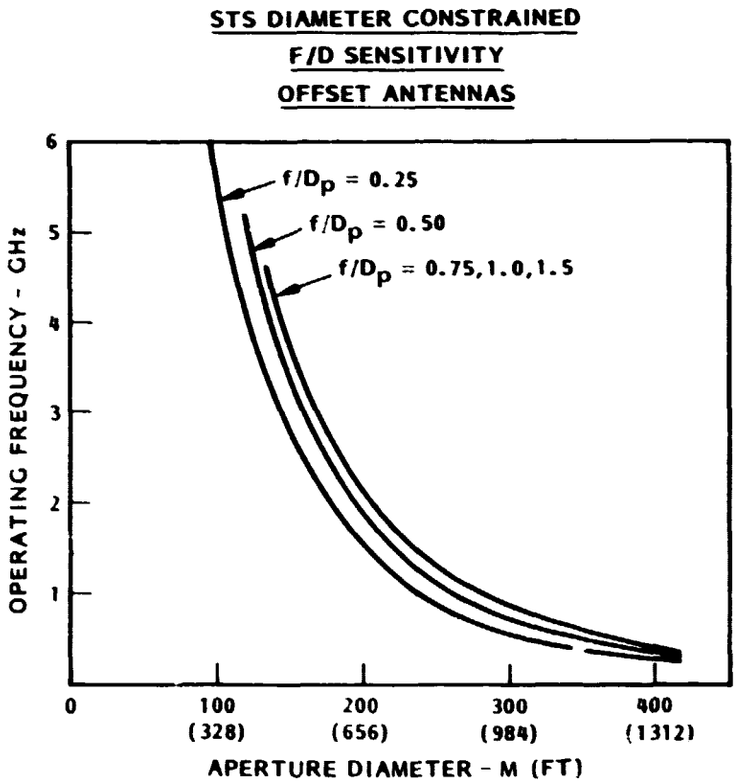

Figure 18.- Antenna system sensitivity to F/D.

Because of the impact of thermal distortion on the antenna performance, it is important to understand the causal parameters. One of the major contributors is the coefficient of thermal expansion (CTE). For the majority of the analyses performed on this study, a CTE of 1 x $10^{-7}/^{o}F$ was chosen to reflect a graphite epoxy reference structure. The performance sensitivity to this property can be seen in Figure 19.

Another property of the structure materials that has a significant effect on performance is the thermal conductivity. The advent of metal matrix composites (MMC), which combine the distortion coefficient of the graphite fibers with the thermal conductivity of metals, has had a significant effect on the projection of antenna performance.

The top curve on this chart was prepared using the properties typical of graphite magnesium MMC. The CTE used is 1 x $10^{-7}/^{o}F$ and the thermal conductivity is 18 BTU/HR-^{o}F-FT. The corresponding K for the graphite epoxy structure is 13.5 BTU/HR-^{o}F-FT.

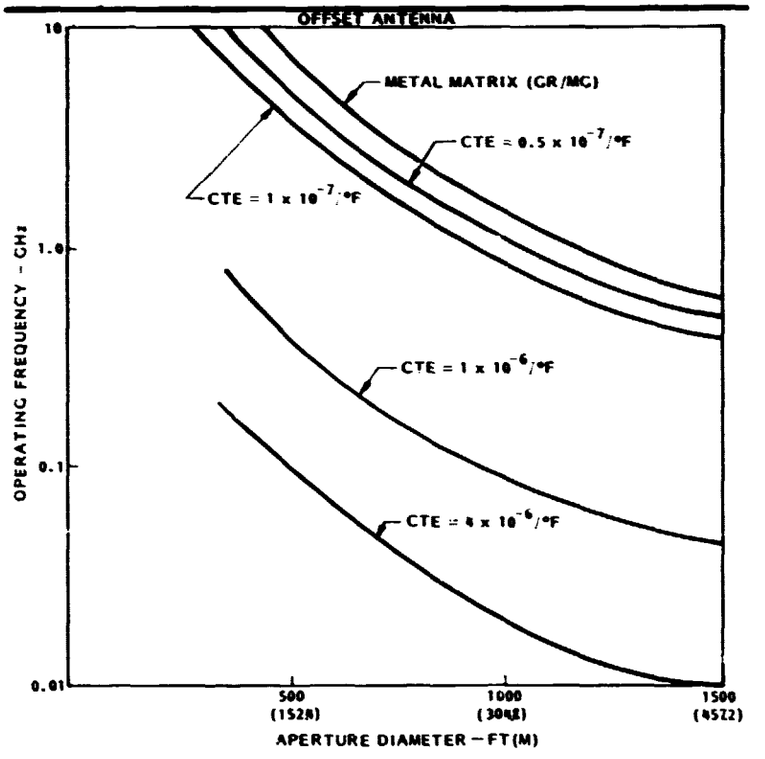

Figure 19.- Antenna sensitivity to material characteristics.

Application of the MMC properties to the analysis of the offset reflector results in reduced surface figure errors due to the lower thermal distortion and thereby increases the useable aperture diameter at a given frequency. Note also, on Figure 20, the MMC materials will not exhibit the viscoelastic creep error associated with graphite resin composites.

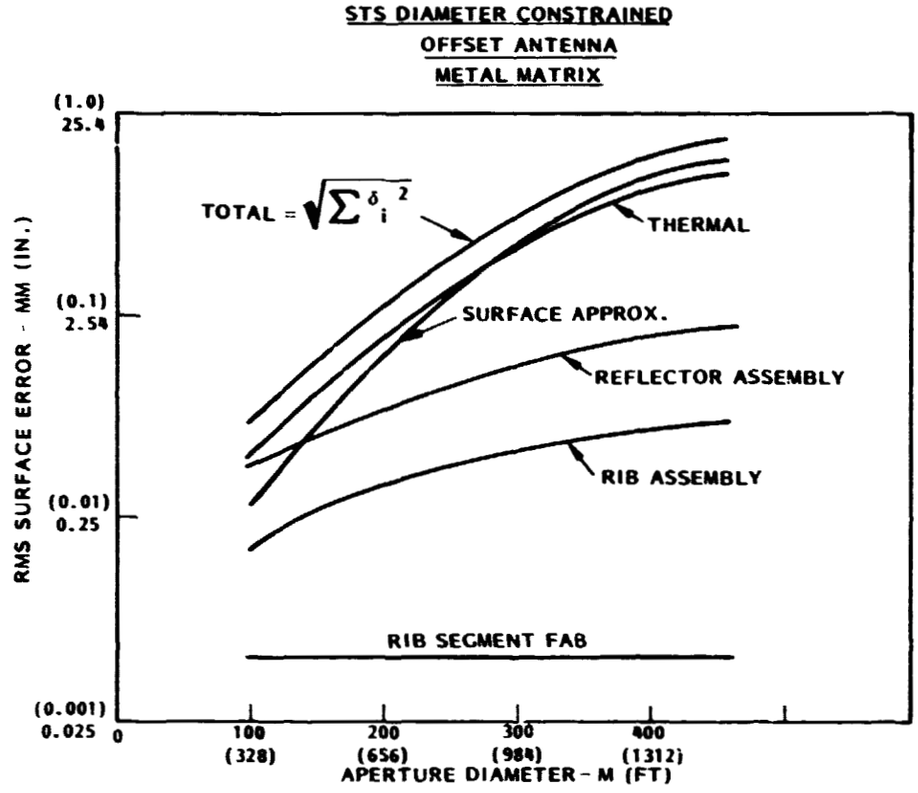

Figure 20.- Surface figure characteristics with metal matrix ribs.

Throughout the analyses thus far presented, the rib configuration has been held as a constant varying only in length and parabolic shape. This lenticular rib has a hub attachment cross section (rib root) of one inch wide, 4 inches high and a width taper of 2:1. The effect of changing the rib root geometry to 5 inch wide, 20 inches high can be seen in Figure 21. Increasing the rib width and height of the rib has the effect of reducing the number of ribs that can be attached to the hub. This in turn, reduces the useable operating frequency at a given diameter.

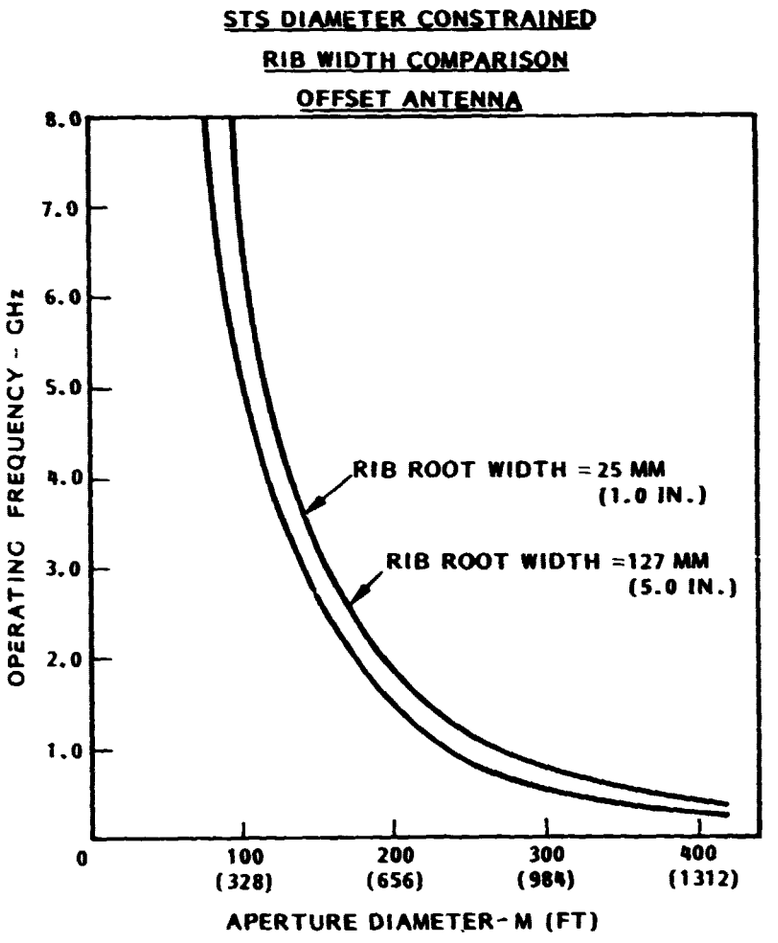

Figure 21.- Antenna system sensitivity to rib design.

PROJECTED ANTENNA COSTS

Figure 22 presents the projected cost for an offset antenna as a function of aperture size, weight and operating frequency. The data show that for low frequency apertures the cost is reasonably proportional to weight or diameter. As operating frequency limits are pushed the costs start to rise rapidly. This seems to occur in the 50 to 100 million dollar range for frequencies greater than 2 GHz.

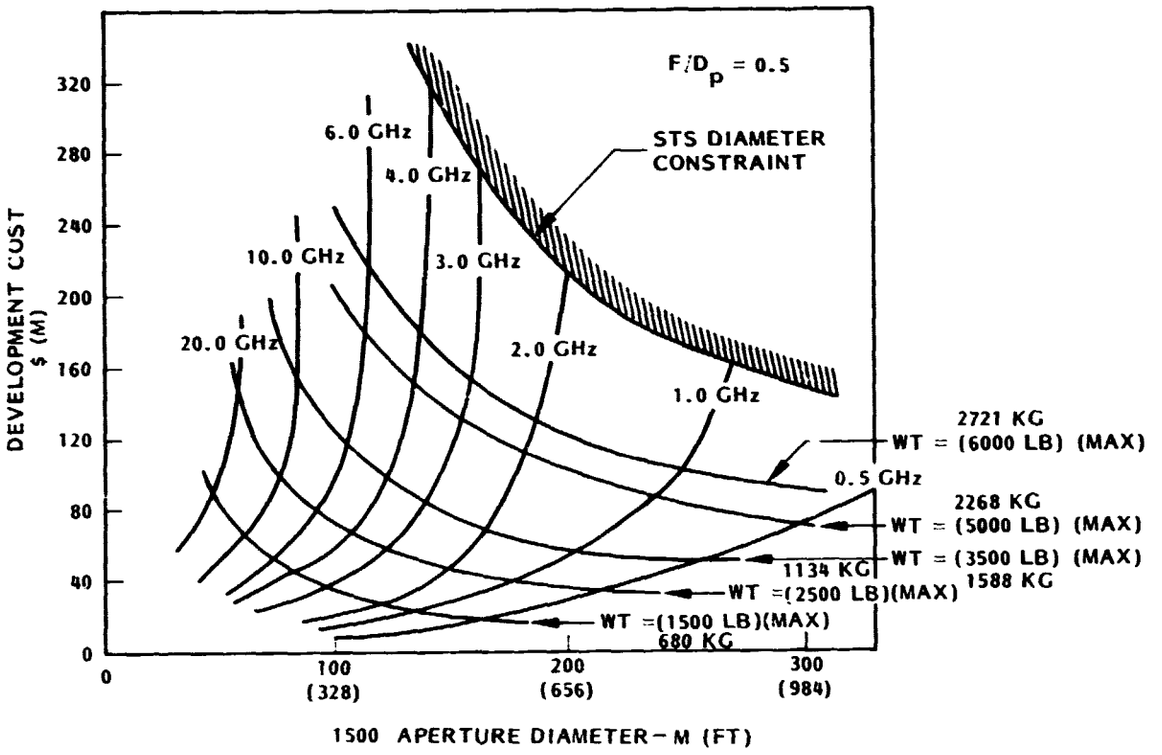

Figure 22.- Offset antenna cost projections.

OFFSET VS SYMMETRIC COST COMPARISON

The data presented in Figure 23 present the cost factor for an offset antenna. This increase is between 15 and 30%. The 30% factor is dominated by size and extra mast length costs, while at the higher frequencies the costs for maintaining a highly accurate reflector surface dominate.

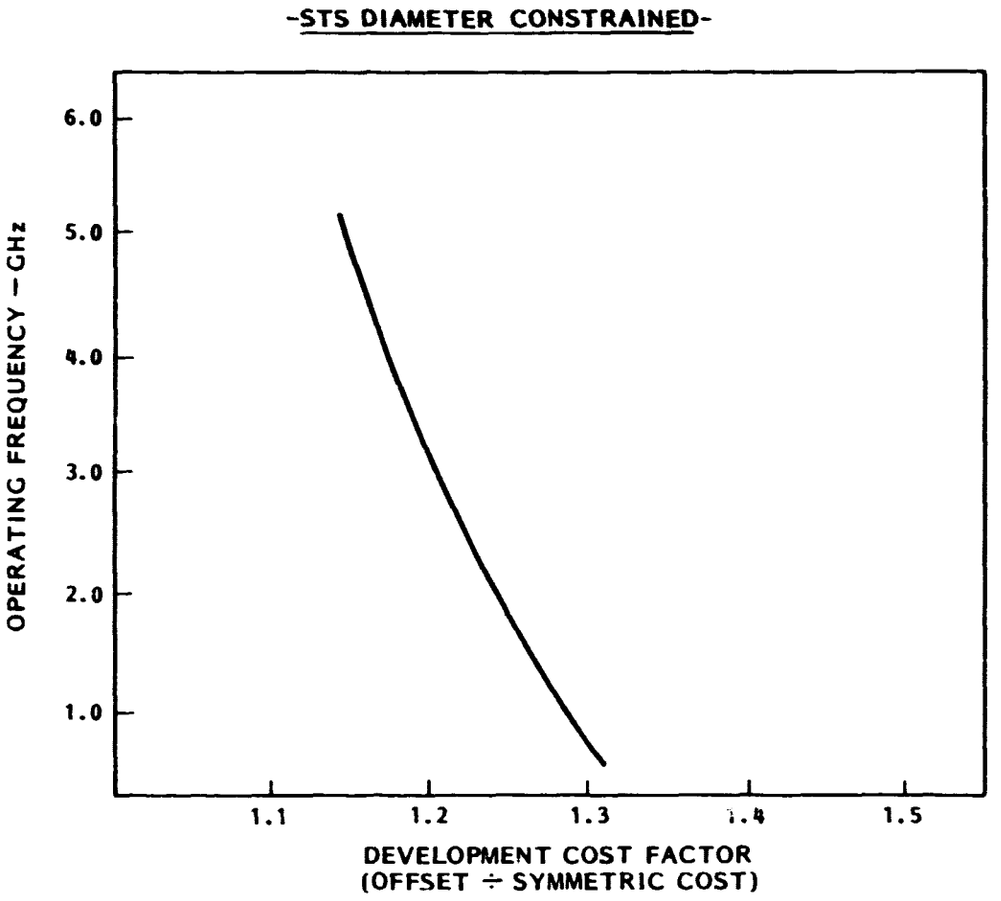

Figure 23.- Offset vs. symmetric antenna cost comparison.

TECHNICAL CONCERNS

The results of the investigation were surprising and satisfying. Earlier projections indicated the appropriateness of the Wrap Rib for large diameter antennas, and these projections have been reinforced. Technically, however, these are some concerns which must be addressed prior to a program undertaking. Figure 24 summarizes these concerns. The first four items can only be satisfactorily addressed through a hardware program. Further studies will resolve the latter three.

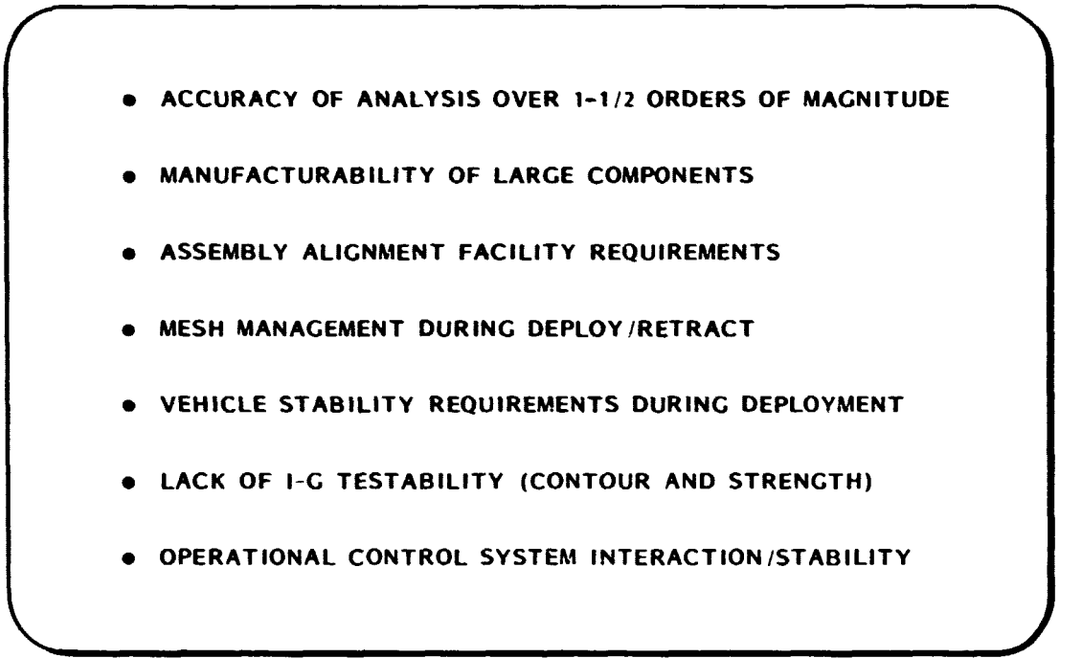

Figure 24.- Performance projection technical concerns.

PROGRAM PLAN

The final study activity was expended reviewing the concerns with undertaking a space flight program demonstration of a large diameter Wrap Rib antenna. The projected costs and technical risks identified the necessity of developing an early data base at a size which could comfortably be analytically scaled and which would reduce risk through demonstration. This program, identified in Figure 25, would involve developing a testable segment of a 50 M aperture. This would be used to validate the design and provide a scaling factor of 2 or 3 for the 100 to 150 M missions. The dominant effects of thermal distortions in the performance projections indicate orbital surface adjustment may prove cost effective and should be investigated. Finally, since the design is being defined, the stability and control system interactions and limitations should be identified.

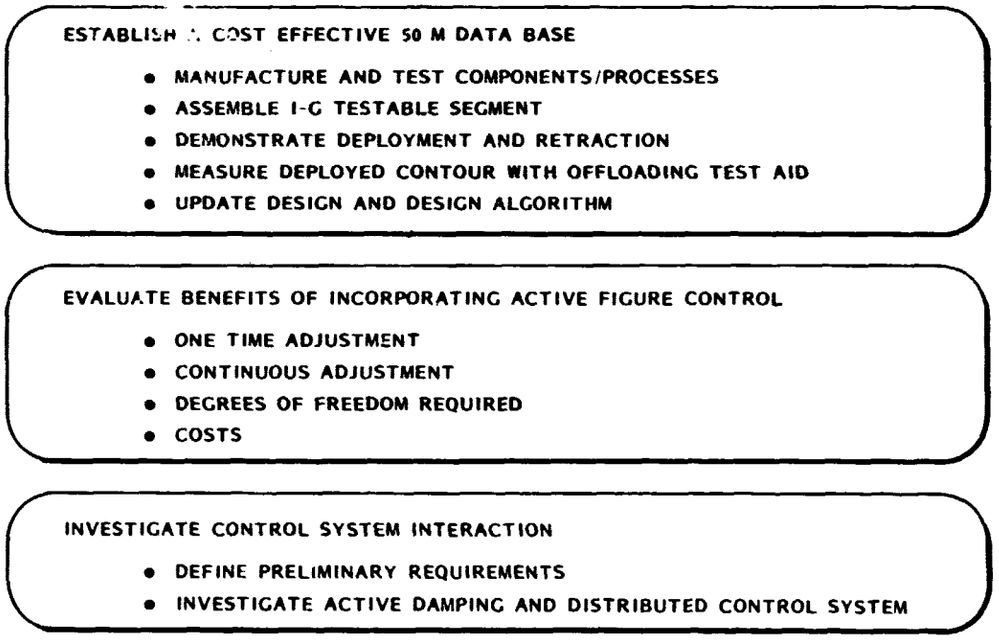

Figure 25.- Risk resolution/development plan.

STUDY CONCLUSIONS

As with any study one must be conservative when drawing conclusions. In this case we can conservatively draw those indicated in Figure 26. It is hoped that further activity will defend the reasonableness of designs which are at the limits indicated by the technical work performed.

- OFFSET WRAP RIB ANTENNAS UP TO 150 M DIAMETER ARE FEASIBLE FOR OPERATION AT 2 TO 3 GHz
- STS COMPATABILITY IS NOT A DESIGN DRIVER
- COST AND TECHNICAL RISKS INDICATE A NEW DATA BASE REQUIRED PRIOR TO UNDERTAKING 100 TO 150 M DESIGNS
- FURTHER ACTIVITY SHOULD INCLUDE ACTIVE SURFACE CONTROL AND CONTROL SYSTEMS INTERACTION STUDIES

Figure 26.- Study conclusions.

D2

N80-19147

ADVANCED SUNFLOWER ANTENNA CONCEPT DEVELOPMENT

J. S. Archer
TRW

LSST 1ST ANNUAL TECHNICAL REVIEW

November 7-8, 1979

This report is a summary of the results of a study performed at TRW to determine the feasibility of stowing large solid antenna reflectors in the shuttle using the Advanced Sunflower Concept developed at TRW. This work was sponsored by JPL as part of its study of precision self-deployable antenna systems, which in turn is part of the NASA Large Space Systems Technology (LSST) program.

PAGE 32 INTENTIONALLY BLANK

STOWED REFLECTOR CONFIGURATION

The basic deployment concept was originally developed at TRW to meet the requirement for large diameter ($D/\lambda > 1000$), high accuracy reflectors to be used in the 10 to 100 GHz range or higher, within the constraints of the shuttle.

The folded petal concept provides hinged connections along adjacent edges of all panels. Bending and shear continuity is thereby provided throughout the contour in the deployed aspect. All elements are released and deployed simultaneously.

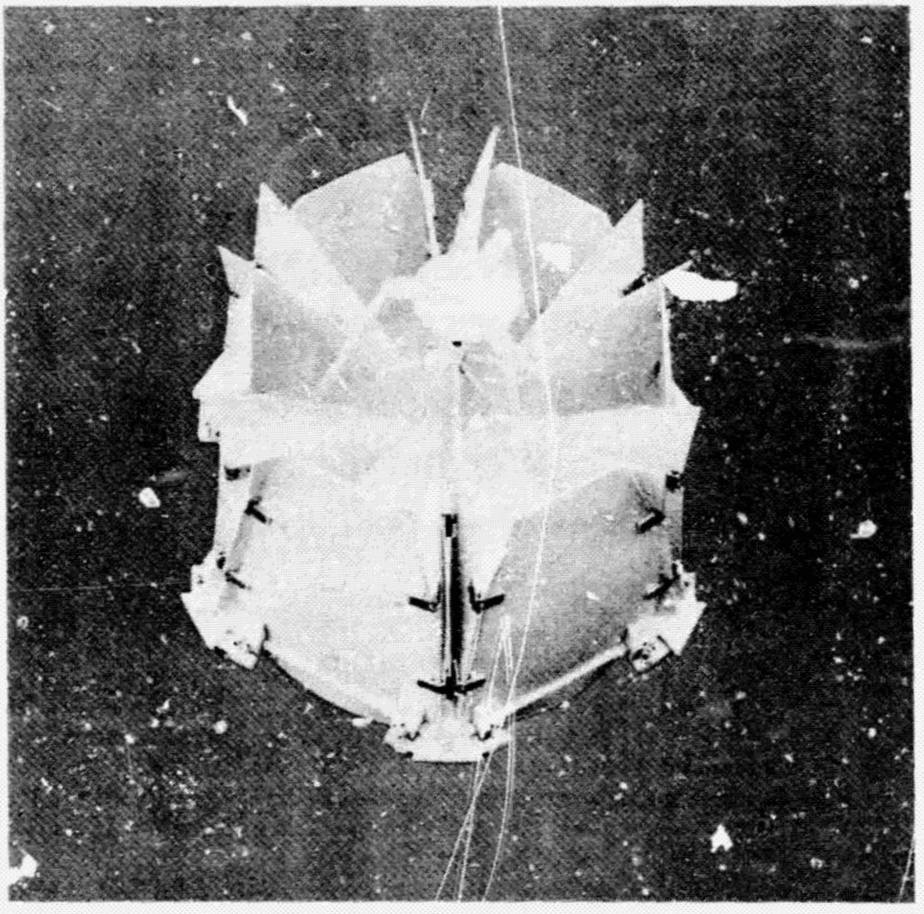

ORIGINAL PAGE IS
OF POOR QUALITY

WORK STATEMENT TASKS

The study focused on two major tasks. The first was to conduct an investigation of the original deployment concepts, including the following:

1. Determine the largest antenna of this design stowable in the shuttle payload compartment.

2. Determine the upper boundary for surface quality vs. antenna diameter.

3. Determine packing efficiency and weight vs. diameter.

4. Develop ROM cost estimate vs. diameter and surface quality.

5. Perform the above tasks for offset fed antennas.

6. Identify critical technologies required for construction of these antennas.

The second task involved the development of advanced designs which would allow antennas up to 100 feet in diameter to be accommodated by the shuttle. The same information as in the first task was to be obtained for the most promising of these designs.

PRECISION DEPLOYABLE REFLECTOR STUDY
FOR JPL, NASA LANGLEY
WORK STATEMENT TASKS

- DETERMINE LARGEST DIAMETER REFLECTOR THAT CAN BE STOWED IN SHUTTLE - CURRENT CONFIGURATION
- ESTIMATE SURFACE CONTOUR ACCURACY FOR A RANGE OF SIZES - CURRENT CONFIGURATION
- ESTIMATE ROM COSTS AS A FUNCTION OF REFLECTOR DIAMETER AND CONTOUR ACCURACY - CURRENT CONFIGURATION
- IDENTIFY AND QUANTIFY THE CRITICAL TECHNOLOGIES REQUIRED TO DEVELOPE THE REFLECTOR ABOVE
- DETERMINE PACKAGING EFFICIENCY AND WEIGHT AS A FUNCTION OF REFLECTOR DIAMETER - CURRENT CONFIGURATION
- NEW CONCEPTUAL DESIGNS TO IMPROVE PACKAGING EFFICIENCY FOR REFLECTORS UP TO 100 FT. DIA.
- CHOOSE PREFERRED CONCEPT AND PROVIDE ROM COST ESTIMATES, PACKAGING EFFICIENCY, WEIGHT AND CRITICAL TECHNOLOGIES
- PERFORM THE ABOVE TASKS FOR OFFSET FED REFLECTORS IN ADDITION TO FOCAL FED REFLECTORS

STOWED ENVELOPE PROPORTIONS

The critical parameter which determines the maximum aperture which can be stowed in shuttle is the number of primary panels in the configuration. Preliminary studies provided data on the ratio of stowed diameter to deployed diameter as the number of main panels was varied from 4 to 12. 6, 12 and 18 main panel configurations were examined in more detail for the study.

REFLECTOR CONFIGURATIONS AND RATIOS OF DIAMETER TO STOWED ENVELOPE DIMENSIONS

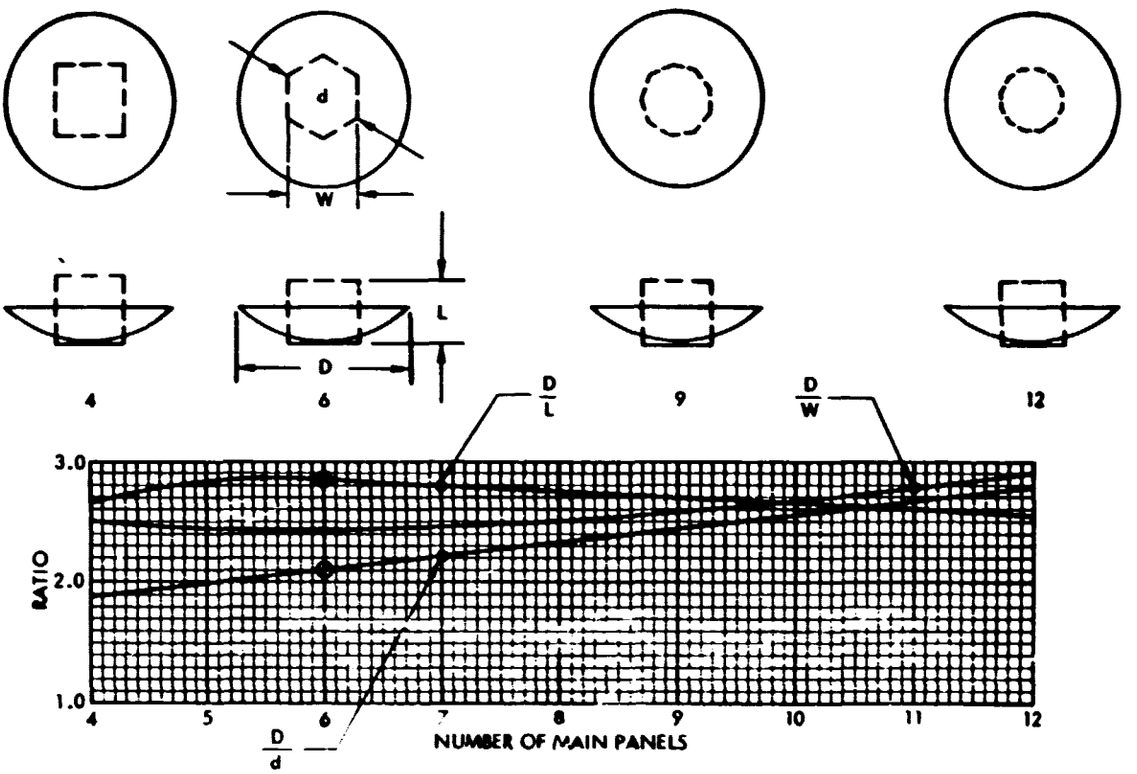

STOWAGE OPTIMIZED STUDIES

The detailed examination of the 6 main panel configuration included an optimization of the configuration to allow a more efficient packing of the panels. This included trimline adjustment to avoid interference between panels when stowed. The optimization studies were accomplished for a F/D ratio of 0.4.

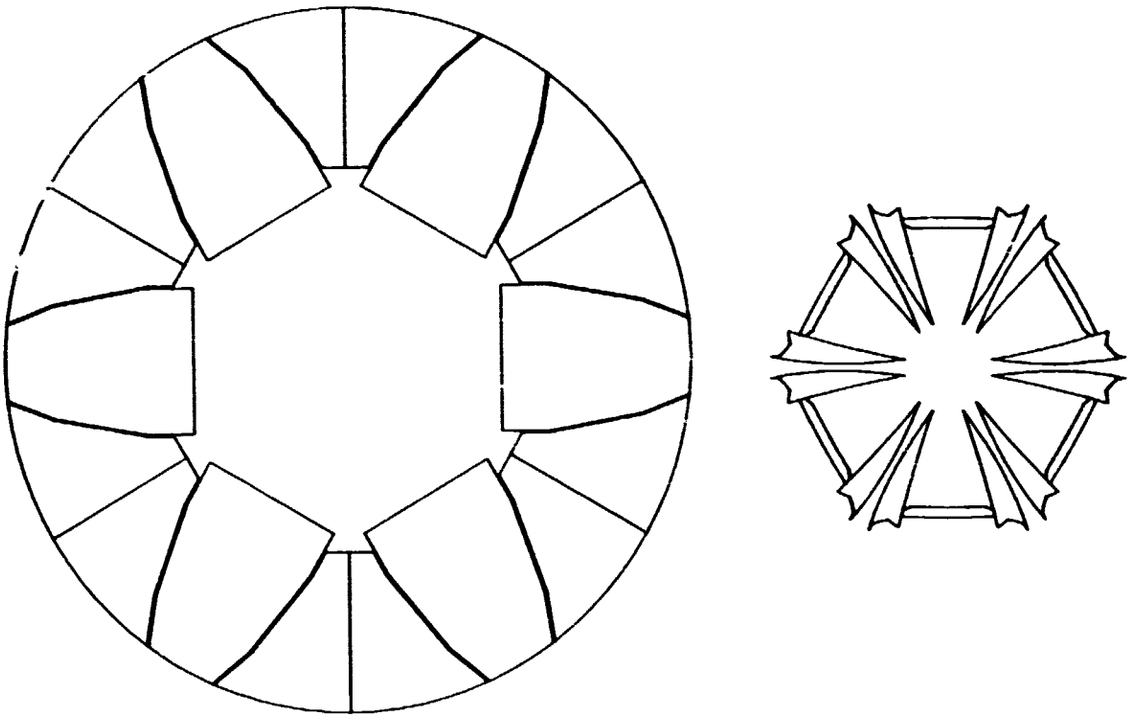

6 MAIN PANEL CONFIGURATION BEFORE OPTIMIZATION

OPTIMIZED 6 PANEL CONFIGURATION

This view is an optimized 6 panel configuration which compares with the original configuration shown previously. Note the increased aperture to stowed diameter ratio. The maximum aperture for the 6 panel configuration is 33.2 feet.

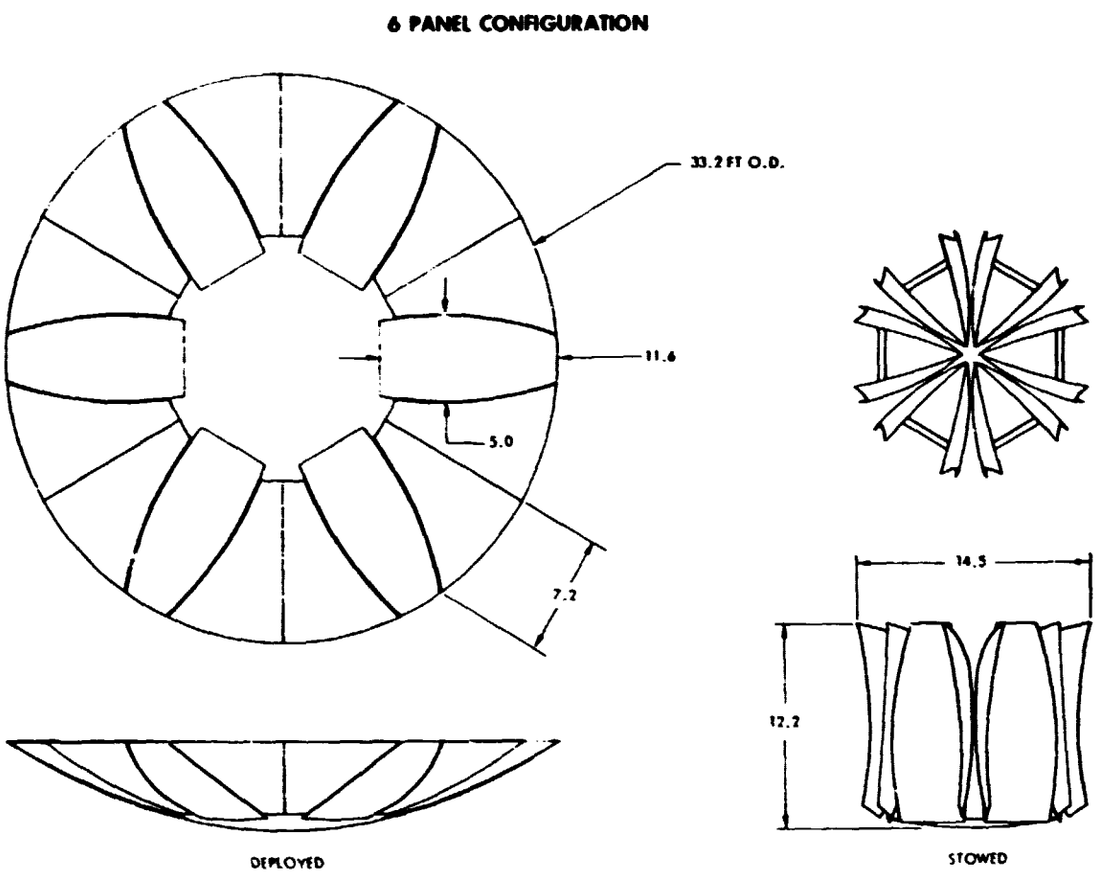

OPTIMIZED 12 PANEL CONFIGURATION

The 12 main panel configuration is illustrated below after optimization. A 37.8-foot aperture may be stowed in the shuttle with a 14.5-foot diameter stowed envelope. Note the long narrow panel envelopes when compared to the 6 panel configuration.

12 MAIN PANEL CONFIGURATION

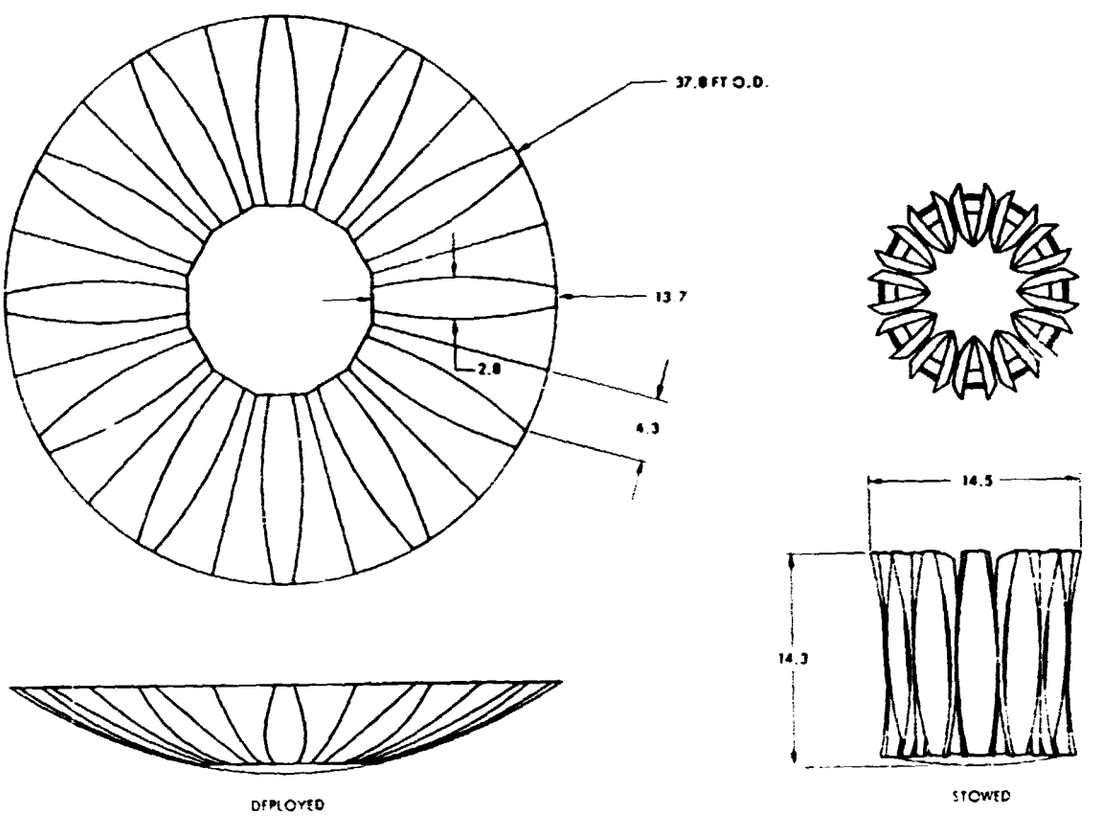

OPTIMIZATION APPROACH

This view illustrates the optimization approach. The goal is to compactly place the triangular panel and half the main panel within the allocated triangular wedge. This was accomplished most conveniently using a CAD graphical display. The influence of displacing various hinge locations was determined individually. Thence, by iteratively adjusting the hinge positions, the most compact arrangement was determined which defined the optimum geometry. A second constraint on the optimization was to minimize the radial envelope of the folded panels.

The cross-hatched areas on the panels were provided to improve the visibility of the projected surfaces.

OPTIMIZATION APPROACH, 12 PANELS

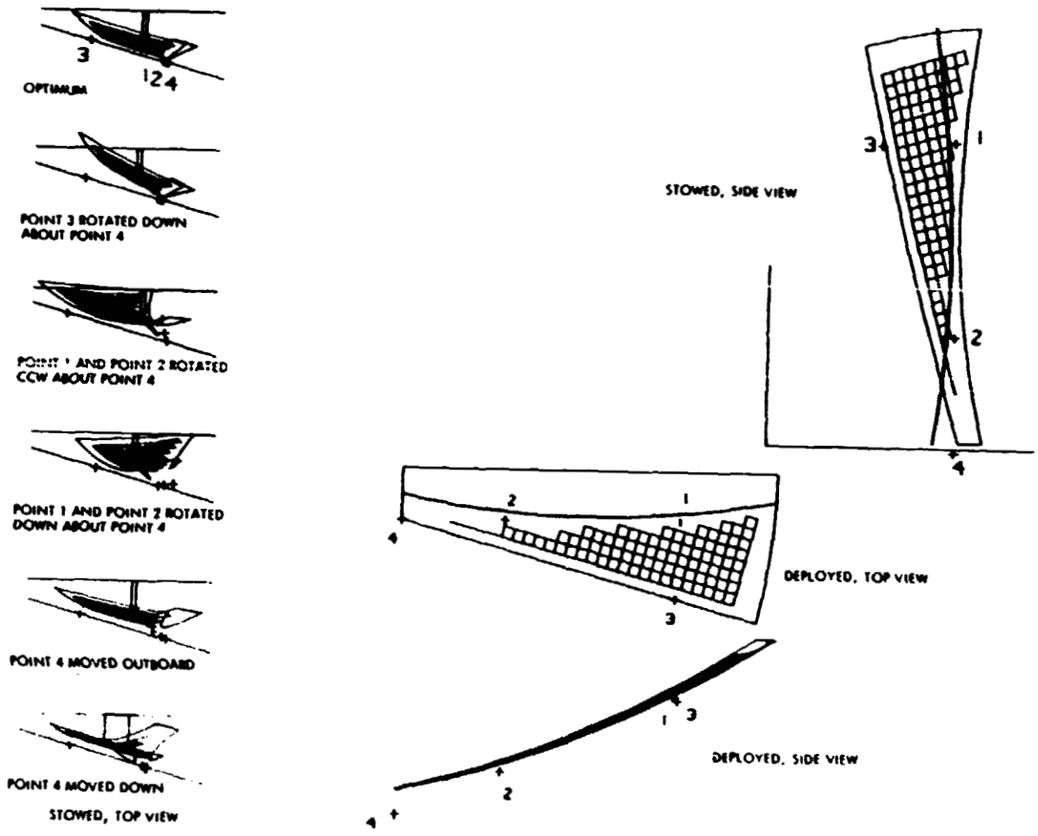

18 PANEL CONFIGURATION

The maximum stowable aperture was attained with the 18 main panel configuration. This provided a 42-foot aperture for the available 14.5-foot stowed envelope. It was determined that more than 18 main panels would not improve the stowing ratio.

18 MAIN PANEL CONFIGURATION

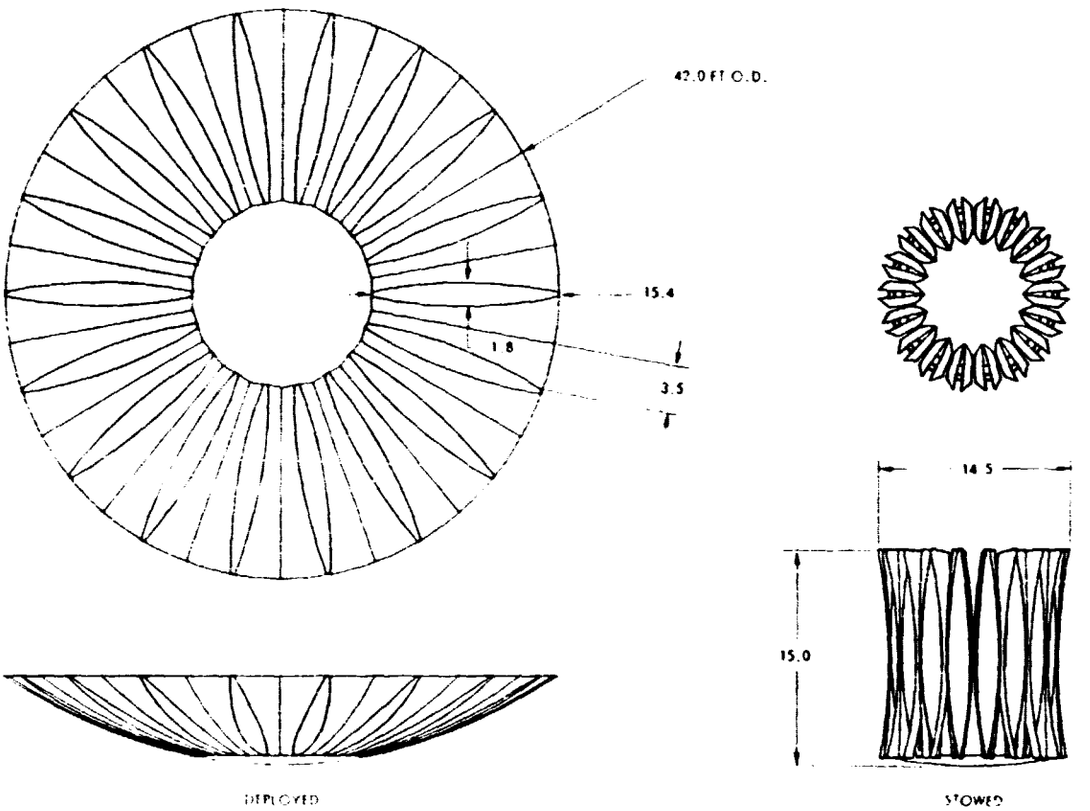

SHUTTLE STOWAGE OF 18 PANEL CONFIGURATION

Stowage of the 42-foot, 18 main panel aperture requires a 15-foot segment of the shuttle bay.

An increase of the F/D ratio from 0.4 to 0.62 for the 18 panel configuration would allow an increase in the aperture from 42 foot to 50 foot for stowage in shuttle. However, a similar F/D increase would not result in significant improvement for the 6 panel configuration, since the panel width is the governing factor rather than the curvature.

18 MAIN PANELS

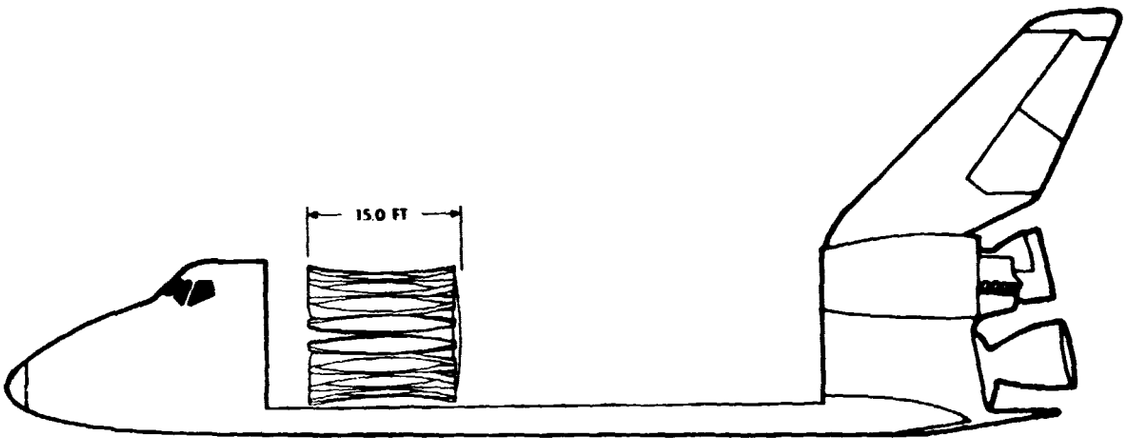

STOWED VIEW OF 18 PANEL CONFIGURATION

This enlarged view of the stowed 18 main panel configuration illustrates the detail which is possible for conceptualizing the complex geometry on the CAD (Computer Aided Design) graphical display. The long narrow envelope of the panels increases the difficulty of achieving a precision contour. Two hinge connections are provided along adjacent edges between panels. Adequate space is available within the folded reflector to provide supporting structure for a feed or subreflector.

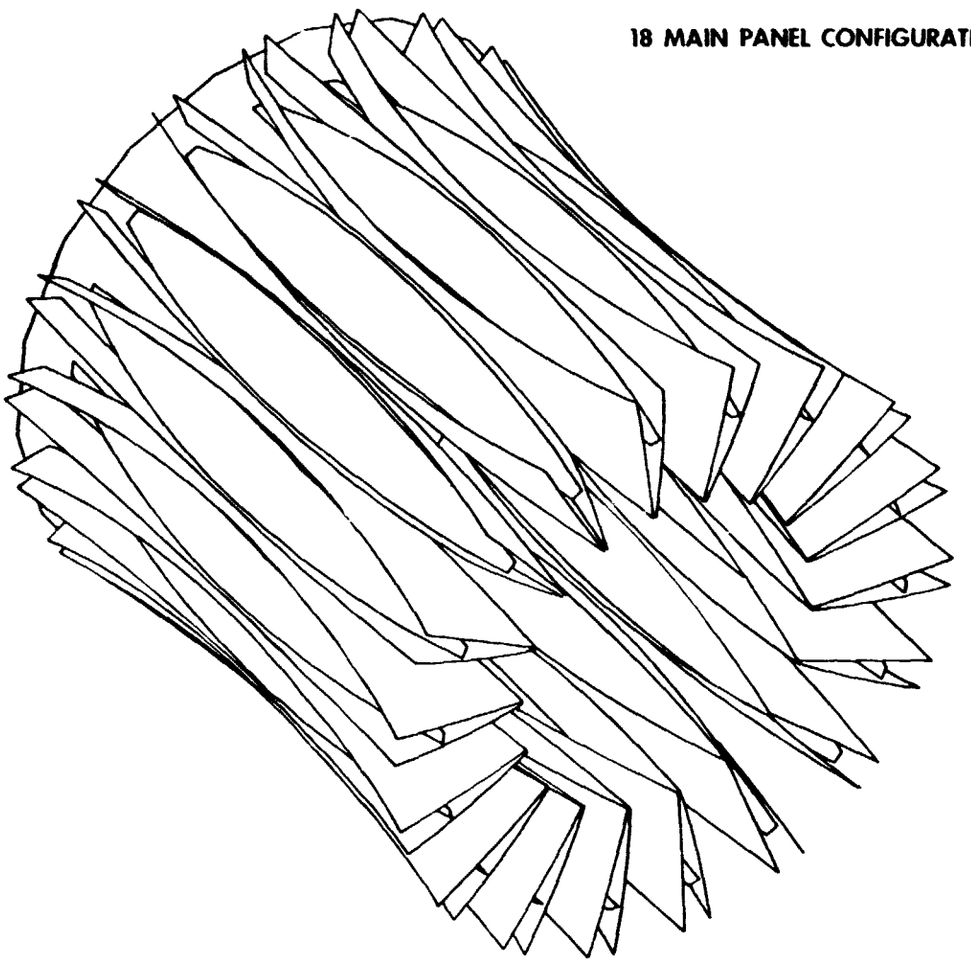

18 MAIN PANEL CONFIGURATION, STOWED

ANTENNA WEIGHT VS. DIAMETER

The weight of antenna reflectors has been estimated for diameters of 16 to 100 feet. The weight of feeds and subreflectors is not included. Since the weight of the reflector predominates, the plot is approximately valid for advanced configurations to be described which may require additional hinges or other hardware. Specific designs were assumed for 16, 24 and 100-foot apertures and intermediate points linearly interpolated. The basic construction assumed a graphite/epoxy aluminum honeycomb sandwich configuration.

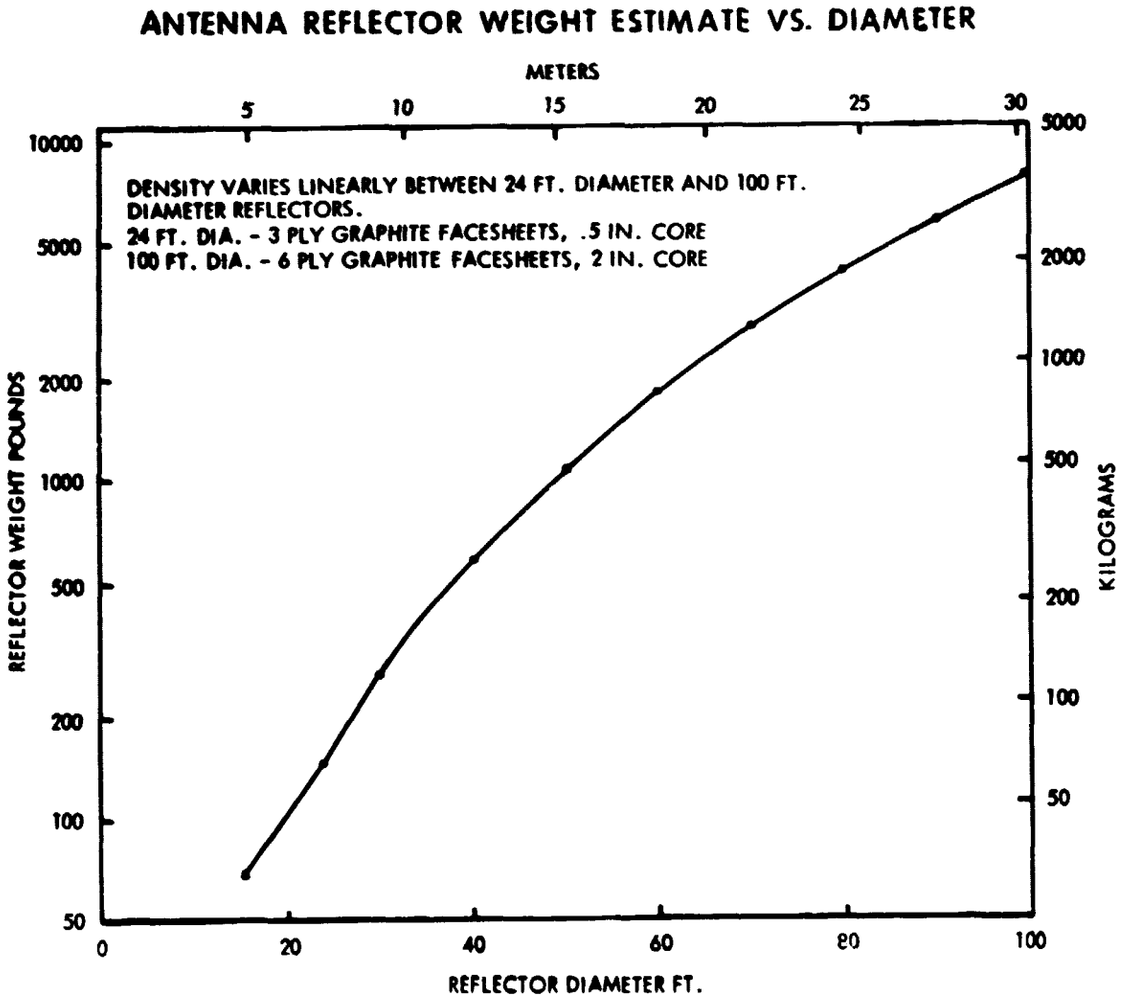

CONTOUR ERROR ESTIMATES

An attempt has been made to estimate the surface quality obtainable for the large aperture antenna reflectors of both the original and advanced designs. Four separate estimates have been made. The first three are based on presently available fabrication technology, improved fabrication technology and post fabrication adjustment of the panels, respectively. The fourth estimate is for a system with an orbit active control of panel contour.

The errors quoted are conservative. They are based on considerations of the long narrow panel shapes and on thermal distortion analyses for a 16-foot aperture.

CONTOUR ERROR ESTIMATES

	RMS DEVIATION	MAX DEVIATION	BASIS OF ESTIMATE/ASSUMPTION
AS FABRICATED			FROM FAB OF SOLID REFLECTORS AND TEST PANELS
CENTER SECTION	$0.9X10^{-4}$ D	$2.7X15^{-4}$ D	
OUTER PANELS	$2.0X10^{-4}$ L	$6.0X15^{-4}$ L	
POST FAB ADJUSTED	.0005"	.0015"	TOLERANCE IN SETUP AND INSTRUMENTATION ASSUMED SAME REGARDLESS OF SIZE MAX PANEL LENGTH 19 FT.
ASSEMBLY	.001"/10' DIA	.003"/10' DIA	ESTIMATE ONLY, ERROR IN LOCATING PANEL IN OPTIMUM POSITION AND ATTACHING HINGES
DEPLOYMENT	.0005"/20' DIA	.0015"/20' DIA	BASED ON REPEATABILITY OF SUNFLOWER
THERMAL	.002"/20' DIA .0034"/100' DIA	.006"/20' DIA .0102"/100' DIA	BASED ON THERMAL DISTORTION ANALYSIS OF 16 FT. REFLECTOR AND MAX DEVIATION = .006 CALCULATED FOR INDIVIDUAL PANELS OF 40' DIA.

NET RMS ERROR ESTIMATE

The total RMS performance of various sized apertures for the basic configuration, as well as advanced configurations, is shown here. This performance is predicated upon the utilization of a post fabrication panel shape adjustment to optimize the contour. This technique is commonly applied and is considered state-of-the-art.

ESTIMATE OF RMS ERROR
POST FAB PANEL ADJUSTMENT

ERROR CONTRIBUTOR	1 RING			2 RINGS			3 RINGS		
	20'	30'	40'	40'	60'	80'	80'	100'	120'
POST FAB ADJUSTMENT	.0005	.0005	.0005	.0005	.0005	.0005	.0005	.0005	.0005
ASSEMBLY	.0010	.0020	.0030	.0040	.0050	.0060	.0070	.0080	.0090
DEPLOYMENT	.0005	.0008	.001	.0015	.0020	.0030	.0035	.0040	.0045
THERMAL	.0020	.0022	.0024	.0024	.0027	.0030	.0030	.0034	.0037
TOTAL	.0040	.0055	.0069	.0084	.0102	.0125	.0140	.0159	.0177

RIGID REFLECTOR PERFORMANCE EXTRAPOLATION

An independent error assessment was accomplished based on extrapolation of existing data for solid contour reflectors. This was performed for a 30-foot aperture, 6 panel configuration. The results are consistent with the previous chart. It is suggested that this performance may be considerably improved by using precision tooling and on-orbit figure control.

EXPECTED MECHANICAL PERFORMANCE
(30 FT APERTURE)

	DEMONSTRATED CAPABILITY	PROJECTED CAPABILITY
MANF RMS	0.002(1)	0.001(2)
ASSY RMS	0.002	0.001(3)
ORBIT RMS	0.002	0.001(4)
R.S.S.	0.004	0.002

(1) POST-FABR ADJUSTMENT OF PANEL CONTOURS
(2) PRECISION LAYUP MOLD
(3) IMPROVED ASSEMBLY TOOLING
(4) IN-ORBIT FIGURE CONTROL

SHAPE CONTROL ACTUATION SYSTEM

On-orbit shape control for minimizing the effect of orbital environments on contour RMS could be readily implemented on the Advanced Sunflower configuration. Actuators for applying linear and angular differential motions between reflector panels can readily be integrated into the design at the hinge assemblies, as illustrated. These would be selectively actuated by a feedback control loop connected to a system of contour distortion sensors.

SHAPE CONTROL ACTUATION SYSTEM
FOR LARGE PRECISION DEPLOYABLE REFLECTORS

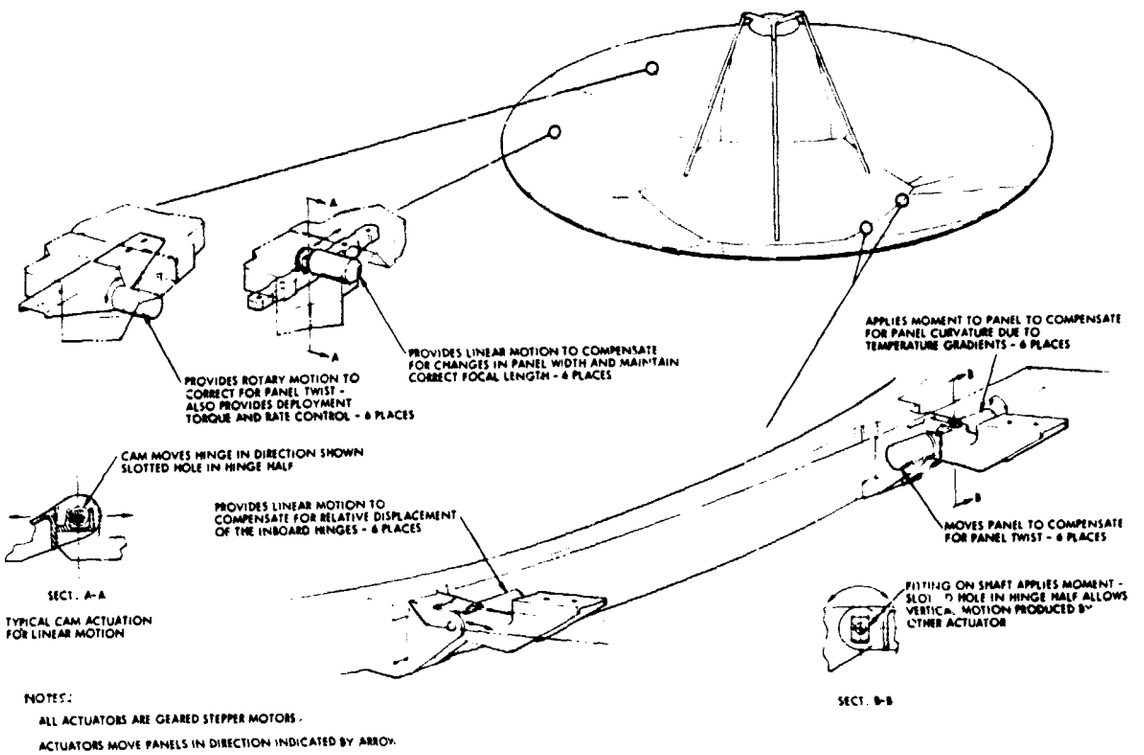

ALTERNATIVE DESIGNS

Several designs have been considered as possible alternatives to improve the stowed to deployed diameter ratio, and thereby increase the size of the antenna stowable in the shuttle. Of the six designs examined, one, the Sunflower concept, is an existing and successful design, one is a modification of the original design, and the other four involve the addition of a second a possibly a third ring of panels to the original configuration.

The Sunflower concept has been used successfully and is capable of providing a 100-foot antenna stowable in the shuttle. The major drawback, however, is that upon deployment the panels are not connected together and would require either complicated latching mechanisms or considerable EVA to achieve a sufficiently accurate reflector.

100 FT. DIA. "SUNFLOWER" REFLECTOR

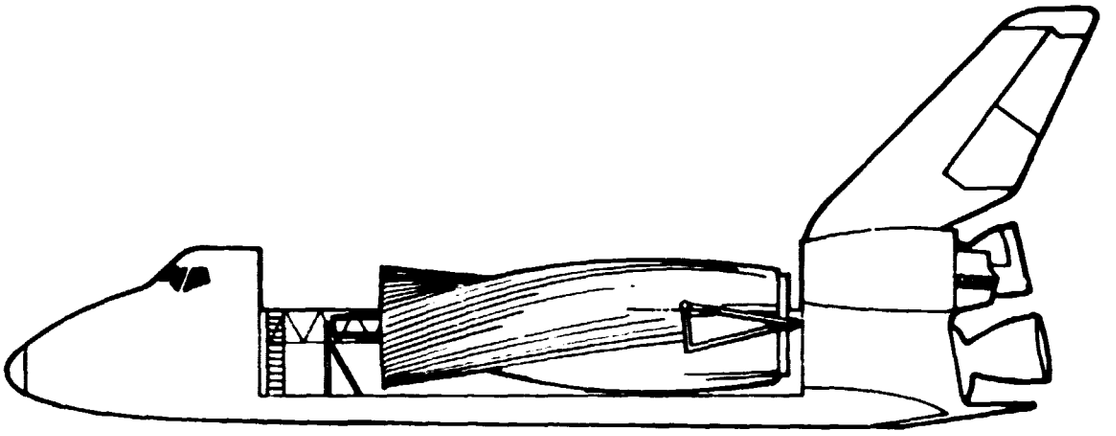

DOUBLE RING CONFIGURATION

The most successful approach so far discovered to improve packing has been to break the antenna into two rings of panels rather than one. By this method, the effect of the panel curvature is reduced and the panels may be folded closer to the axis of the reflector. Several ways of attaching and controlling this second ring have been examined. Some of the concepts have the potential of being extended to a three-ring configuration, perhaps using different concepts for each ring.

The simplest method to build a second ring is simply to split a single ring into two with corresponding panels. The hinges of the single ring are repeated in each new ring. The main panels of the outer ring are hinged to the outboard end of the main panels of the inner ring, while the triangular panels of the two rings are not connected. By utilizing this new degree of freedom, and by manipulation of the outer ring hinges, the second ring can be optimized independently, taking advantage of the reduced curvature of the shorter panels.

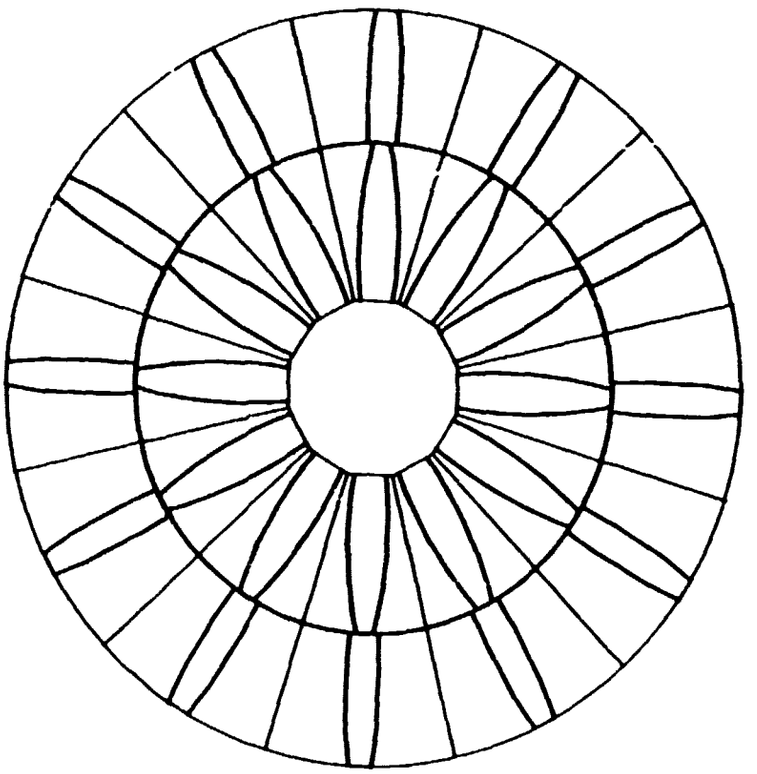

DEPLOYED, TOP VIEW

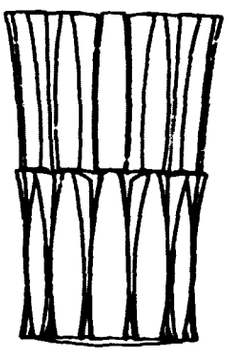

STOWED, SIDE VIEW

12 MAIN PANELS IN BOTH RINGS

HALF PANEL INNER RING

To reduce the number of panels required for the system described above, the inner ring may be composed of half as many panels as the outer, taking advantage of the empty space inside the lower part of the stowed antenna. Since alternate outer ring main panels are then unsupported, additional mechanisms must be added to completely control deployment.

6-12 MAIN PANEL DOUBLE RING CONFIGURATION

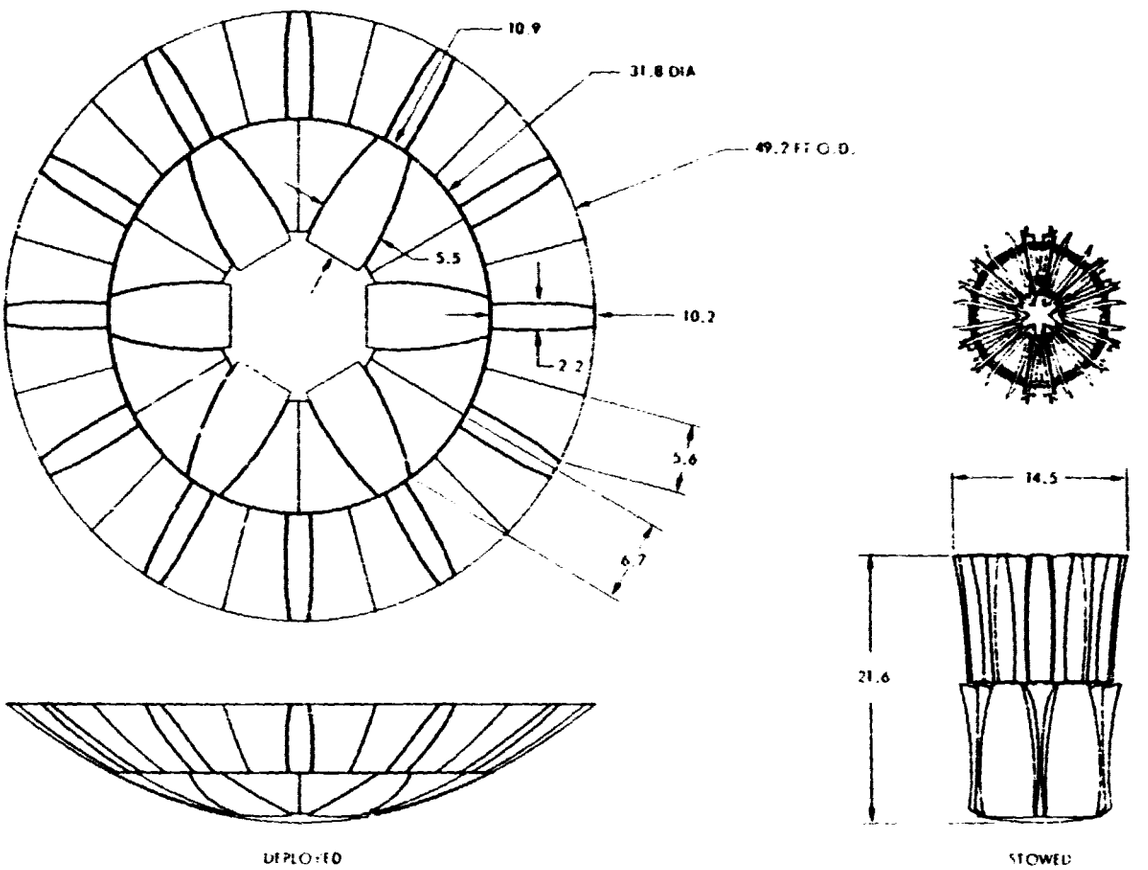

OUTER RING SUPPORT CONCEPT

To substitute for the inner ring panels, control arms may be substituted. These arms are connected to the support ring and are driven by the same drive shaft as for the original panels. This configuration has a six panel inner ring and a twelve panel outer ring. A major drawback of this configuration is that the arms are not connected to the inner ring of panels as are the main panels, which results in a less stiff reflector. The control arms may also add significant weight and complexity to the structure.

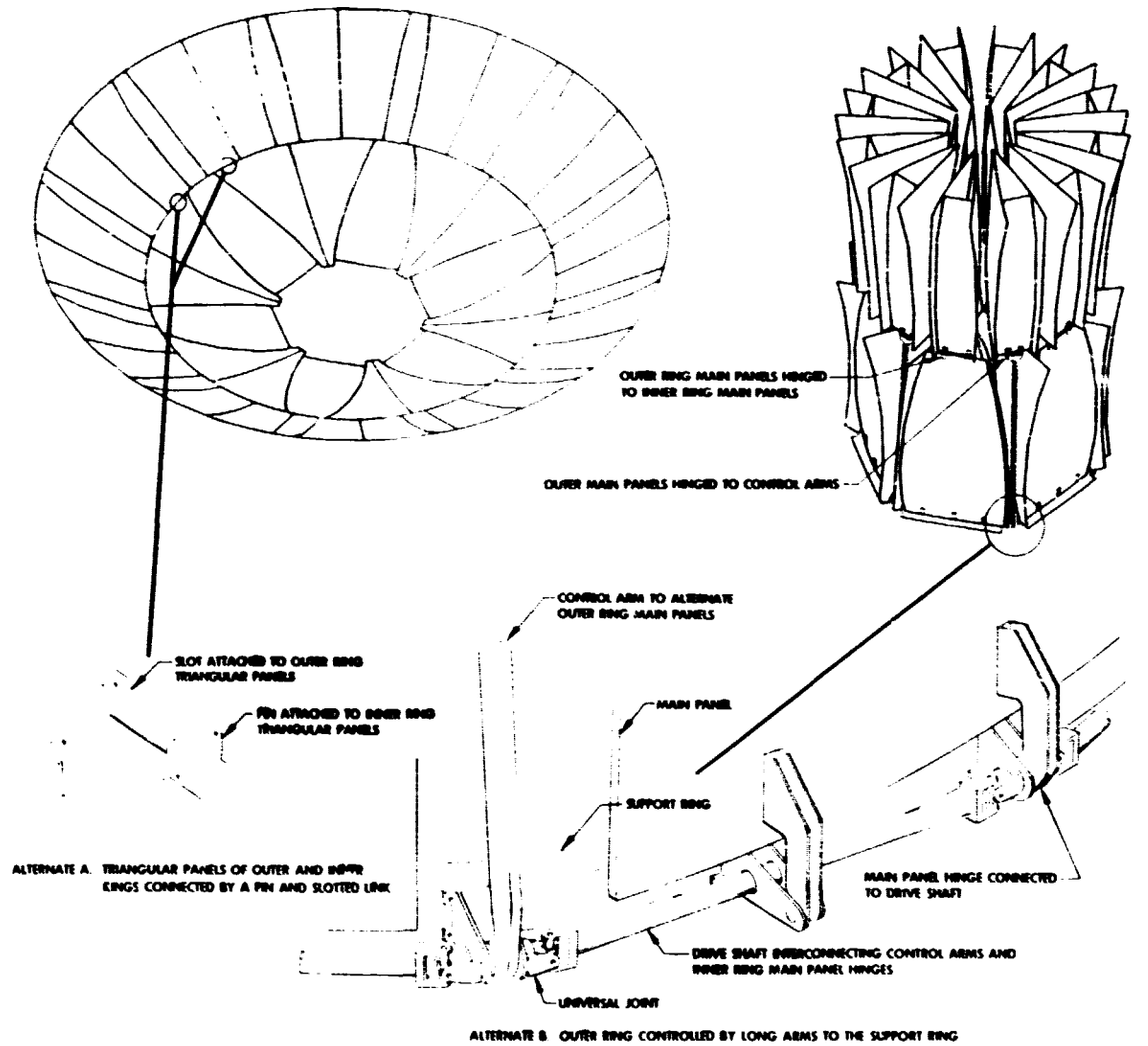

DOUBLE RING CONFIGURATION, 6-12 MAIN PANELS SHOWN

18-36 DOUBLE RING CONFIGURATION

Application of the double ring concept to the 18 panel configuration almost doubles the aperture which can be stowed in shuttle. In the 18-36 concept, the maximum aperture is 80 foot with a F/D of 0.4. The stowed length occupies over half the available shuttle bay capacity.

18-36 MAIN PANEL DOUBLE RING CONFIGURATION

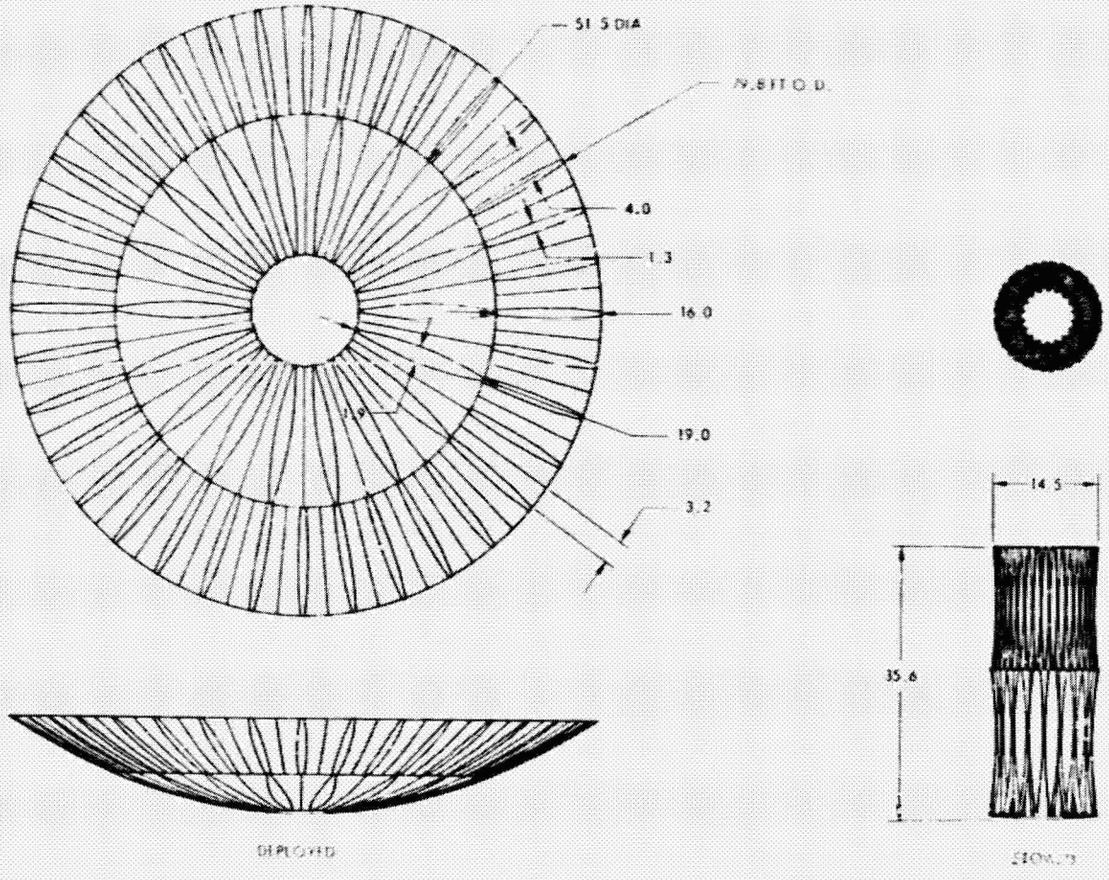

80-FOOT APERTURE ON SHUTTLE

This view illustrates the deployed 18-36 panel configuration, 80-foot aperture supported from within the shuttle bay.

A detailed study of offset reflectors was not performed due to time limitations and the relative priority of other tasks. Preliminary investigation, however, indicates that offset reflectors would stow more compactly than axisymmetric configurations of the same diameter due to the reduced panel curvature. Manufacture would be more difficult due to the loss of symmetry.

80-FT. (24.4-METER) PRECISION DEPLOYABLE REFLECTOR ON SHUTTLE

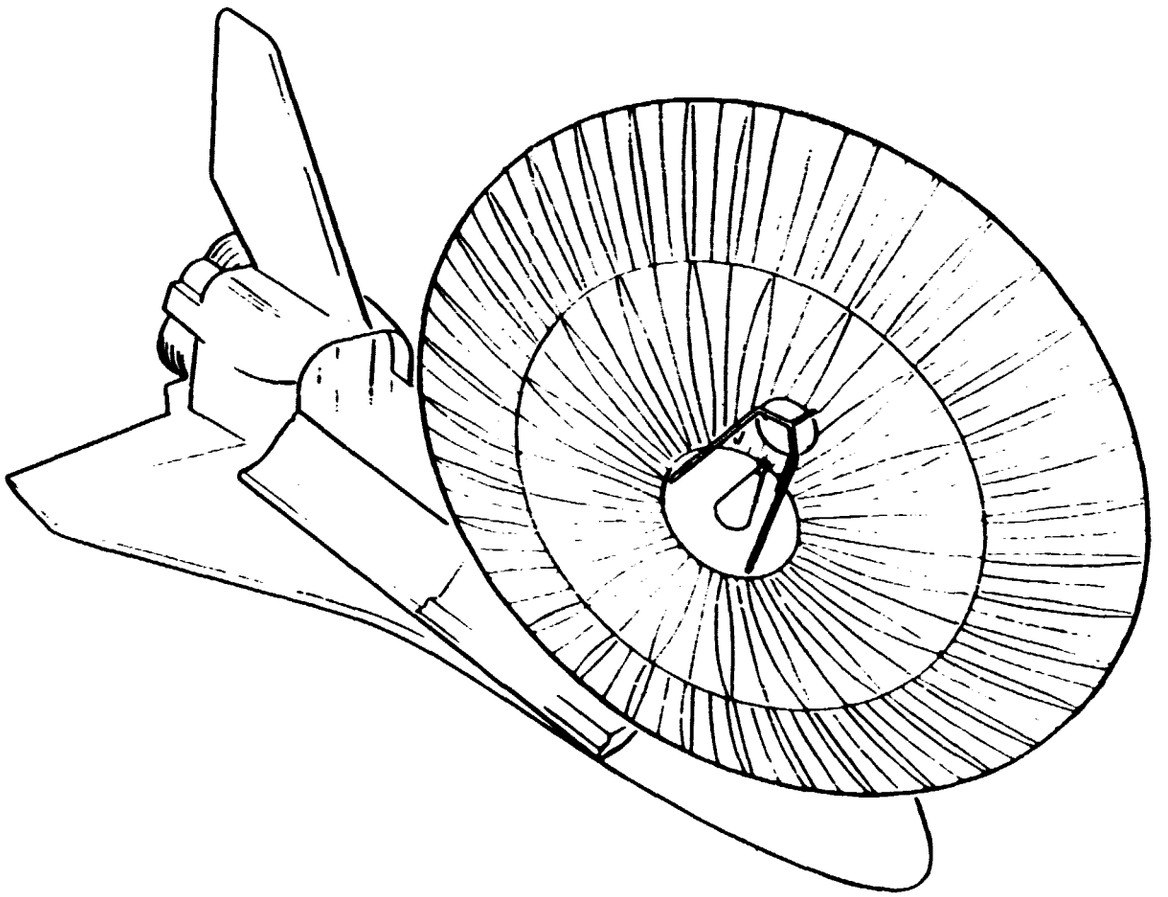

CRITICAL TECHNOLOGY STUDIES

Several critical new technologies judged necessary for the construction of successful large diameter antennas have been identified. These technologies mainly concern the advanced fabrication and adjustment techniques, and related problems. In addition, they apply equally to both the original design and the advanced concepts.

The first study proposed is to investigate designs and processes which reduce the as-fabricated reflector panel errors. The principal parameters in this study are the materials and tooling. Improved tooling precision and room temperature curing should contribute greatly to improved panel contours.

CRITICAL TECHNOLOGY STUDIES

TITLE: CONTOUR ACCURACY CONTROL FOR PRECISION DEPLOYABLE REFLECTORS.

STUDY 1

OBJECTIVE: IMPROVE ACCURACY OF FABRICATING INDIVIDUAL PANELS.

APPROACH: DESIGN, FABRICATE AND MEASURE PANELS TO DEMONSTRATE THE ADVANTAGE OF ONE CONFIGURATION OVER ANOTHER. ANALYTICAL MODELING WILL BE UTILIZED WHERE FEASIBLE TO PREDICT THE EFFECT OF THE VARIOUS PARAMETERS.

TASKS:
- IDENTIFY PARAMETERS THAT COULD CONTRIBUTE TO DISTORTION
- MODEL PANEL AND VARY PARAMETERS TO ASCERTAIN CONTRIBUTION OF EACH
- DESIGN TEST PANELS TO ISOLATE EACH PARAMETER TO DETERMINE ITS CONTRIBUTION
- FABRICATE BOTH FLAT AND CURVED PANELS TO ISOLATE THE PARAMETERS AND PROVIDE CONTROL AND REPEATABILITY OF THE FABRICATION PROCESSES
- MEASURE CONTOUR ACCURACY
- OPTIMIZE THE CONFIGURATION

POST FABRICATION ADJUSTMENT

The second technology study would develop concepts for post fabrication adjustment as an approach to developing high precision contours. This approach has been very successful for rigid contour reflectors. The problems peculiar to this configuration are the high aspect ratio panels.

CRITICAL TECHNOLOGY STUDIES

STUDY II

TITLE: CONTOUR ACCURACY IMPROVEMENT BY POST-FABRICATION ADJUSTMENT OF PRECISION DEPLOYABLE REFLECTORS.

OBJECTIVE: DEVELOP CONCEPT FOR IMPROVING ACCURACY OF INDIVIDUAL PANELS BY POST FABRICATION ADJUSTMENT.

APPROACH: ONE OR MORE CONFIGURATIONS WILL BE CHOSEN FROM TRADE-OFF STUDIES OF VARIOUS CONCEPTS. THE ACCURACY OF THE CONCEPTS WILL BE DEMONSTRATED BY DESIGNING, FABRICATING AND MEASURING THE CONTOUR OF PANELS REPRESENTATIVE OF A DESIRED LARGE DIAMETER REFLECTOR.

TASKS:

- CONCEPTUAL DESIGN OF ALTERNATE CONFIGURATIONS
- USE ANALYTICAL MODEL TO DETERMINE OPTIMUM NUMBER AND LOCATION OF ADJUSTMENT POINTS
- CHOOSE PRIME CONFIGURATION AND DESIGN SHELL, AND BACK-UP STRUCTURE
- FABRICATE SHELL ON EXISTING MOLD OF 98 IN. FOCAL LENGTH IF DEEMED ADEQUATE
- FABRICATE BACK-UP STRUCTURE
- MEASURE CONTOUR
- ADJUST TO OPTIMIZE CONTOUR

ACTIVE CONTOUR ADJUSTMENT TECHNOLOGY

The third critical technology study identified is the development of active contour control techniques for large aperture reflectors. The development of actuation systems, including actuator mechanisms, and their integration into the deployment mechanisms, requires investigation. This would include analytical optimization studies, design and verification tests of breadboard hardware.

CRITICAL TECHNOLOGY STUDIES

STUDY III

TITLE: A STUDY OF ACTIVE CONTOUR CONTROL OF LARGE PRECISION DEPLOYABLE REFLECTORS.

OBJECTIVE: DEVELOP CONCEPT FOR IMPROVING ACCURACY OF COMPLETE REFLECTOR IN SPACE WITH ACTIVE ADJUSTMENT.

APPROACH: AN ANALYTICAL MODEL WILL BE USED TO PERFORM THE TRADE-OFFS OF THE CONCEPTUAL DESIGNS. AFTER THE ADJUSTMENT LOCATIONS AND THE REQUIRED FORCE/MOTION IS DETERMINED THE ACTUATING SYSTEM WILL BE DESIGNED. ONE OR MORE TYPICAL JOINTS WILL BE DESIGNED, FABRICATED AND TESTED TO VERIFY ITS CAPABILITY. A BREADBOARD OF THE SENSOR SYSTEM AND CONTROL ELECTRONICS WILL BE DESIGNED AND BUILT TO DEMONSTRATE THE COMPLETE SYSTEM ON A REPRESENTATIVE PANEL.

SUMMARY

In summary, our study has demonstrated the feasibility of the basic concept for shuttle applications with 40-foot apertures at frequencies of 100 GHz. We have also identified concepts allowing extension of the basic concept to 80-foot apertures, operable at 60 GHz.

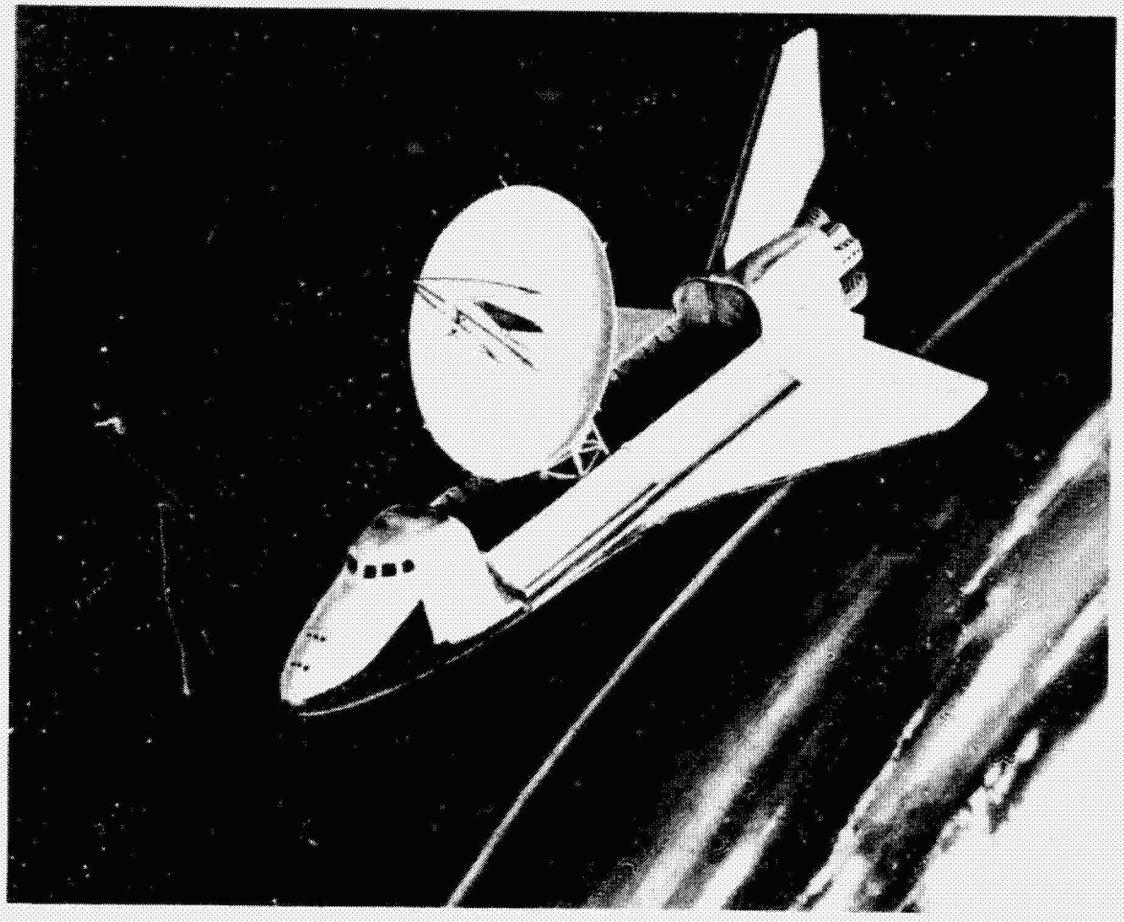

ORIGINAL PAGE IS
OF POOR QUALITY

D3

N80-19148

CONSTRUCTION ALIGNMENT SENSOR FEASIBILITY DEMONSTRATIONS (LASER MEASUREMENT)

R. H. Anderson
Lockheed Missiles and Space Company

Contract no. NAS7-100

LSST 1ST ANNUAL TECHNICAL REVIEW

November 7-8, 1979

ABSTRACT

Lockheed Missiles and Space Company (LMSC) is developing a family of laser heterodyne sensors for use in the active control of spacecraft structures. These sensors include a HeNe distance measuring system for structures requiring accuracies to 0.1 mm and a CO_2 distance measuring system which will measure unambiguously down to 0.01 μm. Vibration sensors, based on both HeNe and CO_2 lasers, are also being developed. These systems will measure fractions of a μm displacement from DC to kHz. All of these sensors have been breadboarded to verify performance and are in various stages of development directed toward prototype engineering models. This paper discusses the design theory and trade-offs required for instrument selection.

PRESENTATION OUTLINE

INTRODUCTION

COARSE MEASUREMENTS

FINE MEASUREMENTS

VIBRATION MEASUREMENTS

TEST RESULTS

CONCLUSIONS

INTRODUCTION

For several years, the Sensor Technology Organization at Lockheed Missiles and Space Company (LMSC) has been developing sensors to be used for the measurement and active control of spacecraft structures. These sensors are all laser heterodyne systems. Both HeNe and CO_2 lasers have been used.

A coarse system, which is designed for applications where high accuracy is not required, uses a modulated beam and a high accuracy phase measurement scheme to obtain resolution on the order of 0.1 mm. With several modulation frequencies, distances on the order of kilometers can be measured. A fine measurement system has been developed which will work either in conjunction with the coarse system or independently. It uses a multi-state, two-color CO_2 laser which can be used to produce unambiguous measurements from 20 cm down to 0.01 μm resolution over distances to 100 m. A summary of the distance measuring capabilities is illustrated in Table 1.

Vibration measurements have been made using both Doppler frequency detection and a beat frequency phase measurement system with capabilities of measuring displacements less than a 0.1 μm at vibration frequencies from essentially DC to several kHz.

A feasibility demonstration of the coarse system capability was made under Contract No. 955130 for the Jet Propulsion Laboratory, California Institute of Technology, sponsored by the National Aeronautics and Space Administration under Contract NAS7-100.

INTRODUCTION

POSITION MEASUREMENT

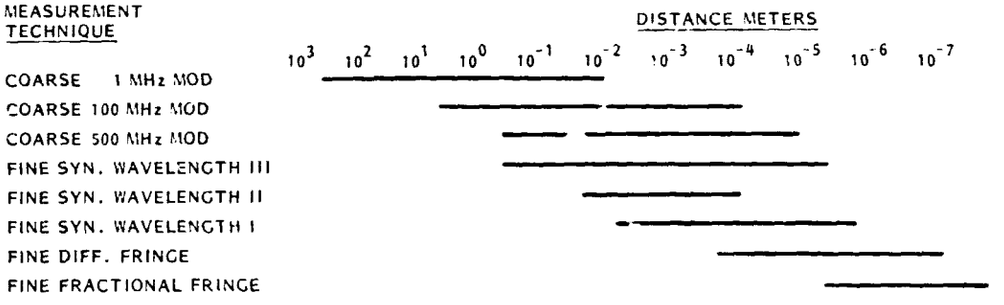

VIBRATION MEASUREMENT
SYSTEM DEMONSTRATED WITH 0.05 METER Hz
CAPABILITY, 0.08 μm RESOLUTION FROM DC TO KHz

Table 1

COARSE MEASUREMENT OPTICAL LAYOUT

The coarse system measures distance by accurately measuring phase of a modulated laser beam. Distance to a reference point is compared with the distance to the target. This method eliminates, through common moding, any drifts prior to the output beam splitter. Actual implementation of both CO_2 and HeNe systems has been accomplished. The following discussion applies to both systems.

An optical layout is illustrated. The beam from the laser is both spatially and frequency shifted by the Bragg cell. The unshifted portion of the beam is used as the local oscillator for the heterodyne receiver. The shifted beam is directed through the phase modulator with mode matching lenses. This modulated beam is split, and one sent to the reference mirror and the other to the target. Two choppers, 180° out of phase, sample the beams alternately for signal processing. For the demonstration, a mirror on a rotary table was used to direct the beam to the targets. Both the reference beam and target beam are returned to combine with the local oscillator beam to be received by the detector.

COARSE MEASUREMENTS — I

OPTICAL LAYOUT

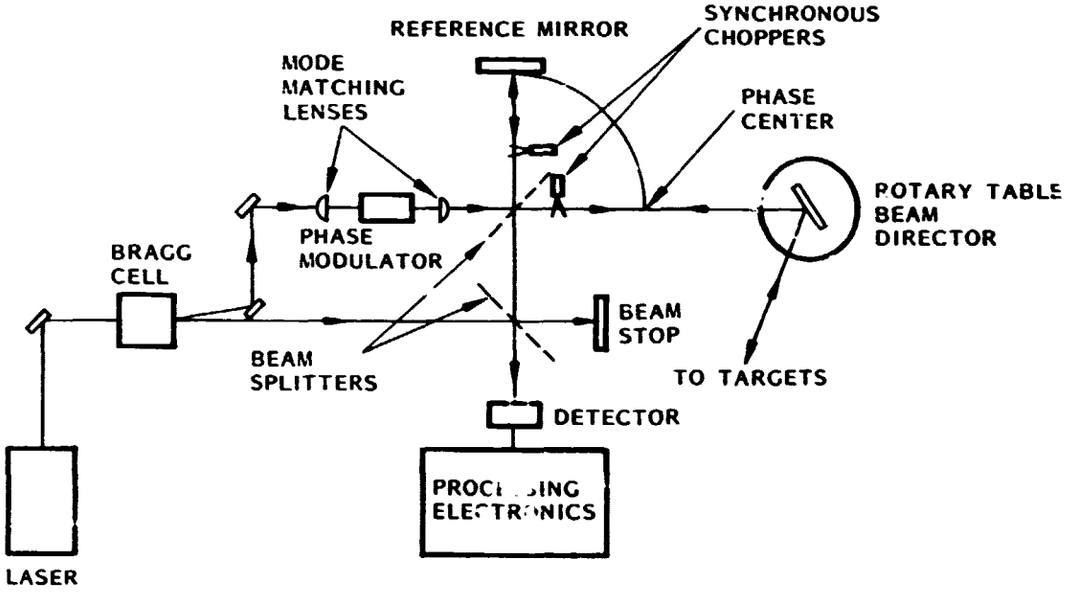

COARSE MEASUREMENT SIGNAL PROCESSING

The processing electronics consist of the system described below, as well as a micro-processor for converting the signals to a digital range output. LMSC has breadboarded the signal processing scheme described and demonstrated its performance.

The processing flow is shown in the figure. Beginning in the upper left-hand corner, FM modulation frequencies of 1.0 or 100 MHz are selectable by the RF switch. The selected RF power is divided and the first fraction passes successively through an adjustable (phase shifting) transmission line, a power amplifier, and a phase modulator for the working beam. The other fraction of the RF power passes to the 90° hybrid divider where about one-half the power is phase shifted and two outputs corresponding to sine and cosine functions are provided. These outputs, each with a phase and amplitude trimmer, go to the inputs of a pair of SPST RF switches. The switch output provides the following RF mixer with sine and cosine inputs on alternate half cycles. The crystal detector, amplifier, and logarithmic voltmeter provide the output shown.

COARSE MEASUREMENT – II

SIGNAL PROCESSING

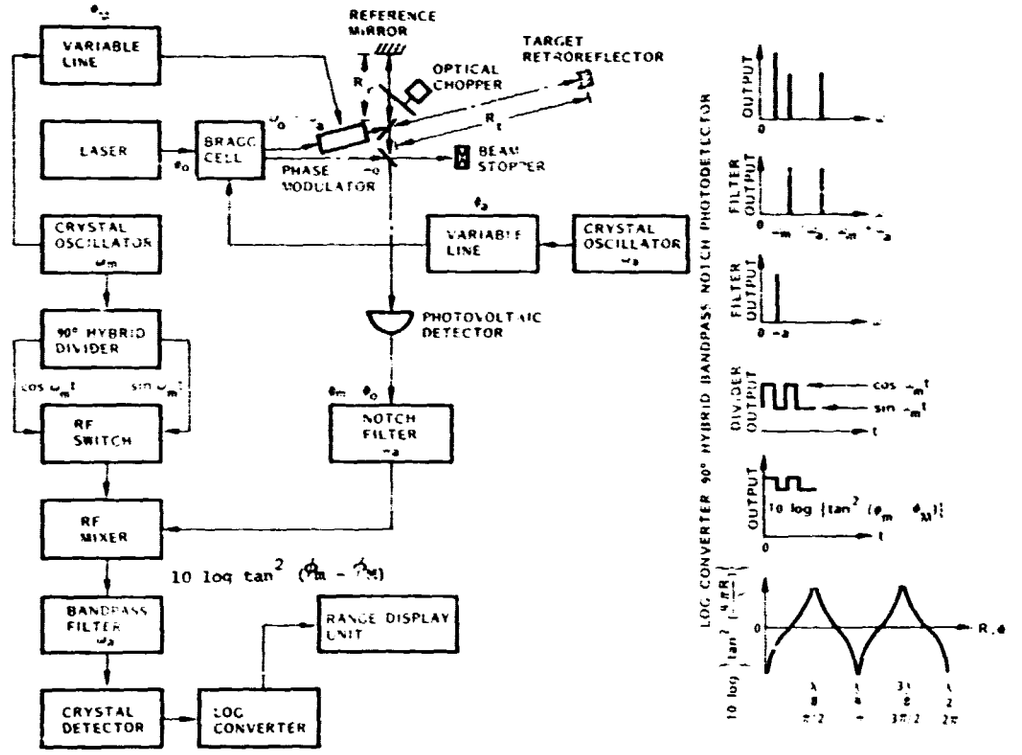

COARSE MEASUREMENT RANGE RESOLUTION AND LASER COMPARISON

The range, R, can be solved explicitly in a simple, straightforward manner as a function of the signal phase ϕ. The target range relative to the reference mirror can be calculated by subtracting two consecutive range measurements, one to the target and another to the reference mirror. The range resolution is

$$(\Delta R_m)_{min} = \frac{\lambda_m}{4} (\Delta\phi_m)_{min} = \frac{\lambda_m^2}{\pi A \sqrt{\left(\frac{S}{N}\right)}}$$

where λ_m = modulation wavelength

A = π x (modulation depth)

(S/N) = signal-to-noise ratio

$$\approx \frac{2\left(\frac{\eta q}{h\nu}\right)^2 P_\ell P_s}{B\left(\frac{2q^2}{h\nu} P_\ell + \frac{4kT_A}{R_L}\right)}$$

where

η = detector quantum efficiency
q = electron charge
$h\nu$ = photon energy
P_ℓ = optical local oscillator power
P_s = optical signal power
B = electronic bandwidth
k = Boltzman's Constant
T_A = equivalent temp. of amp.
R_L = resistance of load resistor

The range of resolution of a HeNe system is found to be comparable with that for a CO_2 system for the typical parameters listed in the table.

COARSE MEASUREMENT – III

$(\Delta R_m)_{min} = \frac{\lambda_m}{4} (\Delta\phi_m)_{min}$

$\frac{\lambda_m^2}{\pi A \sqrt{\left(\frac{S}{N}\right)}}$

WHERE λ_m MODULATION WAVELENGTH
A π x (MODULATION DEPTH)
(S/N) SIGNAL TO NOISE RATIO

$\frac{(\Delta R_m)_{CO_2}}{(\Delta R_m)_{HeNe}} \quad \frac{160\ \mu m}{106\ \mu m} \quad 1.59$

HeNe - CO_2 COMPARISON

PARAMETERS FOR RANGE RESOLUTION CALCULATION

PARAMETERS		HeNe SYSTEM	CO_2 SYSTEM
λ_m	METER	3	
MODULATION DEPTH		0.2	0.02
η		0.8	0.5
q	COUL	1.6×10^{-19}	
$h\nu$	JOUL	3.13×10^{-19}	1.87×10^{-2}
P_ℓ	WATT	10^{-3}	
P_s	WATT	10^{-6}	
B	H_z	10^3	
k	JOUL/K	1.38×10^{-23}	
T_A	K	596°	
R_L	OHM	50	

COARSE SYSTEM RESOLUTION DATA

The coarse system range resolution data is shown for a 100 MHz CO_2 system. The target was translated back and forth in 1 mm steps, with the data averaged over 1 sec per reading.

OPS RANGE RESOLUTION DATA

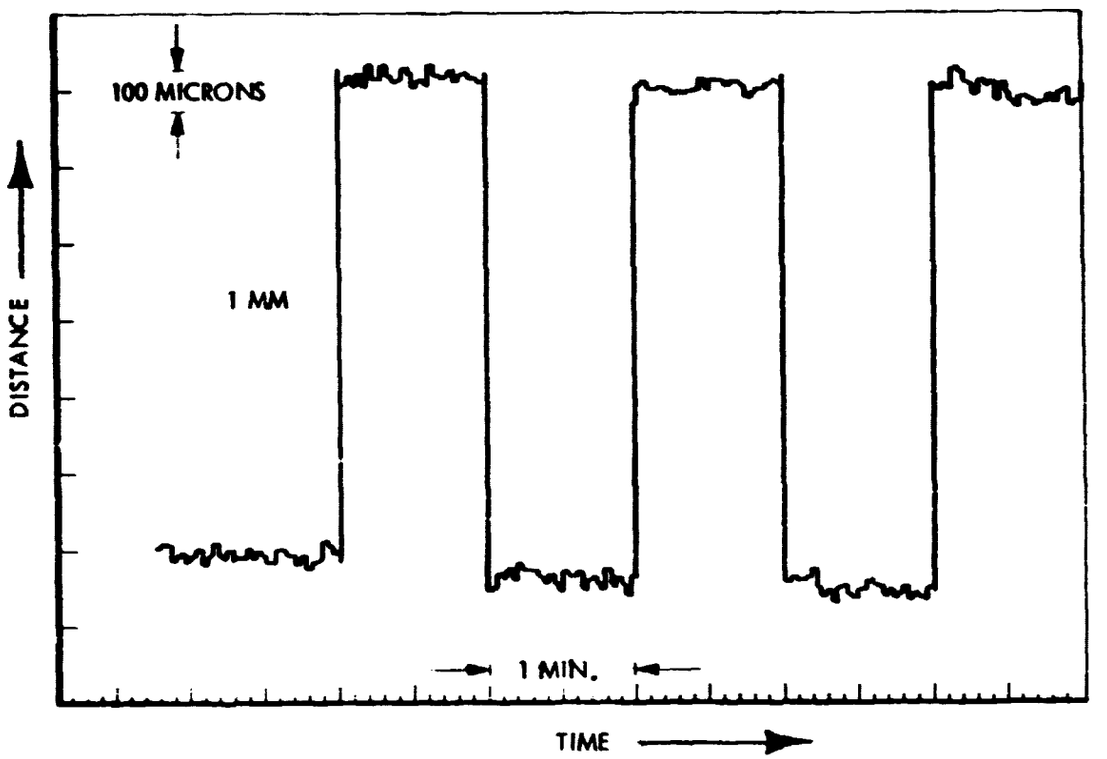

COARSE SYSTEM LINEARITY DATA

The linearity of the system is illustrated by the accompanying data. 1/20-inch steps were input and held for 7.5 sec over a total displacement of 1 inch.

OPS RANGE MEASUREMENT LINEARITY DATA

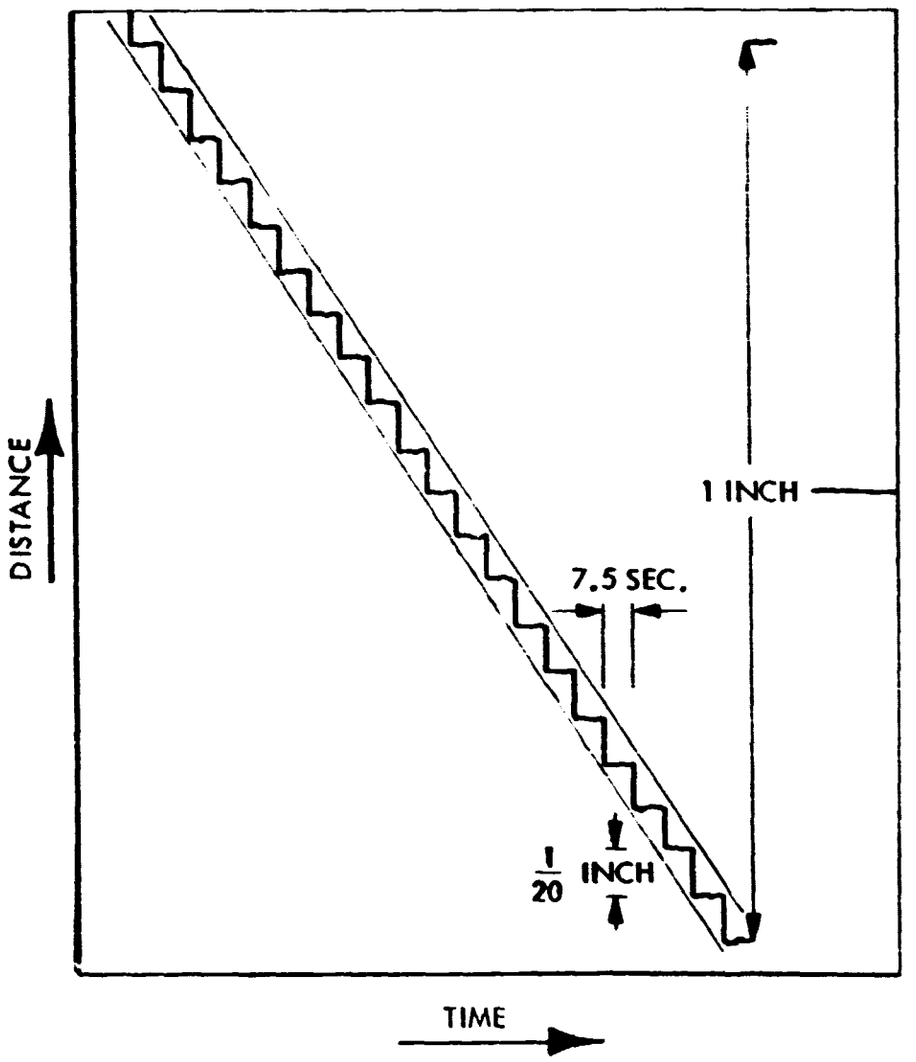

TWO-COLOR LASER OPERATION

The heart of the fine measurement system is the switchable two-color CO_2 laser. Gain occurs in the CO_2 gas mixture in many distinct lines corresponding to a given vibrational transition frequency. These lines, corresponding to R and P branches and numbered in each, are illustrated.

By controlling the cavity length, the line of operation can be established. If the length is such that an R frequency and P frequency have the same gain, they will operate simultaneously. This can be accomplished by separation of the signals (spectrally) and servoing a piezo-electric driven mirror to the proper cavity length. Thus, two-color operation is achieved. This can be refined further by selecting a specific R line and P line within the branches for laser operation. LMSC has developed a laser which can be switched through four pairs of lines.

FINE MEASUREMENTS – I

CO_2 GAIN CURVE 10.4 μM BAND

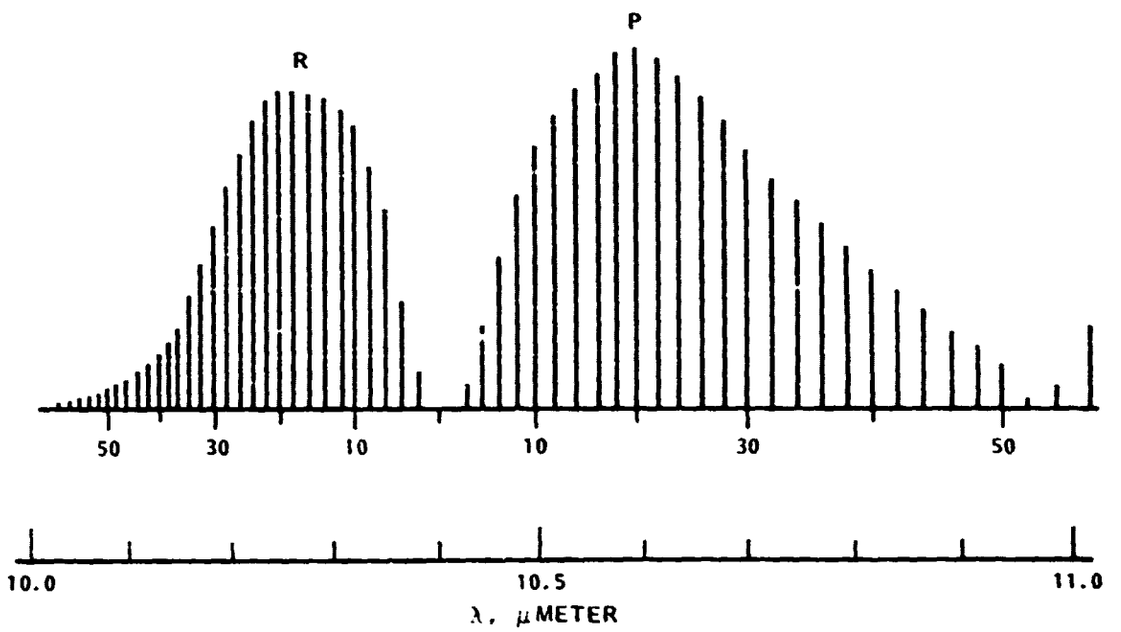

FOUR STATE SWITCHING

The four state switching sequence is illustrated. Starting at 0, the laser switches to positions 1 through 5 and back to 0. Each state is held for 70 msec by balancing the power between the two lines involved. The entire sequence takes about 280 msec.

SWITCHING SEQUENCE SCHEMATIC OF FOUR-STATE T-C LASER

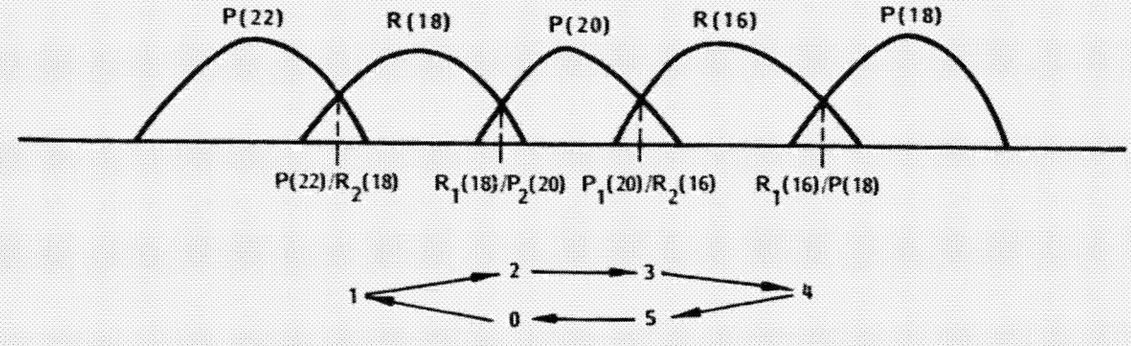

FINE SYSTEM WAVELENGTH HIERARCHY

By obtaining the frequency difference between pairs of lines, longer wavelengths can be produced. By looking at the difference between a pair of differential fringes, still longer wavelengths occur. In the figure, a hierarchy of wavelengths is established which can be obtained from the LMSC laser. The differential fringes are those obtained from a single two-color state. The synthetic wavelengths only exist in the comparison of one state to another. From this, it can be seen that an ambiguity of 40 cm can be obtained in total path length (20 cm in measuring distance). Ambiguities up to 15 m can be obtained by taking the difference of adjacent line center frequencies.

FOUR-STATE T-C LASER FREQUENCY/WAVELENGTH HIERARCHY PYRAMID

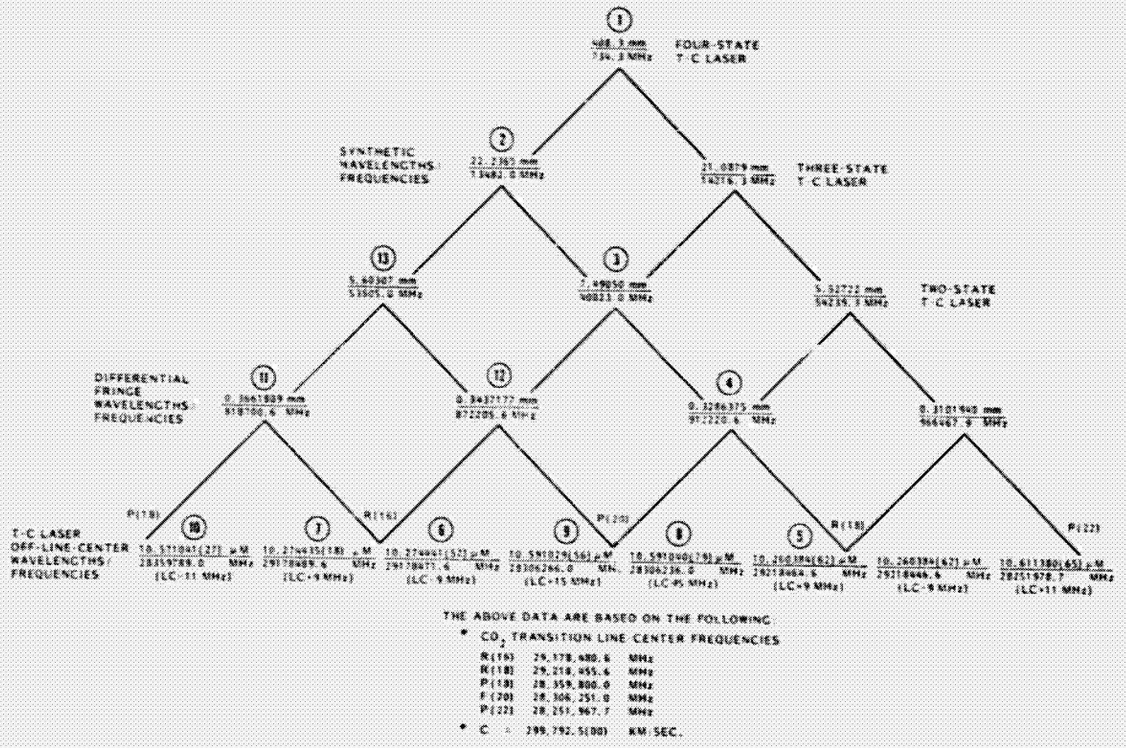

FINE SYSTEM BREADBOARD LAYOUT

This figure illustrates the setup used to make comparitive measurements with an HP Interferometer. The LMSC sensor is chopped so as to alternately look at the reference and target retroreflectors. The HP tracks the target position and the output is compared to that of the LMSC sensor. The Bragg cells frequency shift the beam for heterodyning. The grating is used to separate the two colors for detection.

OPTICAL POSITION SENSOR BREADBOARD LAYOUT

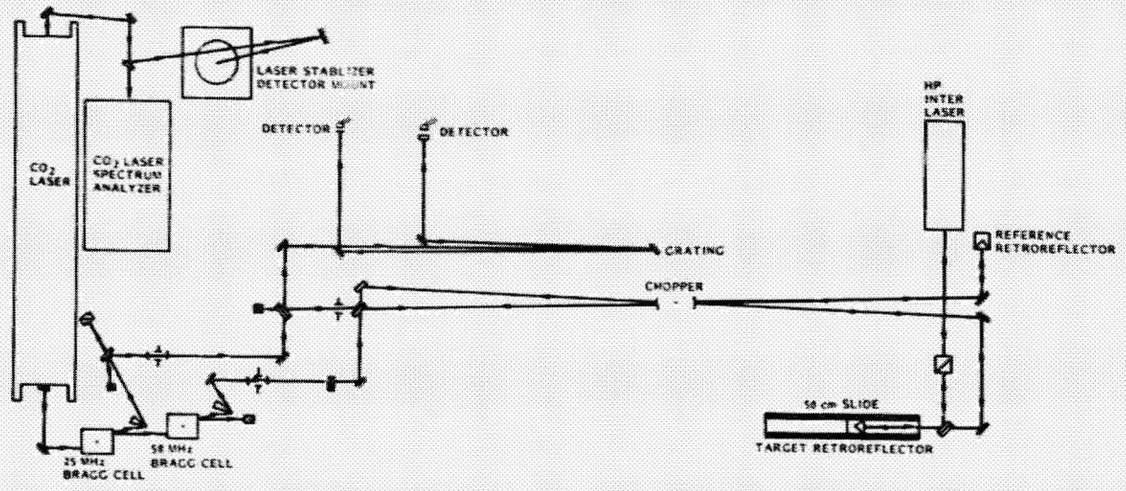

FINE SYSTEM ACCURACY DATA

Recent OPS-HP comparison measurements have been made using the previously shown breadboard wherein the OPS and HP beams were co-located as much as possible. Results achieved with this configuration show that the OPS-HP differential distance measurements vary nearly linearly with range, and that the statistical variation from linearity can be held to within $\pm 0.025\,\mu m$ over a 0-50 cm target excursion provided the temperature in the vicinity of the OPS "interferometer" is held constant to within approximately $\pm 0.01°C$.

This Figure presents typical data. Perfect agreement between OPS and HP would yield measurement data all in a straight line with zero slope. The measurements shown in the Figure, however, show a good linear relationship between OPS and HP, but an apparent wavelength discrepancy indicated for the most part by the linear bias of $+3.82\,\mu m/m$ (some 4 parts in 10^6). The "linear bias" represents an approximate straight line best fit to the OPS-HP differential measurement data; this linear portion of the measurement is removed in the computer and the residuals plotted using an expanded scale to more clearly reveal statistical variations.

DIFFERENTIAL DISTANCE COMPARISON MEASUREMENTS (OPS-HP)

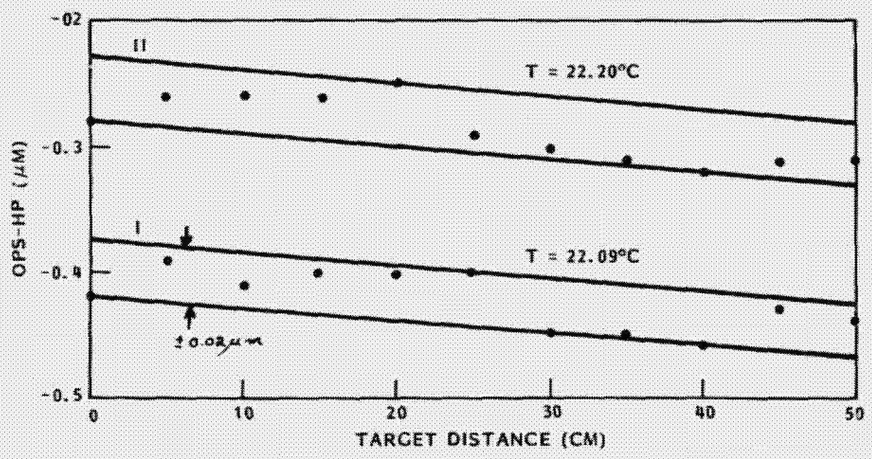

ATMOSPHERIC CORRECTION: -265.57 μm/m

LINEAR BIAS: + 3.82 μm/m

FINE SYSTEM BEAM POINTING

A beam directing scheme needed to be devised which would not affect the path length. That scheme is also shown in the Figure where all errors occurring behind the output beam splitter are in a common mode in the reference and target measurements. It will require calibration of all measurement positions to account for optical differences but no scanner induced errors should occur.

FINE MEASUREMENT – IV

BEAM POINTING SYSTEM

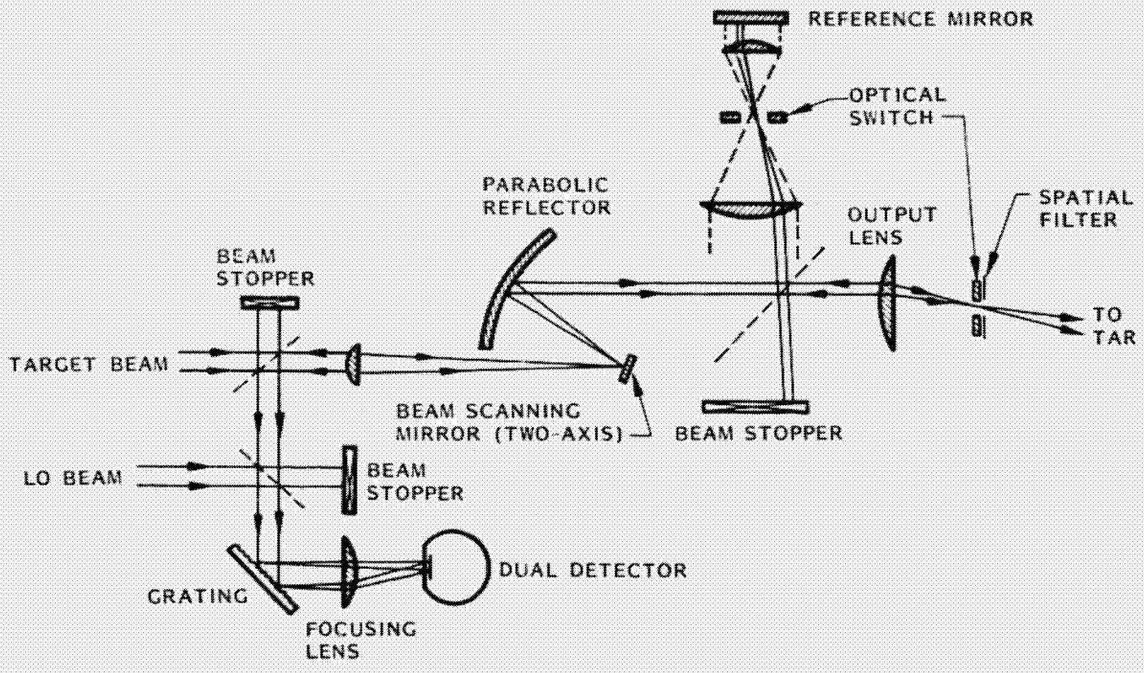

VIBRATION SENSOR SIGNAL PROCESSING

A HeNe laser Vibration Sensor has been demonstrated which features an analog and digital ouput for computational convenience, and which complements conventional vibration sensors by sensing vibratory events at low frequencies - from DC to beyond 50 Hz. Vibration amplitude resolution of the sensor is 0.08 μm, maximum amplitude and frequency product is 0.05 MHz for a 2 MHz electronic bandwidth. For example, the maximum measurable vibration amplitude for a 25 Hz vibration is 2 mm. The time delay of the sensor output from the actual vibration is less than 1 μsec which is essentially real time for measuring the dynamics of structures and vibration sensing for the dynamic damping of structures (active control). By electronically splitting the laser beam using a Bragg cell, it is possible to simultaneously sample and, hence, monitor a large number of points to which retroreflectors have been affixed. Although the laboratory Vibration Sensor employed but two channels, it exhibited the basis for continuously sensing more than 50 independent vibrating targets.

VIBRATION SENSOR – I

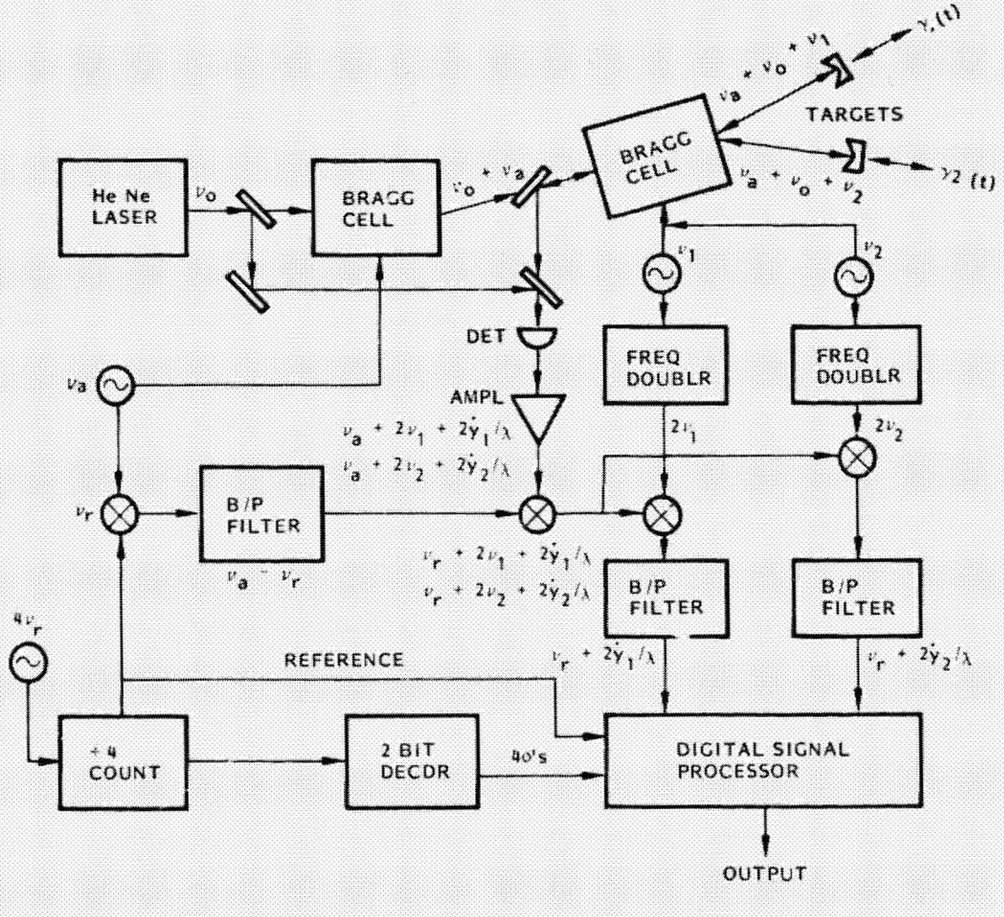

VIBRATION SENSOR DATA

The oscilloscope trace of the displacement of two vibratory targets is shown. In the Figure, the upper trace is the sensor output for channel 1 target vibrating at 30 Hz and an amplitude of 1.5 mm. The middle trace is the sensor output for channel 2 target which measures a 60 Hz vibration at an amplitude of 0.9 μm. It is noticeable that the "stair-like" waveform is a result of digital signal processing. Each step of the stair represents 0.08 μm displacement of target which is the resolution of the present system. The lower trace represents the driving signal to the PZT for channel 2 target. Comparing the output of the Vibration Sensor with the driving signal of the target mirror indicates a time delay of about 1 μsec between the sensor output and the actual vibration, of which, about 500 nsec is contributed by the digital circuitry (between the falling edges of input sampling clock $\emptyset_1$ and output sampling clock $\emptyset_5$), the rest of it is due to the settling time of D/A converter.

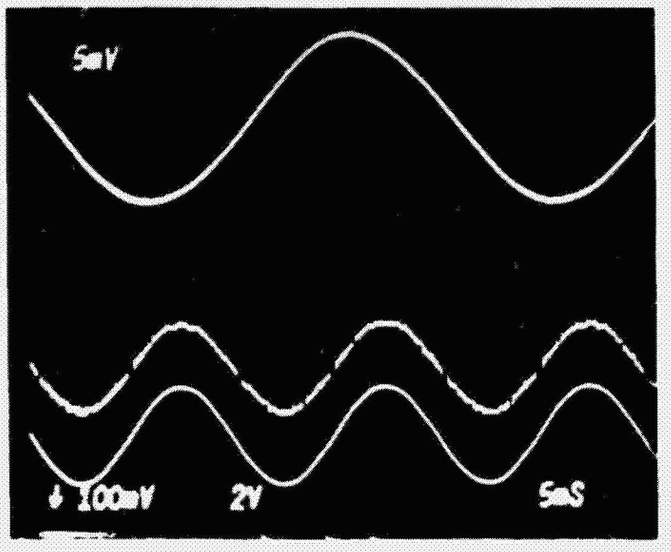

3 mm

1.8 μm

VIBRATION SENSOR OUTPUT FOR TWO VIBRATORY TARGETS (EXHIBITION OF AMPLITUDE RANGE AND SENSITIVITY OF SENSOR)

ORIGINAL PAGE IS
OF POOR QUALITY

VIBRATION SENSOR DC RESPONSE

The DC response of the sensor is shown in the upper trace of this Figure. The only difference between this and the previous experiment is the driving voltage applied to the shaker for channel 1 target. In this experiment, a 0.5 Hz square wave is applied to the shaker. The sensor measures the steady state DC displacement (-1 mm) as well as the transient behavior of the shaker.

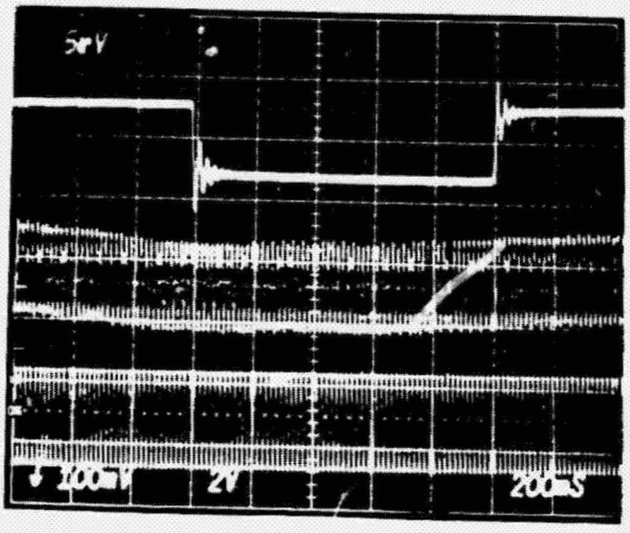

1 mm

1.8 μm

VIBRATION SENSOR OUTPUT FOR TWO VIBRATORY TARGETS

(EXHIBITION OF AC AND DC RESPONSE OF SENSOR)

CONCLUSIONS

Based on the analyses and the breadboard demonstrations performed at LMSC, we have made the following conclusions:

- It is possible to measure distance with HeNe absolutely from km down to 0.1 mm.
- It is possible to measure distance with CO_2 from km down to 0.01 μm.
- Rates on the above measurements can be made from rates of 1 per sec to 100 per sec.
- It is possible to measure vibrations from DC to kHz with up to 50 channels per detector/laser.

The primary concern in the application of the above sensors is one of beam direction and integration into the structural system being controlled. This problem is best approached for each system configuration.

N80-19149

JPL SELF PULSED LASER SURFACE MEASUREMENT SYSTEM DEVELOPMENT

Martin Berdahl
Jet Propulsion Laboratory
Pasadena, California

LSST 1ST ANNUAL TECHNICAL REVIEW

November 7-8, 1979

The technology of accurately describing the surface shape of large space deployed antenna structures is a requirement for performance evaluation.

Surface deviation tolerance is based upon the requirement for close wave phase coherence. In order to achieve the required antenna gain, pointing accuracy, and minimize the cross talk possibilities realized from excessive side lobe energy it is sometimes necessary to use surface figure tolerances of less than one fiftieth of a wavelength. For some of the higher frequencies contemplated for use in space deployed communications antennas, this could require that surface deviations not exceed one twentieth of a millimeter.

A list of some conceptual space deployable antenna designs and their characteristics and surface tolerance requirements are shown in Table 1.

The assurance that an antenna will operate efficiently after deployment is best ascertained by direct measurement of its surface with respect to design geometry. Further benefits derived from post deployment measurement may include the possibility of periodic adjustments in either the surface or in the feed point location which may have distorted or changed due to thermal or other causes.

SATELLITE MISSION	ANT. DIA. METERS	TYPE*	EFFECTIVE WAVELENGTH, MM	σ, MM ALLOW SURF TOLERANCE	APPROX. $\frac{\sigma}{\lambda}$ TOLERANCE
MOBCOMSAT	75	MDC	400	8.0	1/50
ODSRS	45	EC	9.38	0.745	1/15
VLBI	30	MDC	12.58	1.0	1/15
R/A SETI	24	PDC	0.629	0.05	1/15
PUB. SERV.	22.6	MDO	111.5	2.54	1/40
TELECONF.	4.7	PDO	21	0.4	1/50

*C CASSEGRAIN
D DEPLOYABLE
E ERECTABLE
M MESH
O OFFSET
P PRECISION

TABLE 1. FEATURES OF CONCEPTUAL ANTENNA DESIGNS

MEASURING TECHNIQUES EXPLORED

Several of the state-of-the-art measuring techniques have been studied. Among the more interesting for the thirty meter mesh deployable cassegrain measurement are the Payne, LMSC and JPL systems.

The Payne system uses a modulated laser beam and phase detection to achieve a claimed 100 micron resolution but uses only one modulation frequency and thus is ambiguous beyond the half wavelength range of 27 cm.

The LMSC system overcomes ambiguity by modulating the laser beam with two widely different frequencies. The resolution claimed is in the order of 200 microns. Since the system now uses a CO_2 laser, it has possible size and weight problems.

The HP5501 and the Boeing systems are for measuring small strains or changes in distance and may have usefulness as sensors for reference alignment of antenna axis and surface scan position.

The JPL self pulsed system has promise of being very interesting from the standpoints of non-ambiguity, simplicity weight and ease of data reduction.

The TRW angular measurement system is a bidirectional led and detector system capable of resolving angular deviation equivalent to sub millimeter motion.

SURFACE MEASURING SYSTEMS

TYPE	OPERATING PRINCIPLE	CHARACTERISTICS
Simple Optic Radar	Range = $\frac{\text{Speed of Light x Time}}{2}$	Unambiguous 150 mm Resolution
Payne, LMSC Modulated Laser	Phase Difference Measurement $\phi_r - \phi_s = 4\pi \frac{R}{\lambda}$	Ambiguous ~200 μ Resolution Complex
H.P. 5501 Machine Control	Straight Interferometer with Count Accumulation	±1 Count or 1λ Accuracy
Boeing Multi-Channel	Interferometry with Phase Resolution	1/20 λ Resolution (Optical Straingage) Complex
JPL Self Pulsed Laser	Range = $\frac{\text{Speed of Light}}{2 \times \text{Frequency}}$	Non-Ambiguous ~ 50 μ Resolution
TRW Angular Measurement	Bidirectional Angular Deviation Led & Beamsplitter	Very Fine Resolution ~ 0.1 mm in 45 Meters Limited Travel

LMSC STRUCTURAL ALIGNMENT SENSOR CONCEPTUAL DEMONSTRATION

A contract was let to Lockheed Missiles and Space Company to demonstrate a system for measuring distance to a target with high resolution capability. The tasks included measurements using both CO_2 and helium-neon laser equipment. An optional task was to demonstrate the ability to unambiguously measure the absolute distance to any given target.

The basic capability was demonstrated using both types of laser. The resolution obtained was in the order of one to two tenths of a millimeter. The capability of unambiguous distance measurement was not achieved due to lack of necessary equipment although there is little doubt that this could have been achieved.

The LMSC system shows real promise of use in the measurement of large antenna surfaces although it is complex and may present size and weight problems.

LMSC STRUCTURAL ALIGNMENT SURFACE MEASUREMENT SYSTEM HARDWARE CONCEPTUAL DEMONSTRATION

OBJECTIVE

To demonstrate the LMSC developed conceptual breadboard structural alignment sensor system for the high accuracy resolution measurement at a round trip distance in the order of one hundred meters, and to unambiguously measure the absolute distance from a reference to a target.

TASKS

- Demonstrate the operation and resolution capability of the LMSC system with a CO_2 laser
- Demonstrate the operation and resolution capability of the LMSC system with a helium-neon laser
- Demonstrate the LMSC capability to unambiguously measure absolute distance

SIGNIFICANT ACCOMPLISHMENTS

- The LMSC system demonstrated the capability for resolving distances in the order of one to two tenths of a millimeter in ranges up to 50 meters.

LOCKHEED MISSILES AND SPACE COMPANY CONTRACT
"STRUCTURAL ALIGNMENT SENSOR"
OPTICAL LAYOUT

The Lockheed "structural alignment sensor" system for measuring distances from a scan position to several targets is shown. It consists of a laser optic source which is both frequency and phase modulated. The modulated signal is alternately sent to the target and to a reference mirror. The return signals containing distance information are optically mixed with the original laser frequency and detected. The distance from the reference (or scan mirror) to the target is found by electronic processing. Measurement resolution in the order of one tenth millimeter has been achieved by this system.

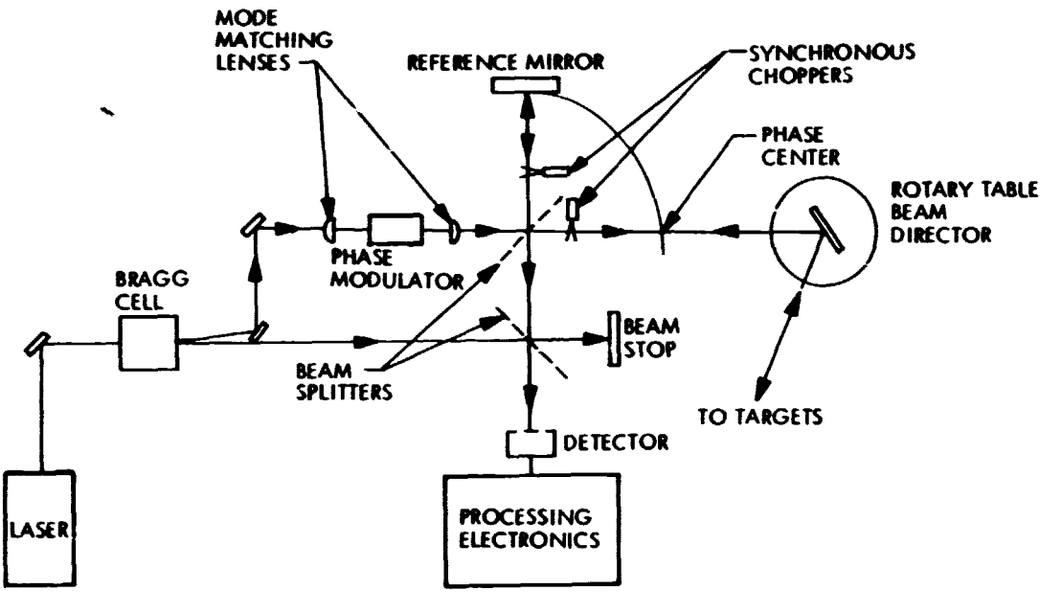

SAS Optical Layout Diagram

JPL SELF PULSED LASER RANGING SYSTEM

The objective was to prove and evaluate the concept of a self pulsed ranging system. This included the ability to produce a frequency inversely proportional to range, and to attempt to project resolution capability in order that the system might be evaluated for further development.

The approach was to design and fabricate a breadboard system sufficient to allow projected capability.

The breadboard was fabricated and tested. It verified functional operation with short time resolution in the order of 0.2 millimeter, non-ambiguous ranging and a maximum range capability in the order of 150 meters. Projected capability of the system is resolution of less than 0.1 mm over a reasonable time period and a range extension to over 300 meters.

The FY80 plans are to upgrade the system and perform distance measurements on simulated antenna geometries.

JPL SELF PULSED LASER SURFACE MEASUREMENT SYSTEM HARDWARE CONCEPTUAL DEMONSTRATION

OBJECTIVE

To develop a functional hardware system to accommodate the demonstration of the basic system concept for the unambiguous determination of range and a system evaluation that addresses the limits of performance and the applicability of the system for further development.

APPROACH

- o Design, fabricate and assemble components for functional system
- o Develop system to the point of a functional demonstration and evaluation
- o Generate estimates of potential system performance based on system evaluation
- o Access applicability of system for flight hardware application

SIGNIFICANT ACCOMPLISHMENTS

- o Functional system operation has been achieved
- o Ranging resolution of 0.2 mm has been achieved for an overall range of 150 meters
- o Approaches for upgrading the system for the next phase of development have been developed

The self pulsed laser ranging system is used for measuring distances from a fixed reference or scan position to several locations on the surface of an antenna reflector. Processing the information thusly obtained is used to define the "Figure" or shape of the surface upon which antenna operational efficiency is directly dependent.

Operation of the system consists of initiating a pulse from the laser emitter which is pointed at the scan mirror. The emitted pulse strikes the scan mirror, is reflected and sent to one of several targets located on the surface of the antenna. Upon reflection from the target, the pulse returns to a detector via the scan mirror. The detected pulse is amplified and used to trigger the next emitted pulse. After the first pulse is emitted, received and used to trigger another pulse the process becomes repetitive with a repetition rate uniquely determined by the distance traveled to the target and back. A measure of the repetition rate or frequency thus created provides the means required for determining range since the total distance traveled is inversely proportional to the frequency.

During its round trip travel, the emitted pulse traverses the distance from the laser to the target and back to the detector at the speed of light. It then proceeds through electronic circuitry with some delay until it triggers another light pulse. A distance equivalent to the time delay realized by the travel time of the returning pulse from the scan mirror to the detector, through the electronics and back to the scan mirror may be subtracted from the total distance to provide a precise measure of the round trip distance from the scan mirror to the target.

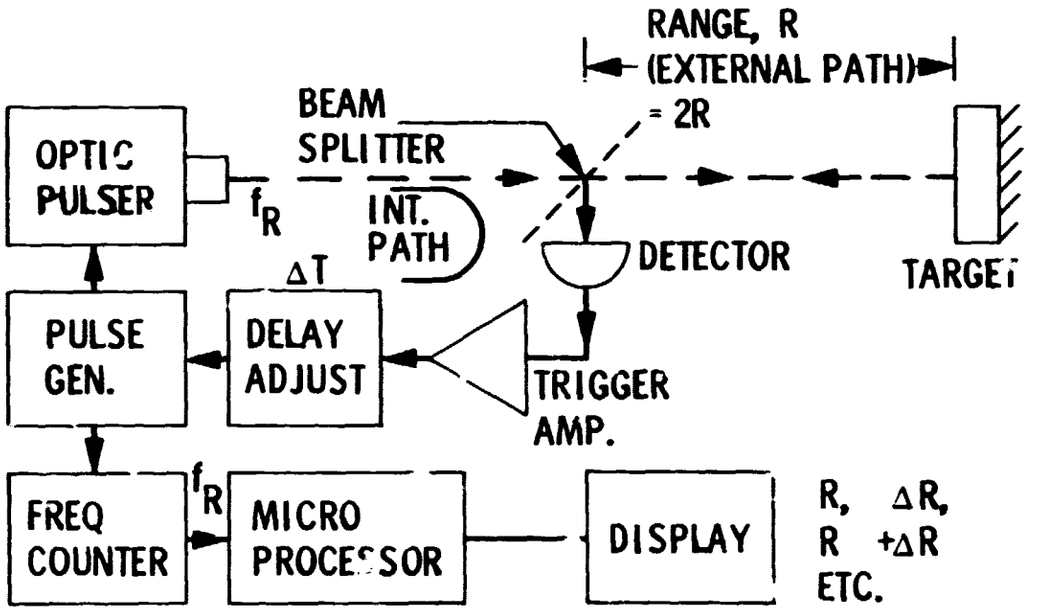

JPL SELF PULSED LASER MEASUREMENT SYSTEM

SIMPLE CALCULATIONS

The self pulsed laser ranging system is made possible by the relation which ties wavelength and frequency to the speed of propagation, in this case the speed of light in a vacuum. (See equation 1). In our case, the wavelength will be the round trip distance to the target and will include any optical and electronic path or equivalent time delay included in the loop containing the electronic equipment out to the reference position from which surface measurements are to be made. A more correct equation relating distance and frequency then is given by equation 2.

The value for the equivalent internal path length is found by reflecting the signal back to the detector by the scan mirror. The frequency thus obtained will uniquely define the equivalent internal path distance. (Equation 3). By subtracting the equivalent internal path from the total path to the target and back, the desired distance from the reference, or scan mirror, to the target is obtained. Since the object is to find the range from a reference position, the total path length is divided by two. (Equation 4). Since the internal path length is a constant when a scan mirror is used, a value for the internal range may be found and subtracted from all target measurements to obtain range from the reference to the target. (Equation 5).

$$\text{Wavelength, } \lambda = \frac{\text{Speed of Light, C}}{\text{Frequency, f}} \qquad (1)$$

$$\text{Round Trip Distance} = \frac{c}{f} - S_{\text{internal}} \qquad (2)$$

$$\text{Internal Path, } S_{int} = \frac{c}{f_{int}} \qquad (3)$$

$$\text{Range, R} = \frac{c}{2f} - \frac{c}{2f_{int}} \qquad (4)$$

$$\text{Range, R} = \frac{c}{2f} - K \qquad (5)$$

$$\text{Where K} = \frac{c}{2f_{int}}$$

SYSTEM PERFORMANCE

System performance is nearly totally dependent upon the stability with which the ringing frequency is established when aimed at a distant target. Most of the stability problems of the self pulsed ranging system occur in electronic circuits in the form of varying component delay time, wave form jitter, and temperature effects. Some problems arise from varying signal strength with target distance; however, this type of problem is more easily handled by using automatic gain control and wave shaping techniques. The former problems are sometimes an inherent characteristic of the equipment and can only be improved by component selection, use of state-of-the-art devices and careful attention to thermal problems.

When the ranging system uses a standard frequency counter for measuring the pulse repetition rate, it is interesting to note that using a one second time gate will automatically provide an average of one million round trip samples if the ringing frequency were one megahertz. At one megahertz the round trip path would be three hundred meters or would correspond to a range of one hundred fifty meters. Such a total range might easily correspond to a scan mirror to target distance of the order of one hundred meters or to the measurement of an antenna dish of one hundred meters diameter. Resolution of measurement in this case would be one part in a million corresponding to one one millionth of three hundred meters. Since range is one half of the round trip distance this resolution is halved along with the division to obtain range. (See equation 6). It may be seen that resolution, providing the sample time gate remains constant, will increase with shorter distances and smaller antennas. This is fortunately in the right direction since smaller antennas may operate at shorter wavelengths and require higher resolution measurement. The relation between a change in frequency with respect to a change in wavelength is obtained by differentiating equation (1). (See equation 7).

$$\text{Resolution (1 count)} = \frac{\text{Range}}{10^6} = \frac{150 \times 10^3 \text{ mm}}{10^6} \qquad (6)$$

Resolution = 0.15 millimeters

$$f = \frac{c}{\lambda} \qquad (1)$$

$$\frac{df}{d\lambda} = -\frac{c}{\lambda^2} \qquad (7)$$

Inverting and substituting $\lambda = 2R$ gives the distance increment resolvable as

$$\frac{dR}{df} = -2\frac{R^2}{c} \qquad (8)$$

from which resolution also = 0.15 mm/Hz

INCREASING RESOLUTION BY GATING A HIGH STANDARD FREQUENCY

As antenna size increases and frequencies become lower, the resolution is decreased by the significance of plus or minus one hertz error in the length of sample time for frequency measurement. In order to overcome this problem a predetermined number of pulses of the ringing frequency may be used to define the time gate through which a precision high frequency is passed and counted. The time gate may be made very precise by edge triggering the opening and closing of the gate on the leading edges of pulses of the ringing frequency. If the count of N_f pulses of the ringing frequency, f, is used for determining the gate time t, the gate time will be N_f divided by f. (See equation 9).

If a standard high frequency, F, is passed through a gate of time duration, t, the count accumulation, N_F, of standard frequency, F will be given by equation 10.

$$\text{Gate time,} \quad t = \frac{N_f}{f} \tag{9}$$

$$\text{Count Accumulation,} \quad N_F = Ft \tag{10}$$

$$\text{from which} \quad t = \frac{N_F}{F} \tag{11}$$

Equating (9) and (11)

$$\frac{N_f}{f} = \frac{N_F}{F} \tag{12}$$

and

$$f = \frac{FN_f}{N_F} \tag{13}$$

using $\lambda = \frac{C}{f}$ or $2R = \frac{C}{f}$ and substituting in (13)

$$\text{gives} \quad \text{Range,} \quad R = \frac{CN_F}{2FN_f} \tag{14}$$

which gives range in terms of the high frequency standard. Resolution then may be as good as one count of the standard frequency in the number of counts passed through the gate, or one part in N_F parts of the path distance.

CONCEPTUAL DESIGN TEST RESULTS

A breadboard test setup was made using a separate pulsed led source, a reflecting target mirror placed at about four meters distance, and a pin diode detector to receive the reflected pulses. The detected pulses were amplified, shaped and transmitted through a length of RG58 coaxial cable. The combined equivalent optical path of cable, range and internal electronic delay was approximately three hundred meters corresponding to a range of the order of one hundred fifty meters. The signal from the delay cable was fed to the led pulse driver to initiate new pulses and produce a self oscillating system. The system repetition rate was very nearly one megahertz.

After several modifications to electronic circuitry, stabilization of power supplies, and adjustments to optic components some promising results were obtained. Criteria for system feasibility include stability of frequency and data point scatter. Several short runs were made over one minute time intervals and the data plotted. The results of one such run are shown. It may be seen that the standard deviation fell within 0.74 millimeters and that the drift rate was in the order of one half a millimeter per minute. With improved electronics, optics and delay means, it is entirely feasible that readings may approach the one tenth millimeter or one hundred micron achievement goal.

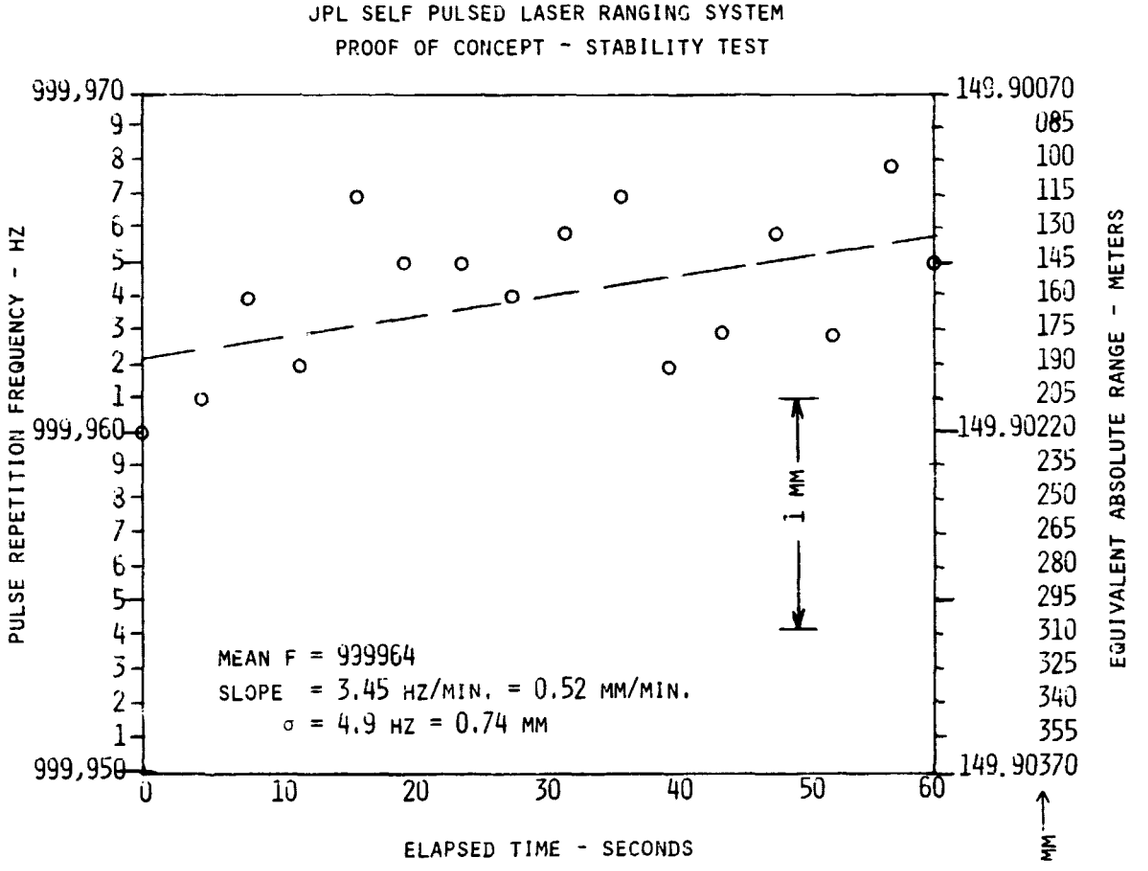

IMPROVED HARDWARE SYSTEM

The promising results obtained using relatively crude breadboard encouraged the design and construction of more sophisticated hardware and electronics with which to obtain feasibility information. The objectives of the improved system include a demonstration of the system to scan and unambiguously measure distances to several targets as would be required for measuring the contour of an antenna surface. A simplified layout of the complete pulsed laser ranging system is shown. The laser is located in a fixed position and transmits pulses to a conveniently located scan mirror. The mirror is programed to scan surface targets, a reference target and to reflect the pulses back on themselves to the detector. Subtraction of the path from the transmitter to the scan mirror and return from measurements made to the various targets provides the distances from the scan mirror, or reference position, to the targets. A microprocessor is used to control the scan process, to compute distances and to possibly analyze the surface figure in real time so that it may be used for active control.

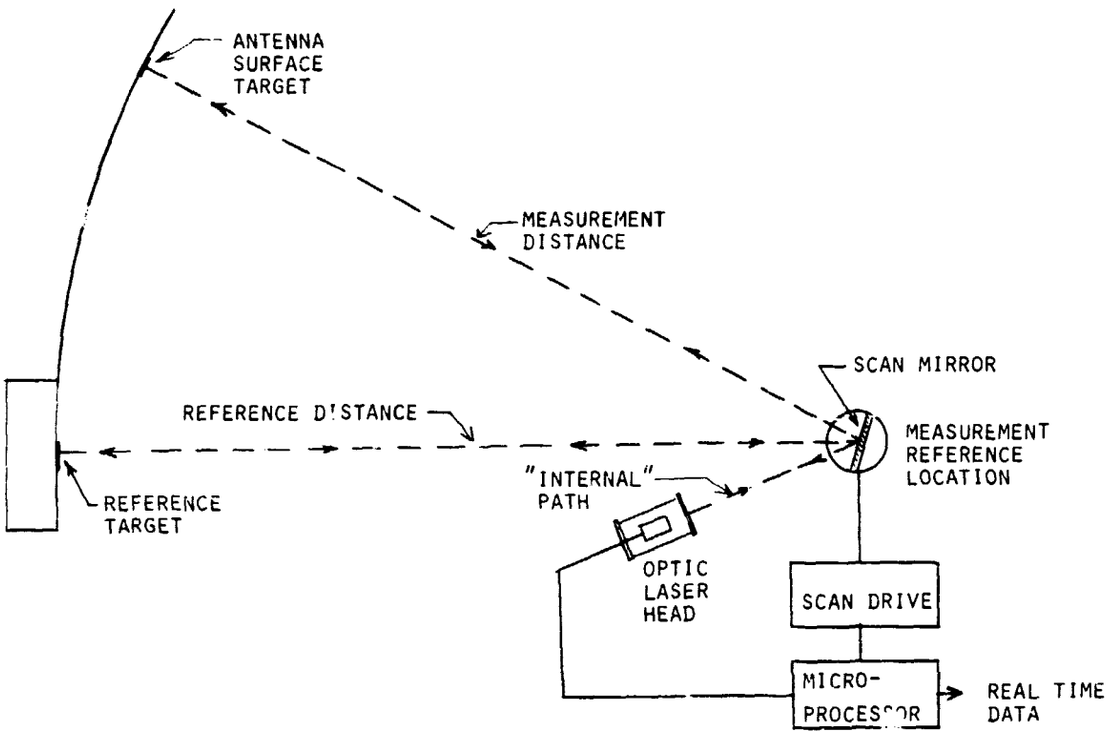

JPL SELF PULSED LASER RANGING SYSTEM

FEASIBILITY TEST HARDWARE OPTIC/ELECTRONIC HEAD

A new combined optical head has been designed and constructed. The head contains both led transmitter and pin diode detector together with driver and pulse conditioning electronics. The optic axis of the led transmitter is coincidental with the receiving optics so that transmitter and detector pointing is achieved simultaneously.

The led/laser pulser is located near the forward end of the small diameter axial tube. Its output is better collimated by a lens and transmitted. The beam expands slightly as it proceeds to the target and returns to the collector mirror in the rear of the head. The collector mirror focuses the return beam to a point near the rear entrance of the axial tube. Upon entering the tube the beam is collimated and reflected to the detector box on one side of the large tube. The small collimated beam is focussed on the pin diode detector which converts it to an electrical signal. The electrical signal is processed, conditioned and leaves the detector through a delay line to the pulser driver on the opposite side of the large tube. It is also split off to the microprocesser to provide range information. The electronics for both pulser and detector receive power from an external source. The head is intended to be a stationary device pointed only at the scan mirror.

OPTIC HEAD SECTION VIEW

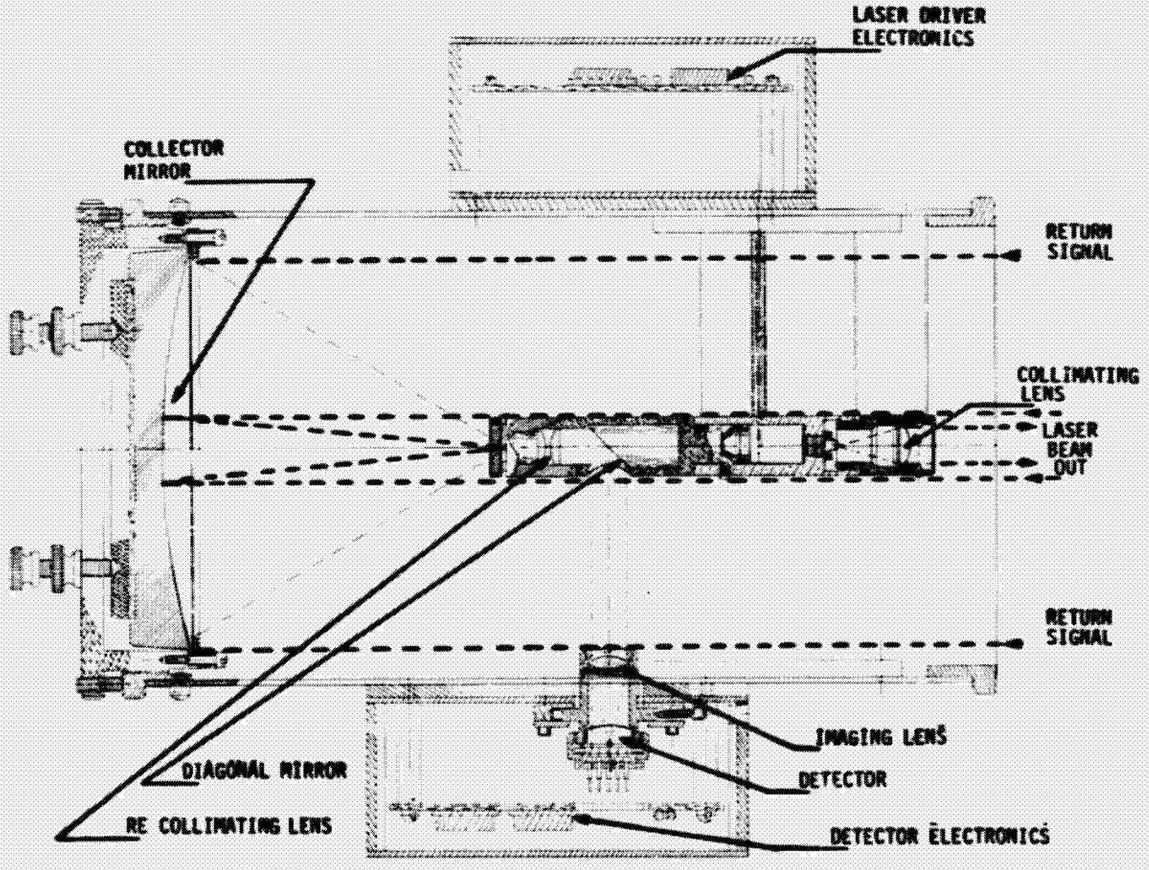

C-2

OPTIC LASER HEAD
ALIGNMENT CONFIGURATION

The photograph below shows the improved laser head with alignment optics mounted for use. No signals are transmitted or received during alignment of the head to the scan mirror or a target. The telescope mounted on top of the case looks into a periscope whose exit window allows the telescope optic axis to be displaced to coincide with the optic axis of the laser head. The periscope is uniquely located and attached to the laser head with a registration ring and pin to permit rapid and accurate alignment when attached.

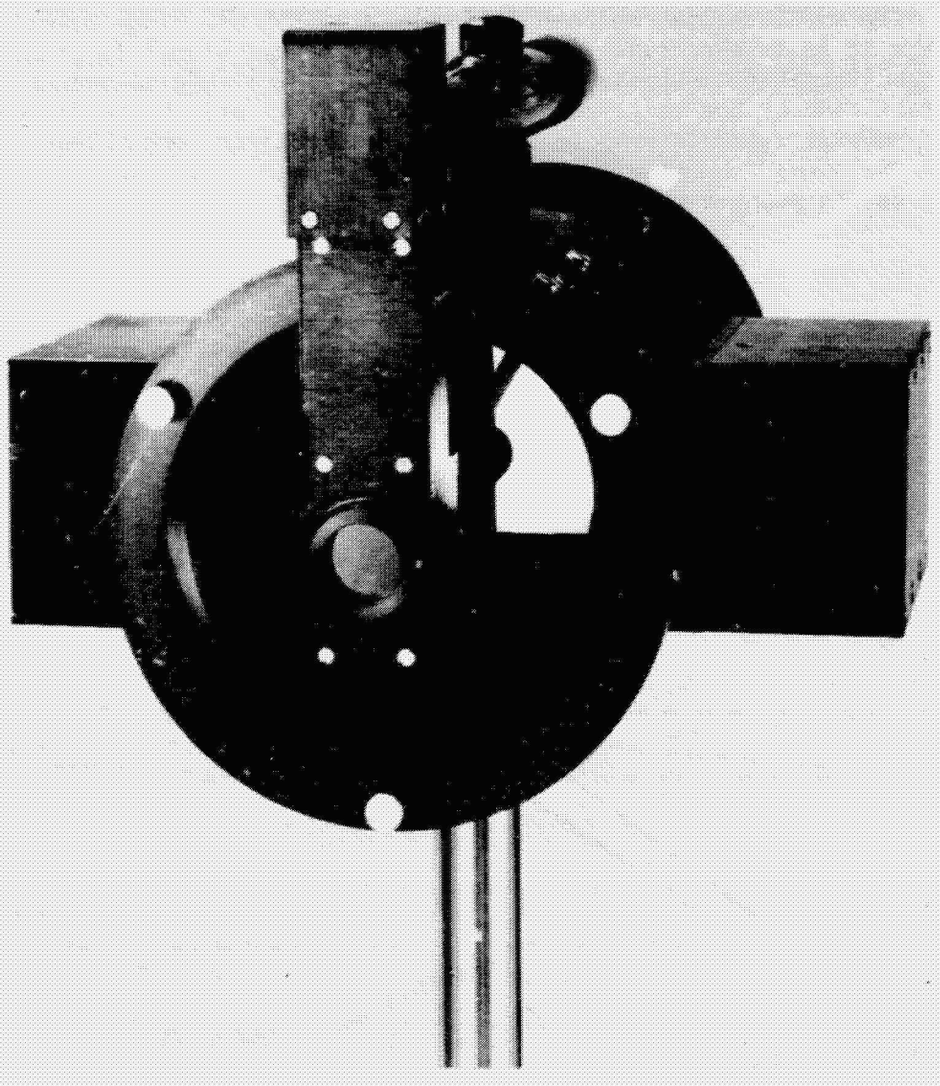

ORIGINAL PAGE IS
OF POOR QUALITY

OPTIC LASER HEAD
USE CONFIGURATION

The photograph below shows the optic laser head with alignment optics removed. The laser collimating lens may be seen in the small centrally located tube. Most of the return beam misses the small central tube and is collected by the mirror at the rear of the case. The collected beam is focussed to enter the rear of the small central tube where it is collimated and reflected out to the detector electronics in the box at the right. The box at the left contains the laser pulse driver. The case is approximately thirteen centimeters in diameter by thirty centimeters long and weighs approximately three kilograms including electronics in the use configuration.

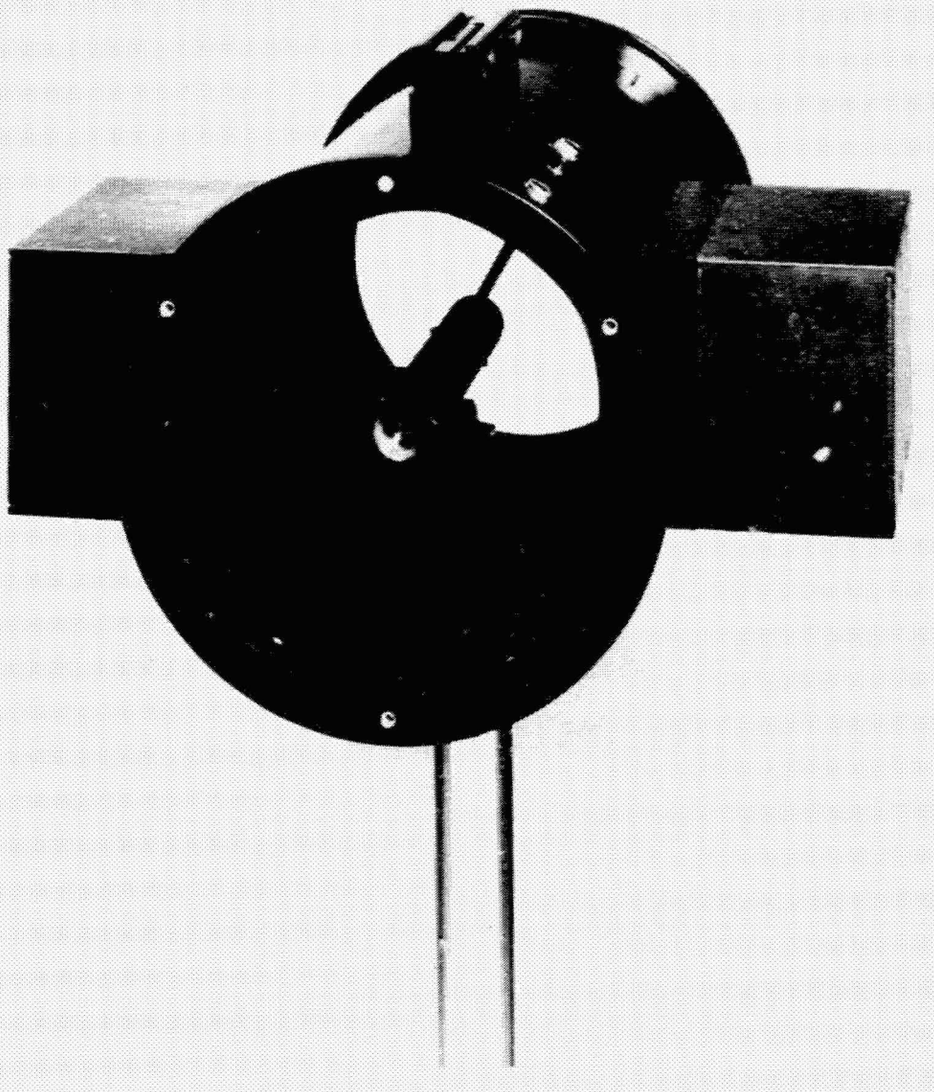

OPTIC LASER HEAD
LASER PULSE DRIVER

In a box mounted to the side of the optics case is shown the laser pulse driver electronics. The electronics are mounted on a double sided printed circuit board measuring five and one half by nine centimeters. In the pulse driver, signals are received from the detector by way of a delay line, shaped and power amplified to the level required for driving a led or laser. Heat dissipation and temperature control of this package and the laser may have a significant bearing on the system performance. Precautions were taken to radiate laser heat.

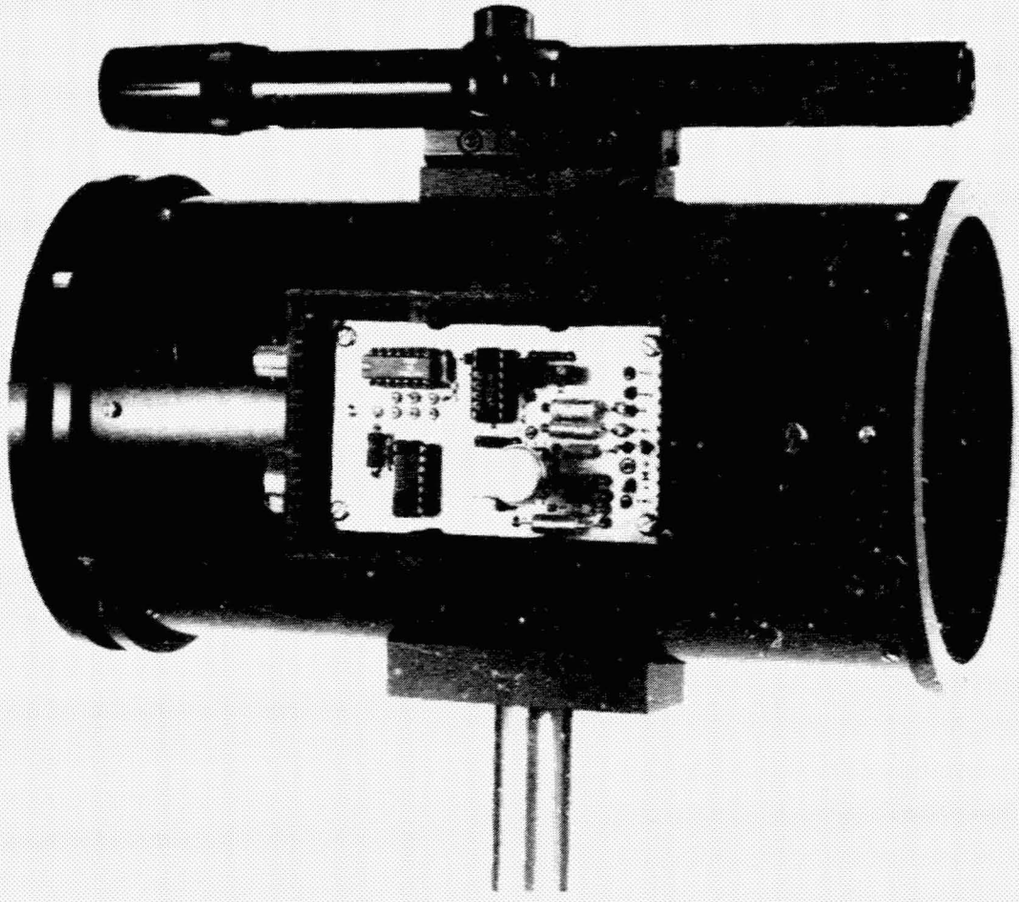

ORIGINAL PAGE IS
OF POOR QUALITY

OPTIC LASER HEAD
DETECTOR ELECTRONICS

The accompanying photograph shows the detector electronic circuit board required to amplify and shape the received pulses for precise time triggering and for driving the transmission/delay line to the laser pulser. The receiver electronics also includes provision for automatic gain control to assure that pulses from different distances and targets will time trigger consistently. The detector and concentrating optics are located below the electronics and are adjustable by means of screws and holes in the sides of the housing box. The box and printed circuit board are approximately the same size as those used for the pulse driver.

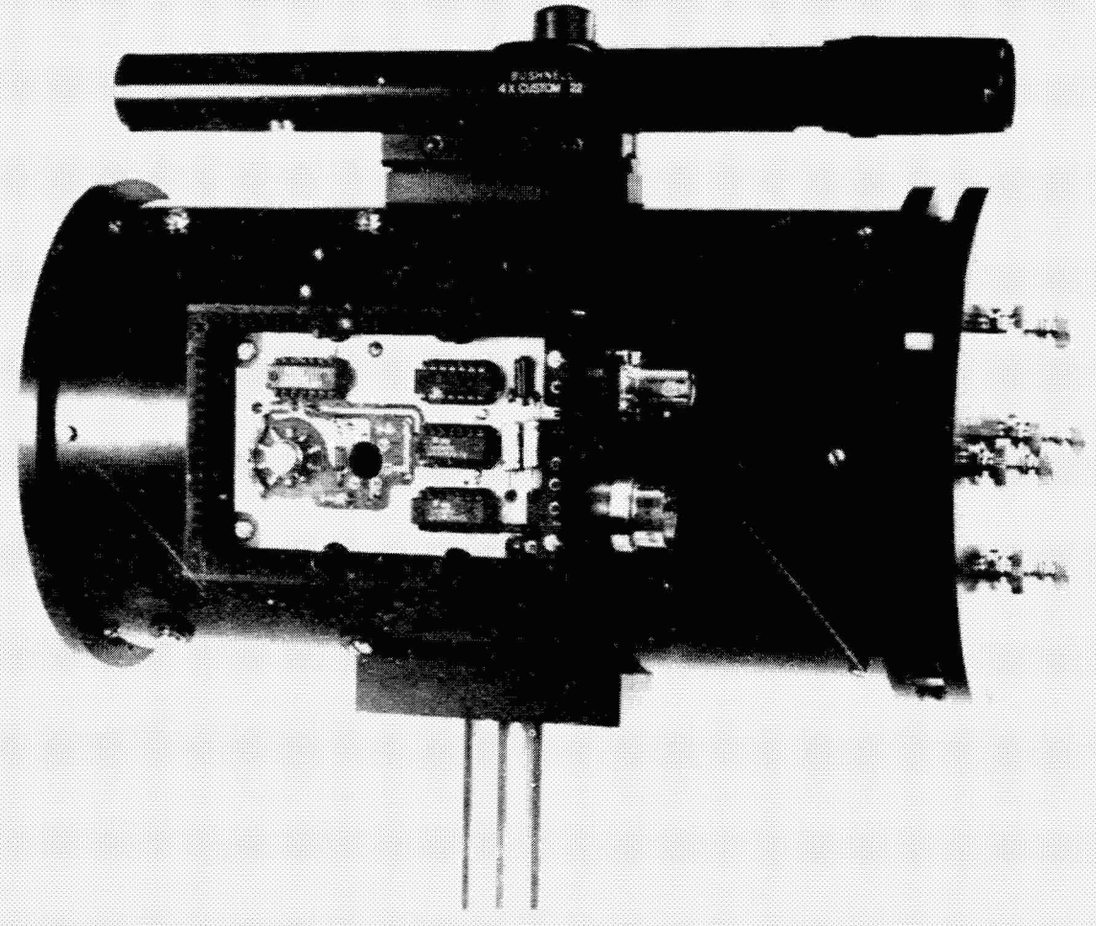

LSST - STRUCTURAL CONCEPT - DEPLOYABLE REFLECTORS
ANTENNA SURFACE MEASUREMENT SUMMARY

Many possible systems for use in measuring antenna surface contour were investigated. Most of these systems were optical types capable of fine distance or angle resolution. Complexity varied as the capability to resolve distance.

Of the systems investigated, there were at least three which showed promise of use on early deployed antennas. The Lockheed Missiles and Space Company's "structural alignment sensor" has the capability desired and may be a logical choice although it is not yet perfected and its present complexity indicates that there may be problems with size and weight. The TRW angular measuring system has the capability of resolving very small angles and would be useful where a dependably stiff panel of confident contour must be aligned to become a part of an overall surface. It appears to have fine resolution and cost effectiveness for what it does although it does not have the capability of measuring local distortions in a large surface. The JPL self pulsed laser ranging system has resolution limitations; however, at this time it appears to be a viable candidate for measurement of large antenna surfaces where cost, weight, and simplicity are important factors.

At the present time, we are working on the JPL system which shows promise of resolving distances in the order of less than one tenth of a millimeter. Our goal for FY80 will be to set up a practical demonstration to show the capability of the JPL system. Other activities will include continuation to explore other surface measuring systems and to perform some studies with regard to the application of measuring systems to specific selected antenna candidates.

SUMMARY

- Concept Successfully Demonstrated
- Present Capability Includes
  - Greater Than 150M Range Capability
  - Less Than One Millimeter Resolution
  - Unambiguous Distance Measurement
- Projected Performance
  - One Tenth Millimeter Resolution
  - Low Power Consumption
  - Low Volume and Weight
  - Relatively Low Cost
- Probable Measurement Applications
  - Early Deployed Antennas
  - Large, Low Frequency Antennas

Research described in this publication was carried out by the Jet Propulsion Laboratory, California Institute of Technology under NASA contract NAS 7-100.

N80-19150 25

FY 79 - LSST ANTENNA TECHNOLOGY DEVELOPMENT

Thomas G. Campbell
NASA Langley Research Center
Hampton, VA 23665

LSST 1st ANNUAL TECHNICAL REVIEW

November 7-8, 1979

For review purposes, the objective and near-term technology requirements of the LSST antenna development effort are listed below.

LSST
REFLECTOR CONCEPT DEVELOPMENT

OBJECTIVE

- TO DEVELOP TECHNOLOGY NEEDED TO EVALUATE, DESIGN, FABRICATE, PACKAGE, TRANSPORT AND DEPLOY LARGE ANTENNA SYSTEMS FOR CLASSES OF POTENTIAL APPLICATIONS.

TECHNOLOGY REQUIREMENTS (NEAR TERM)

- TO DEVELOP DEPLOYABLE ANTENNA SYSTEMS
- SIZE RANGE UP TO 100 METERS IN DIAMETER
- FREQUENCY RANGE 1 TO 15 GHz
- TECHNOLOGY AVAILABLE CY 1983

The deployable reflector concept development effort for FY 79 was divided into two concept areas--the Maypole (Hoop/Column) for near term applications, and the Erectable Truss Concept for far term mission applications.

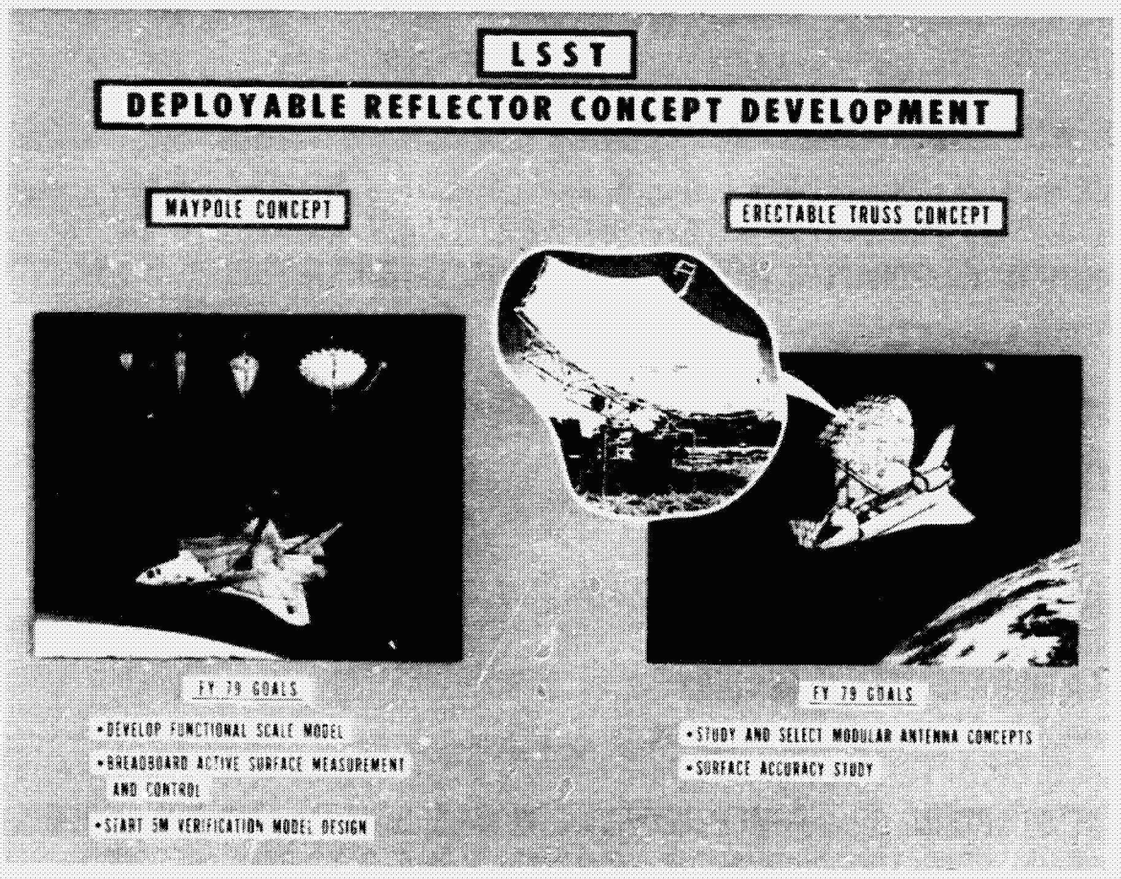

ORIGINAL PAGE IS
OF POOR QUALITY

Associated with the Maypole and Erectable Truss development efforts are the following tasks for FY 79.

LANGLEY RESEARCH CENTER

- DEPLOYABLE REFLECTOR CONCEPT DEVELOPMENT - MAYPOLE (HOOP/ COLUMN); PHASE I TASK DEVELOPMENT CONTRACT AWARDED TO THE HARRIS CORPORATION MAY 1, 1979. (NAS1-15763)

- MODULAR REFLECTOR STUDY CONTRACT AWARDED TO GENERAL DYNAMICS APRIL 5, 1979. (NAS1-15753)

- DEVELOPMENT OF ELECTROMAGNETIC ANALYSIS METHODS FOR LARGE APERTURE ANTENNAS. (CONTINUING IN-HOUSE ACTIVITY AT THE LANGLEY RESEARCH CENTER)

- DEVELOPMENT OF SURFACE ACCURACY MEASUREMENT SYSTEM FOR LARGE SPACE STRUCTURES; PHASE-I CONTRACT AWARDED TO TRW, REDONDO BEACH, CA; SEPTEMBER 12, 1978. COMPLETION OF PHASE-I FEBRUARY 15, 1980. (NAS1-15520)

The technology development plan for the modular reflector concepts is shown below. After completing the parametric evaluations, design configurations for 100-meter diameters using the PETA and the rigid panel concepts were to be developed for concept comparison and trade-off studies.

MODULAR REFLECTOR CONCEPT DEVELOPMENT

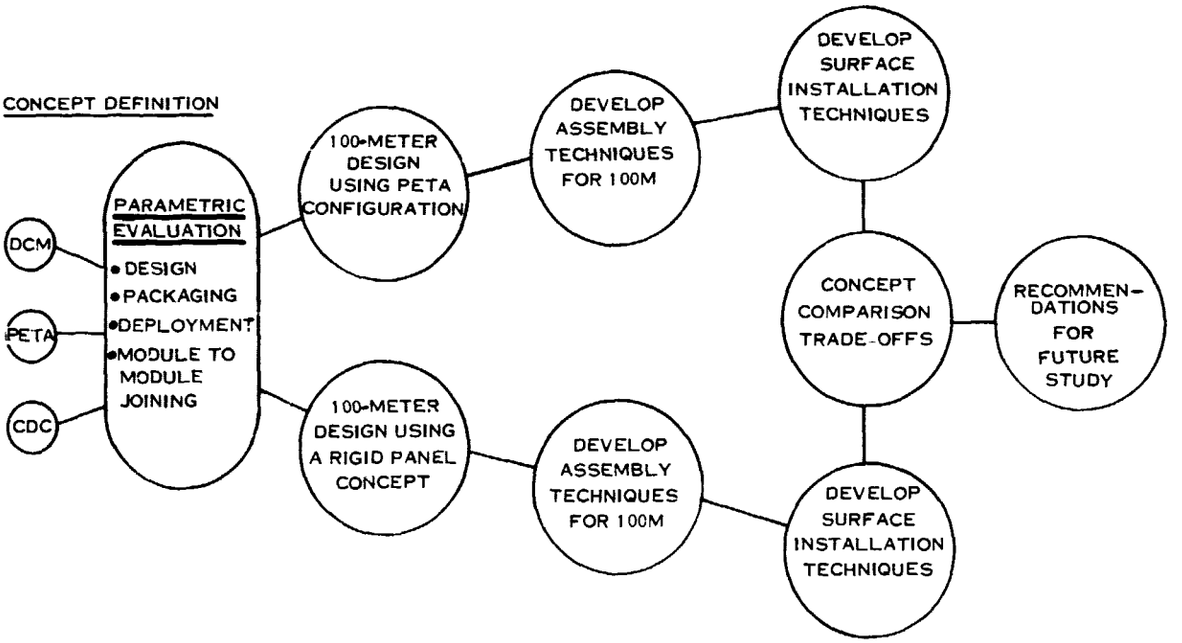

The following accomplishments were made in FY 79 related to the development of modular reflector concepts.

MODULAR REFLECTOR CONCEPTS STUDY

NAS1-15753
GENERAL DYNAMICS

ACCOMPLISHMENTS

- PARAMETRIC CURVES HAVE BEEN DEVELOPED TO SIZE FACETTED ANTENNA SURFACES
- PACKAGING AND DISPENSING ARRANGEMENTS HAVE BEEN DEVELOPED FOR DCM AND PETA CONCEPTS
- PRELIMINARY ASSEMBLY STUDIES OF PETA ASSEMBLY TECHNIQUE COMPLETED
- PRELIMINARY DESIGNS FOR 100 METER REFLECTORS BEING ESTABLISHED

In the deployable reflector area for near term mission applications, a Maypole (Hoop/Column) concept is being developed by the Langley Research Center for LSST. Shown below is an artist's view of the antenna as deployed from shuttle.

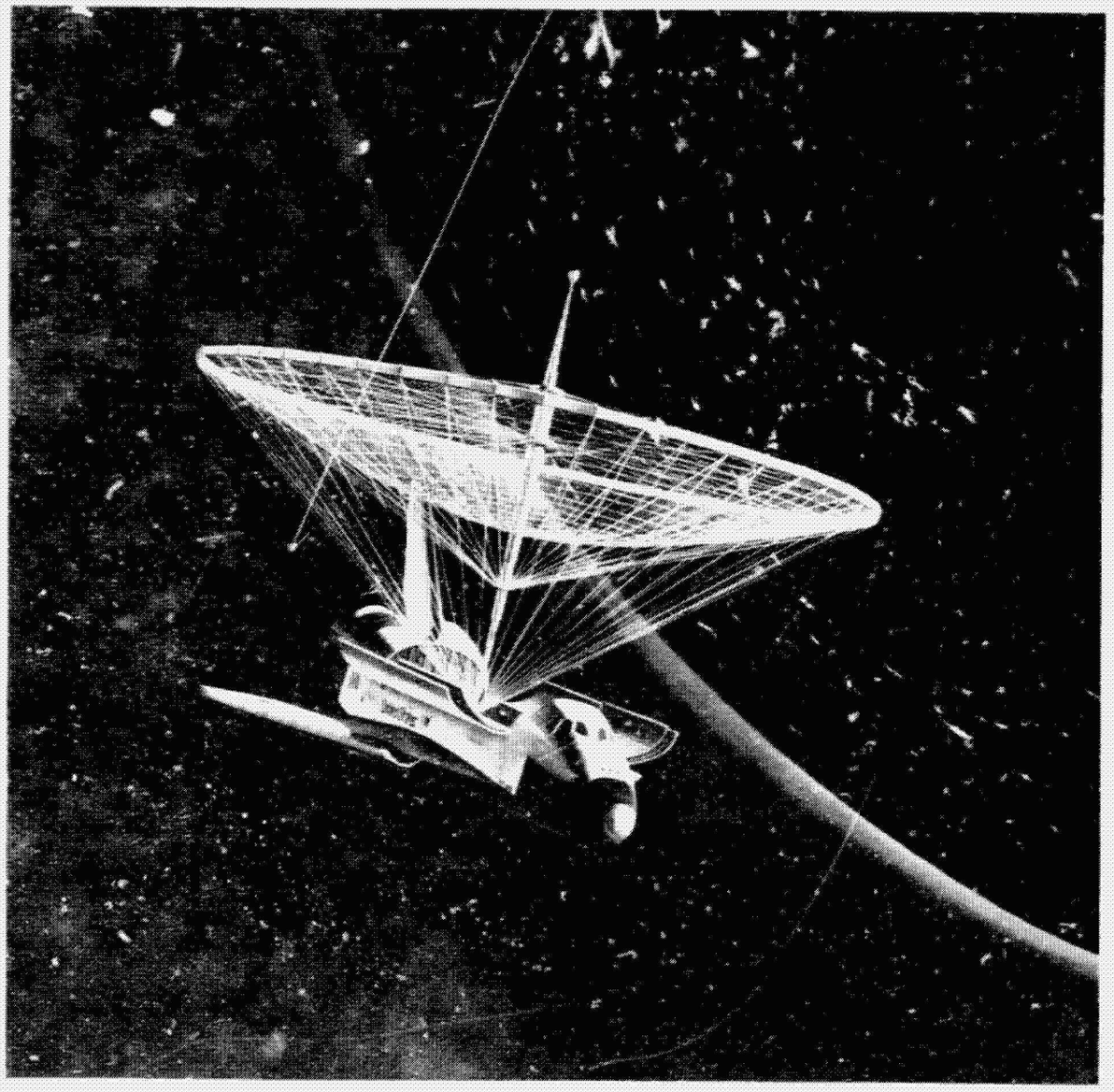

ORIGINAL PAGE IS
OF POOR QUALITY

Shown below is the technology development philosophy that is underway for the Maypole (Hoop/Column) development effort. Included in this plan shall be: (1) a review of the mission requirements; (2) an economic assessment of the reflector technology; (3) concept review; (4) preliminary design using subscale and intermediate scaled elements; and (5) the integration of the surface measurement system with the reflector. Throughout this technology development activity, confidence in the design of critical items shall be obtained through the fabrication and test of subscale, intermediate, and full scale components. All of these outputs shall input the development and verification of the predictive analysis methods.

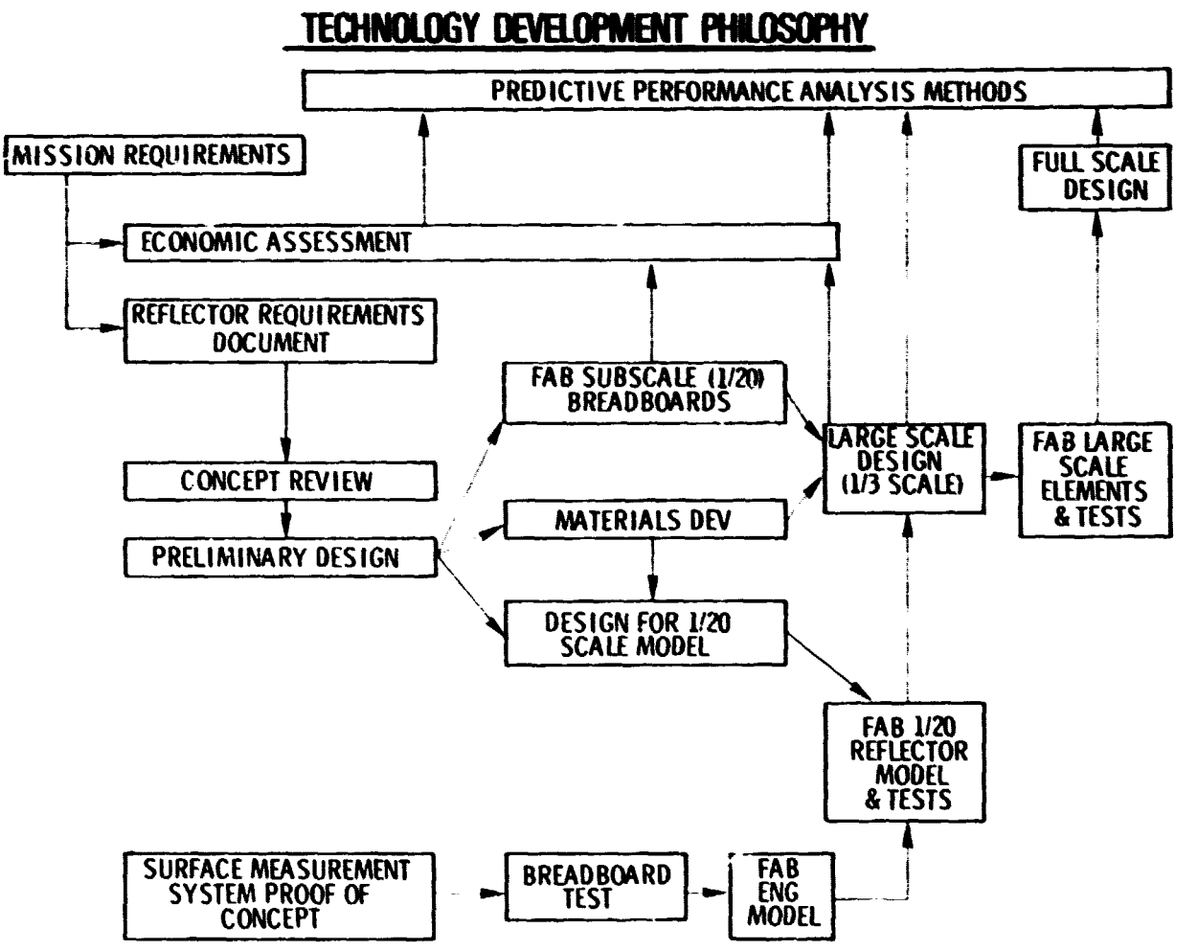

One of the first activities associated with the Maypole development effort is to develop possible mission scenarios (using the LSST near term focus mission) so that the reflector configuration and requirements could be determined. The following view graph presents the approach used in defining the technology drivers and the subsequent "point" design for the reflector activity.

LSST CONFIGURATION/REQUIREMENT DEFINITION APPROACH FOR THE MAYPOLE (HOOP/COLUMN) DEVELOPMENT ACTIVITY

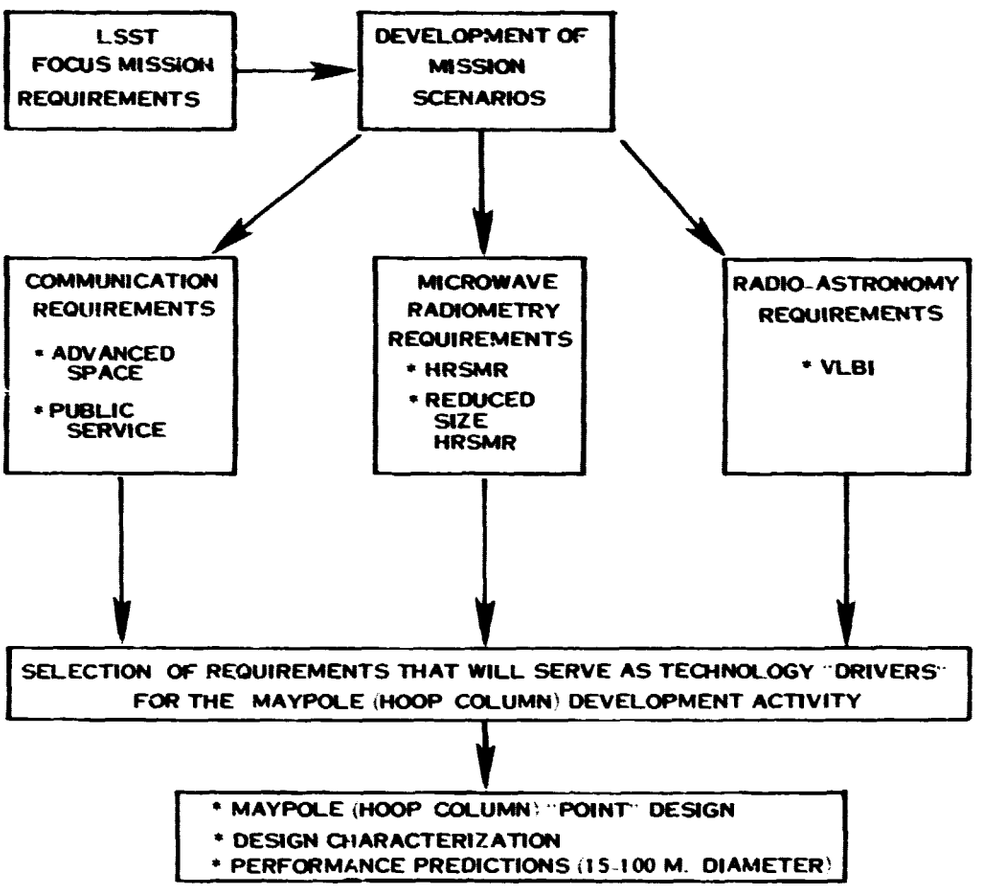

In developing the scenario for the communications mission, the recent results of a Langley contract with TRW are prevalent and shall influence the LSST activity. The TRW multiple beam antenna study represents the only known multiple beam work that has been undertaken by NASA during the past several years. Therefore, it was believed to be important to briefly report on the results of this work during this RTR review. The following view graph presents the objectives of the multiple beam study.

KU-BAND MULTIPLE BEAM ANTENNA PROGRAM OBJECTIVES

CONUS SPOT BEAM ANTENNA

- DEVELOP A 12/14 GHz MULTIPLE BEAM ANTENNA FOR CONTIGUOUS SPOT BEAM COVERAGE OF CONUS PLUS ALASKA AND HAWAII
- FREQUENCY REUSE ACHIEVED THROUGH A COMBINATION OF FREQUENCY PLAN, POLARIZATION ORTHOGONALITY, LOW SIDELOBE BEAMS
- APPLICATION IS HIGH CAPACITY POINT-TO-POINT COMMUNICATIONS AND DIRECT BROADCAST SERVICE
- BUILD AND TEST A BRASSBOARD MODEL ANTENNA TO:
  - EVALUATE THE MULTIPLE BEAM ANTENNA DESIGN CONCEPT
  - ESTABLISH ACHIEVABLE BEAM ISOLATION AND GAIN
  - DETERMINE PERFORMANCE CHARACTERISTICS OF KEY ELEMENTS OF ANTENNA HARDWARE
  - PROVE FEASIBILITY OF A FLIGHT MODEL ANTENNA

CONUS SPOT BEAM ANTENNA

DESIGN SPECIFICATIONS AND MEASURED CAPABILITIES

	SPECIFICATIONS	MEASURED CAPABILITIES
DOWNLINK FREQUENCY	11.7 TO 12.2 GHz	11.7 TO 12.2 GHz
UPLINK FREQUENCY	14.0 TO 14.5 GHz	14.0 TO 14.5 GHz
POLARIZATION	ORTHOGONAL LINEAR	ORTHOGONAL LINEAR
COVERAGE	CONTIGUOUS CONUS, ALASKA AND HAWAII	CONTIGUOUS CONUS, ALASKA AND HAWAII
NUMBER OF BEAMS	ABOUT 25 BEAMS	17 BEAMS
SIDELOBE LEVEL	-32 dB	-36 dB AT BORESIGHT -32 dB OFF BORESIGHT
CROSS POLARIZATION	-28 dB	-32 dB
BEAM CROSSOVER LEVEL	-7 dB FOR DOWNLINK -9 dB FOR UPLINK	-6 dB FOR DOWNLINK -8 dB FOR UPLINK
BEAM ISOLATION	28 dB	TBD
FEED CIRCUIT LOSS	<0.30 dB	<0.20 dB
INPUT VSWR	<1.4:1	<1.2:1
REFLECTOR DIAMETER	200 CM APPROXIMATELY	200 CM
POWER HANDLING CAPACITY	100 WATTS AVERAGE POWER	100 WATTS

CONUS SPOT BEAM ANTENNA

KEY DESIGN FEATURES

- 15-BEAM COVER CONUS PLUS TWO SEPARATE BEAMS FOR ALASKA AND HAWAII
- EACH BEAM UTILIZES ONE-HALF OF THE 500 MHz BANDWIDTH AVAILABLE FOR BOTH UPLINK AND DOWNLINK COMMUNICATIONS
- BEAMS OF THE SAME COLOR ARE COPOLARIZED AND IN THE SAME FREQUENCY BAND
- BEAMS IN ADJACENT ROWS ARE ISOLATED BY FREQUENCY SEPARATION
- ADJACENT BEAMS IN A ROW ARE ORTHOGONALLY POLARIZED
- 17-BEAM SYSTEM REQUIRES TWO 2-METER OFFSET REFLECTORS WITH 17 FEEDS
- EACH FEED CONSISTS OF A 9-HORN CLUSTER TO PRODUCE ONE SPOT BEAM
- EACH OFFSET REFLECTOR IS CONFIGURED WITH A WIRE GRID SUBREFLECTOR TO DIPLEX ORTHOGONALLY POLARIZED FEEDS (BEAMS)
- EACH FEED IS LINEARLY POLARIZED AND OPERATES BOTH DOWNLINK (11.7 - 12.2 GHz) AND UPLINK (14.0 - 14.5 GHz)

A conceptual satellite configuration using the multiple beam design is shown below. In order to meet the requirements, two offset fed reflectors are needed for beam interleaving.

CONCEPTUAL SATELLITE CONFIGURATION

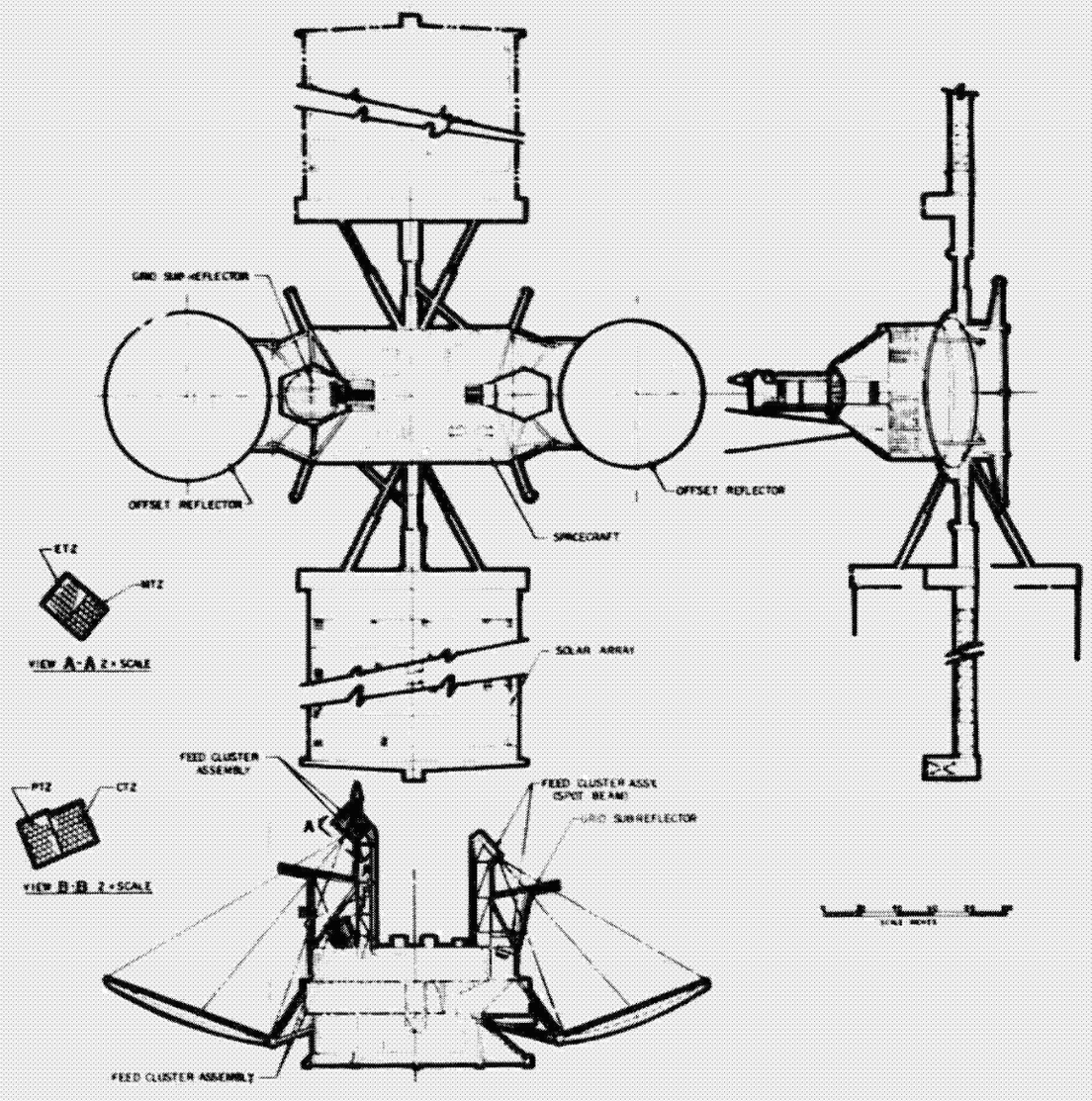

Shown below is how the Maypole (Hoop/Column) could be used to produce the 17-beam CONUS coverage as described in the TRW study. This configuration is for an F/D <1.0.

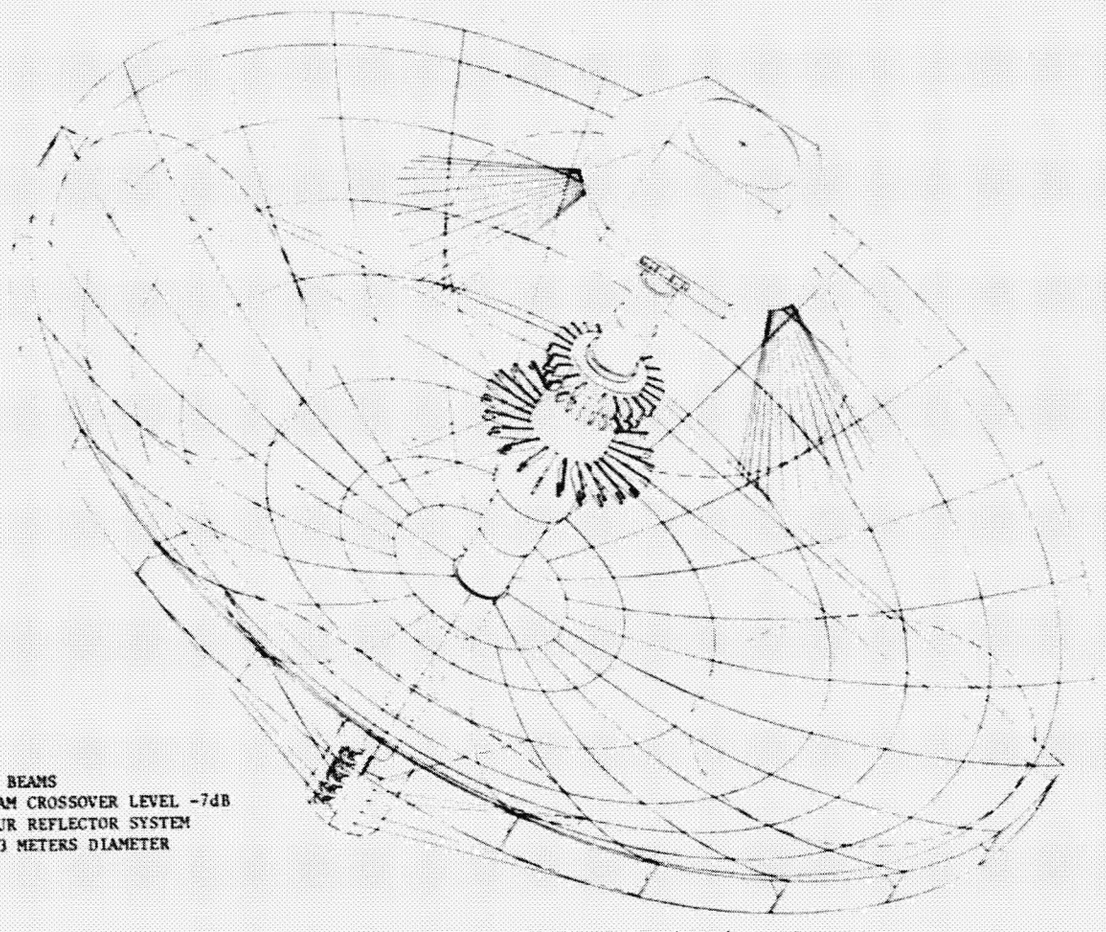

17 BEAMS
BEAM CROSSOVER LEVEL -7dB
FOUR REFLECTOR SYSTEM
7.3 METERS DIAMETER

MULTIPLE BEAM ANTENNA CONFIGURATION USING THE (HOOP/COLUMN) MAYPOLE CONCEPT FOR PROVIDING CONUS COVERAGE AT KU-BAND (ISOMETRIC VIEW).

Shown below is how the Maypole (Hoop/Column) could be used to produce 308 beams for CONUS coverage. A longer F/D = 2.0 would be required. This is basically the QUAD Aperture approach that will be discussed in the next paper by D. C. Montgomery and L. D. Sikes.

HIGH PERFORMANCE FEED CLUSTER
308 BEAMS
BEAM CROSSOVER LEVEL -3.75dB
FOUR REFLECTOR SYSTEM
CORRUGATED HORN FEED ELEMENTS (5.75λD)
61.0 METERS DIAMETER

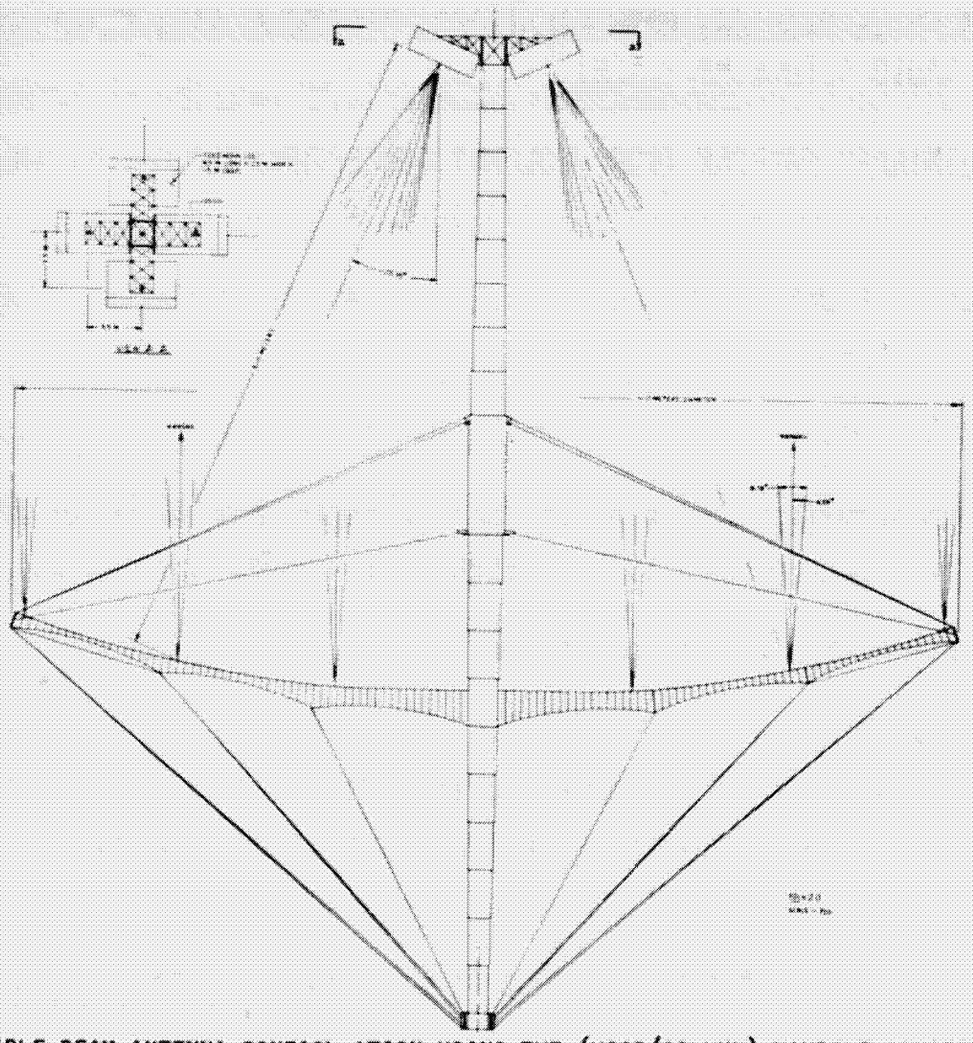

MULTIPLE BEAM ANTENNA CONFIGU ATION USING THE (HOOP/COLUMN) MAYPOLE CONCEPT FOR PROVIDING SUBCONTINENT, C INENT, CONTIGUOUS BEAM COVERAGE (SECTION VIEW).

SUMMARY OF ACCOMPLISHMENTS

I. REFLECTOR DEVELOPMENT

- REQUIREMENTS DEFINITION: DEVELOPED SCENARIOS FOR LSST NEAR TERM FOCUS MISSION; COMMUNICATIONS, MICROWAVE RADIOMETRY, AND RADIO ASTRONOMY - VLBI.

- PRELIMINARY MAYPOLE (HOOP/COLUMN) CONCEPTUAL DESIGN OBTAINED FOR THE COMMUNICATIONS FOCUS MISSION.

- CONCEPTUAL DESIGNS OBTAINED FOR CRITICAL COMPONENTS OF HOOP/COLUMN REFLECTOR.

- PUBLICATIONS:

  A. "DEPLOYABLE REFLECTOR ANTENNA TECHNOLOGY DEVELOPMENT FOR THE LARGE SPACE SYSTEMS TECHNOLOGY PROGRAM", BY R. E. FREELAND, AND T. G. CAMPBELL. PRESENTED AT AIAA CONFERENCE MAY 1979 HAMPTON, VA.

  B. "DEVELOPMENT OF MAYPOLE (HOOP/COLUMN) DEPLOYABLE REFLECTOR CONCEPT FOR 30 TO 100 METER APPLICATIONS", BY DR. B. C. TANKERSLY, HARRIS CORPORATION. PRESENTED AT AIAA CONFERENCE MAY 1979.

  C. "NASA TECHNOLOGY FOR LARGE SPACE ANTENNAS", BY R. A. RUSSELL, T. G. CAMPBELL, AND R. E. FREELAND. PRESENTED AT 49TH STRUCTURES AND MATERIALS PANEL MEETING, OCTOBER 7-12, 1979, COLOGNE, WEST GERMANY.

Included in FY 79 was the development of Electromagnetic Analysis methods for large aperture antennas. Shown below are a few of the accomplishments.

SUMMARY OF ACCOMPLISHMENTS CONT'D.

II. ELECTROMAGNETIC ANALYSIS

° PUBLICATIONS:

A. "A PRELIMINARY STUDY OF A VERY LARGE SPACE RADIOMETRIC ANTENNA", NASA TM 80047/P.K. AGRAWAL.

B. "A METHOD FOR PATTERN CALCULATION FOR REFLECTOR ANTENNAS WHOSE GEOMETRY IS DESCRIBED BY A FINITE NUMBER OF DISCRETE SURFACE POINTS", IEEE SYMPOSIUM, JUNE 1979, P. K. AGRAWAL, AND W. F. CROSWELL.

The final activity conducted during FY 79 was the development of a Surface Accuracy Measurement Sensor for Large space systems. These accomplishments are listed below.

SUMMARY OF ACCOMPLISHMENTS CONT'D.

III. SURFACE ACCURACY MEASUREMENT SYSTEM

- SUCCESSFUL PROOF OF CONCEPT DEMONSTRATION AT TRW, SEPT 1979.
- PUBLICATIONS:

  "SURFACE ACCURACY MEASUREMENT SENSOR FOR DEPLOYABLE REFLECTOR ANTENNAS", R. S. NEISWANDER, TRW. PRESENTED AT AIAA CONFERENCE, HAMPTON, VA. MAY 1, 1979.

This view graph shows how the TRW system would be implemented using the Maypole (Hoop/Column) reflector.

HARRIS MAYPOLE (HOOP-AND-COLUMN) MESH DEPLOYABLE ANTENNA

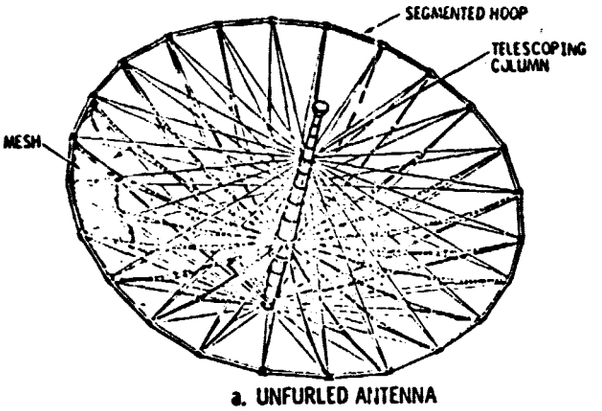

a. UNFURLED ANTENNA

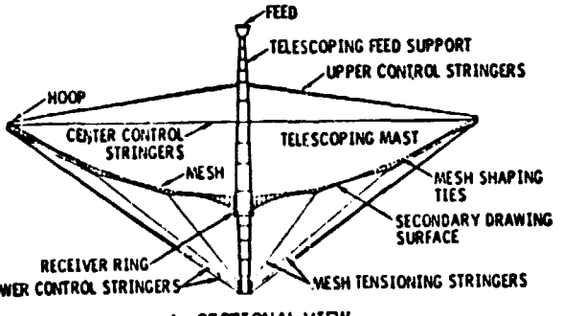

b. SECTIONAL VIEW

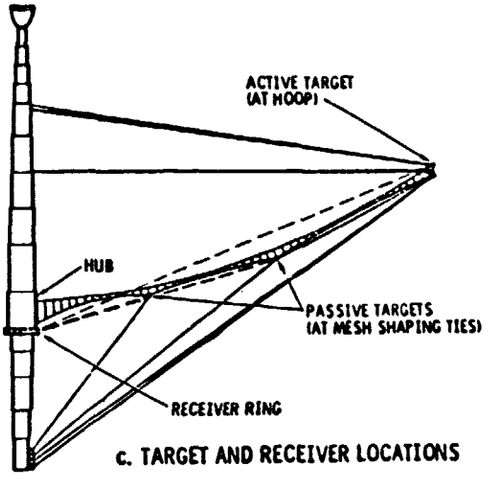

c. TARGET AND RECEIVER LOCATIONS

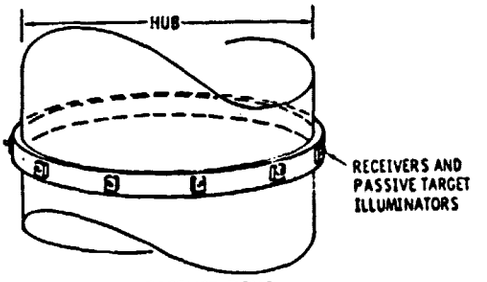

d. RECEIVER RING

This photograph shows the set-up for the proof of concept demonstration of the SAMS at TRW. This set-up is basically a 1/10-scale configuration of the 100-meter reflector application.

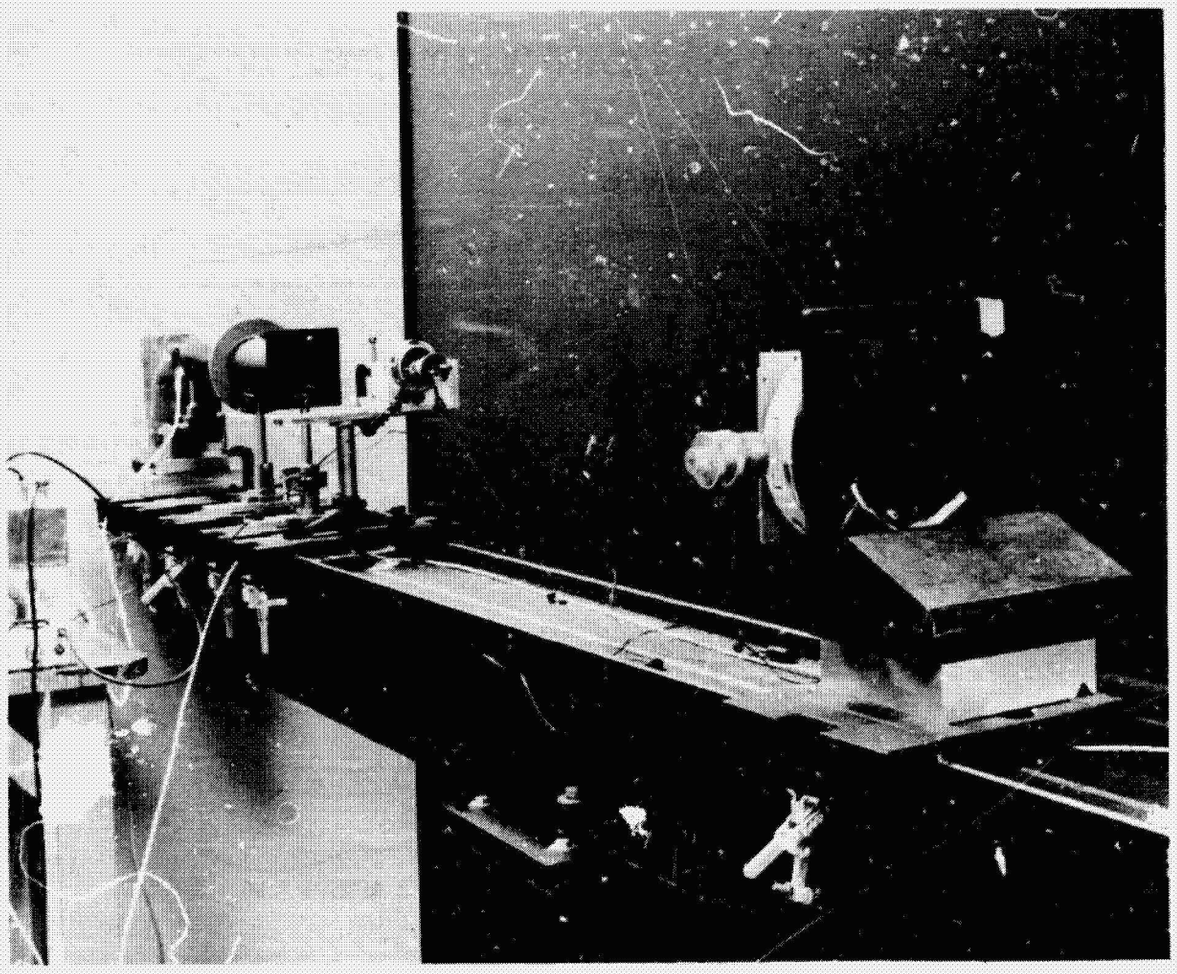

ORIGINAL PAGE IS
OF POOR QUALITY

D6

DEVELOPMENT OF THE MAYPOLE (HOOP/COLUMN) DEPLOYABLE REFLECTOR CONCEPT FOR LARGE SPACE SYSTEMS APPLICATIONS

D. C. Montgomery and L. D. Sikes
Harris Corporation
Government Systems Group

NASl - 15763

LSST 1ST ANNUAL TECHNICAL REVIEW

November 7-8, 1979

HOOP/COLUMN REFLECTOR

The Hoop/Column reflector concept is being developed for mission applications in the mid 1980's and beyond. The accompanying artist's conception shows a 30 meter diameter reflector in the LDASE (Large Deployable Antenna Shuttle Experiment) configuration. This concept was generated during a previous NASA sponsored AAFE program.

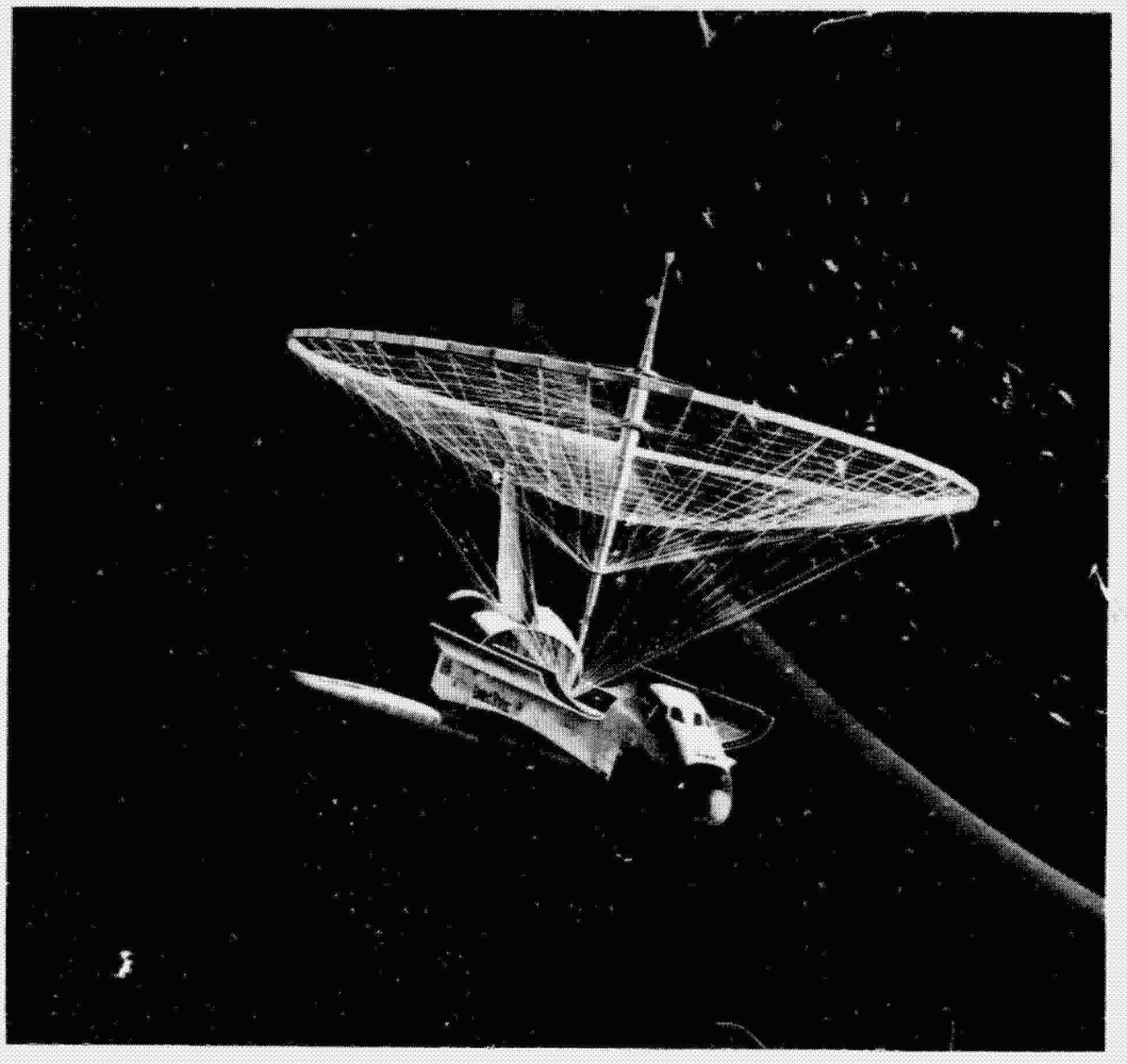

ORIGINAL PAGE IS
OF POOR QUALITY

N80-19151

PROGRAM OBJECTIVE

The program is a technology development study. The specific technologies to be developed are stated below.

PROGRAM OBJECTIVE

TO DEVELOP THE TECHNOLOGY NEEDED TO EVALUATE, DESIGN, FABRICATE, PACKAGE, TRANSPORT AND DEPLOY THE MAYPOLE HOOP/COLUMN REFLECTOR

PROGRAM DESCRIPTION

The program is organized by specific tasks. Each task has specific objectives which, when combined, are directed at meeting the overall program objective. Two tasks have been initiated to date. They will be highlighted later in this report. The remaining tasks are summarized below.

Task 3 is an Advanced Concepts task which permits the study of spinoff technologies or other TBD areas of study. Task 4 is the hardware phase of the contract. This task will be used to build demonstration models of the Hoop/Column antenna which show how it satisfies various focus mission requirements. Additionally, an active surface adjustment breadboard model will be built to demonstrate this capability. Other elements of the design will be fabricated for evaluation. Task 5 will utilize the PRICE routine to provide parametric cost data or a family of antennas based on size, configuration, etc. Task 6 is a task intended to design a 5 meter dia. verification model which will be built and tested subsequent to this contract.

PROGRAM DESCRIPTION

- TASK 1 – CONCEPTUAL DESIGN AND PERFORMANCE PROJECTIONS FOR THE MAYPOLE (HOOP/COLUMN) REFLECTOR CONCEPT FOR LARGE SPACE SYSTEMS APPLICATIONS
- TASK 2 – MATERIALS DEVELOPMENT
- TASK 3 – ADVANCED CONCEPTS
- TASK 4 – DEMONSTRATION MODELS AND FULL SCALE ELEMENTS
- TASK 5 – ECONOMIC ASSESSMENT
- TASK 6 – 5-M DIAMETER VERIFICATION MODEL

HOOP/COLUMN CONCEPT

The following three figures illustrate the basic concept approach. The conceptual design shown was the direct result of the previously mentioned AAFE program and formed the basis of the present LSST Hoop/Column development study effort. The basic elements described are the telescoping mast, the rigid articulating hoop and a series of cords used to shape the surface and position the hoop.

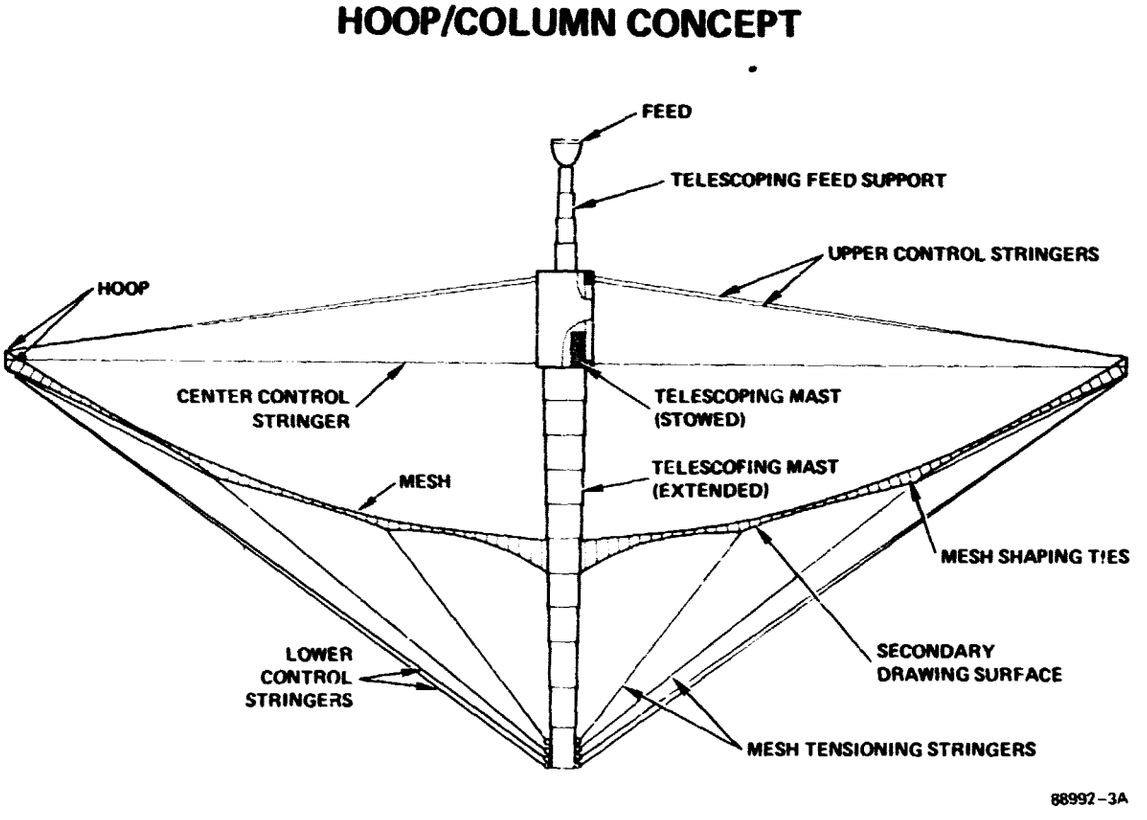

Hoop/Column Deployment Sequence

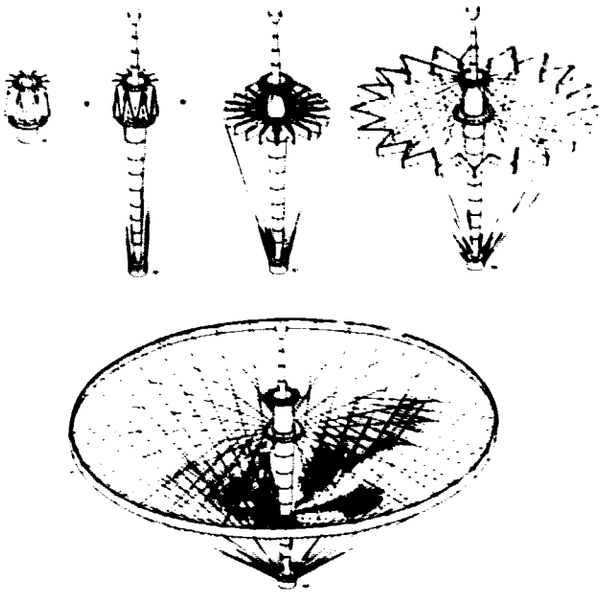

SURFACE SHAPING TECHNIQUE

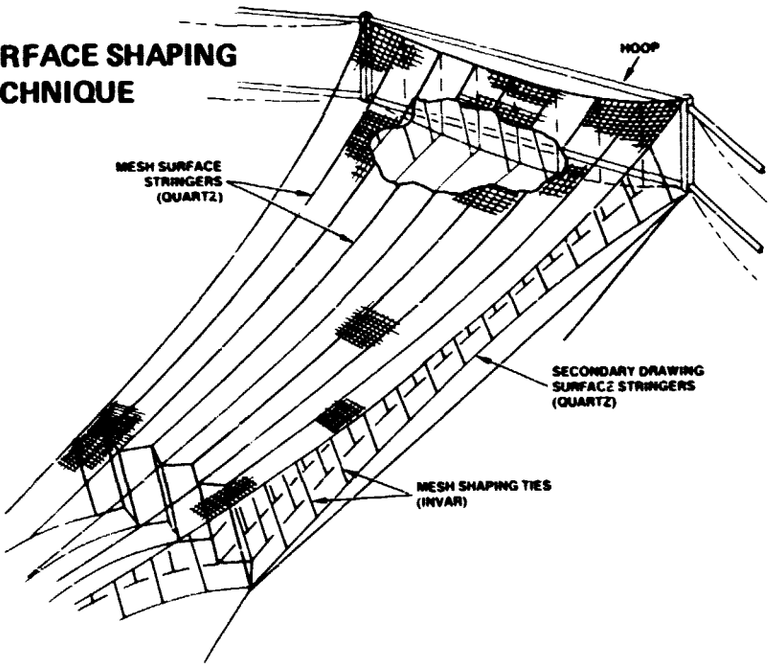

TASK 1

CONCEPTUAL DESIGN AND PERFORMANCE PROJECTIONS FOR THE MAYPOLE (HOOP/COLUMN) REFLECTOR CONCEPT FOR LARGE SPACE SYSTEMS APPLICATIONS

TASK 1 OBJECTIVES

This task is the primary design and analysis portion of the program. The first objective is key to performing all subsequent activities in this task. By reviewing the focus mission scenarios provided by NASA, specific configuration requirements have been determined. Upon completion of this review, technology drivers are identified and organized into a document (Reflector Requirement Document) which will serve as the design specification for the balance of the program. These requirements will define the configuration or "point design" which may or may not be one specific mission.

A detailed conceptual design must then be established around the requirements of the RRD. Full analyses will be accomplished in order to provide performance projections for the design. Related to this analysis will be the development of a scaling technique which will permit performance estimates for a given configuration over the range of sizes from 15 to 100 meters in diameter.

Additional objectives include the development of both manufacturing and testing methods consistent with structures of this size.

OBJECTIVES

- DEFINE "POINT DESIGN" CONFIGURATION RESULTING FROM TECHNOLOGY DRIVERS IDENTIFIED DURING MISSION SCENARIO STUDIES
- DEVELOP A REFLECTOR REQUIREMENTS DOCUMENT (RRD)
- ESTABLISH A DETAILED CONCEPTUAL DESIGN AROUND REQUIREMENTS OF THE RRD
- PERFORM ANALYSIS TO PREDICT ANTENNA PERFORMANCE
- ESTABLISH A "SCALING" PHILOSOPHY AND TECHNIQUES TO PREDICT PERFORMANCE OF ANTENNAS OVER THE RANGE OF 15-M TO 100-M DIAMETER
- ESTABLISH A MANUFACTURING PLAN CONSISTENT WITH THE REQUIREMENTS OF THE DESIGN
- DEVELOP A TEST PHILOSOPHY AND APPROACHES REQUIRED TO VERIFY PERFORMANCE

TASK 1 FLOW

The plan for meeting the objectives of this task is shown in the figure below. Present activities are centered around identification of the technology drivers necessary to define the point design.

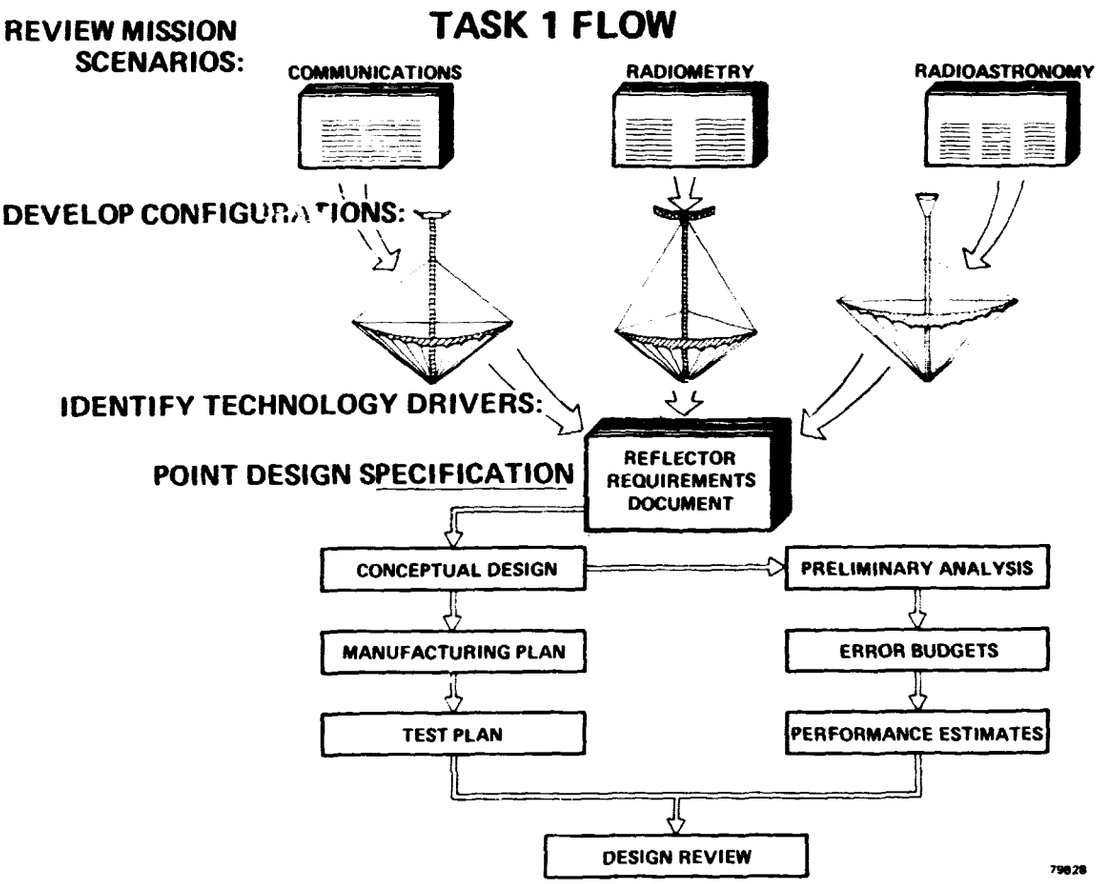

LSST MISSION SCENARIO SUMMARY

Mission scenario data was provided by the NASA Langley Research Center in the form of a report given by ref. 1. Therein was described mission data for advanced communications and public service satellite, soil moisture radiometry, and radio astronomy. An exercise of evaluating various system configuration alternates based on the individual missions was implemented with the intent of choosing the most optimum design approaches. The only scenario which was not clearly defined was the public service satellite mission. It seemed most reasonable during preliminary evaluations to postulate maximum mission requirements to conform to that of advanced communications. If this is done, and as this mission becomes more clearly defined with indications that the requirements are not as complex as previously assumed, the proposed system can be reduced in complexity.

LSST MISSION SCENARIO SUMMARY

MISSION / PARAMETER	COMMUNICATIONS				MICROWAVE RADIOMETER SYSTEM	RADIO ASTRONOMY (VLBI)
	ADVANCED		PSS			
FREQUENCY (GHz)	4-6	11-14	0.87	2.0	1.4	1.4-22
POINTING ACCURACY (DEGREES)	0.035	0.035	0.035	0.035	0.1	0.01
BEAM NUMBER	219	219	TBD	219	200-300	1
BEAM ANGLE (DEGREES)	0.256	0.256	TBD	0.256	0.06	FREQUENCY DEPENDENT
BEAM ISOLATION (dB)	-30	-30	-30	-30	N/A	N/A
ORBIT ALTITUDE	GEO	GEO	GEO	GEO	LEO	LEO
RESOLUTION (km)	N/A	N/A	N/A	N/A	1	10^{-5}/SEC* / 10^{-3}/SEC**
REVISIT COVERAGE (DAYS)	N/A	N/A	N/A	N/A	3	N/A
SWATH ANGLE (DEGREES)	N/A	N/A	N/A	N/A	$\pm$30	N/A
LIFE TIME (YEARS)	>20	>20	>20	>20	>20	>20

*TARGET
**GOAL

FACTORS INFLUENCING CONFIGURATION CHOICE

(ADVANCED COMMUNICATIONS)

The Advanced Communication mission scenario calls for a multiple beam antenna capable of producing 219-100 mile highly isolated spot beams covering the Continental United States. Selection of appropriate designs fulfilling this coverage requirement places great stress on configuration dependent parameters. These parameters greatly influence the ability of the proposed system to meet the coverage requirement while at the same time meeting the isolation and efficiencies required. Trade studies must be performed to define acceptable bounds on reflector size, F/D, feed array configuration geometries and array sizes, each of which influence multibeam performance, blockage and intrabeam isolation. Depending on whether a large symmetrical reflector or an offset reflector system is used, the feed system may either be extremely complex or simple. This will influence internal system losses and overall system efficiency.

FACTORS INFLUENCING CONFIGURATION CHOICES

(ADVANCED COMMUNICATIONS)

- MULTIPLE BEAM PERFORMANCE
  - REFLECTOR F/D
  - REFLECTOR SIZE/MULTIPLE REFLECTORS
  - AVAILABLE FEED ARRAY REAL ESTATE
  - FEED ARRAY ELEMENTS
- BEAM-TO-BEAM ISOLATION
  - REFLECTOR F/D
  - BLOCKAGE
  - FEED ARRAY ELEMENTS
  - BEAM USAGE SCHEMES
- INTERNAL SYSTEMS LOSSES
  - FEED ARRAY CONFIGURATION CHOICES
  - BEAM ISOLATION SCHEMES

RESOLUTION OF RF DESIGN CONCERNS

(ADVANCED COMMUNICATION)

Use of the total aperture of the symmetrical reflector system is desirable since this appears to be the most efficient use of the total system. Trade studies have been conducted which indicate that to use the entire reflector implies that an extremely large feed array must be employed where each feed element is small. The reflector system is over illuminated with a lare percentage of blockage, resulting in high sidelobes. Additionally, the secondary beams are too narrow for this application. This requires that the beams be combined in such a way that the overall combining process produces a flat topped beam with high sidelobes. The isolation will be acheived by utilizing frequency and polarization diversity tc provide guard bands which will contain the sidelobes.

Alternatively, an offset system may be designed which produces the appropriate secondary pattern size. The blockage will not be present but the feed array real-estate availability will dictate that several offset reflectors will be required. Use of this type of system buys the added advantage of low coma distortion and low scan loss as indicated by ref. 2.

RESOLUTION OF RF DESIGN CONCERNS
(ADVANCED COMMUNICATIONS)

- THE OBVIOUS INHERENT RF DESIGN CONCERN FOR A LARGE SYMMETRICAL REFLECTOR CAN BE RESOLVED BY DEVISING A BEAM PLAN WHICH ISOLATES SIDE LOBES BY UTILIZING GUARD BANDS GENERATED BY PROPER USE OF POLARIZATION AND FREQUENCY DIVERSITY
- RF BLOCKAGE AND LOW F/D PROBLEMS CAN ALSO BE OVERCOME BY USING MULTIPLE OFFSET REFLECTORS
  - AS F/D INCREASES THE ASSOCIATED COMA DISTORTIONS DECREASE, BUT SO DOES THE AVAILABLE FEED ARRAY REAL ESTATE; HENCE A MULTIPLE REFLECTOR SYSTEM MUST BE EMPLOYED USING BEAM INTERLEAVING
  - BEAM ISOLATION IN THESE DESIGNS OBTAINED BY USING FREQUENCY DIVERSITY AND ORTHOGONAL POLARIZATIONS

ANTENNA CONFIGURATION CANDIDATES

(ADVANCED COMMUNICATIONS)

The Maypole Hoop/Column concept lends itself quite well to two configurations—a symmetrical reflector system and a quad offset design. The basic configuration in either case is what appears to be a symmetrical reflector system with F/D of approximately one. Referring to the discussion on the previous page, the symmetrical system is very complex where each individual 0.25^{o} beam is comprised of nine narrower beams. Total array size is 1317 feeds. The offset design is achieved by generating a surface in each quadrant of the symmetrical Hoop/Column which represents an offset reflector system having a boresight axis parallel to the Column axis. Since the available area for feed elements has been increased by four, the number of feeds per reflector is 55 full sized scalar feeds. The total structural size is the same for the offset geometry as it is for the symmetrical system; hence, the offset F/D is effectively doubled to two.

ANTENNA CONFIGURATION CANDIDATES
(ADVANCED COMMUNICATIONS)

- SINGLE SYMMETRICAL FOCAL POINT FED PARABOLOID
  - F/D ≈ 1
  - 219 BEAMS (BEAM WIDTH = 0.25^{o})
    - o EACH SPOT BEAM COMPOSITE OF NINE SUMMED BEAMS
    - o BEAM ISOLATION ACHIEVED BY USING POLARIZATION AND FREQUENCY DIVERSITY
    - o SINGLE FEED ARRAY – 1317 FEEDS
- CUSPED QUAD APERTURE DESIGN
  - SINGLE REFLECTOR WITH QUADRANT SUBDIVISIONS
    - o EACH QUADRANT CONTAINS SINGLE OFFSET SYSTEM
    - o 55 BEAMS (FEEDS)/OFFSET REFLECTOR SPACIALLY INTERLEAVED TO PRODUCE 219 EQUALLY SPACED SPOT BEAMS
  - F/D ≈ 2 FOR OFFSET SYSTEM

SINGLE SYMMETRICAL REFLECTOR

As has been discussed, the array feed geometry for the symmetrical reflector is very imposing and causes the symmetrical system to have several serious R.F. problems. The aperture blockage problem causes the overall gain loss to be appreciable. This can be partially compensated for by adjusting the aperture size slightly. A total buy back cannot be achieved in this way, however. The system sidelobe level is also increased, but this may be compensated for by generating guard bands by properly utilizing the band channelization. The system network loss will be higher than normal due to the requirement of using multiple diplexers, many power dividers and yards of waveguide.

SINGLE SYMMETRICAL REFLECTOR

(ADVANCED COMMUNICATIONS)

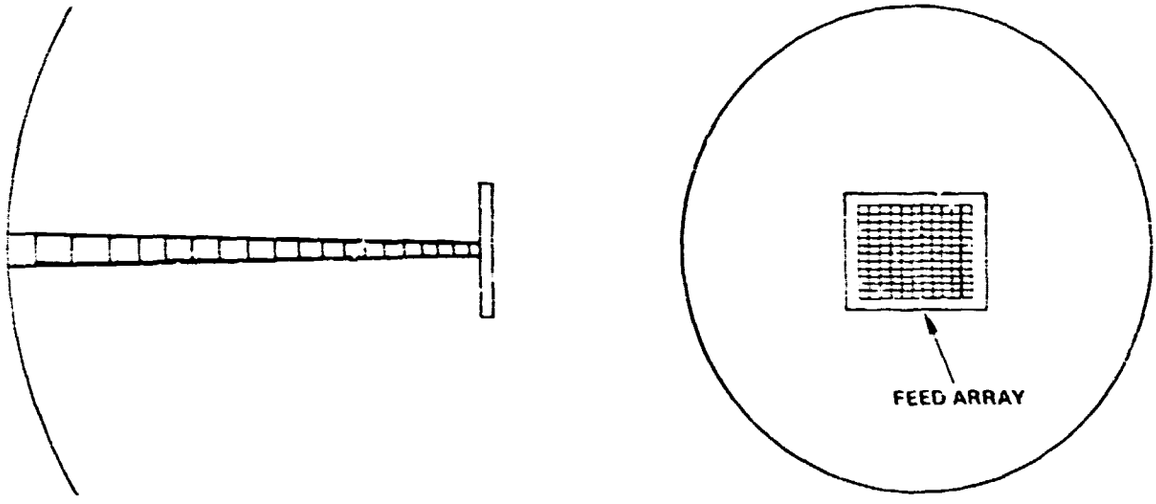

QUAD APERTURE/FEED CHARACTERISTICS

The Quad Aperture system employing the Maypole Hoop/Column concept requires four individual surfaces whose boresights are parallel to the Column axis. The focal point of each offset is totally offset so that the aperture is unblocked. The feed arrays for each reflector are attached to the central columns via a five axis gimballing system. This gimbal is required on each feed array to do an orbit adjustment of reflector illumination in the situation where small amounts of compensation are required due to deployment misalignment. This function is performed by two axes of the five axis system by rotating the array in two planes. The beam interleaving is adjusted by translating the feed array in two dimensions. This effectively scans the beam bundle in space and fixes the beam crossover levels. Beam focusing adjustments are performed by a single dimensional translation along the offset boresight.

QUAD APERTURE/FEED CHARACTERISTICS
(ADVANCED COMMUNICATIONS)

- INDIVIDUAL CUSPED APERTURE CONFIGURED IN OFFSET GEOMETRY
- OFFSET REFLECTOR SURFACE COMPRISED EITHER OF MULTIPLE MESHES OR SCALLOPED OFFSET OUTLINE
  - MULTIPLE MESHES
    - OFFSET REFLECTOR MESH HIGHLY REFLECTIVE AT 4-6 GHz BAND
    - SURROUNDING MESH LOW DENSITY OR COMPRISED OF FREQUENCY SENSITIVE SURFACE (FSS) ELEMENT
  - SCALLOPING TO OUTLINE OFFSET REFLECTOR SURFACE
- FEED SYSTEM FOR EACH QUAD SECTION ADJUSTED BY FIVE AXIS GIMBAL
  - REFLECTOR EDGE ILLUMINATION ADJUSTMENT
  - BEAM INTERLEAVING POSITION ADJUSTMENT
- FEED GEOMETRY IS AREA COVERAGE DEPENDENT

QUAD APERTURE APPROACH

(ADVANCED COMMUNICATION)

The mesh region shown in each quadrant must be comprised of multiple meshes, or the offset reflector outline must be defined by a scalloped exterior. If the wedged shaped region in each quadrant was developed from a single mesh, the feed energy would not be efficiently used. The circular regions shown in the figure represent the -15 dB feed pattern main beam levels. Past this circular area several high level sidelobes exist. The first sidelobe is -17 dB compared to the main beam, and the second and third sidelobes are relatively high as well. If these sidelobes fall on the reflector surface, they will cause substantial gain loss. The region per quadrant beyond the circular area must be either open mesh or frequency sensitive surface elements tuned to a sufficiently displaced out-of-band frequency so that sidelobe energy is leaked through that region of the reflector.

QUAD APERTURE APPROACH

(ADVANCED COMMUNICATIONS)

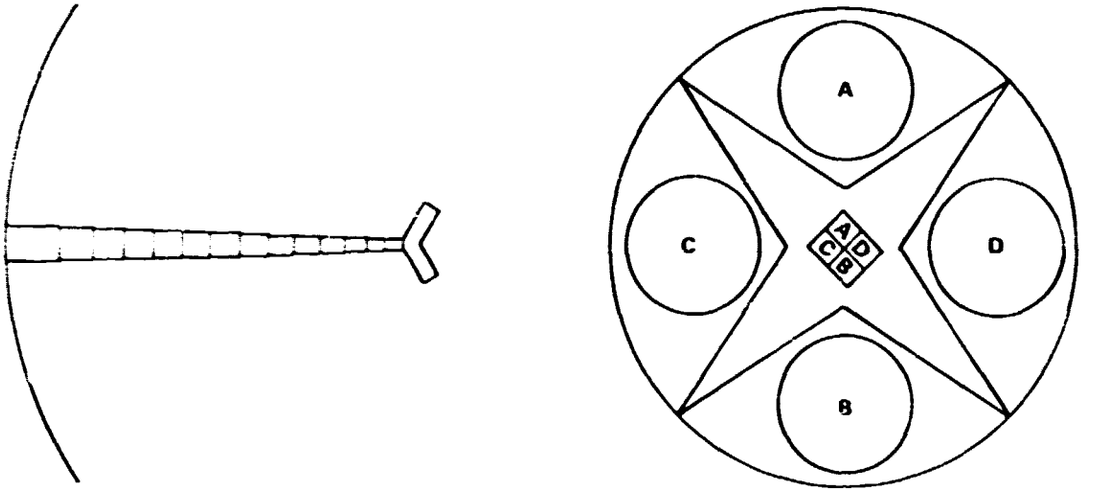

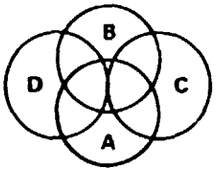

SPACIALLY INTERLEAVED BEAMS

SYMMETRICAL/QUAD APERTURE TRADES

(ADVANCED COMMUNICATIONS)

Comparisons of the symmetrical reflector to the offset system have been made on a qualitative basis without applying exacting scrutiny to system related performance parameters. However, enough investigative rigor has been applied to feel that selection of one of these approaches can be clearly made. The symmetrical reflector system appears to fail on several important counts. Network losses make this system less efficient than is desirable for a communications mission. Other inefficiencies relating to gain loss due to blockage and loss in beam efficiency due to high sidelobe level make this approach unattractive. Conversely, the quad aperture design wins on all counts and is clearly the most appropriate use of the Maypole Hoop/Column geometry for advanced communications.

SYMMETRICAL/QUAD APERTURE TRADES
(ADVANCED COMMUNICATIONS)

PERFORMANCE PARAMETER	EVALUATION SUMMARY	
	SYMMETRICAL	QUAD APERTURE
LOSSES		
• SCANNING	MEDIUM	LOW
• COMBINING	-9 dB	LOW
• NETWORK	LOSSY	NEGLIGIBLE
COMA DISTORTION	MODERATE	NEGLIGIBLE
CROSS POLARIZATION	NONE	NEGLIGIBLE
ISOLATION	GOOD	EXCELLENT
BLOCKAGE	LARGE	NONE
FEED SYSTEM COMPLEXITY	EXTREME	MODERATE
GAIN VARIATION (BEAM-TO-BEAM)	NEGLIGIBLE	-3 dB
OVERALL GAIN (COMPARATIVE)	-9.5 dB + NETWORK LOSSES	-9 dB + NETWORK LOSSES

ALTERNATIVE METHOD FOR USING CUSPED QUAD APERTURE

DESIGN FOR 4-6 GHz AND 11-14 GHz

(ADVANCED COMMUNICATIONS)

As defined by the mission scenario information, the advanced communication system should employ both C-band and Ku-band capability. However, such a dual band system would require individual antennas per band unless a scheme for using a single Maypole antenna could be devised. This is, in fact, the intent. Before this method is discussed, some of the physics of aperture antennas should be addressed. Recalling that the system requirement is for 219-100 mile spot beams, the angular half-power beam width is approximately 0.25 degrees. The reflector size required for this beamwidth can be determined by a commonly known formula relating reflector size in wavelengths to half power beamwidth. The relationship is linear so that since the C-band wavelength is 2.5 times longer than the Ku-band wavelength the apertures must be 2.5 times different in size to produce the same beamwidth.

ALTERNATE METHOD FOR USING CUSPED QUAD APERTURE DESIGN FOR 4-6 GHz AND 11-14 GHz
(ADVANCED COMMUNICATIONS)

- INDIVIDUAL OFFSET REFLECTOR EMPLOYS TWO MESH ARRANGEMENTS
  - CENTRAL MESH ASSEMBLY HAS GOOD REFLECTION CHARACTERISTICS IN BOTH BANDS; HOWEVER, PROJECTED CIRCULAR APERTURE DIAMETER DESIGNED TO GIVE 0.25^{o} HPBW AT 12.5 GHz
  - FSS_1 DESIGNED TO PASS 11-14 GHz ENERGY WHILE REFLECTING 4-6 GHz ENERGY; DIAMETER OF FSS_1 PROJECTED APERTURE DESIGNED TO GIVE 0.25^{o} HPBW AT 5 GHz
  - FSS_2 TRANSPARENT TO BOTH 4-6 GHz AND 11-14 GHz ENERGY
- 11-14 GHz FEEDS LOCATED IN VERTEX REGION OF HOOP/COLUMN SYSTEM; SPLASH PLATE FSS SUBREFLECTOR USED TO ILLUMINATE OFFSET REFLECTOR
- 4-6 GHz FEEDS LOCATED AT FOCAL POINT OF OFFSET SYSTEM

4-6 GHz/11-14 GHz SYSTEM

(ADVANCED COMMUNICATIONS)

The mesh system that is used for the two bands of operation can be designed to be frequency sensitive so that portions of the mesh are reflective only at the appropriate design frequencies. As shown in the figure the central region of the C/Ku reflector is highly reflective to both bands while being the correct diameter to produce a 0.25 degree pencil beam at Ku-band. The mesh immediately attached to the central area is composed of frequency sensitive surface (FSS_1) elements which are resonant (reflective) at C-band only and transparent to Ku-band energy. The immediate surface (supporting surface) surrounding FSS_1 (FSS_2) is transparent to both C/Ku band energy. The FSS_1 surface and central region correspond to a circular aperture size required to produce a 0.25 degree spot beam in C-band. Since the C/Ku-band feeds cannot occupy the same area, the Ku-band feeds must be placed along the central column out of the focal region of the offset, hence, the requirement for the FSS splash plate.

4-6 GHz/11-14 GHz SYSTEM
(ADVANCED COMMUNICATIONS)

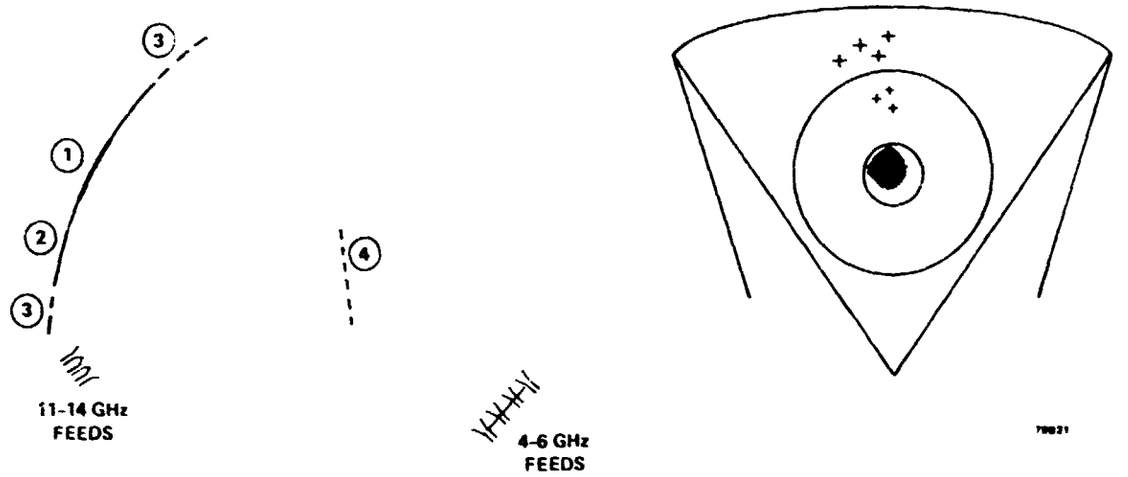

(1) CENTRAL MESH ASSEMBLY
(2) FSS_1
(3) FSS_2
(4) FSS SENSITIVE TO 11-14 GHz ENERGY

PUBLIC SERVICE SATELLITE MISSION

As discussed previously, public service satellite mission scenario data was not as definitive as was advanced communications data. Since advanced communications appeared to be a most difficult mission to accomplish systems wise, it was felt that the same systems description should be applied to the bands of application. Hence, a simple scaling operation was performed on the offset reflectors. The feed array geometry does not change since the required real estate is determined by the area coverage requirement. Therefore, the dimensions shown were chosen on that basis. The 870 MHz system is a very formidable structure; however, it is felt to be an achievable size.

PUBLIC SERVICE SATELLITE MISSION

- EMPLOY SAME CONFIGURATION AS ADVANCED COMMUNICATION DESIGN
- FREQUENCIES OF INTEREST: 0.87 AND 2.0 GHz
- DIRECTLY SCALE ADVANCED COMMUNICATIONS DESIGN
  - 0.87 GHz : 200 METERS
  - 2.0 GHz : 97 METERS

LSST MICROWAVE RADIOMETER MISSION

The soil moisture radiometer/advanced crop forecasting study data has shown an extremely large structure (upwards to a 660 meter reflector). Since it is felt that this requires a far term technology commitment, a reduced size radiometer addressing the same mission must be investigated to define a more practical approach for a near term LSST focus mission. Several reduced size concepts were investigated including a low earth orbit confiquration requiring reboost. The reboost geometry is interesting, but the propellant required to occasionally reboost is excessive. The non reboost geometry still involves large structural components, which places this LSST mission in the far term application category.

LSST MICROWAVE RADIOMETER MISSION

- FURTHER SYSTEM DEFINITION REQUIRED BY ADDITIONAL TRADE STUDIES
- POTENTIAL MISSION REDUCTION TRADE-OFF ANALYSES ONGOING
- CURRENT CONCEPTUAL CONFIGURATIONS TEND TO PLACE THIS MISSION IN THE LSST FAR TERM APPLICATIONS CATEGORY
  - REDUCED SIZE RADIOMETER EXTREMELY DIFFICULT
    - CENTRAL COLUMN LENGTH 400 METERS
    - FEED ARRAY LENGTH 100 METERS
  - REBOOST CONFIGURATION INVOLVES EXCESSIVE PROPELLANT

PROPOSED RADIO ASTRONOMY (VLBI)

The orbiting very long baseline interferometer reflector system requirements were investigated and a Cassegrain antenna system was suggested. The specifics of the reflector and subreflector shaping were not addressed, but gross parameters of the system were defined. It is felt that very specific aspects of the systems' design can be defined at a later point since major antenna performance dependence is defined by the seperation distances of the antennas on the baseline. Other antenna characteristics which should be considered early in the program are receiver front ends, feeds and the associated cryogenics. An important systems aspect which should not be overlooked is the beam squint compensation problem which can be solved by employing a pointable subreflector. Actual implementation of this compensating means has not been defined; however, illustrations of proposed mechanisms shall be shown later.

PROPOSED RADIO ASTRONOMY (VLBI)

- INITIAL STUDIES INDICATE THAT A 30-METER CASSEGRAIN SYSTEM WILL SERVE VLBI NEEDS
  - F/D = 0.7
  - ~3-METER SUBREFLECTOR
- FREQUENCY BANDS OF INTEREST: 1.4, 2.3, 5.0, 7.9, 11, 15, 22 GHz
- SINGLE BEAM PER FREQUENCY
- FEED ARRAY CONSISTING OF CIRCULAR ARRAY OF SCALAR HORNS
- FEED ARRAY/SUBREFLECTOR SYSTEM COMMONLY SUPPORTED BY CENTRAL MAST IN HOOP/COLUMN CONFIGURATION
- POINTABLE SUBREFLECTOR COMPENSATION FOR SQUINTED BEAMS

LSST ANTENNA REQUIREMENTS BASED ON MISSIONS

To this point in the LSST program the following data has been compiled, outlining clearly defined antenna configurations. Parameters for each antenna including surface accuracy and gain have been included. Work is still being done in the radiometry area and as acceptable mission scenario reductions are done to allow for a more realistic near term design, this will be presented. However, to the date of this publication those mission reductions have not been forthcoming. It is clear that for such large structures, for cost amortization, the system must remain operational for at least a 20 year period. This is felt to be a realistic and achievable goal from a structural lifetime standpoint.

LSST ANTENNA REQUIREMENTS BASED ON MISSIONS

MISSION / PARAMETER	COMMUNICATIONS				RADIO ASTRONOMY (VLBI)
	ADVANCED		PSS		
FREQUENCY (GHz)	4-6	11-14	0.87	2.0	1.4-22
REFLECTOR DIAMETER (METERS)	55	55	200	97	30
F/D	2	2	2	2	0.7
SURFACE ACCURACY	λ/50	λ/50	λ/50	λ/50	λ/30
GAIN (dB)	60.3	60.3	60.3	60.3	52.6-76.0
BEAM NUMBER	219	219	219	219	1/FREQ
BEAM ISOLATION (dB)	-30	-30	-30	-30	N/A
LIFE TIME (YEARS)	>20	>20	>20	>20	>20

MAJOR ELEMENTS - AREAS OF CONCENTRATION

During the period involving the study of the mission scenarios and configuration definition, design activities continued in parallel on non-mission dependent elements. The major elements are listed below.

MAJOR ELEMENTS

AREAS OF CONCENTRATION

- TELESCOPING MAST
- HOOP
- CONTROL SYSTEM

CABLE DRIVEN MAST

One mast design which was pursued is the cable driven mast. This concept is a variation on several state-of-the-art designs presently being utilized as high-lift personnel platforms. The figure below depicts a mast cross section which is typical 3 places around the central axis. The basic design consists of multiple shells nested inside each other. Attached to the flange of each section is a pulley. A cable is fastened to the inner-most section and routed over pulleys on the upper and lower flanges of adjacent sections. The opposite end is routed through a level wind device and terminated on a spool.

Three drive motors are provided for redundancy. Each motor is connected to a level wind drive screw and the main take-up spool by means of gears. As the cable is wound on to the spool, the mast sections are driven outward until latching of each section is accomplished. The reverse cycle (retracting) is accomplished by means of a single cable (not shown) attached to the inner-most section. By pulling this cable, unlatching of the lst section takes place and it is retracted. Each section is unlatched by the motion of adjacent inner sections.

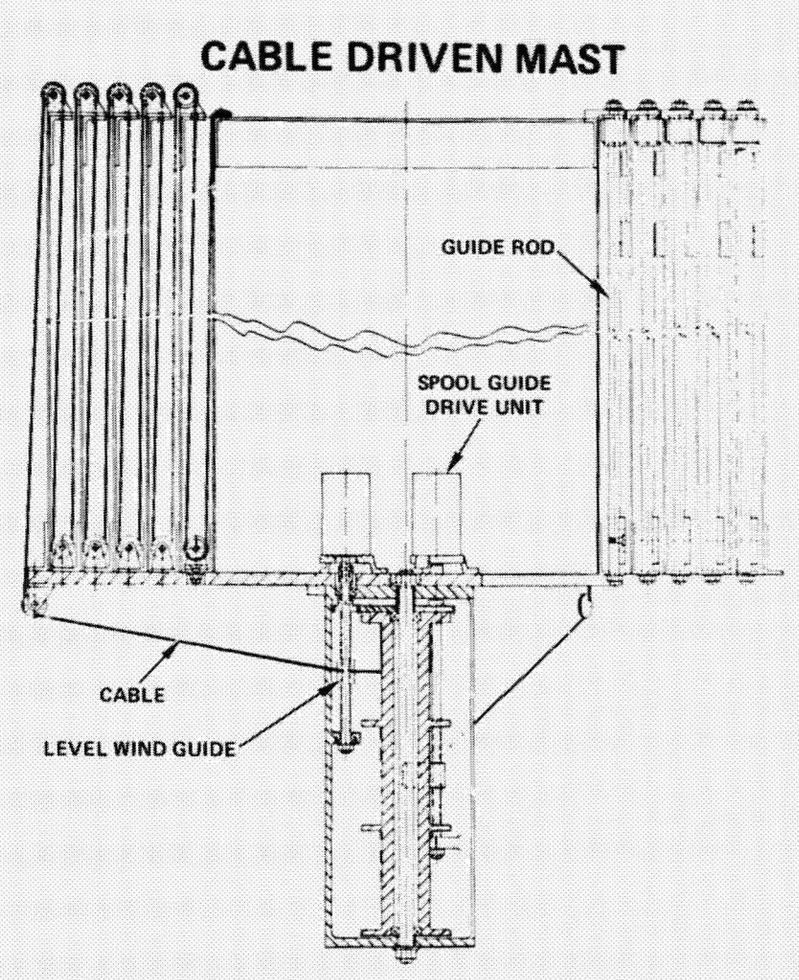

SINGLE SCREW MAST

A second mast configuration under study is the single screw mast concept. Deployment is accomplished by a jack-screw type mechanism. The telescoping shell members are nested inside each other when stowed. The inner-most section has a nut element which is engaged on the threaded portion of the single screw along the central axis. All these sections have floating nuts which are not engaged on the threaded portion of the screw. As the screw is rotated, the inner section translates outward. Three guide rods provide alignment and rotational restraint for each section. When the inner section contacts the upper flange of the adjacent section, it forces that section to translate upward also. This motion causes the floating nut of the second section to engage on the threaded portion of the screw.

The floating nut is required to ensure the thread lead of the screw mates properly and causes no binding or jam nut type action. The cycle continues in the same manner for all subsequent sections.

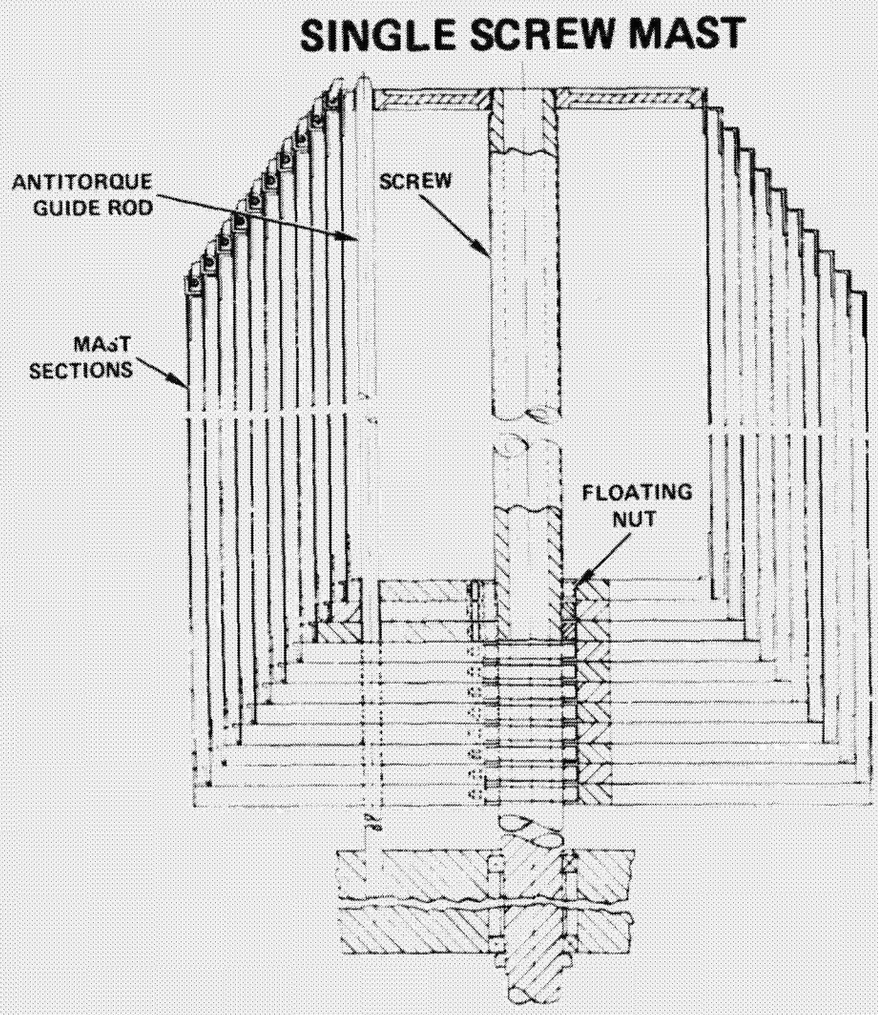

SINGLE REVERSIBLE BALLSCREW MAST

The third mast concept described here is similar to the single screw mast. It differs in the fact that a single nut element is used to drive all sections. As in all the concepts, the mast sections are nested inside each other when stowed. Deployment takes place by rotating the screw which in turn causes the nut to translate. The nut contains a mechanism which unlatches all sections, plus a hook element that captures the base of each section and provides a means to drive the sections outward.

When the first section nears the end of its travel, it latches with the upper flange of the adjacent section. When latching is complete, the drive unit reverses direction causing the nut element to return down the screw until it unlatches the second section and engages its base. The drive unit again reverses direction and drives the second section outward in the same manner as the first section. The sequence is repeated until all sections are deployed.

SINGLE REVERSIBLE BALL SCREW MAST

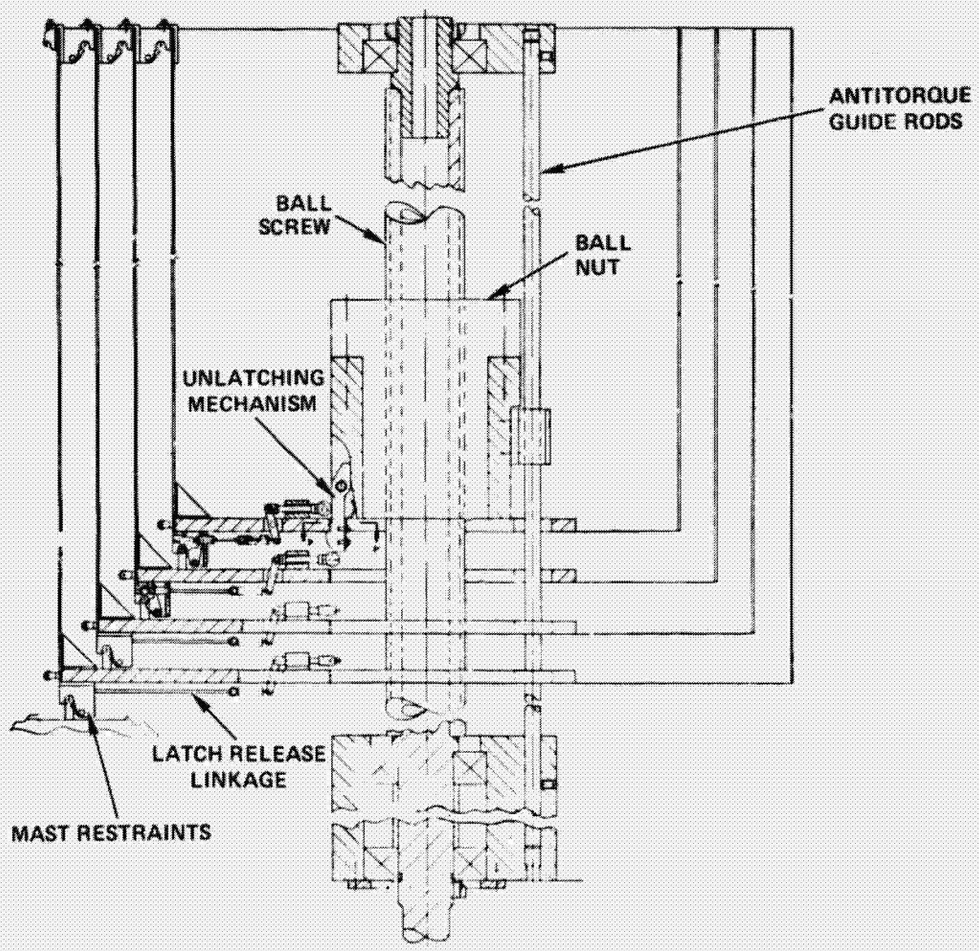

CABLE PULLEY SYNCHRO

The initial work done on hoop development consisted of improving the deployment reliability of the AAFE designed hoop. The approach was taken that if a synchronization method could be incorporated into the design, the overall reliability would be enhanced greatly. The method developed is described below.

The figure below shows a schematic representation of a portion of the hoop at some intermediate deployment position. Consider the hoop members which are shown cross-hatched.

A pulley is attached to the end of each of these members at the outer joints. A cable is routed over each pulley in a figure "8" pattern with the cross-over point on the center of rotation of the inner joint between the two outer joints shown. The cable is also fixed to each pulley so that sliding is not possible. If the hoop member attached to the left most outer joint under consideration is rotated clockwise about the outer joint, it can be seen that the right most hoop member will be driven counterclockwise by the same amount. In other words the angle formed by one outer joint will always equal the angle formed by the next outer joint. The same method is used to synchronize the inner joints.

The basic premise of this method of synchronization is that if all outer joints form equal angles and all inner joints form equal angles, then a regular polygonal shape must be described at any point in the deployment. The regular shape implies synchronization.

CABLE/PULLEY SYNCHRO

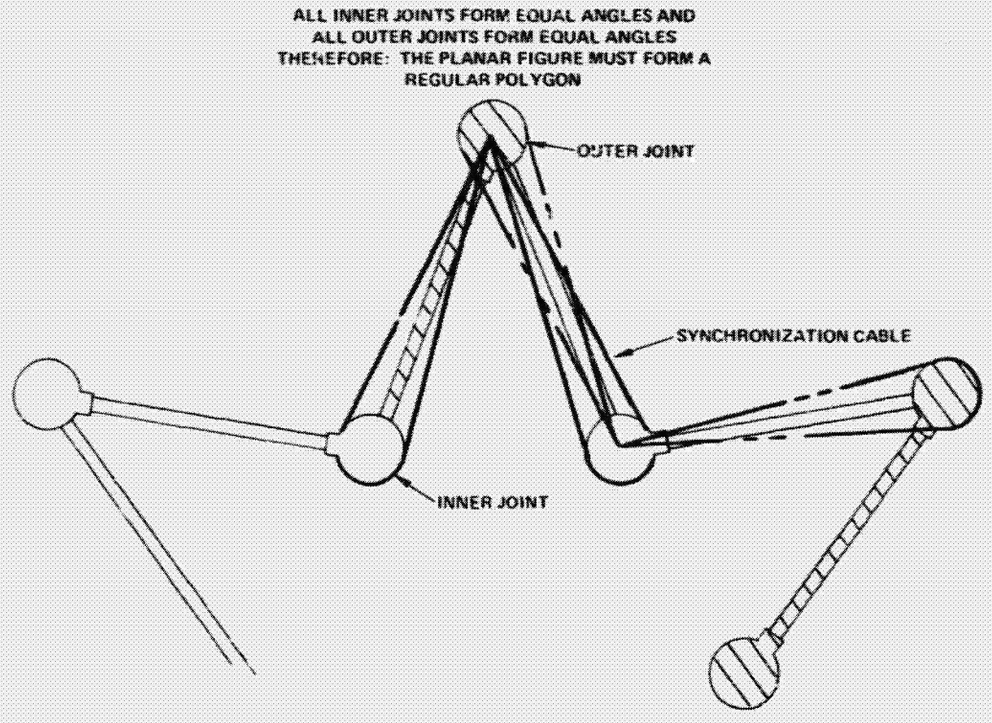

MODIFIED AAFE HOOP

This figure shows a detailed layout of a single hoop joint with the synchronization method just described included.

MODIFIED AAFE HOOP

HINGE JOINT

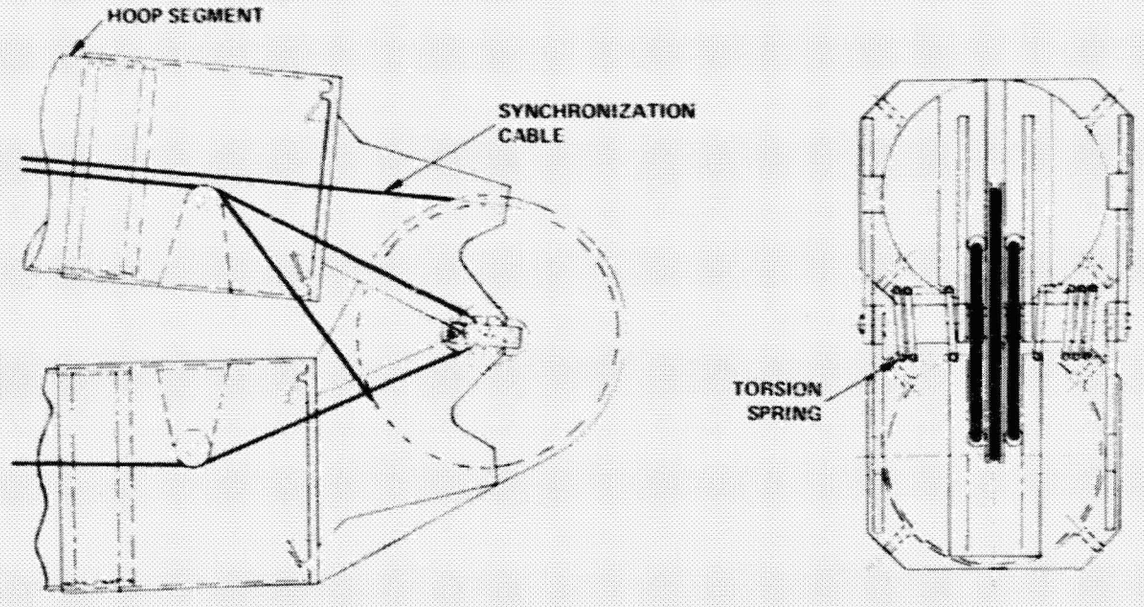

SINGLE STAGE HOOP DEPLOYMENT SEQUENCE

Another hoop concept was developed on this program in an attempt to simplify the deployment and hence control system requirements of the hoop. The deployment sequence of this concept is shown in the figure below. The approach developed utilizes a double hinge at each joint which permits rotation without any torsional wrap-up in the hoop members. The single stage deployment refers to the motion of the hoop throughout its deployment. The joints of the hoop describe a right circular cylinder at all stages of deployment. The individual hoop segments simply rotate from vertical to horizontal about an axis through the center of each member. These axes are radial lines forming a plane normal to the axis of the mast.

Advantages of this hoop deployment method include control system simplification, good mesh handling characteristics, and no toggling action as the hoop completes its deployment.

SINGLE STAGE HOOP DEPLOYMENT SEQUENCE

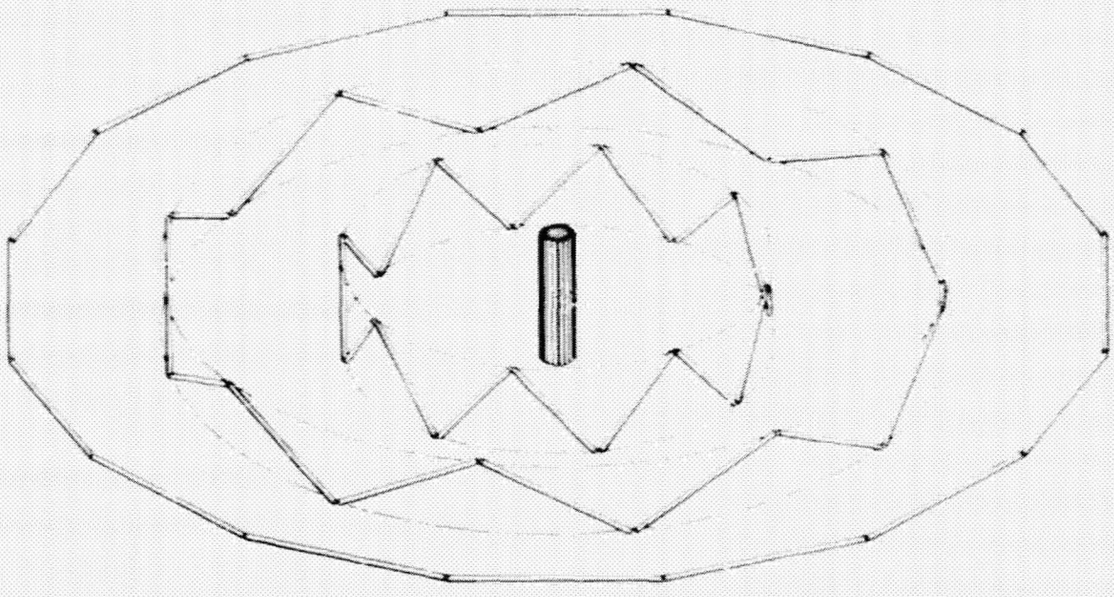

SINGLE STAGE HOOP

This figure shows a schematic of the joint required for the single stage hoop and how one member is coupled to another in different stages of deployment. The hinge platform supports the two hinge points required of this concept. Each hinge axis is along a radial line through the center of the mast and in a plane normal to the mast central axis. Uniform motion is achieved by means of a pushrod connected to offset attach points. Synchronization of this hoop is realized by keeping all hinge platforms parallel during deployment. This occurs by means of strips or cables (not shown) connecting one platform to the next. The system works similarly to a pantograph.

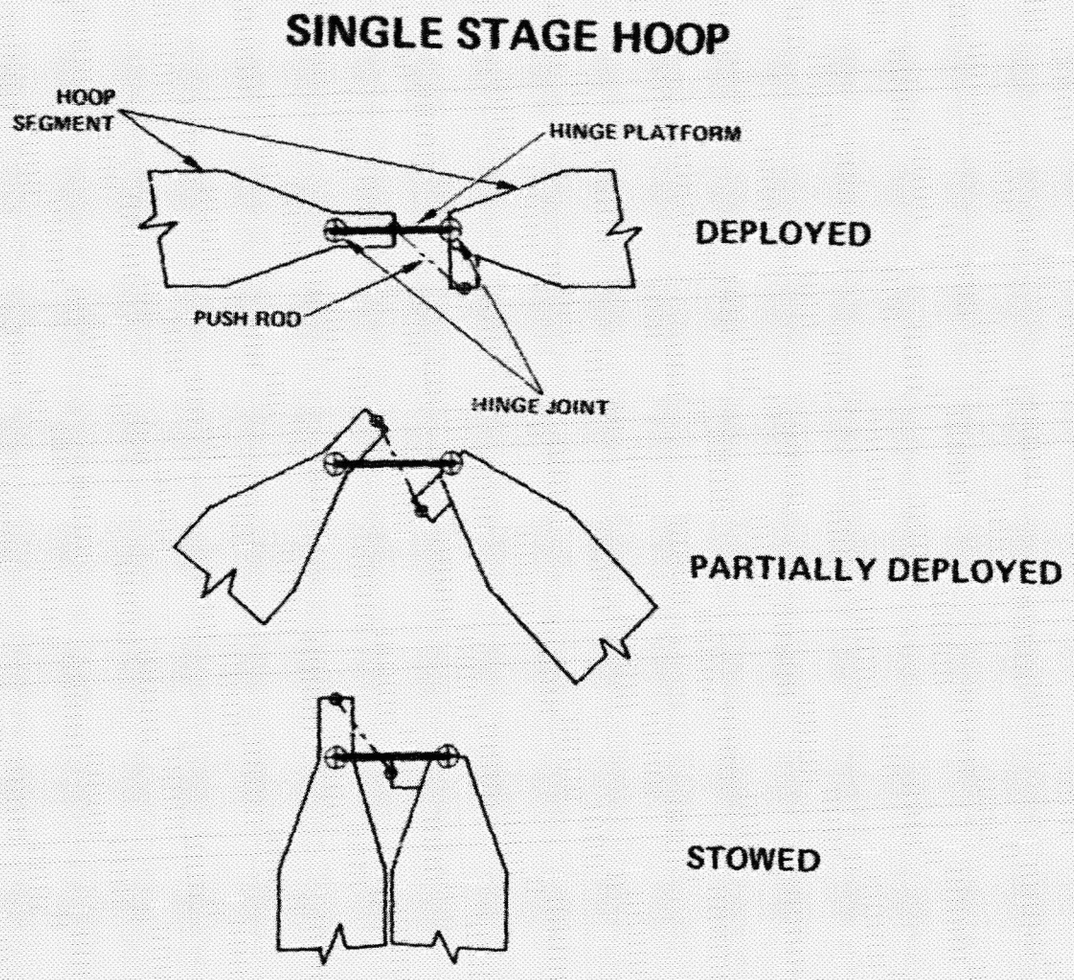

SINGLE STAGE HOOP

PLAN VIEW

This figure and the next figure show detailed layouts of the actual hinge joint. The hinge platform is a truss structure which exhibits high efficiency from a strength and stiffness to weight standpoint. The tubular hoop segments are terminated with bonded fittings which transition from a tubular section to a truss section which mates with the hinge platform.

SINGLE STAGE HOOP – PLAN VIEW

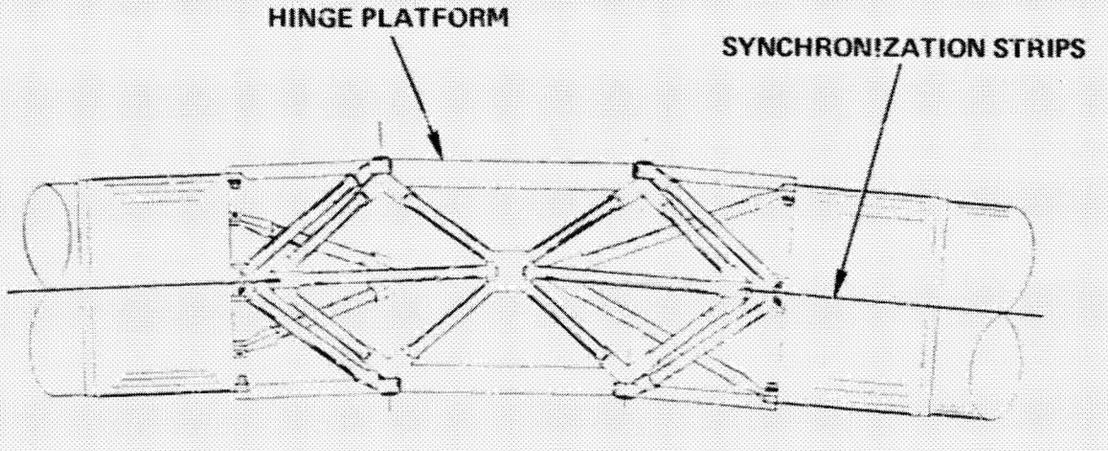

MOTOR NOT SHOWN FOR CLARITY

SINGLE STAGE HOOP

SIDE VIEW

This figure shows the joint previously described from a side view. The pushrod is visible in this view and can be seen connecting the adjacent hoop segments. The synchronization strips can also be seen attaching to the hinge platform. Also described in this figure is a method for driving the hoop. A linear actuator is used to drive one section which in turn drives the adjacent section.

SINGLE STAGE HOOP – SIDE VIEW

DEPLOYED POSITION

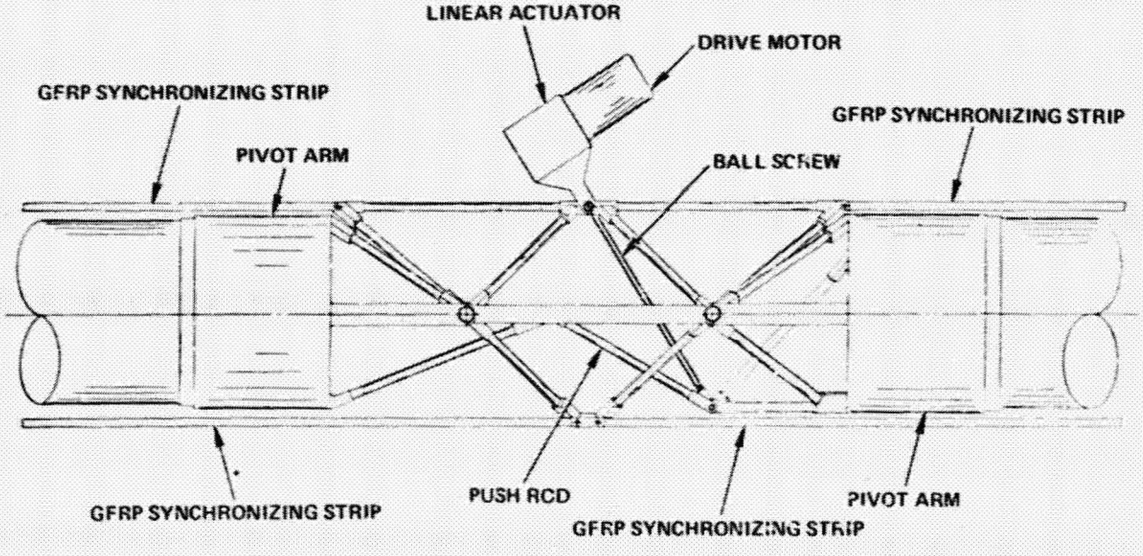

COMMUNICATIONS MISSION

Configuration studies previously described have established the requirements for various Hoop/Column configurations which meet the focus mission applications. The first configuration described is for the communications mission.

The figure shows an isometric representation of the Quad Aperture approach. Four individual regions of the reflector are formed in an offset configuration. A separate offset feed array illuminates each cusp or quadrant of the reflector. The mast shown utilizes a telescoping concept for the primary structural member and an Astromast, manufactured by ASTRO Research Corporation, for the feed support.

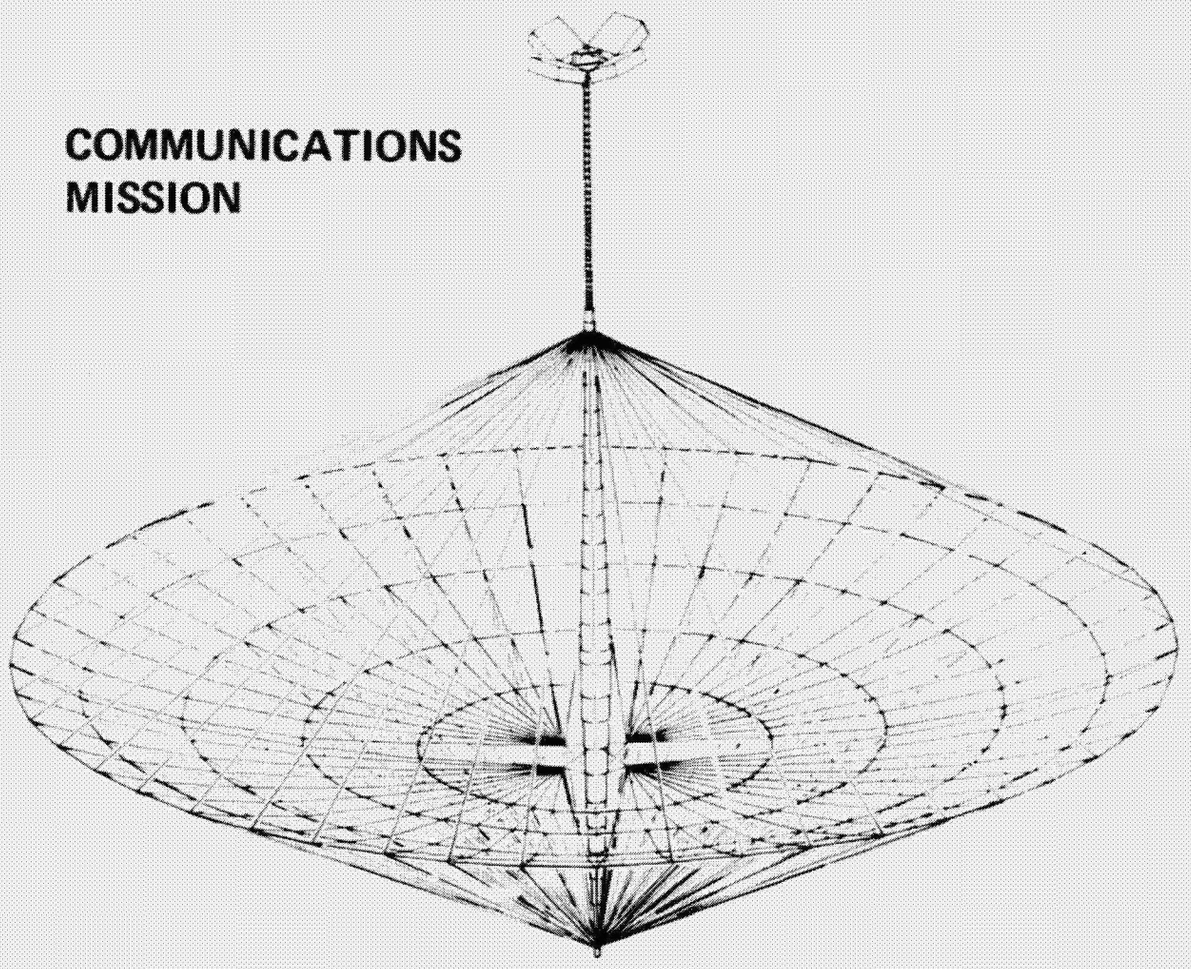

COMMUNICATIONS MISSION DEPLOYED

This figure shows a top view of the deployed antenna. The circular areas represent the individual feed array illumination areas on each quadrant.

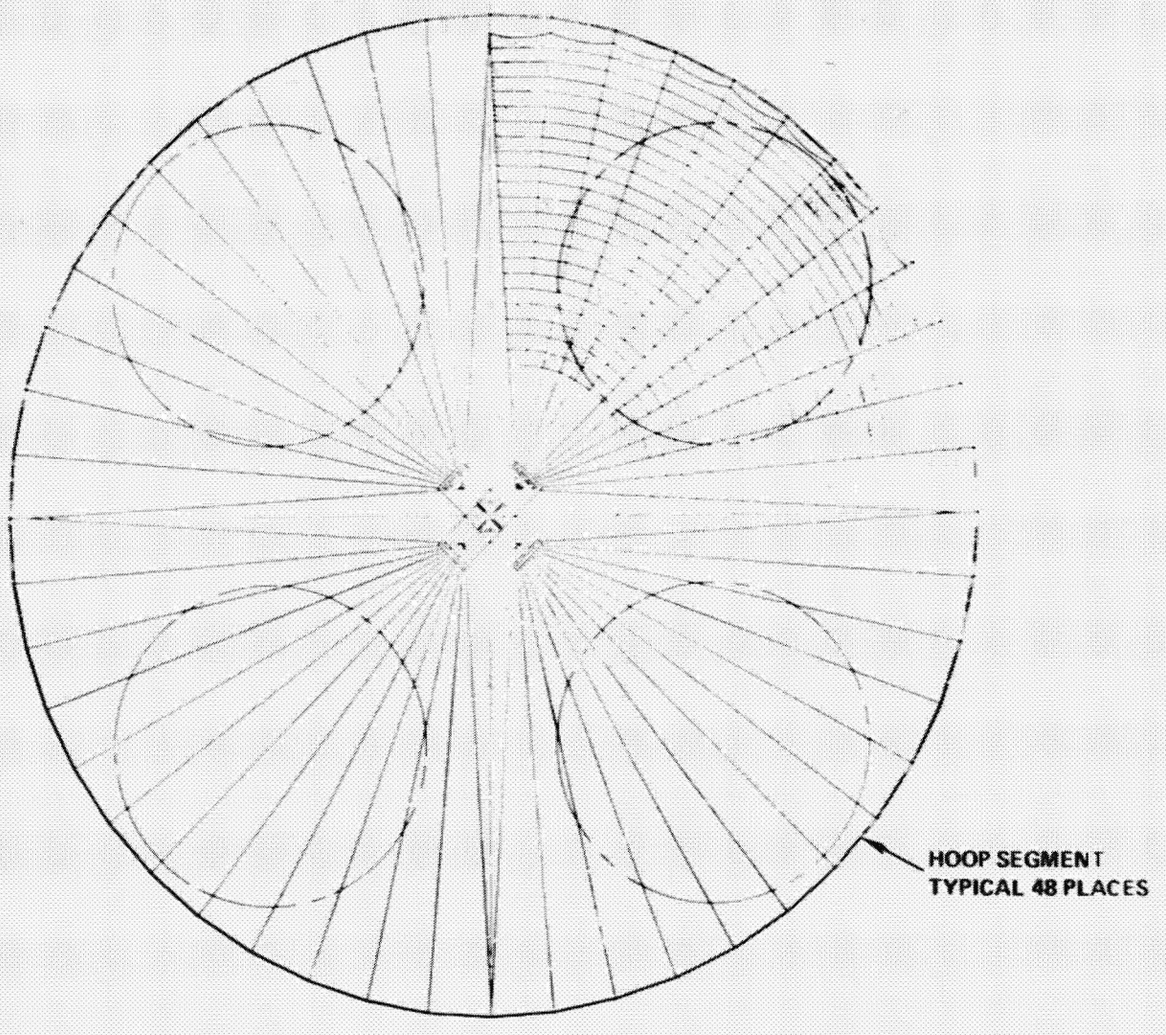

COMMUNICATIONS MISSION STOWED

This figure shows a representation of the basic stowed configuration. The feed arrays are attached to a supporting beam by 5-axis gimbals. These gimbals provide all adjustment capabilities necessary to align all R.F. beams after deployment. The lower end of the configuration shows a mechanism which permits the required offset attach point for the surface control stringers.

COMMUNICATIONS MISSION STOWED CONFIGURATION

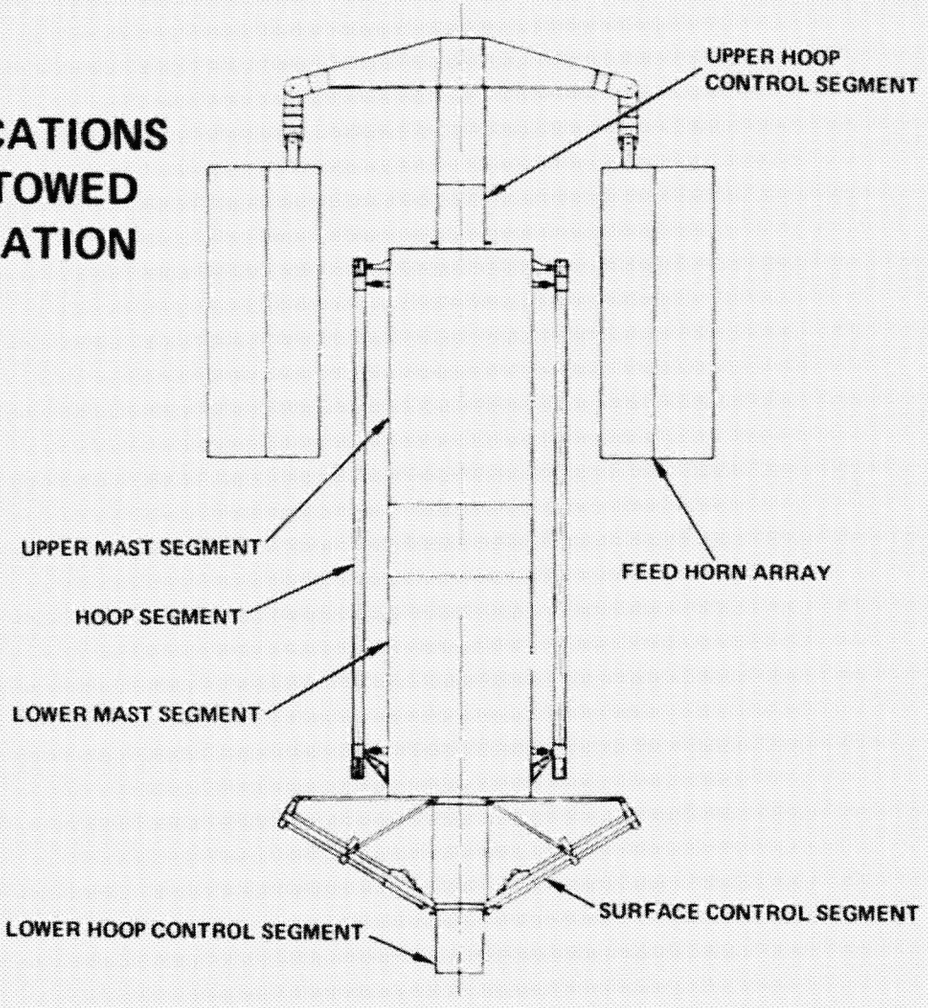

RADIO ASTRONOMY

A second mission for which the Hoop/Column concept was configured is Radio Astronomy. This approach utilizes a symmetrical reflector and a multi-horn Cassegrain system. The subreflector is supported by extendable Astromasts, manufactured by ASTRO Research Corporation, in a tripod arrangement. This permits pointing of the subreflector as well as axial defocusing adjustments. The antenna is sized at 30 meters in diameter.

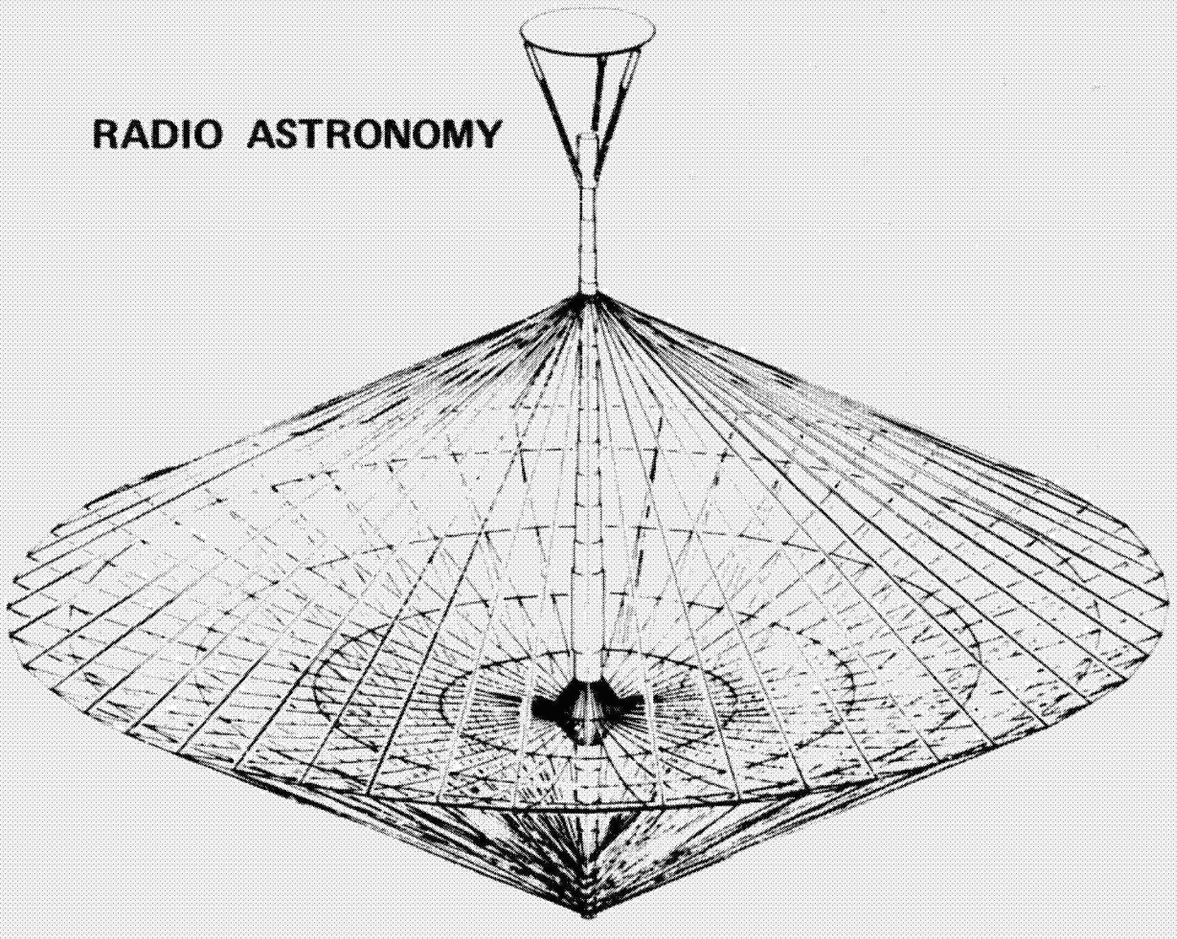

RADIO ASTRONOMY STOWED

The figure below depicts the antenna configuration in the stowed position. The solid subreflector is the driving constraint on stowed diameter. The stowed package is readily accommodated by the shuttle cargo bay.

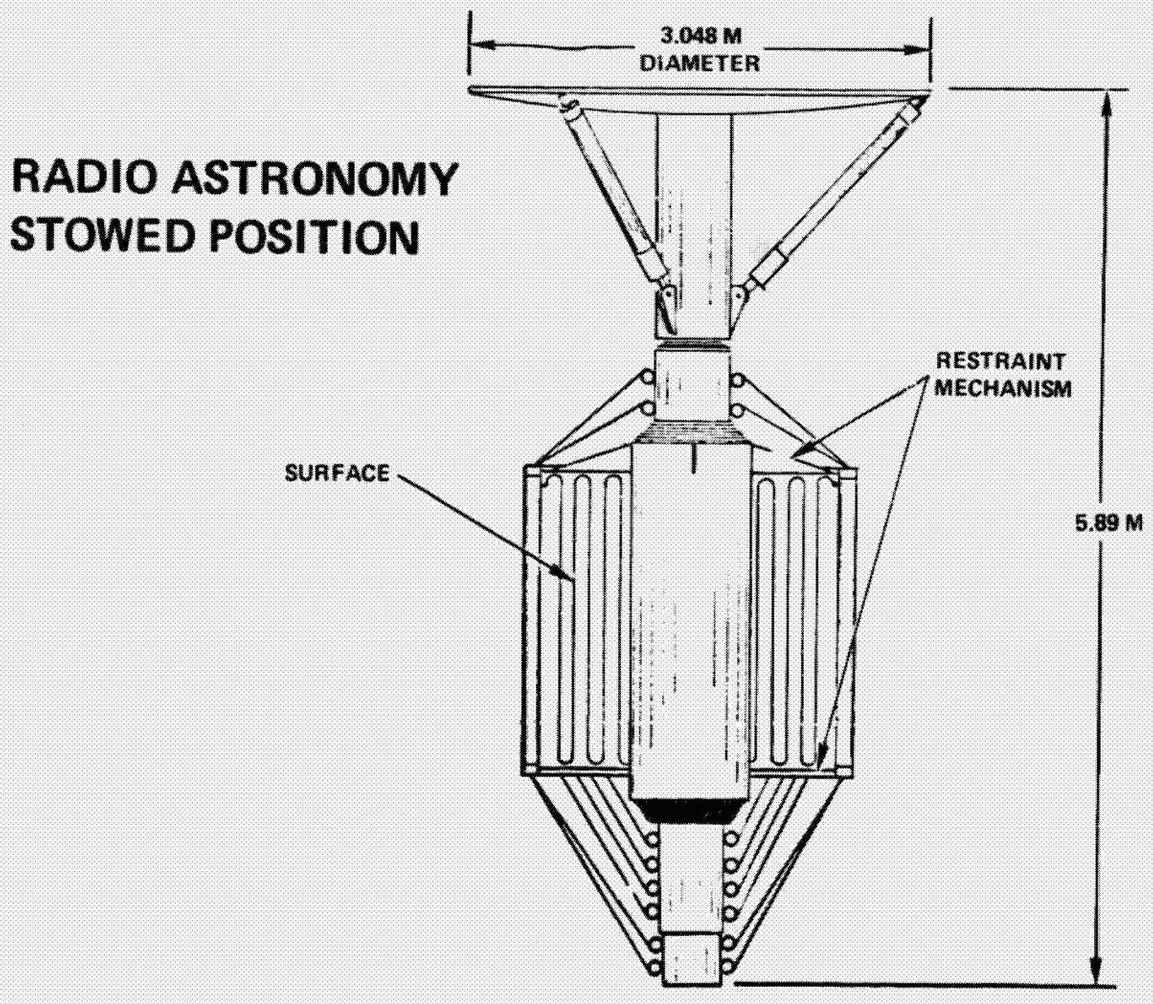

TASK 2 MATERIALS DEVELOPMENT

This task is the only other task initiated to date. The entire task funding is directed toward development of cable technology. The applications of this technology reach well beyond the Hoop/Column antenna to many of the proposed large space structures using cable tensioned structural elements.

TASK 2

MATERIALS DEVELOPMENT – CABLE TECHNOLOGY

TASK 2 OBJECTIVES

This development activity is tailored toward the specific environmental requirements of earth orbits. Detailed requirements must be defined in order to limit the scope of the task toward particular applications. A review of available data is required to provide background information and clues to what approaches appear feasible or worth pursuing.

Basic material candidates will be generated and samples fabricated in various configurations. Material properties data will be developed through a number of tests. Finally, a cable configuration will be selected and its properties used in the analytical models of task 1 which are used for performance projections.

OBJECTIVES

- DEFINE CABLE REQUIREMENTS, STRUCTURAL, THERMAL, ENVIRONMENTAL
- PERFORM DATA RESEARCH
- EVALUATE CANDIDATE MATERIALS AND CONFIGURATIONS
- FABRICATE SAMPLES OF SELECTED CABLE MATERIAL/CONFIGURATION COMBINATIONS
- DETERMINE MATERIAL PROPERTIES OF SELECT CONFIGURATIONS VIA APPROPRIATE TESTS
- PROVIDE DESIGN DATA AS INPUT TO TASK 1 ANALYSIS

FIRST YEAR OBJECTIVES AND STATUS

The joint NASA/HARRIS objectives and milestones for the first year of the program are shown below. The status of the activities underway to meet these objectives are also listed.

FIRST YEAR OBJECTIVES	STATUS
• DEVELOP REFLECTOR REQUIREMENTS DOCUMENT	• MISSION SCENARIOS RECEIVED AND EVALUATED • TECHNOLOGY DRIVERS IDENTIFIED • PRELIMINARY DOCUMENT DEVELOPED • FINAL DOCUMENT COMPLETE, 1980
• PRELIMINARY POINT DESIGN TO MEET LSST REFLECTOR REQUIREMENTS DOCUMENT	• ELEMENT CONCEPT DESIGN TRADE STUDIES IN PROGRESS • CONCEPT DESIGNS DEVELOPED FOR FOCUS MISSIONS • POINT DESIGN SELECTION SCHEDULED THIS MONTH • POINT DESIGN CONCEPT REVIEW IN FEB, 1980
• DESIGN AND PERFORMANCE ANALYSES FOR MAYPOLE HOOP/COLUMN	• TRADE ANALYSES SUPPORTING ELEMENT CONCEPT SELECTION UNDERWAY • PRELIMINARY PERFORMANCE ANALYSES FOR POINT DESIGN SCHEDULED FOR FEB 1980 COMPLETION • EXTRAPOLATED PERFORMANCE FOR VARIOUS SIZE REFLECTORS AND FOCUS MISSIONS SCHEDULED FOR MAY, 1980
• DESIGN AND FABRICATE SCALED FEASIBILITY MODELS FOR FOCUS MISSION APPLICATIONS	• TO BE INITIATED UPON ACTIVATION OF THE DEMONSTRATION MODELS TASK • COMPLETION SCHEDULED FOR FEBRUARY, 1980
• DESIGN SURFACE CONTROL BREADBOARD	• TO BE INITIATED AFTER POINT DESIGN SELECTION • COMPLETION SCHEDULED FOR MAY, 1980

REFERENCES

1. Campbell, T.G.; and DiBattista, J.: Focus Mission Scenarios for Communications, Radiometer and Radio Astronomy—LSST Technology Requirements Definition, NASA Langley Research Center, May 1979.

2. Ruze, J.: Lateral-Feed Displacement in a Paraboloid, IEEE Transactions on Antennas and Propagation, September 1965.

N80-19152

SURFACE ACCURACY MEASUREMENT SENSOR FOR DEPLOYABLE REFLECTOR ANTENNAS (SAMS DRA)

Robert S. Neiswander
TRW
Redondo Beach, California

NAS1-15220

LSST 1ST ANNUAL TECHNICAL REVIEW

November 7-8, 1979

OBJECTIVE

The objective of the Surface Accuracy Measurement Sensor program is to develop an optical measurement technology base from which a wide range of sensor systems for space applications can be derived. Example systems include:

Attitude transfer of isolated remote instruments: A typical instrument is positioned remote to the parent vehicle to minimize contamination of its functioning: it may be restrained at the end of a long flexible mast, or by a tether, or possibly at a short range free flyer.

Measurement of large antenna surface distortion: Distortions in the reflecting surfaces of large space antennas are to be measured in real time, providing 1) a means of assessing the antenna behavior, and 2) the sensor input for active surface control.

Aid in the manufacture and assembly of structures in space: The bending and twist of composite beams during the forming operation can be monitored, and the deformations of the resultant long beams during assembly can be continuously measured.

For the immediate program effort, however, the sensor system application is limited to large antenna surface distortion measurements.

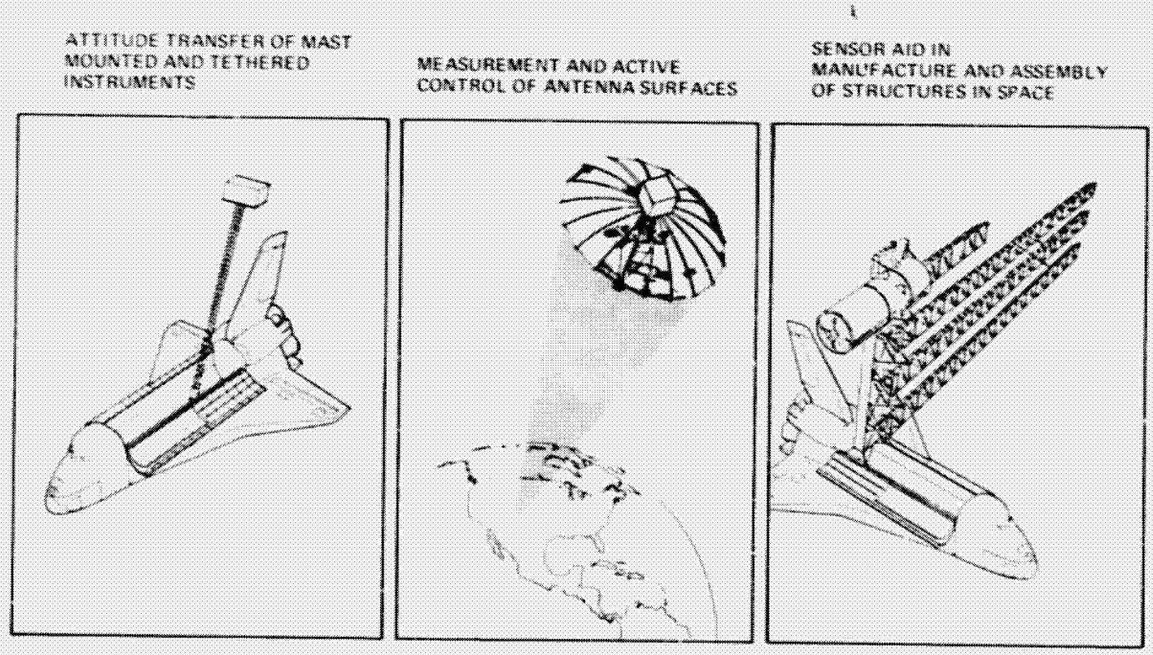

Figure 1

REPRESENTATIVE LARGE SPACE ANTENNAS

Of the candidate antennas for space applications, the nondeployable are limited (to be Shuttle compatible) to something less than 5 meters diameter, and the erectable antennas, although showing promise of hundreds of meters expanse, demand robotics, manipulators and/or extra-vehicular activities unavailable currently or in the near future. The deployable antenna, an antenna that can be stowed aboard the Shuttle in a single package and unfurled independent of Shuttle support, fills the gap, providing the technique for near-future realization of large, advanced space antennas. The current SAMS DRA program, thus, is specifically aimed at sensor systems for deployable antennas.

Representative of the deployable antennas are 1) the Harris Inc. Hoop-and-Column antenna, 2) the TRW Advanced Sunflower precision deployable antenna, 3) the Lockheed Wrap-rib configuration and 4) the General Dynamics Precision Erectable Truss Antenna (PETA). The Hoop-and-Column, the Wrap-rib and the PETA antennas provide mesh reflectors up to about 100 meters diameter. The TRW Advanced Sunflower, a solid surface antenna, may have a diameter perhaps as large as 30 meters.

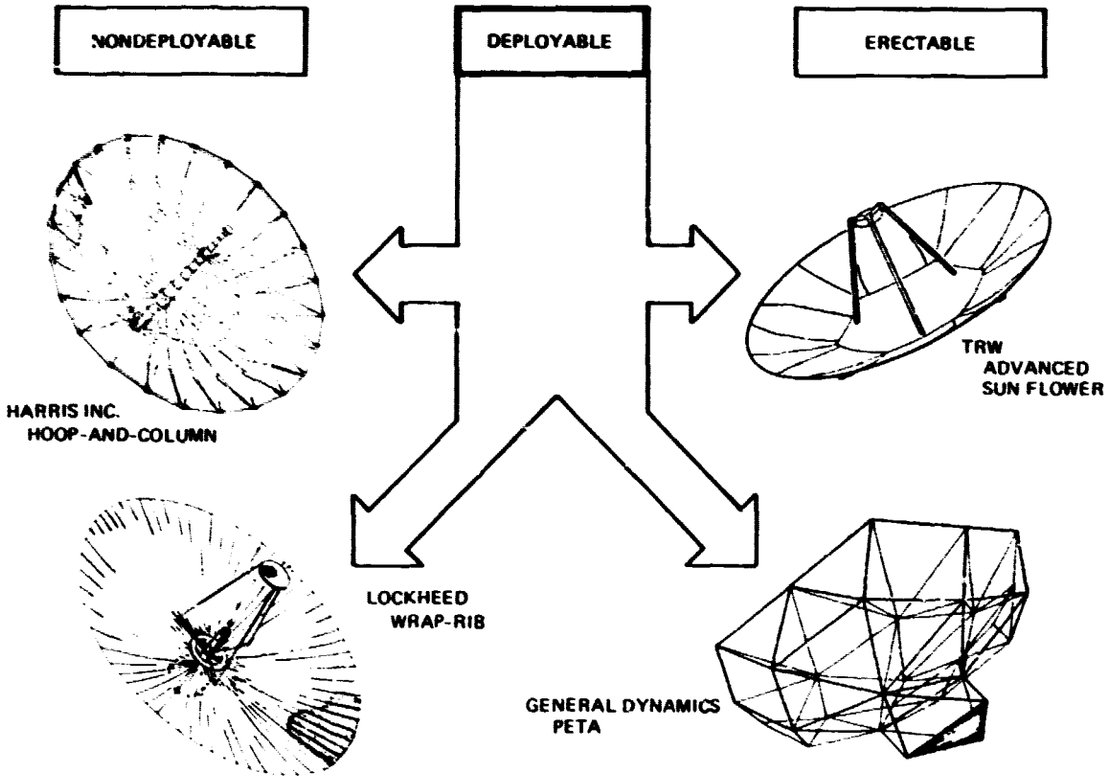

Figure 2

SENSOR SYSTEM REQUIREMENTS

In addition to providing the necessary measurement range and required accuracy, the SAMS DRA must be compatible with the space operation. If it is part of an active surface control system, its measurements must be made in real time, with signal outputs that conveniently interface with on-board microprocessors and that do not demand excessive computer manipulations. The measurement system must have long term stability, and must be unconfused by bright backgrounds such as glints from local structure and the sunlit earth.

Since the sensor likely will be operating with the antenna activated, the sensor elements cannot degrade the microwave properties of the antenna and cannot be affected by microwave interferences from the antenna and drive.

And for maximum assurance of success, the sensor system must rely solely upon established component technologies.

- REAL-TIME MEASUREMENT OUTPUTS
- IMMUNITY TO BACKGROUND (SUNLIGHT GLINTS, EARTHSHINE, ETC.)
- MEASUREMENT STABILITY
- COMPATIBILITY WITH SIMPLE REAL-TIME DATA PROCESSING (I.E., LINEAR RESPONSES)
- DIRECT INTERFACE WITH MICROPROCESSORS, FEEDBACK CONTROLLERS AND CONVENTIONAL RECORDERS
- MODULAR SYSTEM ELEMENTS: SIMPLE, RUGGED, INEXPENSIVE (EXPENDABLE IF NECESSARY)
- RELIANCE UPON EXISTING TECHNOLOGY BASE

Figure 3

TECHNICAL APPROACH

The two approaches toward the optical measurement of remote target displacements or deformations are: 1) optical ranging, in which the basic measurement is target-to-sensor range, and 2) optical angular sensing, in which the principal measurements are of target angular displacements lateral to the line of sight. For antenna distortion measurements, the techniques have constraints as illustrated in Figure 4.

Target ranging: Ideally, the range measurement is made from the center of curvature of the reflecting surface, at a distance approximately twice the height of the feed point. More practically, the sensor head is at or just below the feed. Angular definition of the target requires auxiliary sensing, such as angle encoders at the sensor pointing means.

Angular measurement: The ideal angular measurement is from a line of sight tangent to the reflecting surface; and here, the best position for the sensor is at or below the apex of the reflecting surface. Conversion of angular deflections to lineal deflections at the target requires a knowledge of target-to-sensor range (at reduced accuracy).

It is quite possible that the ultimate sensor system may be a hybrid, with both ranging and angle sensing capabilities. For its simplicity and compatibility with the antenna configurations, however, the angle sensing (triangulation) technique is the focus of the current effort.

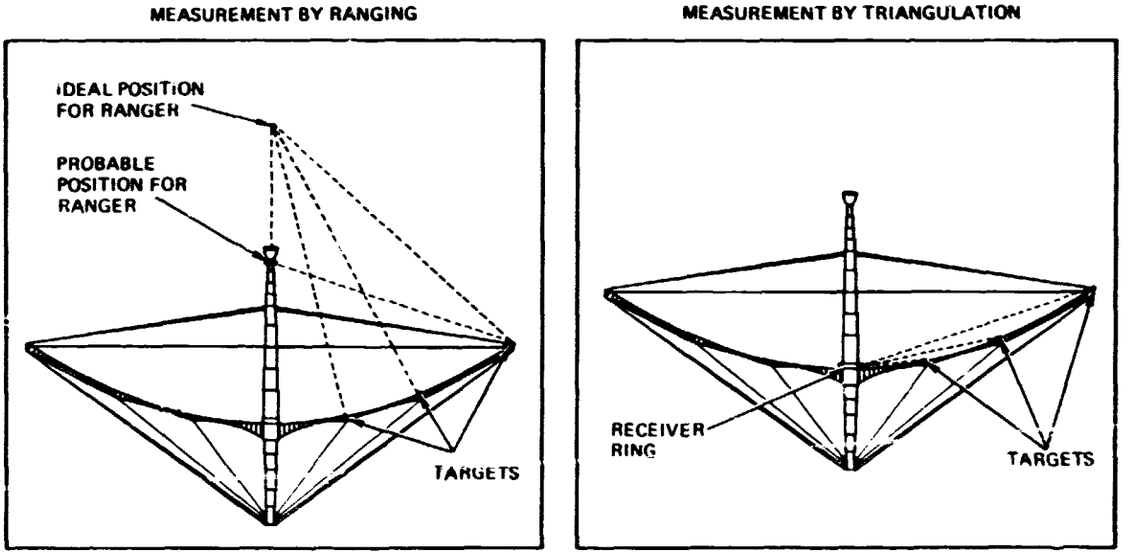

Figure 4

CURRENT PROGRAM

The following pages summarize the programmed effort under Contract NAS1-15520 for NASA Langley Research Center. This effort has been divided into three phases:

Phase 1: System Definition and Conceptual Design: After a review of the requirements for the four representative deployable antennas, conceptual sensor designs for each configuration are formulated and performance estimates made.

Phase 2: Proof of Concept Demonstration: The most critical areas, as pointed up by the conceptual design studies, are to be simulated in the Proof of Concept test. Results of the test establish the initial level of verification of the ultimate sensor system performance.

Phase 3: Fabrication and Test of a Breadboard Unit: The deliverable breadboard unit is a basic sensor receiver and suitable targets for test and evaluation by LaRC.

PROGRAM DESCRIPTION AND SUMMARY OF RESULTS

Figure 5

PROGRAM FLOW CHART

The central line of development is an iterative series of conceptual designs that become the basis for the breadboard. Paralleling this sequence, sensor system requirements, as established by the various antenna configurations and their interfacing, are continuously updated and refined, with the changes reflected in the sensor configurations. Along another parallel route, the characterization of the key components in the sensor system are validated and refined, leading to a final component selection for the breadboard.

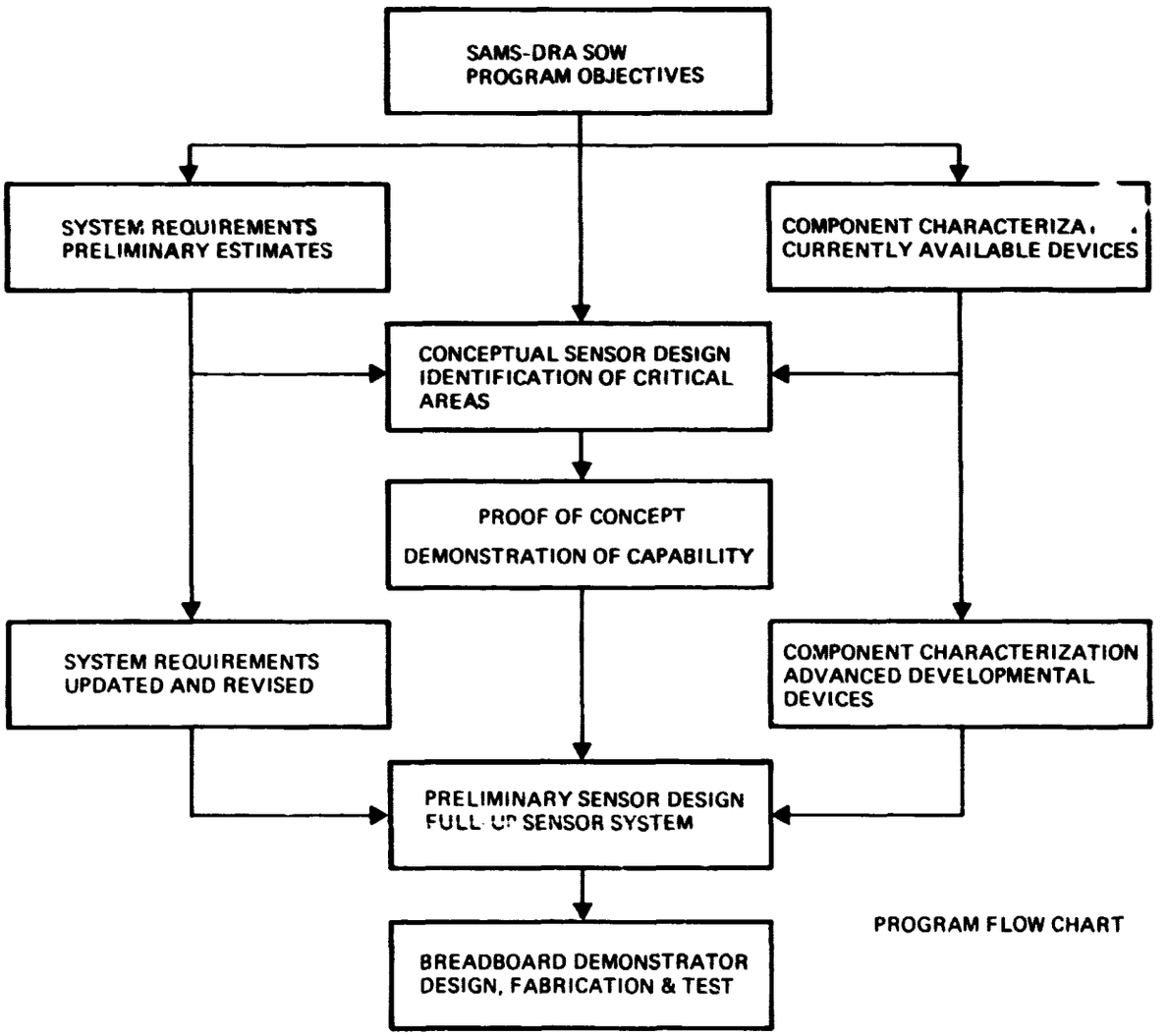

Figure 6

PROGRAM SCHEDULE

Starting in September of last year, Phase 1, System Definition and Conceptual Design, was completed in March, 1979, and Phase 2, Proof of Concept Demonstration testing was completed in August (Demonstration for NASA in September). Phase 3, Breadboard Fabrication and Test, is in progress.

The following pages gives a very brief review of the Phase 1 effort, and then discuss the tests and results of the Proof of Concept Demonstration.

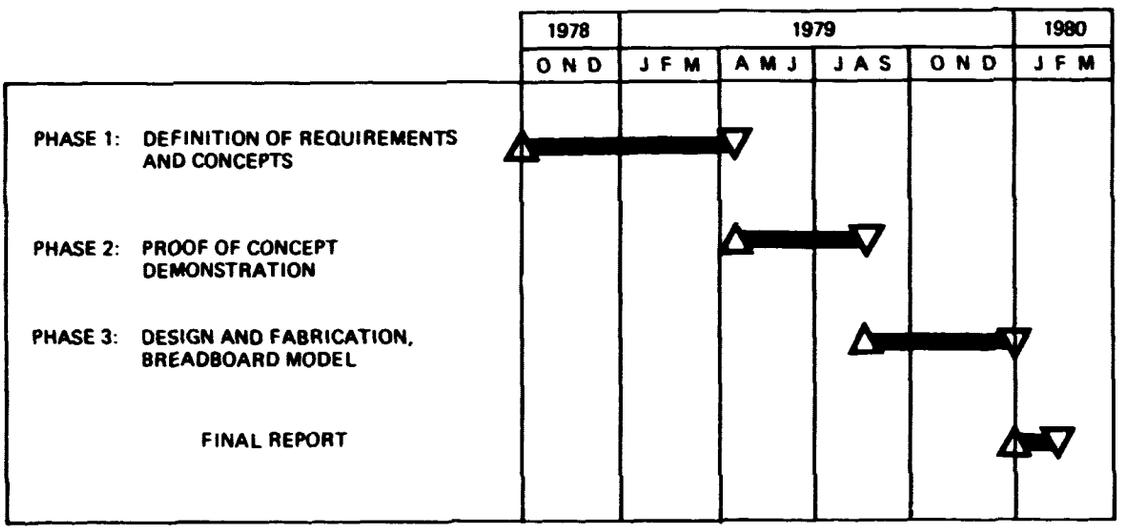

Figure 7

PHASE 1. DEFINITION OF REQUIREMENTS AND CONCEPTS

As discussed earlier, requirements for the four representative deployable antennas are to be defined; and from these requirements, conceptual designs for a suitable sensor system for each configuration is to be made. It is assumed at the outset that primary intent of the measurement system is to determine the behavior of an active, in-operation antenna. A reduced number (perhaps a hundred or less) target sample points at the antenna surface are adequate. It assumes that the fine-grain characterization of the antenna surface, demanding thousands of sample points, has been established by non-operational (e.g., photogrammetric) testing.

- SENSOR REQUIREMENTS FOR FOUR REPRESENTATIVE DEPLOYABLE ANTENNAS ARE TO BE DEFINED
- CONCEPTUAL SENSOR SYSTEM CONFIGURATIONS ARE TO BE ESTABLISHED FOR EACH OF THE ANTENNAS
- SENSOR COMPONENT CHARACTERISTICS ARE TO BE DEFINED
- PRELIMINARY ESTIMATES OF SENSOR SYSTEM PERFORMANCE ARE TO BE MADE

Figure 8

TYPICAL SENSOR SYSTEM CONFIGURATION

A typical sensor configuration is shown for the Harris Hoop-and-Column antenna. The coordinate reference system for all measurements is established at the antenna hub, near the apex of the reflecting surface. At this hub, a ring of optical, dedicated (i.e., non-scanning) receivers provide simultaneous coverage of the entire reflecting surface as represented by sample point targets at the mesh tie points and at the hoop. The targets may be active (i.e., light emitting diodes) or passive (i.e., retroreflectors, illuminated by light emitting diode projecters situated at the receivers). To minimize the number of receivers, each has multiple target coverage.

Range to the hoop segments, needed to convert the angular motions to lineal displacements, is determined stoichiometrically (noting that the separation between two adjacent targets at the hoop can be estimated, for example, by the hoop segment temperature). Range interpolation appears adequate for the intermediate targets between the hoop and the hub.

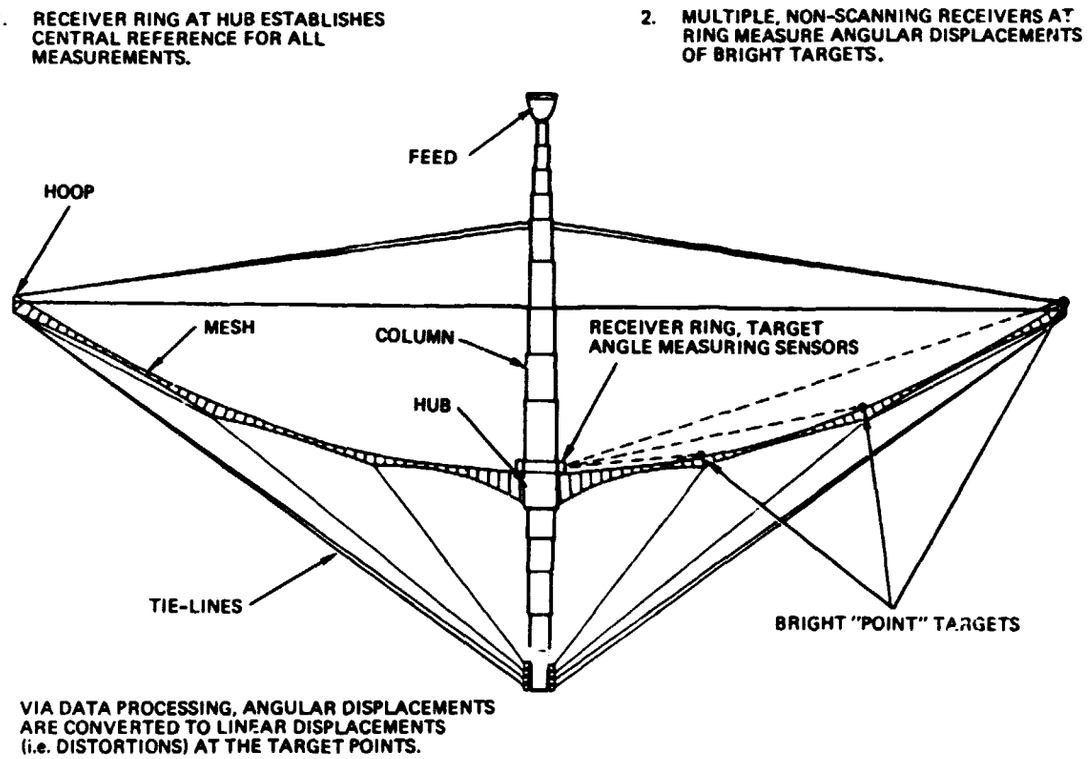

Figure 9

CONCEPTUAL CONFIGURATIONS SUMMARY

In the baseline antennas selected, it was assumed that the maximum diameter, Shuttle compatible, for the TRW Advanced Sunflower was 12.5 meters (this has later been revised upward), while the three deployable mesh antennas were 100 meter diameter. For all antennas, the minimum wavelength usable corresponded to 90 dB theoretical gain (10^4 wavelengths across the antenna). At this mimimum wavelength, the required accuracy in measuring surface deformation was a thirtieth of a wavelength. These requirements thus represent the most difficult cases (excluding the special applications where exceedingly high side lobe rejection is demanded).

From a sensor system viewpoint, the most challenging configuration is that for the Harris Hoop-and-Column. The preliminary estimate is that 120 sample points are needed for a 40 gore antenna, and two-thirds of these samples are at the unsupported mesh tie-points.

	TRW ADVANCED SUNFLOWER	HARRIS MAYPOLE	GENERAL DYNAMICS PETA	LOCKHEED WRAP-RIB
ANTENNA CHARACTERISTICS				
ANTENNA TYPE	PRECISION DEPLOYABLE	MESH DEPLOYABLE	MESH DEPLOYABLE	MESH DEPLOYABLE
DIAMETER RANGE	3 METERS TO 30 METERS	15 METERS TO 100 METERS	15 METERS TO 100 METERS	15 METERS TO 100 METERS
FREQUENCY RANGE	100 GHz TO 30 GHz	0.6 GHz TO 30 GHz	0.6 GHz TO 30 GHz	0.6 GHz TO 30 GHz
BASELINE ANTENNA MODEL				
CONSTRUCTION	36 FOLDING STIFF PANELS	40 GORE	8 BAY	80 RIB
DIAMETER	12.5 METERS	100 METERS	100 METERS	100 METERS
MAXIMUM FREQUENCY	240 GHz	30 GHz	30 GHz	30 GHz
MINIMUM WAVELENGTH	1.25 MILLIMETERS	1 CENTIMETER	1 CENTIMETER	1 CENTIMETER
SURFACE MEASUREMENT REQUIREMENTS				
MAXIMUM EXCURSION OF SURFACE (NORMAL TO OR TANGENTIAL IN SURFACE)	5 CENTIMETERS	50 CENTIMETERS	10 CENTIMETERS	20 CENTIMETERS
REQUIRED MEASUREMENT ACCURACY	40 MICROMETERS	333 MICROMETERS	333 MICROMETERS	333 MICROMETERS
NUMBER SAMPLE POINTS	36 AT PANEL TIPS	40 AT HOOP - 80 AT MESH	48 AT NODES	80 AT RIB TIPS
LOCATION	-	AT TENSION STRINGER TIE POINTS	-	-
TOTAL NUMBER OF SAMPLES	36	120	48	80

Figure 10

PHASE 2. PROOF OF CONCEPT DEMONSTRATION OBJECTIVES

Of the sensor configurations for the four representative deployable antennas, that for the Harris Hoop-and-Column is the most demanding. Sampling targets at the hoop segments are at a range of about ' meters from the receivers. These targets, however, can be active (l : emitting diodes). Intermediate targets at the mesh tie points are at lesser range, but may be required to be passive. Therefore both sensing modes, active with a light emitting diode target and passive with a retroreflector target, must be demonstrated. Moreover, estimated excursions of the targets from their nominal positions may be as large as 50 centimeters, total. With these conditions, the overall measurement accuracy at any target point is to be 333 micrometers.

Since it is impractical to realize a full scale demonstration, the Proof of Concept test was devised for a tenth scale. That is, the target-receiver distance was about 4.5 meters, the consequent maximum target excursion, 5 centimeters, and the required accuracy, 33.3 micrometers. To account for the change in target radiant power received, the target brightness was correspondingly scaled down.

- MOST DEMANDING APPLICATION IS THE HARRIS HOOP-AND-COLUMN ANTENNA
- BOTH ACTIVE (LED) AND PASSIVE (RETROREFLECTOR) TARGETS ARE TO BE USED
- TARGET-RECEIVER RANGE IS TO BE ONE-TENTH SCALE
- MEASUREMENT ACCURACY AND TARGET EXCURSION ARE SCALED ACCORDINGLY
- TARGET BRIGHTNESS IS REDUCED TO ACCOUNT FOR SCALING
- DEMONSTRATION IS TO BE:
  1) MEASUREMENT ACCURACY
  2) MAXIMUM TARGET EXCURSION
  3) SIGNAL - TO - NOISE

Figure 11

PROOF OF CONCEPT SETUP

The Proof of Concept setup consisted of a single axis receiver viewing a target mounted on a precision two-axis traverse. Incremental adjustment accuracy of the traverse was 2.5 micrometers (.001 inches). Signals from the detector were amplified, electronically bandpassed, and fed to a systems voltmeter. Its digital output was sent to a mini-processor that computed the measured coordinate, X, of the target. Additionally, the computer gave as outputs 1) the signal sum (measure of the incident flux at the detector) and 2) the rms variation, or noise, in the signals.

The test consisted of performing a traverse at the target, recording the computer output at each traverse increment. From the results, the maximum measureable excursion at the target, the linearity of the response, the measurement accuracy, and the system noise could be determined. From the scale factor. these values could immediately be extended to the full size antenna sensor.

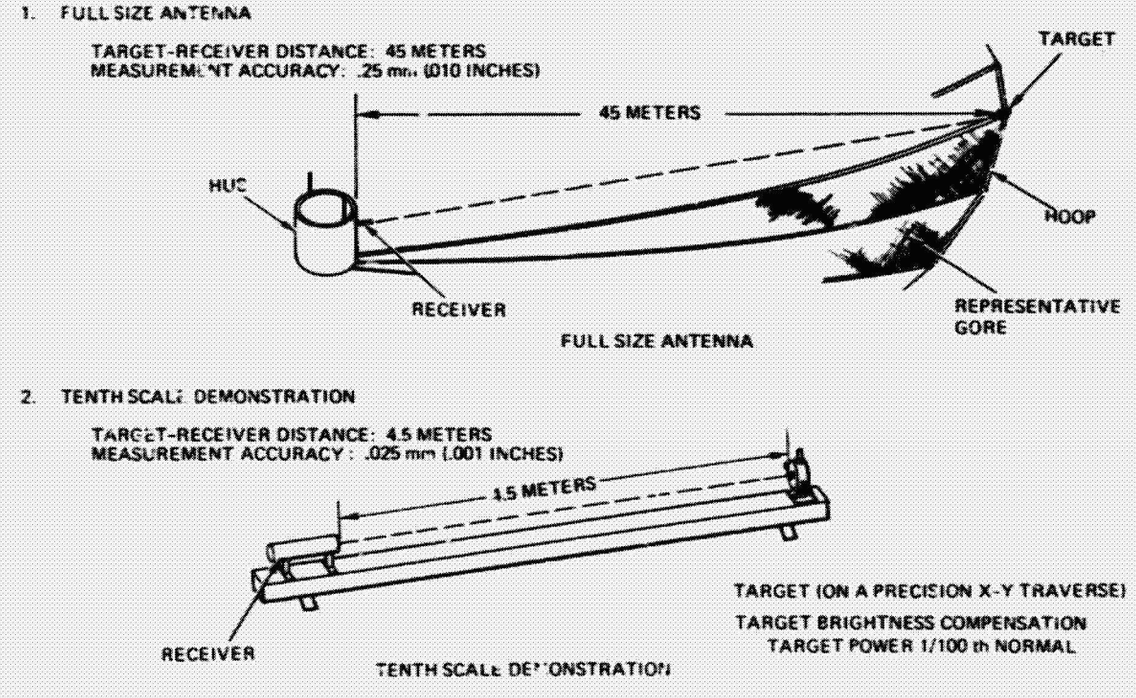

Figure 12

PROOF OF CONCEPT SETUP PHOTO

As shown in the photo, the setup was made on a 5 meter optical bench. At the extreme right the x-y traverse (moved forward in the picture) carried either a light emitting diode target or a retroreflector. In the retroreflector (passive target) mode, the target was illuminated by a light emitting diode projector - diode and beam shaping horn shown to the right of the receiver aperture. At the receiver, an objective lens imaged the target on a single axis, silicon PIN detector. Immediately aft of the detector is an electronic box enclosing the dual channel preamplifier-postamplifiers. Support electronics, including the 9825A Hewlett-Packard computer, are to the left of the setup shown.

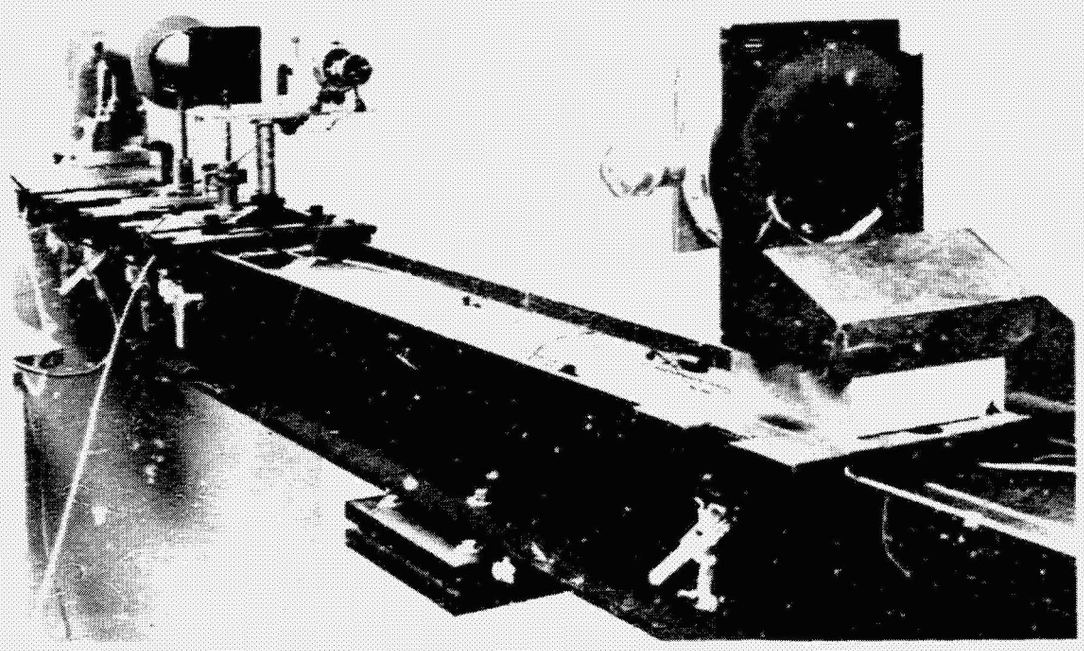

Figure 13

ORIGINAL PAGE IS
OF POOR QUALITY

PROOF OF CONCEPT RESULTS

A comparison of the required and the measured performances for the Proof of Concept is made below:

	Required	Measured
Max. Target excursion		
At test setup	± 2.3 cm*	± 2.75 cm
Extrapolated to antenna	± 29.7 cm	± 25 cm
Deviation from linearity		
At test setup	31 μm**	8.8 μm
Extrapolated to antenna	333 μm	94 μm
Noise		
At test setup	31 μm	1 μm
Extrapolated to*** antenna	333 μm	11 μm

* The scaling was actually 10.7:1.
** This is the total measurement error allowed. In an error budget, at least half of this can be allocated to the sensor itself.
***Noise measure for the active target.

	DEMONSTRATION	FULL SIZE ANTENNA
RECEIVER - TARGET RANGE	4.5 METERS	45 METERS
MAXIMUM DEFORMATION MEASURED	± 2.5 CM	± 2.5 CM
MEASUREMENT SYSTEMATIC ERROR (DEVIATION FROM LINEAR)	7.5 μm (.0003 IN)	75 μm (.003 IN)
RANDOM ERROR (APPROXIMATELY ONE SECOND RESPONSE TIME)	2.5 μm (.0001 IN) RMS	25 μm (.001 IN) RMS

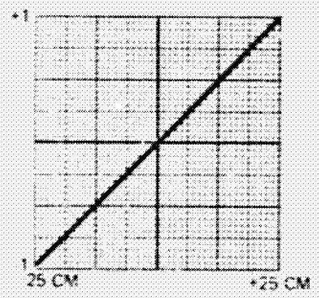

FULL EXCURSION RESPONSE

TARGET DISPLACEMENT

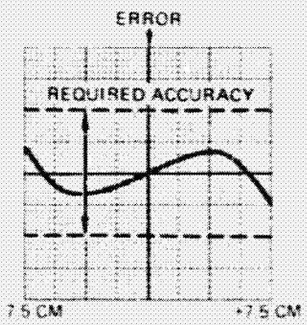

MEASUREMENT ERROR

Figure 14

N80-19153

DEVELOPMENT OF ELECTROMAGNETIC ANALYSIS METHODS FOR LARGE APERTURE ANTENNAS

C. R. Cockrell and L. D. Staton
NASA Langley Research Center

P. K. Agrawal*
RCA - Moorestown, N. J.

LSST 1ST ANNUAL TECHNICAL REVIEW

November 7-8, 1979

*Formerly with George Washington University at NASA Langley Research Center

PAGE 172 INTENTIONALLY BLANK

OBJECTIVES

- TO ESTABLISH AND VERIFY TECHNIQUES FOR PREDICTION OF EM PERFORMANCE OF LARGE SPACE ANTENNAS
- TO DEVELOP STATISTICAL AND DETERMINISTIC MODELING TECHNIQUES-INCLUDING EFFECTS OF SURFACE ROUGHNESS, DISTORTION, AND SEGMENTATION

DESCRIPTION OF WORK

- EXTENSION OF PRESENT TECHNIQUES OF APERTURE INTEGRATION FOR LARGE, SEGMENTED REFLECTORS
  - Planar Segmentation
  - Curved Segmentation
- ANALYSES OF DETERMINISTICALLY DISTORTED LARGE REFLECTORS WHOSE SHAPE IS DETERMINED BY SAMPLED POINTS
- UNIFIED APPLICATION OF STATISTICAL CORRELATION THEORY FOR BOTH SURFACE ROUGHNESS AND LARGE SCALE SURFACE DEVIATIONS
- CONSTRUCTION AND TESTING OF EXPERIMENTAL MODEL TO VERIFY THEORETICAL MODEL

GEOMETRY OF THE REFLECTOR ANTENNA

The geometry of figure 1 is used to compute the radiation patterns of reflectors. The aperture integration technique is employed in obtaining these patterns: First, rays are traced from the feed to the reflector surface and then to an aperture plane located in front of the reflector. Next, using geometric optics for each ray, the tangential electric field is found at many points in the aperture plane and, by numerically performing a double integration over the aperture plane, the secondary far-field radiation pattern is computed. The relatively slow lateral variation of the fields in the aperture plane compared with that of the surface currents on the reflector allows a more economical computation than does the direct integration of surface currents.

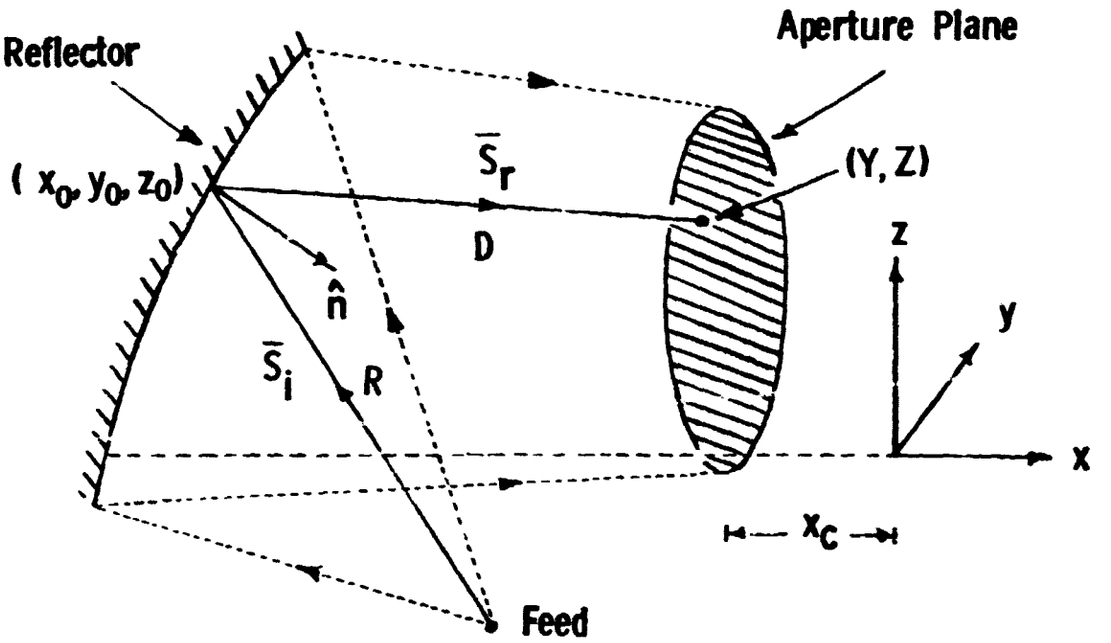

Figure 1

COMPUTED RADIATION PATTERNS FOR SEGMENTED REFLECTORS USING APERTURE INTEGRATION METHOD

Shown in figure 2 are calculated H-plane radiation patterns for a spherical reflector which is approximated by a number of planar hexagonal, triangular, and square facets placed on the ideal sphere such that the RMS surface deviation in each case is the same (.012m). On the average the surface deviation is more slowly varying over the reflector approximated by planar hexagons than over that approximated by planar triangles. The pattern for the hexagonal approximation agrees better with the pattern for the exact spherical reflector (not shown). The pattern for the square approximation, however, has higher side lobes which are apparently caused by the regular surface deviation associated with this shape.

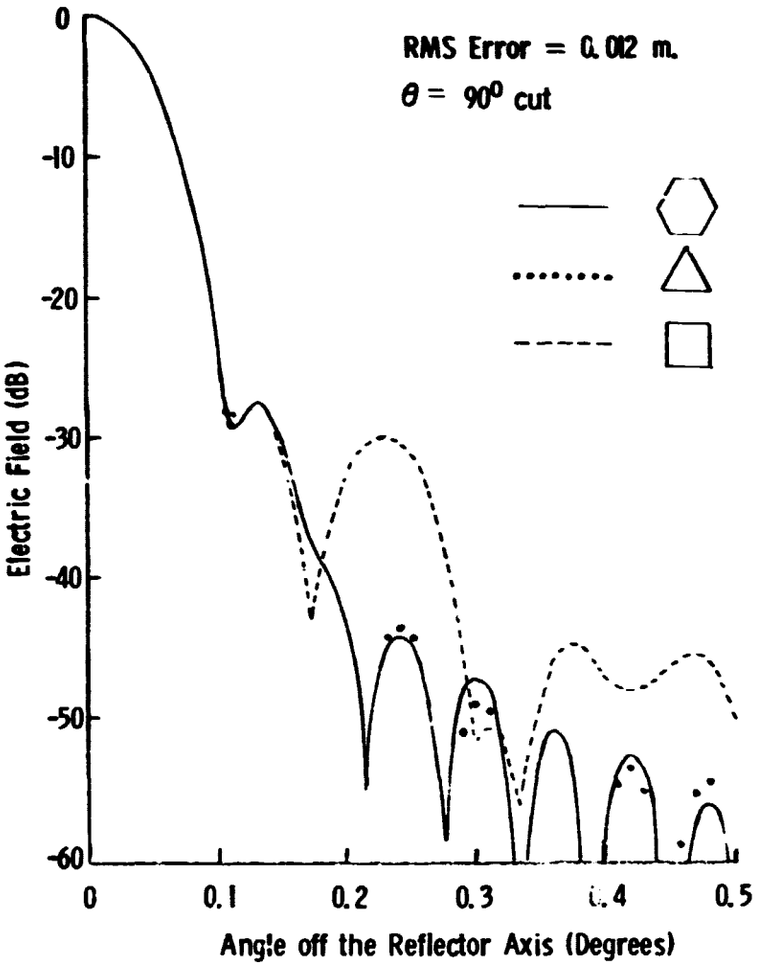

Figure 2

EFFECTS OF LARGE SCALE SURFACE ERRORS ON EM PERFORMANCE

An example of large scale deterministic type phase error (quadratic) effects on the radiation patterns of an aperture antenna is shown in figure 3. The solid curve corresponds to zero error ($\Delta=0$); i.e., the aperture distribution varies only in amplitude. The cases $\Delta=\lambda/8$ and $\Delta=\lambda/4$ correspond to increasing quadratic phase error with the same amplitude distribution. Increase in phase error results in an increase in power radiated in the side lobes.

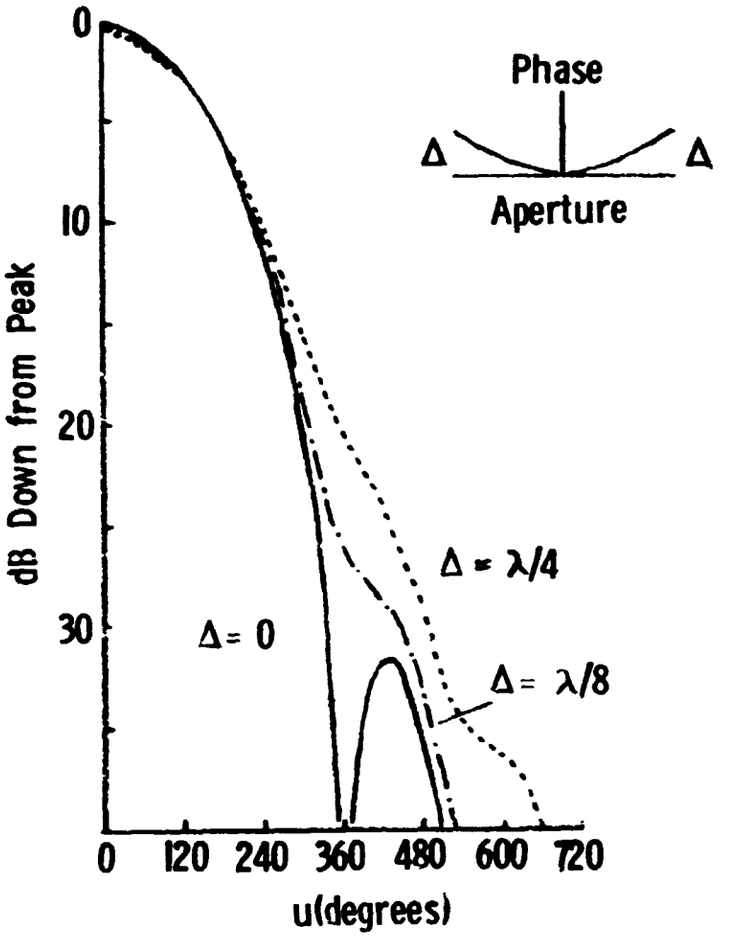

Figure 3

ENVELOPES OF RADIATION PATTERNS FOR QUASI-RANDOM PHASE ERRORS

Figure 4 illustrates for a circular aperture antenna (diameter D) how the radiated power in the side lobes increases for a class of irregular phase errors (see inset) which may be characterized as quasi-random (ref. 1). The curve labled 0 is error-free and the remaining curves represent indicated amounts of maximum peak to peak phase errors. Aperture tolerances corresponding to these phase errors are shown in the parentheses. The general effect of such irregular,but deterministic, phase errors is almost always to raise the side lobe levels and hence to lower the antenna beam efficiency.

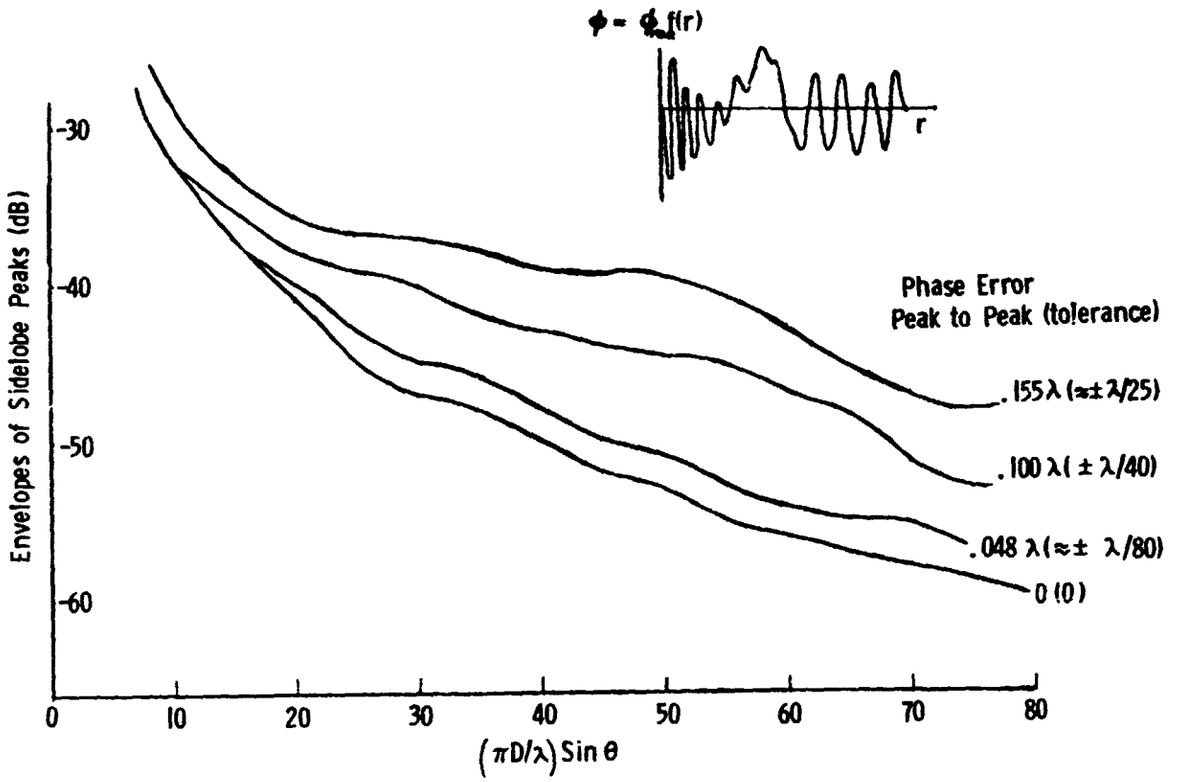

Figure 4

RADIATION PATTERNS OF 20-SEGMENT APERTURE ANTENNA WITH GAUSSIAN DISTRIBUTED PHASE ERROR

Figure 5 shows the calculated radiation patterns of 20-segment aperture antennas of width D with assumption of uniform amplitude on all segments and Gaussian distributed phase error on each segment. The solid curve represents the radiation pattern when no phase error exists across the aperture. The dotted curve represents the expected (ensemble average) pattern which is obtained through random process analyses. The remaining radiation patterns come from two members of the ensemble of 20-segment aperture antennas.

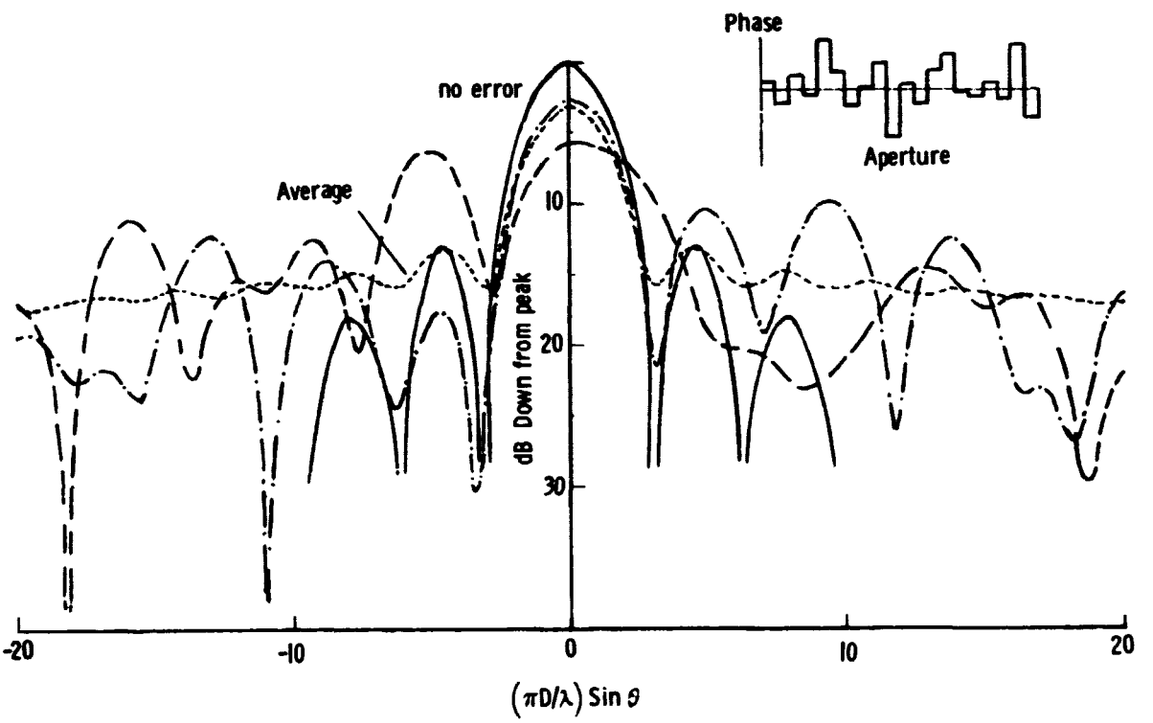

Figure 5

SECONDARY PATTERN BEAM EFFICIENCY vs. RMS SURFACE ERROR IN WAVELENGTHS FOR DIFFERENT CORRELATION LENGTHS

The effects of surface errors on the beam efficiency of a large aperture antenna can be illustrated by applying the theory developed by Ruze (ref. 2). In Ruze's work the phase error (surface error) is chosen from a Gaussian population which is statistically uniform over the entire reflector surface. The auto-correlation function of the phase is also taken to have a Gaussian form with a constant variance (square of the correlation length). Based on his work the beam efficiency (assumed to be 100 percent for the unperturbed aperture) is plotted in figure 6 as a function of rms surface error with normalized correlation length (C/λ)as a parameter. It is seen that the smaller C/λ values (i.e., more rapidly varying surfaces) give rise to more stringent requirements on surface rms error for high beam efficiency. For more slowly varying surface (large C/λ) the surface rms error can be relaxed and still allow relatively high beam efficiency.

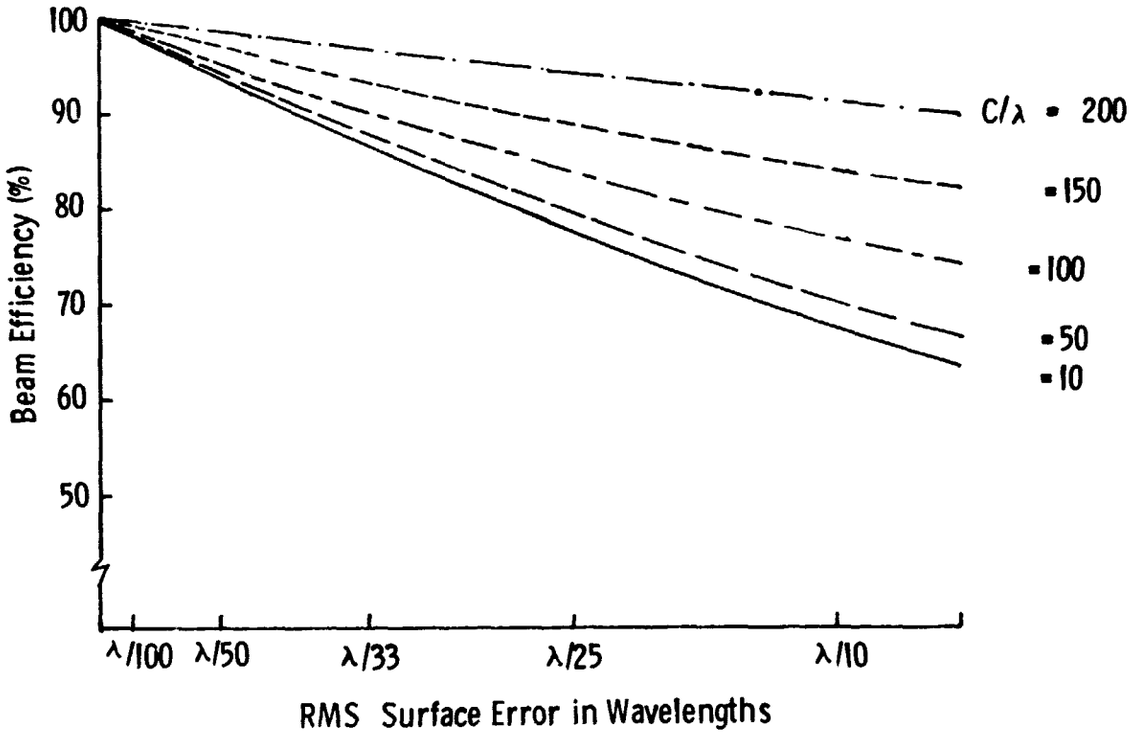

Figure 6

REAL PART OF THE AUTO-CORRELATION FUNCTION OF
20-SEGMENT APERTURE ANTENNA WITH
GAUSSIAN DISTRIBUTED PHASE ERROR

Figure 7 shows the real part of the auto-correlation function of a 20-segment aperture antenna with the assumption of uniform amplitude and Gaussian distributed phase error on each segment. The solid curve is the zero error case and the dotted curve is the ensemble average obtained through random process analyses. The two remaining curves are the real parts of the auto-correlation functions of two members of the ensemble of 20-segment aperture antenna. The Fourier transforms of the total auto-correlation functions (given in part in figure 7) are the power pattern curves given in figure 5.

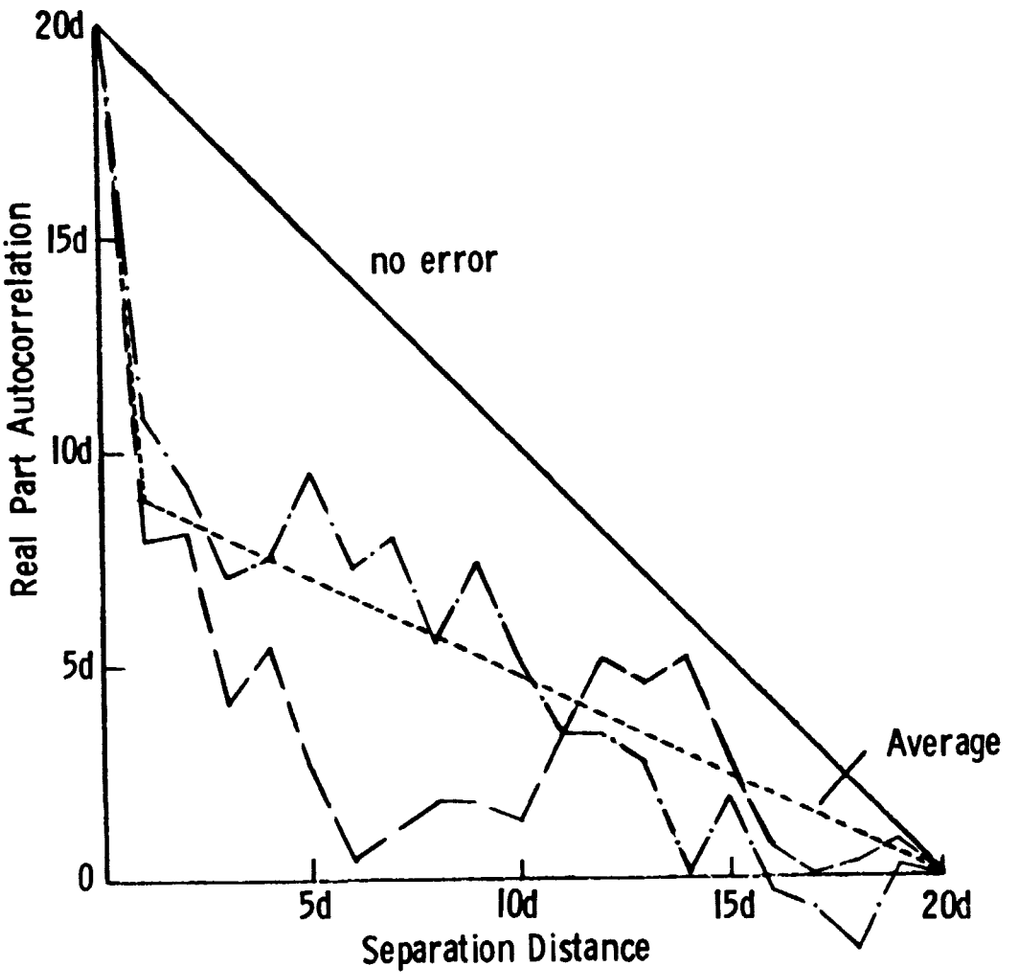

Figure 7

RATIOS OF STANDARD DEVIATION TO THE MEAN AS A FUNCTION OF AUTO-CORRELATION SEPARATION DISTANCE

By observing figure 7, it can be seen that the auto-correlation functions from members of an ensemble of 20-segment aperture antennas can deviate from their ensemble average auto-correlation function (dotted curve in figure 7). The ratio of the standard deviation to mean for the 20-segment aperture antenna as a function of auto-correlation separation distance is given by the circles in figure 8. By increasing the number of segments within each antenna, the auto-correlation functions of the separate antennas approach arbitrarily close to the ensemble average (expected) auto-correlation function predicted by random process analyses. The increase in the number of segments clearly reduces the ratio of standard deviation to the means shown by the square and triangle symbols in figure 8.

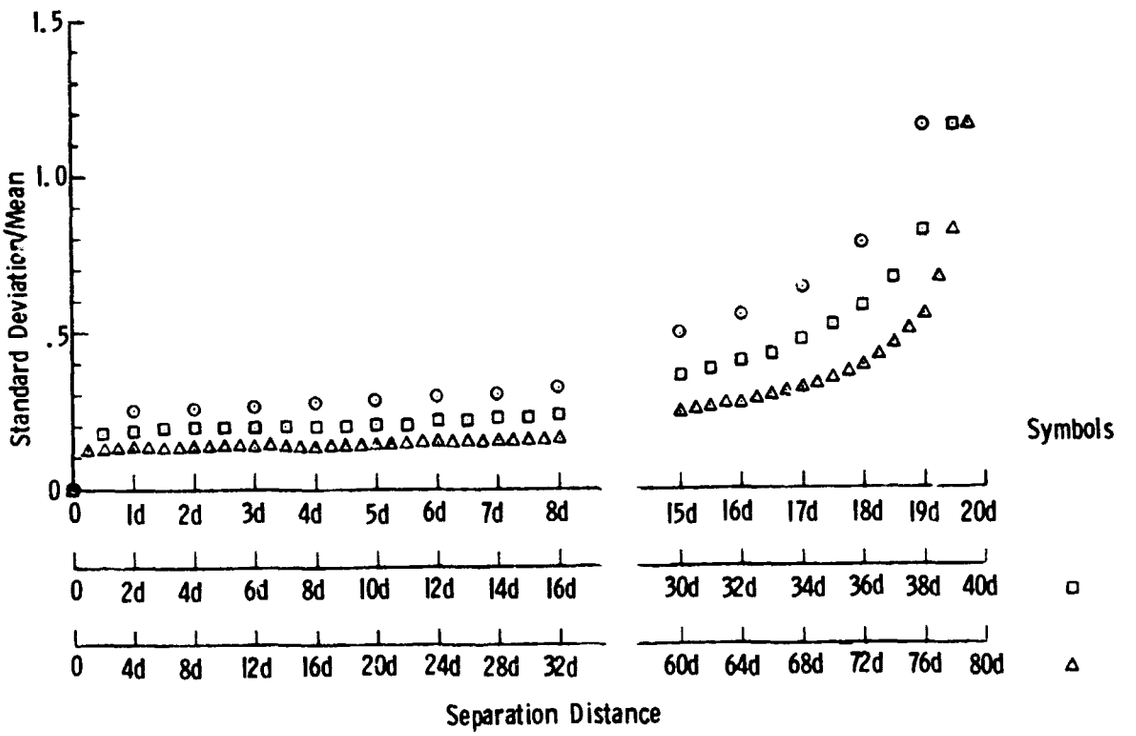

Figure 8

CONCLUDING REMARKS

- Deterministic Analyses
  - assumes exact knowledge of surface
  - true radiation patterns
  - both scale distortions
  - a range of possible distortions can lead to wide variance about the designed pattern
- Random Process Analyses
  - assumes statistical knowledge of surface
  - average radiation patterns
  - both scale distortions, provided correlation region is small compared to the aperture size
  - large correlation region can lead to large variance about the average pattern
- General Effects of both Analyses
  - broaden main beam
  - side lobe radiation increases with phase amplitude and variation
  - requirement of high beam efficiency in a very large antenna demands utmost care in EM analysis

C - 3

PLANS FY'80

- EXPERIMENTALLY VERIFY SEGMENTED REFLECTOR PROCRAM
- EXPERIMENTALLY VERIFY SAMPLED POINT PROGRAM
- CONTINUE ANALYSES OF ANTENNAS THROUGH AUTOCORRELATION TECHNIQUES
- CONTINUE SEGMENTED REFLECTOR ANALYSES

PUBLICATIONS

- "A PRELIMINARY STUDY OF A VERY LARGE SPACE RADIOMETRIC ANTENNA," NASA TM 80047 , JAN. 1979, P. K. AGRAWAL
- "A METHOD FOR PATTERN CALCULATION FOR REFLECTOR ANTENNAS WHOSE GEOMETRY IS DESCRIBED BY A FINITE NUMBER OF DISCRETE SURFACE POINTS," IEEE APS SYMPOSIUM, JUNE 1979, P. K. AGRAWAL, J. F. KAUFFMAN, AND W. F. CROSWELL
- "PRELIMINARY DESIGN OF LARGE REFLECTORS WITH FLAT FACETS," NASA TM 80164, P. K. AGRAWAL, M. S. ANDERSON, M. F. CARD

REFERENCES

1. Dragone, C. and Hogg, D. C.: Wide-Angle Radiation Due to Rough Phase Fronts, Bell System Technical Journal, Vol. XLII, No. 5, September 1963.

2. Ruze, John: Antenna Tolerance Theory - A Review, Proc. IEEE, Vol. 54, pp. 633-640, April 1966.

N80-19154

ELECTROSTATIC FORMING

J. W. Goslee
NASA Langley Research Center

LSST 1ST ANNUAL TECHNICAL REVIEW

November 7-8, 1979

PAGE 186 INTENTIONALLY BLANK

ELECTROSTATIC FORMING

Electrostatic forming of antenna or reflector surfaces was proposed to Langley in 1978 by General Research Corporation (GRC). A small 0.91-m (3-foot) diameter reflector was fabricated by GRC and demonstrated to various groups both at Langley and NASA Headquarters.

This viewgraph demonstrates the concept and shows how the membrane deflects when a voltage is applied between the membrane surface and back electrodes.

ELECTROSTATICALLY CONTROLLED MEMBRANE CONCEPT

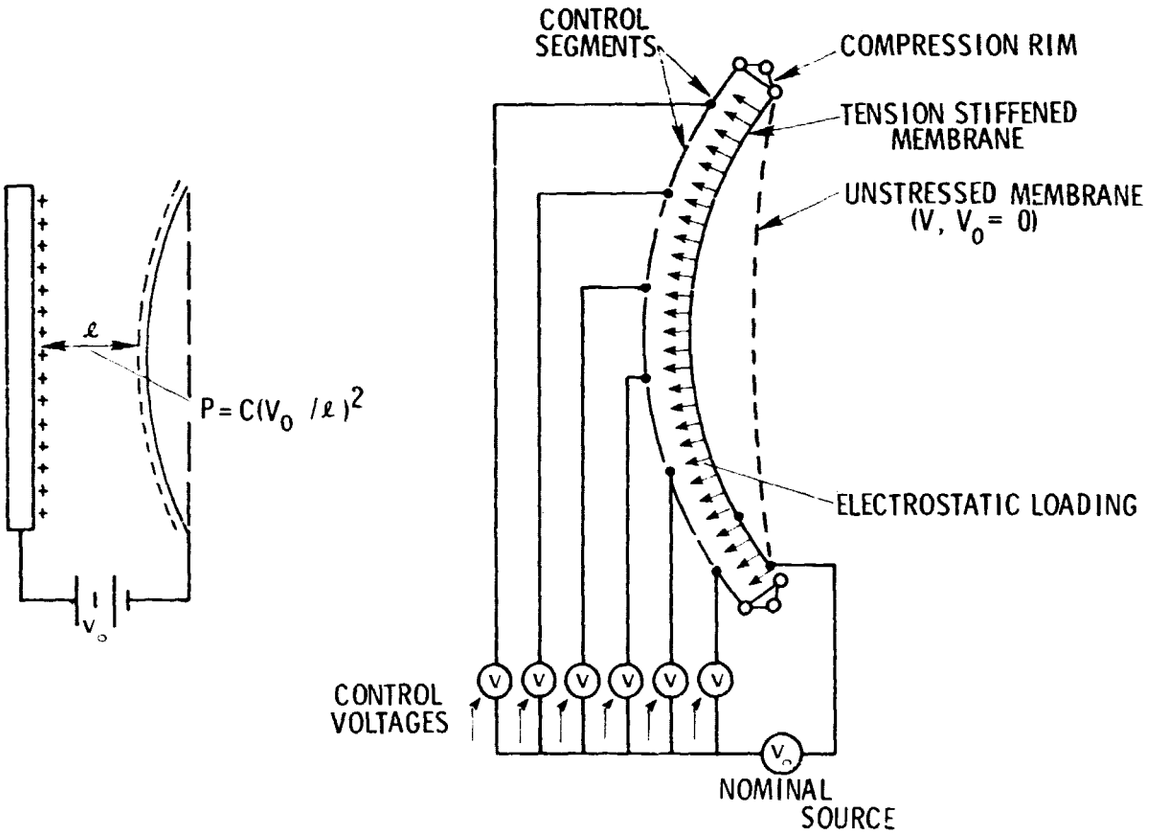

ELECTROSTATIC FORMING

Langley funded a study by GRC to conduct a parametric study and preliminary design of a 4.88-m (16-foot) diameter test fixture which is to be used to prove that the electrostatic forming technique is a viable means of forming antenna surfaces. After the study was completed in February 1979, Kentron was given the job of producing a working design of the test fixture. The final drawings were completed in September 1979.

In connection with developing the details of the 4.88-m (16-foot) test fixture, Kentron fabricated a 1.83-m (6-foot) diameter preprototype test fixture which was used to try out some of the ideas which went into the design of the 4.88-m (16-foot) test fixture. The 1.83-m (6-foot) fixture is set up at Langley along with the laser surface sensing device which Robert Spiers will discuss in the next paper.

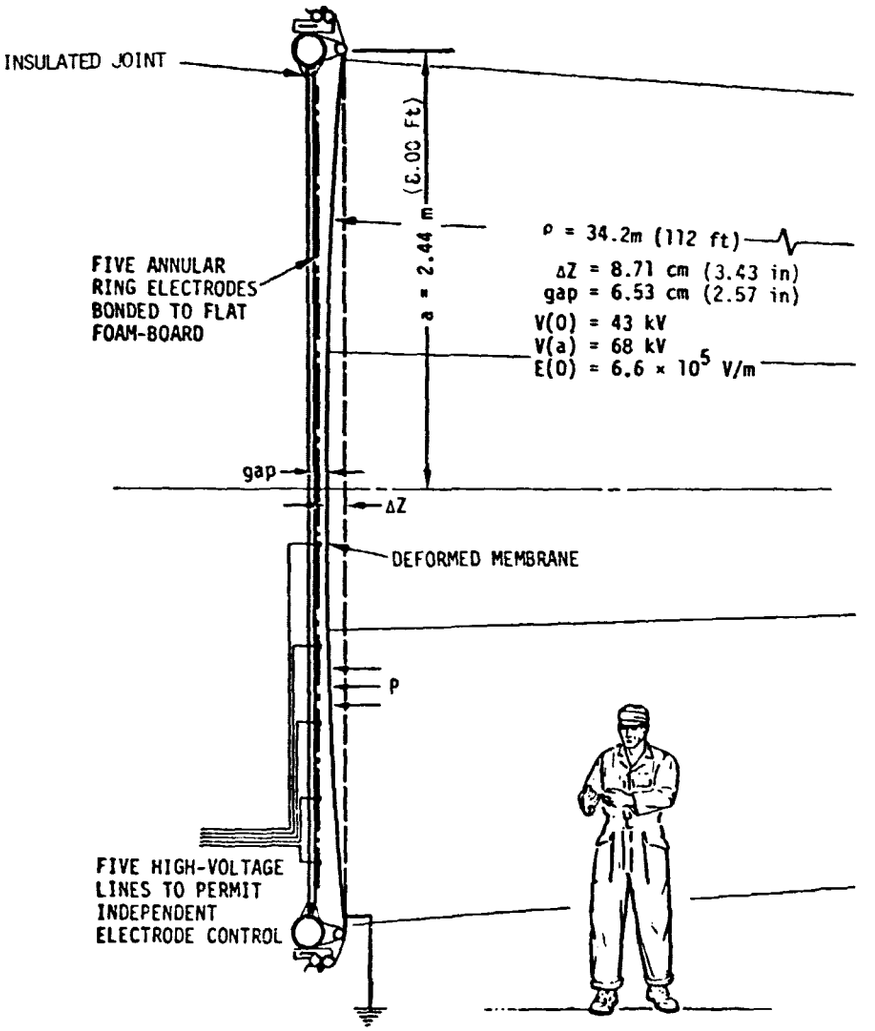

ELECTROSTATIC FORMING

The drawings of the 4.88-m (16-foot) diameter test fixture have been released to the shops and we anticipate that it will be completed in March 1980. Also, by that time, we hope to have a surface sensing technique clearly defined.

This viewgraph shows how the 4.88-m (16-foot) diameter test fixture will be set up with the surface sensing device at the radius of curvature which will be at 34.2 meters (112 feet) from the surface.

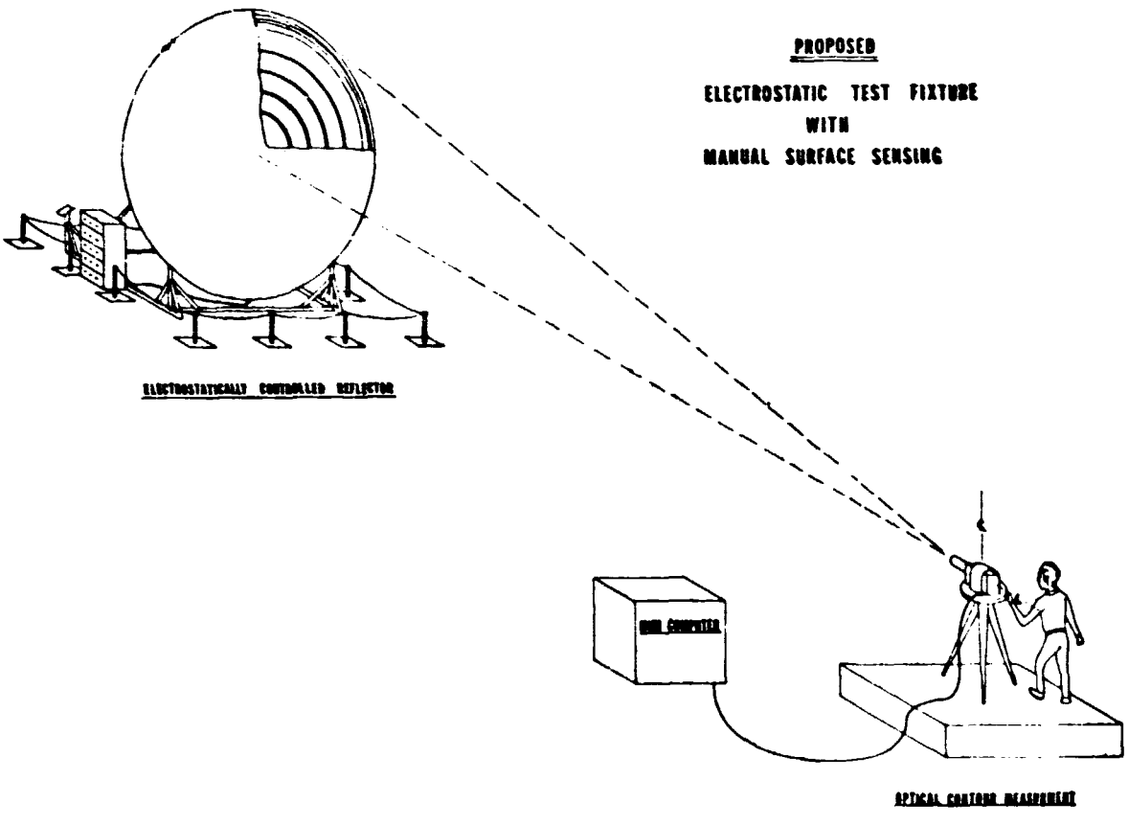

ELECTROSTATIC FORMING

The initial material we intend to test is 0.3 mil. Aluminized Kapton which will have several seams after fabrication. Later on, we want to test other plastic materials as well as some of the meshes that are being used for antennas.

This viewgraph shows the proposed schedule for the F. Y. 1980 efforts.

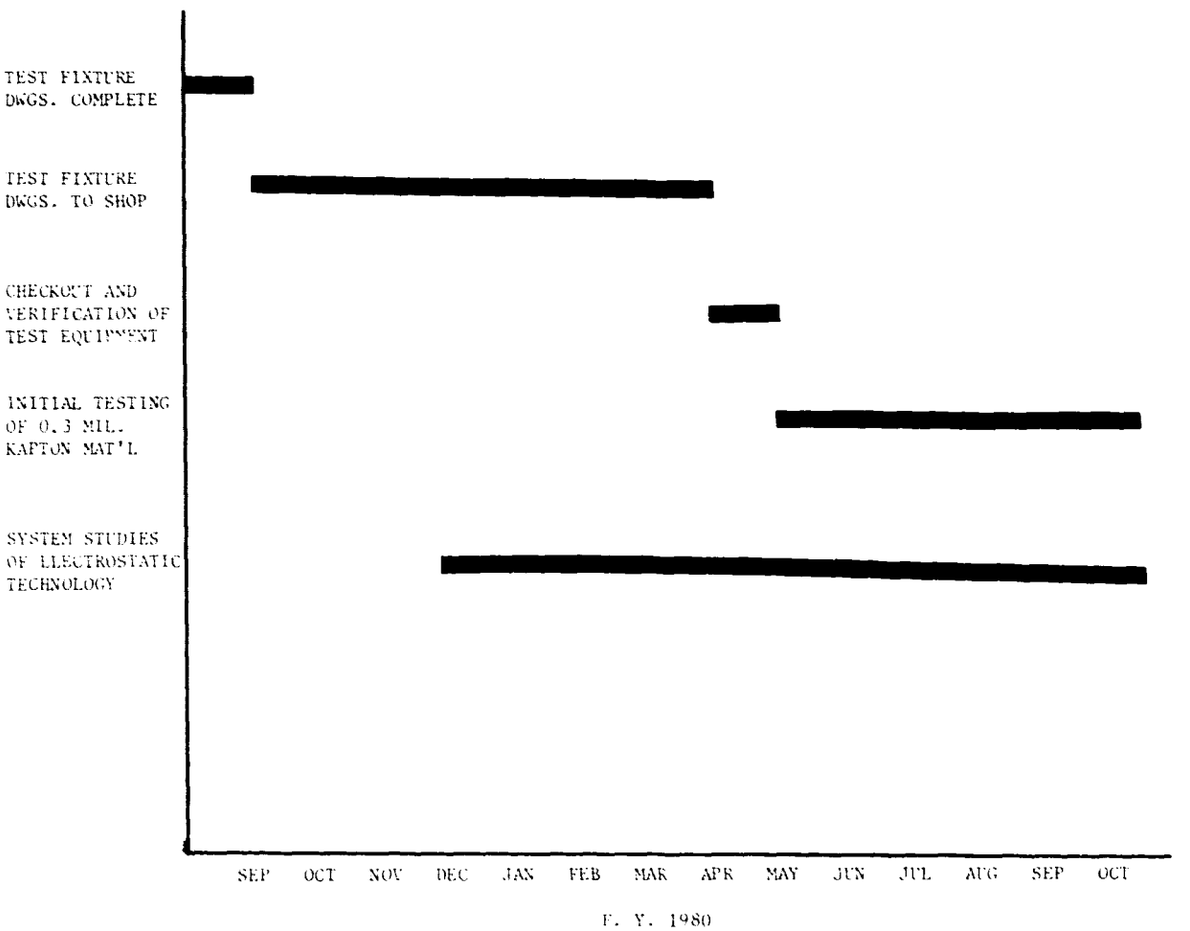

ELECTROSTATIC FORMING

We also intend to examine the electrostatic forming technique from a system technology viewpoint during F. Y. 1980 to determine some of the potential antenna characteristics. Also, we want to determine if space charging effects would create any potential problems on an electrostatically formed antenna. From an analytical viewpoint, we want to develop further understanding of the electrostatic technique and how it can be used in future applications.

This viewgraph shows the areas to be investigated in system technology.

ELECTROSTATIC SYSTEM STUDY AREAS

- Study of LEO and GEO Environmental Effects on Electrostatically Charged Surfaces
  - Determine Floating Potential
  - Determine Vacuum and Plasma Effects on Electrostatically Charged Surfaces
  - Determine Stress in Insulation Due to Electrical Field
- System Study of Technology Involved in Electrostatically Formed Antennas
  - Mechanical Interface Between Reflector and Supporting Structure
  - Thermal Effects on Antenna System
  - Structural Configuration
  - Deployment Concept
  - Mass of System
  - Stowed Volume
- Analysis and Scaling of 4.88-m (16-Foot) Diameter Test Data
  - Test Data Analytic Representation
  - Validation of Reflector Shape
  - First Order Scaling to Large Sizes

N80-19155 D/0

SURFACE MEASURING TECHNIQUE

Robert B. Spiers, Jr.
NASA Langley Research Center
Hampton, VA 23665

First Annual LSST Program Technical Review
held at
Langley Research Center
Hampton, VA 23665
November 7-8, 1979

SURFACE MEASURING TECHNIQUE

A modified Foucault or knife edge test (ref. 1) is applied to measure the surface contour of a large circular electrostatically formed concave reflector. The technique is diagramed in the figure. The aperture of a 3 milliwatt HeNe laser is placed at the estimated center of curvature of the reflector with its beam directed toward the geometric center of the reflector. A projection screen to receive the reflected laser beam is attached to the laser and remains normal to the emerging laser beam as the laser scans the surface of the reflector. If the concave surface is a true spherical surface the reflected beam always returns to the laser aperture in the center of the screen. For a nonspherical surface the reflected beam falls on the screen at a distance, ℓ, from the laser aperture. From geometry the reflector surface deviations, Δd, from a truly spherical surface are related, to a good approximation, to the linear distance ℓ. The reflector's contour is calculated by summing the incremental Δd's for all incremental Δy's. An error analysis of the measurement technique indicates a 50 percent error in surface deviations is likely. Propagation errors due to the summing operation are known to contribute strongly to the error. More exact solutions are being sought.

REFLECTOR SURFACE MEASUREMENT TECHNIQUE
(MODIFIED FOUCAULT OR KNIFE EDGE TEST)

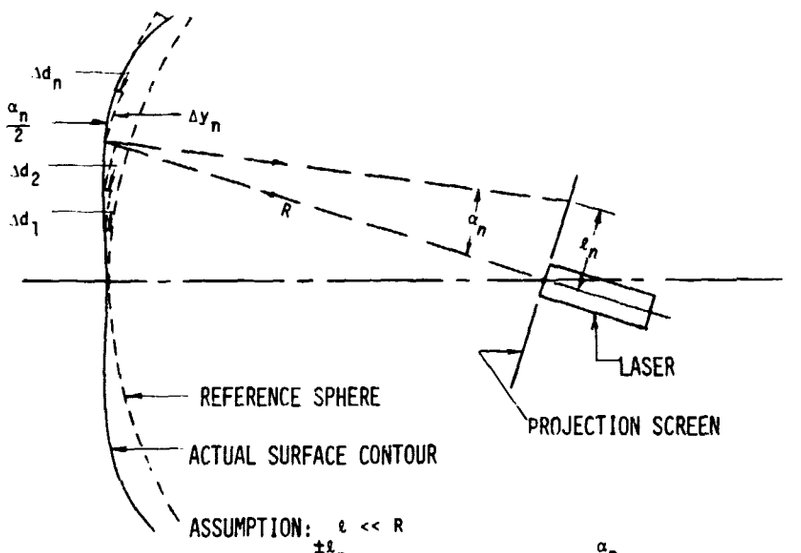

ASSUMPTION: $\ell \ll R$

THEN $\pm\alpha \approx \frac{\pm\ell_n}{R}$ (RADIANS) AND $\pm\Delta d_n \approx \pm\frac{\alpha_n}{2}\cdot\Delta y_n$ (METERS)

APPROXIMATE SURFACE DEVIATION FROM REFERENCE SPHERE $d \approx \Delta d_1 + \Delta d_2 + \ldots \Delta d_n$

CHARACTERIZING SMALL SCALE SURFACE ROUGHNESS

Additional characterization of surface roughness on a scale small compared to the laser spot size at the reflector can be obtained from the increased laser spot size at the project screen. The maximum surface deviation, $h_{max.}$, from an average surface over the spot size, d, is given in terms of the laser parameters, the projection geometry and the increased laser spot size, x. The particular energy distribution in the increased laser spot size on the screen indicates a particular characteristic reflector surface roughness. Such indicators are helpful to characterize the surfaces of aluminized membranes applied to large space structures.

CHARACTERIZING SMALL SCALE SURFACE ROUGHNESS

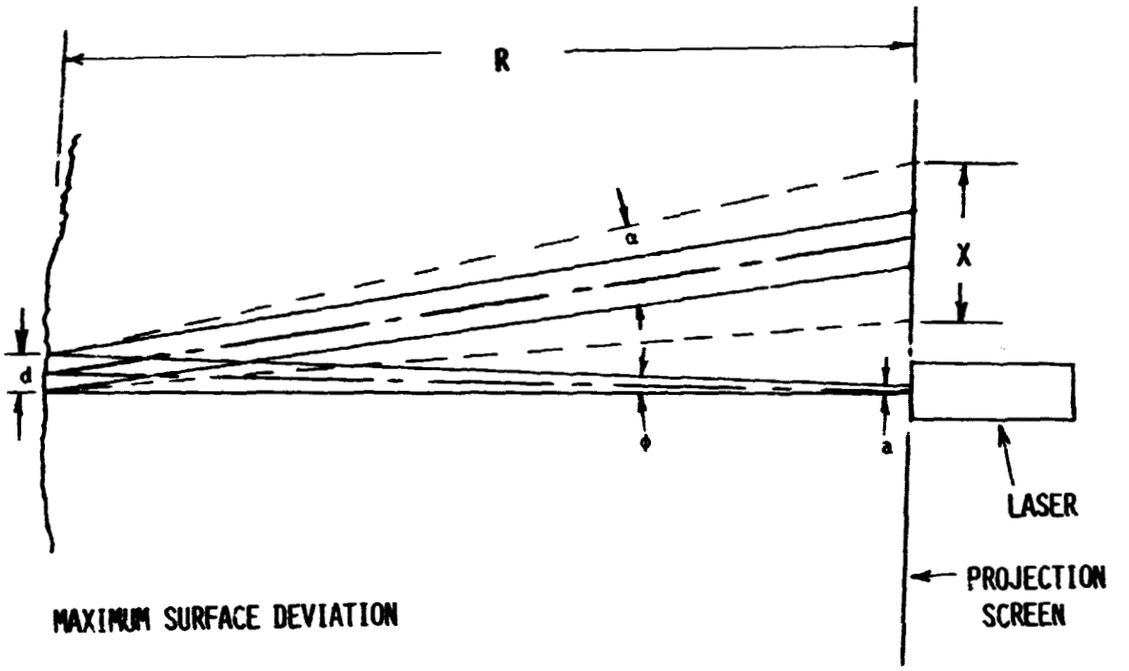

MAXIMUM SURFACE DEVIATION

$$h_{max.} = d \cdot \alpha \text{ (METERS)}$$

WHERE

$$\alpha = \frac{\frac{1}{2}x + \frac{1}{2}(a + 2\phi R)}{R} \text{ (RADIANS)}$$

CONCAVE REFLECTOR PARAMETERS

The reflector was formed by loosely stretching an aluminized Kapton film over a plastic tube circular form. Two electrostatic electrodes are attached to the back of the reflector surface, one at the center of the circular surface and one concentric ring electrode located between the center and the edge of the reflector. Opposite potential electrodes are spaced a small distance behind those attached to the reflector. When potentials of 40,000 to 50,000 volts are applied the Kapton film tensions to form a concave surface. The surface material retains some creases which comes from handling and a few wavy wrinkles which are caused by material fabrication nonuniformities and assembly tensioning nonuniformities. Typical surface roughnesses due to creases are of the order of 0.1 mm while wrinkles are typically 1.0 mm.

CONCAVE REFLECTOR PARAMETERS

- DIAMETER - 1.83 METERS (72 INCHES)
- FOCAL LENGTH - 7.32 METERS (288 INCHES)
- MATERIAL - ALUMINIZED KAPTON
- SURFACE FORMING - ELECTROSTATIC FIELD

MEASUREMENT RESULTS

A smooth curve of the actual electrostatically formed reflector surface is compared to a curve representing a reference sphere. Measurements of surface slope and deviation were calculated every 15 cm along the reflector's horizontal and vertical diameters using the modified knife edge measurement technique. The reference sphere and the actual surface were adjusted to coincide at the geometric center of the circular reflector. The maximum deviation from a sphere is approximately 6 mm. No effort was made to electrostatically control the figure of the surface during these measurements.

REFLECTOR SURFACE ACCURACY MEASUREMENT RESULTS

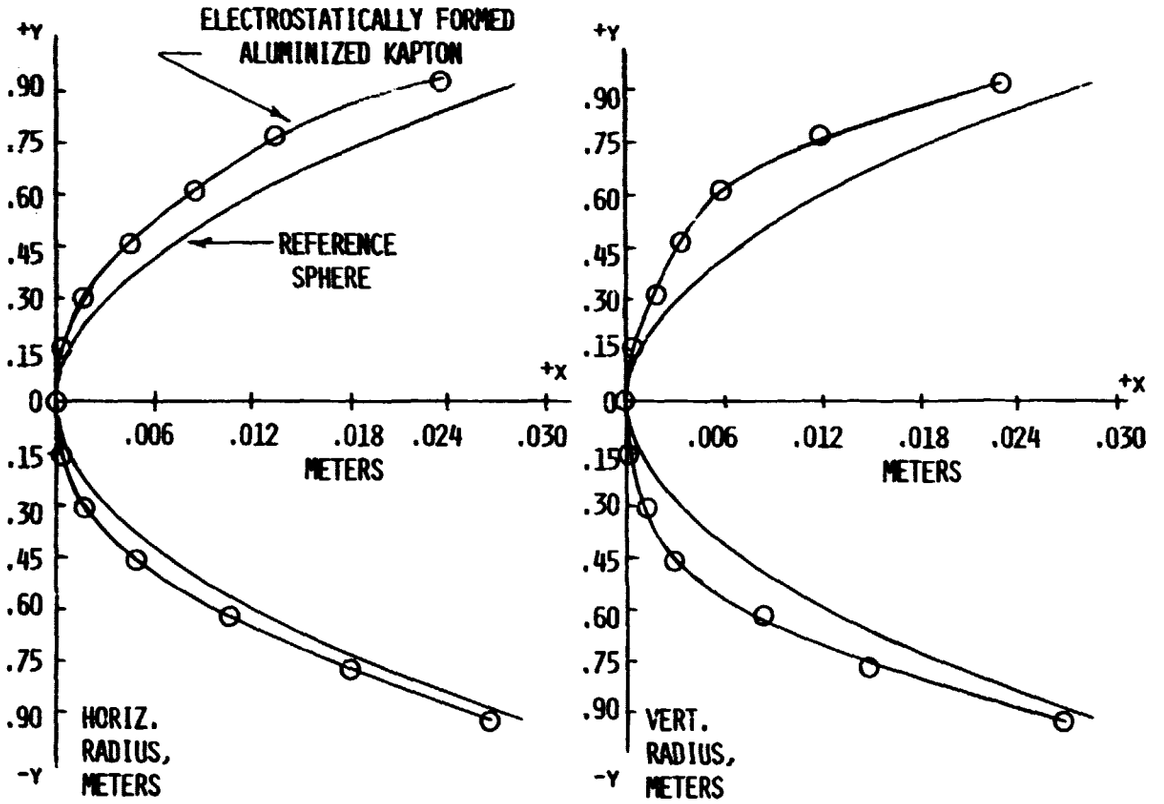

REFERENCE

1. Smith, Warren J.: Modern Optical Engineering, The Design of Optical Systems, pp. 439-443, McGraw-Hill Book Company, New York, New York.

N80-19156

STRUCTURAL CONCEPTS FOR LARGE SPACECRAFT

H. G. Bush, W. L. Heard, Jr.,
and J. E. Walz
Langley Research Center
Hampton, Virginia

LSST 1ST ANNUAL TECHNICAL REVIEW

November 7-8, 1979

The cost of transporting spacecraft to low earth orbit, even using Shuttle, is extremely high. It is imperative that the most efficient use be made of the transportation system. In order to minimize the amount of mass which must be orbited, and to determine spacecraft designs which meet the multiplicity of design conditions and system constraints, it is necessary to employ an optimization approach. A preliminary analysis and design code for sizing hexagonal planform spacecraft is currently being developed at LaRC. The minimized structural mass/area for reflector class spacecraft of various spans (D) is shown in figure 1 (F-1) for several design values of platform fundamental frequency. The results are for tetrahedral truss platforms with inward folding surface members. The truss depths of the results shown were constrained to 18m - the length of the Shuttle cargo bay. In F-2, the sensitivity of package size dimensions for a 300m platform are illustrated as a function of platform fundamental frequency. The results show that package size changes from long and slim for low frequencies to short and fat for higher frequencies. The impact of this dimensional change on transportation requirements is shown in F-3 for two different spacecraft classes. The results show that below a critical stiffness value (frequency) the spacecraft can be transported in a mass critical mode, indicated by the horizontal lines. However, above the critical stiffness value, transportation requirements become dominated by package geometry and increase rapidly as indicated by the near vertical lines. Thus, a deployable spacecraft for any mission would appear to have a limiting stiffness value above which it becomes impractical to transport, even in segments.

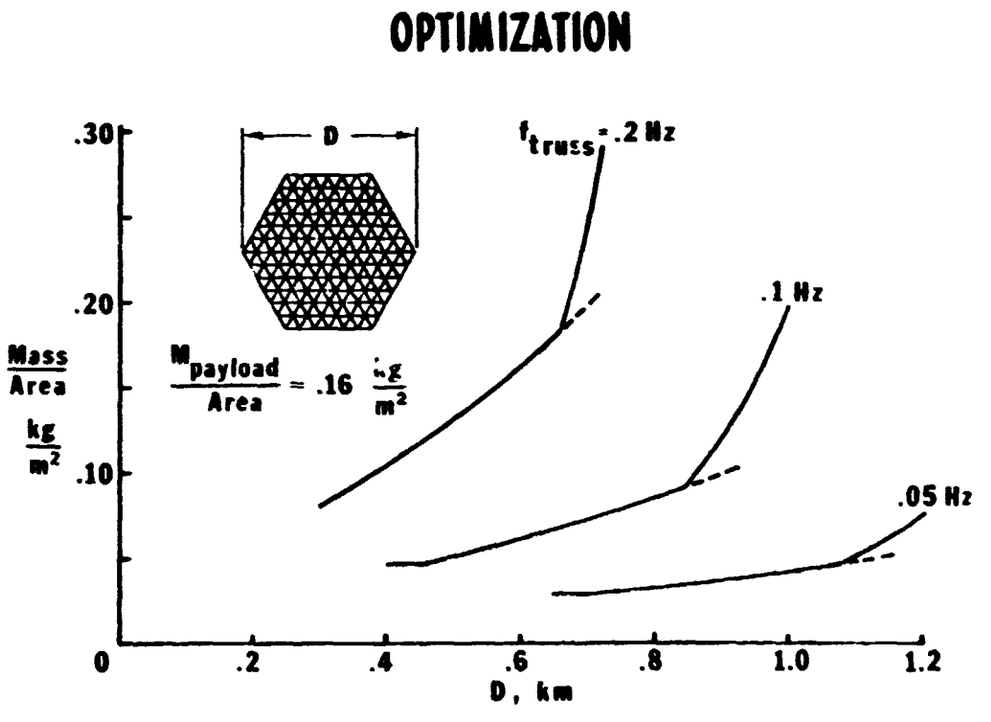

F-1

PACKAGING

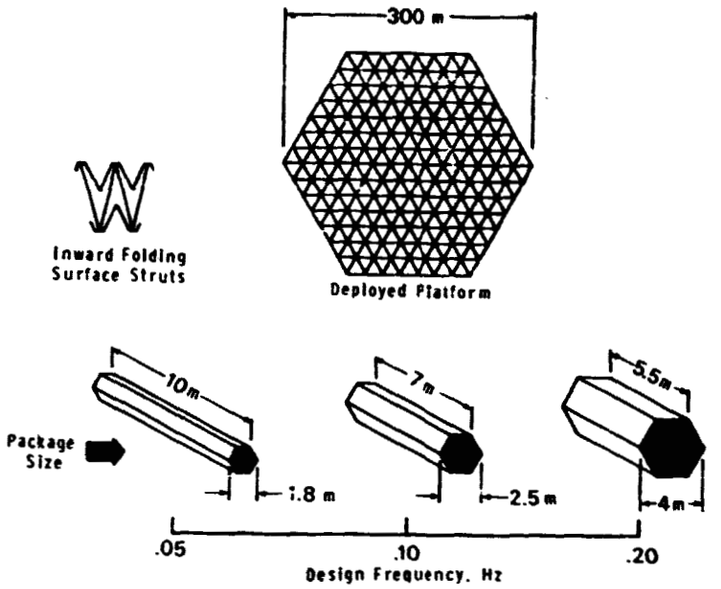

F-2

TRANSPORTATION

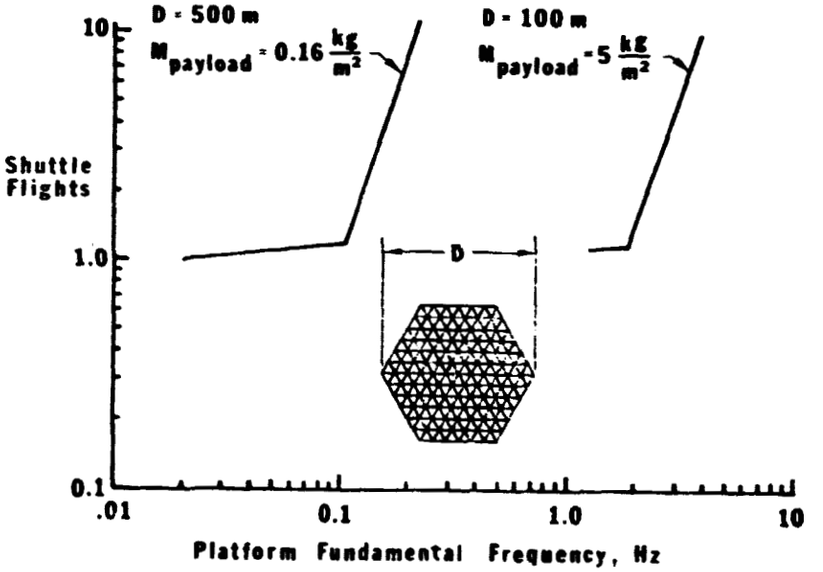

F-3

ANALYSIS AND DESIGN - PLATFORMS AND REFLECTORS

The spacecraft sizing activity requires an analysis for each design requirement considered. As appropriate design requirements are identified, analyses are developed and included in the sizing code for simultaneous consideration with all constraints. Results from one such analytical study (reference 1) are shown in F-4 where load concentrations resulting from missing members in truss plates were examined. The table shows that using a "classical approach" to estimate load concentration effects would result in concentration factors which are over a factor of 2 higher than those predicted by a discrete analysis.

Results from a preliminary analysis for sizing curved reflectors (reference 2) are shown in F-5. This figure shows the approximate dimension (L) of a triangular facet arrangement which is used to approximate a curved reflector surface for a specified surface error (δ_{rms}) and focal length (F). The triangular apices are assumed to coincide with supporting truss hard points (nodes). Therefore, L becomes the required strut length for the truss and must be considered in the design process.

MISSING MEMBER EFFECTS

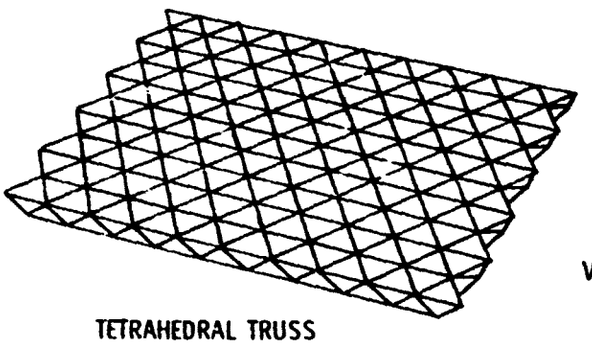

TETRAHEDRAL TRUSS

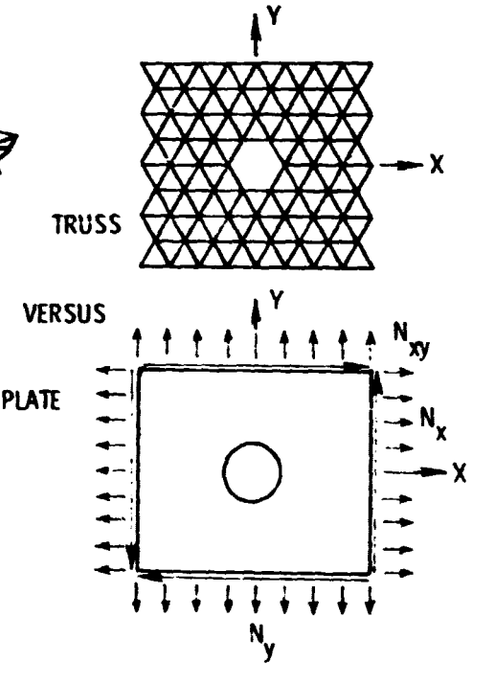

LOADING	TRUSS LOAD CONCENTRATION FACTOR	PLATE STRESS CONCENTRATION FACTOR
N_x	1.30	3.00
N_y	1.48	3.00
N_{xy}	1.56	4.00

F-4

FACETED ANTENNA DESIGN

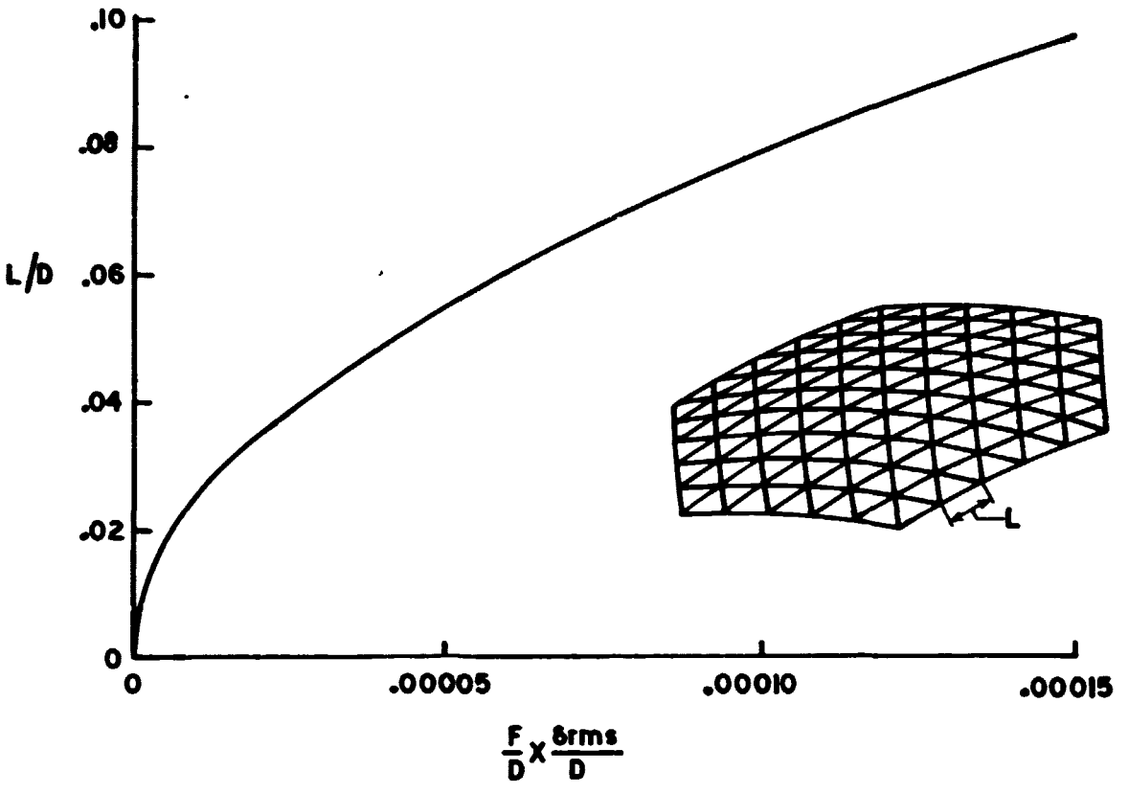

F-5

ANALYSIS AND DESIGN - BASIC ELEMENTS

A comprehensive characterization of various structural configurations for long columns was presented in reference 3, which compared structural efficiencies to identify preferred minimum mass concepts. Transportability of the structural configurations to orbit was not examined. In reference 4, a derivative of the cylindrical column which can be stacked for transporting is identified and is illustrated in F-6. This element-denoted the nestable column - is being studied and developed (reference 5) as a basic building block applicable to many types of built-up spacecraft structure. However, for extremely lightly loaded or long length applications, the solid skin nestable columns are minimum gage thickness constrained. Preliminary design calculations, based on analyses similar to reference 3, indicate that open or lattice skin configurations would offer significant mass savings as shown in F-6. In order to analyze and design this type of reticulated structure more accurately, a new buckling theory has been developed (reference 6). Some typical analytical results are shown in F-7 for a three longeron column which show that the discrete analysis predicts buckling, for some column proportions, at a lower load than is predicted by conventional methods.

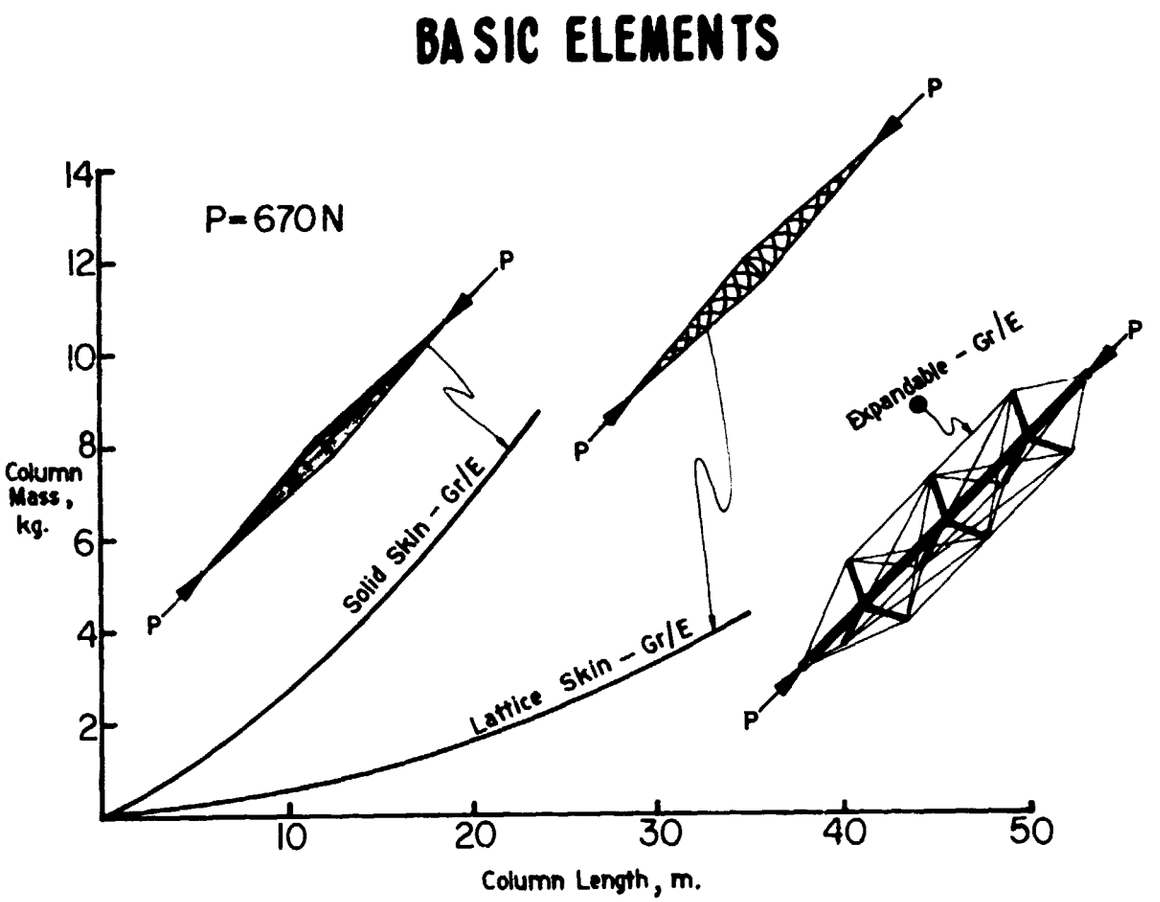

F-6

NEW BUCKLING THEORY PREDICTS DISCRETE EFFECTS IN LATTICES

TYPICAL CONFIGURATIONS

REPEATING GRID COLUMN

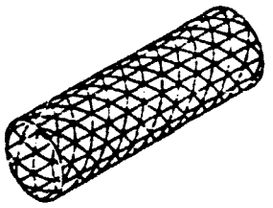

THREE ELEMENT BOOM

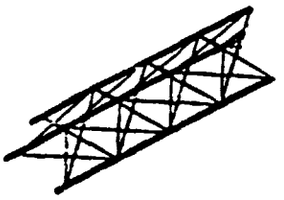

BUCKLING OF THREE ELEMENT BOOM

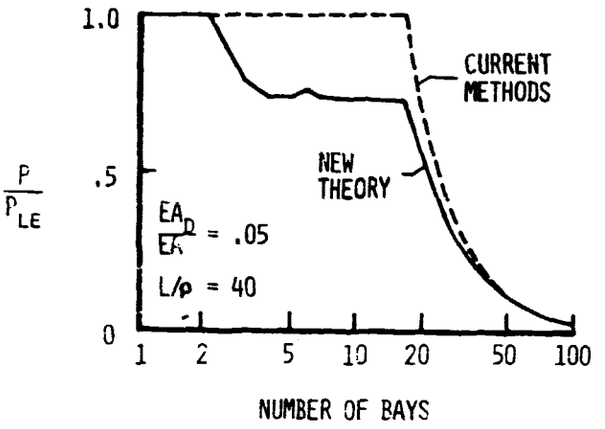

FEATURES OF THEORY

- o CONFIGURATIONS WITH EACH NODE HAVING SIMILAR GEOMETRY
- o FINITE ELEMENT BASED ON BEAM-COLUMN THEORY
- o PERIODIC MODE SHAPE
- o 6x6 DETERMINANT FOR BUCKLING OR VIBRATION

F-7

CONCEPT DEVELOPMENT

Pretensioned Column

One potential way in which the mass and volume of a compression strut may be reduced, is through the use of pretensioned elements which stabilize a central compression carrying member. The efficiency of one such column is shown in F-7 (previous page). Another example of this type of structure is shown in F-8, where a deployable pretensioned column is illustrated in the stowed and deployed position. This column is 5m in length, weighs approximately 0.4kg and was designed to buckle at 220 N. Preliminary testing indicated that it would carry approximately 260 N before buckling.

Joint Concepts

Along with the development of basic elements, ways to join erectable components are being studied. Several joint concepts which have been fabricated are shown in F-9. All models exhibit side entry and can be manually removed from, or inserted into, existing structure. However, disassembly of two joint models requires special tools. Also, all models are designed to be compatible with automated assembly of erectable structures. The joints were designed to represent actual flight quality components so that meaningful evaluations of each model's operational, structural and dynamic characteristics may be made.

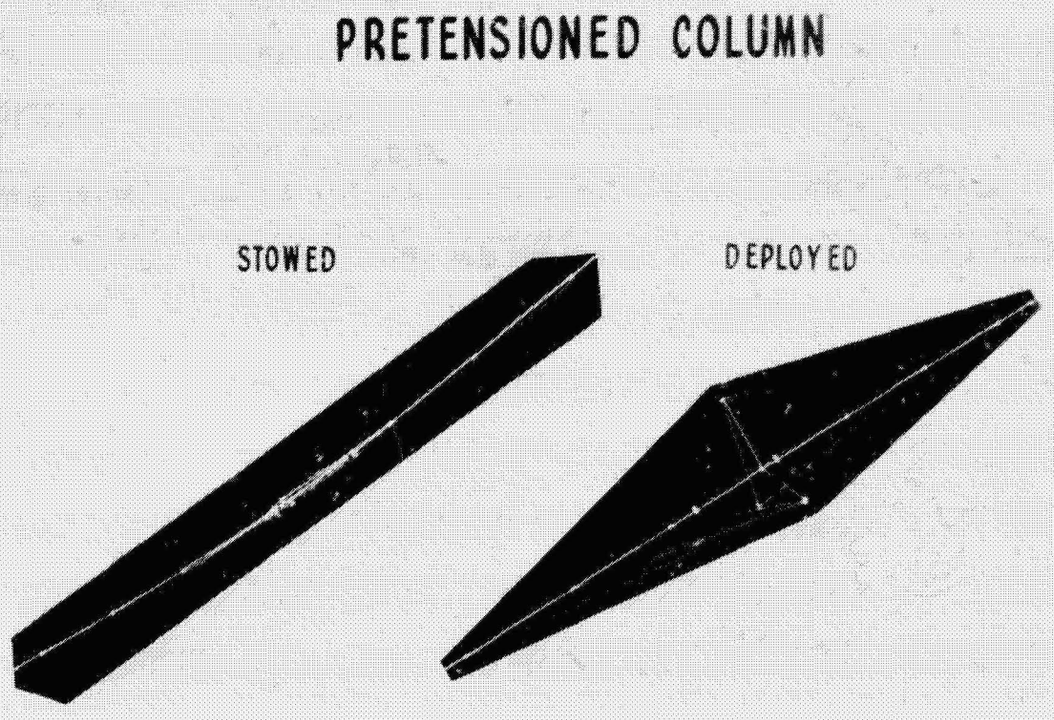

F-8

ORIGINAL PAGE IS
OF POOR QUALITY

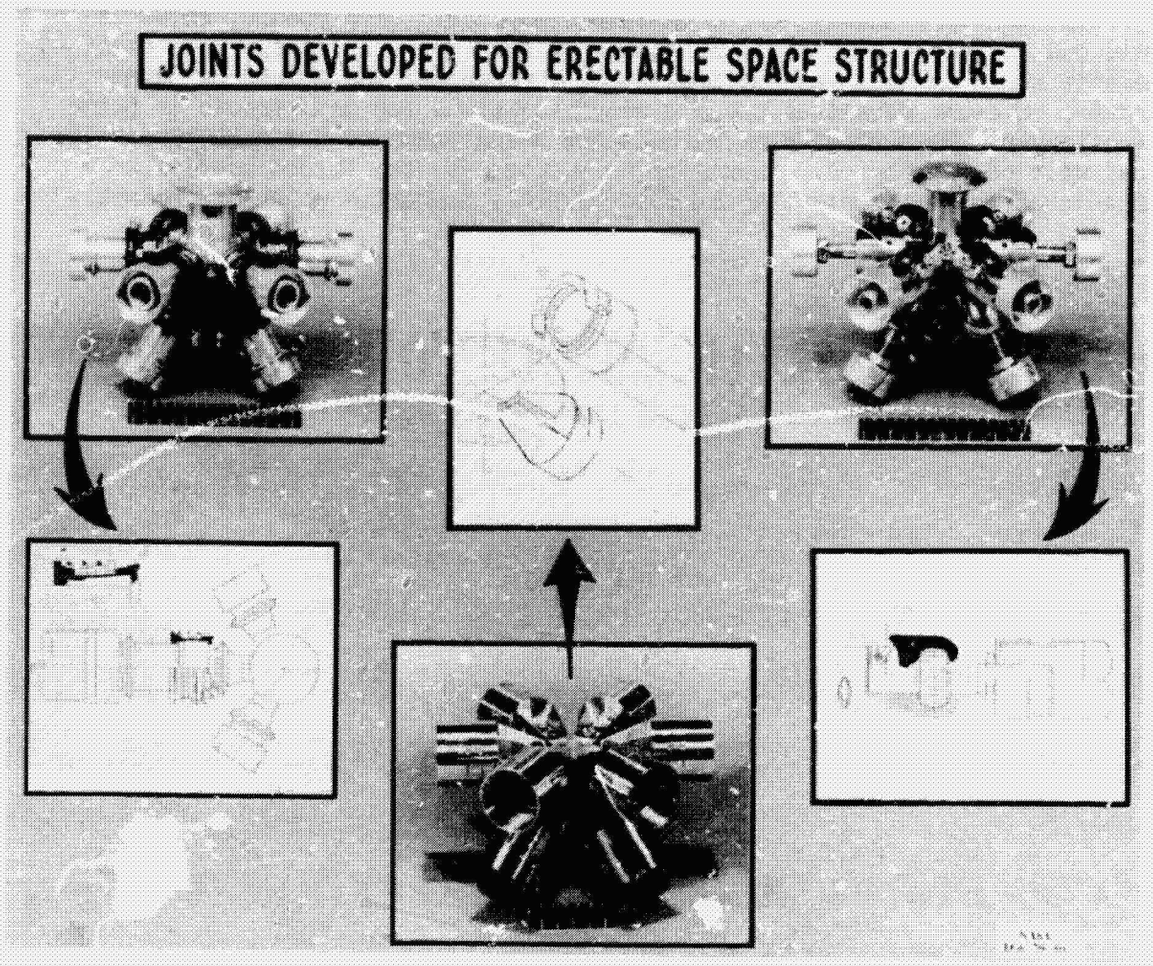

F-9

CONCEPT DEVELOPMENT

Deployable Module

A modular concept for constructing reflectors is shown in F-10 and F-11. The modules are connected together at three points in each surface. When assembled, the hexagonal planform of one side forms the closed reflector surface as shown in F-10. This concept incorporates a flat triangular facet approximation to a doubly curved reflector surface. Each module, shown in F-11, can be folded with all members stowed parallel for transport to orbit where it would be deployed and assembled. Currently, the necessary joint hardware is being developed and a deployment method for each module is being investigated. Mesh attachment methods are being examined and an engineering model will be fabricated. Packaging techniques for the folded modules are being investigated along with on-orbit assembly scenarios which are compatible with use of the Shuttle.

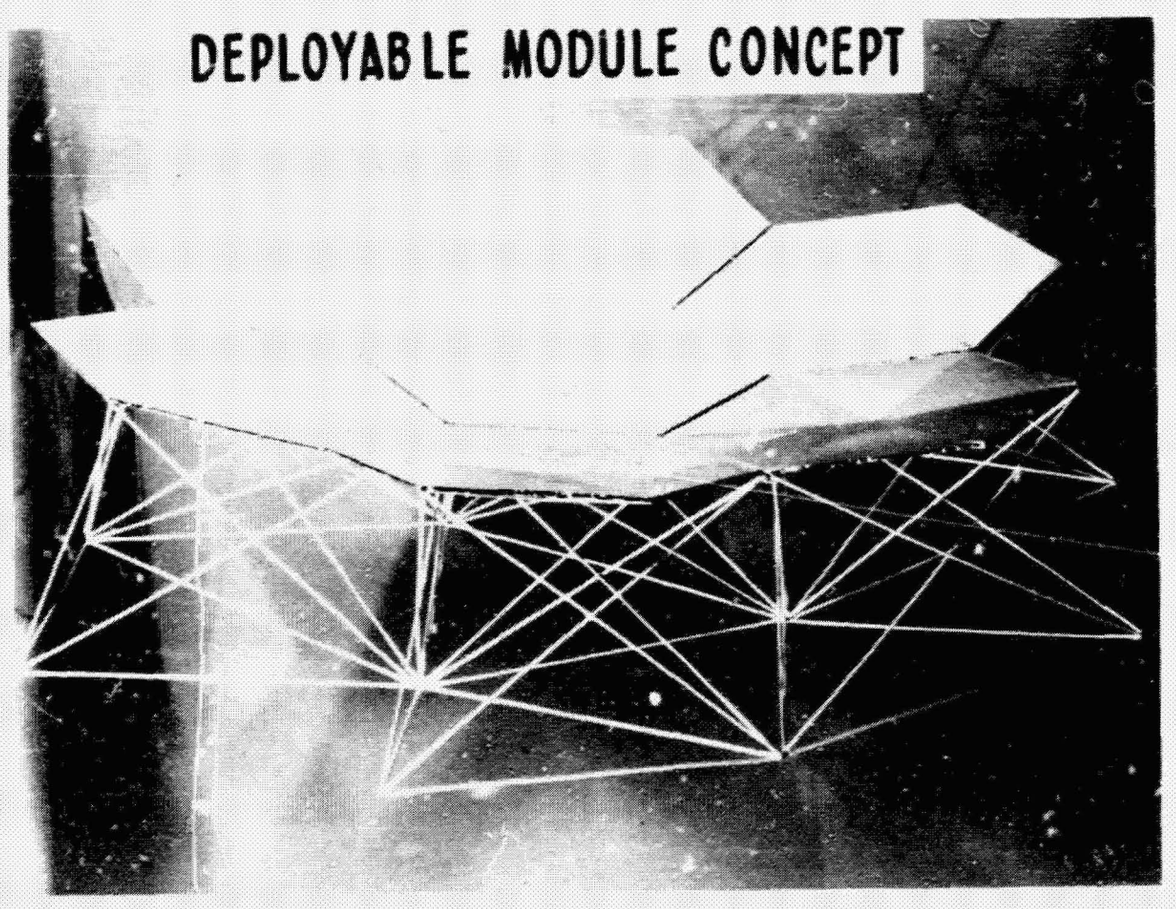

F-10

ORIGINAL PAGE IS
OF POOR QUALITY

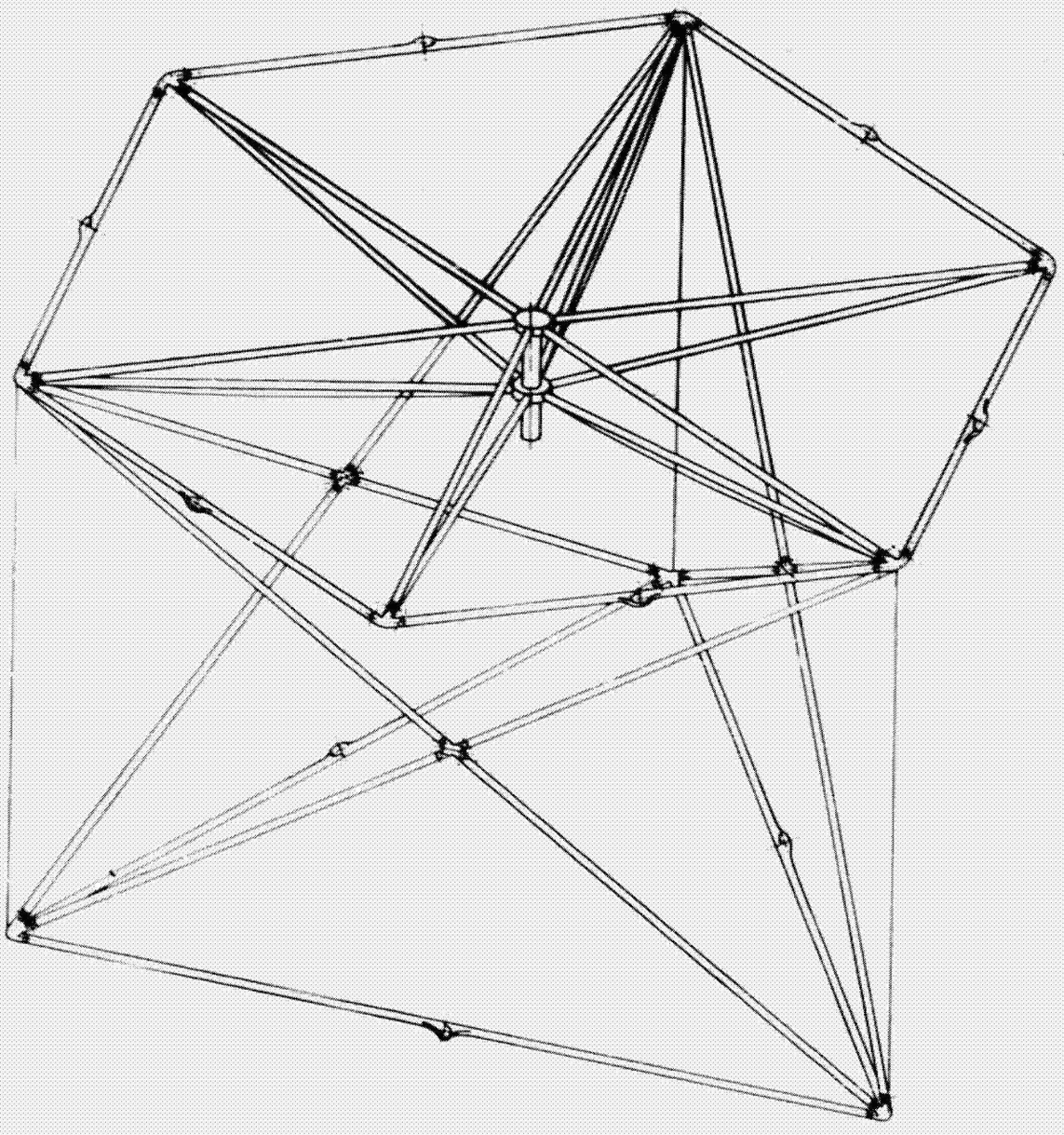

F-11

CONCEPT DEVELOPMENT

Deployable Truss Test

Deployable trusses are an important class of spacecraft structure. The ability to fabricate and package an entire spacecraft on earth for transfer to orbit where it is deployed into a functional status is a desirable goal. Foldable trusses, however, exhibit several features which can limit their utility unless overcome. Deployment kinematics of many folding truss members pose a challenge to designers to eliminate potential mechanical anomalies. To investigate this feature, and to determine member loads during an unrestrained deployment, the tetrahedral truss model shown in F-12 was fabricated and successfully deployed in zero-g. The truss was deployed using springs at the joints to provide deployment energy during the freefall experiment. Strains recorded during member lockup compared favorably with pretest analytical predictions.

DYNAMIC QUALIFICATION MODEL

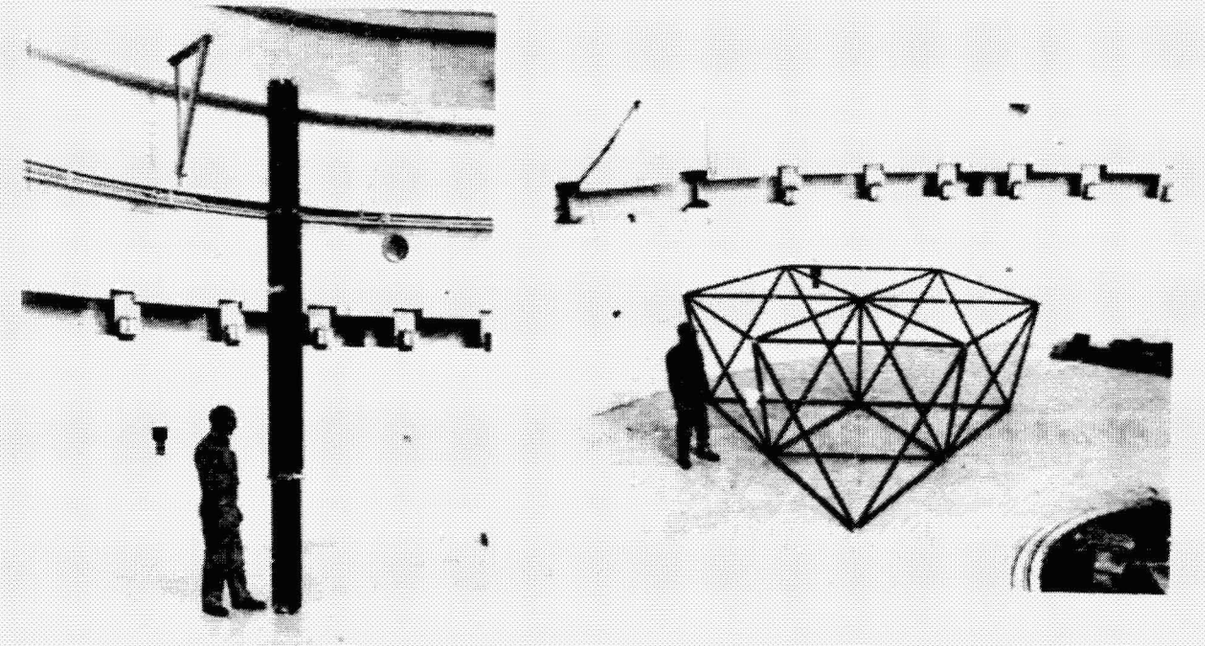

F-12

ASTRONAUT ASSEMBLY STUDIES

Man's capability for assembling structural components in a weightless environment has been investigated in the MSFC Neutral Buoyancy Facility. The test purposes were to develop preliminary timelines for various construction scenarios using Astronaut subjects and to obtain information on the types of hardware and assembly aids required by pressure suited workmen. A six strut tetrahedral cell, shown in F-13, was assembled by two pressure suited Astronaut subjects. The average assembly times (min/strut) for various pairs of subjects are shown in F-14. The bounding lines around the data indicate the general learning curve trend. As more tests were conducted, experience was gained and the assembly times decreased, appearing to plateau at about 5 min/strut for the tests shown. Using this preliminary labor rate, an estimate may be made of the size spacecraft which could be assembled during one Shuttle flight. Such an estimate is shown in F-15 where the Shuttle is assumed to have an operational on-orbit limit of seven days. The calculations are based on the crew being able to assemble 96,20 m struts/day. The figure shows that approximately a 200 m span spacecraft can be assembled. This result should not be considered in a quantitative sense but rather in a qualitative sense of whether man can make a significant contribution participating in the assembly process. The results to date, from a productivity viewpoint, indicate that man's capability should be further considered, particularly for proposed nearer term activities.

NEUTRAL BUOYANCY FACILITY TESTS

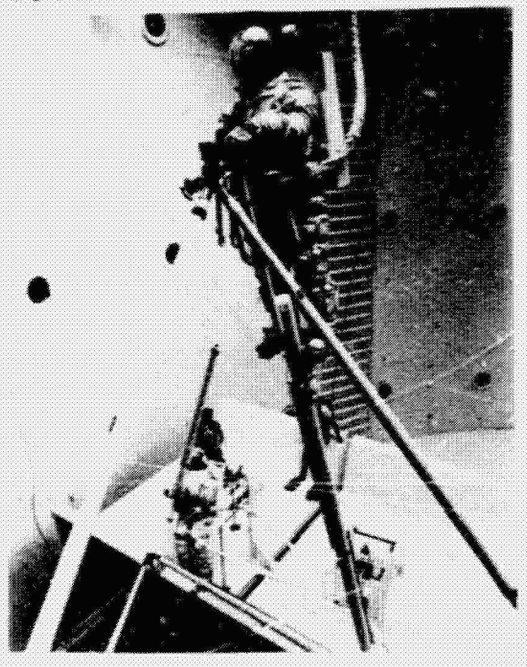

F-13

ASTRONAUT ASSEMBLY - NBF SIMULATION

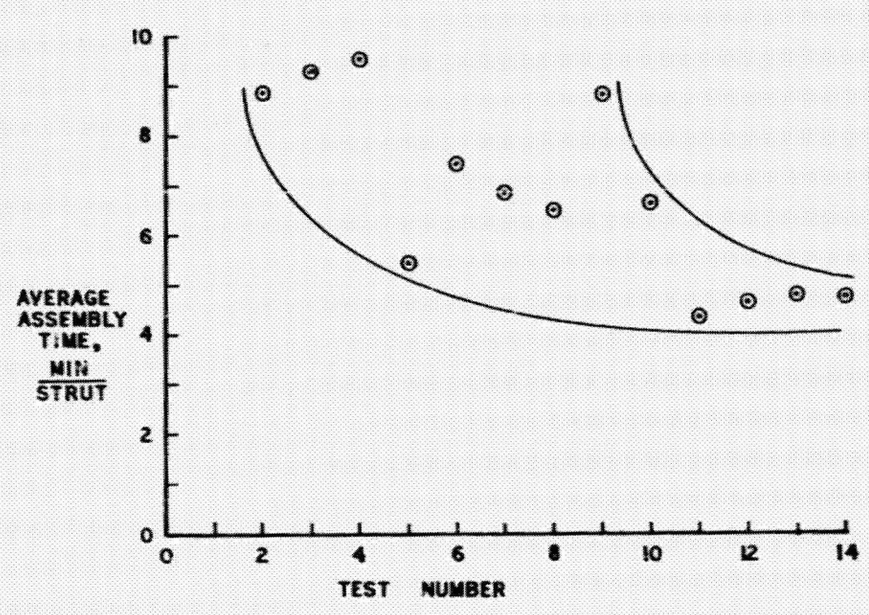

F-14

ESTIMATED CONSTRUCTION TIME

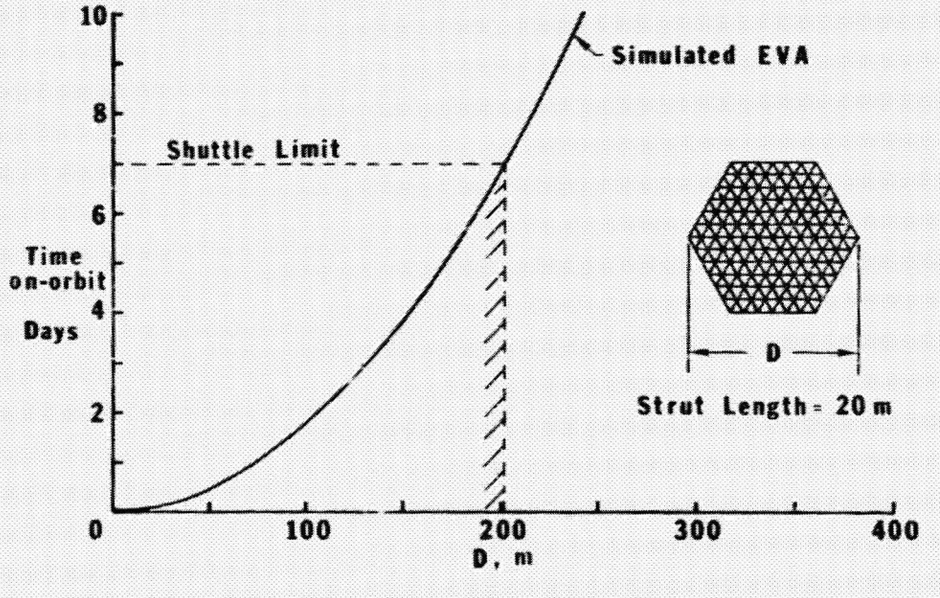

F-15

AUTOMATED ASSEMBLY STUDIES

Some proposed missions require structures sufficiently large that they are impractical to deploy or assemble by Astronauts. For such structures, it would be desirable to automate the assembly process as much as possible. Several automated concepts have been studied over the past year. An artist's illustration of preferred concept is presented in F-16, where the automated assembler is shown constructing a truss platform. A detailed sketch of the machine is shown in F-17. Conceptually, the machine is envisioned to be an assemblage of simple mechanisms which perform specific, sequential, repetitive operations to construct a repetitive truss structure using nestable struts. The machine consists of two pairs of swing arms, each pair connected by a tie rod (F-17), and a gimballed four-sided main frame. Cannisters, containing nested half-struts and/or nodal joints are attached to the arm and frame members. The machine operates by alternately swinging the upper and lower arms to walk from node to node (hardpoints) along the platform edge inserting struts and nodes which are dispensed from the cannisters as it progresses. Strut halves are snapped together as the machine steps using a strut assembly mechanism, an example of which is shown in the figure. Theoretically, in two days of operation this machine could assemble all of the 20 m nestable struts which Shuttle could transport to orbit in a mass critical mode (approximately 2600). The assembled structure would have an area of approximately 0.1 km^2.

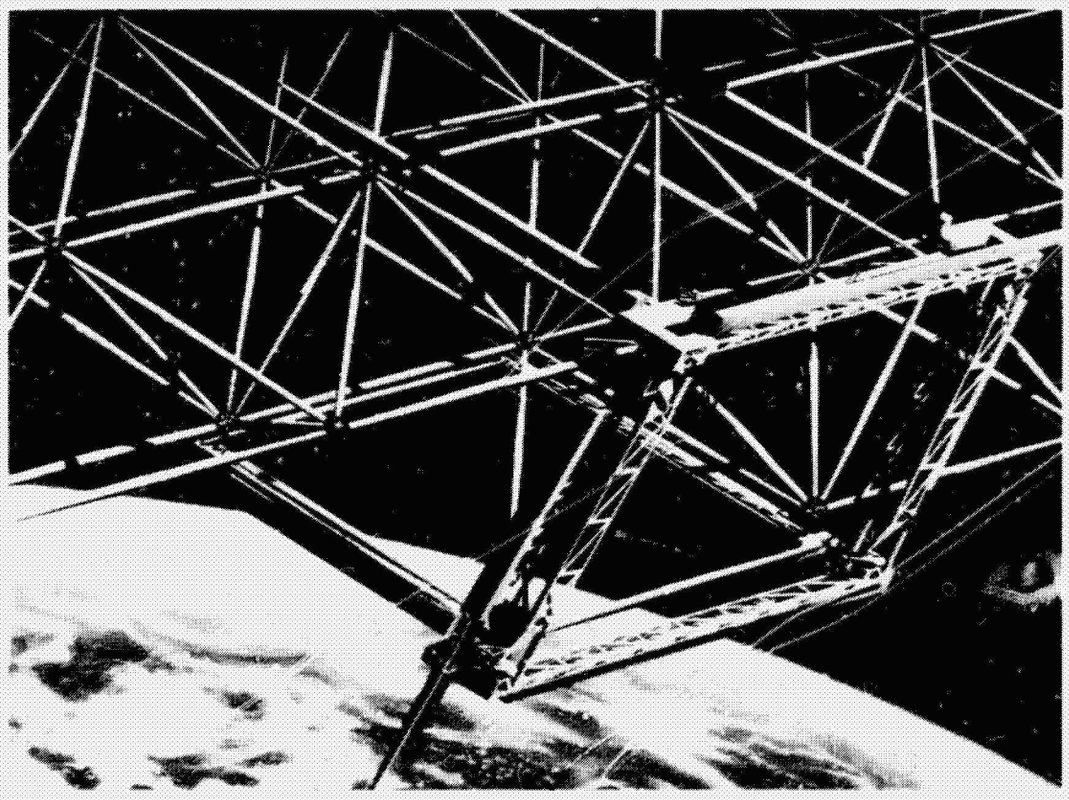

F-16

ORIGINAL PAGE IS
OF POOR QUALITY

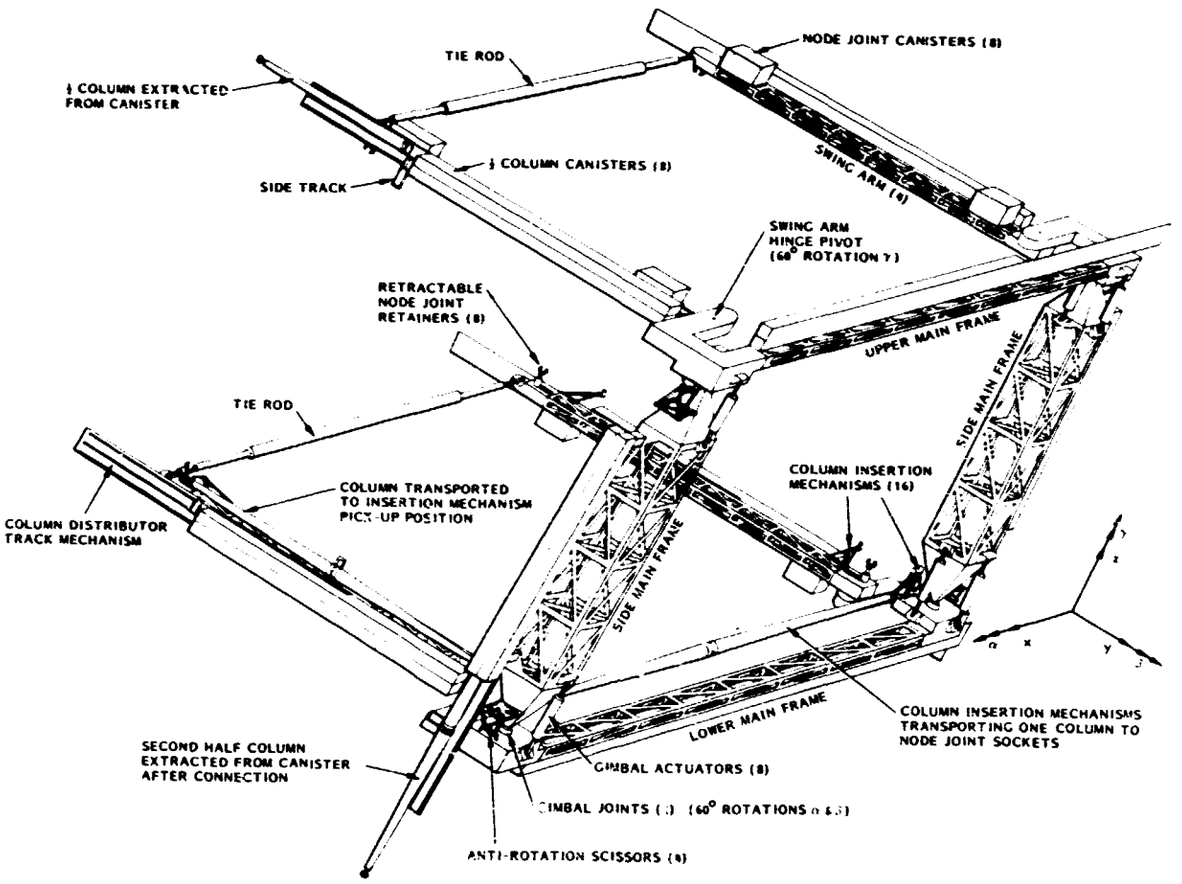
NODE JOINT CANISTERS (8)
TIE ROD
½ COLUMN EXTRACTED FROM CANISTER
½ COLUMN CANISTERS (8)
SIDE TRACK
SWING ARM (4)
SWING ARM HINGE PIVOT (60° ROTATION)
RETRACTABLE NODE JOINT RETAINERS (8)
UPPER MAIN FRAME
SIDE MAIN FRAME
TIE ROD
COLUMN TRANSPORTED TO INSERTION MECHANISM PICK-UP POSITION
COLUMN DISTRIBUTOR TRACK MECHANISM
COLUMN INSERTION MECHANISMS (16)
SIDE MAIN FRAME
LOWER MAIN FRAME
COLUMN INSERTION MECHANISMS TRANSPORTING ONE COLUMN TO NODE JOINT SOCKETS
SECOND HALF COLUMN EXTRACTED FROM CANISTER AFTER CONNECTION
GIMBAL ACTUATORS (8)
GIMBAL JOINTS (8) (60° ROTATIONS α & β)
ANTI-ROTATION SCISSORS (8)

F-17

REFERENCES

1. Walz, Joseph E.: Load Concentration Due to Missing Members in Planar Faces of a Large Space Truss. NASA TP-1522, 1979.

2. Agrawal, Pradeep K.; Anderson, Melvin S.; and Card, Michael F.: Preliminary Design of Large Reflectors With Flat Facets. NASA TM-80164, 1978.

3. Mikulas, Martin M., Jr.: Structural Efficiency of Long Lightly Loaded Truss and Isogrid Columns for Space Applications. NASA TM-78687, 1978.

4. Bush, Harold G.; Mikulas, Martin M., Jr.; and Heard, Walter L., Jr.: Some Design Considerations for Large Space Structures. AIAA J., vol. 16, no. 4, Apr. 1978, pp. 352-359.

5. Heard, Walter L.; Bush, Harold G.; and Agranoff, Nancy: Buckling Tests of Structural Elements Applicable to Large Erectable Space Trusses. NASA TM-78628, 1978.

6. Anderson, Melvin S.: Buckling of Periodic Lattice Structures. NASA TM-80187, 1979.

7. Jacquemin, G. C.; Bluck, R. M.; and Grotbeck, G. H.: Development of Assembly and Joint Concepts for Erectable Space Structures. Final Report: NAS1-15240, NASA CR-3131.

N80-19157

ERECTABLE/DEPLOYABLE CONCEPTS FOR LARGE SPACE SYSTEM TECHNOLOGY

W. E. AGAN
VOUGHT CORPORATION

CONTRACT NO. NAS8-33431

LSST 1ST ANNUAL TECHNICAL REVIEW

NOVEMBER 7-8, 1979

PAGE 216 INTENTIONALLY BLANK

OUTLINE

This presentation reports the progress and status that the Vought Corporation has made on the Erectable/Deployable Concepts Contract for the Marshall Space Flight Center. Mr. Erich Engler is the Contract Monitor. The order of presentation starts with a statement of the objective and scope which sets the stage for the work that has been completed. A brief schedule and the six individual tasks are identified along with what has been accomplished in each of those areas. A short, 16 mm, film of the deployment of a structural module demonstrates the applicability of this effort toward near term missions.

Outline

- Objective and scope
- Schedule
- Development of new erectable space structure concepts
- Preliminary design of selected systems
- Preliminary development of assembly techniques and aids
- Component fabrication and test
- Tolerance and utility analysis
- Payload/experiment carrier design study
- Module deployment film
- Summary

OBJECTIVE

The objective of this program is to develop new joints and/or elements to build a technical data base for near term space platform missions. This objective is fulfilled by identifying new structural members and attachments.

Objective

Contribute to the overall data base for various proposed missions/projects using erectable/deployable structures through the identification and analysis of new structural elements approaches and end attachments.

SCOPE

The contract is basically comprised of six tasks. The first task is a review of what work had been done in the past. From that data base, new designs are developed and compared to each other and existing designs. The most promising concepts are selected for preliminary design. Next is the development of preliminary assembly techniques and aids followed by a component fabrication and proof of concept test. Two additional tasks were added to the contract to emphasize utility incorporation and tolerance analyses into the overall design of the joints and members. The sixth task was a payload experiment design study.

Scope

Task 1: Development of new erectable space structure concepts

- **Review all LSS missions to date**
- **Review all LSS structural concepts proposed to date**
- **Generate new concepts**

Task 2: Preliminary design of selected systems

- **Evaluation and selection criteria**
- **Investigate existing concepts**
- **Establish new concepts**
- **Evaluate all concepts**
- **Preliminary design**

Task 3: Preliminary development of assembly techniques and aids

- **Requirements**
- **Definition and evaluation**
- **EVA/manned assembly demonstration and simulation program**

Task 4: Component fabrication and test

Task 5: Tolerance and utility analysis

- **Tolerance study**
- **Incorporation of utility provisions**

Task 6: Payload/experiment carrier design study

The contract go ahead was in April and completion will be in December. There are three tasks yet to complete: Task 4, the component fab and test which is now underway; the utility and tolerance analysis; and payload experiment carrier study, which will also be concluded in December. The final report will be issued in February.

Erectable Concepts for Large Space System Tech

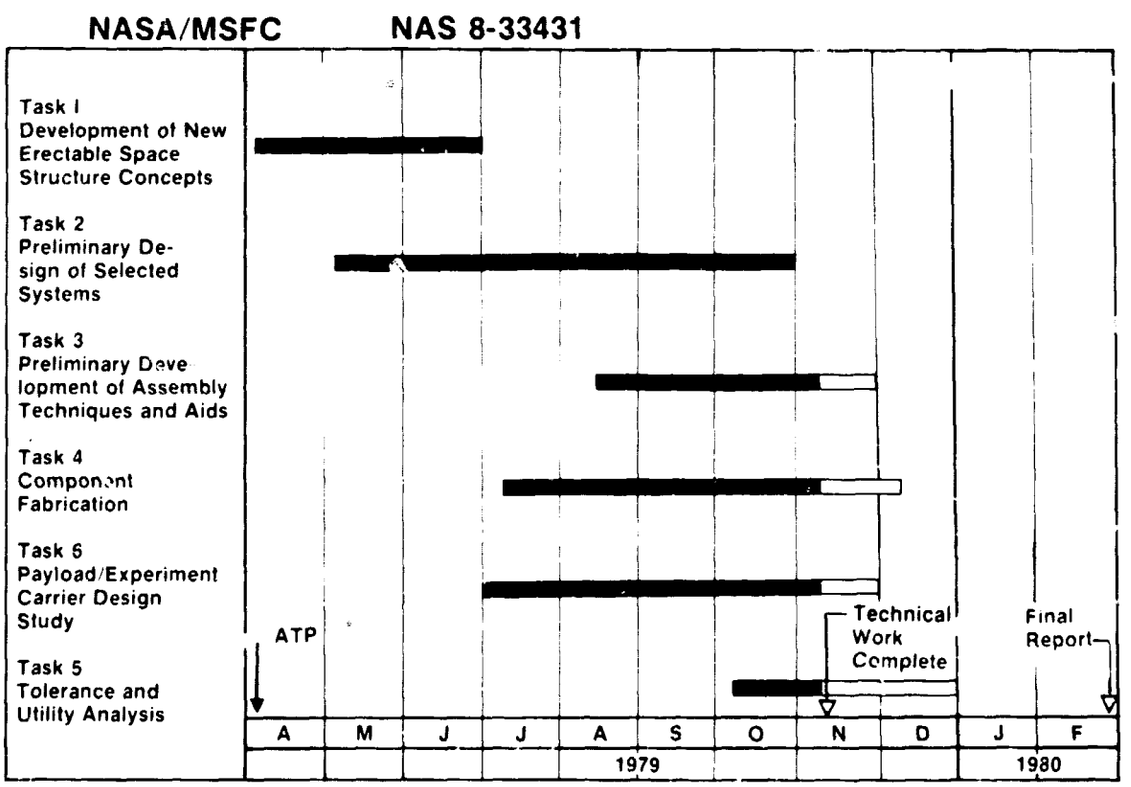

DEVELOPMENT OF NEW ERECTABLE
SPACE STRUCTURE CONCEPTS

The first task was to review the missions expected in the next five to fifteen years. As previously stated, the objective of the contract was to make our work applicable to the near term missions. Guidelines for the study included a 1985 to 1990 low earth orbit platform as a primary consideration, and geostationary structure as a secondary consideration. The resulting structure would have to function with or without Spacelab pallets and it would be assembled by man with machine assistance. That particular philosophy may be changing in the future for man to be an observer only. At least two RMS's would be available for deployment and assembly. The task was to develop either members or modules such that platforms or other applications could be built in a building block fashion. In this way the sequential assembly of the modules will permit constructing a variety of platform configurations. Attention was also to be given how to incorporate utilities, either electrical or fluid, into the members or into the joints or across the joints. Utilities provisions may very well influence the configuration or assembly procedure/equipment and must be considered upfront. Eleven (11) missions were considered applicable. Some examples reviewed are, Electronic Mail, Pin hole Satellite, deployable antennas and Science and Applications Space Platform that was studied toward the end of 1978. The Science and Applications Space Platform was believed the most applicable; therefore, our work has been directed at joints and/or members that would be useful in that endeavor.

Development of New Erectable Space Structure Concepts

Review of LSS Missions to Date

Objective: Identify near-term missions that would use erectable/deployable structures to provide applicability to concept evaluation and selection

Guidelines:
- 1985-1990 LEO platform
- GEO requirements on secondary basis
- Function with or without spacelab pallets
- Assemble by man with machine assistance
- Two RMSs available for deployment and assembly
- Utility provisions

Results: Eleven (11) LSS missions are applicable
Science and application space platform most applicable

ORIGINAL PAGE IS
OF POOR QUALITY

DEVELOPMENT OF NEW ERECTABLE

SPACE STRUCTURE CONCEPTS

Out next task was to look at what industry had done in the past. The reasons for that approach were to establish a point of departure, to avoid duplication and also to stimulate thought process for generating new ideas. At a minimum, 43 existing joint ideas that had a practical merit were identified. A patent search, going back to the 1890's, revealed 73 different insertion type joints that could possibly work. Approximately 45 structural elements were identified.

Development of New Erectable Space Structure Concepts

Review of LSS Structural Concepts Proposed to Date

Objective: To collect previously proposed structural joints and elements to

- Establish point of departure for new ideas
- Avoid duplication
- Stimulate idea spinoff

Results:

— Forty-three (43) joining methods were identified

— Seventy-three (73) patented joining methods were reviewed

— Forty-five (45) structural elements or methods were identified

DEVELOPMENT OF NEW ERECTABLE
SPACE STRUCTURE CONCEPTS

Prior to the generation of new ideas through brainstorming, the types of joints that would actually be required were identified. Single member strut or unions basically require either a side latching type of joint or insertion type of joint, or possibly a hybrid of the two. Deployable modules, which are comprised of several members and go through kinematic motion to a final configuration, require approximately nine (9) different types of joints or nodes. Examples are single pivot or double pivot, telescoping members, etc. From the background of previous ideas and the above requirements 72 different types of joints were generated. Very simple to very complex ideas were considered. The 72 ideas did not necessarily have practicality; they were just ideas. Similarly, 38 different structural members were generated. Again, they ranged all the way from the very simple linear members to a multi-member deployable module. This wide range of concepts was considered to be a structural member.

Development of New Erectable Space Structure Concepts

Generate New Concepts

Objective: Develop new structural joints and elements

Required joint types:

Deployable Modules:	Strut/union erectables:
1. Single pivot node	1. Side latching joints
2. Double pivot node	2. Insert joint
3. Rotating intermediate pivot fitting	3. Hybrids
4. Stretch members (telescope)	
5. Shrink members (telescope or knee joint)	
6. Removable members	
7. Module-to-module attachment	
8. Nodal knee joint	
9. Mission equipment attach	

Results:
— Seventy-two (72) new joining ideas were generated
— Thirty-eight (38) new structural member ideas were conceived

PRELIMINARY DESIGN OF SELECTED SYSTEMS

Having the multitude of ideas, a screening process was used to eliminate the impractical ones. This was done on an engineering qualitative basis. The 72 joints and 38 members were screened to 14 joining devices and 8 members, including the joints and members that had been previously proposed. Those results were then subjected to a more detailed figure of merit type of evaluation. Examples of evaluation parameters are ease of capture, ease of locking, alignment, adjustment, durability, thermal distortion, etc. From that paired comparison evaluation, 7 joints and members were selected for further development in preliminary design. Those seven (7) concepts will be discussed.

Preliminary Design of Selected Systems

Objective: Evaluate and select most promising structural concepts and develop through preliminary design

Procedure:

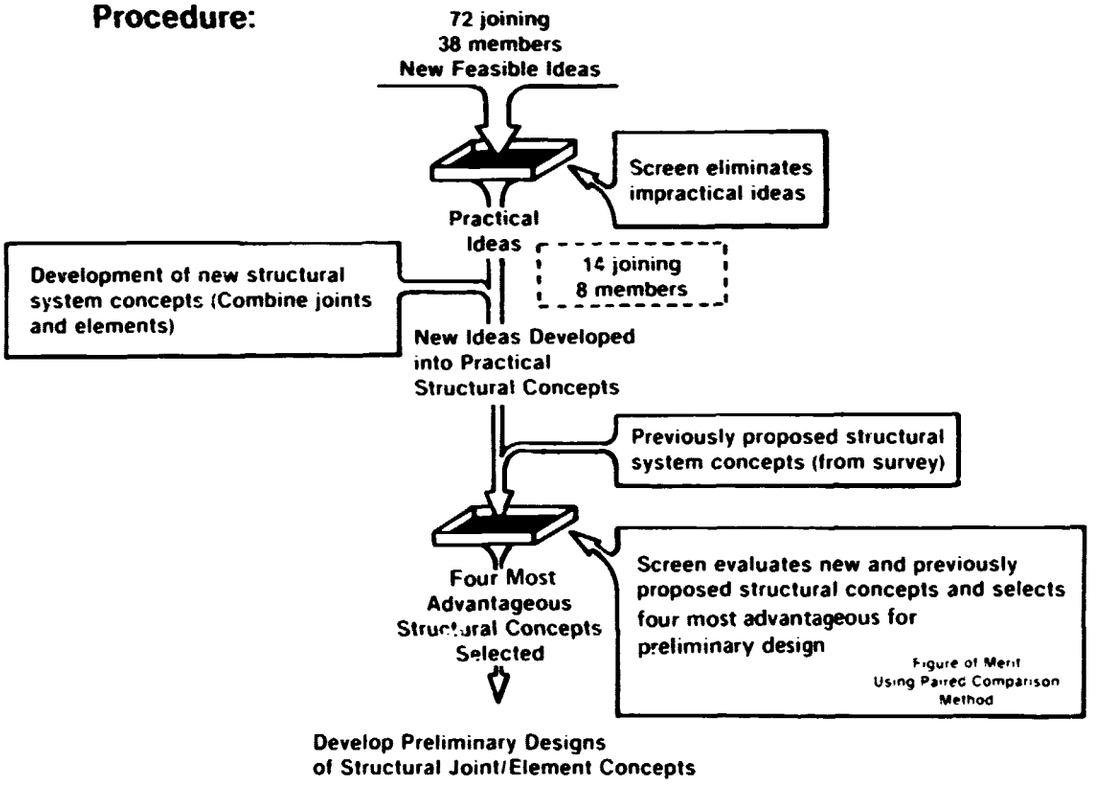

The first joint is an automatic coupler. Its characteristics are that it can be inserted either in the axial direction or from the side. It is a hybrid; it can be inserted in either direction. It has $\pm$ 12.5 mm gathering range and a soft capture misalignment of $\pm 5^{o}$. Another feature of this particular joint is that the release mechanism, although not finely perfected here, is on the member end as opposed to the union end. In this case the release mechanism can be operated by a person using one arm or one RMS such that removal after release can be in one motion. This is as opposed to releasing from the union end and pulling the member away, which would require two (2) appendages.

Preliminary Design of Selected Systems

Automatic Coupler Clevis Joint

Design 36

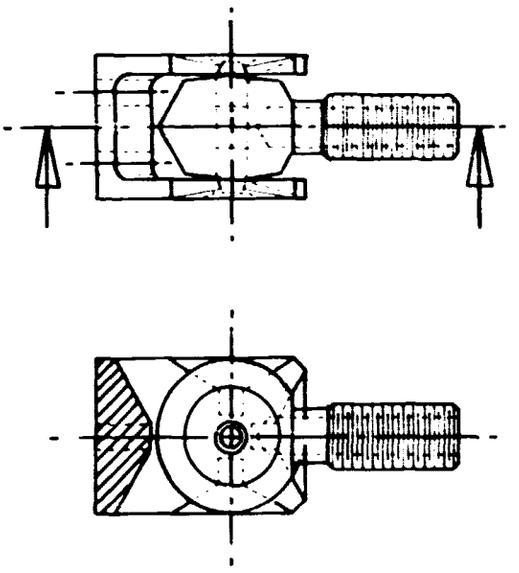

Characteristics:

1. Insert either side or end
2. ± 12.5 mm gathering range
3. Soft capture misalignment: ±5° out of plane or ± 1 mm axial
4. Hard locks automatically as misalignment is removed
5. ±90° pivot as a clevis
6. Can be released

The second concept is a side latching detent joint. It has the same characteristics as the automatic coupler in that it has a wide angle of insertion. It can be inserted in the 0° or 90° direction. Both of these parts have been fabricated and have gone through proof of concept testing.

Preliminary Design of Selected Systems

Side Latching Detent Joint

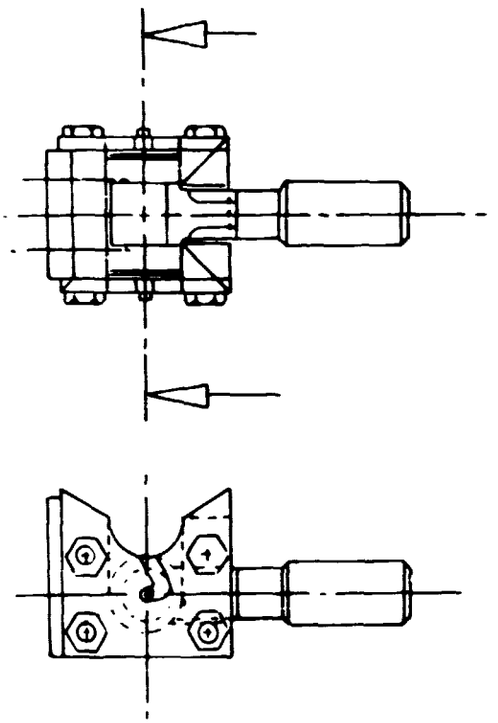

Design 27

Characteristics:

1. Insert one side
2. ±12.5 mm gathering range
3. Hard locks when fully inserted as misalignment is removed
4. +90° pivot as a clevis

Photograph of the automatic coupler and side latching detent joints disassembled.

The black scale is 15 cm long.

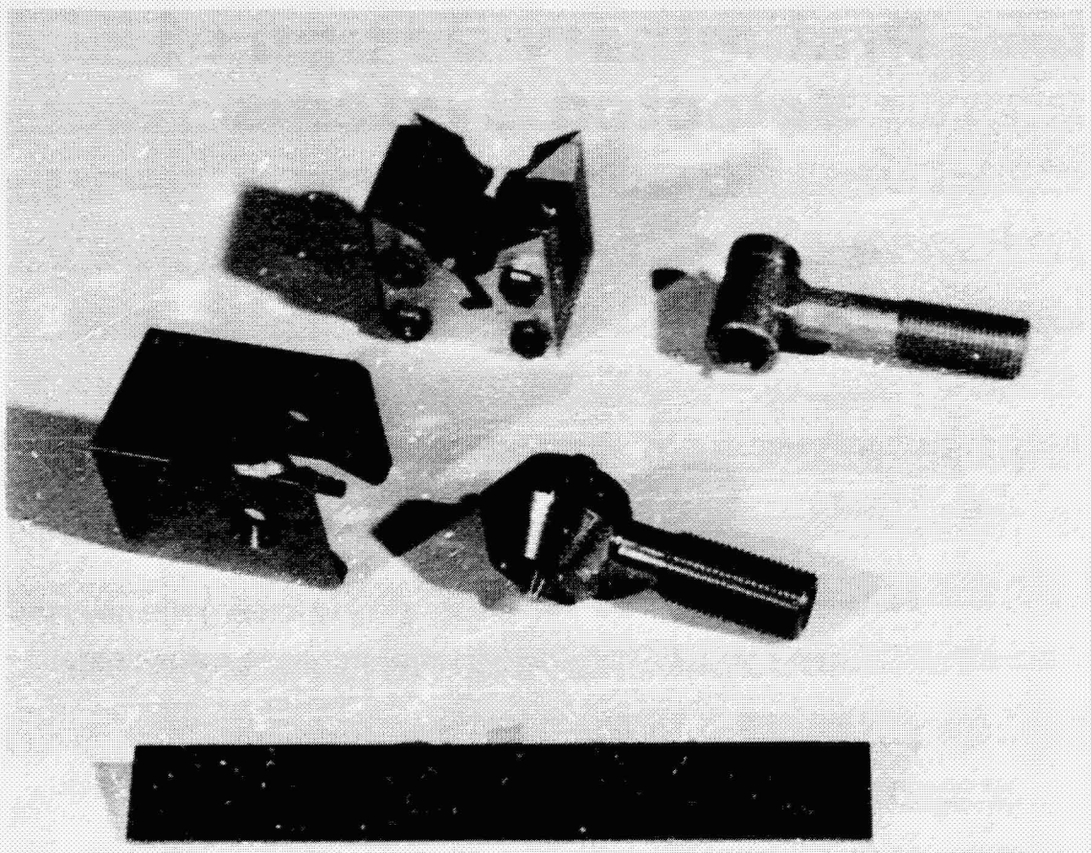

ORIGINAL PAGE IS
OF POOR QUALITY

This is a photograph of the automatic coupler and side latching detent joints assembled. The black scale is 15 cm long.

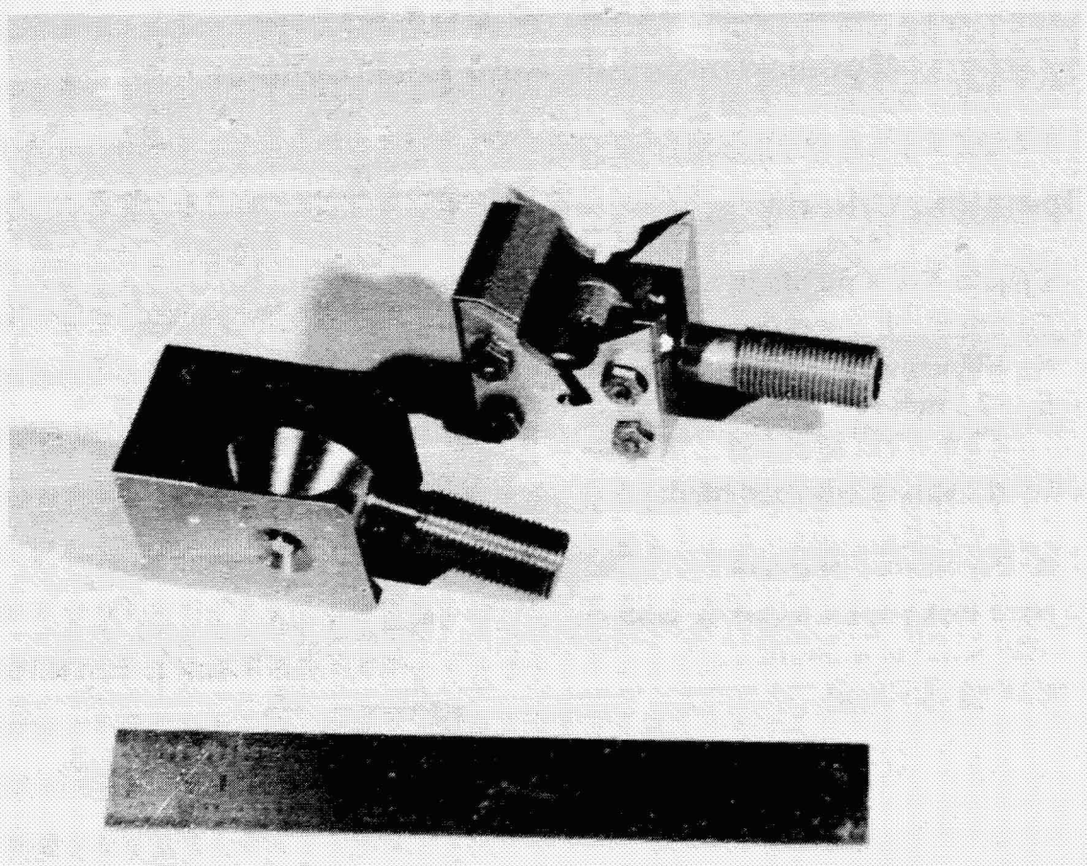

The third joint concept is called a module-to-module coupler. Because the other four selected elements were modules, a method of connecting two modules together was required. Most likely the two modules will never be perfectly aligned. Therefore criteria were established so that one of the four joints would connect or soft capture when there is a 10° misalignment between modules. Once the modules are aligned, possible joint mismatch due to tolerances may exist in the mating plane (radial) and perpendicular to the mating plane. Soft capture in the plane is $\pm$ 12.5 mm radial and 1 mm radial for hard capture. Capture perpendicular to the mating plane will occur if all four joints are within 2.5 mm.

Preliminary Design of Selected Systems

Module-To-Module Auto Lock Coupler

Concept 22A and 22B

Operating Criteria:

1. Couple 3 or 4 points in a plane
2. Soft capture misalignment:
   A. 10° angular
   B. 12.5 mm R
      2.5 mm out of plane
3. Hard capture misalignment:
   A. 1 mm R
   B. 2.5 mm out of plane
4. Hard locks upon insertion with no additional operations
5. Can be released

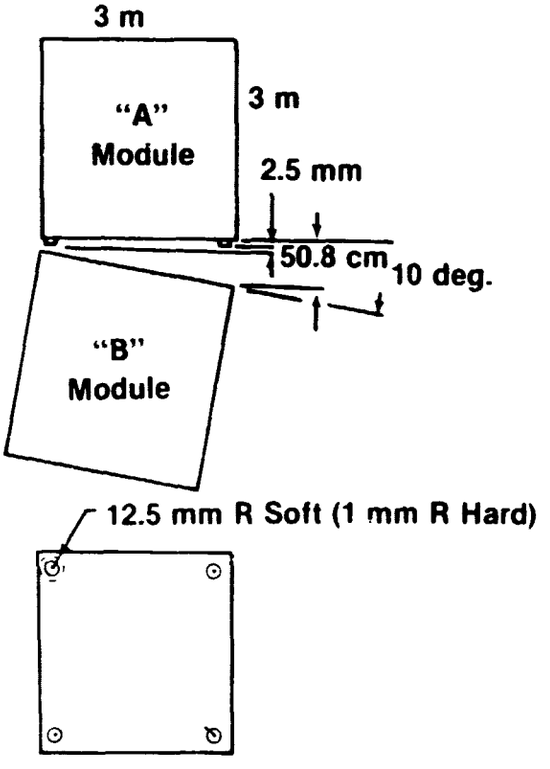

The module-to-module concept is a typical probe drogue type of joint, a conical surface on the front and spherical surface on the back. The probe part is the less expensive; it is mounted to the corner of the modules. There are three fingers around the circumference of the drogue part. As the probe enters the drogue, the fingers are pushed back out of the way and after passing over center, the fingers - which are spring loaded - return to capture the probe. There is 2.5 mm of forward motion permissible at that position. This allows the four joints to be engaged and locked and able to carry loads while misaligned by 2.5 mm perpendicular to the mating plane. As the probe proceeds into the drogue the fingers continue to capture the element thus preventing reverse motion.

Preliminary Design of Selected Systems

Module-To-Module Auto Lock Coupler

Design 22B

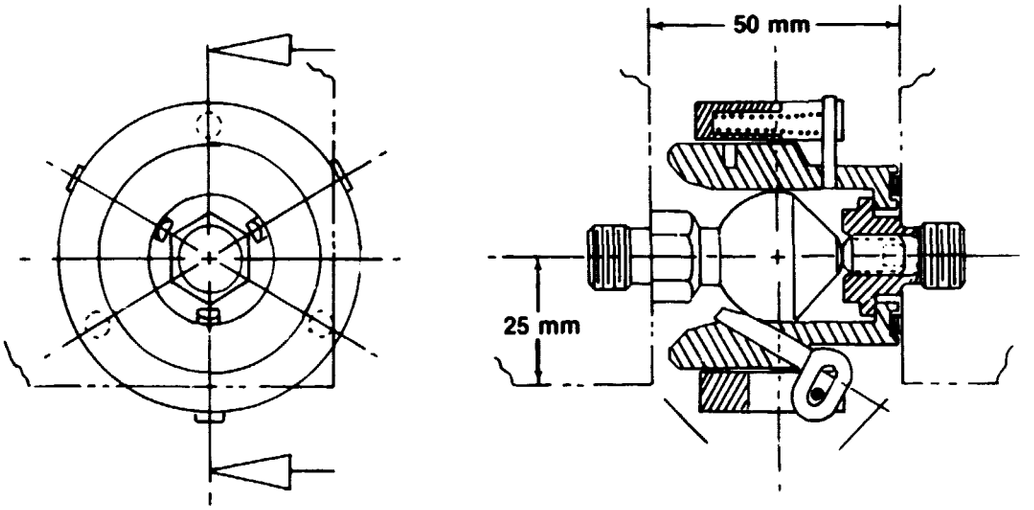

The fourth element is a deployable module. The 1/10 scale model shown below is a double cell double fold configuration. Each cell is a 3 m cube. A variety of joints and members exist in this structure. There are telescoping diagonals, single clevis joints, and double swivel clevis joints. The maximum number of members at a node is nine (9). The probe part of the module-to-module coupler shown previously will be located externally at each node to provide attachment of another module or experiment pallets.

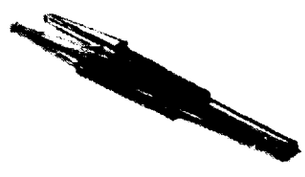

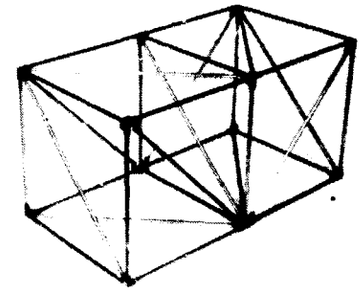

PRELIMINARY DESIGN OF SELECTED SYSTEMS

Packaging is an important aspect in the transportation of space structures. The remaining three (3) concepts studied are different packaging arrangements for the 3m cubic cell. The total packaging volume required to assemble a nominal structure arm, 3m x 3m x 18m, of the Science and Application Space Platform is shown. Concept 35 has a large cross section but is very thin. The longitudinal members are loose and will require additional orbital assembly time. Concept 38 is a single fold configuration and requires the largest volume. Concept 39 stows in a long narrow space. The hybrid configuration is similar to Concept 35 except that it does not have any loose members. Therefore, assembly time is reduced at the expense of cargo volume. These four packaging configurations offer different form factors which may be coordinated with Orbiter cargo manifests.

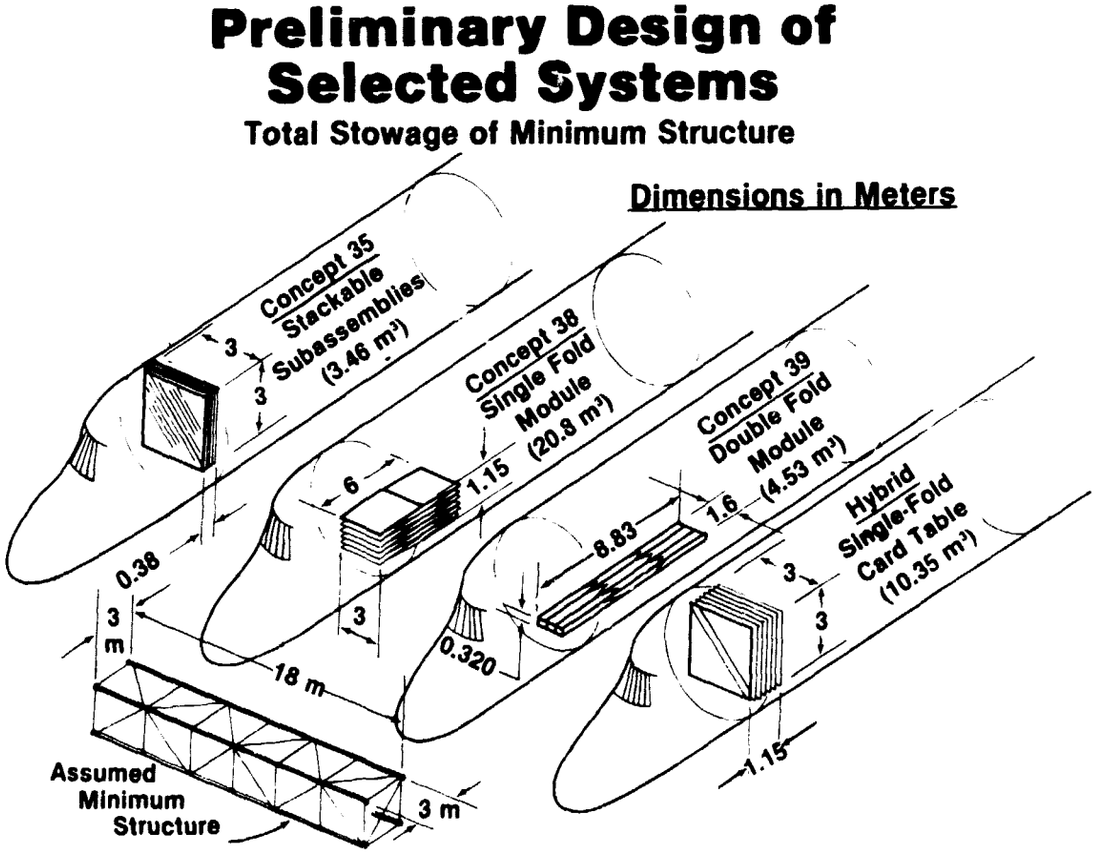

Additional dimensional details are shown for the four packaging schemes.

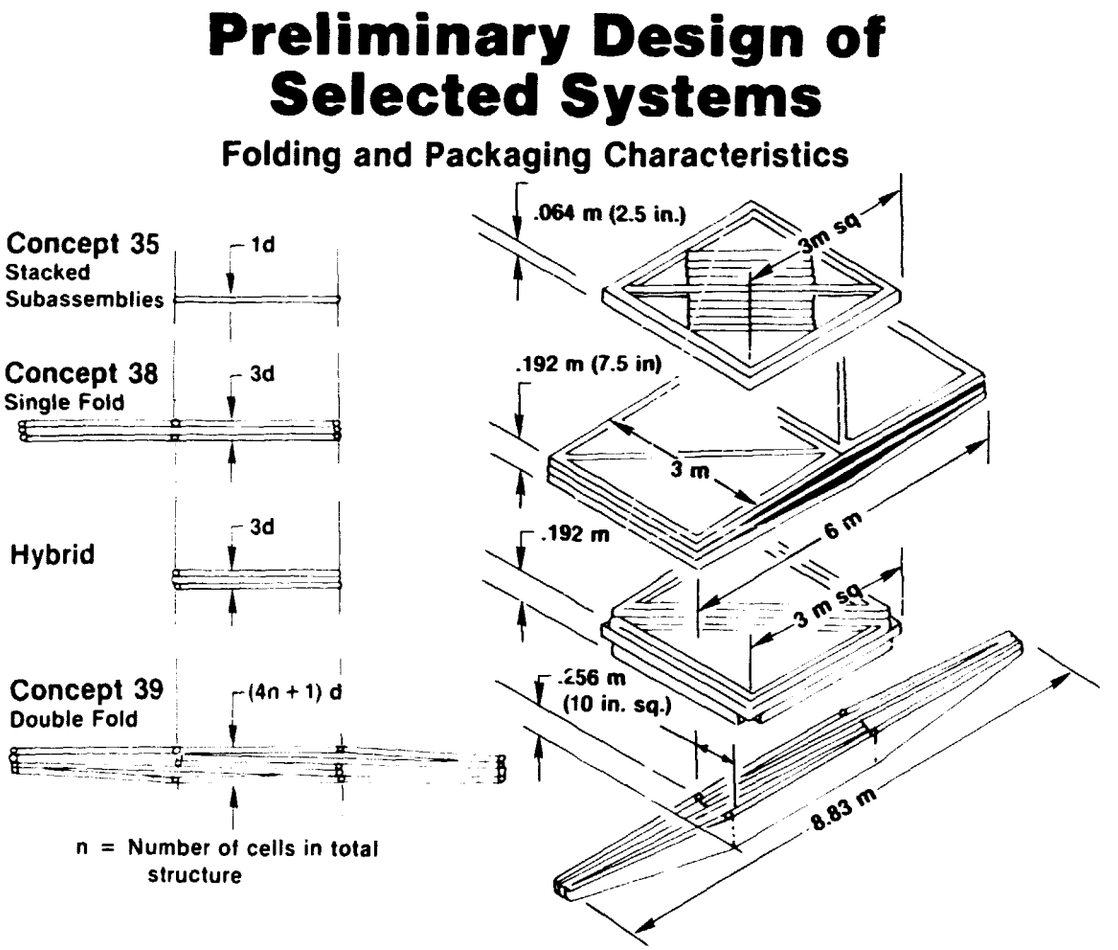

The results of those four packaging schemes are presented on a comparative basis. The lengths or areas of various types of structures that could be developed with the four configurations are shown. For example, the double fold concept will provide a 3 meter by 3 meter linear type platform 984 meters long if a full cargo bay was available. If the EVA and OMS kits are in the Orbiter then 492 meters of linear platform can be transported. Similar data are shown for a frame, cube, and wide area platform. The double fold element can be configured with 6m elements and still fit within the cargo bay and provide a linear platform 6m x 6m x 984m.

Preliminary Design of Selected Systems

Platform Configuration Options and Size Comparisons 1.5 and 3m Struts

		Concept →	35 Subassembly		38 Single Fold		39 Double Fold		Hybrid "Cardtable"	
		Strut Size →	3m	1½m	3m	1½m	3m	1½m	3m	1½m
A	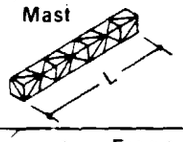	Full Bay	864	1.728	144	288	984	984	288	576
		With EVA & OMS	675	1.350	96	216	492	738	225	450
B	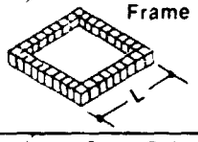	Full Bay	216	432	36	72	246	246	72	144
		With EVA & OMS	166	338	24	54	123	184	56	112
C	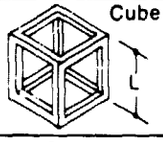	Full Bay	72	144	12	24	82	82	24	48
		With EVA & OMS	-	12	8	18	41	62	18	38
D	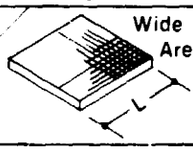	Full Bay	50.9	50.9	20.8	20.8	54.3	38.4	29.4	29.4
		With EVA & OMS	45.0	45.0	17.0	18.0	38.4	33.3	26.0	26.0

* Numbers in table are dimension "L"

PRELIMINARY DEVELOPMENT OF
ASSEMBLY TECHNIQUES AND AIDS

Preliminary development of assembly techniques and aids task was required to develop timelines and identify the construction aids and transportation requirements that would be necessary to fulfill the near term applications for the joints and members developed.

Preliminary Development of Assembly Techniques and Aids

Objective: Identify and define steps, procedures, equipment, complexity/timeline estimates for transportation and construction of reference platform using selected design concepts.

PRELIMINARY DEVELOPMENT OF
ASSEMBLY TECHNIQUES AND AIDS

An example of the double fold double cell module packaging arrangement with the 25 KW Power System is shown below. Other arrangements may also be used.

Preliminary Development of Assembly Techniques And Aids

Typical Orbiter Installation

18m Strongback with Existing Concept — 25 kw Power System

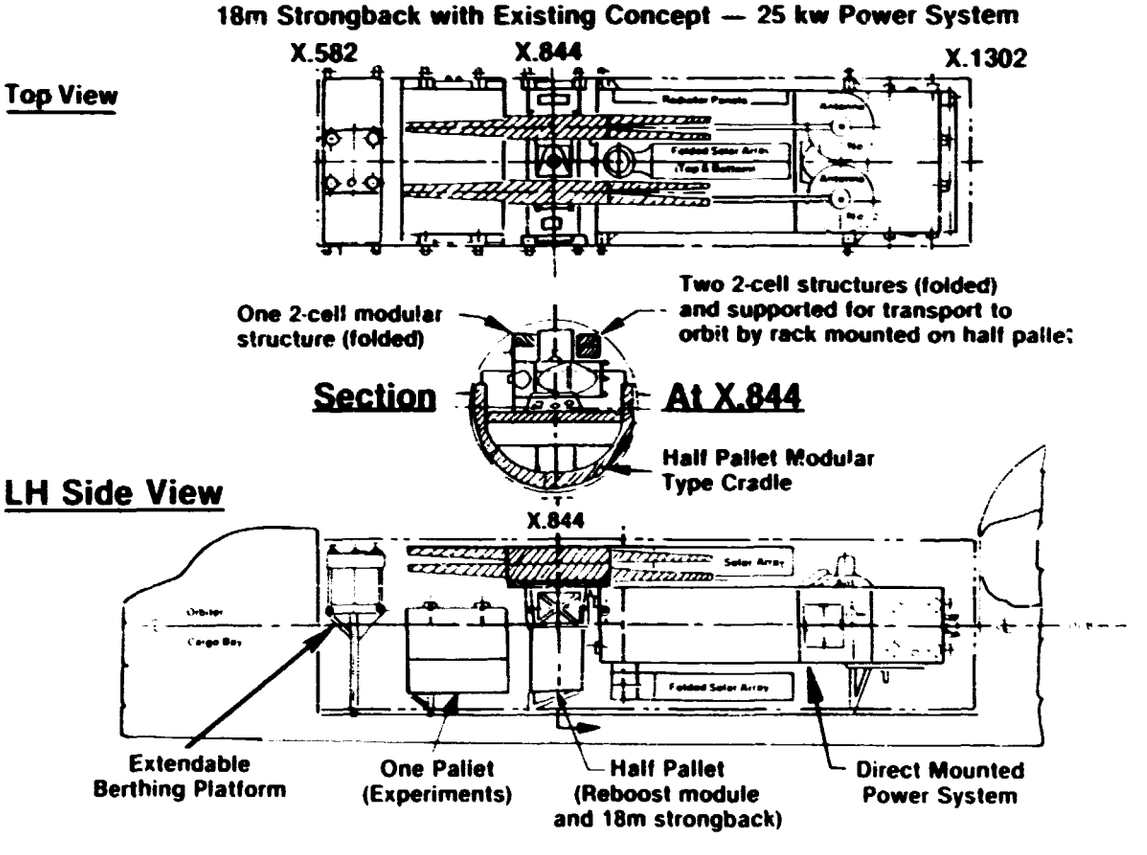

PRELIMINARY DEVELOPMENT OF
ASSEMBLY TECHNIQUES AND AIDS

One (1) 3m x 3m x 18m platform arm is shown being deployed by the RMS from its stowed (collapsed) position. A 16mm movie has been taken of this operation. Deployment feasibility has been verified.

Preliminary Development of Assembly Techniques And Aids

Kinematics of Deployment for an 18m Strongback from Orbiter Cargo Bay

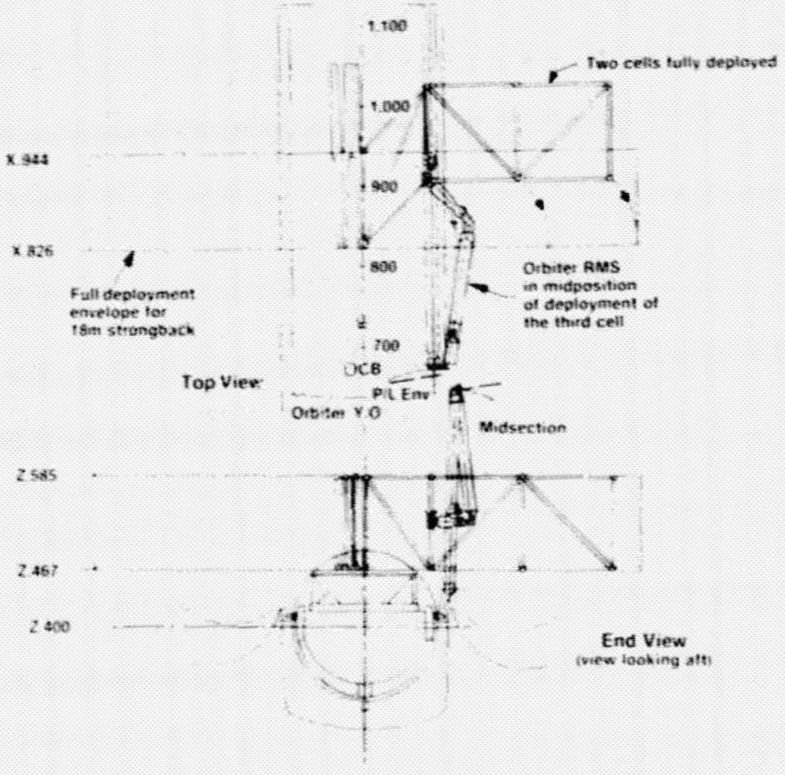

COMPONENT FABRICATION AND TEST

The fourth task was component test and fabrication with the objective being to provide proof of concept. The three joints built will go through an assembly, static, dynamic, and thermal test. Two of the joints have been fabricated; the third is now in fabrication. A ½ size length double cell module with full size joints is being fabricated and will undergo assembly testing.

Component Fabrication And Test

Test Matrix Overview

Test	General Information			Test Specimens		
	Setup	Purpose	Data	1 Full Scale Joint	2 Subscale Deployable Module	
Assembly	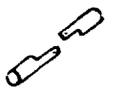	• Check Joining and Locking Features. Ease of Operation. Deployment Features	• Clearances • Binding. • Difficulty Factor	X	X	Objective: Demonstrate proof of concept
Static	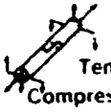 Tension Compression Shear Moment Torsion	• Check Joint Integrity. Strength. Stiffness	• Deflection • Rotation • Functional • Binding	X		
Dynamic	Electro Magnetic Shakers Low-Level Short Duration	• Check Locking And Unlocking Wear. Binding. Looseness	• Clearances Functional	X		
Thermal	Heat °C Cold °C With and Without Load	• Check Expansion and Contraction. Binding Fit and Function	• Temperature Deformation	X		

The static/thermal test setup for the automatic coupler joint is shown. Tension, compression, shear, moment, and torsion loads were applied at room temperature and -106°C (-160°F).

ORIGINAL PAGE IS
OF POOR QUALITY

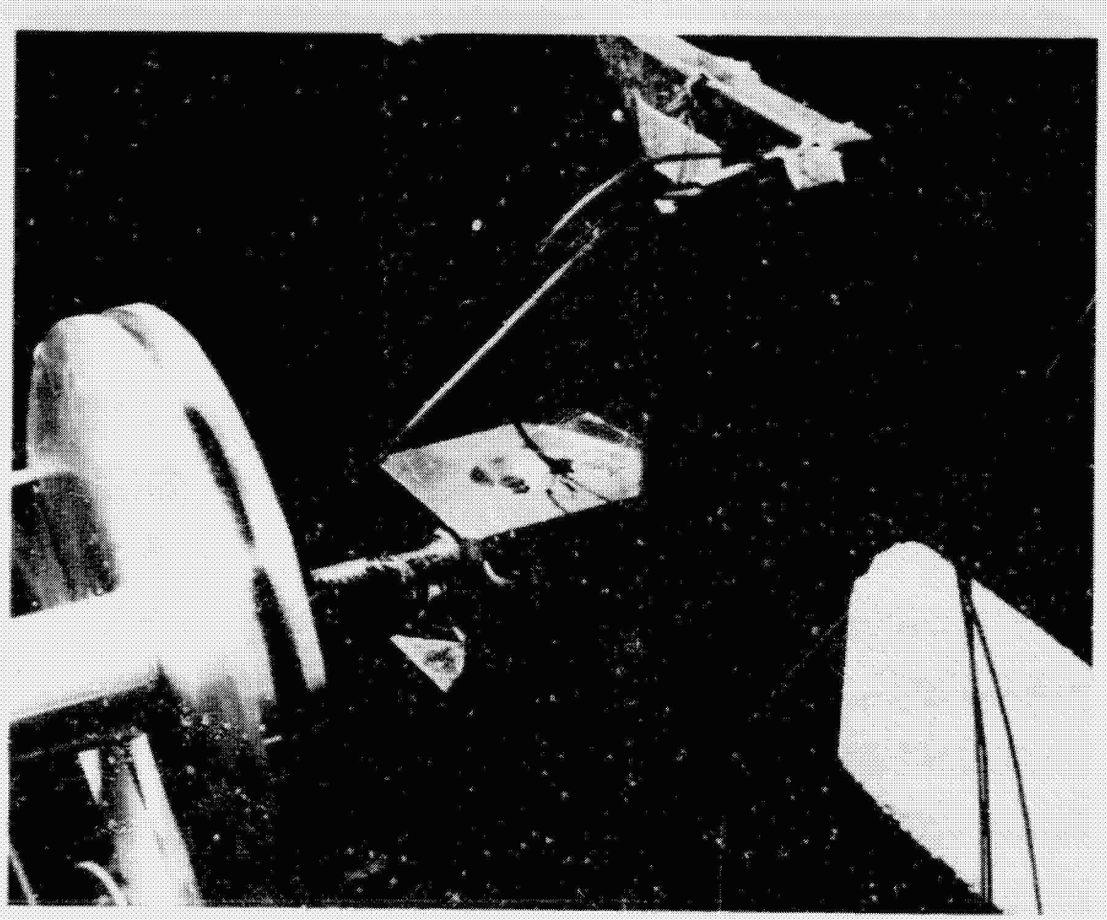

TOLERANCE AND UTILITY ANALYSIS

The purpose of this task is to investigate, in greater detail, the effect of tolerances within a joint relative to an assembly. Considering a long linear platform, what types of limits should be put on joints such that the tolerances would not accumulate to provide an excessively loose fitting or non linear structure? The utility incorporation is not to develop new connectors but merely to incorporate existing connectors into the structural arrangement in some fashion such that their incorporation enhances the assembly and construction and does not become a burdensome item.

Tolerance and Utility Analysis

Objective: To concentrate on the effect of tolerances for systems using selected concepts. To provide means of incorporating state-of-the-art electrical and fluids connectors into candidate joints concepts and wires/lines into members

Results: Effort just begun — completion expected December 1979

PAYLOAD/EXPERIMENT CARRIER
DESIGN STUDY

The payload/experiment carrier design study was primarily intended to develop a carrier to transport the elements or modules developed; but it also needed to be sensitive to other space experiments and to be responsive to the requirements of the Shuttle and the reference Science and Application Space Platform. A modular approach has been developed which emphasizes versatility, light weight, and cost effectiveness plus being accommodative to the interfaces that will be present.

Payload/Experiment Carrier Design Study

Objective: Accomplish conceptual design of carrier structure for elements/ modules and space experiments responsive to requirements of shuttle and reference platform.

Approach: Modular design that is

- Versatile
- Lightweight
- Cost effective
- Easy attachment to primary structure
- Clean packaging scheme
- Convenient transportation and handling characteristics

And will accommodate

- Interfaces and integration — thermal, power, data
- Experiment requirements — mounting, viewing

PAYLOAD CARRIER SYSTEM

The modular system is basically a thin wafer type of base/platform that fits into the Orbiter in vertical fashion. It has the side and keel segments of variable lengths. Cradle halves or a "y" load truss can be used if necessary or for the larger experiments. From these basic components a variety of carrier configurations can be constructed to meet the structural and experiment requirements.

Payload Carrier System

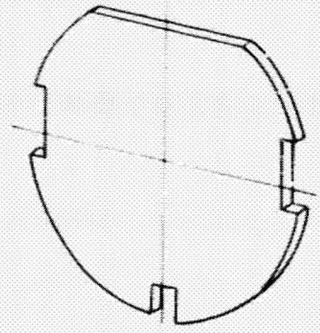

1. Base common to all platform mounted carriers

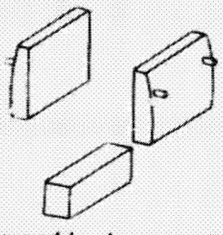

2. Side and keel segments — length depends on payload requirements

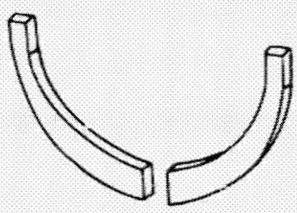

3. Cradle halves

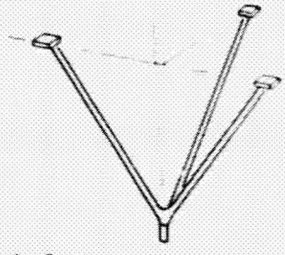

4. Optional "Y" load truss

Components

1. Base: Forward surface — orthogrid
   Aft surface attaches to probes on platform structure.
2. Side and keel segments: Contain sill and keel trunnions
3. Cradle halves
4. Options: A. Shelves
   B. Support struts with remote operated latches
   C. Radiators — 2.8m²/Radiator
   D. Share-a-carrier pallet
   e. Pivot table for IPS

STRONGBACK/CARRIER COMBINATION

An 18 meter platform arm is shown supporting a family of experiments. The smaller experiments are on the thin wafer sections. With the optional keels, sides and cradles, larger payloads can be supported. The module to module coupler is shown connecting the experiment carrier to the platform. Each carrier has an RMS pickup attachment for handling purposes.

Strongback/Carrier Combination

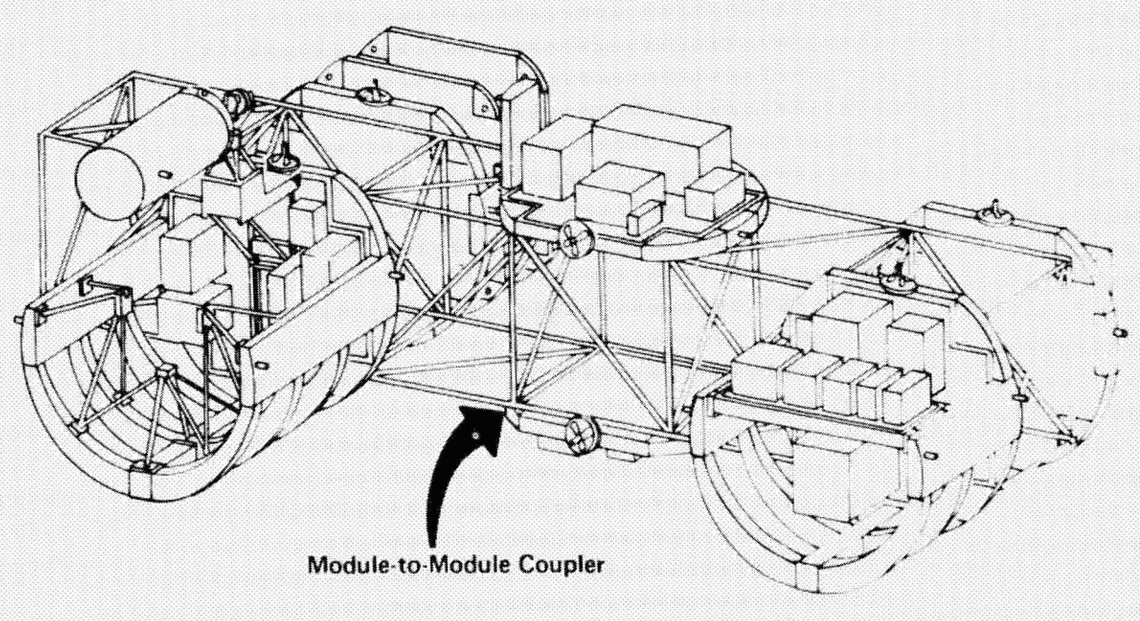

TYPICAL ORBITER INSTALLATION

Three double cell double fold modules are connected to provide 18 m total length and installed in the Orbiter bay with three other experiments. Deployment of this 1/10 scale platform arm was shown in 16 mm film strip.

Typical Orbiter Installation

18 m Strongback with Three 1984 Payload Concepts

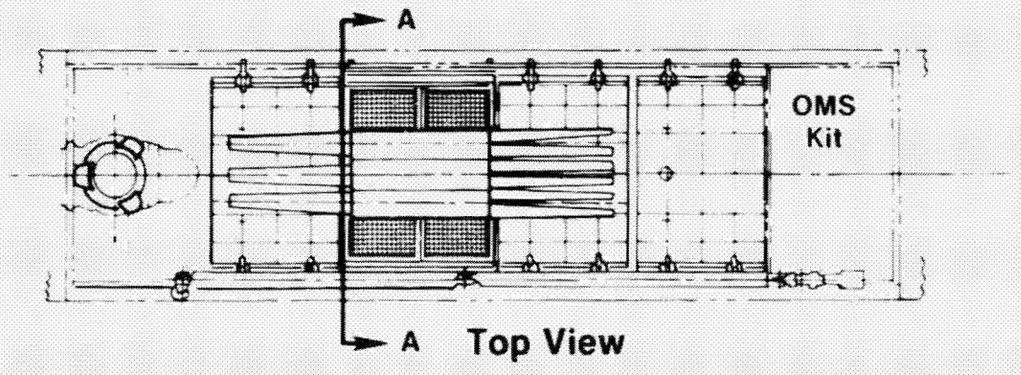

Top View

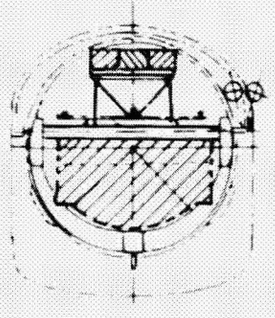

Section A-A

Stowage space available for strongback to PS mounting adapters(s) and other accessories

KEY SUMMARY ITEMS

Previous work has been reviewed and the effort has been directed primarily toward near term applications, such as the smaller linear or strongback type of platforms. Seventy-two joint and member ideas have been evaluated with the most promising concepts being selected by a figure of merit evaluation. Two of the joints have been fabricated and the other one is in fabrication. Four structural modules are being developed. The double cell double fold configuration will be fabricated in a ½ length size full joint module. The double fold module is a promising concept from a packaging point of view because it will more than adequately supply the length of the platform arm that is needed for the near term.

Key Summary Items

- All previous work reviewed
- Application of joints and elements directed toward 1985-1990 LEO platforms
- Seventy-two (72) joining ideas and thirty-eight (38) member ideas were generated
- Most promising concepts selected on FOM evaluation
- Two (2) promising strut joints designed and fabricated
- One (1) module-to-module coupler joint designed and in fabrication
- Multicell deployable module designed with ½ length struts and full size joints — in fabrication
- Double-fold module is promising, considering packaging/ assembly requirements

N80-19158

SPACE FABRICATION: GRAPHITE COMPOSITE TRUSS WELDING AND CAP FORMING SUBSYSTEMS

L. M. Jenkins, NASA/Johnson Space Center
D. L. Browning, General Dynamics Convair Division

LSST 1ST ANNUAL TECHNICAL REVIEW

November 7-8, 1979

LSST SPACE FABRICATION

Although funding limitations have precluded extensive support, LSST has provided some resources for beam builder subsystem technology studies. The contract with General Dynamics-Convair is for nine months beginning September 25.

LSST SPACE FABRICATION

- SPACE FABRICATION OF STRUCTURE BY A BEAM BUILDER IS NOT A MAJOR LSST ACTIVITY
- FORMING AND WELDING OF COMPOSITES HAS BEEN SUPPORTED WITH $125,000
- GENERAL DYNAMICS-CONVAIR IS UNDER CONTRACT TO DO FORMING AND WELDING WITH EXISTING BENCH TEST EQUIPMENT AND TO BUILD A PROTOTYPE TRUSS

Figure 1

PROGRAM DESCRIPTION

The Graphite Composite Truss Welding and Cap Forming Subsystems contract was begun in late September 1979. This program description provides basic contractual data, identifies all milestones and shows the time spans planned for accomplishing each subtask within the three major task groups. The program is being conducted in accordance with the following groundrules:

Cap forming
- On existing bench model machine

Welding
- On existing commercial welder
- General Dynamics Convair-developed horn tips/schedules

Truss
- Geometry, element/joint details, material per SCAFEDS, Part III (NAS9-15310)
- Length: 4.90m (3 bays + std end cutoff)
- Die-formed cross-members
- Instrumentation & load intro fittings provided
- Tests conducted at JSC

Material
- Consolidated strip for testing at LaRC: woven single-ply graphite/glass; polysulfone resin

- Contract data
  - — NAS 9-15973 — Value: $120,102
  - — Agency: NASA/JSC — Contractor: General Dynamics Convair Division

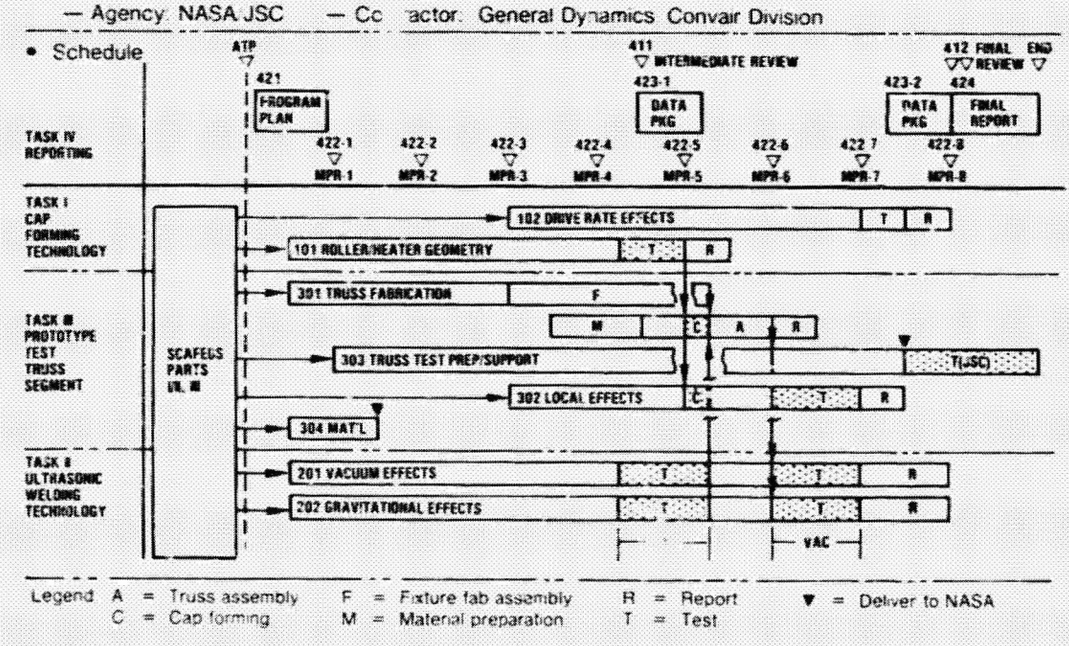

Figure 2

AUTOMATED BEAM BUILDER CONCEPT

The beam builder concept developed during the SCAFEDS forms a triangular truss 1.3 meters on a side. Flat strips of preconsolidated graphite fiber fabric in a polysulfone matrix are coiled in a storage canister. Heaters raise the material to forming temperature then the structural cap section is formed by a series of rollers. After cooling cross members and diagonal tension cords are ultrasonically welded in place to complete the truss.

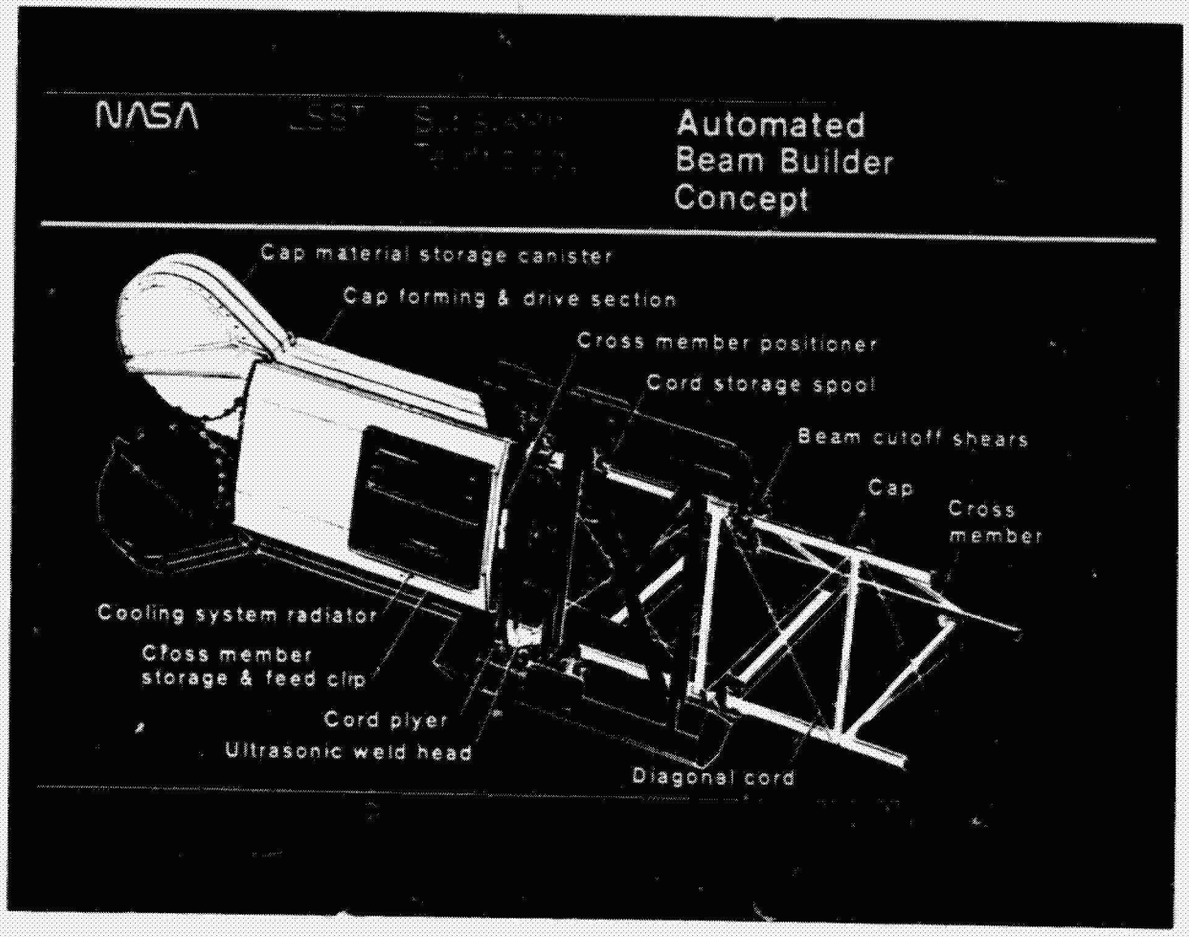

Figure 3

ORIGINAL PAGE IS
OF POOR QUALITY

PROTOTYPE COMPOSITE TRUSS TEST

Because no performance data existed on the lightweight graphite composite truss configuration planned for automated space fabrication, a test was performed using a display article fabricated under the Space Construction Automated Fabrication Experiment Definition Study (SCAFEDS). Although the graphite fiber and polysulfone matrix were representative, the cap forming technique was not. Schedule incompatibility dictated hand lay up/vacuum cure on aluminum tooling in lieu of continuous roll-forming as originally planned. This resulted in undetected cracks on the free edges which in turn led to premature failure during compressive tests. A repeat test is planned with the truss built under this contract.

PROTOTYPE COMPOSITE TRUSS TEST

TEST OBJECTIVE: TO OBTAIN EARLY DATA ON TORSIONAL STIFFNESS, DAMPING AND SHORT COLUMN STRENGTH.

TEST ARTICLE: SCAFEDS DISPLAY, 3 BAY, 1.3 M X 4.9 M, 6.4 KG, GRAPHITE FIBER-POLYSULFONE COMPOSITE

TEST RESULTS: CRACKS IN EDGE OF OPEN CAPS AT 500 KG (1216 LB) LOAD, TEST STOPPED SHORT OF 1230 KG PREDICTED

TEST ANALYSIS:

- PREMATURE COMPRESSIVE FAILURE DUE TO UNDETECTED FIBER DAMAGE DURING FABRICATION LAYUP
- TORSIONAL STIFFNESS LOWER THAN PREDICTED
- DAMPING IN 2% RANGE

CONCLUSIONS:

- HIGH RISK IN TESTING ARTICLE NOT BUILT FOR THAT PURPOSE
- REPEAT TEST WITH NEW TRUSS

Figure 4

TRUSS TEST SETUP

The white SCAFEDS truss test article is shown against the structural test "backstop" at JSC. Compressive load is applied to end loading fixtures by a hydraulic cylinder from the Apollo-Soyuz docking test rig. Bending and torsional loads were applied to the upper fixture.

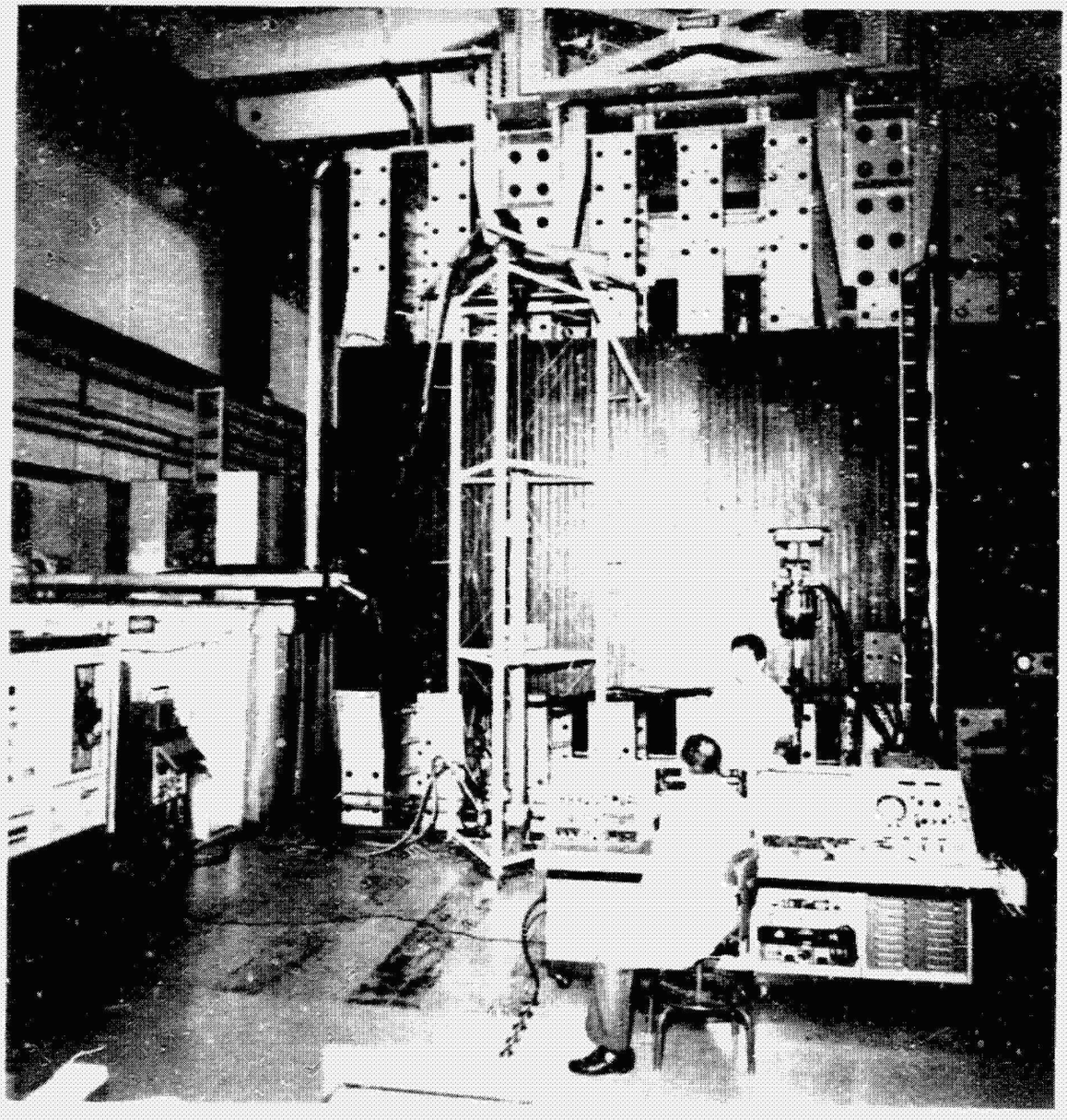

Figure 5

ORIGINAL PAGE IS
OF POOR QUALITY

PROTOTYPE TRUSS CAP EDGE CRACK

This is a photograph of one of twenty edge cracks observed during the compression test. The cracks were less than one centimeter long and occurred in all three caps. They were randomly spaced, but none closer than 20 cm to each other. Some cracks had been detected and patched during fabrication while others went undetected until exposure under test loads. Non-linear analyses as well as the results of several tests show that the edge cracking failure mode does not reflect the behavior of representative specimens.

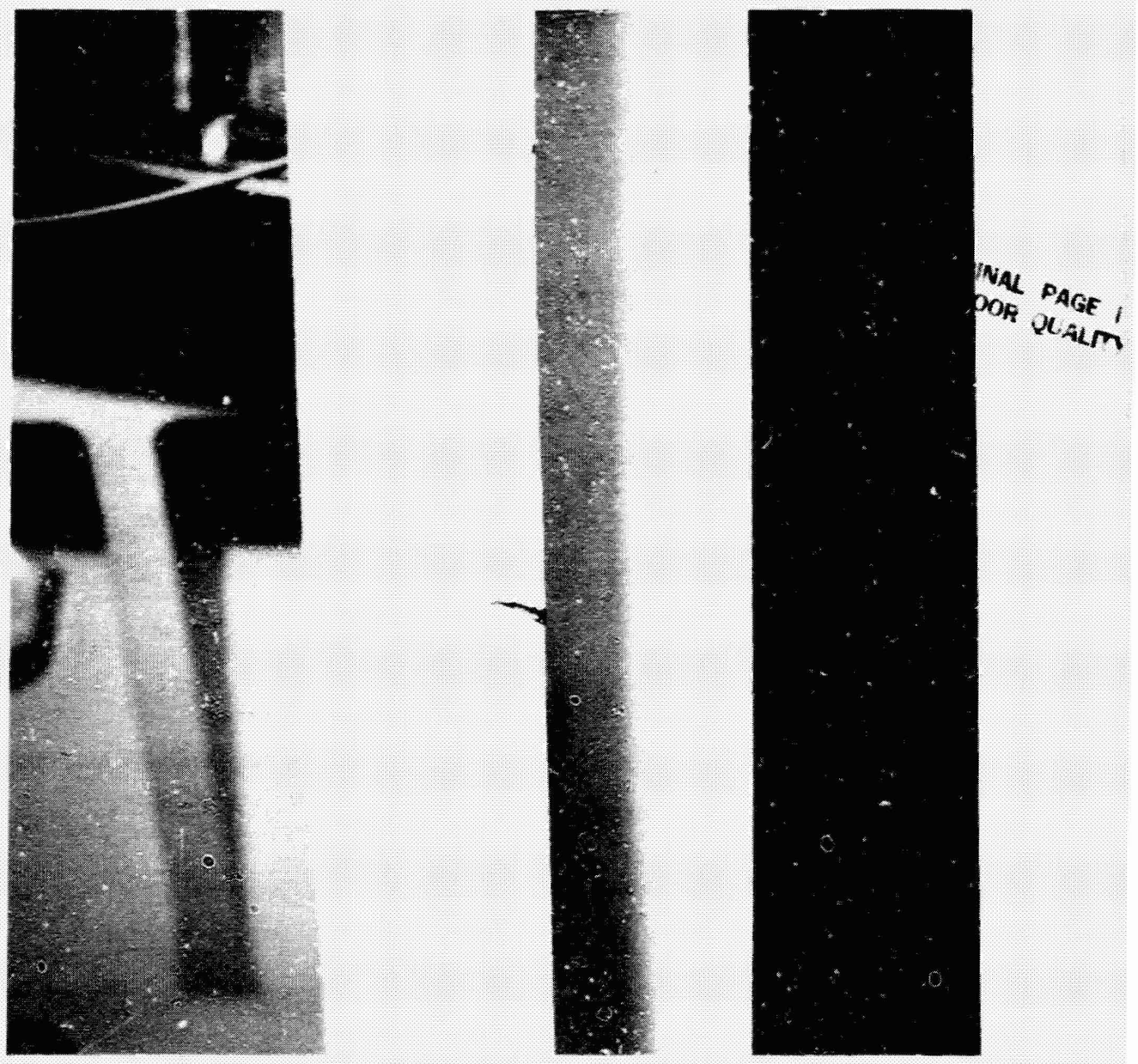

INAL PAGE I
OOR QUALITY

Figure 6

OPEN CAP STABILITY ANALYSIS

The compressive stability of open triangular caps was assessed for both round- and sharp-cornered sections of equal perimeter using the STAGS C computer code (ref 1). Linear bifurcation analyses showed that local buckling of the side flats occurred first in both sections and the dashed lines show a load-carrying advantage of about 7.6 times for the round-cornered section.

A non-linear collapse (crippling) analysis was also conducted to determine the ultimate strength of the round-cornered section. The solid curve shows load vs. deflection for this analysis, which was continued to a load of 6583N without indication of failure. Flexural (Euler) and torsional buckling allowables were also predicted by linear analyses, with torsional failure occurring first at a load of 13646N. Thus, the correct compression allowable lies between the crippling cutoff and torsional instability loads, resulting in a very large margin over the anticipated maximum SCAFE cap load of 316N.

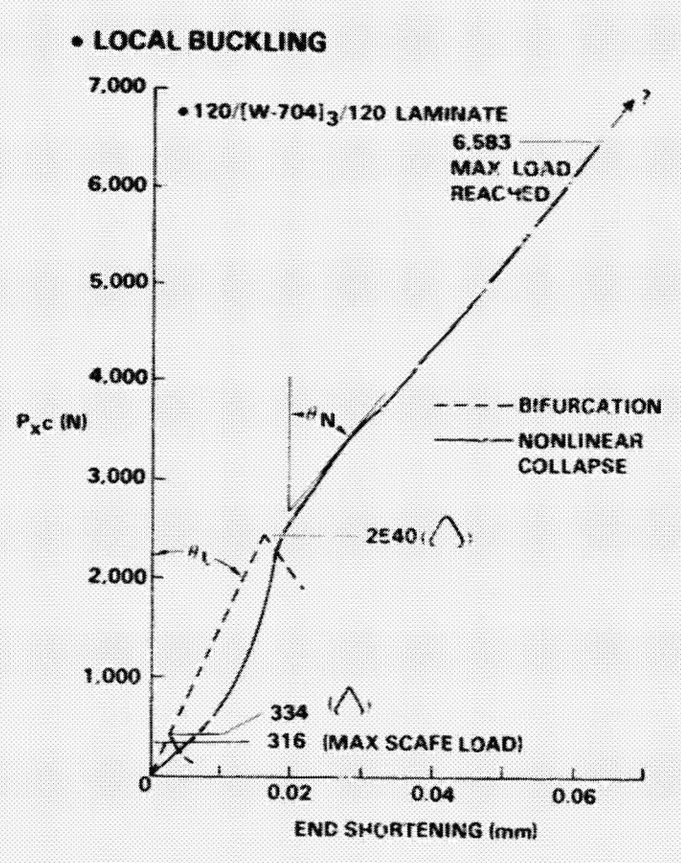

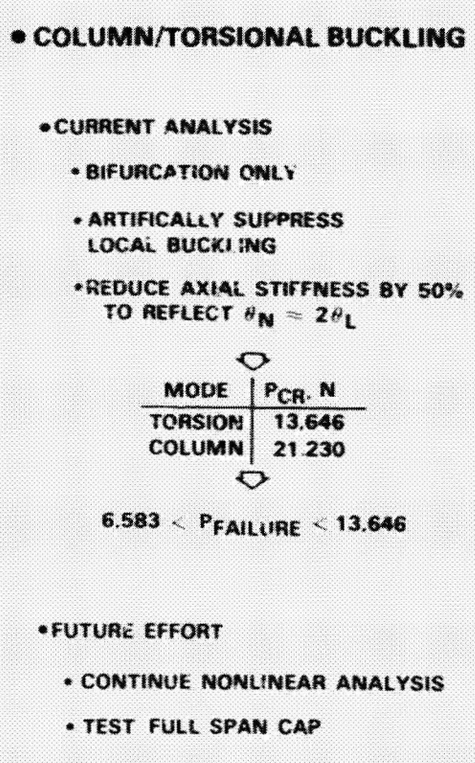

Figure 7

CAP SECTION TESTS

Cap strength and failure mode characteristics have been determined through several tests employing a setup similar to the one shown here. Low slenderness ratios are chosen to assure crippling failure, and strain gages are used during setup to assure uniformity of load introduction to the cross-section. Both the original laminated and later single ply materials have been tested. Results of laminated specimen tests and their close correlation with bifurcation analyses are given in ref. 1. Results for roll-formed single-ply specimens are shown and appear to indicate substantial benefit in initial buckling load due to the woven fiber construction.

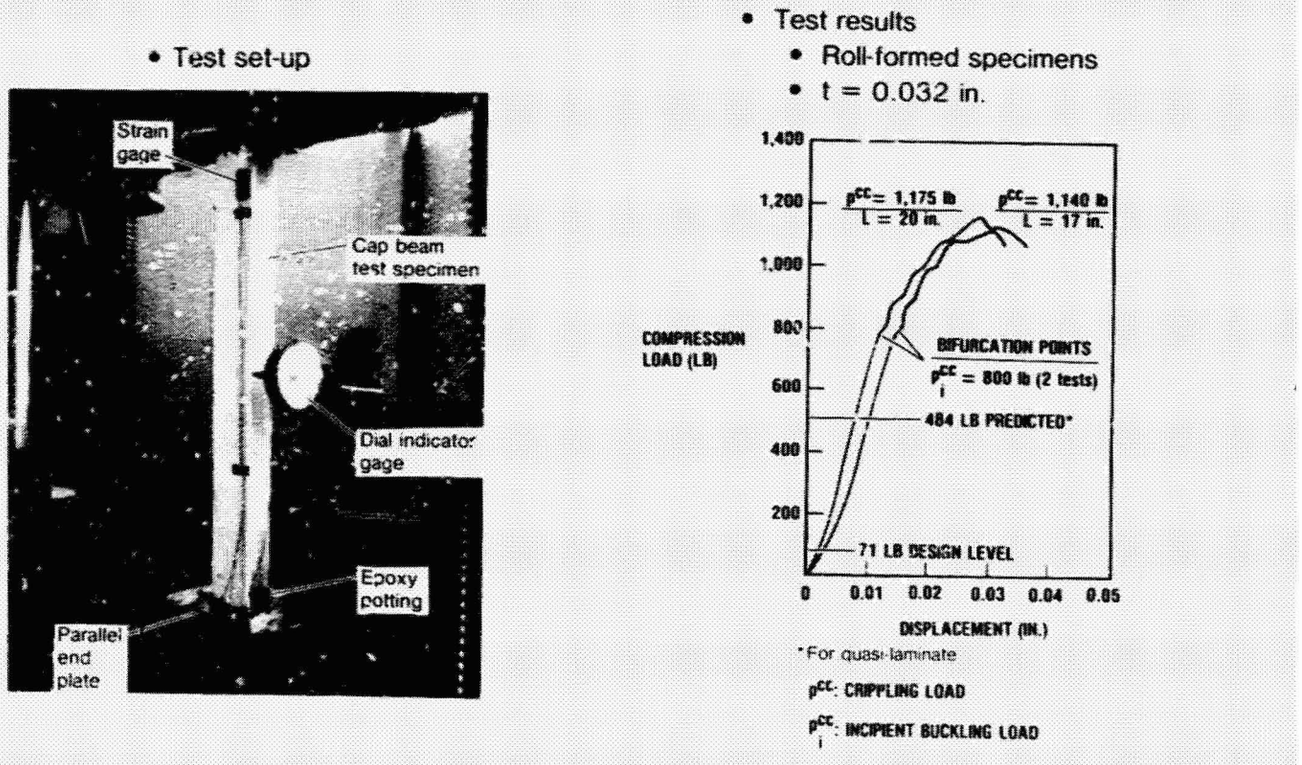

Figure 8

CAP SECTION CRIPPLING FAILURE MODE

The cap failure mode seen in all tests to date is shown in the photo, with the direction of view as indicated. Typically, cracks initiate at the edges of a buckled side flat, and propagate into the adjacent corners as the load is increased to ultimate. At failure the free edges remain uncracked.

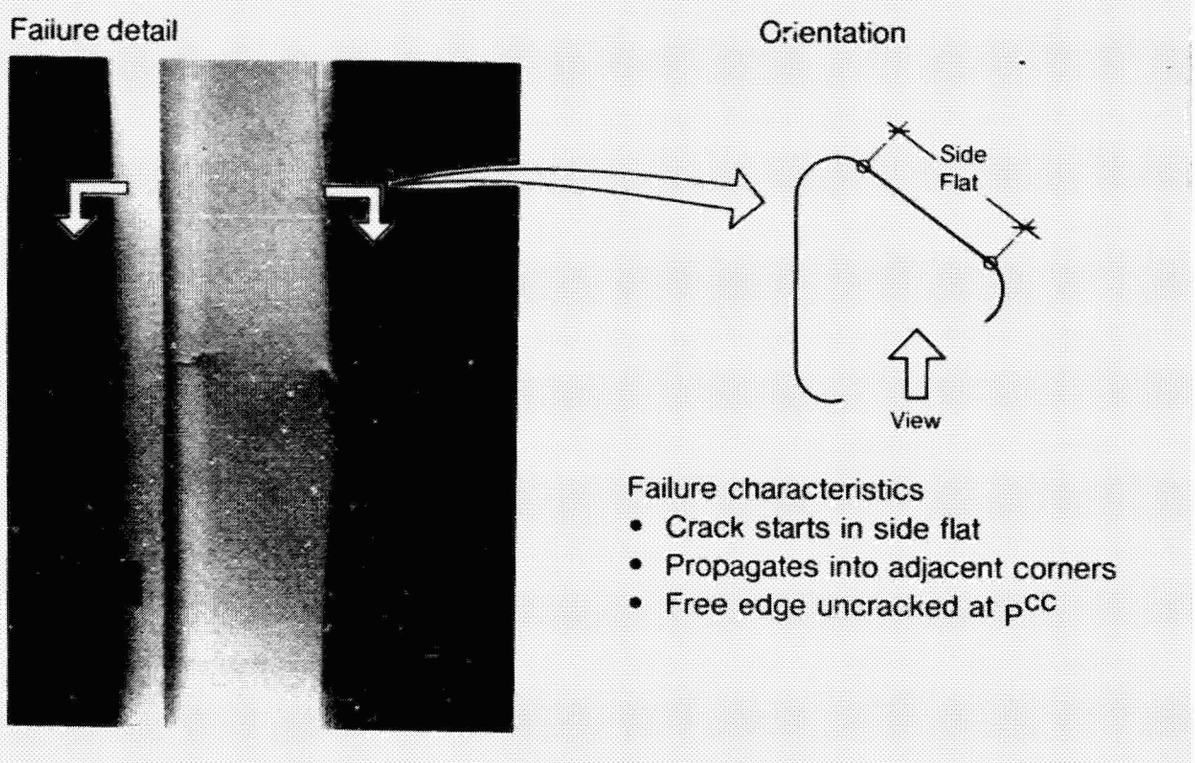

Figure 9

SINGLE-PLY STRIP MATERIAL

During initial SCAFED study effort a material design evolved which combined the benefits of two fibers (glass and graphite), thermoplastic resin, and a white pigmented coating into a strip material suitable for the SCAFE fabrication process and service environment. Properties of this "sandwiched-graphite" multi-ply laminate, using then-available materials, were first predicted using conventional analytical techniques, and later verified by coupon tests. At the start of laminate evolution, however, the processing and forming benefits to be achieved by combining the desirable features of the constituent materials into a single-ply woven strip were already recognized. As weavable high-modulus graphite yarn became available, private development of single ply strips began, adopting the SCAFE cap laminate as a baseline for fiber percent/orientation and thickness.

However, a further valuable asset of single-ply material is the flexibility in gage selection since the ply thickness and stacking symmetry constraints of the laminate approach are eliminated. Consequently a new material, designed for increased stiffness plus improvement in various "second-order" characteristics is now in development. Comparison with the original laminate shows a 20% gage reduction, significant weight decrease, a small but acceptable reduction of beam fundamental frequency and essentially unchanged local stability of the cap side flats. As an added benefit, it also permits cap/crossmember material commonality.

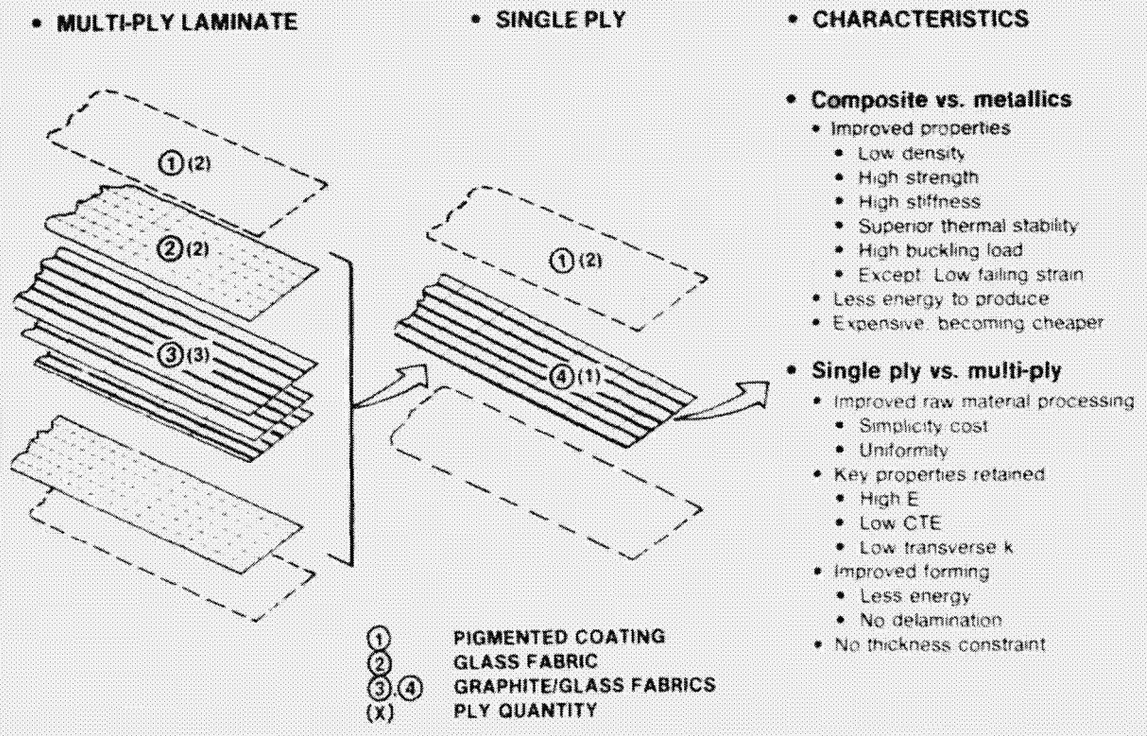

Figure 10

CAP FORMING

The beam builder system is comprised of eight subsystems, each of which consists of one or more subsystem modules. This concept permits each subsystem module to be developed separately before integrating the complete subsystem into the beam builder.

The cap forming subsystem, for example, consists of three cap forming machines. General Dynamics Convair Division has built and demonstrated the prototype cap forming machine shown. It is being used to develop the materials, processes and techniques to be incorporated in the flight beam builder cap forming machines. It will also be used to meet the objectives of this program by producing cap members for the test truss and cap test specimens for determining local effects of column loaded cap members. Cap forming technology will be further advanced by the improvements to be made in forming roller and heater geometry, and through an evaluation of drive rate effects.

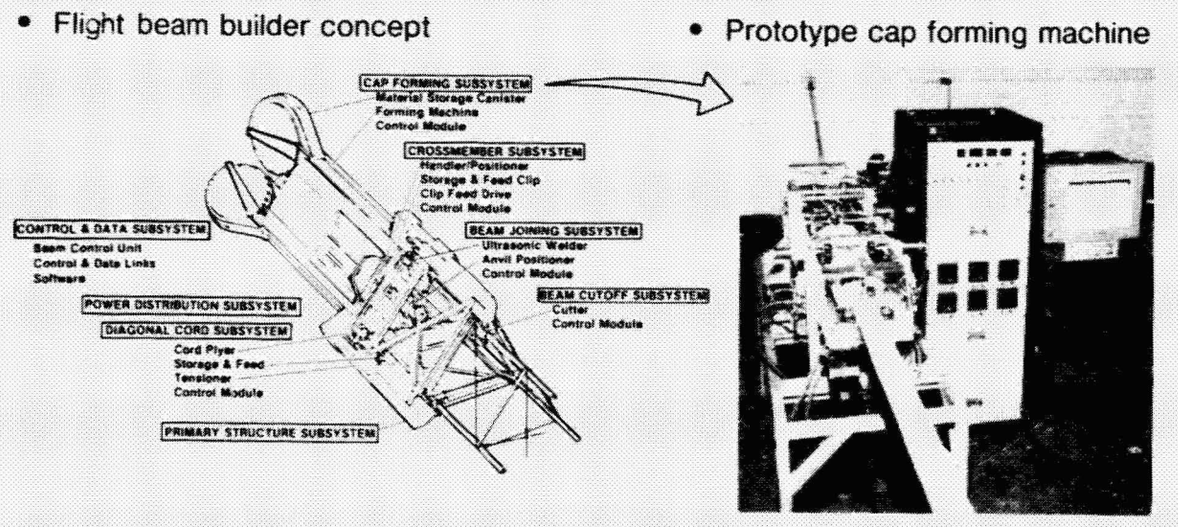

Figure 11

WELD PROCESS DEVELOPMENT AND APPLICATION

Early development of ultrasonic welding technology for joining graphite polysulfone composites started with the evaluation of weld tips and welding schedules using small samples of both bare and coated material. This led to a joint design for the triangular truss beam, which not only connects the beam caps and crossmembers together but captures the diagonal cord within the welded zone as well.

This joint design was demonstrated with the fabrication and assembly of the first prototype truss demonstration article produced during the initial phase of the SCAFEDS program. Improvements in this joint design have occurred through subsequent development activity and will be employed in the truss test article to be produced under this contract.

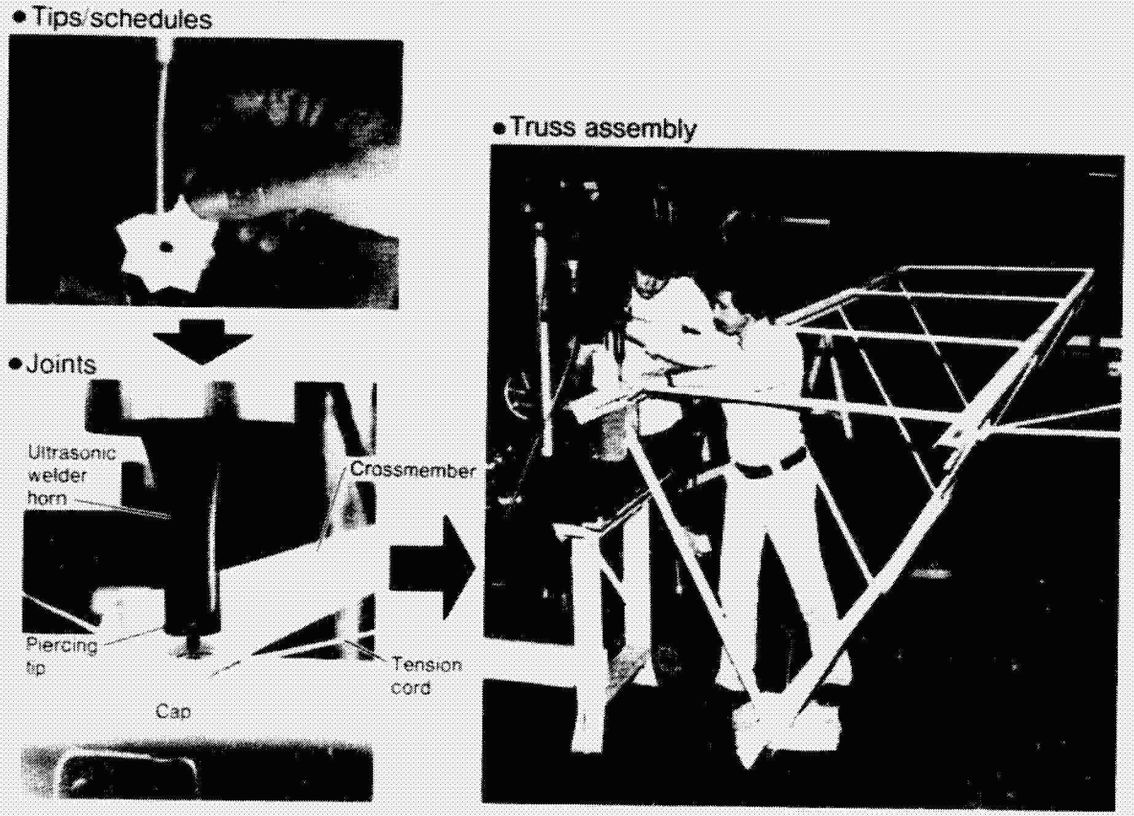

Figure 12

ORIGINAL PAGE IS
OF POOR QUALITY

WELDING IN PARTIAL VACUUM

The existing data base for the ultrasonic welding of graphite/polysulfone composite material includes the performance of welds in partial vacuum using a vacuum chamber which encloses only the weld horn and weld specimen as shown. Results indicate no reduction of weld strength down to the vacuum levels achieved with this approach.

By placing the entire welder inside a vacuum chamber, the overall effects of in-vacuum welding on both the weld specimens and machine performance will be more thoroughly assessed, at vacuum levels approaching those to be experienced by the flight beam builder.

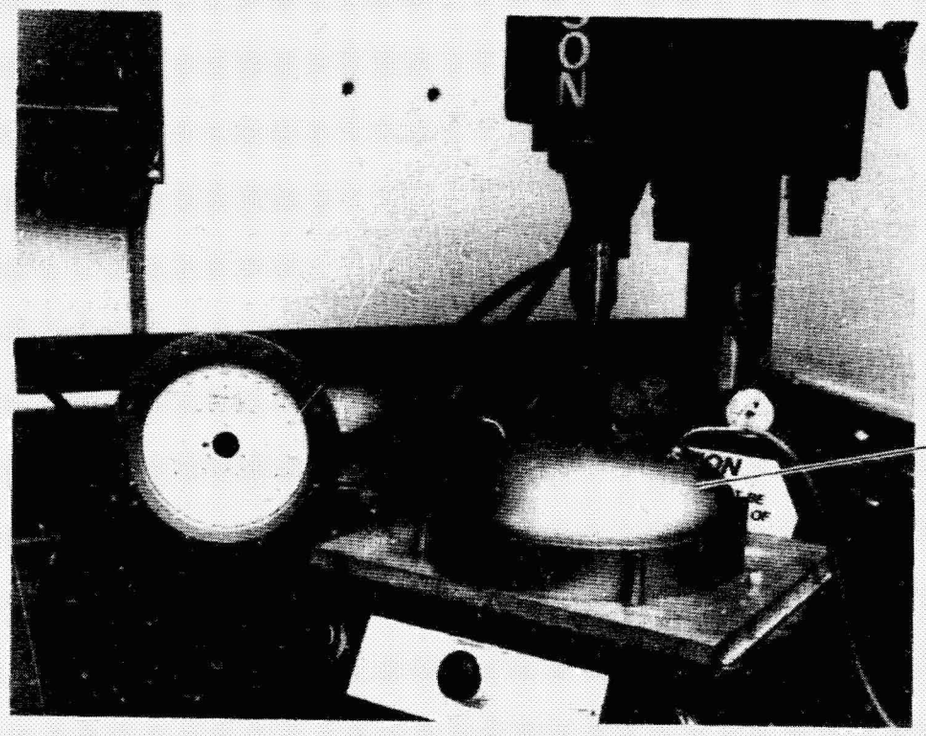

Figure 13

REFERENCES

1. Spier, E.E.: Stability Analysis and Testing of Thin-Walled Open-Sectioned Graphite/Thermoplastic Structures; in the Proceedings of the 10th National SAMPE Technical Conference, Oct. 1978.

N80-19159

STRUCTURAL ASSEMBLY IN SPACE

By

Jack W. Stokes
National Aeronautics and Space Administration
George C. Marshall Space Flight Center

and

Edwin C. Pruett
Essex Corporation

Presentation to LSST Program Technical Review
Langley Research Center
Hampton, Virginia
November 7 and 8, 1979

PAGE 262 INTENTIONALLY BLANK

PART A

OVERVIEW

We wish to share with you our thoughts, accomplishments, and plans in large structures assembly. I will present an overview of our three-year study plan for Large Space Structures Technology (LSST). Ed Pruett (Essex Corporation) will report on the work Essex is performing this year in support of structural assembly definition and evaluation.

The role of man and machine in assembly operations has been given a great deal of consideration and debate over the last few years. Emphasis on one or the other as an assembly mode fluctuates each year.

We believe that, depending upon the packaging and orbital characteristics of a structure, as well as its complexity and mission requirements, there is a role in assembly for both man and machine. Figure 1 indicates a spectrum for mixing man and machine for any typical structure assembly. Totally manual operation appears at one end of the assembly spectrum, while totally automated operation appears at the other. Such operating factors as economics, nature of assembly tasks, and availability of technology, skills, etc. should direct design to some optimum man/machine mix for assembly.

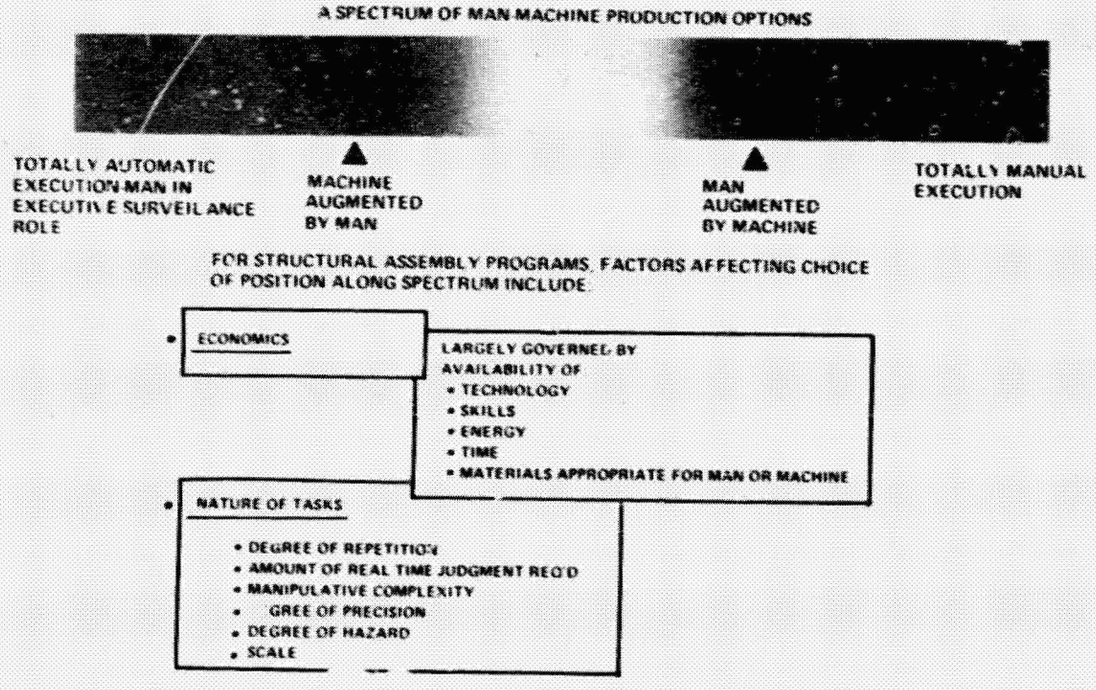

Figure 1 .../Machine Spectrum for Assembly

From Skylab we have demonstrated and proven that manned Extravehicular Activity (EVA) is a viabl technique for relatively simple one-time assembly functions. However, as depicted in figure 2, we recognize that as structure characteristics and requirements become more complex we must emphasize the role of remote/automated systems in structural assembly, using man as an overseer.

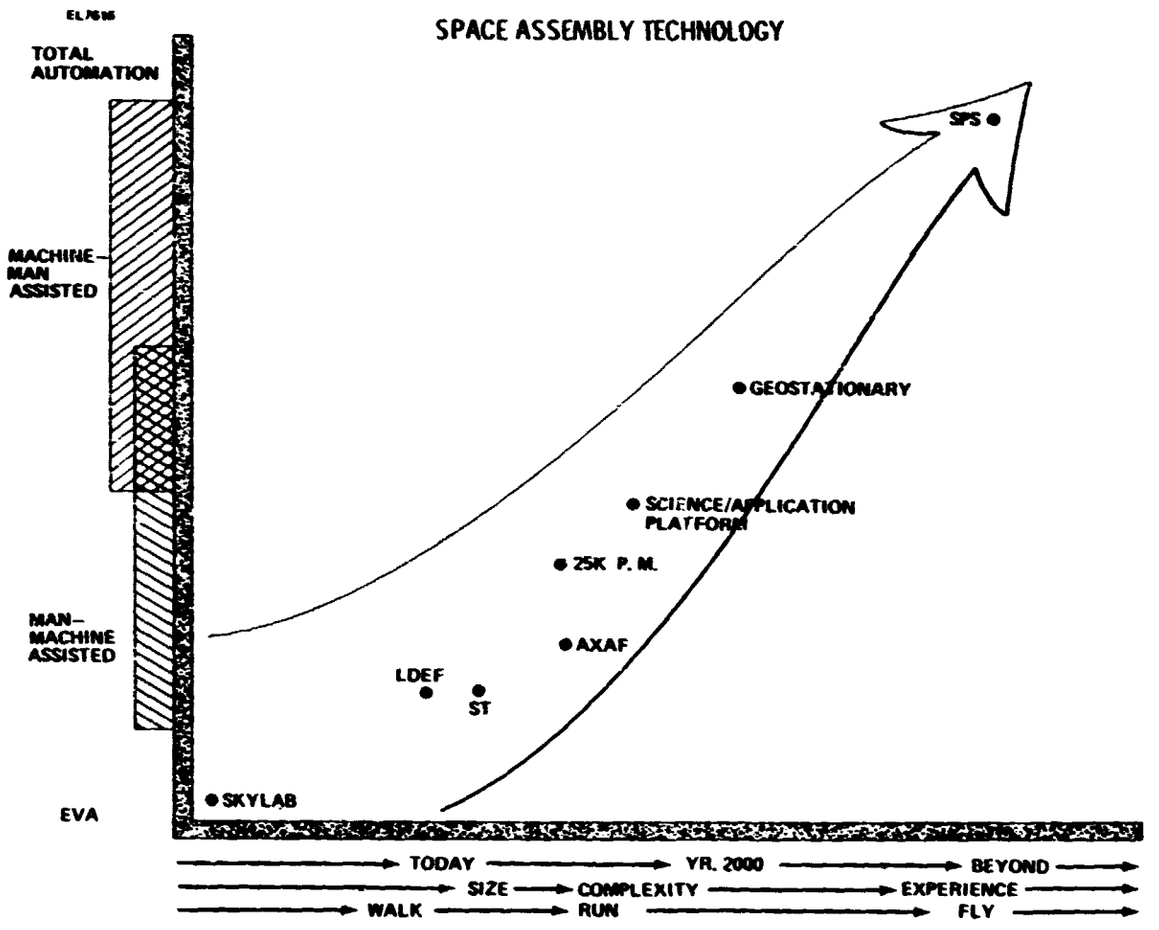

Figure 2 Man/Machine Role in Assembly

Manual assembly is very feasible (figure 3) when mechanical assembly methods remain simple or when the structure to be assembled is in close proximity to the Orbiter payload bay. However, assembly with manual crew aids becomes less efficient as construction moves to repetitious functions for large scale structures. Here, remote or automatic assembly aids may best perform the assembly fuctions.

OPERATIONS/ASSEMBLY AIDS	CREW INVOLVEMENT	APPLICATION/ADVANTAGES
AUTOMATIC ASSEMBLY MACHINES (EG "SPACE SPIDER") 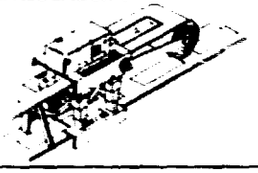	• ESTABLISH INITIAL CONDITIONS • START AND STOP AUTOMATIC SEQUENCES. • MONITOR EXECUTION, TROUBLE SHOOT HARDWARE AND SOFTWARE	• LARGE SCALE OPERATIONS • REMOTE OPERATIONS • LOW OR CONTROLLED CONSTRUCTION LOADS
FREE FLYING TELEOPERATORS	• PILOT TRANSPORT VEHICLE • CONTROL MANIPULATOR ARMS • MONITOR SYSTEM STATUS, TROUBLE SHOOT HARDWARE, SOFTWARE	• REMOTE OPERATIONS • NON -REPETITIOUS OPERATIONS • TASKS WITH HIGH DEXTERITY REQUIREMENTS • CAN BE GROUND CONTROLLED
SHUTTLE–ATTACHED MANIPULATORS, CRANES, CHERRY PICKERS 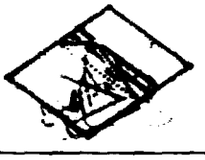	• PROVIDE STABLE STS PLATFORM FOR CONSTRUCTION OPERATIONS • OPERATE MANIPULATOR TO UNSTOW POSITION AND MATE STRUCTURAL ELEMENTS	• LOCAL (LOW EARTH ORBIT) CONSTRUCTION • CONTROLLED CONSTRUCTION FORCES • CONTINGENCY EVA POSSIBLE
HAND TOOLS & AIDS FOR EVA USE	• EVA CREWMAN SERVES DIRECTLY AS SPACE CONSTRUCTION WORKER	• MINIMAL COST FOR EQUIPMENT DEVELOPMENT EXISTING CAPABILITY • HIGH FLEXIBILITY FOR UNFORSEEN TASKS • LOCAL CONSTRUCTION, SMALLER SCALE CONSTRUCTION

Figure 3 Orbital Assembly Aids and Crew Involvement

Our interest in the determination of efficient, cost effective structural assembly is manifested in a three year plan (figure 4). Through 1982 we will:

a. Continue to develop the cost analysis begun last year. This analysis is intended to establish a method for economically mixing large structure assembly techniques. It will also develop and evaluate procedures for assembling various large structures. We consider this analysis and its output, a working cost algorithm for assembly, to be our major study emphasis. The algorithm will be computerized and maintained such that an organization can determine the most cost effective method for assembling any defined structure.

- CONTINUE TO DEVELOP COST ANALYSIS - MAJOR STUDY EMPHASIS
- SHIFT FOCUS TO SPACE PLATFORMS & DEPLOYABLE STRUCTURES
- SHIFT EMPHASIS FROM MANUAL EVA OPERATIONS TOWARD REMOTE/AUTOMATED OPERATIONS
- CONTINUE TO SUPPORT ANALYSIS THROUGH SIMULATION - NEUTRAL BUOYANCY, ZERO-G, COMPUTER, OTHER PROGRAM SIMULATIONS
- CONTINUE TO DEVELOP & UPGRADE DEFINITION OF ASSEMBLY AIDS & CREW AIDS
- DEVELOP ASSEMBLY GUIDELINES DOCUMENT

Figure 4 Three-year Plan for LSST Operations

Figure 5 defines the functions required to complete the three-year plan. Typical structure scenarios, based on benchmark large structures, are being examined and expanded in the area of assembly. Data collected from documentation and simulation feed into functional analyses for each scenario. From such analyses can be determined crew tasks and associated times, as well as assembly and crew aid requirements. Such data can be converted to number of Space Transportation System (STS) flights to determine manual assembly costs, and definition of assembly and crew aids. This can be compared to other cost factors determined through further analysis. The resulting cost algorithm will provide a useful tool for defining the proper mix of functions for man and machine.

b. Our study emphasis previously has been on erectables. Since we have established some definition on erecting structures through manual EVA operations, we will concentrate on deployable structures, with some emphasis on fabricated assemblies. In line with LSST Program Office interests we will address space platforms in lieu of antennas.

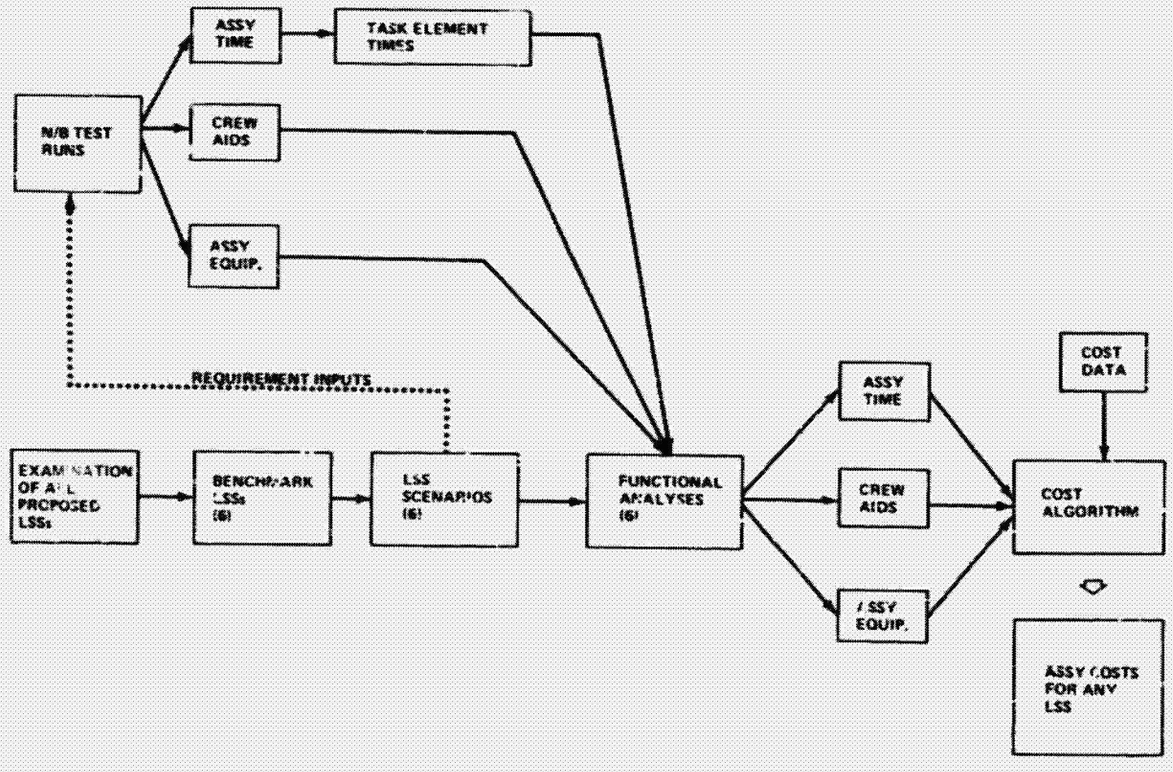

Figure 5 LSST Three-year Functional Flow for Assembly

c. We have established an initially adequate amount of baseline data for manual EVA assembly. We need to better understand the specifics of remote/automated assembly in order to determine proper man/machine mixes for building structures. Therefore, emphasis will shift toward remote assembly, though we will continue to evaluate manual techniques as required.

d. We have performed and will perform various relevant neutral buoyancy assembly simulations as defined in figure 6. Our analysis will continue to be supported through underwater simulation. More realistic simulations will be possible with our new cargo bay mockup including a soon-to-be-delivered functional Remote Manipulator System (RMS). However, new simulation modes will be considered, since neutral buoyancy testing has several inherent shortcomings. Such simulation methods as zero-g (KC-135 Aircraft) and computer-aided techniques will be investigated. We also will continue to monitor those simulations performed for other programs which may supply relevant data toward the analysis.

- √ TEST AND EVALUATION OF LaRC NESTABLE COLUMN ELEMENTS WITH LOCKHEED-SUPPLIED JOINTS/UNIONS.
- √ ASSEMBLY OF TETRAHEDRAL CELL USING SELECTED BEAMS AND ROCKWELL-SUPPLIED JOINTS
- √ NEUTRAL BUOYANCY EVALUATION OF ROCKWELL-SUPPLIED EVA ELECTRICAL CONNECTOR.
- √ CONTINUED EVALUATION OF A VARIETY OF POSSIBLE ELEMENTS, JOINTS AND ASSEMBLY TECHNIQUES.
- √ EVALUATION OF 36-ELEMENT STRUCTURE BY MIT
- √ ON-ORBIT MAINTENANCE OF SPACE TELESCOPE

Figure 6 Neutral Buoyancy Activities for FY79-FY80

e. As a part of the analysis and simulation activity we will continue to define and develop assembly aids and crew aids required to assemble large structures. We will consider those aids available through STS, but will not limit ourselves to them. We understand that assembly can occur either in the payload bay or from a remote site. Therefore, assembly aid requirements may vary from structure to structure.

f. An assembly guidelines document will be generated from data collected from analysis, simulations, and early STS flights. Such a document will assist in the planning and development of the assembly techniques.

Figure 7 describes the schedule for meeting the six functions listed above.

A detailed explanation of the study, as well as the accomplishments for the year, are described in Part B.

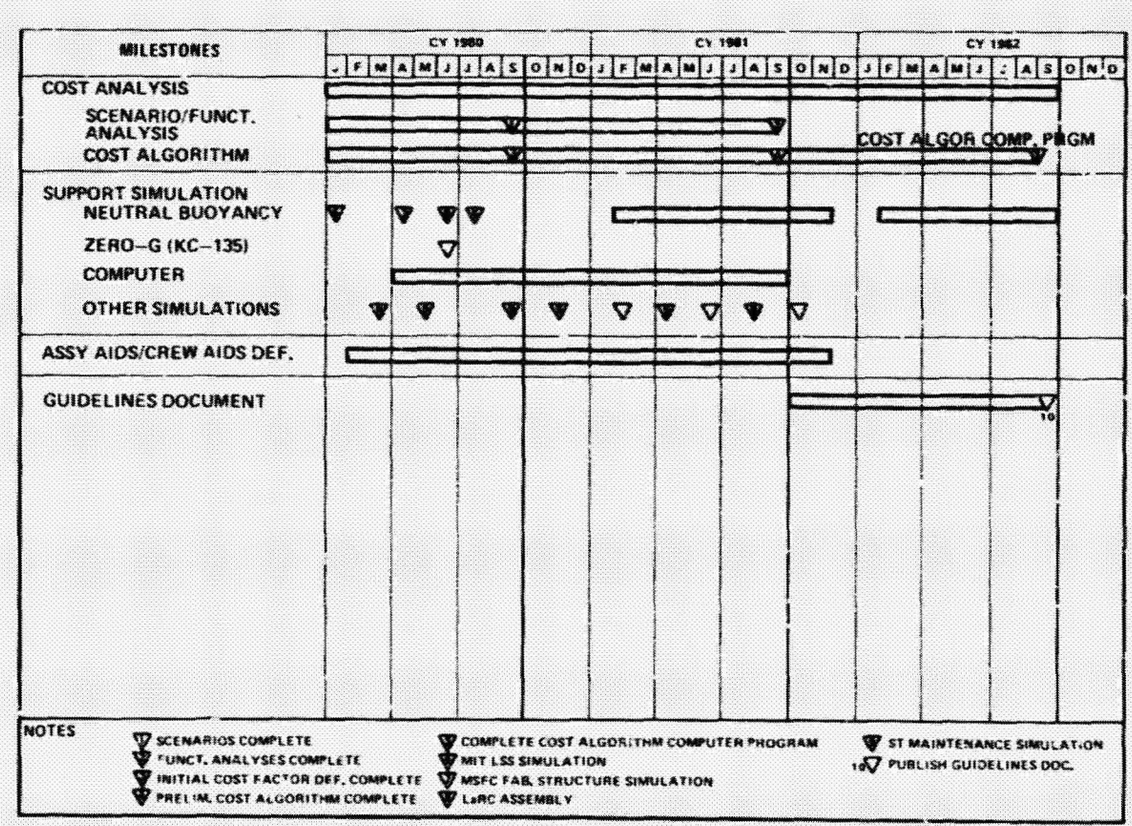

Figure 7 Assembly Three-year Schedu

In summary, let us address what we have learned about assembly in space (figure 8). From Skylab we know that man can perform large scale planned and unplanned operations. Both erectable and deployable assembly have been successfully demonstrated.

We further have demonstrated in a water environment, that under controlled conditions an EVA subject with minimal crew aids (dual handrails) can manipulate masses up to 17,000 lb.

Underwater simulations of payload-related EVA tasks have demonstrated that a crewman can perform contingency EVA operations. However, this is dependent upon early planning in design for manned participation in such contingencies.

Neutral buoyancy simulations investigating the transport, positioning, and assembly of large structural elements have simulated assembly with unaided one and two man operations, EVA operations with manipulator assistance, and EVA operations with small piloted vehicle support. From such tests we have determined that EVA assembly is possible and feasible. Results indicate that, even though one crewman can accomplish assembly, it is more efficient with two men and in some cases with machine aid.

WHAT HAS BEEN DONE TO HELP US LEARN ABOUT ASSEMBLY IN SPACE?	
ACTIVITY	RESULTS
√ SKYLAB REPAIR OPERATIONS	ESTABLISHED THAT CREWMEN CAN PERFORM LARGE SCALE PLANNED AND UNPLANNED OPERATIONS
√ EXPERIMENTS WITH MANUAL MANIPULATIONS OF VERY HIGH MASSES	NB SUBJECTS MANIPULATE 17,000 LB. MASSES
√ NEUTRAL BUOYANCY SIMULATIONS OF SPACELAB PAYLOAD-RELATED EVA TASKS	• CREWMAN PERFORM CONTINGENCY EVA OPERATION IN PAYLOAD BAY • PLAN FOR CREW INVOLVEMENT EARLY IN DESIGN
√ NEUTRAL BUOYANCY TRANSPORT, POSITIONING AND ASSEMBLY OF LARGE STRUCTURAL ELEMENTS (MSFC & LaRC) • UNAIDED ONE AND TWO MAN EVA OPERATION • EVA OPERATION WITH MANIPULATOR ASSISTANCE • EVA OPERATION WITH SMALL PILOTED VEHICLE SUPPORT	• EVA ASSEMBLY POSSIBLE; TWO MAN, OR MACHINE AIDED TASK PREFERRED TO ONE MAN OPERATION • CREW WORKSTATION/RESTRAINTS REQUIRED: CREW MOVEMENT IS COSTLY • STRUCTURAL ELEMENTS MUST HAVE FLEXIBILITY DURING ASSEMBLY • ASSEMBLY TIME FOR TETRAHEDRAL CELL APPROXIMATELY 1/4 HOUR • CONSIDER CREW FOR NONREPETITOUS TASKS, CONSIDER MACHINE FOR ERECTING/DEPLOYING STRUCTURES

Figure 8 Lessons Learned in Large Structure Assembly

It is important to note that assembly time is greatly reduced, and hardware damage is kept to a minimum when the crewman has a proper work-station, which includes foot restraints, and continuous visual and manipulative access to the components being assembled. It should also be emphasized that there must be flexibility among structural elements during the actual assembly operation. Unions on columns or beams which do not allow some play during assembly are strong candidates for damage.

We have found that a two-man EVA team can assemble a tetrahedral cell in about 15 minutes when properly restrained and with minimized crew activity. However, the water environment and its inherent drag on large volume, low mass equipment may make this a very conservative number. Use of other simulation modes may demonstrate that this number can be reduced.

Lastly, we should emphasize that manual EVA is an acceptable mode for nonrepetitious assembly tasks. However, if repetitious tasks are required or if assembly occurs remotely from the Orbiter cargo bay, we should consider remote controlled assembly equipment for large scale construction.

PART B - RESULTS TO DATE

BACKGROUND AND SCOPE

Essex Corporation is currently supporting MSFC's LSST program under a contract entitled "On-Orbit Assembly of Large Space Structures" (NAS8-32989). The overall purpose of the effort is to learn more about the cost for assembling a large structure by EVA crewmen working unaided or using available assembly aids such as the manned maneuvering unit (MMU), shuttle remote manipulator system (RMS), or a teleoperator. Although the total cost for a large structure would include costs for such activities as research and development, ground fabrication, checkout, and ground support, the cost for assembling a platform or antenna in space will be a major cost driver and should be considered when evaluating any proposed LSS as a candidate for further development and flight. The work being performed by Essex is aimed at developing assembly cost data so the assembly costs for any proposed structure can be estimated before any significant development expenses are incurred. Although embryonic in nature, this work could eventually have a tremendous impact on the selection of proposed structures for further evaluation.

CONTRACT TASKS

The two major activities being performed within the contract are (1) development of a cost algorithm for predicting assembly costs (Task 1), and (2) support of the LSS testing effort at MSFC's Neutral Buoyancy Simulator (Tasks 2, 3 & 4). The four tasks and their major outputs are shown below.

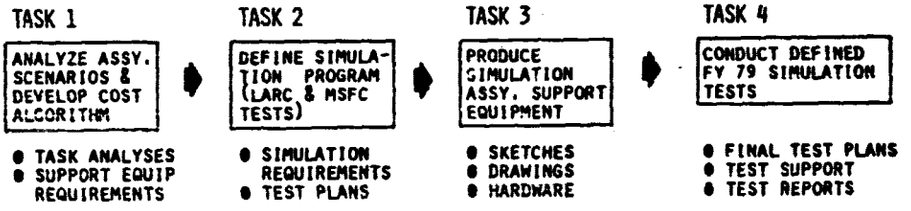

Task 1 is by far the most difficult and consuming of the four tasks. In this task, several LSS scenarios are being prepared that describe a wide range of structure configurations and assembly operations. These scenarios are used to develop more detailed functional analyses that describe the assembly steps and the hardware required to support the assembly task. The seven Task 1 subtasks are listed below.

SUBTASK

1.1 Develop Generic Assembly Scenarios
1.2 Define Assembly Tasks
1.3 Define Support Equipment
1.4 Develop Equipment Performance Requirements
1.5 Develop Cost Algorithm
1.6 Identify Cost Parameters
1.7 Determine Costs for the Six LSSs Studied and Other Proposed LSSs to Evaluate Cost Options

In Task 2, the neutral buoyancy test program is being defined in terms of the simulation requirements and support hardware required for the tests. Preliminary test plans are being prepared for evaluation of two types of joints and two types of columns. Preliminary test plans for evaluation of a 36 element structure to be provided by the Massachusetts Institute of Technology (MIT) are also being prepared.

The purpose of Task 3 is to provide hardware needed during the neutral buoyancy tests but not provided by MSFC or some other NASA center. This includes handrails, foot restraints, assembly fixtures, and data recording equipment.

In Task 4, the simulation test plans are updated to reflect the as-built hardware configurations and any additional procedural changes. During the tests Essex provides a test conductor as well as data recorders and test observers.

PROJECT STATUS

The major output from Task 1 is the cost algorithm for predicting assembly costs. To develop this algorithm, several supporting activities have been started that will provide input data to the algorithms such as the wide range of crew and aided assembly tasks and the cost for providing various labor and hardware elements. Although the cost algorithm is not complete, many of these supporting activities are near completion.

Five assembly scenarios have been prepared that describe the erection, deployment, and fabrication tasks for the structures listed below. These structures were selected not because of their probability of further development and flight but because of the wide range of assembly tasks they included that should be reflected in the algorithm.

- LaRC/RI Pentahedral Area Nodal Mount (Ref. 1)
- JSC/MDAC Single Trapezoidal Box with Nested Pallets (Ref. 2)
- JSC/MDAC Telescopic Spine (Ref. 2)
- MSFC Space Fabricated Platform (Ref. 3)
- MSFC 50m Deployable Antenna (Ref. 4).

Each of these scenarios includes the following major headings:

1.0 Outline
2.0 Description of Structure
3.0 Packaging Plan
4.0 Major Assembly Steps
5.0 Assembly Equipment and Aids
6.0 Problem Areas.

These sections describe the major activities that might impact total cost for structure assembly from launch through component deployment and assembly to scientific instrument installation and checkout.

Functional analyses that describe these structures in more detail have also been prepared. These documents describe in more detail the individual assembly

tasks, the crewmen and their locations, the crew aids and LSS hardware required to perform the task, and the time required.

Individual cost elements such as assembly fixtures, handrails, or remote manipulators have been identified and are presented in Table 1. The specific costs for each of these elements is currently being assessed in terms of dollar cost, volume, weight, etc. The costs for these items will not remain static, and some will be entirely structure-dependent. Any uncertainties associated with the individual cost elements are being recorded in addition to the projected cost per unit, flight, pound, foot, hour, etc.

Table 1 - LSS Assembly Cost Elements

(1) Labor
- EVA Astronauts
- IVA Support Crew
  - o RMS Operator
  - o Assy Coordinator
- Ground Support Crew
- Training Time, Materials & Development
- Development Simulations

(2) LSS Hardware
- LSS Beams or Columns
- Utility Conduits & Junction Boxes
- Experiment Pallets
- LSS Subsystem
  - o Attitude Control System
  - o Power System
  - o Thermal System
  - o Sensors
- Alignment Tools
- Jigs & Fixtures
- Crew Tools
- Crew Aids
  - o Handrails
  - o Foot Restraints
  - o Tethers
  - o Lights
  - o Cameras & Monitors
  - o Portable Work Stations
- RMS & End Effectors
- MMU
- Materials (Sheet Stock, Welding Materials, etc.)
- Fasteners

(3) Crew Support Equipment
- Pressure Suits
- Suit Resupply
- Suit Stowage & Handling
- Food & Other Consumables
- Time On Orbit
- Assy Procedures, Checklists, Diagrams
- Communication Equipment

(4) Flight Operations
- No. of Flights
- Duration of Flights
- No. of Onboard Crewmen
- No. of Ground Crewmen
- No. of EVAs
- EVA Duration
- Orbital Maneuvers

(5) Other
- Assy Error Probability
- Assy Destruction Probability
- Power (Aug & Peak)
- Hydraulics, Pneumatics
- Ground Prep. Time (Packaging)
- Development Costs

Development of the initial cost algorithm should be completed by February, 1980.

In Task 2, a generic simulation test plan was prepared for distribution by MSFC to contractors and other NASA centers who are planning test activities in MSFC's Neutral Buoyancy Simulator. This plan identifies the step-by-step task descriptions required, the data recording capabilities and other information needed by personnel not familiar with the MSFC test procedures.

Additionally, preliminary test plans were prepared for evaluation of the LaRC snap joint/unions, Rockwell ball and socket joints, and the 18 ft and 30 ft columns (NB-18A, B and C).

In Task 3 a video tape recording system was provided for recording the test runs. This system has been tremendously useful for analyzing the crew assembly operations after the test runs.

A manned maneuvering unit (MMU) mockup is also being designed for use in the simulator to support the LSS test runs.

In Task 4 six member tetrahedral cells were assembled 38 times during 21 test runs. During the runs Essex provided a test conductor, data collectors, and test observers. Final test plans were provided prior to each run, and quick-look test reports were prepared after each run. Final test reports were also prepared describing the results of all the tests. Figures 9 through 14 illustrate the assembly of the tetrahedral cell from initial conditions through installation of the simulated equipment module (SEM) at the apex at the end of the run. Figures 15 and 16 show the two joints evaluated.

MAJOR STUDY OUTPUTS

Three study outputs are presented below in addition to the results already discussed in the above project status summary. These study outputs are:

- Neutral buoyancy test results
- Task element times
- Status of cost algorithm.

NEUTRAL BUOYANCY TEST RESULTS

The results of the 21 neutral buoyancy test runs to evaluate the snap joint/unions, ball and socket joints, and 18 ft and 30 ft columns are presented in detail in the quick-look and final test reports. However, the following paragraphs summarize the results and conclusions.

Assembly Time - The lowest assembly times for unaided operations (no RMS or MMU) for the 18 ft columns were on the order of 30 min for the six element structure. The best assembly times using the simulated RMS for column handling and a simulated MMU for crew translation for three union/column combinations are listed below.

	Time (Min)
• Ball and Socket w/ 30 ft Columns	10.6
• Ball and Socket w/ 18 ft Columns	11.1
• Snap Joint w/ 18 ft Columns	14.5

This represents an evaluation of two types of unions and columns from dozens of possible alternatives. Obviously no firm hardware tradeoff data should be drawn from these preliminary tests. However, it does appear that the assembly operation is possible with existing STS equipment and EVA technology and the assembly time for a six element structure is in the 15-30 min. range.

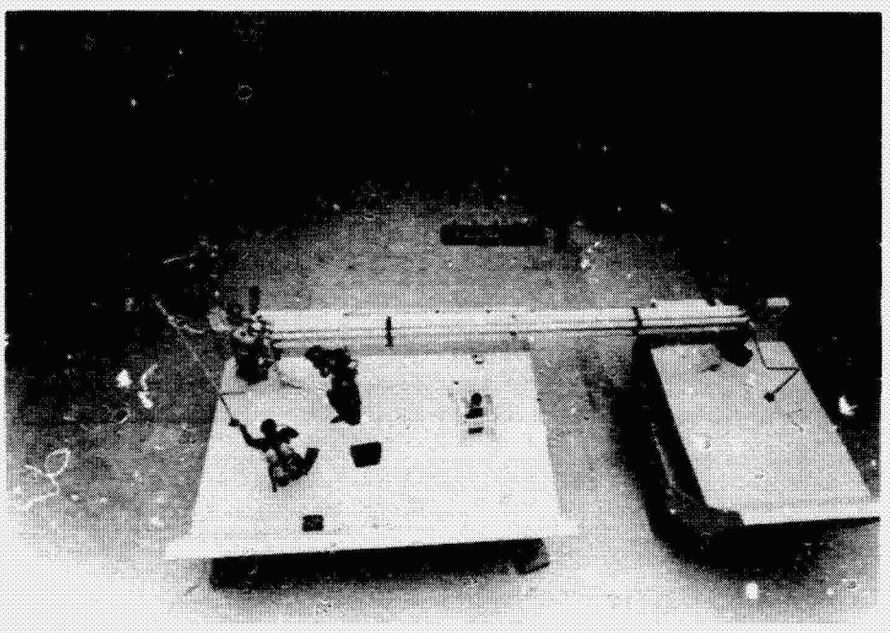

Figure 9 - Test Setup for LSS Tetrahedron Assembly

ORIGINAL PAGE IS
OF POOR QUALITY

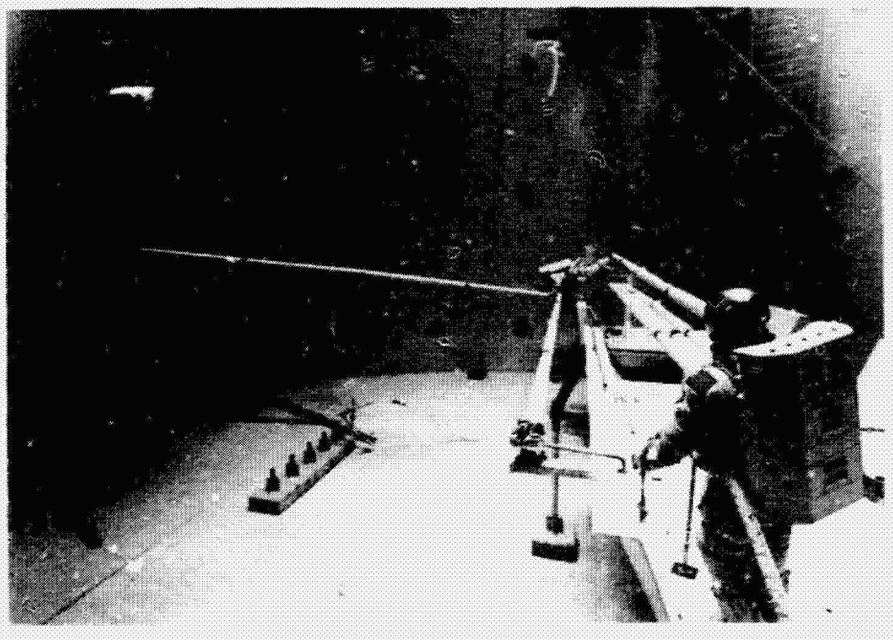

Figure 10 - Installation of Second Column

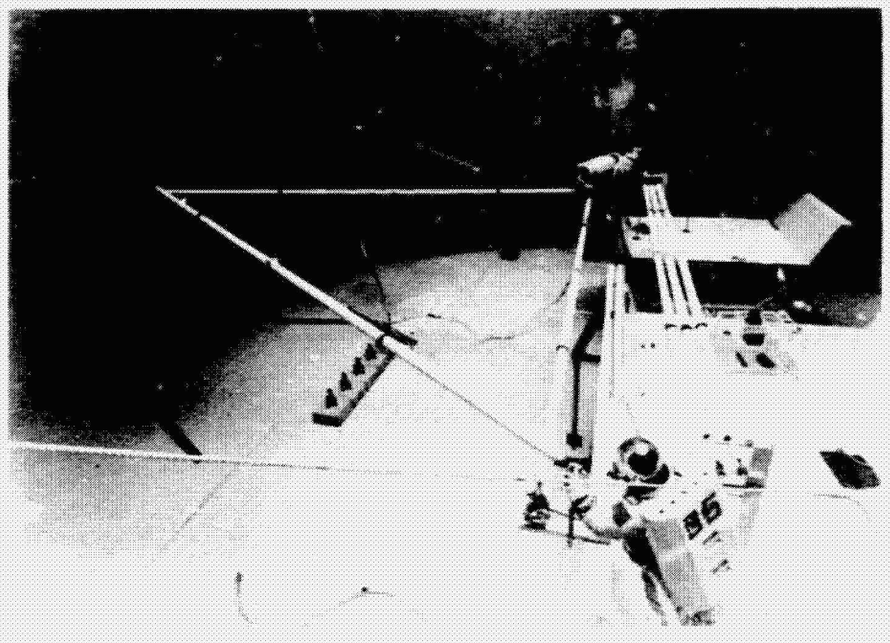

Figure 11 - Completion of Base Triangle

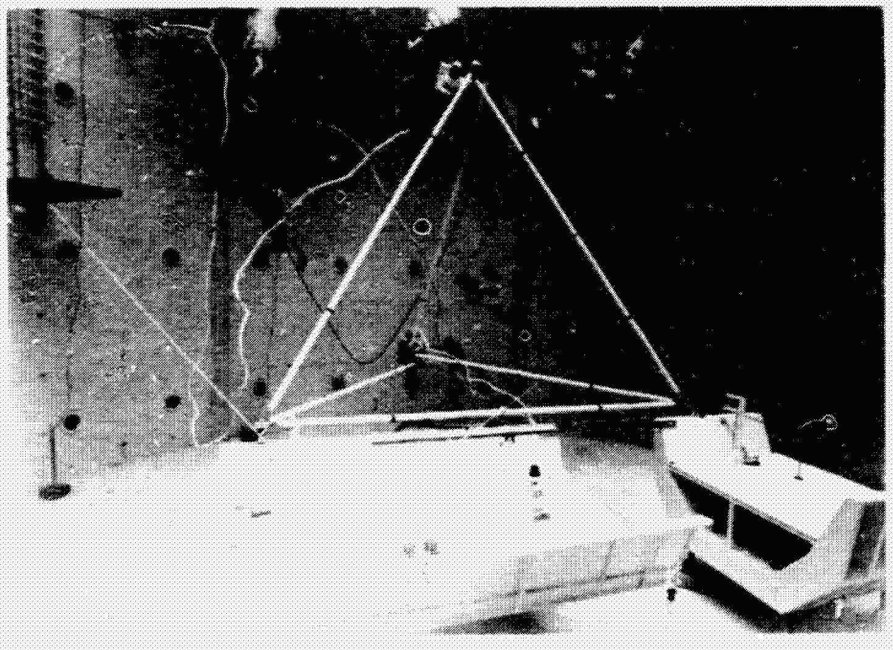

Figure 12 - Completion of Tetrahedron Structure

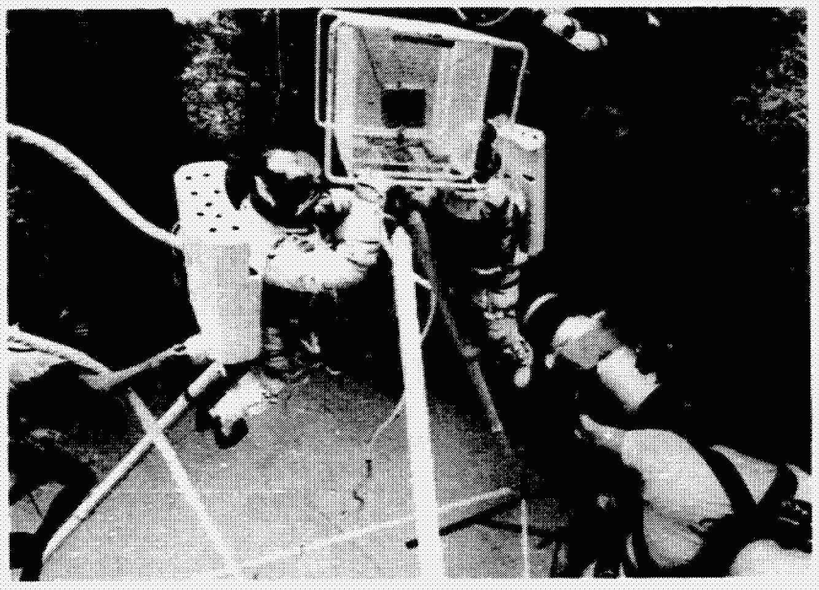

Figure 13 - Installation of Simulated Equipment Module

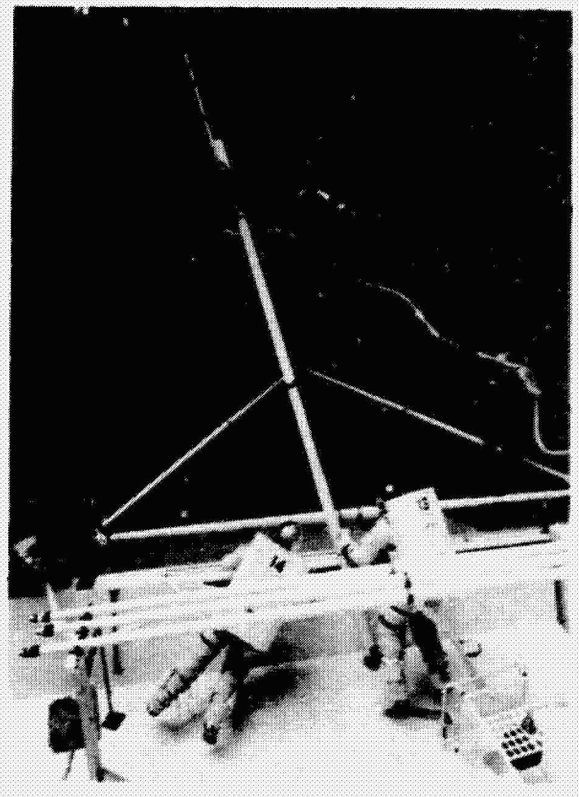

ORIGINAL PAGE IS
OF POOR QUALITY

Figure 14 - Erection of Apex Assembly Aid (Not used on all runs)

Figure 15 - Ball and Socket Joint

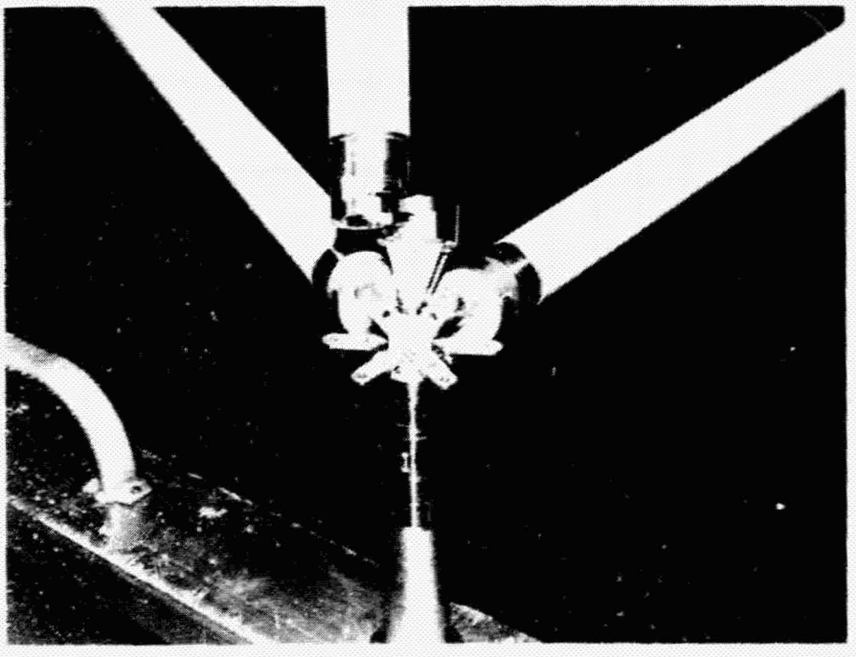

Figure 16 - Snap Joint/Union

ORIGINAL PAGE IS
OF POOR QUALITY

Ease of Operations - Subjectively, the crew preferred the ball and socket joints. It appeared from the run times that more training was required for the snap joint/unions for the crew to become proficient at mating the unions.

Support Equipment Needed - The snap joint/union was more easily operated when a positive crew restraint such as a foot restraint was used. The crew could easily use the ball and socket joint without the aid of a foot restraint.

Reliability - The snap joint/union often could not be mated by the crewman because of column or assembly fixture misalignment. This required that the utility divers make the connection or verify that the crewman had successfully made the connection. This was not true for the ball and socket joints.

TASK ELEMENT TIMES

The evaluation of video tapes from the LSS test runs and some of the Space Telescope test runs revealed 10 major task categories. All the crew operations can be described in terms of these task categories and 83 subtask categories or individual task elements. The 10 task categories are:

- Remove
- Translate
- Position Body
- Ingress
- Egress
- Attach
- Transfer
- Mate
- Verify
- Hand Tool Use

The task elements shown in Table 2 can be used to describe all the crew operations observed in the LSS and Space Telescope test runs. The Space Telescope runs were used to include large module handling and the use of tools which were not observed during the LSS runs.

The task element data presented in these charts can be used along with detailed assembly procedures for any proposed structure to estimate the structure assembly time. The validity of the task element time data will be determined by comparing estimated versus actual assembly times for LSS structures assembled in the neutral buoyancy simulator in the future (e.g., the MIT test scheduled for January, 1980).

STATUS OF COST ALGORITHM

The initial cost algorithm for predicting total LSS assembly costs is currently a collection of independent sets of data with no connecting logic. The major parts of the algorithm are the task element times, cost elements, and functional analyses that define support hardware the labor requirements. It is anticipated that the initial algorithm will be completed in February, 1980 and will be continually updated and expanded throughout the LSST program.

Table 2 - LSS Assembly Task Element Times

TASK ELEMENT		TIME (sec)
1.0	REMOVE	
1.1	Equipment Module from Receptacle (3'x3'x2' - push/pull, no latch)	21
1.2	Union from Box	7
1.3	Union from Post	NA
1.4	Pin from Post	NA
1.5	Column from Rack	8
1.6	Waist Tether from Handrail	12
1.7	Wrist Tether from Union	6
1.8	Wrist Tether from Equipment Module	8
1.9	Module from Base Plate Pins - Critical Alignment	15

TASK ELEMENT		TIME (sec)
2.0	TRANSLATE	
2.1	Along Sill 10 ft.	24
2.2	Along Sill 20 ft.	49
2.3	Over Sill from Outrigger	21
2.4	Over Sill from Cargo Bay	11
2.5	Up Assy Aid Pole 15 ft.	40
2.6	Down Assy Aid Pole 15 ft	22
2.7	Up Assy Aid Pole 15 ft. with Equipment Module (3'x3'x1-1/2')	44
2.8	20 ft. with Columns Using MMU	NA
2.9	30 ft. with Columns Using MMU	NA
2.10	20 ft. Using MMU	NA
2.11	30 ft. Using MMU	NA
2.12	Body 90°	10
2.13	Body 180°	20
2.14	10 ft. Along Straight Handrail	12
2.15	10 ft. Along Curved Handrail	15

TASK ELEMENT		TIME (sec)
3.0	POSITION BODY	
3.1	To Ingress Foot Restraint	19
3.2	To Ingress Leg Restraint	29
3.3	To Attach Waist Restraint	NA
3.4	To Attach or Verify Union Connection	22
3.5	To Verify Column Connection	23
3.6	To Receive Union	NA
3.7	To Receive Column in Leg Restraint	7
3.8	To Receive Column in Foot Restraint	NA
3.9	To Receive Column w/o Leg or Foot Restraint	17

TASK ELEMENT		TIME (sec)
4.0	INGRESS	
4.1	Foot Restraint Using One Handrail	21
4.2	Foot Restraint Using Two Handrails	13
4.3	Leg Restraint Using One Handrail	37
4.4	Leg Restraint Using Two Handrails	NA

TASK ELEMENT		TIME (sec)
5.0	EGRESS	
5.1	Foot Restraint Using One Handrail	8
5.2	Foot Restraint Using Two Handrails	5
5.3	Leg Restraint Using One Handrail	14
5.4	Leg Restraint Using Two Handrails	NA

TASK ELEMENT		TIME (sec)
6.0	ATTACH	
6.1	Waist Tether to Handrail with Foot Restraint	16
6.2	Waist Tether to Handrail w/o Foot Restraint	20
6.3	Union to Own Wrist Tether	17
6.4	Union to Other Crewman's Wrist Tether	NA
6.5	Waist Tether to SEM	12
6.6	Module to Clothesline Hook	12
6.7	Wrist Tether to Clothesline Module	15

Table 2 - LSS Assembly Task Element Times (Continued)

	TASK ELEMENT	TIME (sec)
7.0	TRANSFER	
7.1	Assy Aid to Vertical Position (1 or 2 crewmen)	33
7.2	Assy Aid to Locked Position	26
7.3	18 ft. Column 10° Using Foot Restraint	12
7.4	18 ft. Column 60° Using Foot Restraint	49
7.5	18 ft. Column 60° Using No Foot Restraint	43
7.6	30 ft. Column 10° Using Foot Restraint	NA
7.7	30 ft. Column 60° Using Foot Restraint	NA
7.8	30 ft. Column 60° Using No Foot Restraint	NA
7.9	Module on Clothesline 20 ft.	35

	TASK ELEMENT	TIME (sec)
8.0	MATE	
8.1	Assy Aid Clamp to Pole	56
8.2	Union to Pedestal - Critical Alignment	28
8.3	Column to Union - Critical Alignment	31
8.4	Equipment Module to Union-Critical Alignment	95
8.5	Union to Pedestal - Coarse Alignment	23
8.6	Column to Union - Course Alignment	9
8.7	Equipment Module to Union-Gross Alignment	34
8.8	Union to Assy Pole Clamp	55
8.9	Union to Column - Course Alignment	9
8.10	Tighten Ball Joint Jam Nut	12
8.11	Module to Base Plate Pins-Critical Alignment	90

	TASK ELEMENT	TIME (sec)
9.0	VERIFY	
9.1	Assy Aid Pole Clamp Secure	30
9.2	Assy Aid Union Clamp Secure	35
9.3	Union Mated to Pedestal - Critical Alignment	20
9.4	Column Mated to Union - Critical Alignment	36
9.5	Union Mated to Pedestal - Gross Alignment	NA
9.6	Column Mated to Union - Gross Alignment	NA

	TASK ELEMENT	TIME (sec)
10.0	HAND TOOL USE	
10.1	Grasp Tool	17
10.2	Position Ratchet on Bolt	9
10.3	30° Ratchet Stroke*	3
10.4	45° Ratchet Stroke*	4
10.5	90° Ratchet Stroke*	6
10.6	180° Ratchet Stroke*	10
10.7	Release Bolt Clip	20
10.8	Engage Bolt Clip	25
10.9	Translate 2' Between Bolts	10

*Less than 5 ft-lbs. torque

SUMMARY

The major activities remaining in the existing Essex contract are additional support of the LSS tests planned for January, 1980 and completion of the initial cost algorithm. These activities as well as the tasks already completed will be described in a report due in February.

REFERENCES

1. Final Review, Erectable Space Sciences and Applications Platform Study, SSD 79-0029, February 15, 1979, Contract NAS1-15322.

2. Deployable Orbital Service Platform Conceptual Systems Study, Final Review, MDC G7593, February 14, 1979.

3. Systems Definition Study for Shuttle Demonstration Flights of Large Space Structure, Final Review, Grumman Report No. N55-LS-RP0020, April 1979, Contract NAS8-32390.

4. Final Report, Deployable Antenna Phase A Study, May 15, 1979, Contract NAS8-32394.

N80-19160

SPACE CONSTRUCTION AND UTILITY DISTRIBUTION

K. A. Bloom

Satellite Systems Division
Rockwell International

LSST 1st Annual Technical Review

November 7-8, 1979

A summary of the Rockwell International activities for FY 1979 relating to Large Space Structures Technology, with emphasis primarily on space construction and utility distribution for erectable and deployable platforms.

PAGE 286 INTENTIONALLY BLANK

SPACE SCIENCES AND APPLICATIONS PLATFORM

Derivation of near-term space platform technology requirements was the primary objective of the Space Sciences and Applications Platform Study. Technology advancement to effect an orderly development program leading to construction of space platforms in the 1985 time period was defined, in a program that utilized a viable platform and service module concept with concise OSS/OAST mission ard payload models. Consideration was given to concepts for alternate platform servicing of the payloads described in the model. One of these concepts was selected (Figure 1) for detailed definition and for provision to act as a baseline for technology requirements study.

Using the baseline configuration, issues pertinent to platform development as well as orbit emplacement and operation and on-orbit construction methodology were analyzed. These analyses provided the following data: (a) payload definitions and installation options, (b) identified structural and subsystems options, (c) developed integrated platform system concepts, and (d) identified technology deficiencies and recommended technology development timelines.

SCIENCE AND APPLICATIONS PLATFORM

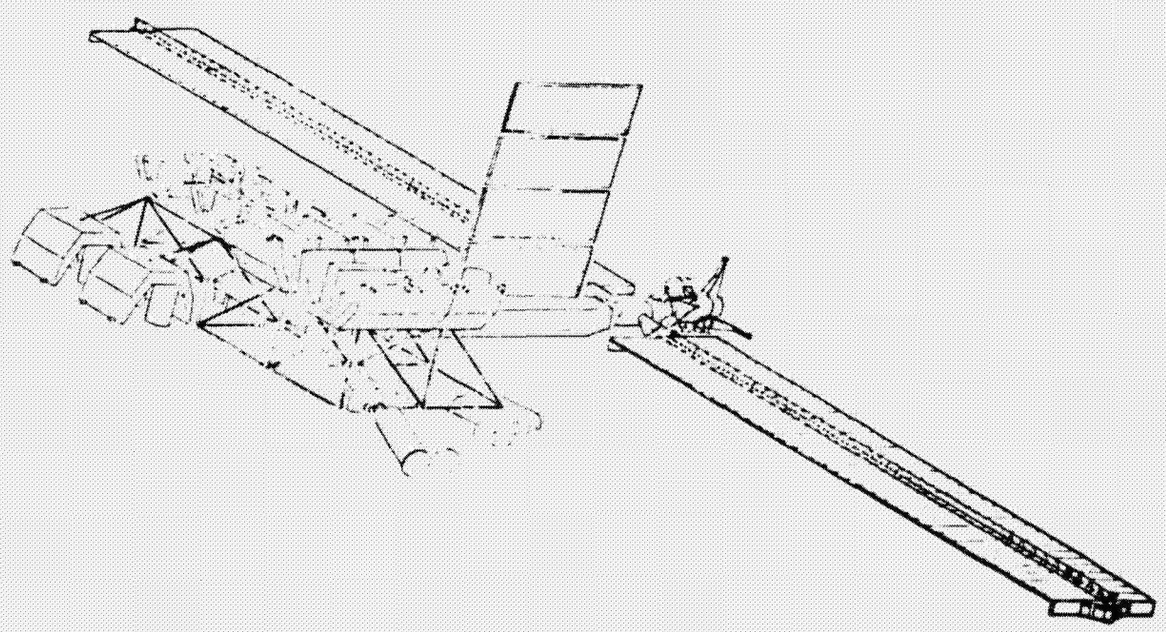

Figure 1

SCIENCE AND APPLICATIONS PLATFORM TECHNOLOGY DEVELOPMENT PLANNING

Utilizing the data obtained from the Science and Applications Platform Study a generalized technique was established for estimating technology development requirements. The schedule period (fifty-eight months for the development program) extended from the determination of the system requirements through the completion of a systems integrated ground test. Major subsystems applicable to a platform such as would be used in the science and applications mission were defined as well as the interaction of these systems with the structure and associated construction equipment. Scheduling and development requirements encompassed the activities/tasks relevant only to the construction of the platform (i.e., individual subsystems would be completed only to the extent of their effect upon the design of the platform structure and construction equipment). Figure 2 depicts a portion of the development planning schedule done in chart form that incorporates the data used in developing the PERT type program (i.e., the interrelationship between each system and the tasks within each system, including task durations).

It was during the Space Sciences and Applications Platform Study and the subsequent development planning that it became apparent that two major challenges exist in large space systems (LSS) construction. These are: (a) the installation of utility distribution systems and (b) the design/development of construction fixtures required for construction of the space platform.

SCIENCE AND APPLICATIONS PLATFORM
TECHNOLOGY DEVELOPMENT PLANNING

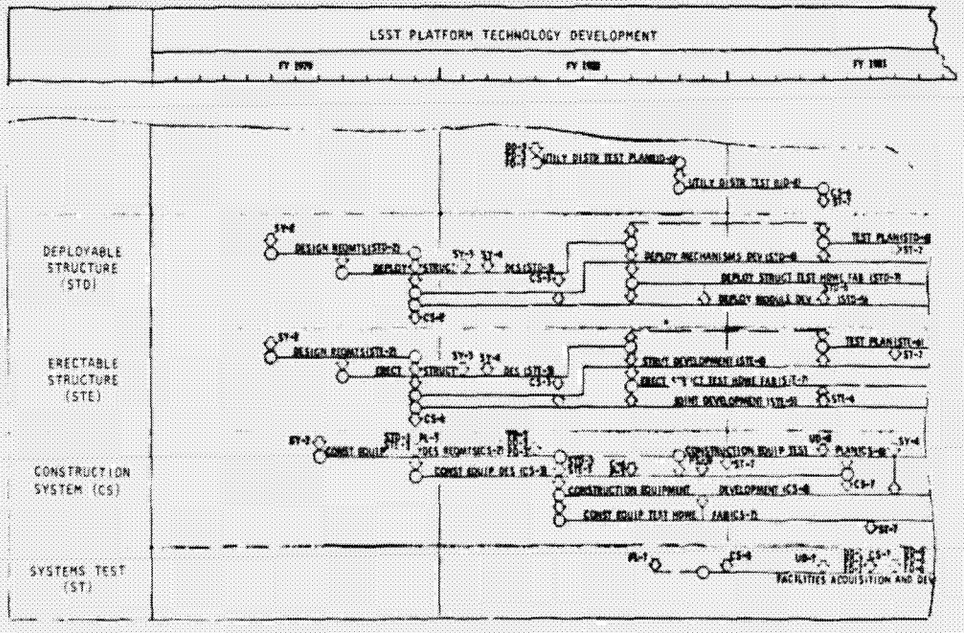

Figure 2

ORIGINAL PAGE IS
OF POOR QUALITY

UTILITIES DISTRIBUTION

The technique of distributing power and data lines and fluid (e.g., cooling, if necessary) lines to and from the various payloads on a large space system is an important consideration in the design and development of the system. It is as significant as the platform structure design. Some of the more important factors to consider when designing the utility distribution system are shown in Figure 3. Options that must be considered in implementing the distribution of utilities, range from the methods by which the system is installed, or integrated, to the actual form the utility is to take. A thorough study and tradeoff analysis are required to arrive at an optimum configuration.

The options are subject to the influence of many drivers. The physical design of the structure and its construction process have a great influence on the distribution system design. Variations in the platform design, and construction sequence would in many cases provide more impact than variations in the magnitude of the utilities. The entire scenario of stowage, installation, servicing, etc., establishes a basis for the design of the distribution system.

Detail problems associated with utility distributions are similar to those encountered in earth-bound systems; however, the solutions are not necessarily the same. Considerable research and development is necessary to resolve the problems associated with space environment and to bring them into state-of-the-art.

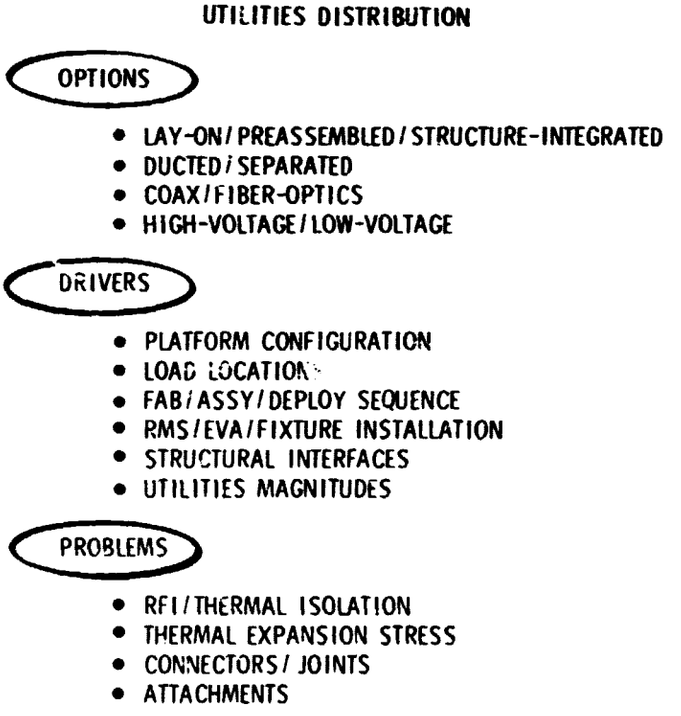

Figure 3

DEPLOYABLE/ERECTABLE UTILITY DISTRIBUTION CONCEPT

A concept for a utilities distribution system was developed utilizing the Space Sciences and Applications Platform as a model. The concept provides power, cooling and data service to various payload pallets mounted on the node points of a tetrahedral truss structure. This concept is shown in Figure 4. Utilities, originating at the side-mounted power module, are routed underneath the node points, to preserve the pallet access and follow the path of the surface columns. High/low voltage regulators are incorporated into the distribution runs to minimize the cable size in the sections that must transmit higher power.

Pallet interface points are located near the centers of the surface columns to service each pallet location. The upper ends of these lines would interface with standard payload connectors such as those proposed for standard mounted payload pallets. Shut-off and selection valves would interface the coolant line runs to a standardized connector plate in the vicinity of the payload.

DEPLOYABLE/ERECTABLE UTILITY DISTRIBUTION CONCEPT

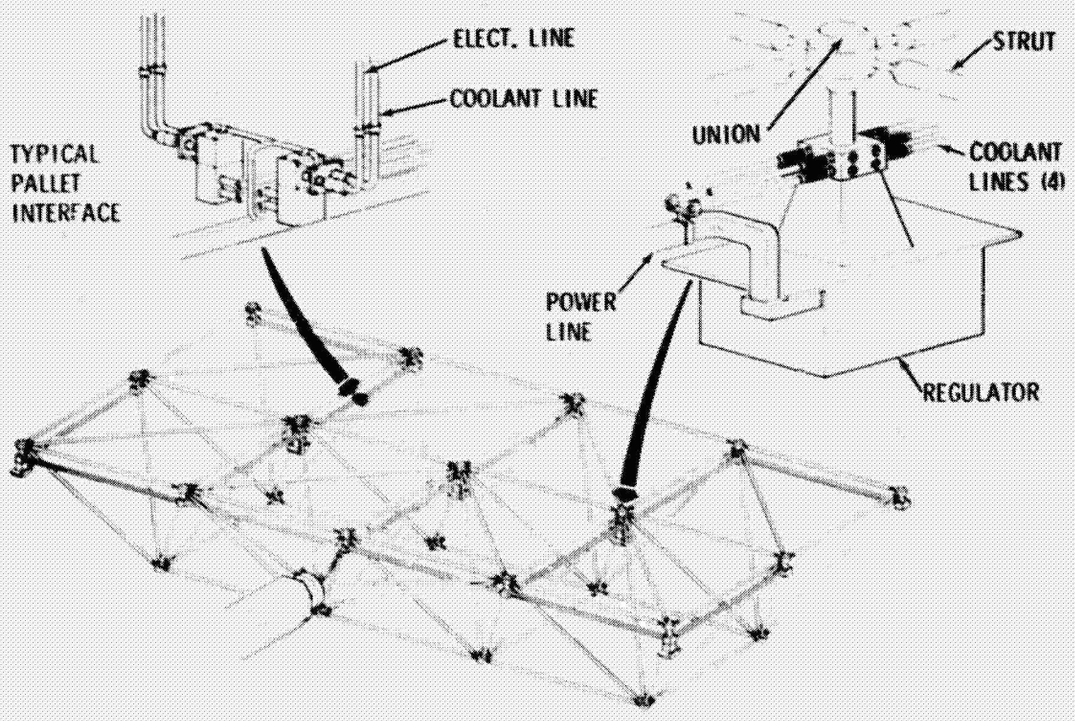

Figure 4

SPACE FABRICATED ELECTRICAL POWER AND DATA DISTRIBUTION CONCEPT

In contrast to the semi-rigid/rigid line installation shown in Figure 4, a flexible line concept for a space fabricated platform shown in Figure 5 has been defined in a space construction system analysis study. This concept allows for continuous installation of electrical power and data lines during beam fabrication. A fabricated utility bundle, complete with branch connectors, would be attached to the space fabricated structure as one of the automated operations of the platform construction fixture. Interconnection of the utility lines on the longitudinal beam with similar lines on the cross beams may require Astronaut Extravehicular Activity (EVA).

SPACE FABRICATION
ELECTRICAL POWER AND DATA DISTRIBUTION CONCEPT

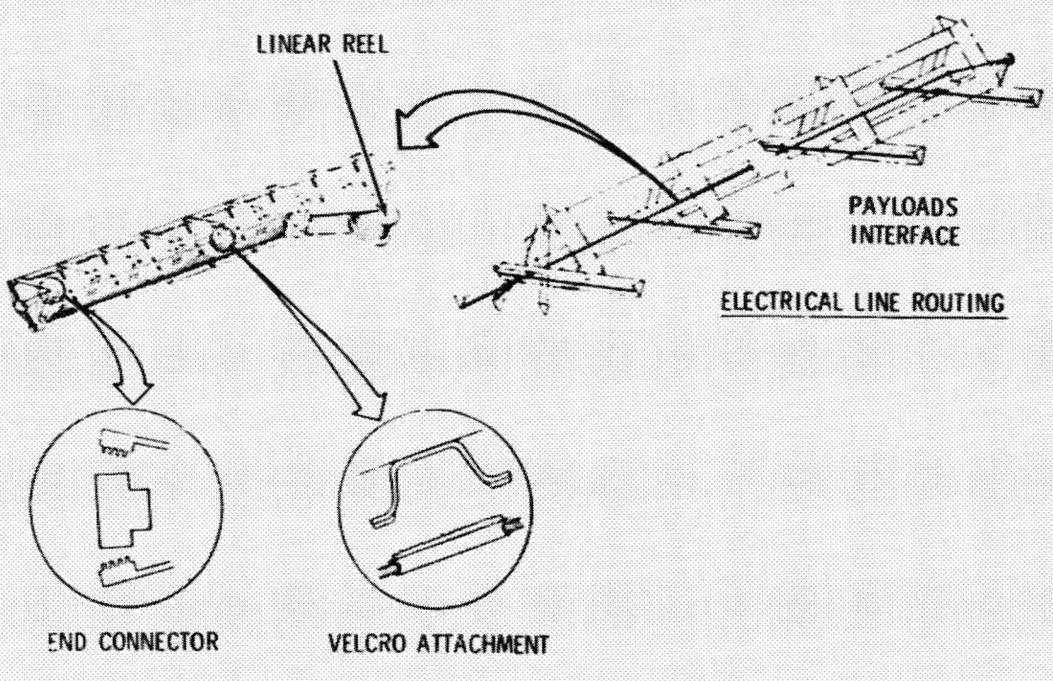

Figure 5

INTEGRATED FIBER-OPTIC CONNECTOR

Data transmission through fiber optics (F/O) for LSS applications has additionally been concluded as acceptable for use in relay satellites for digital transmission of mail, control and regulation of power status, etc.. A design study was conducted to determine a feasible method to integrate the F/O capability into the space platform construction. The objective of the study was to develop methods for connecting erectable structure type unions and struts that have F/O connectors as an integral part of the assembly. Specifically, the design objective was to provide a mechanism that would mate and align a F/O connector plug/receptacle set during a strut/union on-orbit assembly operation using the Remote Manipulator System (RMS) or Astronaut Extravehicular Activity (EVA). From a comprehensive set of mechanism concepts the design shown in Figure 6 was selected. Subsequently, design of the concept was generated in sufficient detail to permit fabrication of a test article. Tests will be performed using the test article to assess the contributions of the mechanism toward the overall attenuation of the optical path.

INTEGRATED FIBER-OPTIC CONNECTOR

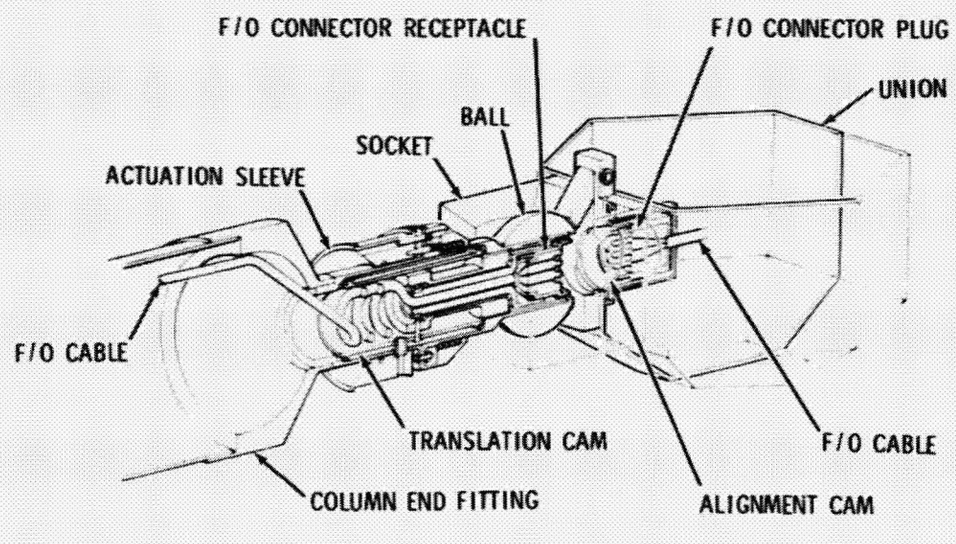

- EVALUATE OPTICAL LOSSES DUE TO ALIGNMENT
- TESTS TO START 12/79

Figure 6

ERECTABLE STRUCTURE ASSEMBLY SIMULATION

The utilities distribution system is not solely comprised of lines and connections. A significant item for installation of the utilities is the installation/attachment of such items as regulator boxes, systems modules and payloads after the platform has been assembled. Figure 7 illustrates one method by which such attachments could be made. The device is an adaptor that interfaces with the union socket assembly on one end with provision for module attachment at the other end. When inserted into the union it is self-aligning and mechanically activates a mechanism which drives an acme threaded screw into a receiving nut in the union; a rigid joint is thereby provided. The energy source for the adaptor is a set of two clock springs. A test article was fabricated and successfully tested in the Neutral Buoyancy Simulator (NBS) at Marshall Space Flight Center (MSFC) by pressure-suited subjects in a simulated EVA mode. Installation time for the adaptor was under three minutes.

LARGE SPACE SYSTEMS
ERECTABLE STRUCTURE ASSEMBLY SIMULATION
AT MSFC'S NEUTRAL BUOYANCY SIMULATOR

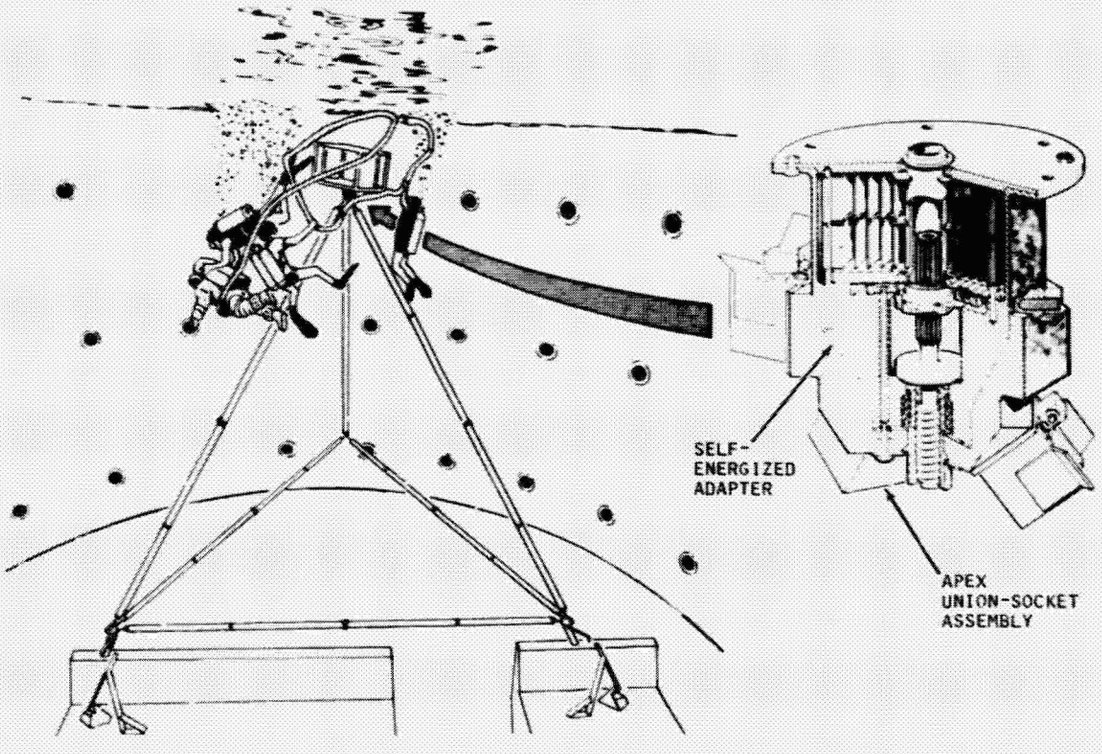

Figure 7

ERECTABLE STRUCTURES ASSEMBLY SIMULATION
PRELIMINARY TEST RESULTS

During 1979, other LSS tests of interest were performed at the MSFC/NBS by pressure-suited subjects to investigate operational procedures and techniques for the assembly of large erectable space structures. Timeline data for assembly of a repeating cell of a tetrahedral truss platform was obtained for varied parameters. The test variables included:

(a) Assembly Techniques
- Manual - Subjects performed assembly tasks as well as transportation tasks.
- Augmented - Subjects performed assembly tasks but transportation tasks were performed by RMS simulations.

(b) Column Lengths
- 30 Foot tubular column, hinged in center (NB-18B Assy. Test)
- 18 Foot nestable column (NB-18C Assembly Test)

(c) Hinged Design (30 Foot Column Only)
- Sleeve Lock (S)
- Latch Lock (L)

(d) Deployment Methods
- Manual
- Anchor - Manual with one column end anchored
- Anchor + Fulcrum - Manual with one column end anchored and a fulcrum used as a deployment aid.

Preliminary test results are shown in Figure 8.

LSS ERECTABLE STRUCTURES ASSEMBLY SIMULATION
PRELIMINARY TEST RESULTS

TEST			NO. OF TRIALS	AVG (RMS) TIME (MIN:SEC)
NB-18B ASSEMBLY	MANUAL		4	22:40
	AUGMENTED		4	14:54
NB-18C ASSEMBLY	MANUAL		2	13:38
	AUGMENTED		2	10:40
NB-18B COLUMN DEPLOYMENT	MANUAL	S	5	1:16
		L	5	1:09
	ANCHOR + FULCRUM	S	2	1:21
		L	2	1:05
	ANCHOR ONLY	S	2	0:39
		L	2	0:42

Figure 8

LSS CONSTRUCTION FIXTURES

Methods/processes for constructing large space systems, using the Shuttle Orbiter as the construction base, range from the erectable assembly of structure from components pre-fabricated on the ground to pre-assembled deployable structure to fully automated in-space fabrication using beam machine facilities. Figure 9 illustrates several types of construction fixtures that would accommodate various configurations of platforms.

Erectable Platforms - Assembled on-orbit from unions and struts by RMS and/or EVA.

(a) Small Area Erectable - A platform similar to the Science and Applications Platform that can be assembled in one orbiter flight.

(b) Large Area Erectable - Similar to a small area erectable but much larger and would require multiple orbiter flights to assemble with orbiter return capability.

(c) Linear Erectable - A long slender platform 200 meters or greater in length with width no greater than the length of a strut. It also would require multiple orbiter flights to assembly with return capability.

Deployable platforms - Pre-assembled on the ground and folded for packaging in the orbiter payload bay. When in orbit the platform is removed from the orbiter, and deployed to form the platform either by RMS or by a self-contained deployment mechanism. The platform size is generally dependent on one orbiter mission transportation capability.

Space Fabrication - On-orbit fabrication of the main structure of LSS platforms using a beam fabricating machine. Beam material is brought to orbit in the orbiter in an unformed stage (e.g., flat stock on reel) where it is formed and welded together to produce a platform structure. Multiple orbiter flights are required for assembly completion, thus requiring orbiter return capability.

Assembly Fixture and Aids - This study presently being performed will derive concepts and requirements for assembly fixtures and aids necessary to the assembly and maintenance of the erectable and deployable space platforms. The results of the study are necessary for the initiation and definition of planning to develop cost effective, Shuttle compatible space systems for the 1985-2000 time frame. Initial tasks of the study included literature search of previous studies to summarize the construction equipment requirements previously defined and to use this information as a data base for further construction definition.

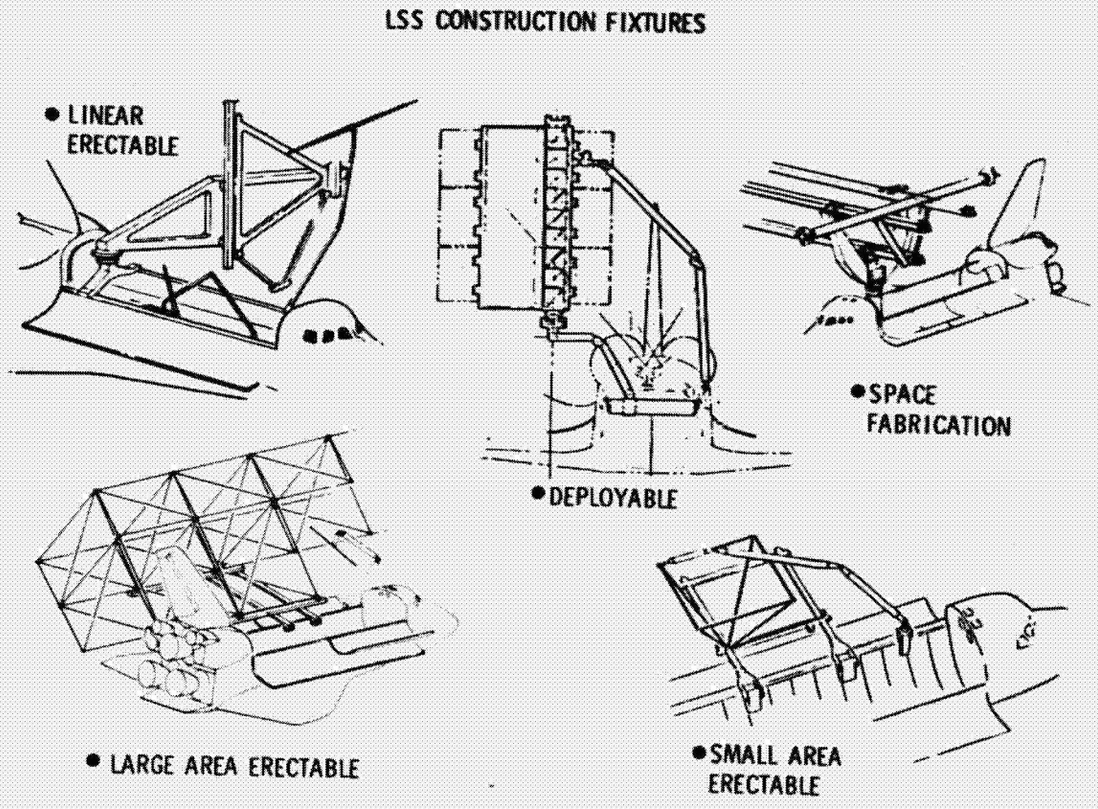
LSS CONSTRUCTION FIXTURES
• LINEAR ERECTABLE
• DEPLOYABLE
• SPACE FABRICATION
• LARGE AREA ERECTABLE
• SMALL AREA ERECTABLE

Figure 9

CONSTRUCTION ACTIVITIES AND EQUIPMENT REQUIREMENTS

Four model platforms were selected for an in-depth analysis of fixture requirements. The platforms were categorized into:

Class I - Platforms that would be assembled during one orbiter flight.
- o Small Area Erectable
- o Deployable

Class II - Platforms requiring more than one orbiter flight or assembly.
- o Large Area Erectable
- o Linear Erectable

For each platform a matrix of construction activities versus equipment requirements (see Figure 10) was generated. This matrix defined the construction activity, fixture requirements (including orbiter and platform interfaces), visual aids and other equipment required (i.e., RMS, Cherry Picker, etc.). Commonality of requirements for construction fixtures for all platforms included: (a) platform secure/release capability, (b) platform translation, (c) provision for electrical interface - orbiter to platform, (d) indicating sensors for operations (deploy, capture, etc.), and (e) lighting and TV installations. The fixture requirements analysis also pointed out the impact that size and shape of the platforms have on the construction fixture. For example, the large area platform requires additional construction equipment to assemble as compared to the small area platform or the linear platform where the RMS reach is more effective. Additionally, installation of systems (utility distribution) and payloads can be drivers in the design of the fixture insofar as reaching to distant points of a platform to install or service a system may require rotation or tilting of the platform for accessibility.

CONSTRUCTION ACTIVITIES AND EQUIPMENT REQUIREMENTS
CLASS I AREA ERECTABLE STRUCTURE

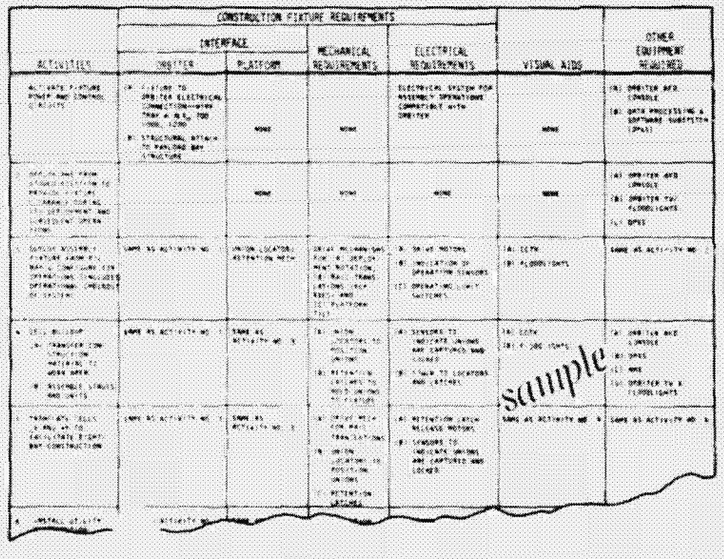

Figure 10

CONSTRUCTION FIXTURE DESIGN FUNDAMENTALS

From the studies performed to date certain fundamental design criteria have been generated (see Figure 11). During construction operations the fixture must not only include platform retention and mobility (translation, rotation, tilting) but should incorporate provisions to support EVA activity in the form of foot restraints, hand holds, equipment stowage, etc.. Large platform construction requiring more than one orbiter flight to assemble would impose the requirement in the fixture to provide an attaching module containing libration damping capability as well as orbiter return capability (i.e., docking port, rendezvous lights/transponders, etc.). The fixture design must also include consideration for packaging in the orbiter payload bay. In most cases volume in the bay is the critical factor; therefore, the least volume required for the fixture should be a design goal. Lastly, the fixture to platform interface must be compatible structurally and mechanically as well as providing utilities transfer if required.

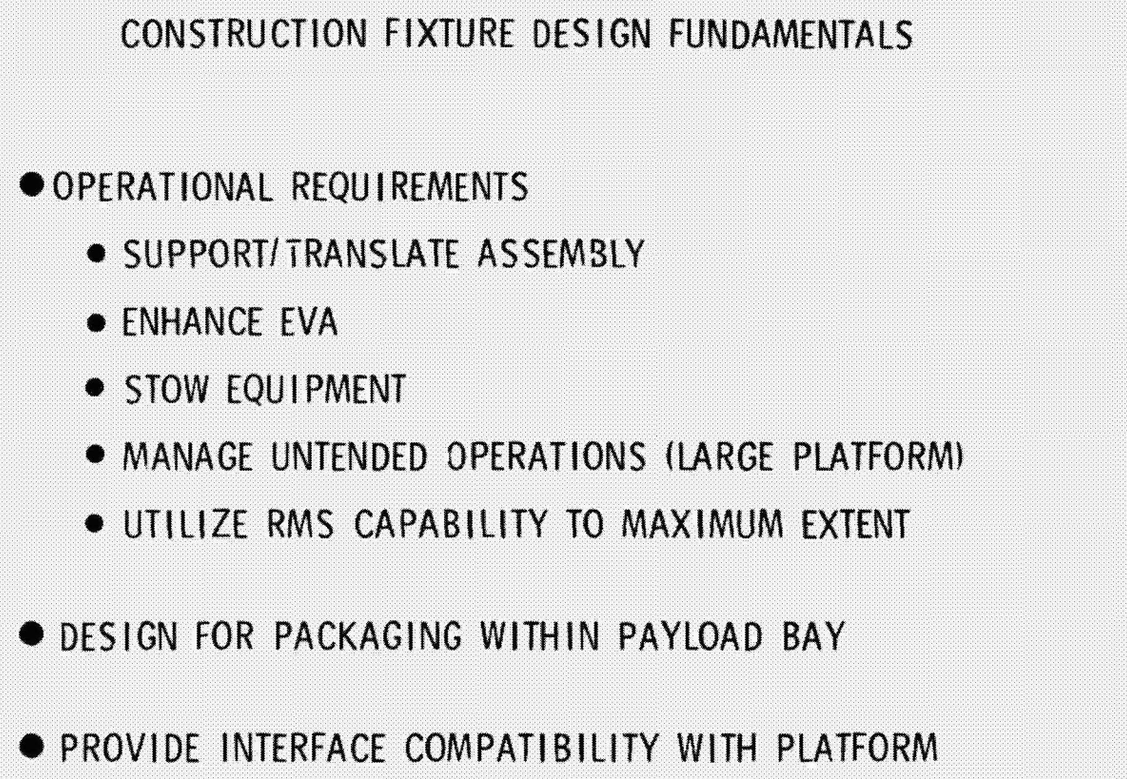

Figure 11

DUAL-USAGE FIXTURE, DEPLOYABLE/ERECTABLE

A design concept is presently being formulated which will provide an interchangeability in components to accommodate the construction of the following platforms: (a) a small area erectable, (b) a deployable, and (c) a linear erectable. This concept will be developed in sufficient detail to provide a rough order of magnitude (ROM) estimate for fabricating a test article for subsequent systems tests. A preliminary concept of this fixture is shown in Figure 12. The concept incorporates a deployable arm, which can be mounted either on the orbiter payload bay longeron or on a special structural member, and a translating rail fixture. One or both portions of the fixture can be used dependent on the platform to be constructed. The addition of the translating rail fixture would allow larger platforms to be assembled with the RMS.

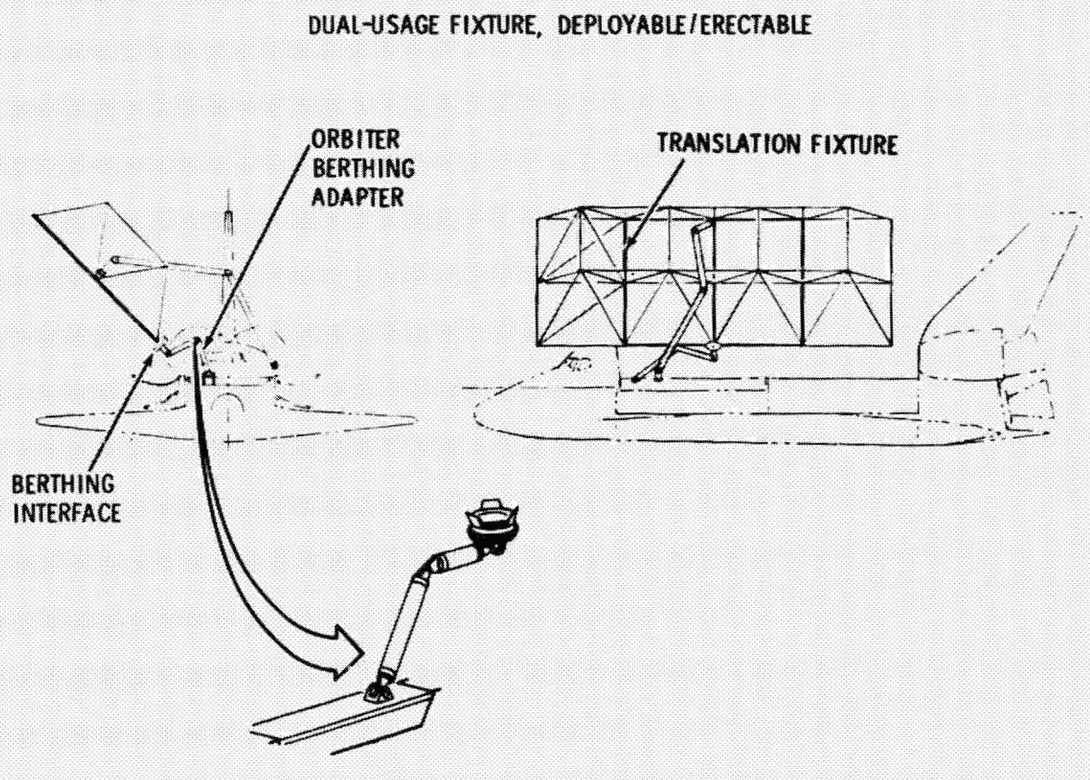

Figure 12

THINGS WE HAVE LEARNED

Important conclusions to be emphasized from the studies/activities performed to date on space construction and platform design are summarized in Figure 13. These include:

Installation of Systems Dominates Construction - Design of the platform and construction fixture(s) must incorporate the requirements for utility systems and payload installation.

Space Platforms Should be Designed to be Compatible with Fixture, Support Equipment and Systems - Parallel design of platforms, fixture, support equipment and systems must be accomplished to provide the necessary design interaction during the early stages of design and carried throughout.

Support Equipment Currently in Development and Planned is Suitable with Some Recommended Changes - The Manned Maneuvering Unit (MMU), Cherry Picker, RMS, etc., appear to satisfy the requirements for support equipment. Additional rotational requirements of the RMS may be necessary for the complete mobility required.

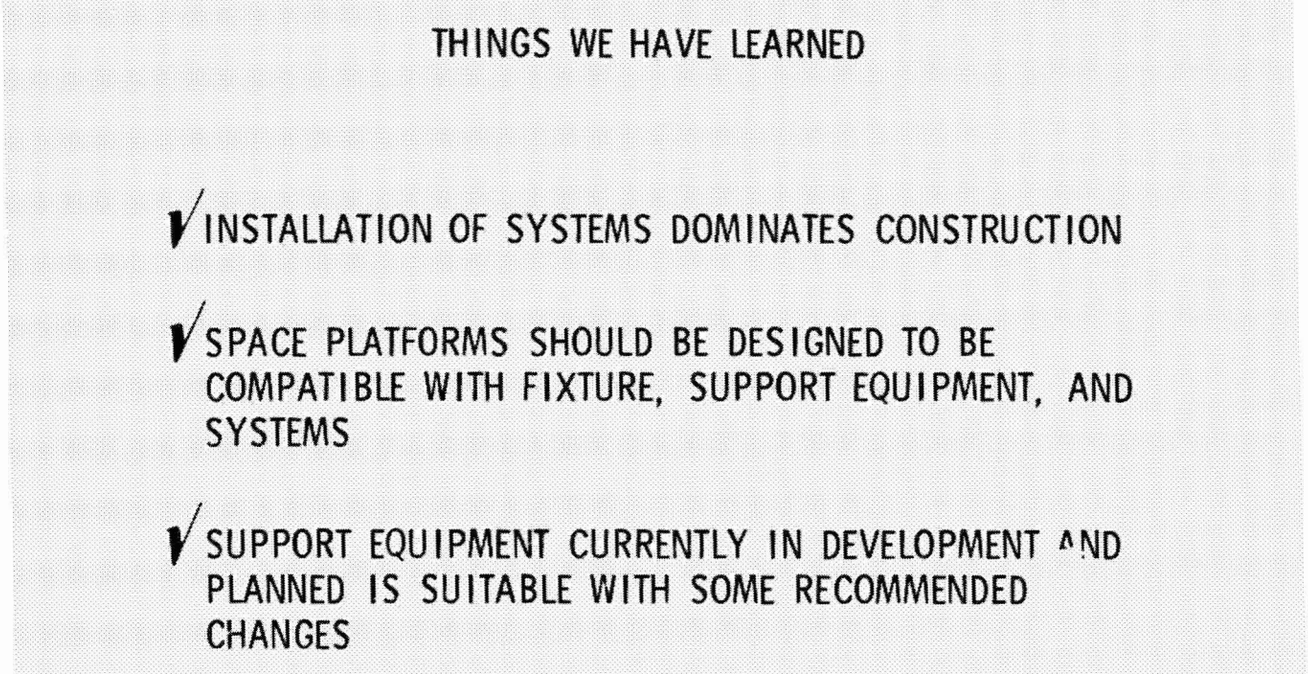

Figure 13

N80-19161

A HIGH RESOLUTION SOIL MOISTURE RADIOMETER

L. R. Dod
Goddard Space Flight Center
Greenbelt, Maryland 20771

LSST 1ST ANNUAL TECHNICAL REVIEW

November 7-8, 1979

PAGE 302 INTENTIONALLY BLANK

This report covers a design study (ref. 1) for an advanced L-Band High Resolution Soil Moisture Radiometer - HRSMR - for the late 1980 time period conducted by General Electric for NASA Goddard Space Flight Center over the period from June to November 1978. The selected system is a planar slotted waveguide array at L-band frequencies as shown in figure 1. The square aperture is 74.75 m by 74.75 m subdivided into 8 tilted sub-arrays The system has a 290 km circular orbit and provides a spatial resolution of 1 km. The aperture forms 230 simultaneous beams in a cross-track pattern which covers a swath 420 km wide. A revisit time of 6 days is provided for an orbit inclination of 50°. The 1 km resolution cell allows an integration time of 1/7 second and sharing this time period sequentially between two orthogonal polarization modes can provide a temperature resolution of 0.7° K.

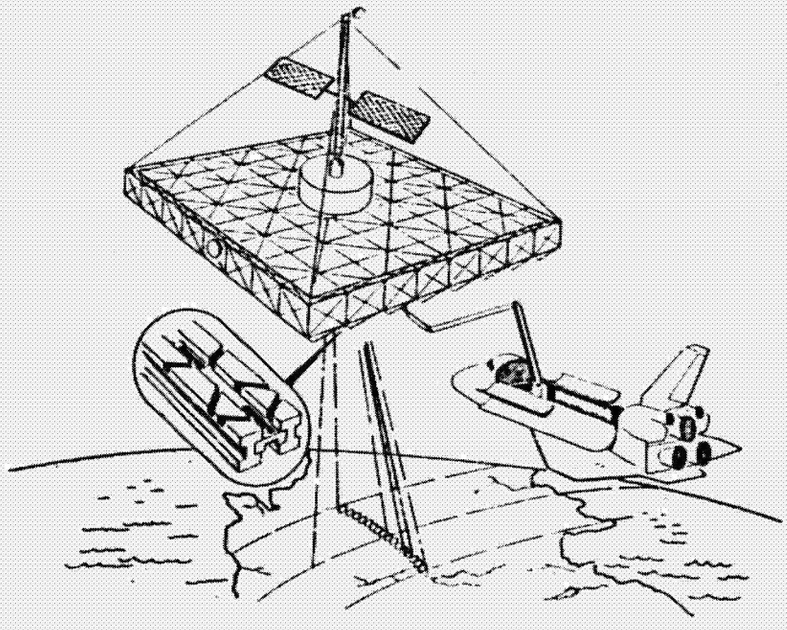

Figure 1.- HRSMR - High resolution soil moisture radiometer.

The relevent systems' parameters and performance characteristics are listed in Table 1. The antenna beam is tilted forward 20° along the satellite track to provide resolution of the two orthogonal linear polarizations.

Table 1-1 HRSMR - Selected System - Major Characteristics

		Comments
Type	Dual Waveguide Array	Graphite Fiber Epoxy Technology
Frequency	1400-1407 MHz	1400-1428 MHz available astronomy band
Size	74.75 m x 74.75 m	(245 ft. x 245 ft)
Number of Subarrays	8	
Subarray Length	9.34 m	(30.6 ft)
Orbit Height	290 km, circular	(180 miles)
Footprint Resolution	1.0 km x .92 km	3 dB, 0°-scan (.62 x .57 miles)
Orbit Plane Inclination	50°	
Revisit Time	6 days	
10 dB-Beamwidth	.313°	
Number of Simultaneous Beams	230	Crosstrack
Scan Angle	±36°	Crosstrack
Swath Width	±210 km	(±130.4 miles)
Tilt Angle	20°, forward	11° electrical + 9° mechanical tilt
Polarization	Dual linear	Switched
System Temperature	600°K	
Temperature Resolution	0.7°K	Total power radiometer
Total Weight	89,200 lbs	
- Spacecraft Weight	73,100 lbs	
- Orbit Maintenance Weight	16,100 lbs	
Total Cost	322 M$	
- Development Cost	50 M$	
- Hardware Cost	110 M$	
- # of Shuttle Flights	3-4	
- Transportation Cost	162 M$	
Orbit Maintenance System	2 SEPS/0.23 lbs thrust each/4.7 KW Power required each	
Attitude Control System	Thrusters and control moment gyros/2500 lbs	
Power Supply System	Articulated roll-out solar array 279 m^2/11.4 KW/800 lbs	

The selection of an array over a reflector is based upon two factors: First, the array has the advantage of a repetitive, modular design with the inherent advantages of reduced initial design and development, reduced ground assembly and testing, reduced modular space testing and reduced complete space transportation and erection. Secondly, the symmetrical, streamlined array configuration, compared to an offset, asymmetrical parabolic torus reflector of about 3 times the aperture, has significant advantages from the viewpoint of attitude control and orbit maintenance against the disturbing forces of atmospheric drag and to a lesser degree, of solar pressure and gravity gradients effects.

With respect to systematic evolution, the array appears to lend itself well for a gradual development program based on the modular array concept, as shown schematically in Figure 2.

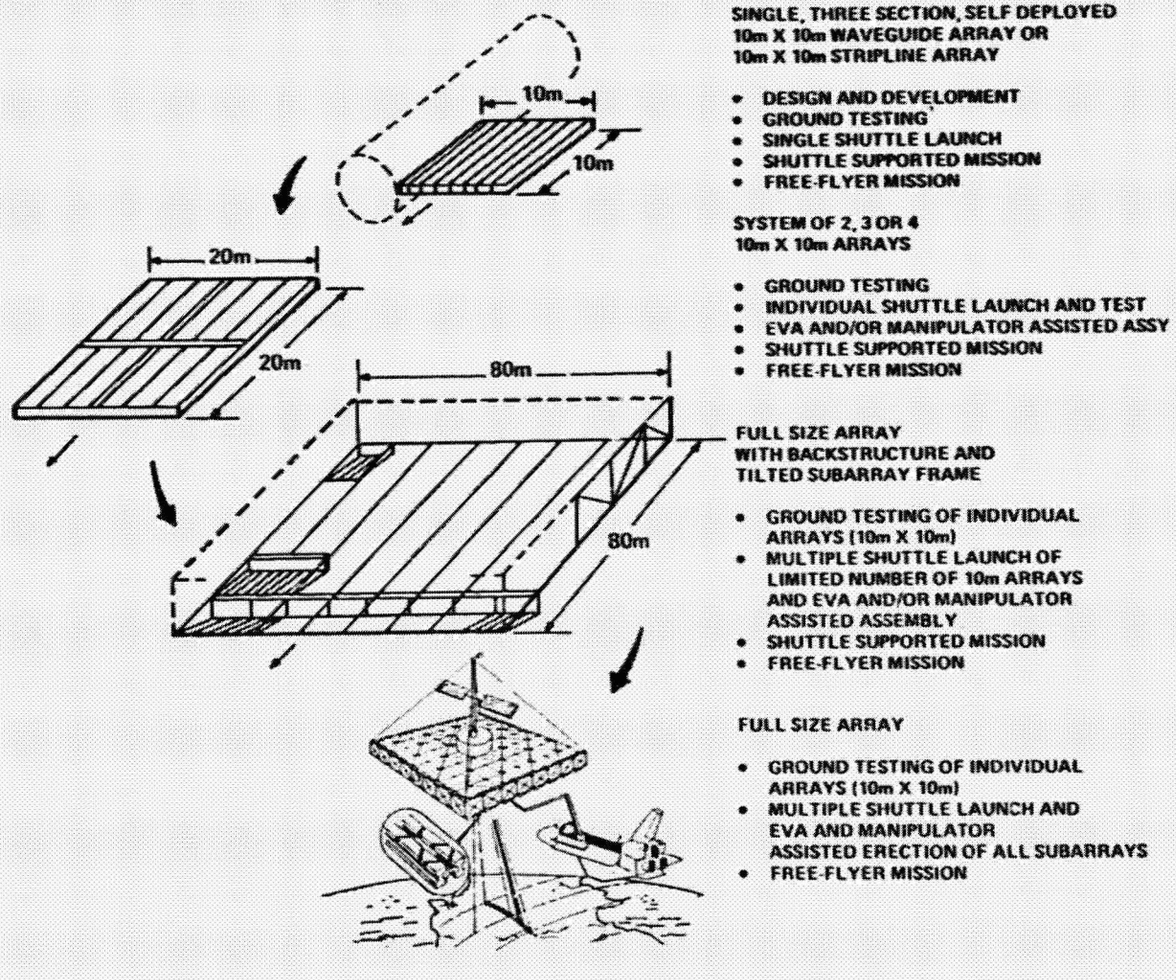

Figure 2.- HRSMR - evolution of array technology.

Considerable iterative effort was expended on the assessment of drag effects as a function of altitude and corresponding aperture size for constant footprint resolution. It was realized that this trade-off was most critical to the determination of the optimum antenna type as well as the optimum aperture size and orbit altitude in terms of overall mission cost. The characteristic cost minima for various candidate systems are shown in Figure 3.

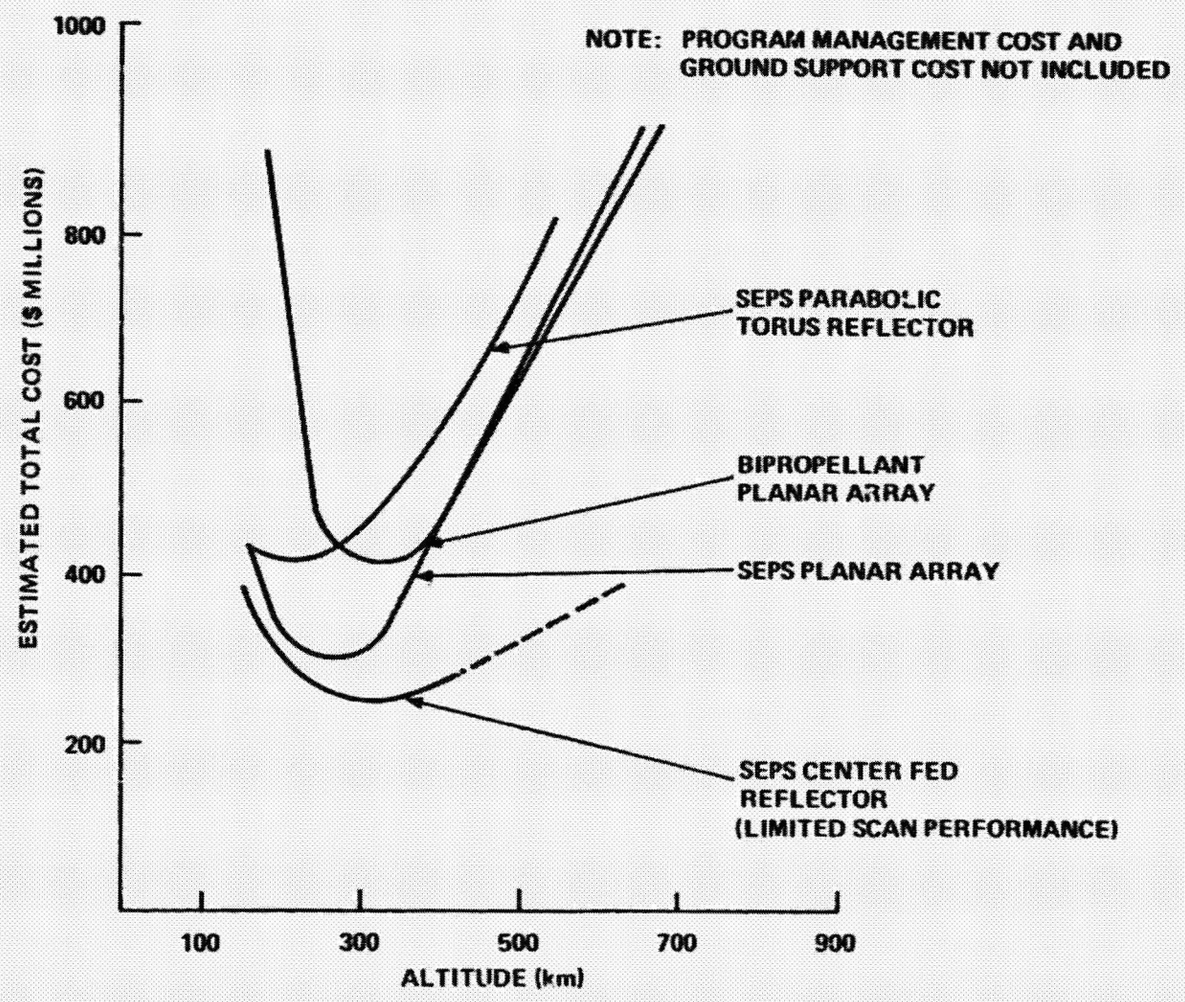

Figure 3.- HRSMR - Cost vs orbit altitude.

Several candidate waveguide array systems were considered. It was found that the beam smear of the antenna due to the dispersion in the waveguide and feed network prevented the use of a full-length waveguide array. Not only would the beam smear be excessive, but the manufacturing tolerances to maintain the desired slot excitation in phase and amplitude over the length of the waveguide would be severe. This system would have the minimum number of receivers and least complexity, but the performance degradation due to beam smear and manufacturing tolerances are not acceptable.

The selected system is a planar waveguide array consisting of 8 subarrays. The 8 subarrays are necessary to prevent the beam smear discussed in the above paragraph. It was found in the trade-off studies of orbit height, drag coefficient, and orbit maintenance propellant, that a 74.75 m by 74.75 m array in a lower orbit met the 1 km resolution requirement with an increased fraction of overall weight devoted to orbit maintenance fuel. The selected system is shown in Figure 4.

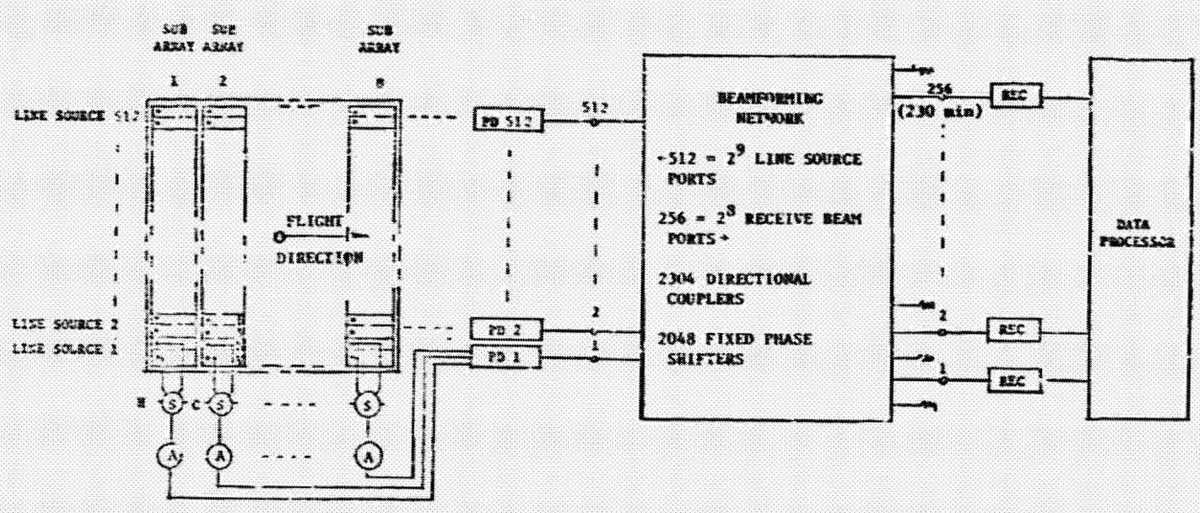

8 SUBARRAYS

512 LINE SOURCES (DUAL POL)

8 X 512 = 4096 EACH { SWITCHES, RF AMPLIFIER, HOT LOADS, COLD LOADS, TRANSMISSION LINES }

512 8-WAY POWER DIVIDERS

1 BEAMFORMING MATRIX

256 RECEIVERS

1 DATA PROCESSOR

LEGEND: S - SWITCH
A - RF AMPLIFIER
H - HOT LOAD
C - COLD LOAD
PD - POWER DIVIDER
REC - RECEIVER

HRSMR - SELECTED SYSTEM

74.75 M X 74.75 M

WAVEGUIDE ARRAY

1.4 GHz

Figure 4.- HRSMR - Selected system 74.75 m x 74.75 m waveguide array, 1.4 GHz.

The antenna array consists of 512 dual line sources. To reduce dispersion and resultant beam smear to acceptable levels, the line sources are divided into eight subarrays, each approximately 9.34 m long. The line sources, oriented parallel to the flight direction, consist of dual slotted waveguides. In order to accommodate dual waveguides for orthogonal, linear polarization and at the same time to maintain a small spacing between waveguides for grating lobe suppression, it is necessary to use ridged waveguide. This results in smaller overall waveguide width and allows an interlaced geometry as shown in Figure 5. In order to tilt the beam 20° forward from nadir, the entire array must be mechanically biased by 9° from the orbit tangent. To prevent grating lobes in visible space, the beam must not be tilted more than 11° electrical. The 20° forward tilt is then accomplished by a mechanical subarray tilt of 9° and an electrical beam tilt of 11° as shown in the figure. The discontinuities in the array aperture are corrected by an electrical compensation method.

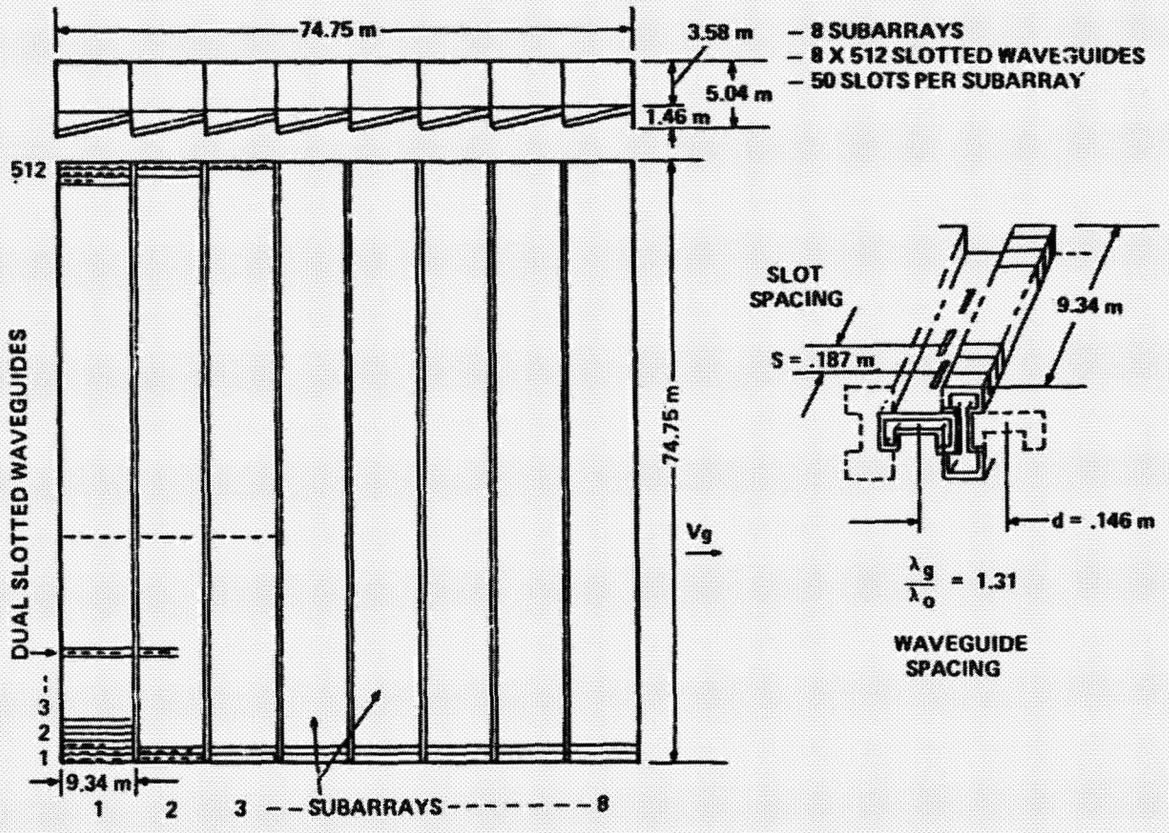

Figure 5.- HRSMR - Waveguide array, 1.4 GHz.

The success of the large aperture radiometer depends critically on a design approach and technique that will permit the maintenance of adequate dimensional tolerances. A rigorous analysis will be performed in the next phase of the study program. A preliminary analysis has been performed to define the various kinds of tolerances and their effects on performance and to determine boundaries within which the design must operate. The total tolerance can be conveniently broken up into four parts. Figure 6 shows one subarray in its deformed state. The four component parts are: (1) Δz represents the dislocation of the center of mass of the subarray from its nominal (X,Y) reference plane, (2) $\Delta\alpha$ represents the tilt angle of an ideal planar subarray, (3) dz represents a systematic bowing of the panel, and (4) σ represents the random distortion.

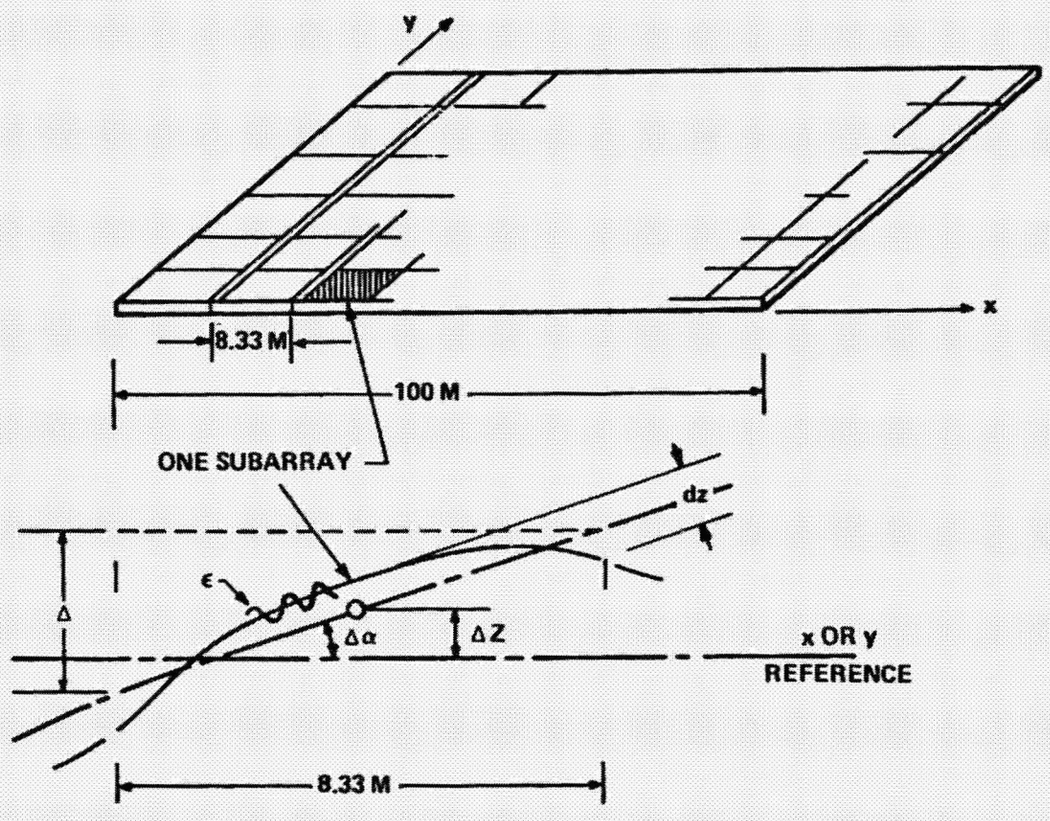

Figure 6.- HRSMR - Array tolerance definition.

Each antenna subarray is joined by bayonet joints and supported every 9.34 m by graphite-epoxy truss work to provide increased stiffness, load stability and to provide support for the auxiliary systems module and for the distributed network of R F amplifiers, switches, hot and cold loads and transmission lines. The truss work supporting the antenna is held in tension by a deployable boom (such as an Astromast) and cable system designed to control and reduce the array overall thermal distortion. Multi-layer insulation blankets cover the array for passive thermal control. The instrument is assembled from multiple shuttle payload deliveries to 290 km altitude. The first flight will bring the system module and solar array, thus providing a controlled assembly platform. Subsequent shuttle loads contain the array, structure, and SEPS hardware. The structure (truss work) is of a collapsible type with attachment joints permitting EVA-assisted RMS deployment and attachment including harness connection. The antenna arrays are stacked in the cargo bay as shown in Figure 7.

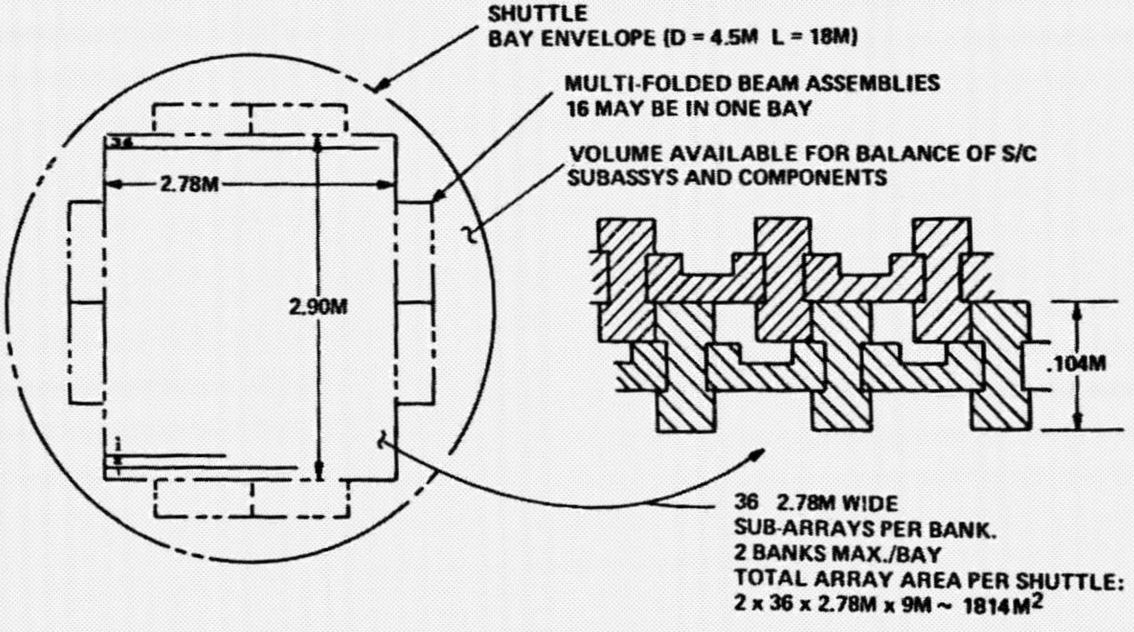

Figure 7.- HRSMR - Packaging concept for dual waveguide planar array.

Reference

1. A Design Study for a High Resolution Soil Moisture Radiometer. General Electric Company Final Report 78SD4241, November 1978.

N80-19162

D17

LARGE SPACE SYSTEM CONTROL TECHNOLOGY OVERVIEW

Gary Parker
Jet Propulsion Laboratory
Pasadena, California

LSST 1ST ANNUAL TECHNICAL REVIEW

November 7-8, 1979

LSST CONTROLS

The controls discussion will be presented by 3 speakers. First, the nature of the problem will be described in an attempt to establish a frame of reference for the more detailed reports to follow. Descriptions of the work that has been done at JPL and at Purdue under contract to JPL will be provided by G. Rodriguez and R. E. Skelton respectively.

LSST CONTROLS

- NATURE OF CONTROLS PROBLEMS
- ADVANCED CONTROL CONCEPT DEVELOPMENT AT JPL
- MODEL ORDER REDUCTION WORK AT PURDUE

THE LSST CONTROLS PROBLEM

The basic LSST Controls problem is simply one of meeting the performance requirements in the face of very complicated vehicle characteristics. Some of the specific requirements might be pointing accuracy and stability, slew rate or perhaps surface contour accuracy. The complications include vehicle flexibility, imperfect knowledge of the structural characteristics, disturbances and the fact that more surface accuracy is required than can be achieved passively. The next series of figures will address these factors individually.

THE LSST CONTROLS PROBLEM

- PROBLEM IS MEETING PERFORMANCE REQUIREMENTS -
  - STABILITY
  - POINTING ACCURACY
  - INSTRUMENT POINTING SLEW RATES
  - SURFACE OR FIGURE ACCURACY
- IN THE FACE OF COMPLICATING VEHICLE CHARACTERISTICS
  - VEHICLE FLEXIBILITY AND SUBSYSTEM INTERACTIONS
  - LESS THAN PERFECT KNOWLEDGE OF STRUCTURAL DYNAMICS
  - DISTURBANCES RELATED TO LARGE VEHICLES
  - PASSIVE SURFACE OR FIGURE CONTROL MAY BE INADEQUATE

VEHICLE FLEXIBILITY

The basic performance requirements such as slew rates and settling times determine the minimum control system bandwidth. If there are structural modes that are not within this bandwidth, they may pose a threat to meeting the performance requirements. Specifically, any uncontrolled motion at the base of an instrument mount that is of a higher frequency than the bandwidth of the instrument mount control system will show up directly in the pointing of the instrument. The motion may be the result of structural modes excited by disturbances. The instrument mount control system bandwidth must be increased to control or compensate for this motion.

VEHICLE FLEXIBILITY

- PERFORMANCE REQUIREMENTS DETERMINE THE MINIMUM CONTROL SYSTEM BANDWIDTH
- STRUCTURAL MODES OUTSIDE THE CONTROL SYSTEM BANDWIDTH PRESENT A THREAT TO MEETING EXPERIMENT OR ANTENNA POINTING ACCURACY REQUIREMENTS
  - FOR EXAMPLE

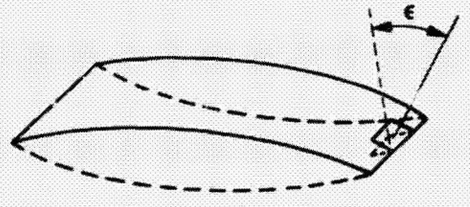

FIRST FREE BENDING MODE

  - POTENTIALLY EXCITED BY DISTURBANCES
- THEREFORE, TO INSURE SATISFYING PERFORMANCE REQUIREMENTS THE BANDWIDTH MAY HAVE TO BE OPENED TO INCLUDE MORE MODES

VEHICLE FLEXIBILITY (Cont'd)

Increasing the bandwidth to include structural modes can only be done if stability can be guaranteed. Stability requires precise knowledge of the motion in each of the modes to be controlled. It also requires knowledge of the effect of applying control on all of the modes. The measurements that are made on the spacecraft structures are of the combined effect of the motion in all of the modes. An estimator is used to derive the required modal motion from the measurements. The estimator consists of an analytical model of the vehicle in which the modal motions are adjusted so that its overall response best correlates with the vehicle measurements. The modal motions that achieve this best correlation are used as the estimates for the control process. It follows that these estimates will be in error and stability will be threatened by inadequacies of the analytical model.

VEHICLE FLEXIBILITY (contd)

- STRUCTURAL MODES WITHIN THE BANDWIDTH PRESENT A THREAT TO STABILITY
  - PRECISE KNOWLEDGE OF THE MOTION IN EACH MODE IS REQUIRED TO PROVIDE DAMPING
  - MEASUREMENTS REFLECT THE COMBINED MOTION RESULTING FROM THE SUM OF ALL MODES
  - INDIVIDUAL MODAL MOTION INFORMATION IS DERIVED FROM AN ESTIMATOR BASED ON AN ANALYTICAL MODEL OF THE STRUCTURE
  - THE ANALYTICAL MODEL IS ADJUSTED TO MAKE THE MODEL OVERALL BEHAVIOR BEST CORRELATE WITH THE MEASUREMENTS OF THE SPACECRAFT - MODAL MOTIONS REQUIRED IN THE MODEL FOR THE "BEST CORRELATION" ARE THE "ESTIMATES" USED FOR ACTUAL CONTROL
  - ESTIMATES WILL BE IN ERROR AND STABILITY WILL BE THREATENED BY INADEQUACIES OF THE MODEL

STRUCTURAL MODEL ERRORS

The models used in the estimation process are in error by two factors: 1) errors of form or parameter values due to lack of knowledge and 2) modifications made to the model to make it practically implementable. The complexity and untestability of very large structures create basic uncertainty of mode frequencies and shapes. The truncating process consists of selecting the modes to be retained in the estimator model. The development of rational truncation criteria is the subject of the work that will be reported on by R. E. Skelton.

STRUCTURAL MODEL ERRORS

- BASIC UNCERTAINTY OF MODE FREQUENCIES AND SHAPES
  - COMPLICATED DYNAMIC DESCRIPTION
  - UNTESTABILITY OF VEHICLE DYNAMICS
  - VARIABLE CONFIGURATION
- MODEL TRUNCATION TO PERMIT PRACTICAL CONTROL SYSTEM IMPLEMENTATION
  - USE OF A LIMITED SET OF ALL OF THE MODES FOR THE ESTIMATOR MODEL
  - DEVELOPMENT OF RATIONAL TRUNCATION CRITERIA REQUIRED

DISTURBANCES

Certain disturbance processes pose a greater problem to large space structures than to current generation S/C just on the basis of the large dimensions. Solar pressure, gravity gradient torques, and aerodynamic drag all have effects related to size. Disturbance from thermal transients, onboard mechanisms and control interaction must also be accommodated.

DISTURBANCES

- LSS ARE SUBJECT TO DISTURBANCES THAT CAUSE MODAL DEFLECTIONS (INTERNAL AND EXTERNAL - MODELED AND UNMODELED)
  - THERMAL TRANSIENTS
  - THRUSTER FIRINGS AND MOMENTUM INTERCHANGE DEVICES
  - ON BOARD MECHANISMS
  - SOLAR PRESSURE
  - GRAVITY GRADIENTS
  - GRAVITY FIELD VARIATIONS
  - AERODYNAMIC DRAG

SURFACE OR FIGURE CONTROL

Distributed sensing may be required to determine the static shape with sufficient fidelity. In addition, if modal vibrations are to be controlled, distributed sensors may provide information not present at any single point and thus minimize estimation errors. Distributed actuation may be required to effect the geometric control required, while minimizing actuator size and complexity. It is also unlikely that all of the modes to be controlled can be influenced at a single point. In cases where continuous high accuracy figure control is required, onboard, closed loop, distributed systems will be required to control the static shape as well as modal vibrations.

SURFACE OR FIGURE CONTROL

- DISTRIBUTED SENSING MAY BE REQUIRED TO MAKE NECESSARY MEASUREMENTS
  - STATIC SHAPE DETERMINATION
  - INFORMATION ON ALL PERTINENT MODES MAY NOT BE AVAILABLE AT ANY ONE LOCATION
  - ESTIMATION ERROR REDUCED BY USING MORE SENSORS
- DISTRIBUTED ACTUATION MAY BE REQUIRED TO ACHIEVE SHAPE ADJUSTMENT
  - REDUCE ACTUATOR SIZE AND STRUCTURAL STRESS CONCENTRATION
  - NOT ALL MODES MAY BE CONTROLLABLE AT ANY GIVEN LOCATION
- ON-BOARD CLOSED-LOOP SYSTEMS REQUIRED FOR MANY APPLICATIONS

SUMMARY OF LSST CONTROL PROBLEMS

Modal vibrations of large space structures can preclude satisfaction of mission requirements. No means exists to directly measure the modal motion that must be controlled. The motion must be estimated and the estimation process is imperfect. We need to improve it. If perfect knowledge of the motion was available, no means exists to influence the modes desired without affecting others in a possible deleterious way. The estimation and control inadequacies are interactive and must be addressed jointly by advanced concepts.

SUMMARY OF LSST CONTROL PROBLEMS

- NO DIRECT MEASUREMENTS AVAILABLE OF MOTION TO BE CONTROLLED
  - MOTION MUST BE ESTIMATED
  - ERRORS ARE INHERENT IN ESTIMATION PROCESS
  - ADVANCED CONCEPTS NEED DEVELOPMENT TO MINIMIZE ERRORS
- EVEN AFTER KNOWLEDGE OF MOTION IS ESTABLISHED, CONTROL ACTUATORS CANNOT DIRECTLY INFLUENCE THE MOTION TO BE CONTROLLED
  - MOTION EXTENDS OVER LARGE DIMENSIONS
  - CONTROL EFFORT MAY CAUSE UNDESIRABLE EXCITATIONS
  - ADVANCED CONCEPTS WILL MINIMIZE INTERACTIONS
- ESTIMATION AND CONTROL PROBLEMS ARE INTERACTIVE AND COMPLICATE EACH OTHER

D18

N80-19163

LARGE SPACE SYSTEM CONTROL TECHNOLOGY STATUS AND ACCOMPLISHMENTS

G. Rodriguez
Jet Propulsion Laboratory

LSST 1ST ANNUAL TECHNICAL REVIEW

November 7-8, 1979

This is a report of technical progress made in FY'79 by JPL in the development of control technology for the LSST program. The report was presented at the first Annual LSST Program Technical Review held at Langley Research Center (LaRC) on November 7 and 8, 1979. Although the report was prepared by G. Rodriguez and G.L. Parker, the progress reflects the collective efforts of R.S. Edmunds, S.M. Gunter, J.N. Juang, E. Kan, Y.H. Lin, D.B. Schaechter, and C.J. Weeks of JPL.

The presentation includes topics which can be outlined as follows:

1. A summary of major objectives of FY'79 tasks
2. A description of major results and accomplishments
3. An outline of FY'80 planned developments
4. A current documentation list reflecting accomplishments to date.

PAGE 322 INTENTIONALLY BLANK

CONTROL TASKS OVERVIEW

Basic technology developments were carried out in the areas of: 1) distributed control to achieve precision attitude and shape control; 2) model order reduction to find the best preflight dynamical models that retain the most significant vehicle dynamics in the controller design; 3) model error estimation to detect inevitable deficiencies in large structural dynamical models; and, 4) disturbance modeling to characterize the external environment for parabolic reflectors.

The applications for the basic technology are in the areas of antenna modeling and control and in the laboratory verification of selected concepts by means of a flexible-beam experiment demonstration.

CONTROL TASKS OVERVIEW

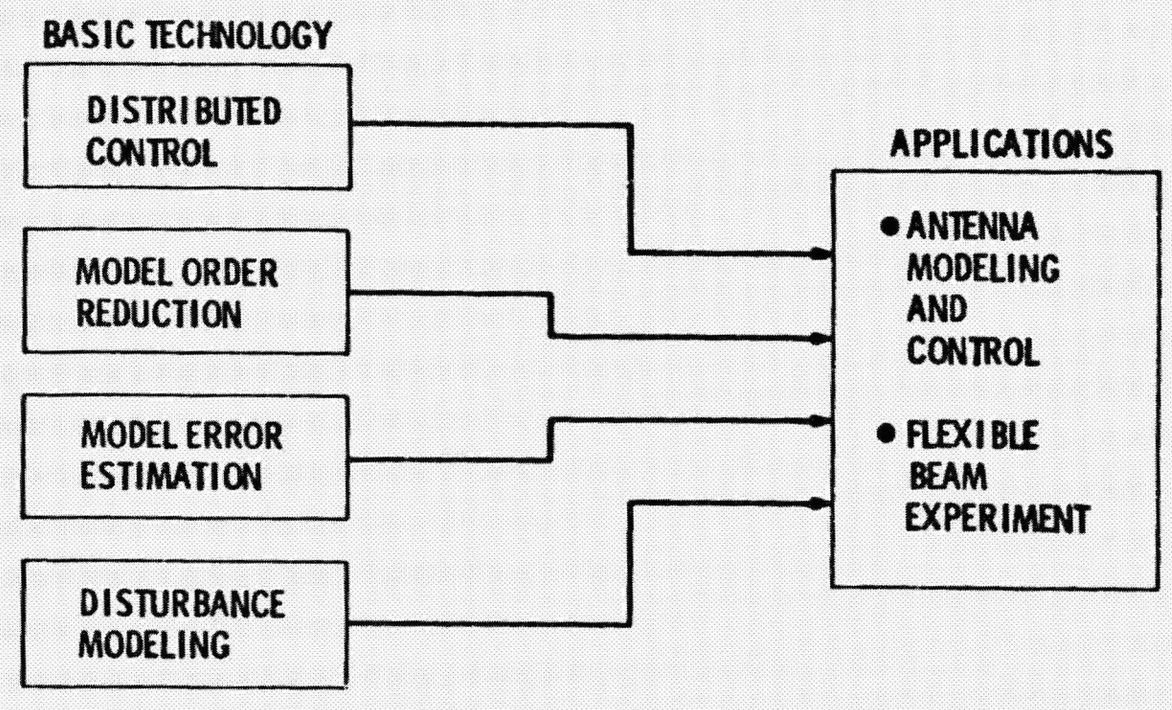

ACCOMPLISHMENTS

1) In the area of antenna modeling and control, preliminary structural models were defined for two representative parabolic reflectors. A control system design evolved for attitude control of the reflectors. The controller design was based on a lumped control concept where the control hardware (sensor and actuators) was mounted at the base of the antenna. 2) In the area of distributed control, static shape control techniques were worked out to establish a prescribed vehicle shape. The corresponding estimation process for determination of vehicle shape from selected sensor measurements was also developed. 3) A model order reduction study was conducted at Purdue University to find the best preflight dynamical models for on-board controller design. The objective of the study was to investigate (and initiate solution of) the problems caused by truncation of the vehicle dynamics required to minimize on-board computations. 4) Estimator designs were developed for on-board detection of large structure model errors. The model error estimators are a natural evolution of state estimation designs crucial to the success of recent JPL spacecraft. They would also constitute a foundation for development and eventual implementation of adaptive estimator concepts. 5) A study was conducted under contract to Lockheed for disturbance modeling of a 100-m diameter antenna in order to study the control/environment interactions. 6) An experimental (flexible-beam) facility was designed for verification of selected distributed control concepts.

ACCOMPLISHMENTS

- DEVELOPED PRELIMINARY STRUCTURAL MODELS AND CONTROL SYSTEM DESIGNS FOR ATTITUDE CONTROL OF PARABOLIC REFLECTORS
- DEVELOPED STATIC SHAPE AND MODAL TECHNIQUES FOR DISTRIBUTED CONTROL OF LARGE SPACE SYSTEMS
- CARRIED OUT A MODEL ORDER REDUCTION STUDY TO FIND THE BEST PRE-FLIGHT DYNAMICAL MODELS FOR CONTROL SYSTEM DESIGN
- DESIGNED MODEL ERROR ESTIMATORS FOR ONBOARD DETECTION OF INEVITABLE DEFICIENCIES IN LARGE STRUCTURE DYNAMICAL MODELS
- DEVELOPED DISTURBANCE MODELS OF A 100-m PARABOLIC REFLECTOR IN LOW-EARTH ORBIT TO STUDY CONTROL/ENVIRONMENT INTERACTIONS
- DESIGNED EXPERIMENTAL FACILITY FOR VERIFICATION OF SELECTED DISTRIBUTED CONTROL CONCEPTS

ANTENNA CONTROL

SUMMARY OF RESULTS

Finite-element models were developed by D.T. DesForges at JPL consistent with two antennas: a 30-m precision deployable design and a 100-m mesh deployable concept. Attitude and surface accuracy definitions were established in terms of structural data in order to allow computation of control performance. Preliminary control designs were developed based on a lumped control concept. Initial performance assessments based on the lumped control concept indicate that a more detailed model is required in order to determine if accuracy requirements can be satisfied with this concept. An assessment of the need for active surface control will be under investigation in FY'80. The disturbance modeling results will provide a tool for assessing the effects of dynamic external environment on the control performance.

ANTENNA CONTROL SUMMARY OF RESULTS

- FINITE-ELEMENT AND MODAL MODELS OBTAINED FOR PARABOLIC REFLECTORS
  - 30m PRECISION DEPLOYABLE
  - 100m MESH-DEPLOYABLE
- ATTITUDE AND SURFACE ACCURACY DEFINITIONS ESTABLISHED IN TERMS OF STRUCTURAL DATA
- PRELIMINARY CONTROL DESIGN AND PERFORMANCE RESULTS DEVELOPED
- DISTURBANCE MODELING STUDY INITIATED

DISTRIBUTED CONTROL CONCEPTS

A distributed control system configuration is illustrated in the figure. In such a control system, sensor measurements of the vehicle deflections are processed by an on-board (possibly decentralized) computer that transmits commands to actuators in order to provide stability and control of the vehicle dynamics. A full-blown closed-loop distributed system as displayed in the figure may be required only in the most demanding applications. However, distributed estimation will be required in most large structures (even the earliest shuttle-based experiment) in order to establish the actual inflight dynamics and control/structure interactions. Consequently, an area of intensive study at JPL is that of estimation for distributed systems and its application to large structure control. The estimators detect both the quasi-static vehicle motions and the dynamics of the structure vibrational modes.

DISTRIBUTED CONTROL CONCEPTS

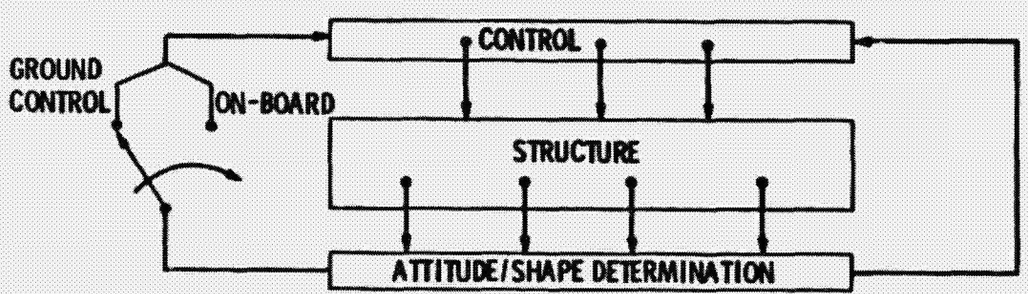

- DISTRIBUTED CONTROL OF LARGE FLEXIBLE STRUCTURES INVOLVES MULTI-STATION SENSING, ACTUATION AND CORRECTION TO MAINTAIN SHAPE
- SHAPE DETERMINATION AND ADJUSTMENT BASED ON GROUND COMMAND REQUIRED IN MOST APPLICATIONS
- ON-BOARD CLOSED-LOOP SYSTEM REQUIRED TO ACHIEVE HIGH PRECISION SURFACE ACCURACY

DISTRIBUTED CONTROL

SUMMARY OF RESULTS TO DATE

1) There are three fundamental options for distributed control system design models: partial differential equations, finite-element and modal models. There are substantial differences in the control systems resulting from these three approaches. The partial differential equation approach is very useful for early control concept design because it can be obtained without a full-blown analysis of the vehicle dynamics. Consequently, such continuum models can be used to study control-related problems that may otherwise be masked by model complexities. The modal approach has the advantage that it retains the physical insight gained by studying the vehicle dynamics in terms of the natural modes of the system. The finite-element models lead to localized controllers where each actuator command depends only on adjoining sensor measurements. An evaluation of each of these approaches is currently under investigation. 2) A fundamental problem in large structure control is that of achieving a prescribed vehicle shape and of establishing shape knowledge based on measurements of the structural deflections. Problems formulated and solved in FY'79 are those of static shape determination and control. In the area of shape estimation, the technique used to achieve the shape reconstruction process is based on the principle of least-squares that minimizes the errors in the system model. A general solution for estimation of distributed parameter systems has been worked out and applied to a flexible-beam structural model. The corresponding solutions for static shape control have also been established. 3) In the area of dynamic shape determination and control, analytical criteria for sensor/actuator placement have been established and applied in the estimation of a single large structure vibrational model.

DISTRIBUTED CONTROL
SUMMARY OF RESULTS TO DATE

- MODELING OPTIONS FOR CONTROL SYSTEM DESIGN
  - CONTROL AND ESTIMATION SCHEMES DEVELOPED BASED ON CONTINUOUS MODELS
  - MODAL CONTROL AND SPILLOVER INVESTIGATED
  - → LOCAL DISTRIBUTED CONTROL SYSTEMS DESIGNED FOR BEAM-LIKE STRUCTURES
- → STATIC SHAPE DETERMINATION AND CONTROL
  - LEAST-SQUARES SOLUTION ESTABLISHED
  - APPLICATION TO FLEXIBLE BEAM-LIKE STRUCTURE
  - FEEDBACK SOLUTIONS FOR STATIC SHAPE CONTROL
- DYNAMIC SHAPE DETERMINATION/ESTIMATION
  - → SENSOR/ACTUATOR PLACEMENT
  - ESTIMATION OF A SINGLE LARGE STRUCTURE VIBRATIONAL MODE

LOCAL CONTROL BASED ON FINITE ELEMENTS

Finite-element analysis is currently the most widely used technique to study the dynamics of flexible space structures. The finite-element method is so versatile and generally applicable that general purpose computer program packages (e.g. NASTRAN, SPAR, etc.) based on this method solve an almost limitless variety of problems in structural mechanics. A finite-element model for an undamped flexible structure typically results in a set of dynamic equations of the form shown in the viewgraph. This set of equations is normally used to set up an algebraic eigenvalue problem whose solution produces the natural frequencies and modes of the vehicle. The resulting eigenvalue problem can be solved very efficiently by making optimum use of the inherent sparsity and bandedness of the matrices in the foregoing formulation.

A uniquely original idea introduced by D.B. Schaechter at JPL (see Ref. 1) is to make similar use of the highly structured format of the mass/stiffness matrices in the finite-element formulation in order to obtain distributed control designs. This design approach leads to localized estimators/controllers where control inputs at any given location are based only on adjoining sensor measurements. This approach takes full advantage of matrix sparsity in order to minimize storage requirements and on-board computations. The local control scheme has proved to be a most promising method for control system design when compared with various other schemes (e.g. modal control) in a representative simplified structure (Ref. 2).

LOCAL CONTROL BASED ON FINITE ELEMENTS

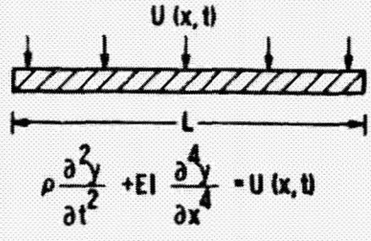

MODEL

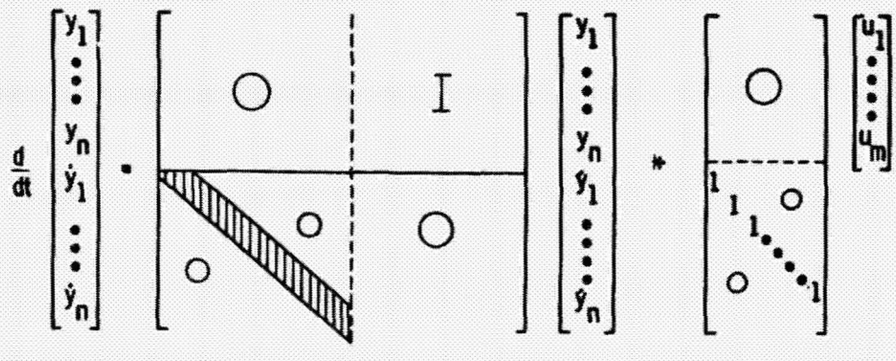

STATIC SHAPE CONTROL

The viewgraph illustrates basic developments in the area of static shape control where the objective is to achieve a prescribed vehicle shape. The results obtained (Ref. 3) are sufficiently general to be applicable to a large class of space systems. The figure shows only the application to a one-dimensional elastic structure. Two plots are displayed in the figure corresponding respectively to deflection and control inputs. The prescribed or commanded shape is a parabola. The objective of the control scheme is to bring the actual structural shape to a configuration that best approximates in a least-squares sense the specified parabola. The resulting control forces that cause the required vehicle deflection are shown in the upper plot in the viewgraph. Current efforts are directed at the extension of the foregoing results to two dimensional configurations.

STATIC SHAPE CONTROL

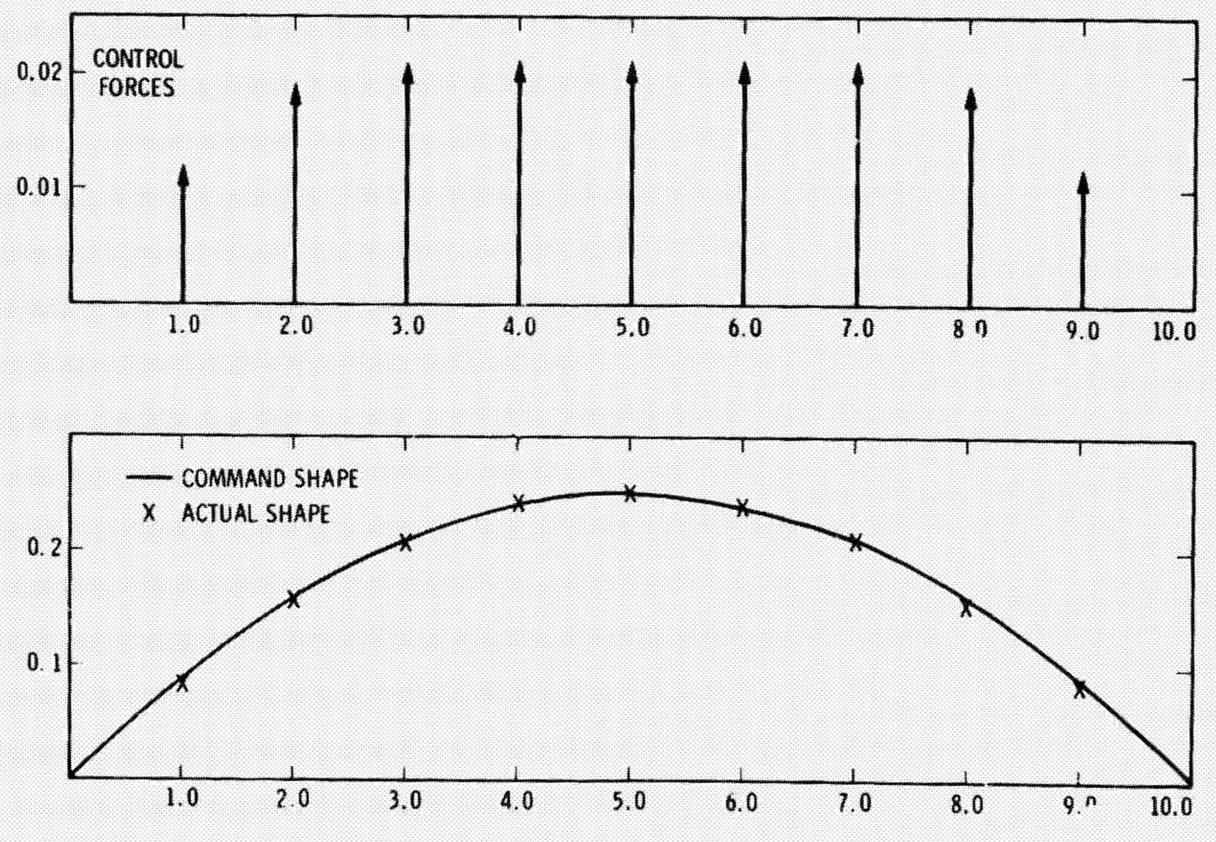

MODEL ORDER REDUCTION

PROBLEM STATEMENT

Modeling for controller design is widely recognized as a major and as yet unsolved problem in achieving precision attitude and shape control. Due to size and flexibility (and the resulting limitations of pre-flight model verifications), a great potential exists for errors in the dynamical models for large structures. In addition, the models used for controller design will be at best reduced-order representations of the structure because 1) large structures are infinite-dimensional systems that cannot be characterized fully by any finite-dimensional model and 2) model order reduction is required to minimize on-board computations.

The modeling process consists of a number of model order reduction stages. The actual large space system corresponding to the left block in the viewgraph is characterized by an infinite number of dimensions and uncertain physical effects. An evaluation model is usually developed based on linearized equations and on a finite-element or modal description of the structure. This evaluation model is used for verification of control system design. In order to obtain the controller model, a further stage of model reduction has to be carried out.

MODEL ORDER REDUCTION PROBLEM STATEMENT

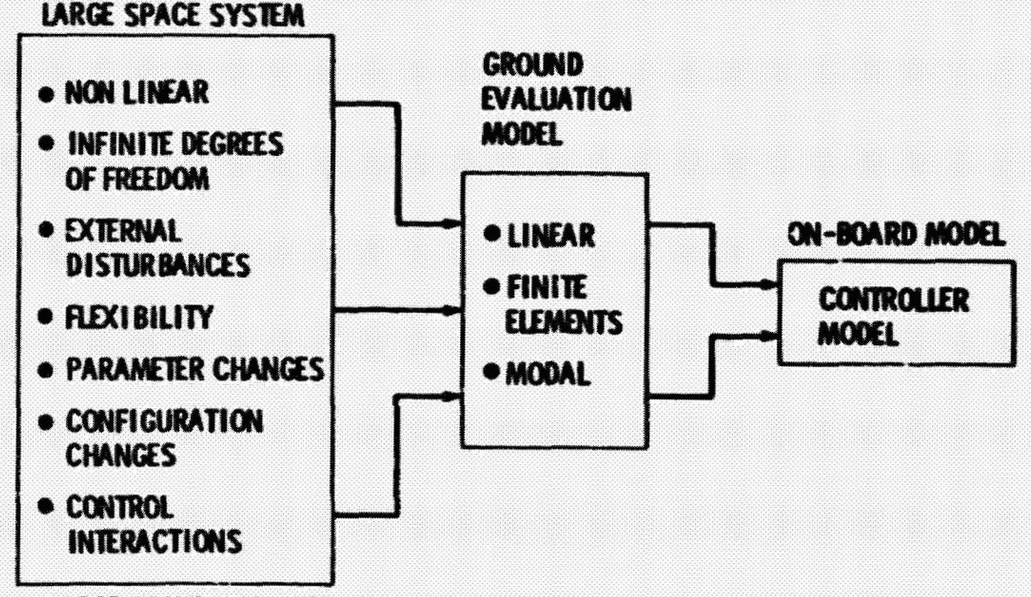

- LARGE STRUCTURES ARE INFINITE-DIMENSIONAL SYSTEMS THAT CANNOT BE COMPLETELY MODELED
- MODEL ORDER REDUCTION IS REQUIRED TO MINIMIZE ON-BOARD COMPUTATIONS AND IMPLEMENTATION COMPLEXITY

The model order reduction study was carried out under contract to Purdue University. The study was initiated by first selecting a generic large structure to illustrate the basic technology developments in model reduction. A number of reduction methods were investigated and a comparative evaluation of selected methods carried out. The method chosen for further investigation is a so-called modal cost analysis technique that tailors reduced-order models to the actual control inputs. Current efforts are directed toward application of the method of modal cost analysis to the generic large structure. A more detailed description of the foregoing results is contained in a subsequent presentation by R.E. Skelton of Purdue University.

MODEL ORDER REDUCTION

- DEVELOP MODEL ORDER REDUCTION METHODS FOR REDUCED-ORDER CONTROLLER DESIGN
- STUDY METHODS FOR MODELING DYNAMICAL SYSTEMS AND ESTABLISH MODEL SELECTION CRITERIA TO CHOOSE TYPES OF MODES TO RETAIN IN THE CONTROLLER DESIGN
- DEVELOP STABILITY, CONTROLLABILITY AND OBSERVABILITY PROPERTIES OF DYNAMICAL SYSTEMS DESCRIBED BY LINEAR MATRIX SECOND-ORDER SYSTEMS
- SELECT A GENERIC SPACE STRUCTURE TO BE USED FOR NUMERICAL ILLUSTRATION
- SUMMARIZE SELECTED MODEL REDUCTION METHODS AND CLASSIFY METHODS ACCORDING TO THEIR SUITABILITY FOR THE GENERIC LARGE STRUCTURE
- INVESTIGATE THE METHOD OF ITERACTIVE MODEL REDUCTION WITH COST-SENSITIVE FORCED MODES TO TAILOR REDUCED-ORDER MODELS TO OPTIMAL CONTROL INPUTS
- SPECIALIZE THE THEORY OF COST-SENSITIVE MODEL REDUCTION METHODS TO LINEAR MATRIX - SECOND-ORDER SYSTEMS
- PERFORM COMPARATIVE EVALUATION OF SELECTED MODEL ORDER REDUCTION METHODS TO GENERIC LARGE STRUCTURE

MODEL ERROR ESTIMATION

Inflight estimation of large structure model errors will have to be carried out in order to detect inevitable deficiencies in large structure estimator models. The models used for controller design will be at best reduced-order representations of the structure because 1) large structures are infinite-dimensional systems that cannot be characterized fully by any finite-dimensional model and, 2) model order reduction is required to minimize on-board computations. Inherent in a reduced-order model are so-called model errors due to four major sources: external disturbances, parameter uncertainties, neglected nonlinearities and truncated dynamics. A formulation for on-board model error estimation based on the principle of least-squares is contained in Ref. 4. The technology base used as foundation to carry out the developments consisted of 1) modeling for dynamics and control of flexible multibody systems, and 2) state estimators critical to recent JPL spacecraft designs. This technology has been found to be essential to all highly flexible and interactive spacecraft. Continued intensive developments in this area could provide an opportunity to have a significant impact on the Galileo attitude estimator design.

The process of model error estimation is illustrated in the next three viewgraphs.

MODEL ERROR ESTIMATION

PURPOSE

- DESIGN ESTIMATORS CAPABLE OF ON-BOARD DETECTION OF INEVITABLE DEFICIENCIES IN LARGE STRUCTURE DYNAMICAL MODELS

EXISTING TECHNOLOGY BASE

- STATE ESTIMATION TECHNOLOGY CRITICAL TO VIKING, VOYAGER, AND GALILEO CONTROL PERFORMANCE
- TECHNOLOGY IS ESSENTIAL FOR HIGHLY FLEXIBLE AND INTERACTIVE SPACECRAFT
- CONTINUED INTENSIVE DEVELOPMENTS WILL PROVIDE OPPORTUNITY TO IMPACT GALILEO ATTITUDE ESTIMATOR DESIGN

ILLUSTRATION OF MODEL ERROR ESTIMATION

A representative vehicle is formed by two rigid elements joined at a single-degree-of-freedom hinge. A perfectly acceptable reduced-order model for this configuration would be the linear single-axis equations for rotational motion of a rigid body. In fact, such an approximation was used in the flight-tested Voyager estimator design. However, the selection of this single-body model for the two-element configuration implies the unavoidable presence of model errors in the characterization of the vehicle dynamics. The model errors are due to four major sources as illustrated in the viewgraph. The model errors can however be lumped and represented in the dynamical model as the variables u and n appearing as forcing terms in the model equations. The objective of model error estimation is to estimate these terms in addition to providing estimates of the state (i.e., angular position and velocity) of the system. The data required to achieve the estimation process consists of measurements of the angular orientation of the vehicle with respect to a celestial reference.

ILLUSTRATION OF MODEL ERROR ESTIMATION

SYSTEM - TWO-BODY

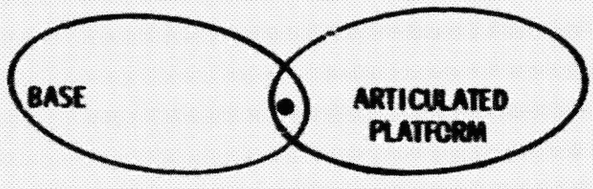

REDUCED-ORDER MODEL

$\dot{\theta} = \omega$ KINEMATICS

$\dot{\omega} = u$ DYNAMICS

$y = \theta + n$ OBSERVATION

MODEL ERRORS

$$\begin{bmatrix} u \\ n \end{bmatrix} = \text{EXTERNAL DISTURBANCES} + \text{TRUNCATED DYNAMICS} + \text{NEGLECTED NONLINEARITIES} + \text{PARAMETER UNCERTAINTIES}$$

INFLIGHT MODEL ERROR ESTIMATION

Estimation of the inflight dynamics of a flexible spacecraft is shown in the figure. The plots correspond respectively to angular position, velocity and estimated model error as functions of time. The available measurements to achieve the required state-variable reconstruction consist of samples of the angular position at the discrete instants in time (see top plot). The data used in the plots corresponds to an actual JPL spacecraft formed by a central rigid bus and an articulated subassembly. The spacecraft dynamics can therefore be represented by the two-element configuration described previously in this presentation. The estimation process was however based on a single-rigid-body model. Consequently, the truncated subassembly motion is reflected as equivalent torques (model errors) in the reduced-order model. The model error estimates shown in the bottom plot very clearly indicate the presence of the truncated motion. Such a model error estimation concept can therefore be used to detect the presence of unmodeled vehicle dynamics. The application of this approach to distributed systems is currently under investigation. A summary of current results is reported in Ref. 4.

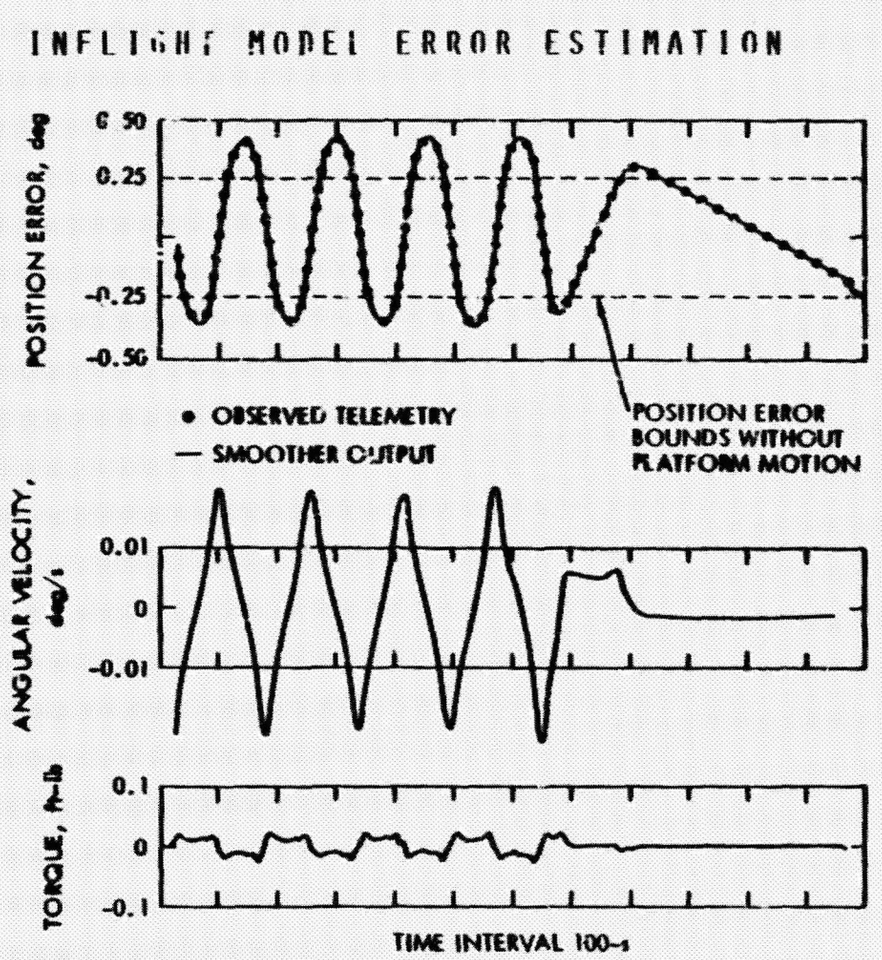

FLEXIBLE BEAM CONTROL OBJECTIVES

The objectives of hardware demonstration using a flexible beam as the "large space structure" (LSS) are to demonstrate active static and dynamic shape control in a real or near-real environment, on which basis our mathematical analysis and simulation are to be verified. This demonstration also provides a test-bed to further development on mechanization and on sensors and actuators.

Not only will the demonstration validate the theoretical analysis but it will bring insight into possible problems in integration and mechanization of the control of LSS. Model inefficiencies, spillover of control or observation, real-world computation limitation and other deficiencies could be detected that will shed light to better and more robust control law and system model design. Such a scaled model demonstration is deemed indispensible as a precursor to full-scaled space demonstration.

LSS FLEXIBLE BEAM CONTROL DEMONSTRATION
OBJECTIVES

- TO DEMONSTRATE ACTIVE STATIC SHAPE CONTROL
- TO DEMONSTRATE ACTIVE DYNAMIC SHAPE CONTROL, I.e., DISTURBANCE DAMPING AND SHAPE CONTROL
- TO FURTHER DEVELOP AND TO PROVIDE TEST-BED FOR TESTING SENSORS AND ACTUATORS
- TO AUGMENT AND TO VERIFY MATHEMATICAL ANALYSIS AND SIMULATION SOLUTIONS UNDER REAL OR NEAR-REAL ENVIRONMENT

FLEXIBLE BEAM CONTROL INSTRUMENTATION

There are four major categories in the instrumentation of the beam control demonstration: (1) flexible beam, (2) actuator, sensor and electronics, (3) digital controller (data processor), and (4) support facilities. The 1/32" x 6" x 12' beam is made of stainless steel. It is hung vertically, hinged at the top and free at the bottom. It has a fundamental frequency, i.e. pendulum rigid-body mode, at 0.3 Hz. Multiple actuators and sensors, with variable location along the beam, are planned. Current configuration has 3 actuators and 4 sensors. Static shape control and multiple mode (<8) dynamic control can be implemented. The actuators and sensors are all off-the-shelf items, the former being d.c. brushless torque motors and the latter eddy current displacement sensors. FY'79 accomplishments include the establishment of the facility; procurement, fabrication and integration of the hardware; software development on the microcomputer to perform static and dynamic shape control: and preliminary experimentation of the control of the beam. With the present set up, various control laws can be tested, such as full-state optimal control, local-state control, and adaptive control. Optimal combination and placement of actuators and sensors can be experimented. Model order reduction and estimation can be investigated using the present facility.

LSS FLEXIBLE BEAM CONTROL DEMONSTRATION
INSTRUMENTATION

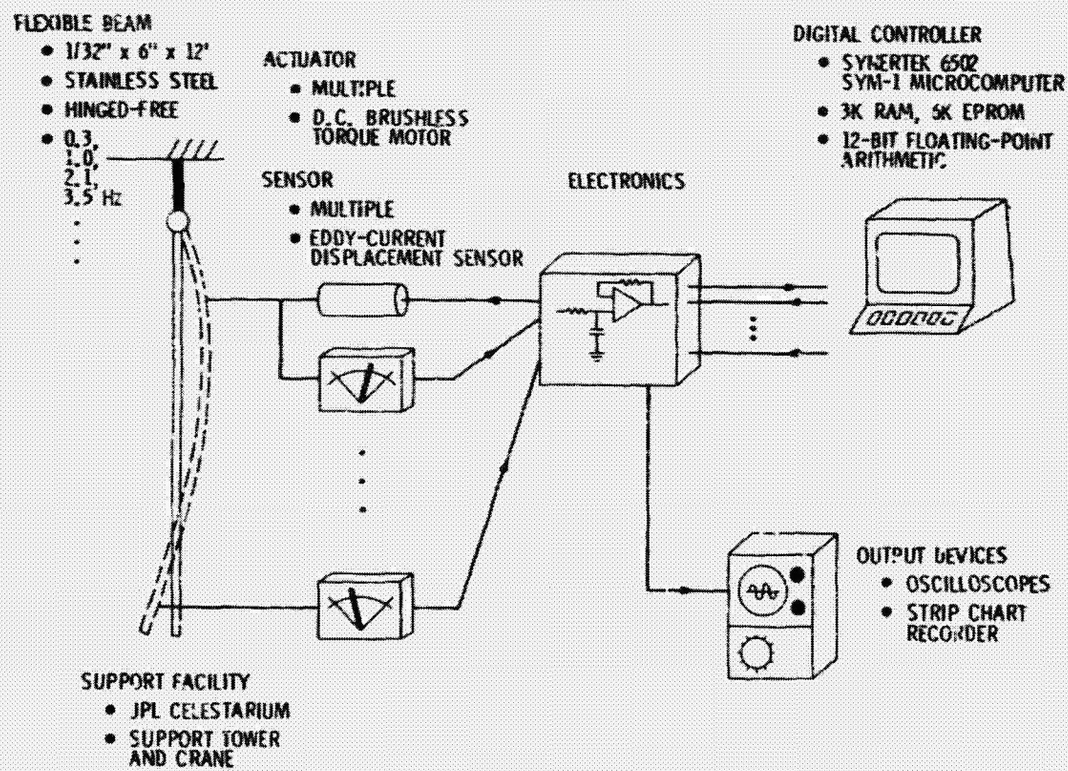

FY'80 PLANNED DEVELOPMENTS

The direction for the FY'80 JPL LSST Controls Program is to characterize, define and initiate solution of the control problems for specific platforms (small science platforms and large multiple payload platforms) and for parabolic reflectors.

The specific tasks to be implemented are tabulated below:

Control of Science Application Platforms

Control of Large Multiple-Payload Platforms

Control of Large Parabolic Reflectors

Analysis and Simulation

Justification of these tasks results from the fact that it is necessary to investigate in detail the performance and stability of specific platforms and antennas in order to achieve an integrated structure and control design approach. The control/structure/performance interaction must be defined and understood in order to develop technology to assure control mechanizations which will accommodate these systems. The specific output of these tasks will be to define and illustrate parametrically control problems and to identify the technology developments necessary to enable subsequent missions.

FY 80 PLANNED DEVELOPMENTS

- PROVIDE A QUALITATIVE DEFINITION OF CONTROL PROBLEMS FOR A SCIENCE APPLICATIONS PLATFORM, A MULTIPLE PAYLOAD PLATFORM AND A PARABOLIC REFLECTOR
- CARRY OUT A COMPARATIVE EVALUATION BETWEEN DISTRIBUTED AND LUMPED CONTROL CONCEPTS
- CARRY OUT PARAMETRIC CONTROL PERFORMANCE STUDIES FOR PLATFORMS AND PARABOLIC REFLECTORS
- PERFORM A MODEL ORDER REDUCTION STUDY TO IDENTIFY AND ILLUSTRATE PARAMETRICALLY CONTROL PROBLEMS CAUSED BY INEVITABLE MODEL ERRORS
- INVESTIGATE PLATFORM CONTROL PROBLEMS CAUSED BY SENSOR AND ACTUATOR SEPARATION BY FLEXIBLE STRUCTURAL ELEMENTS

DOCUMENTATION

Most of the results obtained to date in the JPL control technology development program have been documented. A total of 6 technical conference papers have been presented. The Purdue contract has produced 5 reports in the area of model order reduction. A number of internal JPL reports provide a less formal but nonetheless substantial record of accomplishments to date. This documentation is available from JPL upon request.

TECHNICAL CONFERENCES

Rodriguez, G., "Distributed Control Concepts for Large Space Structures," Conference on Advanced Technology for Future Space Systems," LaRC, Hampton, Virginia, May 1979.

Rodriguez, G., "Optimal Estimation of Large Structure Model Errors," AIAA 17th Aerospace Sciences Meeting, New Orleans, Louisiana, January 1979.

Rodriguez, G., "State and Model Error Estimation for Distributed Parameter Systems," 2nd AIAA Symposium on Dynamics and Control of Large Flexible Spacecraft, Blacksburg, Virginia, June 1979.

Juang, J.N. and G. Rodriguez, "Formulations and Applications of Large Structure Actuator and Sensor Placements," 2nd AIAA Symposium on Dynamics and Control of Large Flexible Spacecraft, Blacksburg, Virginia, June 1979.

Schaechter, D.B., "Optimal Local Control of Flexible Structures," AIAA Guidance and Control Conference, Boulder, Colorado, August 1979.

Rodriguez, G., "Optimal Control of Large Structures Modeled by Partial Differential Equations," AIAA Guidance and Control Conference, Boulder, Colorado, August 1979.

DISTRIBUTED CONTROL REPORTS

Schaechter, D.B., "Candidate Attitude Control Concepts and Tools for Distributed Control," JPL EM 347-20, April 15, 1979.

Schaechter, D.B., "Feedback Solutions for Static Shape Control," JPL EM 347-18, April 13, 1979.

Juang, J.N. and G. Rodriguez, "Formulations for Large Structure Sensor Placements," JPL EM 347-22, May 7, 1979.

Juang, J.N., "Dynamic Characteristics and Control of Large Flexible Structures," JPL IOM 347-79-157, March 9, 1979.

Rodriguez, G., "A Discrete-Time Modal Coordinate Formulation for Evaluation of Large Structure Dynamic Response," JPL EM 347-02, November 9, 1978.

Schaechter, D.B., "Local Control for Structures Described by Finite Elements," JPL EM 347-011, February 22, 1979.

Schaechter, D.B., "Analytical Tools for Local Control of Large Space Structures," JPL EM 347-06, December 15, 1978.

Rodriguez, G., "Optimal Control for Distributed Parameter Systems," JPL EM 347-03, November 21, 1978.

Schaechter, D.B., "LSST: An Optimal Distributed Control Algorithm Using a Maximum Step Size Integration Routine," JPL EM 347-001, October 30, 1978.

Juang, J.N., "A Warning for Modal Control of Reduced Order System," JPL EM 347-23, May 7, 1979.

Gunter, S. and D.B. Schaechter, "Shape Control Flexible-Beam Experiment Objectives and Plans," JPL EM 347-25, May 7, 1979.

Schaechter, D.B., "Further Results for Static Shape Control," JPL EM 347-27, May 24, 1979.

Juang, J.N. and G. Rodriguez, "Formulations and Applications for Large Structure Actuator Placements," JPL EM 347-28, May 30, 1979.

Juang, J.N., "A Pole Assignment Algorithm with Computational Ease," JPL EM 347-31, July 24, 1979.

Juang, J.N., and A.F. Tolivar, "Some Characteristics of a Partitioned Matrix," JPL EM 347-33, September 14, 1979.

Schaechter, D.B., "Flexible Beam Control Software," JPL EM 347-34, September 17, 1979.

Gunter, S.M., "Flexible Beam Experiment Shear and Bending Moment Analysis," JPL EM 347-35, September 19, 1979.

Gunter, S.M., "State-of-the-Art Assessment of Shape Control Techniques," JPL EM 347-37, September 24, 1979.

Lin, Y.H., "A Dynamic Feedback Control Design for Large Space Structures," JPL EM 347-38, September 26, 1979.

MODEL ORDER REDUCTION REPORTS

Skelton, R.E. and P.C. Hughes, "Stability, Controllability and Observability of Matrix-Second-Order Systems," Purdue Research Foundation Report, April 1979.

Skelton, R.E. and P.C. Hughes, "Generic Model of a Large Flexible Space Structure for Control Concept Evaluation," Purdue Research Foundation Report, July 1979.

Skelton, R.E. and P.C. Hughes, "Controllability and Observability for Flexible Spacecraft," Purdue Research Foundation Report, July 1979.

Skelton, R.E. and P.C. Hughes, "Measurement Feedback and Model Reduction by Modal Cost Analysis," Purdue Research Foundation Report, July 1979.

Skelton, R.E., "Flexible Space Structure Model Reduction by Modal Cost Analysis," Purdue Research Foundation Report, September 1979.

MODEL ERROR ESTIMATION REPORTS

Rodriguez, G., "Optimal Estimation for Continuous Systems with Discrete-Time Measurements," JPL EM 347-09, January 24, 1979.

Rodriguez, G., "A Geometrical Interpretation of the Model Error Estimation Concept for Large Structures," JPL EM 347-08, December 20, 1978.

Rodriguez, G., "On-Board Sequential Estimation of Large Structure Model Errors," JPL EM 347-12, February 27, 1979.

Rodriguez, G., "Discrete-Time Estimation of a Single Large Structure Vibrational Mode," JPL EM 347-10, February 24, 1979.

Rodriguez, G., "Test-Case Model for Illustration of the Model Error Estimation Concept," JPL EM 347-16, March 30, 1979.

Rodriguez, G., "Optimal Estimation of a Single Large Structure Vibrational Mode," JPL EM 347-04, November 30, 1978.

Weeks, C.J., "The Optimal Estimation of States with Continuous Dynamics by Means of Discrete Observations," JPL EM 347-36, September 17, 1979.

ANTENNA MODELING AND CONTROL REPORTS

Schaechter, D.B., "Preliminary Attitude Control System Definitions and Designs for the TRW 30 Meter Precision Deployable Antenna," JPL EM 347-014, March 8, 1979.

Edmunds, R.S., "LSST Attitude Control Functional Requirements Outline and Approach," JPL IOM 347-79-004, January 4, 1979.

Edmunds, R.S., "Functional Requirements for LSST Attitude Control, Shape Control, and Stationkeeping," JPL IOM 347-79-184, March 29, 1979.

Gunter, S.M., "Antenna Paraboloid RMS Best-Fit Computer Program," JPL EM 343-370, October 20, 1978.

DesForges, D.T., "Structural Dynamic Model of 100-Meter Diameter Mesh Deployable Antenna," JPL IOM 3545-79-36, June 6, 1979.

DesForges, D.T., "Preliminary Structural Dynamic Model of 30-Meter Diameter Precision Deployable Antenna," JPL IOM 3545-79-27, February 26, 1979.

REFERENCES

1. Schaechter, D. B., "Optimal Local Control of Flexible Structures," AIAA Guidance and Control Conference, Boulder, Colorado, August 1979.

2. Schaechter, D. B., "Candidate Attitude Control Concepts and Tools for Distributed Control," JPL EM 347-20, April 15, 1979.

3. Rodriguez, G., "Optimal Control of Large Structures Modeled by Partial Differential Equations," AIAA Guidance and Control Conference, Boulder, Colorado, August 1979.

4. Rodriguez, G., "Optimal Estimation of Large Structure Model Errors," AIAA 17th Aerospace Sciences Meeting, New Orleans, Louisiana, January 1979.

N80-19164

LARGE SPACE SYSTEM CONTROL TECHNOLOGY
MODEL ORDER REDUCTION STUDY

R. E. Skelton
Purdue University

LSST 1ST ANNUAL TECHNICAL REVIEW

November 7-8, 1979

This is a report on the model order reduction for large space structures performed under contract to JPL by Purdue University with R. E. Skelton as Principal Investigator. The main objective of the contract is to find the best pre-flight dynamical models for large structures and thereby retain the most significant vehicle dynamics in the controller designs.

MISSION CONTROL REQUIREMENTS

Large structures have to satisfy a wide range of mission control requirements including pointing and shape control. Specific missions with these requirements may include platforms and large antennas.

MISSION CONTROL REQUIREMENTS

- POINTING CONTROL
- SHAPE CONTROL
  - ANTENNAS
  - PLATFORMS

PROBLEMS OF ACTIVE CONTROL OF
LARGE STRUCTURES IN SPACE

One of the main problems in active control of large structures in space is that the controller designs require accurate models to represent the structure dynamic response. Present models obtained typically by means of a finite-element analysis of the structural dynamics are not sufficiently accurate as a result of four classes of errors: parameter uncertainties, nonlinearities, neglected variables and external disturbances. In addition the process of model order reduction must be carried out in order to satisfy on-board memory and speed computational requirements.

PROBLEMS OF ACTIVE CONTROL OF LARGE STRUCTURES IN SPACE

- CONTROL DESIGN REQUIRES ACCURATE MODEL
- PRESENT MATHEMATICAL MODELS NOT ACCURATE ENOUGH
  - PARAMETER ERROR
  - NONLINEARITIES
  - NEGLECTED VARIABLES
- LIMITATIONS OF ON-BOARD DIGITAL COMPUTERS
  - MEMORY
  - SPEED

PURDUE MODEL

An Equivalent Distributed Parameter Model of Truss Structure

In order to study the process of model order reduction a generic model has been selected that contains most of the features important in the modeling and control problem for large structures. The model consists of a rectangular array that is an equivalent distributed model of a truss structure. The continuum model is easier to work with as it does not require the complexities of a more detailed numerical model that may tend to conceal the control-related problems. In the center of the model is an articulated rigid body representing possibly a payload that must be pointed to a higher degree of precision than the remainder of the structure. This model has been used to study the problem of model order reduction for large structures. The results obtained, however, are applicable to a wide range of large structures and are not limited to the selected model.

PURDUE MODEL

AN EQUIVALENT DISTRIBUTED PARAMETER MODEL OF TRUSS STRUCTURE

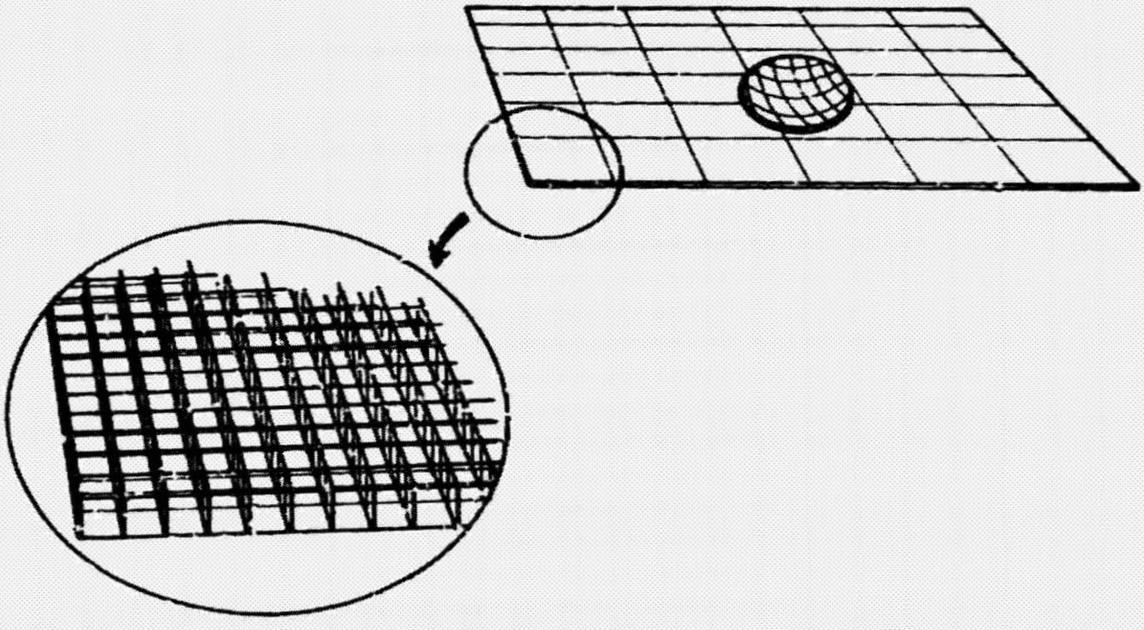

CONTROL/STRUCTURE TRADEOFF

A fundamental tradeoff must be made in developing an integrated control/structure design. Control can either be achieved by means of more software resulting in a lightweight structure or with less software and a heavier structure. One of the results of this study is to provide the necessary methods to perform this tradeoff systematically.

CONTROL/STRUCTURE TRADEOFF

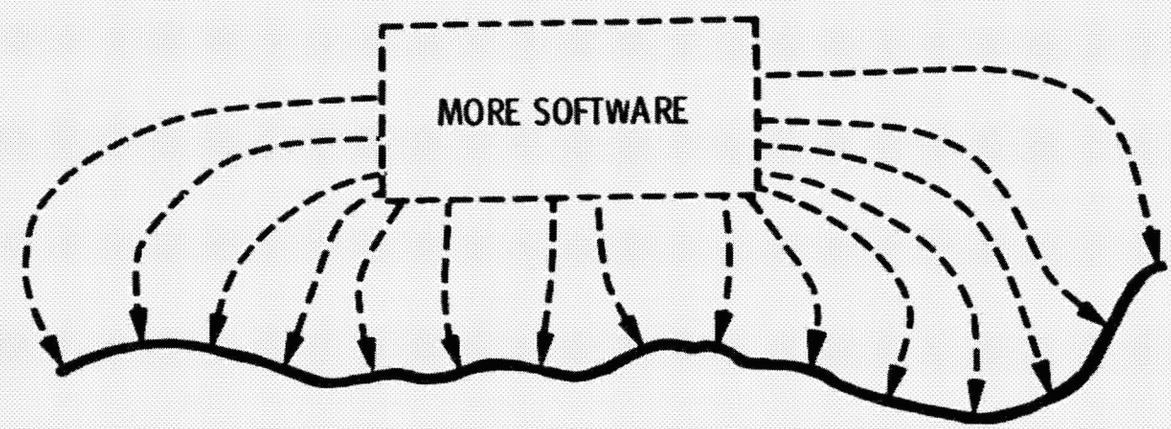

- MORE CONTROL HARDWARE, SOFTWARE (LESS ROBUST)
- LIGHTWEIGHT STRUCTURE

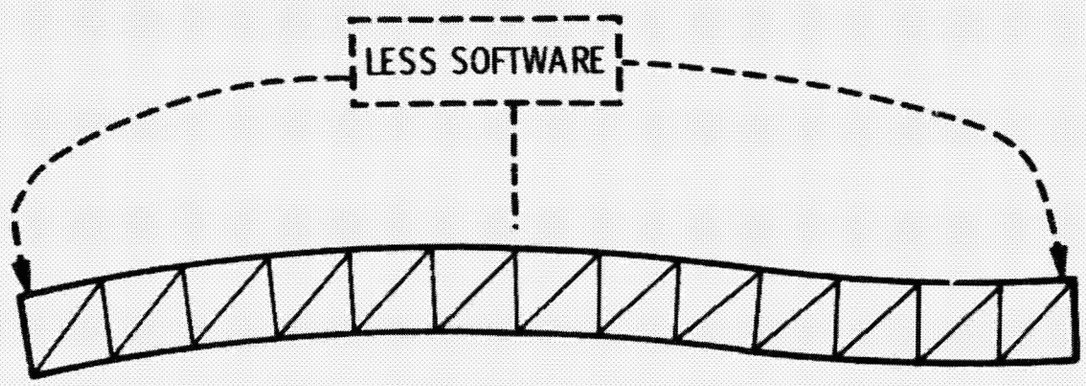

- LITTLE CONTROL HARDWARE, SOFTWARE (ROBUST)
- HEAVY STRUCTURE

DESIRED INTERACTION BETWEEN STRUCTURE
DESIGN & CONTROL ANALYSIS

The desired interaction between structure and control design is displayed in the viewgraph. The objective is to select the critical modes in order to modify the model and the structure and thereby achieve integrated design.

DESIRED INTERACTION BETWEEN STRUCTURE DESIGN & CONTROL ANALYSIS

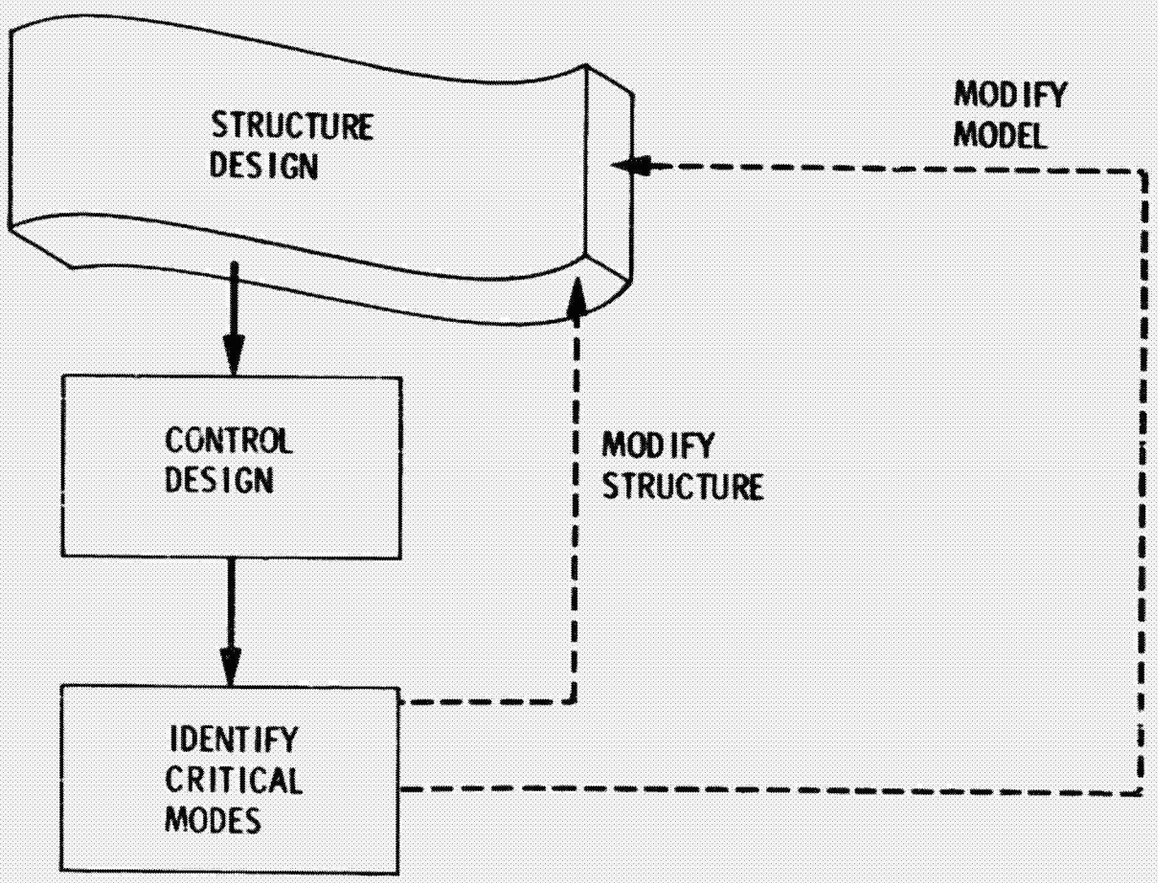

The control study objectives are to suggest desired dynamic structure properties for improved performance and reduced weight. An example of these properties may be the selection of modes that may be damped by introducing passive damping in certain parts of the structure.

CONTROL STUDY OBJECTIVES

- SUGGEST DESIRED DYNAMIC STRUCTURE PROPERTIES FOR
  - IMPROVED PERFORMANCE
  - REDUCED WEIGHT

A number of options exist for dynamical modeling of large structures. The modes selected can be: 1) appendage modes corresponding to the dynamics of individual appendages, 2) spacecraft modes for the overall vehicle dynamic response, 3) open-loop system modes that include also the dynamics of certain elements in the control system, and 4) closed-loop system modes that model the overall system including structure, control and the dynamics of the feedback controllers. The selection is very much dependent upon the configuration. The closed-loop system modes tend to retain the most significant dynamics when the structure is in its operational state.

SELECTION OF DYNAMICAL MODEL

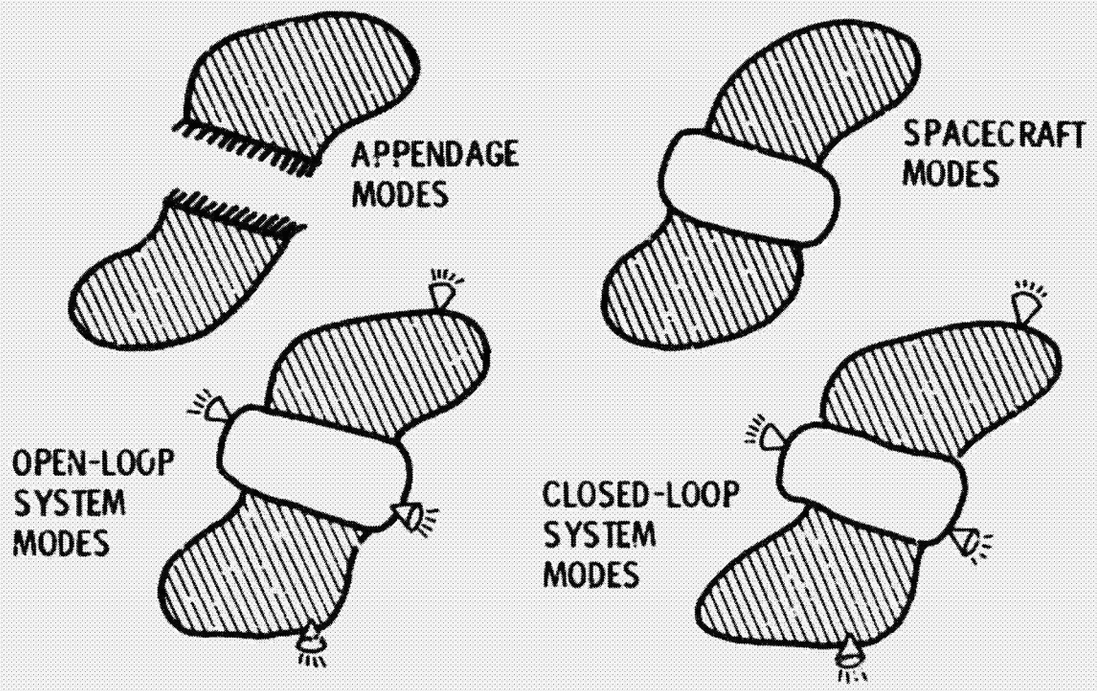

PURDUE MODEL

The figure shows a plot of model completeness index versus the number of modes retained for the Purdue model. The model completeness index gives an indication of the degree of fidelity of a particular modal model with respect to the continuum model which is assumed to be the exact representation of the vehicle dynamics. As more modes are retained, the models become more accurate. A comparison between constrained and unconstrained modes reveals that fewer constrained modes have to be retained in order to obtain a specified model completeness.

PURDUE MODEL

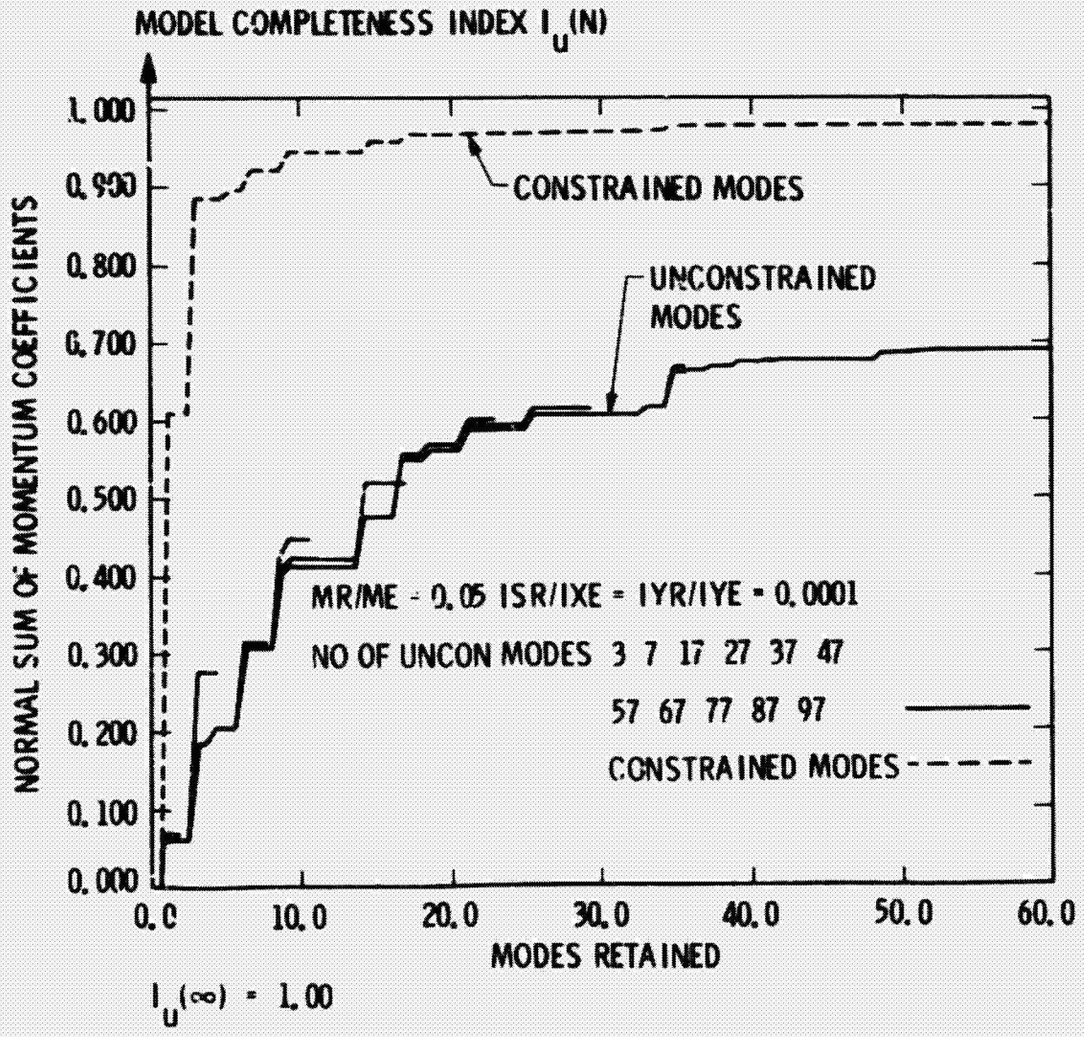

MODAL COST ANALYSIS

COMPONENT COSTS V_i

The method currently under study for model order reduction is modal cost analysis where a so-called cost is associated to each mode. This cost reflects the contribution of each mode to the overall system performance. The component value criterion indicates that the most critical modes are the ones with the largest cost. Conversely, the least critical components have the lowest modal cost.

MODAL COST ANALYSIS
COMPONENT COSTS V_i

$$V = \sum_{i=1}^{M} V_i$$

$$V_i = \frac{1}{2} \sum_{j=1}^{M} (V_{ij} + V_{ji})$$

$$V_{ij} = \mathcal{E}\left[W_i^* K_{ij} W_j\right]_{ZSR} = \mathcal{E}\left[X_i^*(0) K_{ij} X_j(0)\right]_{ZIR}$$

WHERE K SATISFIES

$$0 = KA + A^T K + C^T Q C$$

COMPONENT VALUE CRITERION:

$$V_1 \geq V_2 \geq \ldots \geq V_{M-1} \geq V_M$$

V_1: MOST CRITICAL COMPONENT

V_M: LEAST CRITICAL COMPONENT

ACTUATOR LOCATIONS CONTROLLABILITY SURFACE

In a distributed system, actuator locations are an additional degree-of-freedom in the controller design. A good selection of actuator number and location can lead to improved system performance. A poor selection can at worst lead to overall system instability. The model order selection study also provides criteria for actuator placemen s. The viewgraph shows a so-called controllability surface for the seventh mode of the Purdue model. These actuator locations where the surface is a maximum are where that particular mode is most strongly affected by the control inputs. The points where the surface is zero correspond to locations where the mode is uncontrollable.

ACTUATOR LOCATIONS CONTROLLABILITY SURFACE

SEVENTH MODE

[TWO TORQUE ACTUATORS COINCIDENT AT (a_x, a_y)]

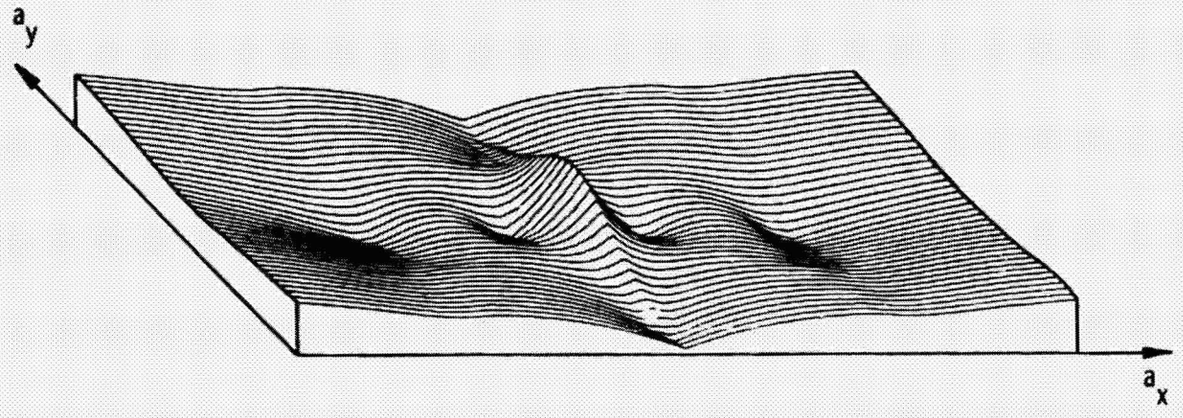

SENSOR LOCATIONS OBSERVABILITY SURFACE

A similar surface can be used for sensor location. The points where the surface is a maximum correspond to sensor locations where the particular mode is most observable by the sensors. Similarly, the points where the surface is zero are those where the mode cannot be observed by means of the sensor measurements.

SENSOR LOCATIONS OBSERVABILITY SURFACE

EIGHTH MODE

[TWO ORTHOGONAL ATTITUDE SENSORS ON R, PLUS ELASTIC DEFLECTION AT (s_x, s_y)]

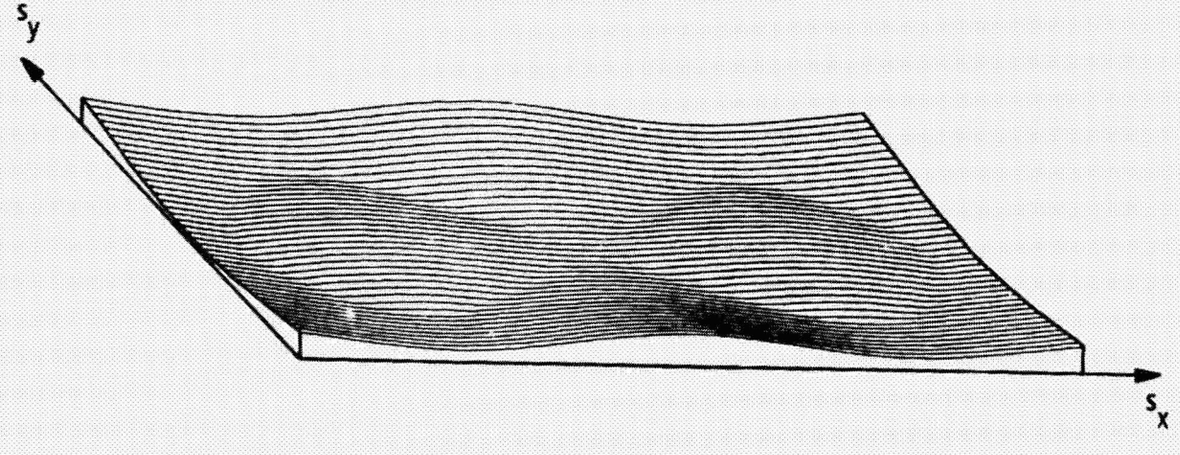

ATTITUDE CONTROL

Modal Cost Analysis

The viewgraph displays results of the application of the technique of modal cost analysis to the problem of attitude control to the Purdue model. By assigning a cost to each individual mode, those modes that have the most effect on the control/structure performance can be selected. The modes with the highest cost are the most important in the control system design and should be retained. Those modes with the lowest cost have little influence on the control performance and are therefore the likeliest candidates for elimination in the controller design.

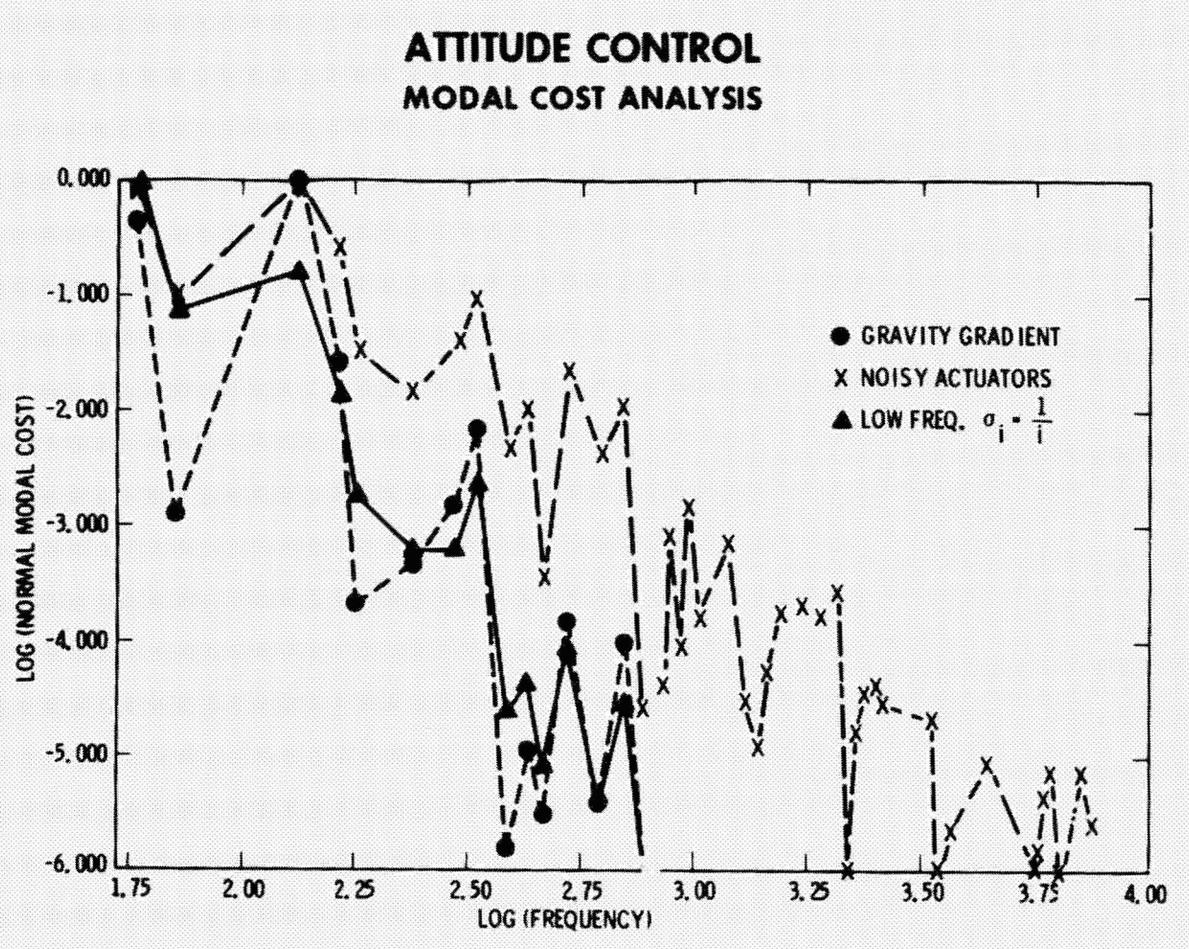

SHAPE CONTROL

Modal Cost Analysis

The viewgraph shows results of the application of the modal cost analysis to the problem of shape control for the Purdue model. By establishing a relative ranking of the modes in terms of their effect on control performance, the most significant modes can be extracted and used in the controller design.

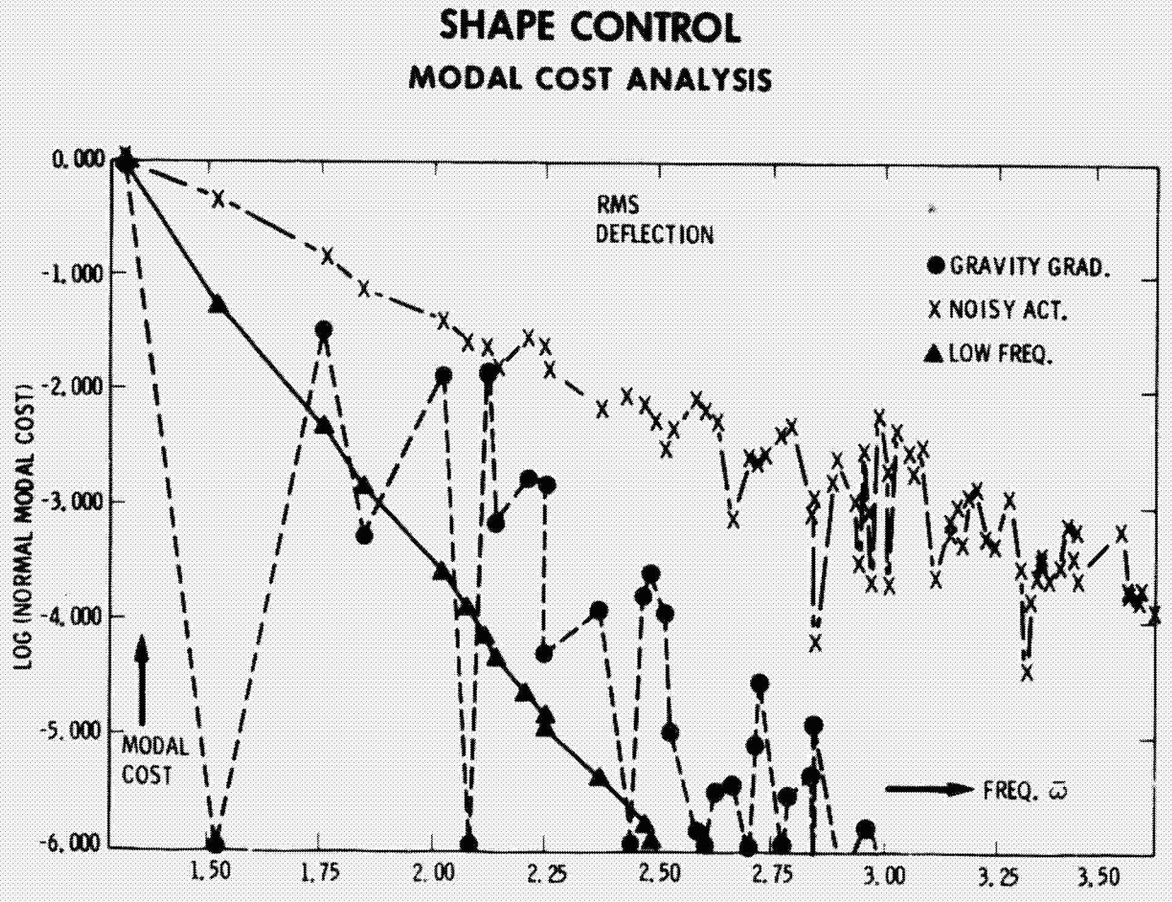

MODEL ERROR VS. CONTROL OBJECTIVE

The plot shows the model error as a result of using an approximate model. As the model order is increased, the model error is reduced in all cases. The plot corresponding to shape control has a larger value for a given model order. This indicates that more modes have to be retained in order to achieve a prescribed fidelity for the shape control problem. Fewer modes have to be retained if attitude control is the desired objective.

MODEL ERROR VS. CONTROL OBJECTIVE

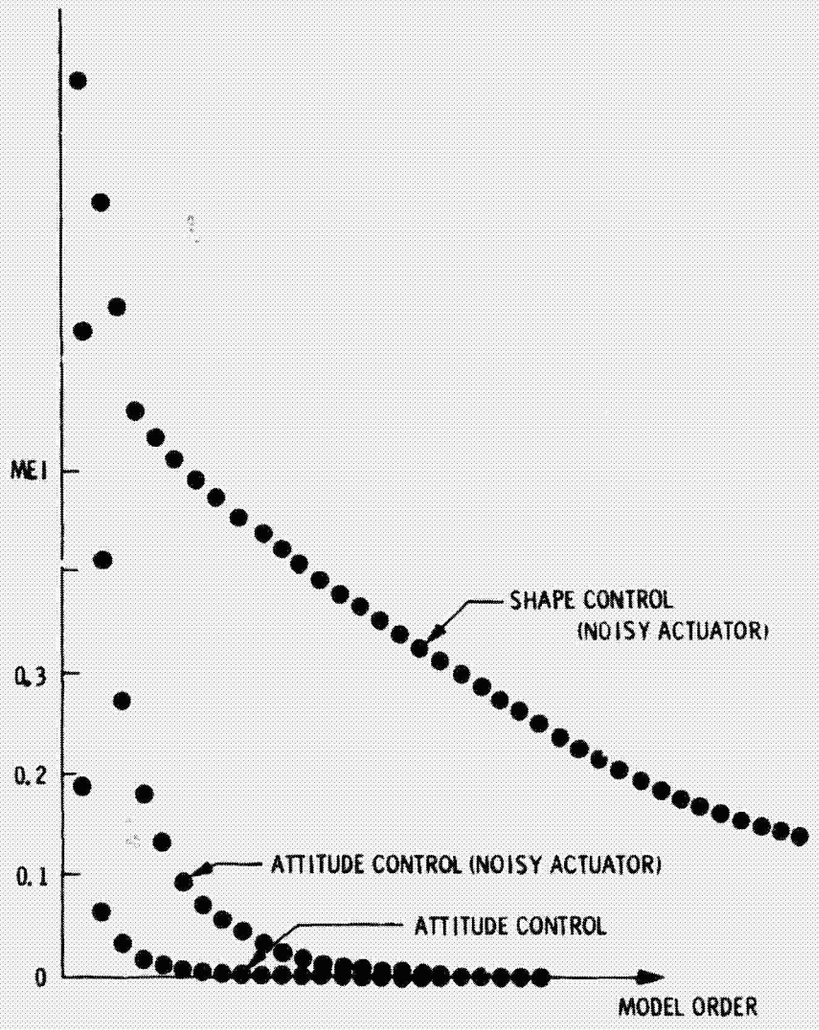

N80-19165

LaRC CONTROLS ACTIVITY FOR LSST

R. C. Montgomery
NASA Langley Research Center

LSST 1ST ANNUAL TECHNICAL REVIEW

November 7-8, 1979

PAGE 358 INTENTIONALLY BLANK

LSST CONTROLS OVERVIEW
LaRC -- FY 79

- o MODELING AND CONTROL OF LSS IN ORBIT
- o REDUCED ORDER DECOUPLING
- o SHAPE CONTROL
- o ATTITUDE CONTROL OF LARGE PLATFORMS USING DUAL AMCD's
- o ADAPTIVE CONTROL OF SPINNING RING
- o LEARNING CONTROL FOR SEP SHUTTLE

Slide 1

As indicated in slide 2 math models have been developed for various types of large flexible structures. These models are being used to study the uncontrolled dynamic characteristics of the structures in orbit and to devise control concepts in order to control their orientation and geometrical shape.

Studies have been made for reduced order decoupled control of the 100-meter long free free beam depicted in slide 3. The objective is to control the in-plane orientation and shape of the beam in a decoupled manner with as few actuators as possible.

Slide 4 illustrates the type of results that are generally obtained when the number of actuators is less than the number of modes considered in the model. Using two controllers, near each end of the beam, to produce a 0.01-radian pitch change, perfect decoupled control is achieved for the rigid body pitch (θ) mode and the first flexible mode (A_1). However, the other two flexible modes cannot generally be included in the decoupling process and hence cannot be controlled.

For a special case where the ratios between the rows of the control-influence coefficient matrix are the same (for example, when the controls are exactly at both ends of the beam) the uncontrolled modes can be included in the decoupling process. Based on information obtained from this special case, a method (referred to as the ratio method) has been developed for adjusting the feedback gains required for control of the complete model. Slide 5 shows the results for the example in slide 4 where these gain adjustments have been made. Almost perfect decoupling is maintained for θ and A_1 and, except for some initial effects, the other two modes are controlled.

Slide 6 illustrates a typical result of the minor effect of modeling errors on the decoupling process. In this case incorrect knowledge of the control characteristics was represented by incorporating random errors of either ±5 or ± 10 percent in the control influence coefficients. The solid curves correspond to the condition where no errors are present.

THE DYNAMICS AND CONTROL OF LARGE FLEXIBLE SPACE STRUCTURES

THRUST - DEVELOP MATH MODELS

INVESTIGATE UNCONTROLLED DYNAMIC CHARACTERISTICS

DEVISE CONTROL LAWS FOR: ORIENTATION, GEOMETRICAL SHAPE

STATUS - LONG THIN FREE-FREE BEAM

CIRCULAR AND RECTANGULAR MEMBRANE

CIRCULAR AND RECTANGULAR PLATE

FUTURE - SPHERICAL AND PARABOLIC SHELL

Slide 2

DECOUPLING STUDIES

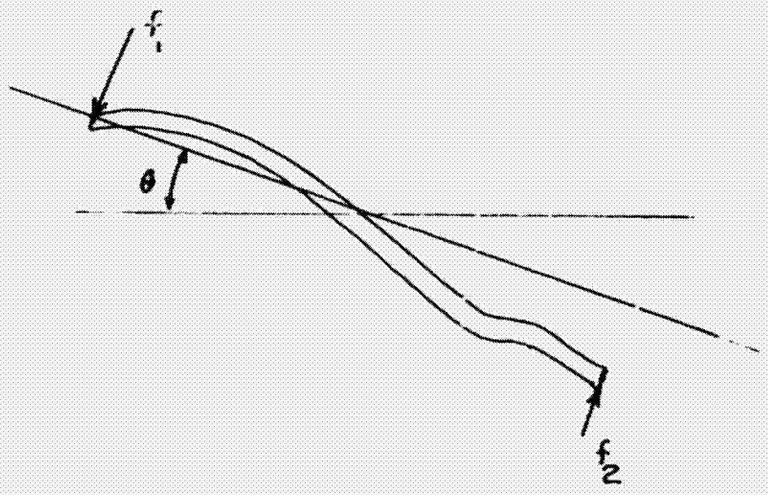

Slide 3

PERFECT DECOUPLING

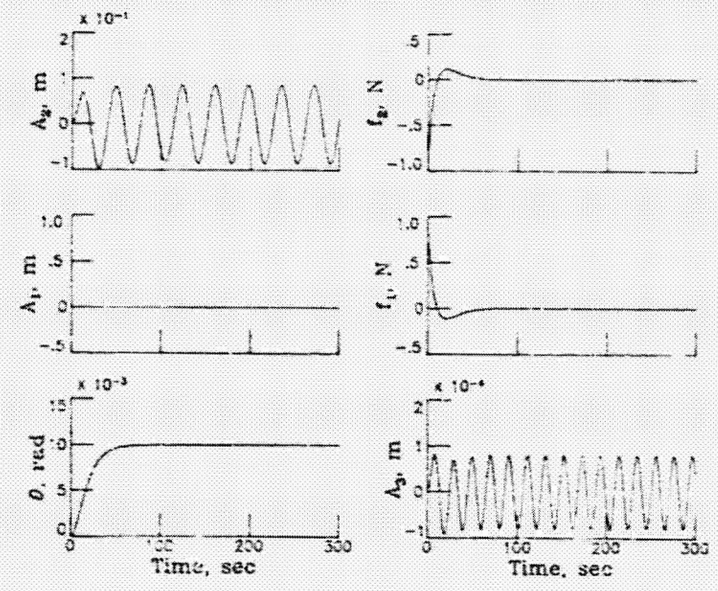

Slide 4

GAIN ADJUSTMENT USING RATIO METHOD

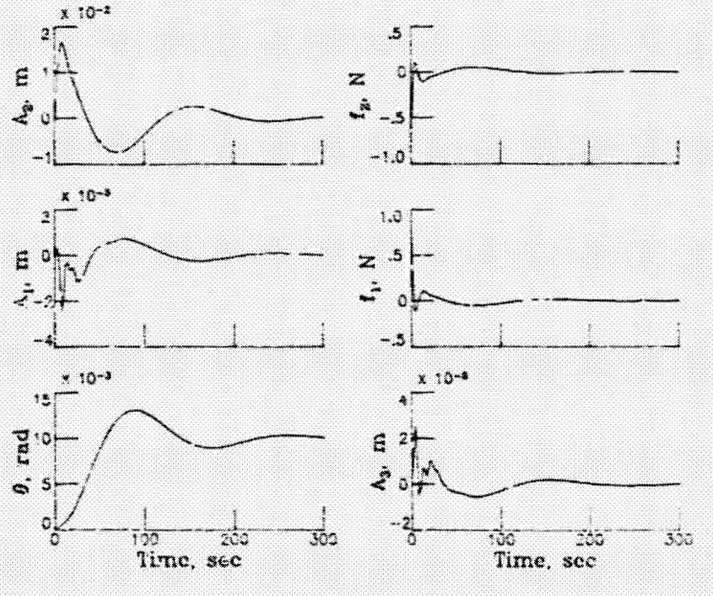

Slide 5

EFFECT OF MODELING ERRORS

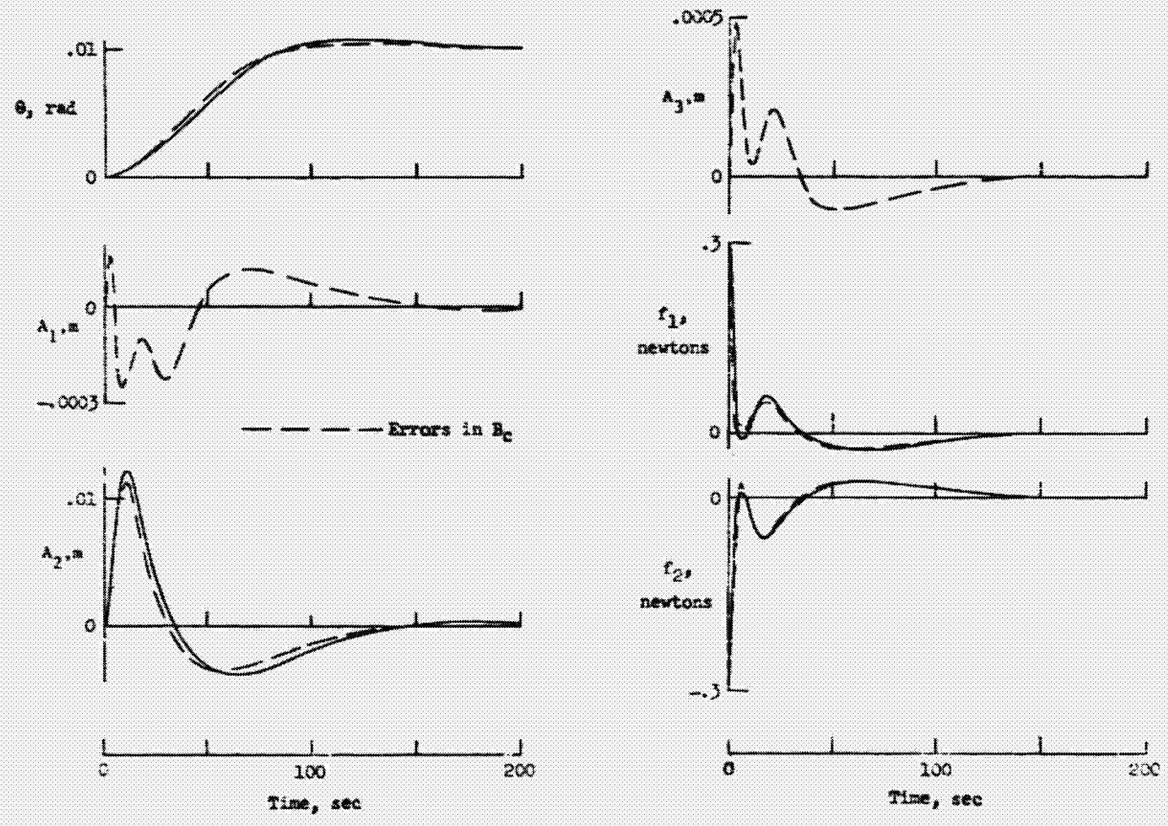

Slide 6

As indicated in slide 7 for shape control three classes of control devices are being considered, boundary control, distributed actuator control, and wave speed control.

Slide 8 is an outline of the time optimal control theory for a string using boundary control and slide 9 is a simulation result. In slide 9, the waves which appear to build up are a result of truncation of the infinite number of system modes to 80 for simulation. The result indicates that some approach <u>other</u> than modal analysis is needed for real time structural control.

SHAPE CONTROL RESEARCH

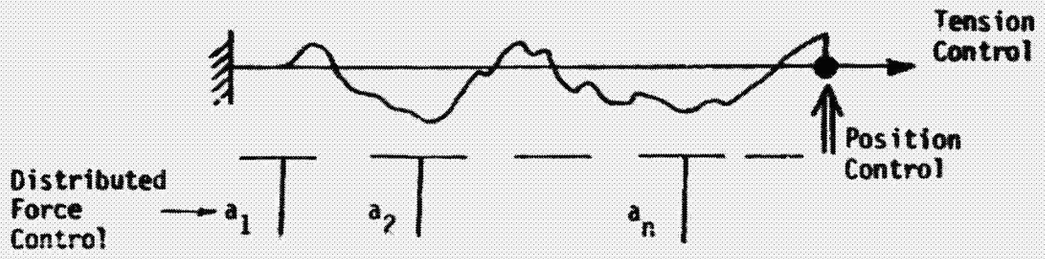

- SIMILAR TO ELECTROSTATIC MEMBRANE CONTROL BUT SIMPLER VERSION
- THREE DISTINCT CONTROL PROBLEMS:
  - (1) BOUNDARY CONTROL
  - (2) DISTRIBUTED ACTUATOR CONTROL
  - (3) WAVE SPEED CONTROL

Slide 7

BOUNDARY CONTROL

PLANAR VIBRATIONS OF A STRING

$$\frac{\partial^2 y}{\partial x^2}(x,t) = \frac{1}{c^2}\frac{\partial^2 y}{\partial t^2}(x,t)$$

$$c = \tau/\rho$$

BOUNDARY CONDITIONS

$$y(0,t) = 0 \qquad y(\ell,t) = u(t) \qquad \left|\frac{du}{dt}\right| \leq 1$$

INITIAL CONDITIONS

$$y(x,0) = g(x) \qquad \frac{\partial y}{\partial t}(x,0) = v(x)$$

TIME OPTIMAL BOUNDARY CONTROL

$$\frac{du^*}{dt}(t) = -c\,\frac{\partial y}{\partial x}(\ell,t)$$

Slide 8

MINIMUM TIME CONTROL IMPLEMENTATION WITH 80 MODES

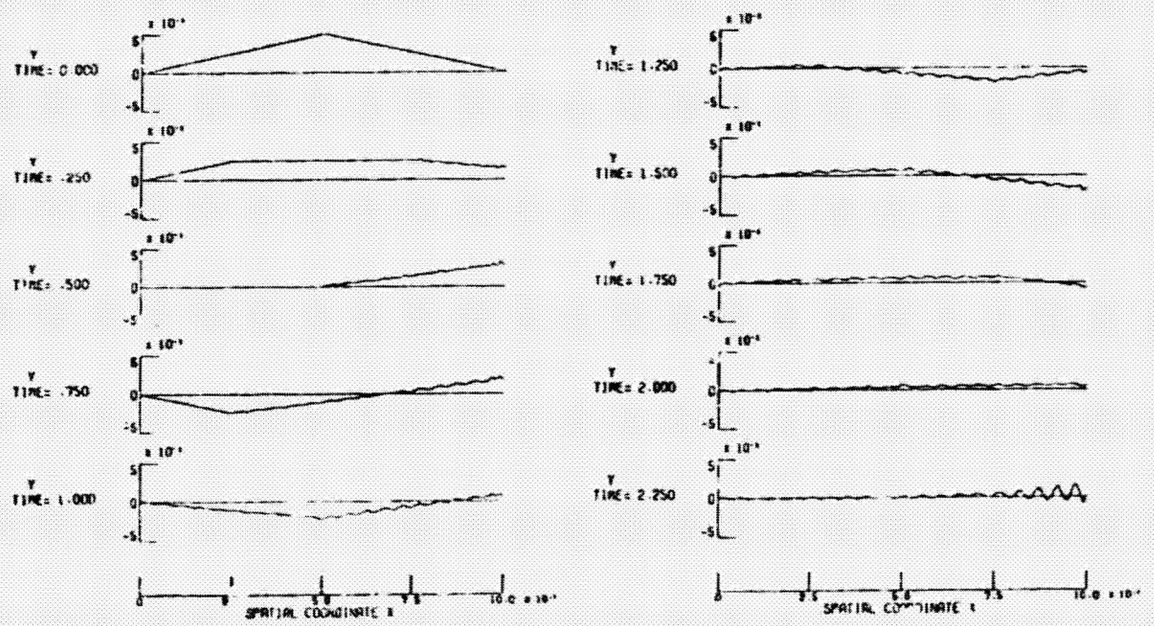

Slide 9

Slide 10 concerns the distributed control of a membrane using electrostatic actuators. An optimal control theory has been derived that minimizes the error, Z, between the desired and actual deflection yet considers the amount of control, U, required to accomplish an error reduction. Slide 11 indicates the form of the graphical output used in simulation to indicate the membrane distortion and the position of the actuators behind the membrane. It also shows the initial membrane distortion used in a simulation to test the control law. Slides 12 through 15 represent the membrane distortion at ever increasing times and show the damping effect of the control laws.

DISTRIBUTED ACTUATION

ACTIVE CONTROL OF A MEMBRANE

EQUATION OF MOTION:

$$z_{tt} + Az = u$$

WHERE

$$Az = -c^2(z_{xx} + z_{yy}) \quad \text{and} \quad c = \sqrt{T/d}$$

COST FUNCTION:

$$C = \frac{1}{2} \int_0^{\infty} \int_0^{b} \int_0^{a} w(x,y) \left[Q z^2 + R u^2 \right] dx\, dy\, dt$$

UNCONS. OPT. PROB: FIND $u^*(x,y,t)$ min. C

OPTIMIZATION WITH CONTROL CONSTRAINT: $u_a(x,y,t) = \sum_{i=1}^{m} v_i(t)\, f_i(x,y)$

$$v^* = \min \left\| \sum_{i=1}^{m} v_i(t)\, f_i(x,y) - u^*(x,y,t) \right\|$$

Slide 10

MEMBRANE DEFLECTION AT TIME = 0. sec.

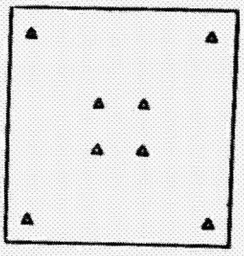

8 Actuators

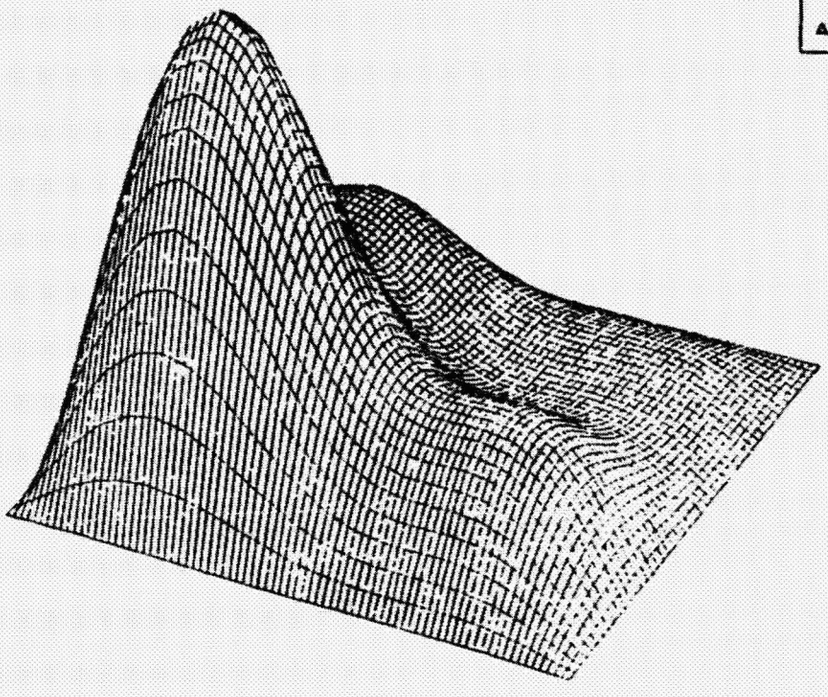

Slide 11

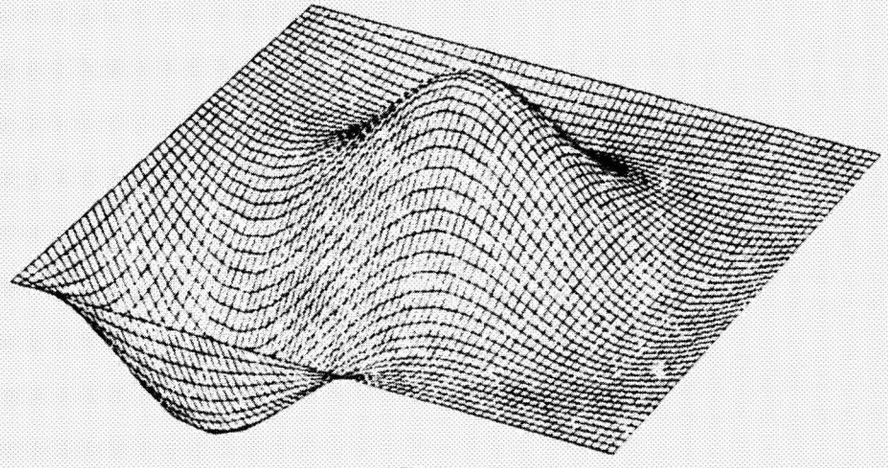

Slide 12

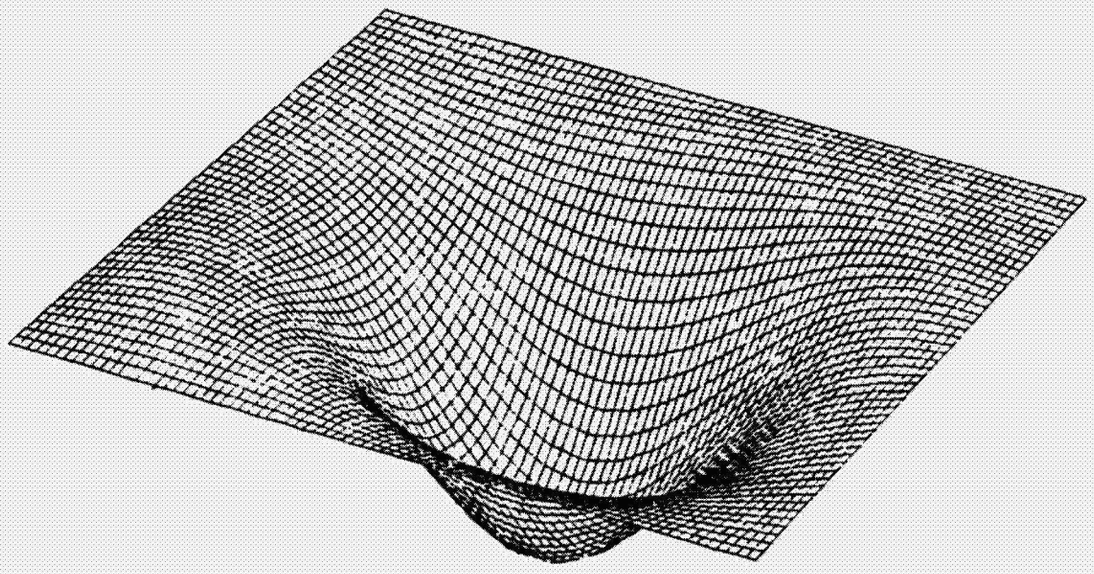

Slide 13

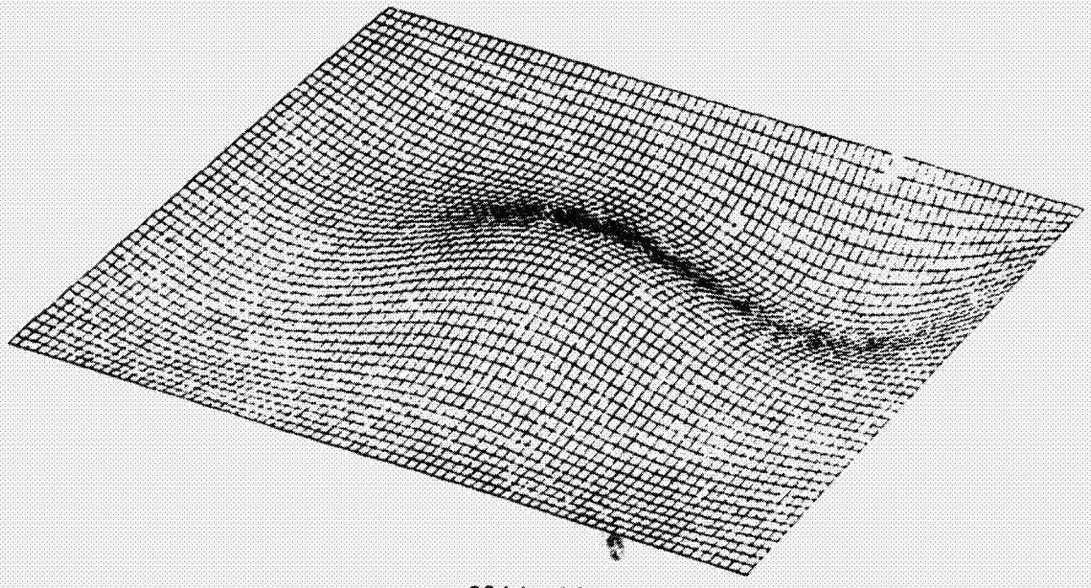

Slide 14

ORIGINAL PAGE IS
OF POOR QUALITY

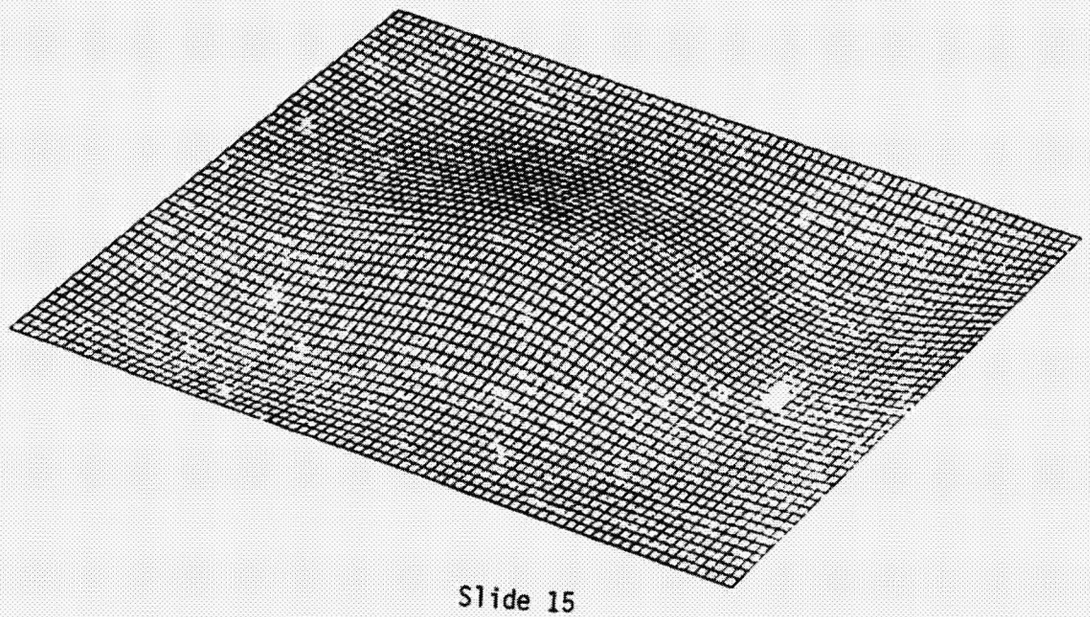

Slide 15

Slide 16 indicated an attitude control concept appropriate for large area platforms. Two large rings spin in the plane of the platform and are scissored to produce a change in momentum that rotates the platform. The rings are attached to the platform by noncontacting magnetic or electrostatic bearings. Because of flexibility a novel adaptive/learning control system concept was developed to suppress elastic marks of the spinning rings while still allowing adequate precisional torques for control.

Slide 17 illustrates the free vibration of the ring as seen by an observer that is spinning with he ring. Points indicated by an * represent where position is sensed by sensors located at fixed points on the platform. The symbol ↑ indicates the application of a force at a bearing fixed to the platform. Slide 18 shows the response of the ring caused by a constant force of 20 N at a bearing station.

Slide 19 shows a desirable ring damping characteristic which requires feedback and knowledge of the modes of motion to achieve.

Slide 20 shows what can happen if the control system is designed with the wrong assumption regarding the modes of motion. In this case the motion does not decay but rather amplifies.

Slide 21 indicates the effectiveness of an adaptive controller. The control system was initially that used in figure 20 which was unstable. Because of the adaptive feature, however, the system identified the required modal information and adjusted the feedback gains to obtain a stable response.

DUAL-MOMENTUM-VECTOR CONTROL CONCEPT

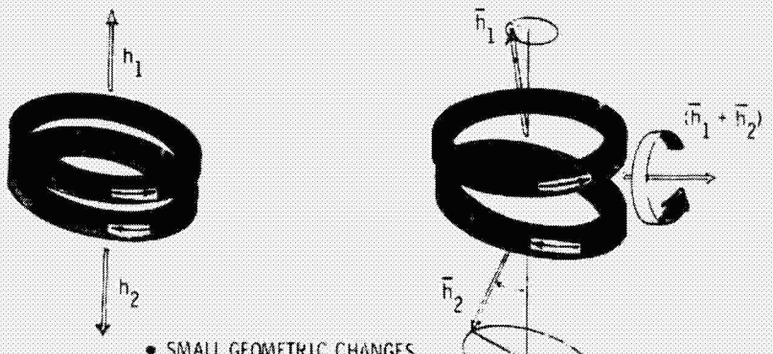

- SMALL GEOMETRIC CHANGES
- LOWEST MASS MOMENTUM CONTROL DEVICE FOR LARGE PLATFORMS
- SMOOTH, DISTRIBUTED CONTROL FORCE

Slide 16

FREE INITIAL CONDITION RESPONSE

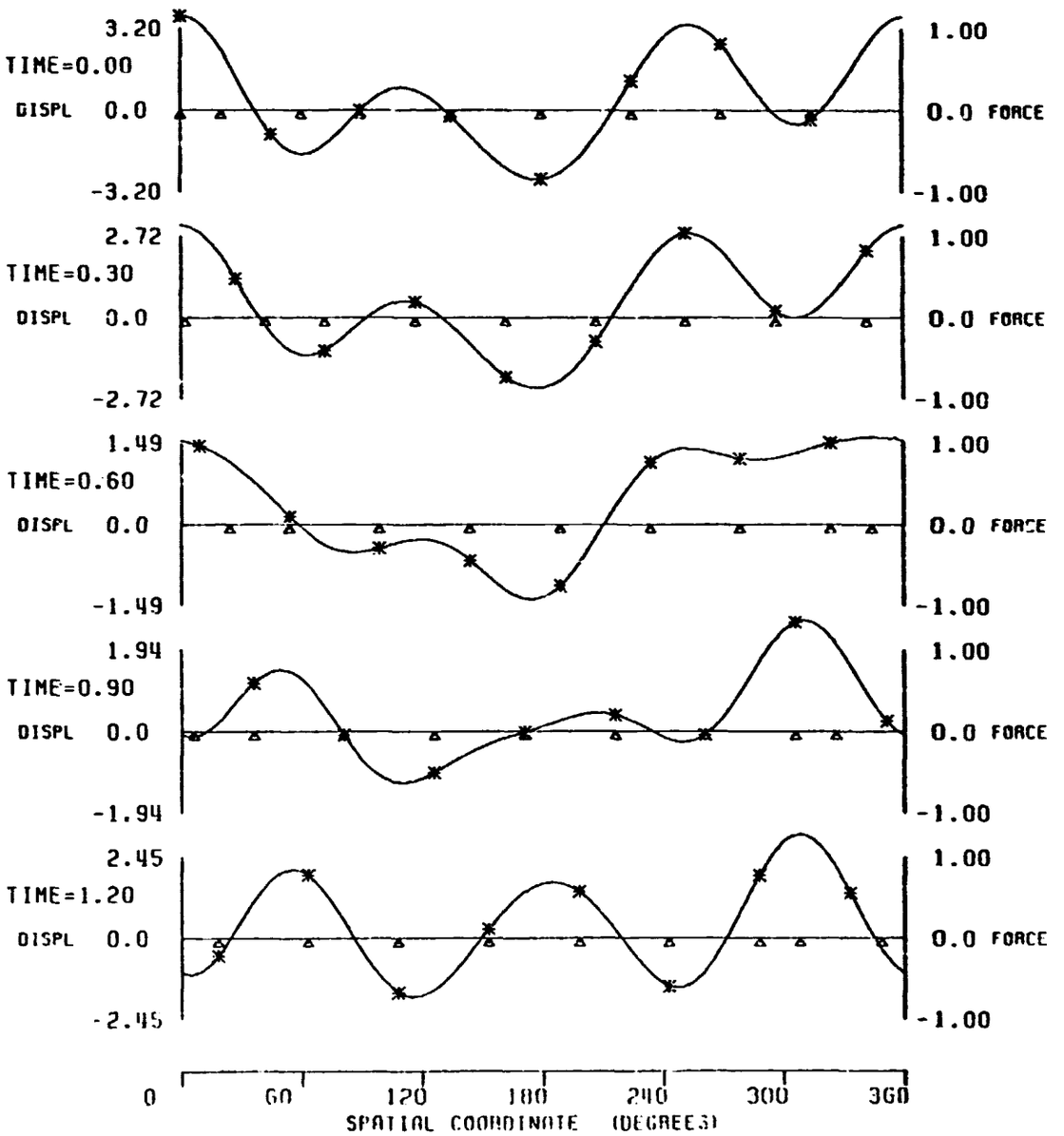

Slide 17

C-5

UNCOMPENSATED STEP RESPONSE

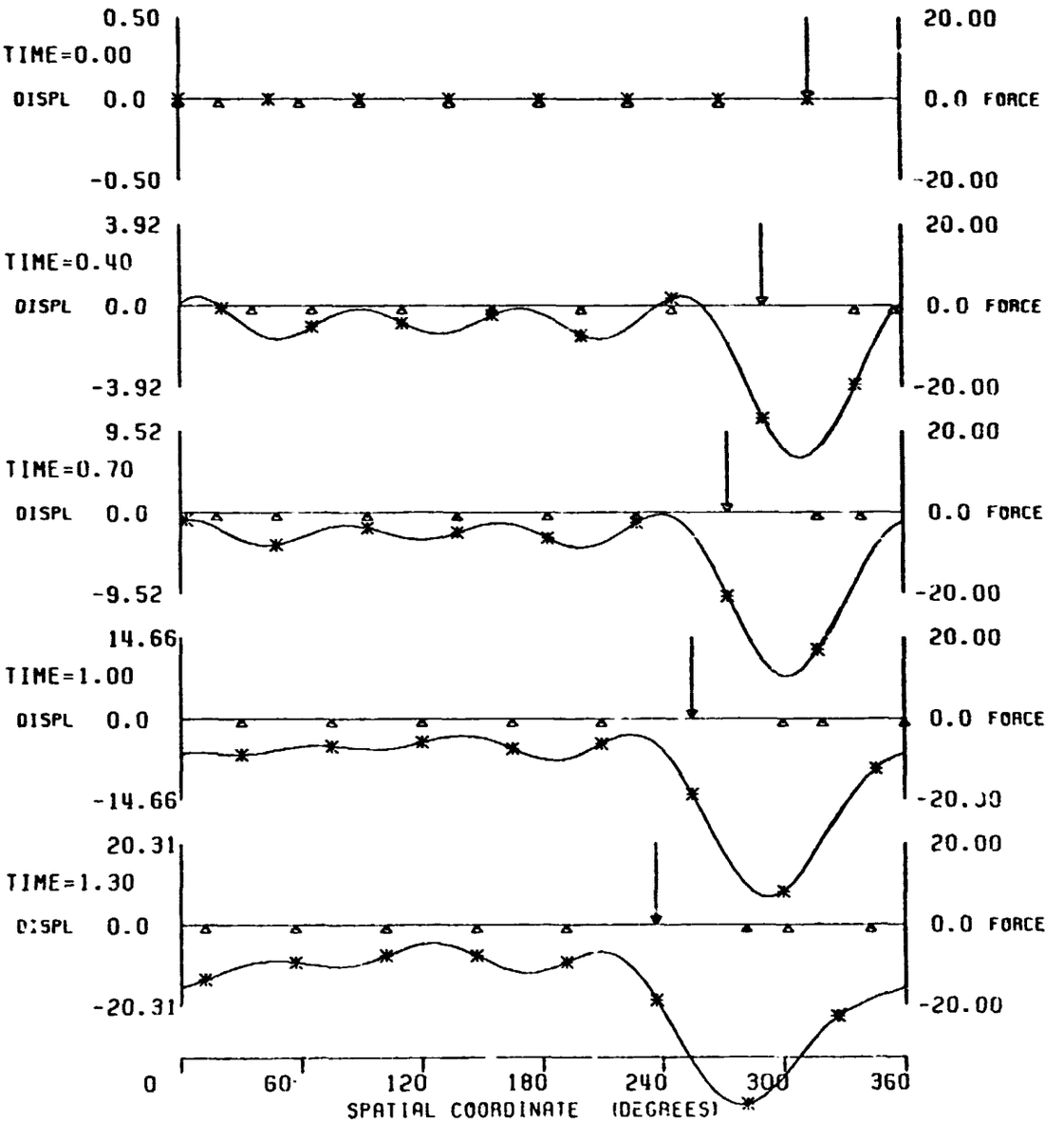

Slide 18

DESIRED DEFORMATION DAMPING

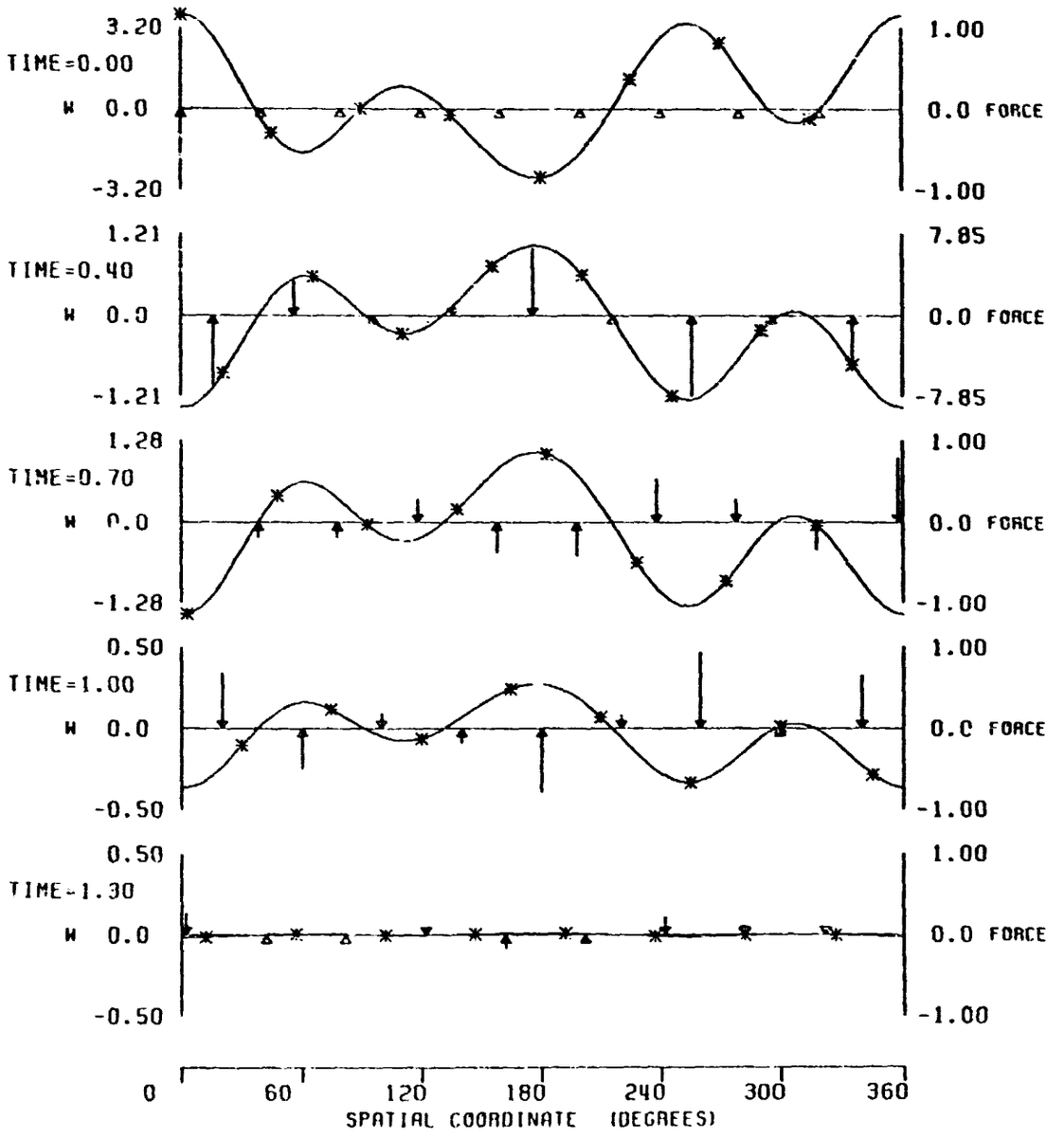

Slide 19

INCORRECT ESTIMATE FIXED CONTROLLER

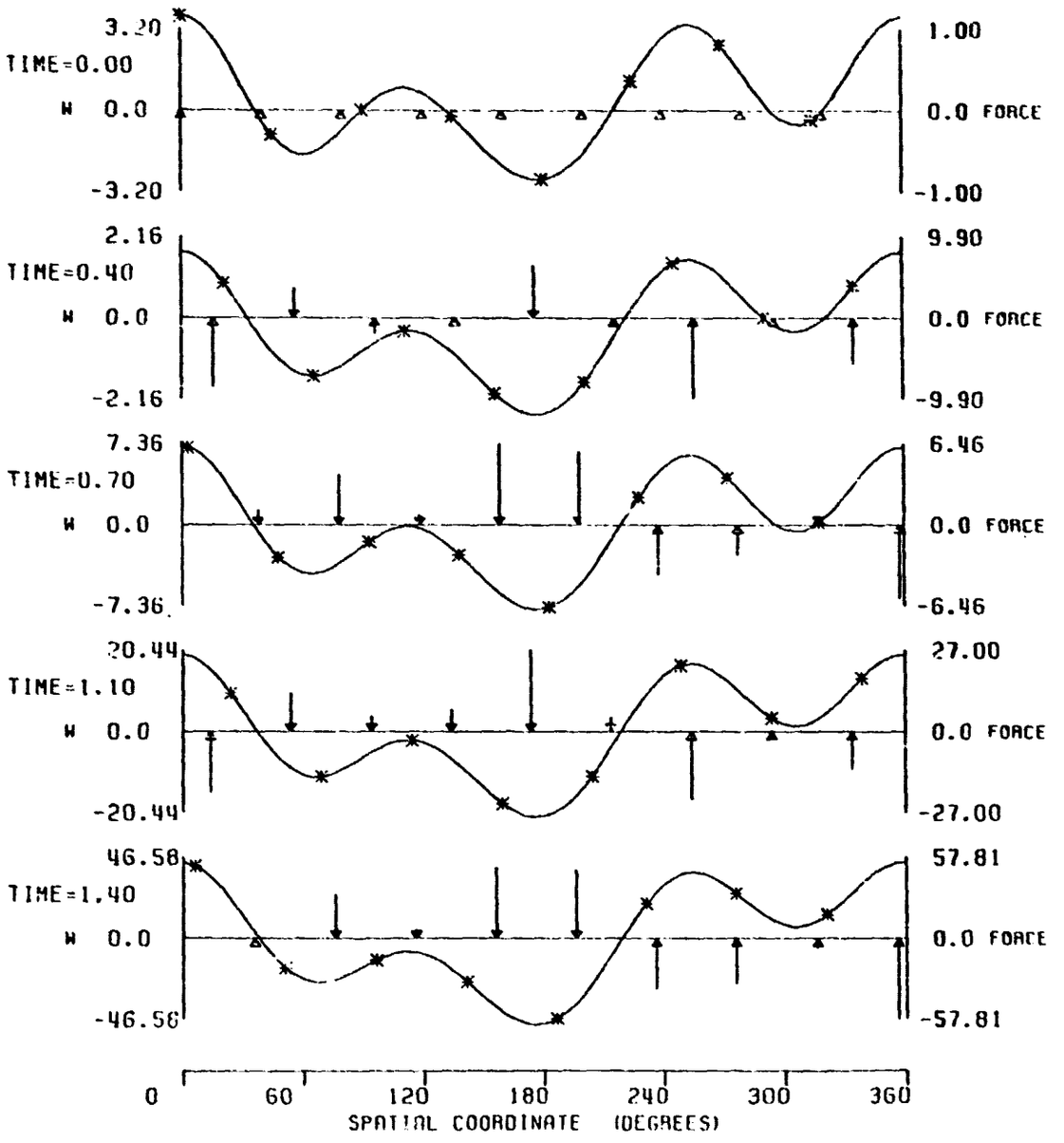

Slide 20

ADAPTION OF UNSTABLE REGULATOR

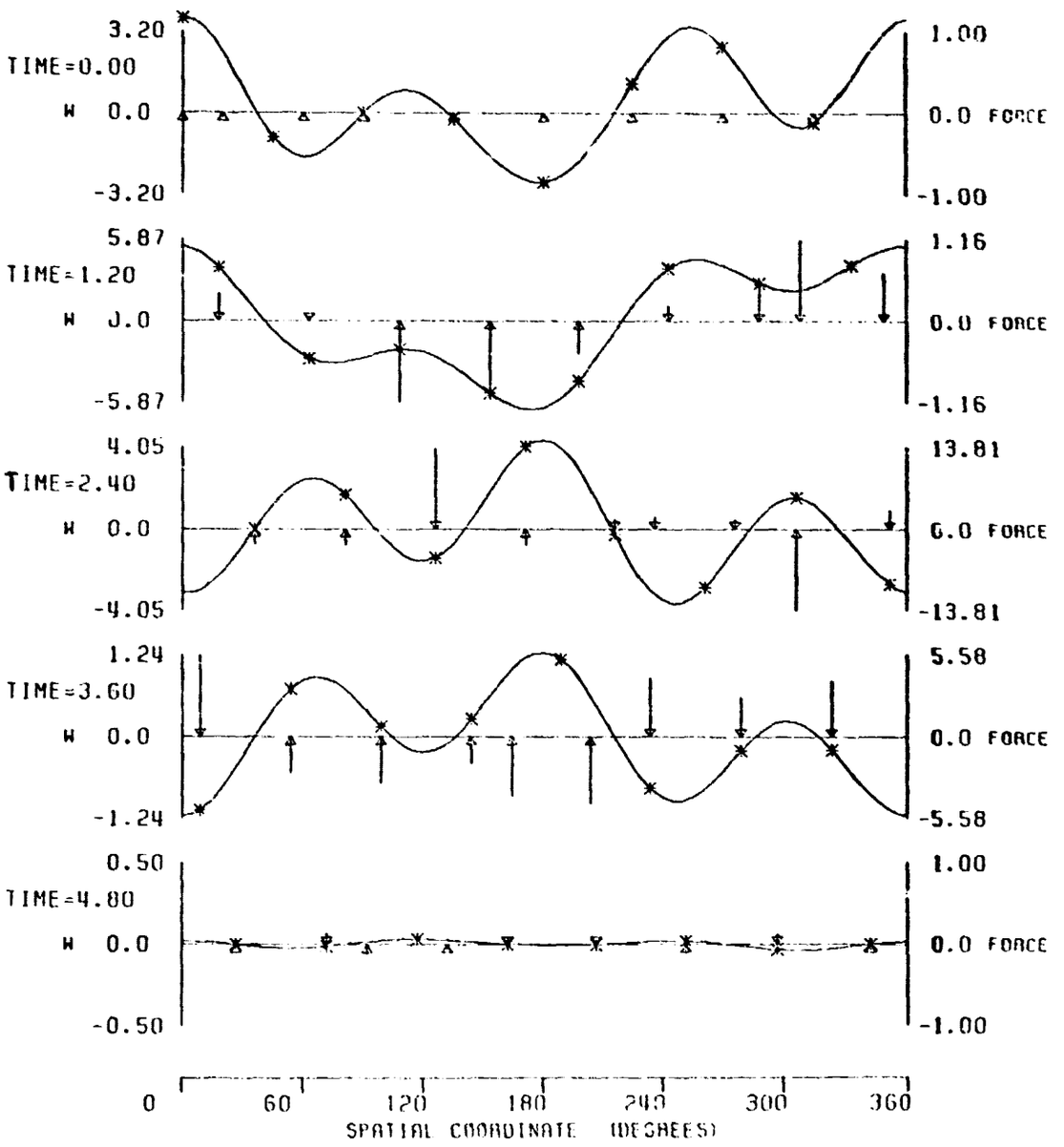

Slide 21

In the area of attitude control, we have considered developing adaptive/learning control system theory for use in handling large space structures. One problem where adaptive/learning theory is needed is in handling of large space objects using the space shuttle. During barging, towing, assembly, and construction operations involving large space structures adequate control requires precise knowledge of the structural dynamics of the objects involved. As indicated in slide 22, this requirement cannot be satisfied using techniques based on analysis or ground testing because of fundamental limitations of these techniques. The adaptive/learning system is conceived on the premise that structural testing must be conducted on the objects involved in the operational space environment. Using in-flight testing, the system identifies parameters of the structures within a class of mission structural models (slide 23). The parameters are used to adjust the control system design to affect acceptable attitude control. Additional tests are required to maintain acceptable attitude control because the dynamics change during operations. The number of such tests is substantially reduced by using model extrapolation based on analysis, thereby conducting tests only when the divergence between the observed dynamics and the model results in unacceptable stability and control margins.

SPACE APPLICATION CONTROL

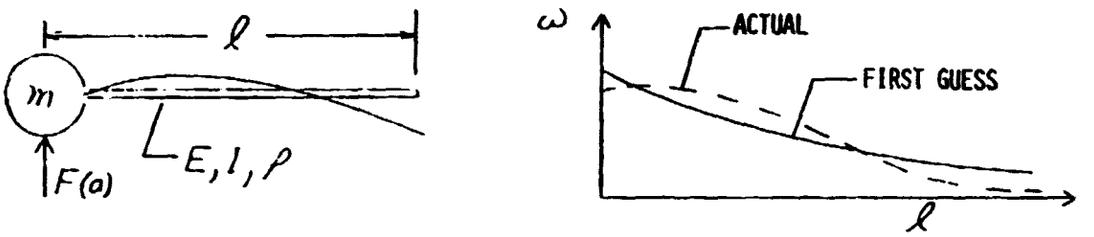

- o PROPER PHASING OF F REQUIRES PRECISE KNOWLEDGE OF THE STRUCTURAL DYNAMICS
- o ADEQUATE ANALYTICAL DEFINITION NOT POSSIBLE FOR COMPLEX STRUCTURES - PROVIDES FIRST GUESS ONLY
- o GROUND TESTING NOT POSSIBLE - GRAVITY, MASS, STIFFNESS CONSIDERATIONS

HENCE: TESTING DURING FLIGHT OF THE ARTICLE TO BE CONTROLLED IS THE ONLY METHOD TO OBTAIN THE REQUIRED STRUCTURAL DYNAMICS KNOWLEDGE

Slide 22

LEARNING SYSTEM DESCRIPTION
(SPACE APPLICATION)

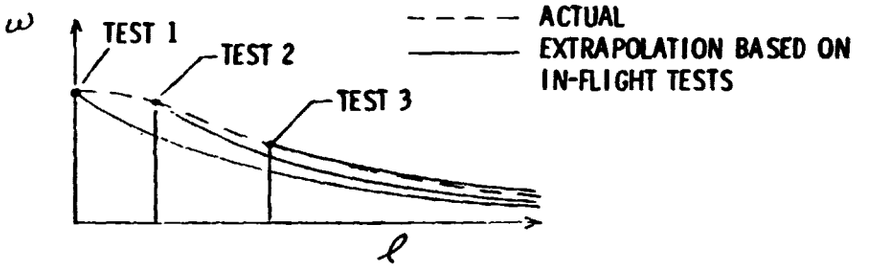

- o AUTOMATICALLY CONDUCTS IN-FLIGHT TESTS WHEN CONFIDENCE IN STRUCTURAL DYNAMICS DEFINITION PRODUCES UNACCEPTABLE STABILITY AND CONTROL MARGINS
- o ADAPTS TO CHANGES IN ORBITAL, MASS, INERTIA, AND FLEXIBILITY CHARACTERISTICS USING GAIN SCHEDULING BASED ON EXTRAPOLATION

Slide 23

The adaptive/learning system important features are listed on slide 24. The system is being developed using an analytical model of the SEP array. The model was created using a finite element model and the SPAR computer program (slide 25).

LEARNING SYSTEM FEATURES

- In-flight definition of structural dynamics
- Optimal decision theory used to initialize testing and adjust feedback law
- Optimal tolerance to control system sensor/actuator failures using analytical redundancy
- "Dither" signal inputs needed for adaptive control are suppressed during operations for which they are not compatible
- Gain scheduling provides adaptation in absence of "dither" inputs based on extrapolation

Slide 24

SEP SPAR MODEL TOP OF SEP

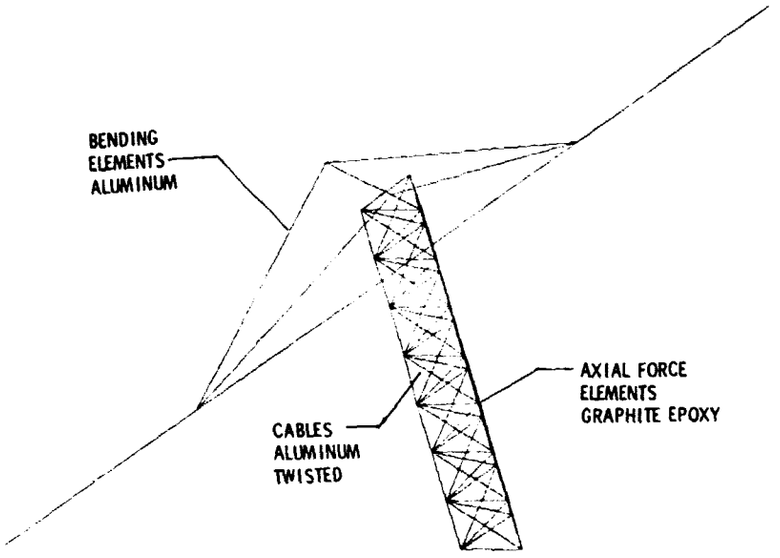

Slide 25

The sensing concept assumed in the adaptive/learning system is a remote sensing concept being studied at LaRC where TV cameras are used in conjunction with a spot pattern on the array. Slide 26 shows the location of the cameras in the shuttle payload bay and the SEP array inclined on angle θ with the shuttle center line. Slide 27 shows the array spot pattern that is used in a simulation program to develop adaptive/learning control schemes.

SEP/SHUTTLE - SENSOR CAMERAS

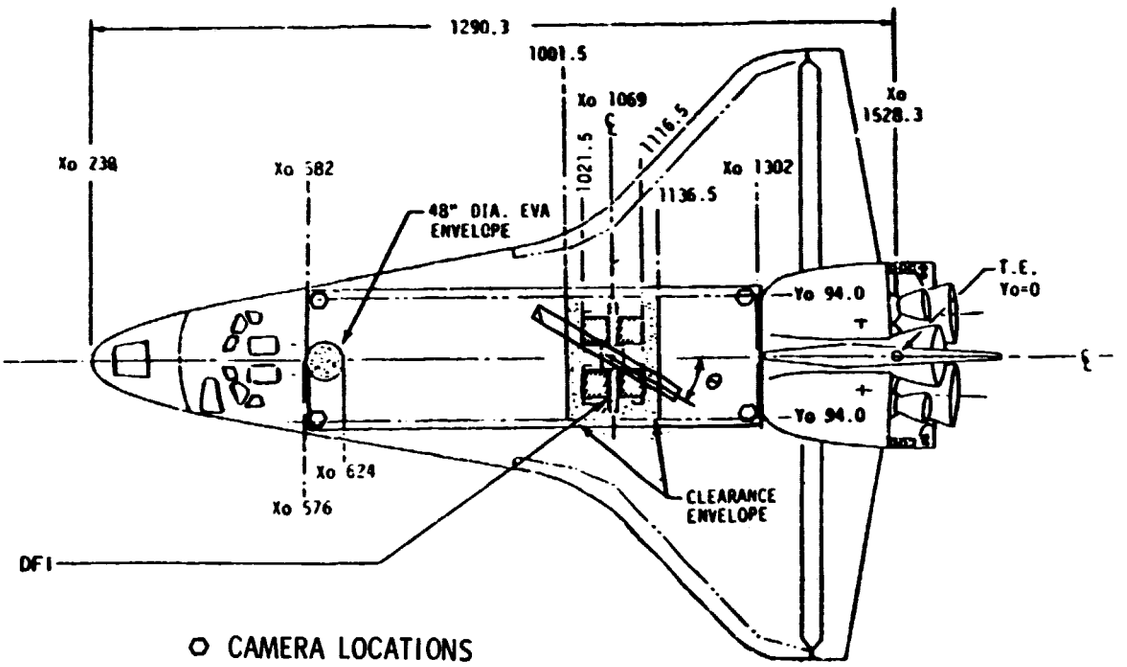

○ CAMERA LOCATIONS

Slide 26

SEP/SHUTTLE - SENSOR-SPOTS

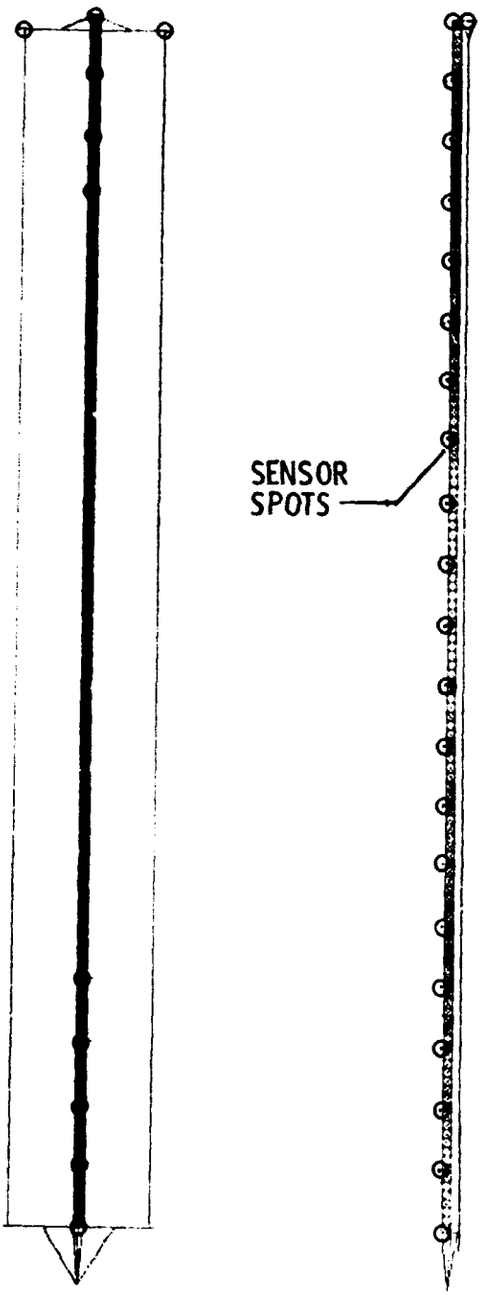

Slide 27

N80-19166

D21

INTERACTIVE ANALYSIS PROGRAM ACTIVITY

J. P. Young, H. P. Frisch, and G. K. Jones
NASA Goddard Space Flight Center

W. J. Walker
Boeing Aerospace Company

LSST 1ST ANNUAL TECHNICAL REVIEW

November 7-8, 1979

PAGE 382 INTENTIONALLY BLANK

OVERVIEW

J. P. Young

INTERACTIVE ANALYSIS PROGRAM ACTIVITY

In order to produce meaningful, alternative large space structure preliminary configurations, designers must have highly flexible and efficient computer codes to evaluate critical interactive effects. These interactive effects arise from the varied parameters of physical plant performance, environments, and forcing functions associated with disciplines such as thermal, structures, and controls. Adverse effects can be expected to significantly impact system design aspects such as loads, structural integrity, controllability, and mission performance. The end product analysis system is conceived to be an integration of individual discipline computer codes into a highly user oriented/interactive graphics based analysis capability. This integration of computer codes must be done in a manner that will greatly accelerate interdisciplinary data flow by maximizing use of modern data base management techniques. By providing computer assisted interdisciplinary preliminary design analysis capability, the designer will be afforded a rapid and efficient system to minimize solution turnaround time.

INTERACTIVE ANALYSIS PROGRAM ACTIVITY

- OVERALL OBJECTIVE

  PRODUCE AN ANALYSIS SOFTWARE SYSTEM CAPABLE OF PERFORMING INTERDISCIPLINARY PRELIMINARY DESIGN ANALYSES OF LARGE SPACE SYSTEMS. DISCIPLINES SUCH AS THERMAL, STRUCTURES, AND CONTROLS ARE TO BE INTEGRATED INTO A HIGHLY USER ORIENTED ANALYSIS CAPABILITY. THE KEY FEATURE OF THE INTEGRATED ANALYSIS CAPABILITY IS TO BE A RAPID AND EFFICIENT SYSTEM THAT WILL MINIMIZE SOLUTION TURNAROUND TIME.

- SPECIFIC GOAL

  HAVE OPERATIONAL INTEGRATED ANALYSIS CAPABILITY (IAC) FUNCTIONING BY END OF FY83

INTERACTIVE ANALYSIS PROGRAM ACTIVITY

In FY79 there was both in-house (GSFC) and contractor activities (Boeing Aerospace Co.). The in-house activities centered around tasks that will provide technical information/analysis techniques to feed into the major contractor activity. In the thermal and structural discipline areas, there is the critical need to identify the individual analysis codes that best match the requirements imposed by an integrated analysis system. In addition, a somewhat new approach to thermal analysis, based on the modal solution techniques, is to be assessed for practical usage. Since no general technique existed for the linearization of sampled data control systems, considerable in-house effort has been devoted to developing this capability. In the systems area, a significant in-house accomplishment has been the development of a general theory for mathematically simulating the coupling of thermal loads into the system dynamics.

A two-phase contract was awarded to Boeing Aerospace Co. in June 1979, for the development of an operational integrated analysis capability. The Phase I effort (10 months performance period) is to produce a detailed development plan and a pilot analysis program designed to demonstrate proof of concept. The Phase II effort is to produce the actual operational software system.

INTERACTIVE ANALYSIS PROGRAM ACTIVITY

IN-HOUSE (GSFC) ACTIVITY

- THERMAL
  - EVALUATE SUITABILITY OF NASTRAN VS. SINDA VS. SPAR
  - ASSESS PRACTICAL LIMITS ON USE OF MODAL SOLUTION TECHNIQUE
- STRUCTURES
  - EVALUATE NASTRAN VS. SPAR VS. SAP-VI
- CONTROLS
  - DEVELOP LINEARIZATION TECHNIQUE FOR SAMPLED DATA CONTROL SYSTEMS
- SYSTEMS
  - DEVELOP GENERAL THEORY FOR COUPLING THERMAL LOADS INTO SYSTEM DYNAMICS

CONTRACTOR ACTIVITY

- TWO PHASE EFFORT WITH END PRODUCT TO BE AN OPERATIONAL INTEGRATED ANALYSIS CAPABILITY
- PHASE I AWARDED TO BOEING AEROSPACE CO. JUNE 79, (10 MONTHS PROGRAM)

CONCEPT OF IAC ARCHITECTURE

In a simplified fashion, the current concept of the IAC system architecture can be represented by the block diagram shown below. As stated earlier, the system is to be highly user oriented and have very efficient interdisciplinary data flow properties. The keys to making this possible are a powerful, yet flexible, data base management system and a highly user oriented executive command/query language and interactive graphics. Not only must the system perform the engineering calculations via the application programs but it must also be designed to efficiently manage, control, and manipulate all the data, input or generated, from the most primitive level to the highest level. This system by itself cannot miraculously solve all the human factor problems associated with interdisciplinary communication and data exchange. The goal is to produce a logical framework that will make this communication much less painful and actually give the practitioners an incentive to interrelate more directly.

The specific application programs shown in the diagram in parentheses are mainly for example purposes only. Final selection will not occur until after start of the Phase II activity.

CONCEPT OF IAC ARCHITECTURE

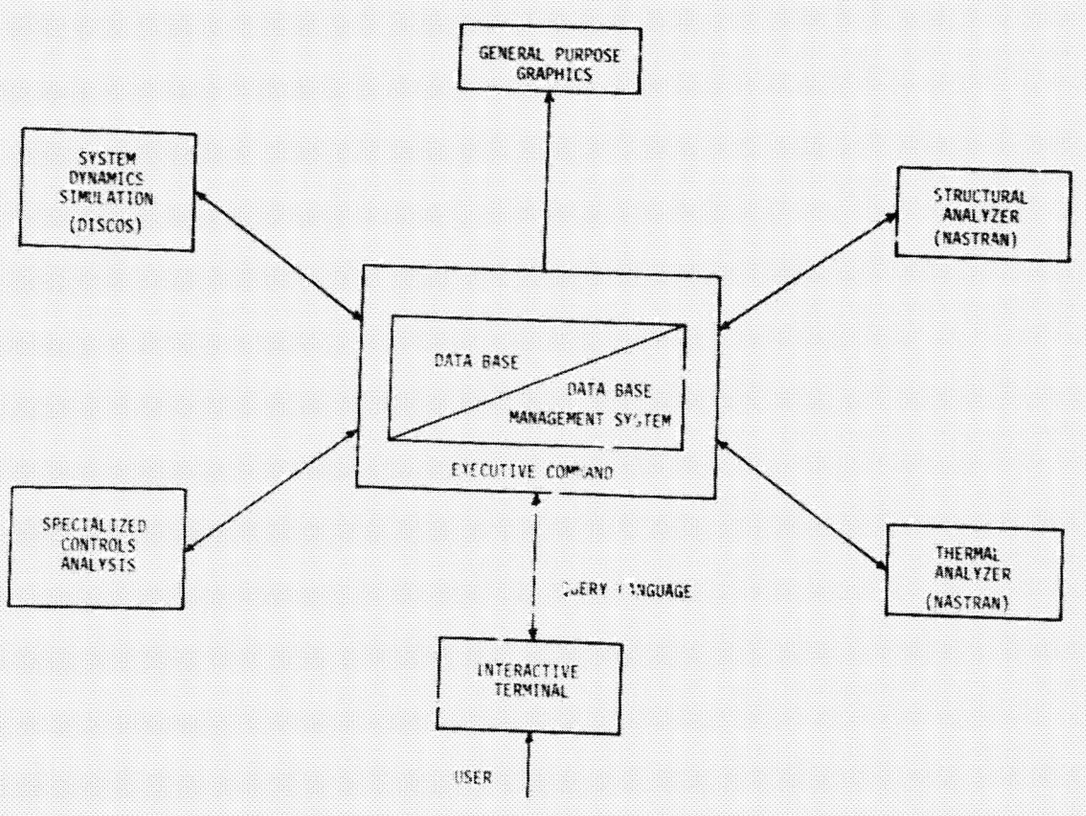

DEVELOPMENT OF SYSTEM DYNAMICS ANALYSIS METHODS

H. P. Frisch

DISCOS PROGRAM IMPROVEMENT ACTIVITY

As shown earlier in the IAC system concept block diagram, DISCOS is designated as a candidate application program to perform the system dynamics analytical simulation. DISCOS basically derives and sets up the computer code necessary to define the plant equations. The user, via FORTRAN code, defines all non-gyroscopic control and environmental loads on the system. DISCOS is structured so as to provide the user with a clean interface between the plant, the controller, and the environment. This clean interface, along with several special interface subroutines, help to minimize the problem associated with non-gyroscopic load definition.

DISCOS PROGRAM IMPROVEMENT ACTIVITY

DYNAMIC INTERACTION SIMULATION OF CONTROLS AND STRUCTURE

MOTIVATION: THE KEY TO BUILDING USEFUL SIMULATION MODELS IS TO MAKE THEM AS SIMPLE AS POSSIBLE. EXCESS DETAIL TENDS TO CONFUSE RATHER THAN CLARIFY.

NEED: A CAPABILITY TO RAPIDLY AND RELIABLY SET UP THE UNABRIDGED EQUATIONS OF MOTION FOR IDEALIZED SPACECRAFT SIMULATION MODELS.

SIMULATION MODELS: FOR CONTROLS RELATED STUDIES SPACECRAFT CAN NORMALLY BE MODELLED AS A SYSTEM OF COUPLED RIGID AND FLEXIBLE BODIES.

DISCOS PROGRAM IMPROVEMENT ACTIVITY

Obviously a full DISCOS capability should not be used for the single rigid or a single flexible body model.

Coupled body problems conceptually look very simple and in most cases they are reasonably easy to understand; however, the derivation and computer implementation of the complete set of coupled non-linear equations of motion, accounting for all gyroscopic effects, can be extremely difficult to obtain and debug.

The DISCOS user need worry only about correctly setting up the input deck to define the problem. The equation derivation and computer implementation portion of the problem has already been taken care of by DISCOS.

COARSE ATTITUDE AND POSITION CONTROL

FINE ATTITUDE AND POSITION CONTROL

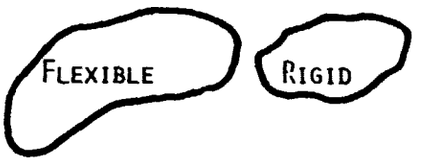

CONTROL DURING CONSTRUCTION OR DOCKING

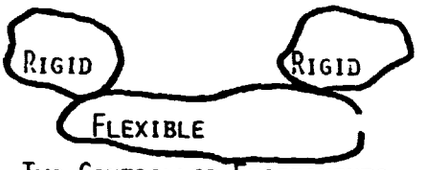

TWO CONTROLLED EXPERIMENTS, COUPLING THROUGH SYSTEM FLEXIBILITY

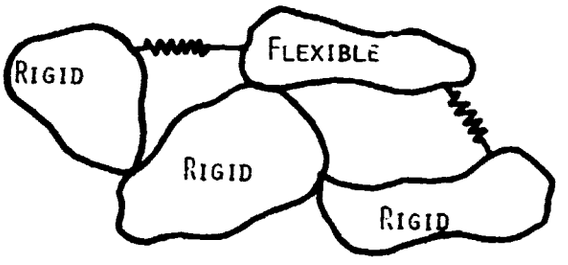

DEPLOYMENT AND SHAPE CONTROL

USE DISCOS--TO AUTOMATICALLY DERIVE AND NUMERICALLY SOLVE THE EQUATIONS OF MOTION FOR THE CONTROLLED COUPLED BODY SYSTEM

DISCOS PROGRAM IMPROVEMENT ACTIVITY

Simulation models are structured with a dual purpose in mind:

1) Expose potential problem areas

2) Provide the engineer with sufficient insight into the problem so that a "fix" can be implemented

Excess detail usually will not hinder the exposure of a problem; however it usually will mask the true cause of the problem.

Coupled rigid-flexible body models, using a minimal number of flexible body modes, are usually adequate for most controls/structure interaction problems.

DISCOS

MODELLING CAPABILITY

- o ARBITRARY NUMBER OF BODIES
- o ANY OR ALL MAY BE FLEXIBLE
- o RELATIVE DEGREES OF FREEDOM MAY BE
  - --KINEMATICALLY FREE
  - --KINEMATICALLY FIXED
  - --CONSTRAINED BY SPRINGS DAMPERS AND/OR MOTORS
  - --DEFINED BY AN APRIORI FUNCTION OF TIME
- o TOPOLOGICAL LOOPS ALLOWED
- o ARBITRARY CONTROL SYSTEM ALLOWED
- o ENVIRONMENTAL LOADS ALLOWED
- o FORCES AND TORQUES MAY BE APPLIED ANYWHERE
  - --DISCRETE LOADS ALLOWED
  - --DISTRIBUTED LOADS ALLOWED

DISCOS PROGRAM IMPROVEMENT ACTIVITY

As presently structured the controller can be defined by an arbitrary set of non-linear logical, algebraic and ordinary differential equations. The linearization procedure is numerical and will not work correctly if the equations cannot be linearized in the continuous time domain. Special techniques, under development, are required for the linearization of sampled data control equations.

DISCOS

ANALYSIS CAPABILITY

- COMPLETE NON-LINEAR TIME DOMAIN SIMULATION
- NUMERICALLY LINEARIZE EQUATIONS OF MOTION

  $\dot{X} = \underline{A}X$

  --IF CONTROLLER IS CONTINUOUS (ANALOG)– PLANT + CONTROL EQUATIONS LINEARIZED

  --IF CONTROLLER IS SAMPLED DATA SYSTEM - ONLY PLANT EQUATIONS LINEARIZED
- FREQUENCY DOMAIN ANALYSIS CAPABILITY

  IF CONTROLLER CONTINUOUS THEN FOR ANY DESIRED SENSOR-ACTUATOR RATIO

  --OPEN LOOP TRANSFER FUNCTIONS SET UP

  --CLOSED LOOP TRANSFER FUNCTIONS SET UP

  --QUASI-OPEN LOOP TRANSFER FUNCTIONS SET UP

  ANALYZED BY

  --BODE

  --NICHOLOS

  --NYQUIST

  --ROOT LOCUS

DISCOS PROGRAM IMPROVEMENT ACTIVITY

Eigenanalysis numerical methods have advanced significantly in the past 5 years. These advances have been incorporated to gain an added measure of numerical error control in the frequency domain analysis section of DISCOS.

Control/structure interaction analysis during orbit adjust requires motion to be measured relative to an acceleration reference to avoid numerical problems.

Last 3 items go together. This capability is essential for docking and appendage deployment problems. It is extremely difficult to implement since proper implementation requires information about the future before it can be computed. The new integration method provides a second order estimate of this future data halfway through the full integration cycle. This permits the proper set up of latching/unlatching logic. The need to conserve momentum during latch/unlatch leads to the last item. Numerical changes in momentum are error; if viewed as a known impulse it can be cancelled by applying an equal and opposite effect.

DISCOS

CAPABILITIES IMPLEMENTED FY79

- NEW STATE-OF-THE-ART NUMERICAL METHODS INCORPORATED IN FREQUENCY DOMAIN ANALYSIS SECTION
- MOTION NOW COMPUTABLE RELATIVE TO AN ACCELERATING FRAME OF REFERENCE
- DEGREES OF FREEDOM MAY BE LATCHED AND UNLATCHED DURING SIMULATION
- NEW INTEGRATION ROUTINE DEVELOPED TO ACCOMMODATE LATCHING/UNLATCHING NEEDS
- ADDITIONAL COMPUTATIONAL ERROR CONTROL LOGIC DEVELOPED FOR COMPUTATION OF GYROSCOPIC CROSS COUPLING EFFECTS

NEW SAMPLED DATA CONTROL ANALYSIS METHOD

Non-linear time domain analysis of a plant subject to a sampled data control can normally be handled without approaching insurmountable numerical or theoretical problems.

The real problems are associated with attempting tc perform a frequency domain stability analysis. Current techniques that are known rapidly become computationally impractical, or theoretically deficient, as one is forced to incorporate multi-rate sampling, many zero order holds of different time duration and several different digital delays.

NEW SAMPLED DATA CONTROL ANALYSIS METHOD

PROBLEM: ZERO ORDER HOLDS AND DIGITAL DELAYS ARE NON-LINEAR ELEMENTS IN THE CONTINUOUS TIME DOMAIN. USUALLY THESE CANNOT BE READILY LINEARIZED

SOLUTION: DEVELOP AN ANALYSIS METHOD WHICH VIEWS THEM AS LINEAR ELEMENTS

METHOD: INTRODUCE THE CONCEPT OF A SET OF LINEAR MIXED OPERATION EQUATIONS

NEW SAMPLED DATA CONTROL ANALYSIS METHOD

Presented here is only the fundamental essence of the method. We first must view the meaning of the dot in the topmost figure. The dot simply says that given an initial state for X and a definition of the function X, then if the mathematical rules of integration are used, the value of X can be obtained for any future time. We now view the use of box in the next figure in the same manner. The box simply says that given an initial state for Y and a definition of the function Y, then if the mathematical rules for zero order hold are used, the value of Y can be obtained for any future time. An analogous statement follows for the use of triangle in the last figure. It is claimed that any linear sampled data control system can be expressed as a set of linear mixed operation equations as shown. Specifically note the zero in the 3,1 slot. Delay of a continuous signal is prohibited. We view the associated computational cost as not being worth the effort.

Next, a periodic pattern of sampling must be assumed. Without this assumption linear stability analysis is not possible. From this point on, the computer takes over to compute the elements of the coefficient matrix associated with the linear finite difference equation shown. This is done by a direct implementation of the mathematical rules of integration, zero order hold and delay. The period implied is that of the periodic pattern of sampling. This is, in effect, the end of the new method since this equation format is compatible with standard Z-domain (frequency domain) stability analysis methods.

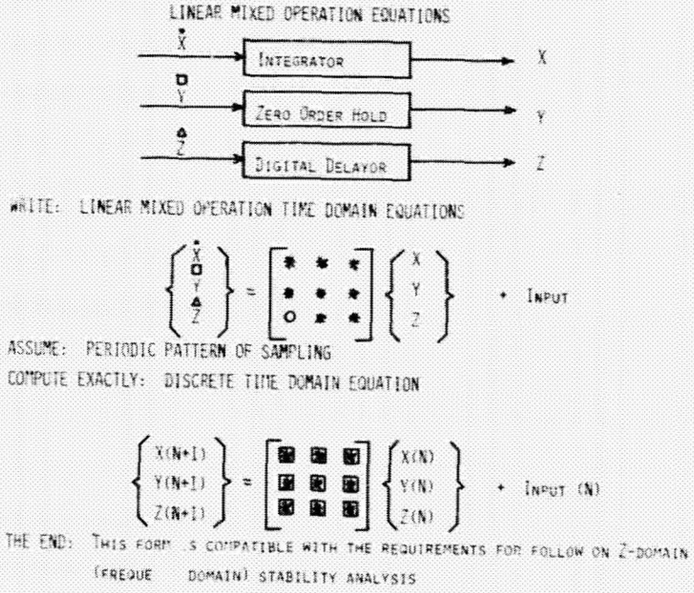

NEW ANALYSIS METHOD FOR THERMALLY INDUCED MOTION

If finite element methods are used to define flexibility, then eventually one arrives at the equation shown and an associated set of vibration modes and natural frequencies. If either finite element or finite difference methods are used for linear thermal analysis then eventually one arrives at the thermal equation shown. This too is amenable to eigenanalysis methods and a set of thermal modes and natural thermal decay time constants can be obtained. Thermal modes define temperature patterns just as vibration modes define displacement shapes. Natural thermal decay time constants define how quickly a temperature pattern would decay to a mean value if the system was placed in a block box, just as natural frequencies define the vibration frequency associated with a particular vibration mode.

The trick to solving the thermally induced motion equation shown is to compute a thermally deformed shape associated with each thermal mode pattern and then to express each of these shapes as linear functions of the vibration modes. From this point more or less standard methods for arriving at generalized displacement and thermal coordinate equations via orthogonality relations are used. The resultant equations blend perfectly with the DISCOS program capabilities. A detail definition of the theory is scheduled for publication in the AIAA Journal of Guidance and Control January-February 1980. The title of the paper is "Thermally Induced Response of Flexible Structures, a Method for Analysis."

NEW ANALYSIS METHOD FOR THERMALLY INDUCED MOTION

BASIC CONCEPTS USED:

- STRUCTURES
  $M\ddot{X} + KX = 0$ — VIBRATION MODES, NATURAL FREQUENCIES
- THERMAL
  $C\dot{T} + DT = 0$ — THERMAL MODES, THERMAL DECAY TIME CONSTANTS
- THERMALLY INDUCED MOTION
  $M\ddot{X} + K(X-X_T) = 0$
  X_T = INSTANTANEOUS POSITION OF THERMAL EQUILIBRIUM
- SOLVED VIA USE OF VIBRATION AND THERMAL MODES
- EQUATIONS THAT DEFINE X_T VIEWED AS CONTROL EQUATIONS TO BLEND WITH DISCOS CAPABILITY
- PAPER TO BE PUBLISHED IN THE JANUARY-FEBRUARY 1980 ISSUE OF THE AIAA JOURNAL OF GUIDANCE AND CONTROL

EVALUATION OF CANDIDATE ANALYSIS CODES

G. K. Jones

ACCOMPLISHMENTS FY79

A VAX 11/730 version of SPAR was developed using as its basis the NASA PRIME version of SPAR. The major tasks were the development of new I/O routines for use with the VAX 11/780 computer and to restructure the code to make it compatible with the VAX data formats. The resulting code is all FORTRAN and makes maximum use of VAX virtual memory system to speed I/O operations.

Four dynamics analyses problems have been defined and three of these problems have been executed on both SPAR and NASTRAN (MSC 52 on VAX). The problems consisted of finding the free-free modes of various size space frame platform models. This class of structure (platform) was selected based on a review of potential LSST structural systems. Modal analyses was selected based on the fact that being able to define the structural modes is essential to the performance of coupled controls-structure analyses. Based on these analyses preliminary observations have been reached as to the relative merits of SPAR and NASTRAN.

LSST TECHNICAL REVIEW
INTERACTIVE ANALYSIS PROGRAM

ACCOMPLISHMENTS FY79

- o VAX 11/780 VERSION OF SPAR DEVELOPED
- o FOUR MODAL ANALYSES PROBLEMS DEFINED
- o THREE OF FOUR PROBLEM EXECUTED ON VAX USING SPAR AND NASTRAN (MSC-52)
- o PRELIMINARY OBSERVATIONS

CANDIDATE STRUCTURAL ANALYSIS CODES

The NASTRAN, SPAR, and SAP VI analysis codes were selected as candidates due to their use within NASA and or the aerospace community. Both NASTRAN and SPAR codes are available through COSMIC and commerical variants of all three codes exist. The NASTRAN program was originally developed by NASA and is a very complex (~300,000 lines of code), but versatile code. It is the most widely used structural analysis code. The other codes SPAR and SAP VI are less complex (~40,000 lines of code) and are not as widely used as NASTRAN. But since they were developed after NASTRAN they incorporate more advanced features in certain areas.

The three codes suitability for use in an interdisciplinary analysis system is being investigated. Of particular concern is how well each codes' would function in an integrated interdisciplinary analysis system. Other factors being assessed are the codes' ability to handle large problem dynamics analyses, their ease of usage, and their documentation.

LSST TECHNICAL REVIEW

INTERACTIVE ANALYSIS PROGRAM

CANDIDATE STRUCTURAL ANALYSIS CODES

CODES:

1. NASTRAN
2. SPAR
3. SAP VI

COMPARISON FACTORS:

- o SUITABILITY FOR USE IN INTERDISCIPLINARY ANALYSIS SYSTEM
- o LARGE PROBLEM ANALYSIS
- o EASE OF USAGE
- o DOCUMENTATION

MODEL C

Four platform models were developed (Models A through D), progressively increasing in size. The smallest model had 8 grid points and the largest model had 500 grid points. Model C is the next to the largest and consists of 200 grid points and about 800 elements. It represents a 500 feet by 500 feet square space frame platform with a thickness of 50 feet. The other models differ from MODEL C only in complexity. The SPAR models were generated using the mesh generators in SPAR; the NASTRAN models were generated using the MOVE preprocessor program.

LSST TECHNICAL REVIEW
INTERACTIVE ANALYSIS PROGRAM

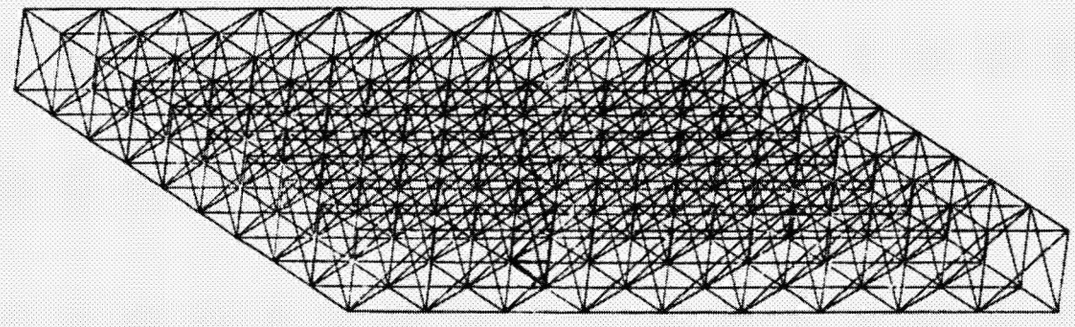

LSST PLATFORM-MODEL C

SPAR-NASTRAN PERFORMANCE

The analysis problems consisted of computing the first 10 to 12 free-free modes of the various platform models. Results for the three smaller models have been obtained. The SPAR run times were about the same as that for NASTRAN when the GIVENS-QR eigenvalue technique was selected in NASTRAN. The INVERSE method in NASTRAN ran substantially slower than the other methods. SPAR appears to use less physical memory than NASTRAN but further investigation is needed to confirm this fact. The input to the SPAR program was much more compact than the NASTRAN input. The NASTRAN rigid format feature is easy to use but lacks the flexibility of the SPAR command language which is also easy to use.

LSST TECHNICAL REVIEW
INTERACTIVE ANALYSIS PROGRAM

SPAR-NASTRAN PERFORMANCE

		SPAR		NASTRAN	
MODEL	DOF	CPU TIME (MIN)	MEMORY (BYTES)	CPU TIME (MIN)	MEMORY (BYTES)
A	48	0.57	100K	1.12(I)	200K
B	108	1.20	124K	2.93(I) 1.03(G)	250K
C	1200	21.2	175K	38.9(I) 21.8(G)	750K 300K

I=INVERSE
G=GIVENS-QR

PRELIMINARY OBSERVATIONS

One tentative conclusion based on the work performed to date is that for modal analysis the performance of SPAR (VAX version) and MSC52 NASTRAN are comparable. SPAR's strong points are that it is easy to use, has compact input, has a built in data base and a simple program structure. This last point is important in that it means that new features can be added to SPAR much more easily than to NASTRAN. The SPAR weak points are its poor documentation, no MPC capability and only one eigenvalue method. In addition the SPAR eigenvalue method was found to be very sensitive to the value of shift parameter selected. More than one run was usually required to find the desired eigenvalues. NASTRAN's strong points are its documentation, MPC capability and its reduction technique. The problem with NASTRAN is that it is a complex code that is difficult to modify and requires a large amount of input. NASTRAN (MSC-52) has two useful eigenvalue techniques (GIVENS-QR, INVERSE) but they are not without their problems either. The GIVENS-QR method when coupled with an appropriate reduction is fast but sometimes has trouble getting good rigid body modes. The INVERSE method exhibits a set of problems similar to the SPAR technique.

LSST TECHNICAL REVIEW

INTERACTIVE ANALYSIS PROGRAM

PRELIMINARY OBSERVATIONS

- SPAR-NASTRAN HAVE ABOUT SAME SOLUTION SPEED PERFORMANCE
- WEAK POINTS
  SPAR--DOCUMENTATION, EIGENVALUE, LACK OF MPC OR REDUCTION TECHNIQUE
  NASTRAN--COMPLEX INPUT, COMPLEX CODE, DATA BASE
- STRONG POINTS
  SPAR--DATA BASE, EASY TO USE, COMPACT INPUT, COMPACT CODE
  NASTRAN--DOCUMENTATION, MPC, REDUCTION TECHNIQUE

THERMAL ANALYSIS COMPUTER CODE ACTIVITY

The SINDA program represents the leading candidate of the "traditional" finite difference type thermal analyzers, whereas NASTRAN and SPAR are of the finite element variety. A comparative evaluation is to be made to accurately document the relative performance capabilities and suitability for incorporation into an integrated analysis environment. The CAVE-3 program, developed by Grumman Aerospace Co. for LaRC, is the only known aerospace oriented program designed to perform thermal analyses via the modal solution method. This program is to be utilized to solve a number of demonstration problems to assess what limitations and usage criteria can be expected when using a modal solution approach.

THERMAL ANALYSIS COMPUTER CODE ACTIVITY

- NASTRAN (MSC-52) INSTALLED ON VAX 11/780, DEMONSTRATION PROBLEMS RUN
- SINDA INSTALLED ON VAX 11/780, DEMONSTRATION PROBLEMS RUN
- SPAR THERMAL ANALYZER PROCESSORS CONVERTED AND INSTALLED ON VAX 11/780
- CAVE-3 MODAL SOLUTION BASED ANALYZER INDENTIFIED AND OBTAINED FROM GAC, INSTALLED ON IBM 360/91, DEMONSTRATION PROBLEMS RUN

DEVELOPMENT OF INTEGRATED ANALYSIS CAPABILITY SYSTEM

W. J. Walker

PROGRAM STATUS

The Integrated Analysis Capability for Large Space Systems is funded under Contract NAS5-25767 by the Goddard Space Flight Center. Mr. J. P. Young of GSFC is the Contract Technical Officer. The current contract is for Phase I of a two-phase effort with Phase II being a pre-negotiated option exercisable by GSFC. Phase I started on June 28, 1979 and continues for a 10-month period. The Statement of Work for Phase I specifies two tasks. The first is to develop a detailed plan for the Integrated Analysis Capability (IAC) computer code. The intent is then to implement this development plan during Phase II. This plan will identify the technical modules to be used with the IAC, its database system and its interactive capability. In addition, a pilot analysis code will be utilized to demonstrate the concepts planned for the IAC. All computer work during Phase I of this effort will be done on the DEC VAX 11/780 machine and use Tektronix's graphics hardware.

Program Status

Contract NAS5-25767

Starting date: June 28, 1979

Duration of phase I: 10 months

Phase I:

Task 1—Generate a detailed development plan for the IAC

Task 2—Produce a simplified pilot analysis code

IAC - CAPABLE OF PERFORMING

The IAC has as its goal the capability of performing the indicated analyses for the conceptual/preliminary design of large space structures. The statements shown describe the necessary technical data flow between the disciplines planned for the IAC; Thermal, Structural and Controls. By Structural is meant both the strength and vibratory considerations as well as the overall system dynamics behavior of a large space system. This capability involves implementing a number of individual computer modules and insuring the interdisciplinary data flow. Depending on the exact configuration of the structural system under study and its level of maturity the analysts can select the appropriate solution. It is felt that this IAC capability encompasses the major anticipated structural needs of the precision/shaped surface structures, low stiffness planar substructures and high stiffness truss structure contained within the large space structures mission model.

IAC—Capable of Performing

- Thermal/structural analysis in a standalone mode
- Thermal/structural coupled analysis in a sequential mode
- Structural/control system coupled analysis
- Quasi-static thermal/structural/control system coupled analysis
- Fully coupled thermal/structural/control system analysis

INTERACTIVE DATA HANDLING

The IAC will provide to the analyst an extensive capability to interactively investigate the behavior of LSS. This is envisioned as occurring within two classes of activity. First, the user interacting with the database in terms of updating existing models in the system and secondly, the user interacting with the data from previous analysis executions in either a query mode or a graphics mode of operations. This activity will involve both the database management system and the database per se. Also, the IAC system will provide an executive system to control the IAC modules and to interact with each module during execution as is necessary. The software development planned for the IAC Interactive Capability must necessarily consider the hardware system. Currently, the computer interactive terminal technology is rapidly changing with vendors developing new products annually. Due to this state of affairs the decision with respect to which interactive terminal hardware systems to use will be postponed as long as possible. For the pilot code, however, Tektronix terminals will be utilized. All graphics software developed for the IAC program will conform to the 1979 SIGGRAPH standards.

Interactive Data Handling

- User/database interface
- User/module interface
- Graphics hardware: Tektronix
- Graphics software: Conform to 1979 SIGGRAPH standards

DATABASE SYSTEM

The database system planned for the IAC will be a relational database system. The organization of this database system is defined by what is known as a two-schema model: logical and physical. The logical organization represents the user's view of the database and will provide security, reliability and relational capability of the system. This organization will establish logical partitions and allow for transfer of data between the partitions, define the organization within a partition and implement the relationships among the data. The physical organization represents the machine implementation of the database and will establish physical segments, records, etc. Among the system's characteristics which will be particularly important from the user's viewpoint will be the permanent nature of the database storage as well as its capability to support multiple users concurrently. The IAC will use a single central processing unit (CPU) and not consider a distributed processing system such as being developed for the IPAD system. The IAC is intended to provide back-up capability and allow recovery in case of computer failure. In addition, a data definition language (DDL) will allow user specification for details of the database schema. Finally, a user oriented query language will provide the interactive access to the database.

Database System

- Two-schema organization
  - Logical
  - Physical
- Characteristics:
  - Multiuser (concurrent usage)
  - Single CPU
  - Recovery
  - Backup
- Data definition/query language

INTEGRATED ANALYSIS CAPABILITY
PILOT PROGRAM

The IAC will have specific modules associated with the structural, thermal, system dynamics and controls technical disciplines shown below on the left. At the present time the specific modules to be used during Phase II have not been selected. For the Phase I pilot code, the technical modules shown below on the right will be used. The NASTRAN thermal and structural analysis will be used in conjunction with the DISCOS program for system dynamics. The DISCOS controls subroutine will be used for purposes of the pilot program. For Phase II a relational database system will be developed for the IAC in conjunction with an interactive tutorial and query capability as well as extensive use of graphics. The pilot program will employ a file oriented database system to demonstrate the interdisciplinary data flow and the user oriented query language. Interactive terminals will also be used along with the pilot program to demonstrate the executive system approach and the interactive graphics. For the graphics output it is planned to use a user oriented menu approach. It should be noted that the pilot program capability will be used to solve a selected demonstration problem. This problem was chosen at the Initial Program Review and is described below.

Integrated Analysis Capability
Pilot Program

- **Structural:** NASTRAN
- **Thermal:** NASTRAN
- **System dynamics:** DISCOS
- **Controls:** DISCOS
- **Database system**
- **Interactive data handling**

PILOT PROGRAM

The function of the pilot program is to provide proof of concept evidence for the IAC system through the execution of a demonstration problem. Thus the pilot program is a restricted subset of the full IAC system capability. The primary software characteristics of this program are shown below. It was specified by the contract that the pilot program be developed for operation on the DEC VAX computer. Boeing Aerospace has a VAX machine at its Kent Space Center and we have remote access to this machine using a Tektronix 4014 from our work area. For the pilot program as discussed previously, a file oriented database system will be utilized to interface the technical modules of NASTRAN and DISCOS and provide a data repository for the user. This system will be accessed interactively to demonstrate the planned capability of the IAC and the IAC/user environment. The graphics capability will use the Tektronix developed Plot 10 package operational on the VAX. This capability will be demonstrated by plotting DISCOS output data. The executive system approach for both the analysis modules and database system will be incorporated into the pilot program.

Pilot Program

- Operational on DEC VAX 11/780
- File-oriented database system
- Interactive graphics
- Executive system–module/data manager

DEMONSTRATION PROBLEM

The demonstration problem selected for the pilot code is a thirty (30) meter antenna structure. This structure has the primary structural elements: spacecraft bus, reflector, and feed truss. A previously developed NASTRAN model of this structure was provided to us by the Jet Propulsion Laboratory (JPL). This model has been exercised generating mode shapes and frequencies for comparison with JPL data (which was excellent). It is planned to perform two types of analysis with this model. One a thermal/structural analysis and the second a structural/control analysis. These analyses will follow the second and third analysis capability shown on the page titled "IAC-Capable of Performing." One purpose of this solution is to demonstrate the user control of the executive system to initiate the thermal and structural analysis. Another is to demonstrate the ability of the system to identify and transfer module generated output to the database and extract data from the database as input to another module. The second analysis performs a similar function but will involve the DISCOS-Controls subroutine and the interactive graphics plotting capability. For this analysis the antenna will be assumed to be gimbaled at the spacecraft bus and one degree of freedom control exercised.

Demonstration Problem

- 30-metre antenna
  - Bus
  - Reflector
  - Feed
- Solve two problem types:
  - Thermal/structural analysis
  - Structural/control analysis

N80-19167

JPL ANALYTICAL PERFORMANCE PREDICTION CAPABILITY

R. Chen
Jet Propulsion Laboratory

LSST 1ST ANNUAL TECHNICAL REVIEW

November 7-8, 1979

PAGE 408 INTENTIONALLY BLANK

JPL Analytical Performance Prediction Capability

OBJECTIVES

The basic long term objective of this task is for JPL to develop simplified analytical capability for the simulation and prediction of performance for large deployable antenna structures. This capability, in the form of a computer code, is expected to account for all phases of hardware use, i.e., ground handling, boost, deployment, on-orbit station keeping, and transfer from LEO to GEO, if applicable. In addition to accounting for static and dynamic loading of the basic structure, the variation in the precision of the reflector surface and the alignment of the feed support structure as a function orbit must be understood and quantified to accommodate electromagnetic analysis.

This development activity is expected to involve the application of the state-of-the-art analysis capability, modification of this capability, the development of entirely new capability and the application of the subject technology by specific antenna structures.

JPL ANALYTICAL PERFORMANCE PREDICTION CAPABILITY
OBJECTIVES

LONG TERM

TO DEVELOP SIMPLIFIED ANALYTICAL CAPABILITY
FOR THE SIMULATION AND PREDICTION OF PERFORMANCE
FOR LARGE DEPLOYABLE ANTENNA STRUCTURES

FY 79

TO DEVELOP ANALYTICAL APPROACHES AND TO INITIATE
THE DEVELOPMENT OF A SIMPLIFIED INTERACTIVE PROGRAM
FOR LARGE DEPLOYABLE ANTENNA STRUCTURES

Specific Tasks

Five tasks were established at the beginning of FY'79 as guidelines for accomplishing objectives.

A. The task involves identifying antenna structures and environment based upon results of recent NASA mission model studies and the specific antennas selected for development from the Wrap-Rib and Precision Deployable Conceptual Development Studies.

B. Construct models to demonstrate computer code capabilities, new capability required, and to establish bases for integrated analysis studies.

C. Investig te different modes for accomplishing structural/thermal coupling based on dissimilar requirements on models used for structural and thermal analyses.

D. Supply dynamic models describing typical modal data to Controls Division to establish interdisciplinary dialogue between Structures and Controls engineers.

E. Determine structural, thermal and dynamic response in terms of structural loading and reflector surface distortion.

SPECIFIC TASKS

A. IDENTIFY CHARACTERISTIC ANTENNA STRUCTURES AND APPLICATIONS

B. DEVELOP ANALYTICAL MODELS

C. DEVELOP APPROACH FOR STRUCTURAL/THERMAL COUPLING CAPABILITY

D. DEVELOP APPROACH FOR STRUCTURAL/CONTROL COUPLING CAPABILITY

E. CHARACTERIZE AND DETERMINE IMPACT OF EXTERNAL DISTURBANCES

Preliminary Plans

A preliminary plan for an analytical program resulting in mid-FY'79 features a centralized data base executive system to be commanded by the user using a precompiler signaled from input information. The data base executive system is capable of storing, managing, indexing, and recalling large amounts of data connecting and sequencing the required analysis tools of various disciplines for proper execution. This feature stresses versatility as well as flexibility in handling interactive analyses for varieties of LSST systems.

LSST - STRUCTURAL CONCEPT - DEPLOYABLE REFLECTORS
SIMPLIFIED INTERACTIVE ANALYSIS COMPUTER PROGRAM

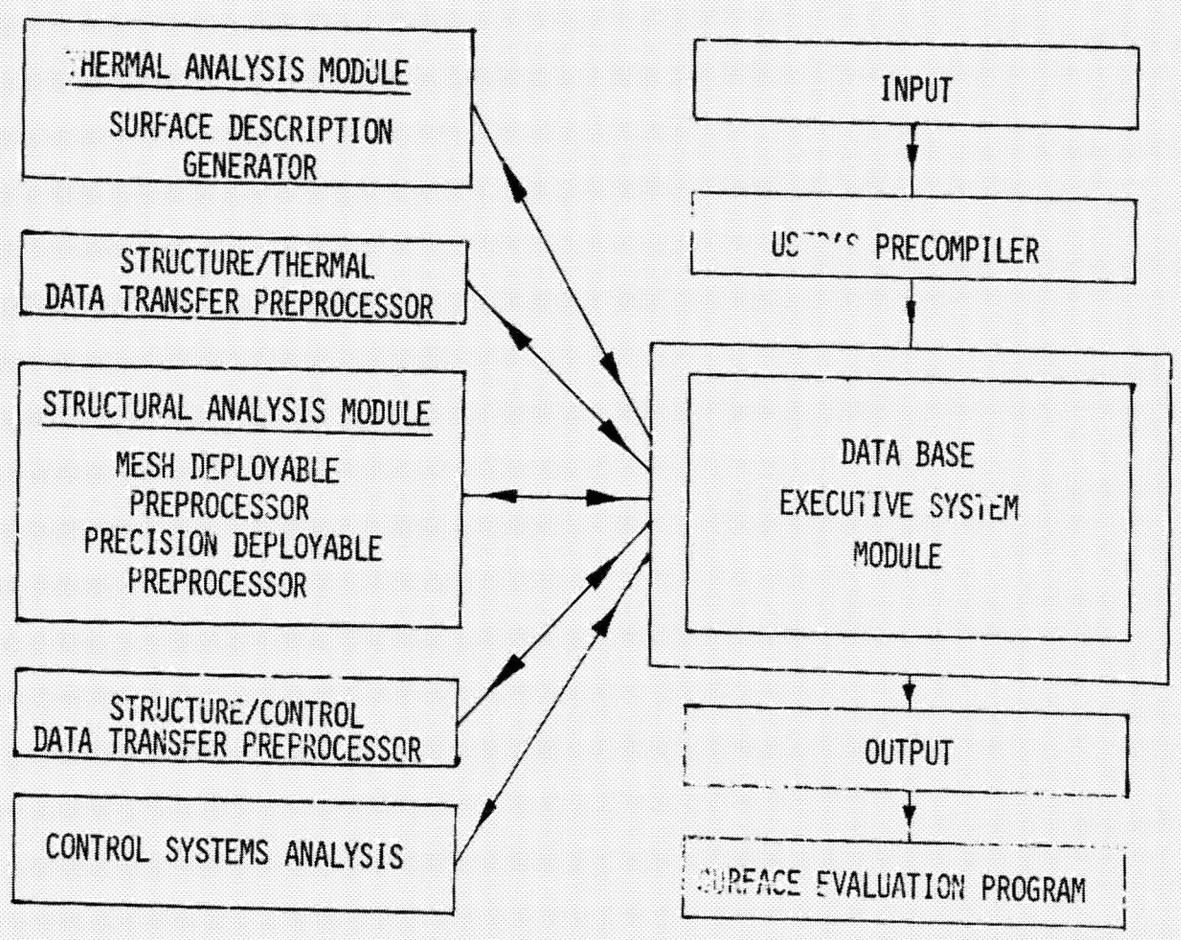

Near Term Plan

The near term (FY'80) objective for implementation of the proposed approach is described in the following figure. The current plan is to develop a thermal/structural analysis capability specifically tailored for the wrap-rib deployable antenna since development of precision deployable antenna has been terminated. In this plan the approach for the structural/controls integrated analysis will be completed in FY'80. Since the analytical capability will be focused only on the mesh deployable antenna, a data base management system is not required here.

NEAR TERM PLAN

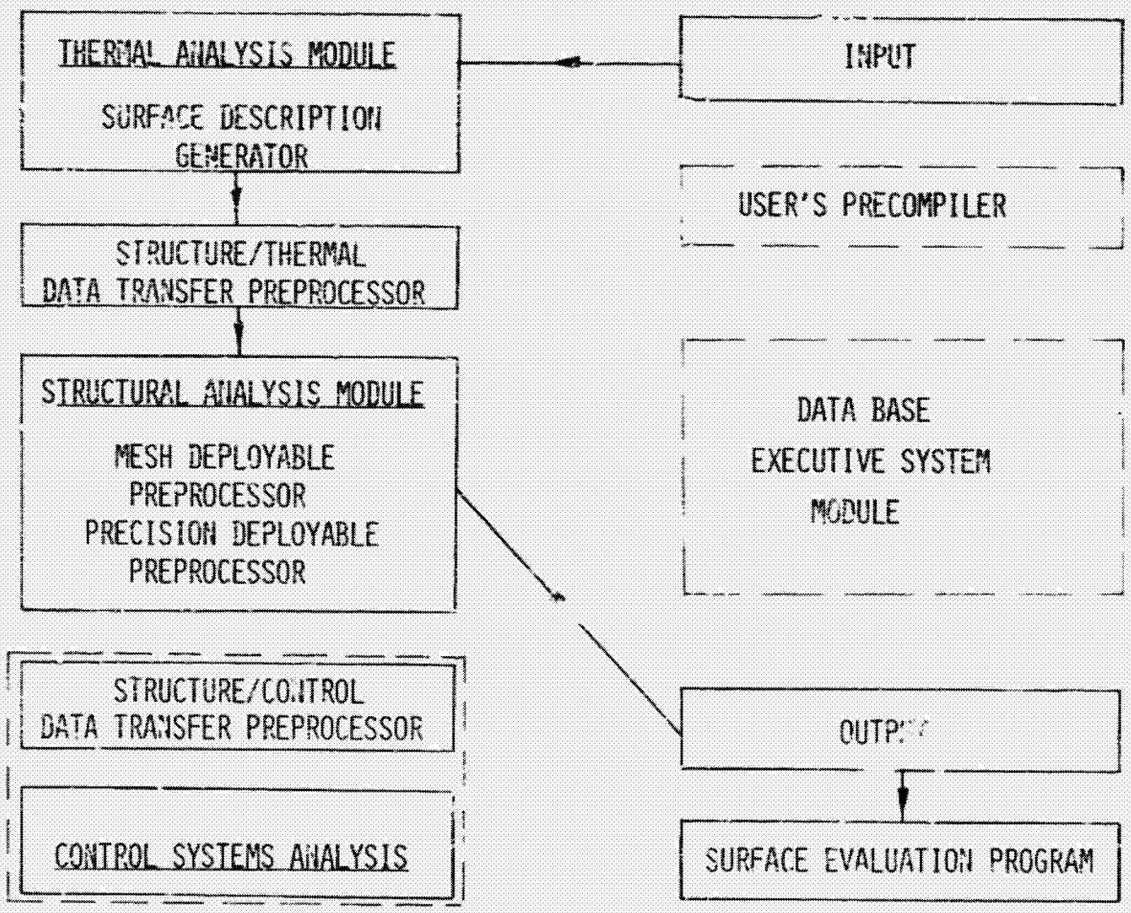

Thermal/Structural Analysis Computer Program

The computer program for the evaluation of thermally distorted wrap-rib antenna consisted of the following main components:

1. LOHARP code to compute heat load input.
2. SINDA code to compute temperature distribution.
3. SAP finite element program to compute thermal/structural distortion.
4. JPL RMS program to compute the total surface RMS deviation to be used in Ruze's formula for evaluation.

Necessary modifications to these programs are to be shown on the following figures.

MESH DEPLOYABLE ANTENNA THERMAL/STRUCTURAL COMPUTER PROGRAM

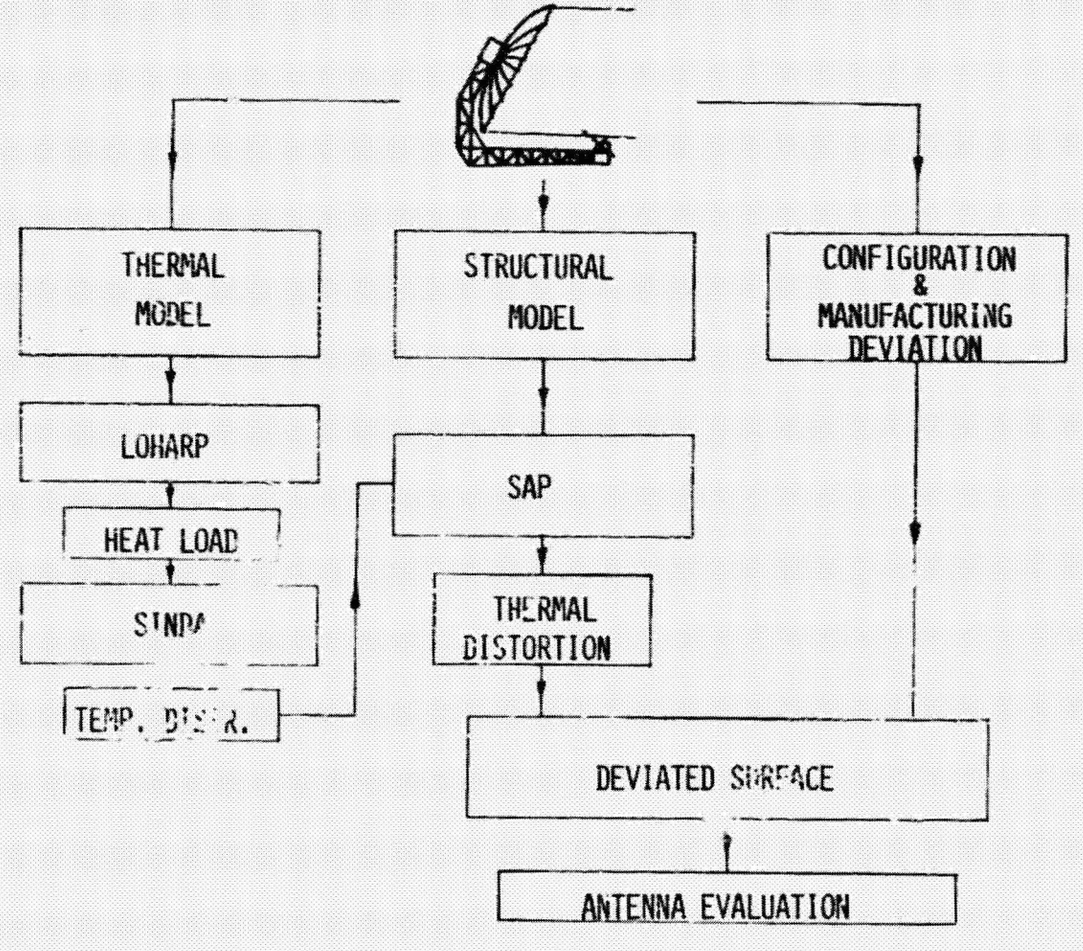

Mesh Deployable Antenna Thermal Analyzer

Three main preprocessors are required to integrate the input information and the computer codes:

1. A preprocessor to generate all surface descriptions of a wrap-rib paraboloid antenna surface. Because of the LOHARP code core limitation, the surface view factors and the radiation exchange factors and therefore the heat loads will be computed on sections of antenna only.

2. A preprocessor to collate the sectional heat loads and compiles the results to yield heat load distribution on a half antenna for use of SINDA code.

3. A preprocessor to transfer temperature distribution information on thermal model to appropriate nodal points of the structural model for use of the structural analyzer.

MESH DEPLOYABLE ANTENNA THERMAL ANALYZER

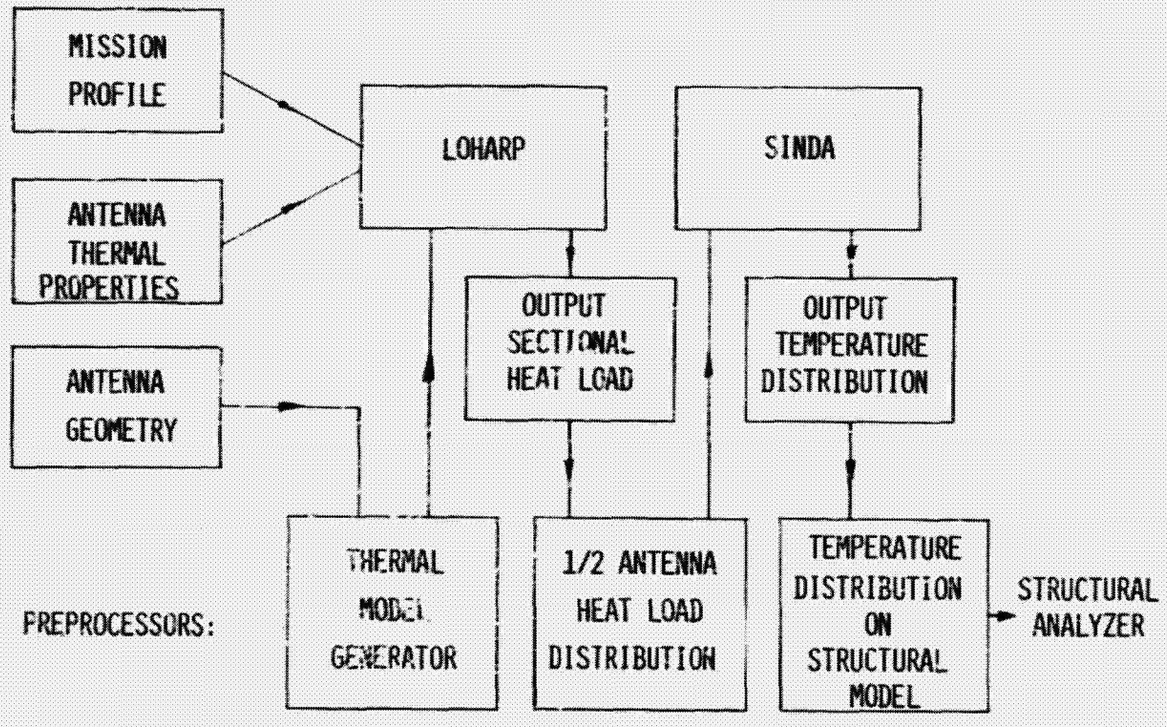

Thermal Model

This figure illustrates a plane and side view of the thermal model of wrap-rib mesh deployable antenna used to find solar and planetary induced heat loads on rib and mesh nodes. As may be seen, only two ribs and included mesh are modeled at one time. The mesh of the rest of the antenna is included for shading purposes only. Heat loads on all other pairs of ribs are found by mathematically rotating the structure shown about the axis by an amount equal to the angle between ribs.

THERMAL MODEL

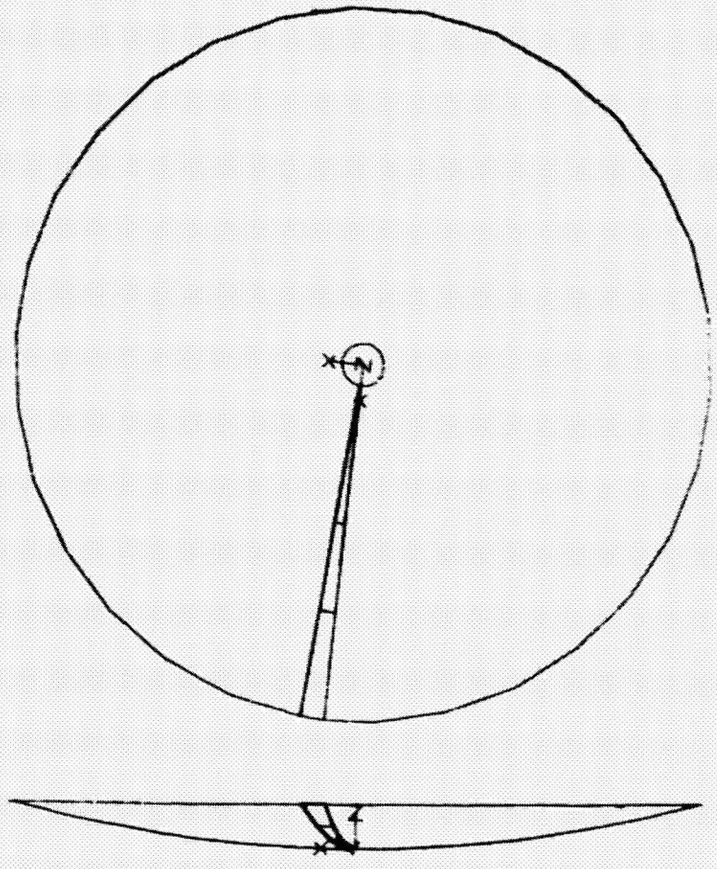

Thermal Model of Outside of Two Adjacent Ribs and Included Mesh

This figure is a close up of the adjacent rib sections appearing in the previous figure. The section shown here is an accurate representation of the actual rib and included mesh surface for a particular set of geometric parameters, and was automatically generated by the preprocessor program given minimal input. View factors and radiant energy interchange factors between the exterior surfaces of adjacent ribs are computed once and subsequently used for all pairs of adjacent ribs.

THERMAL MODEL OF OUTSIDE OF
TWO ADJACENT RIBS & INCLUDED MESH

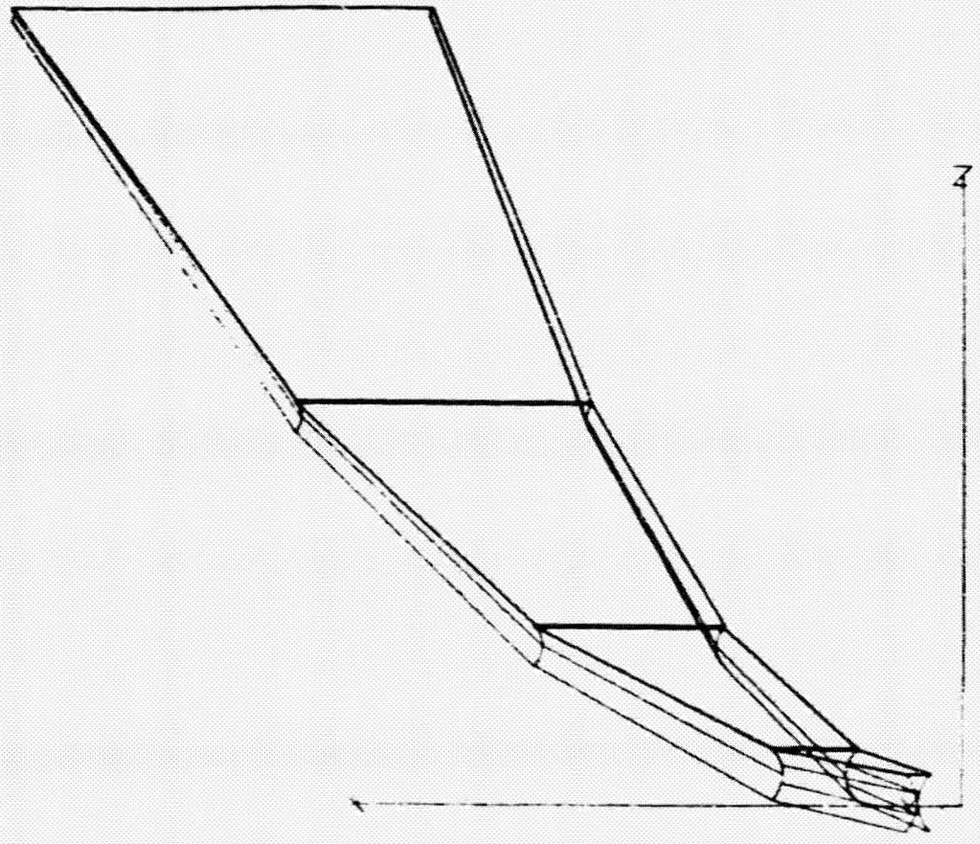

Thermal Model of the Inside of A Single Rib

This figure illustrates the thermal model of one single complete rib and is used to determine view factors and radiant energy interchange factors for intrarib heat transfer. The mathematical model of the single rib is also automatically generated by the preprocessor code. Solar and planetary heat loads do not impinge on the interior surfaces of the rib due to the opaqueness of the rib and multi-layer thermal blanket.

THERMAL MODEL OF THE INSIDE OF A SINGLE RIB

Deployable Reflector Structural Analyzer

Deployable reflectors employ tension type structural components which are in general made from materials having nonlinear elastic properties. For a practical and simplified tool, tension only membrane element is developed by modifying bending elements in the SAP finite element code. The nonlinear behavior of the membrane element is simulated using the perturbation method based upon small linear changes from the undisturbed configuration, the undisturbed configuration being the initial state where the mesh is stretched at the designed pre-stress. The result is a stretched membrane that has a geometric stiffness which gives additional out-of-plane rigidity resulting from the inplane tensile stress.

Other modifications to the structures code include adding capabilities to handle thermal gradients across the rib cross sections, eccentrically applied rib loads, vibrations of the freely supported reflectors, and a cyclic symmetric feature for reducing model size and therefore the computer running time.

MESH DEPLOYABLE REFLECTOR STRUCTURAL ANALYZER

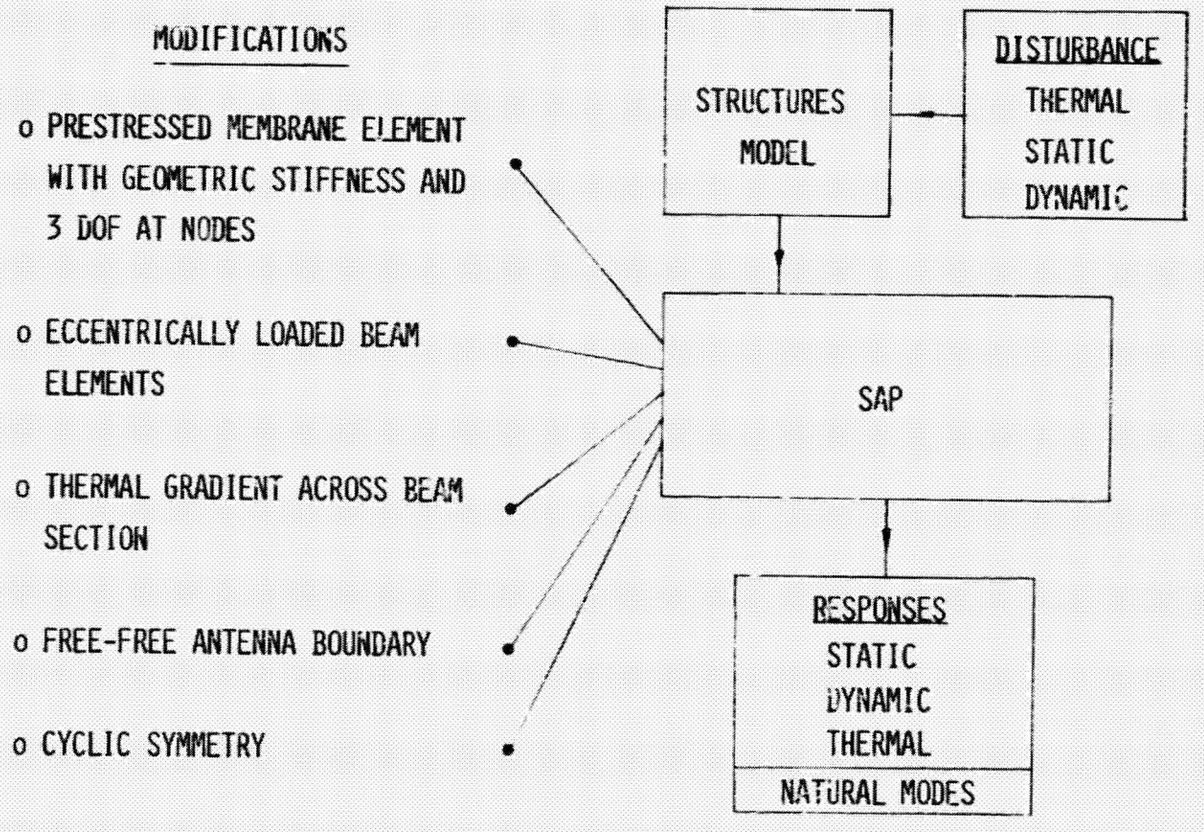

Structural Model 30 Meter Precision Deployable Antenna

A NASTRAN structural model using the 30-m diameter advanced Sunflower antenna concept was constructed. This model was used primarily to obtain samples of structural dynamic characteristics for investigating controls requirements on this type of antennas.

The reflector is assumed to be consisted of aluminum honeycomb panels with 1" core and .020" face sheets. The antenna feed is a triangular plate of the same material, supported by three 16" dia. X .125" w.t. aluminum tubes. A simplified hexagonal spacecraft bus of approximately 100" cube in size is assumed to be attached to the reflector with six aluminum tubes of the same size as the feed supports. The bus and supports have been sized to yield a total weight of 3167 lb.

STRUCTURAL MODEL

30 METER PRECISION DEPLOYABLE ANTENNA

FREQUENCY Hz	MODE
0.00	RIGID-BODY TRANSLATIONS
0.00	RIGID-BODY ROTATIONS
0.43	REFLECTOR BENDING
0.62	FEED SUPPORT TORSION
0.66	REFLECTOR BENDING
0.69	" "
0.95	" "
0.95	" "
1.04	" "
1.23	" "
1.48	FEED STRUCTURE BENDING
6.89	FIRST OVERALL BENDING
6.89	" " "

- F/D = 0.5
- FLEXIBLE SPACECRAFT
- AXISYMMETRIC FEED

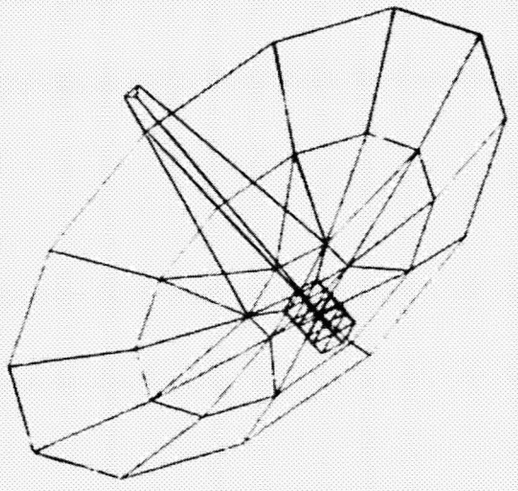

Structural Model 100 Meter Mesh Deployable Antenna

A NASTRAN structural model of a 100 meter mesh deployable antenna using a wrap-rib reflector was constructed. The model consists of 30 tapered ribs of lenticular cross-section made of graphite-epoxy layup. The roots of the ribs are attached to an aluminum central hub which also supports the feed with a tripod of aluminum tubes extended to a distance of 100 meters long.

The mesh membrane reflector surface presented special modeling problems. The normal stiffness of the reflector is contributed purely by the stretching of the mesh membrane which occurs only when the reflector is deployed. This differential or geometric stiffness is not accounted for in the stiffness matrix of conventional finite membrane elements in NASTRAN. To simulate this property, artificial thermal loads were introduced to the model. This generates element differential stiffness terms which were then added to the stiffness matrices for the ribs and mesh to produce the total reflector stiffness properties of the reflector.

STRUCTURAL MODEL

100 METER MESH DEPLOYABLE ANTENNA

FREQUENCY Hz	MODE
0.00	RIGID-BODY TRANSLATIONS
0.00	RIGID-BODY ROTATIONS
.053	REFLECTOR "UMBRELLA" MODE
.065	FEED SUPPORT BENDING
.073	REFLECTOR BENDING
.094	REFLECTOR TORSION
.096	REFLECTOR BENDING
.118	REFLECTOR BENDING
.140	REFLECTOR BENDING
.150	REFLECTOR TORSION

- F/D = 1.0
- AXISYMMETRIC FEED
- "WRAP-RIB" REFLECTOR

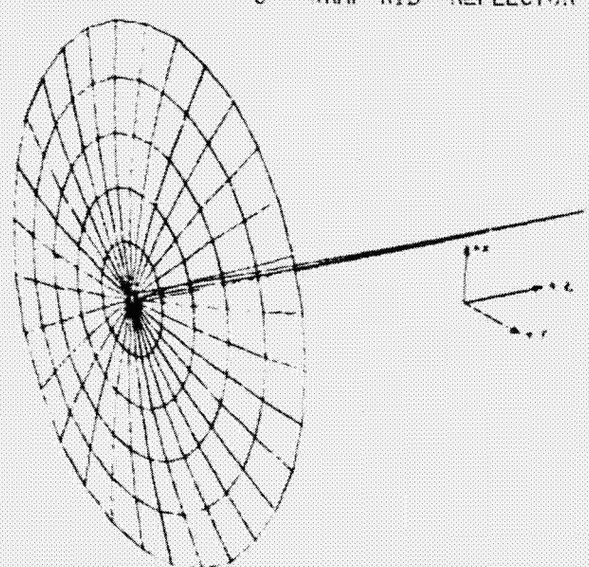

N80-19168

LARGE SPACE SYSTEMS TECHNOLOGY ELECTRONICS - DATA AND POWER DISTRIBUTION

W. G. Dunbar
Boeing Aerospace Company

Contract NAS8-33432

LSST 1ST ANNUAL TECHNICAL REVIEW

November 7-8, 1979

PAGE 422 INTENTIONALLY BLANK

TECHNOLOGY AREA: ELECTRONIC - DATA & POWER DISTRIBUTION

TASK: CABLES AND CONNECTORS; GROUNDING AND BONDING

OBJECTIVE: DEVELOP THE (TASK) HARDWARE TECHNOLOGY AND MANUFACTURING/USAGE TECHNIQUES REQUIRED TO MEET PLATFORM AND ANTENNA SYSTEM NEEDS IN THE MID-1980'S AND BEYOND.

APPROACH: THE APPROACH TO THIS TECHNOLOGY TASK IS ASSEMBLY TECHNIQUE DEPENDENT, AND WILL THEREFORE BE APPROACHED ON TWO FRONTS.

(1) HARDWARE AND TECHNIQUES ASSOCIATED WITH MANNED-EVA, MACHINE ASSISTED ASSEMBLY.

(2) HARDWARE AND TECHNIQUES ASSOCIATED WITH AUTOMATED ASSEMBLY, i.e., MACHINE AS PRIME WITH MAN CONTROLLING OR AS BACK-UP.

TASK DESCRIPTION:

- ASSESS PLATFORM AND ANTENNA SYSTEM REQUIREMENTS.
- ASSESS STATE-OF-THE-ART HARDWARE.
- INVESTIGATE AND EVALUATE HARDWARE, MANUFACTURING/USAGE TECHNIQUES OF OTHER PROGRAMS.
- DEVELOP CONCEPTS/TECHNIQUES BASED ON KNOWN REQUIREMENTS, AND UPON DEVELOPING STRUCTURAL CONCEPTS AND ASSEMBLY TECHNIQUES.
- DO IN-HOUSE DESIGN EVALUATION AND PREPARE TEST PLANS OF NEW CONCEPT HARDWARE.

TASK STATUS: COMBINED TASK CONTRACT INITIATED WITH THE BOEING COMPANY (NAS8-33432) ON MARCH 30, 1979.

- COMPLETED STATE-OF-ART REVIEW FOR GROUNDING AND BONDING; CABLES AND CONNECTORS
- DEFINED DATA AND POWER SYSTEM DISTRIBUTION REQUIREMENTS
- ESTABLISHED GROUNDING & BONDING; CABLE AND CONNECTOR REQUIREMENTS FOR SPACECRAFT WITH LOAD DEMANDS TO 2.5 MEGAWATTS
- DEVELOPED CONCEPTUAL CONNECTOR DESIGNS FOR MANNED AND AUTOMATICALLY MATED SYSTEMS
- EVALUATED MATERIALS COMPATIBILITY FOR BONDING AND CONNECTORS IN STORAGE AND IN SPACE

ACCOMPLISHMENTS ACHIEVED TO DATE

- REVIEWED LSST REPORTS, SUPPLIER DATA AND ACTIVITIES, AND IN-HOUSE REPORTS ON PRESENT AND PRELIMINARY DESIGNS FOR MANNED AND AUTOMATICALLY ASSEMBLED SPACE POWER SYSTEM CABLES, CONNECTORS, AND GROUNDING AND BONDING MATERIALS AND TECHNIQUES.
- DEVELOPED CONCEPTUAL CONNECTOR DESIGNS FOR AUTOMATICALLY CONNECTED/DISCONNECTED ASSEMBLIES IN SPACE
- ESTABLISHED VOLTAGE CURRENT RATINGS FOR LSST DESIGNS TO 10 MEGAWATTS
- DEVELOPED GROUNDING/BONDING PHILOSOPHY CONCEPTS FOR LSST
- DETERMINED THAT THIN ALUMINUM BUSES ARE BEST FOR HIGH CURRENT HIGH VOLTAGE CONDUCTORS
- CONCLUDED THAT GRAPHITE EPOXY MUST BE COATED TO STOP DETERIORATION AND CHAFFING (DUSTING) IN SPACE AND CANNOT BE USED AS A GROUND RETURN.

THRUST FOR NEXT 6 MONTHS PERIOD

- COMPLETE MATERIALS COMPATIBILITY STUDIES
- DEVELOP CONCEPTUAL DESIGNS AND TECHNIQUES - ANALYZE AND EVALUATE USEFULNESS
- DEVELOP ROUTING, TERMINATION METHODS FOR ASSEMBLED DEPLOYMENT BY EVA AND/OR AUTOMATIC/REMOTE COUPLING

PUBLICATIONS

- MONTHLY PROGRESS REPORTS
- FINAL REPORT WHICH INCLUDES:

  RECOMMENDED MATERIALS, CABLE AND CONNECTOR DESIGN CONCEPTS, GROUNDING AND BONDING TECHNIQUES, TEST PLAN, AND INFORMATION OF MONTHLY REPORTS.

SPACECRAFT POWER LEVELS

TYPICAL MISSION POWER REQUIREMENTS (FIGURE 1):

- MISSIONS TO 1980 LESS THAN 5KW
- FUTURE SPACECRAFT POWER DEMANDS STEADILY INCREASING TO 20 MEGAWATTS.
  TYPICAL LOADS - COMMUNICATIONS, EXPERIMENTS, SURVEYS, PHOTOGRAPHY, MINERAL DETECTION, TEMPERATURE SENSING.
- POWER DEMAND SUMMARY CHART (FIGURE 2).
- TYPICAL SPACECRAFT DESIGN:
  FIGURE 3 - ON-ORBIT ASSEMBLY CONCEPT DESIGN FOR COMMUNICATIONS
  FIGURE 4 - COMMUNICATION SATELLITE

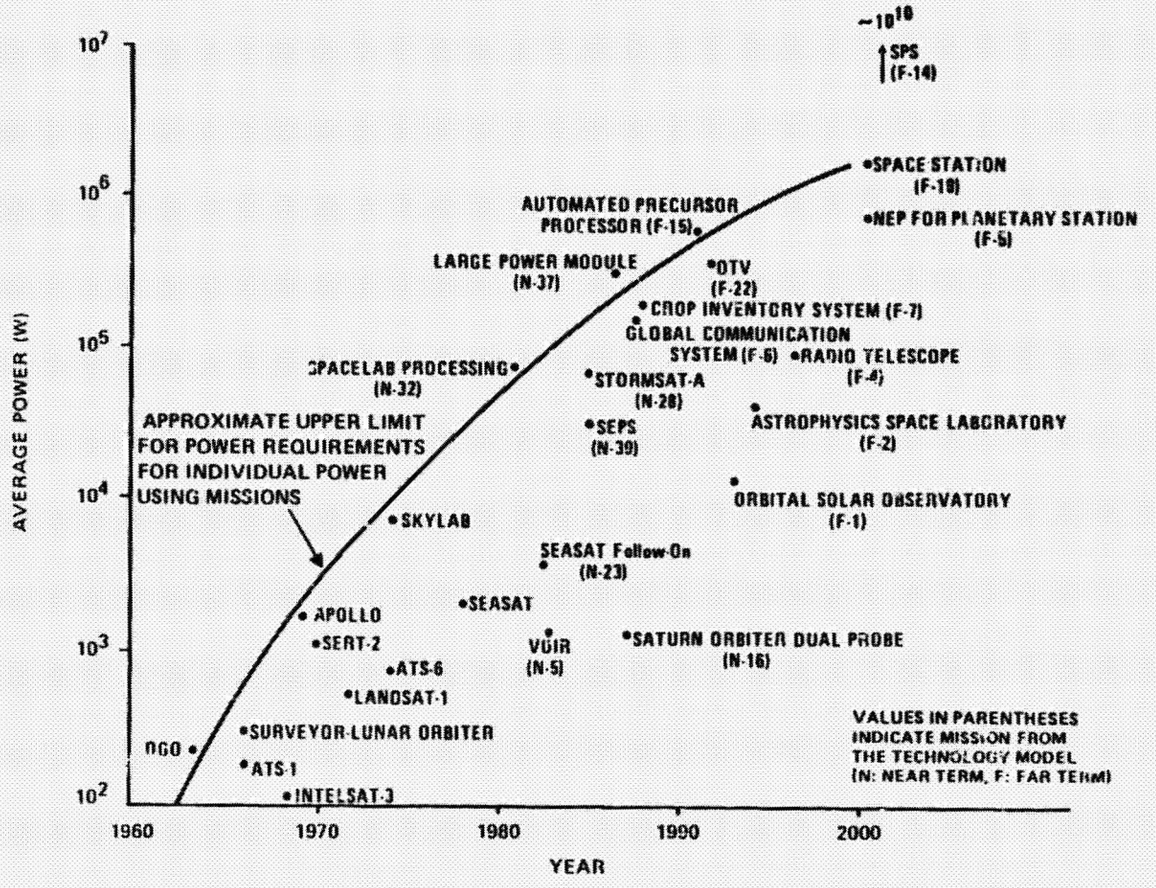

Figure 1.- Mission power requirements.

YEARS	POWER DEMAND - KILOWATTS	
	AVERAGE	MAXIMUM
1980 - 198.	25 - 50	75
1985 - 199.	25 - 200	2,500
1990 - 1995	25 - 750	3,000
1995 - 2000	25 - 2,500	20,000
PAST 2000		TO 10^{10} WATTS

Figure 2.- Spacecraft power demands.

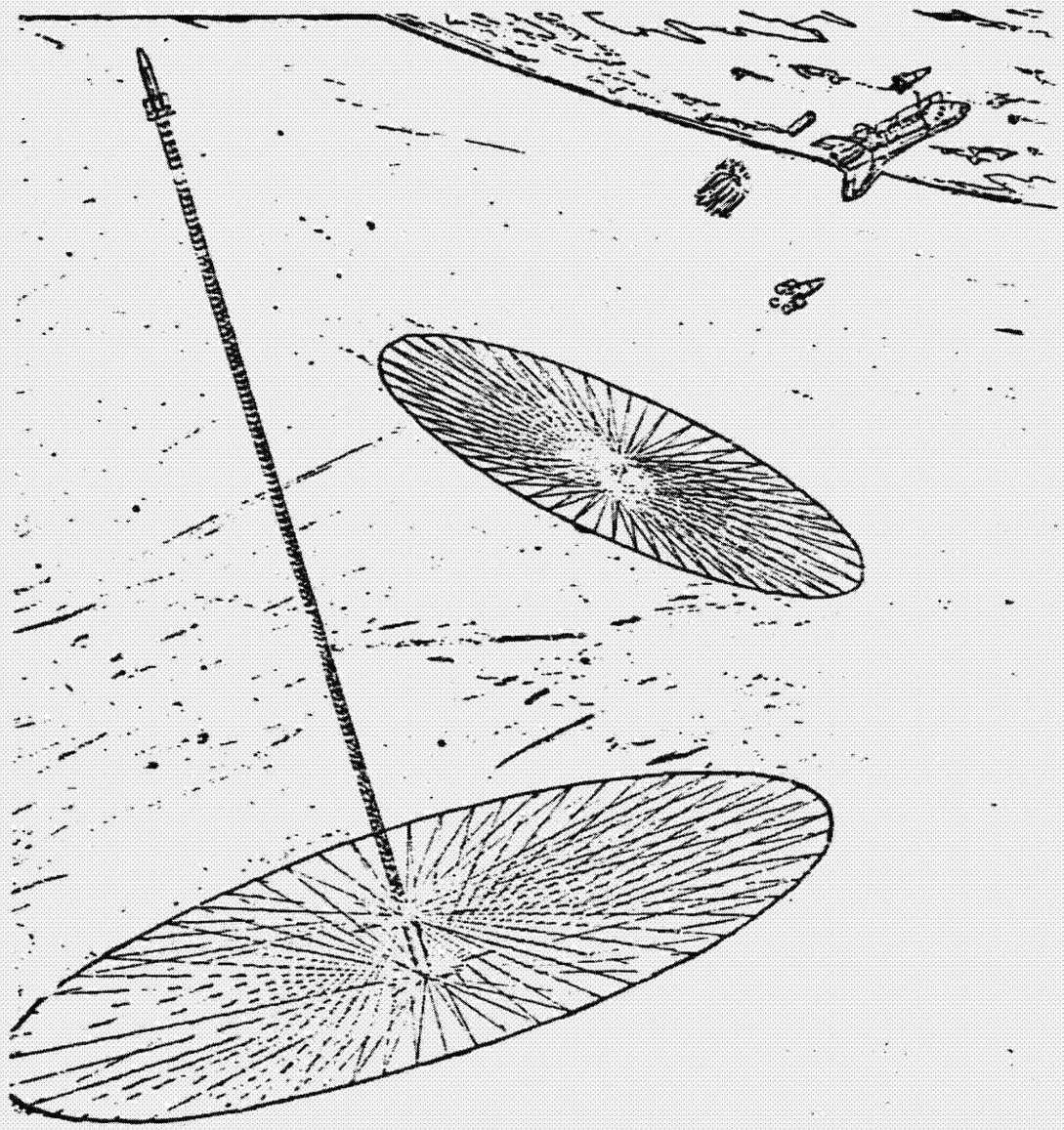

Figure 3.- On-orbit assembly concept design.

ORIGINAL PAGE IS
OF POOR QUALITY

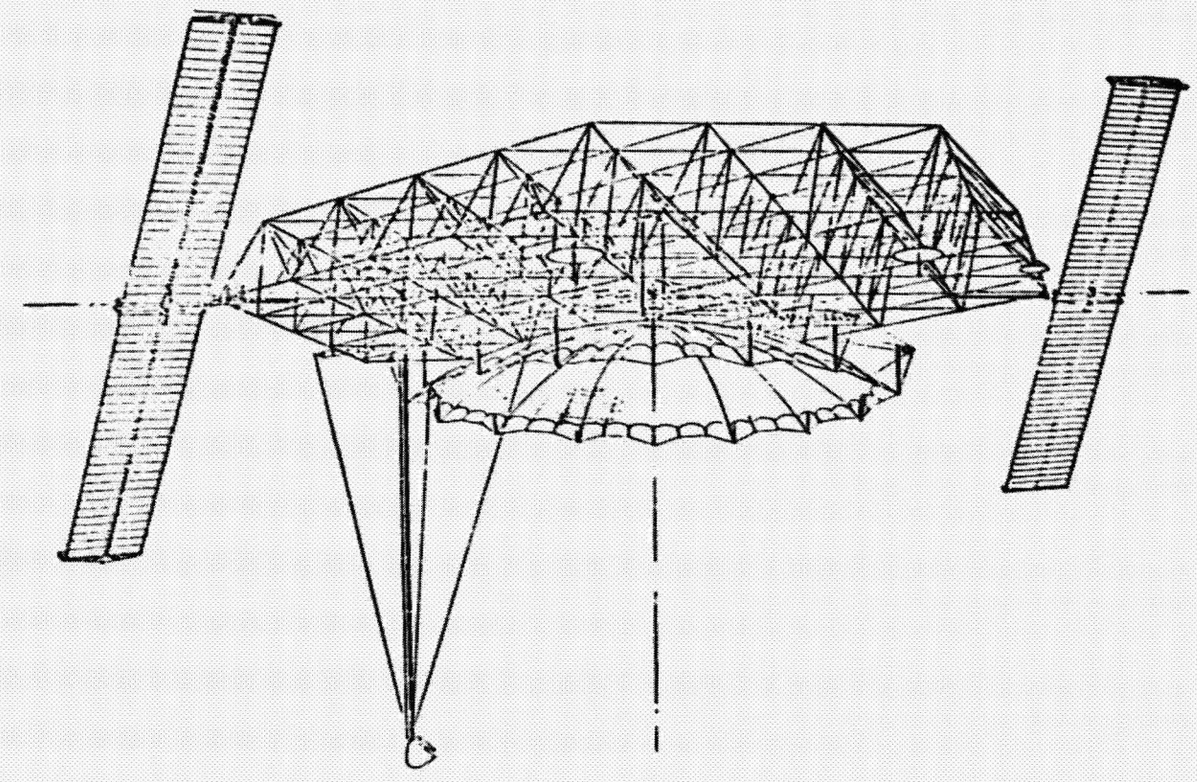

Figure 4.- Dish antenna spacecraft configuration.

DISTRIBUTION SYSTEM

- HIGH POWER LSST DISTRIBUTION SYSTEM (FIGURE 5):
  - CONVERTS LOW VOLTAGE FROM SOLAR CELLS TO HIGH VOLTAGE SYSTEM
  - DISTRIBUTION BY HIGH VOLTAGE LINES TO LOADS
  - USES COMPUTER TO CONTROL CONVERTER
  - SENSOR SIGNALS TRANSMITTED BY FIBER OPTICS
- GROUNDING AND BONDING CONVENTIONAL AND NEW TECHNOLOGY REQUIREMENTS (FIGURES 6 AND 7):
  - LINE VOLTAGES ABOVE 200 VOLTS AND LINE CURRENTS ABOVE 250 AMPERES REQUIRE NEW DESIGN AND MATERIALS TECHNOLOGY; NEW FABRICATING AND INSTALLATION TECHNOLOGY
- CONDUCTOR CONFIGURATIONS CONCEPTS FOR HIGH VOLTAGE AND HIGH CURRENT ARE SHOWN IN (FIGURE 8):
  - PROBLEM AREAS INCLUDE:
    - PLASMA AND DEBRIS
    - COOLING
    - INSTALLATION AND CONNECTIONS

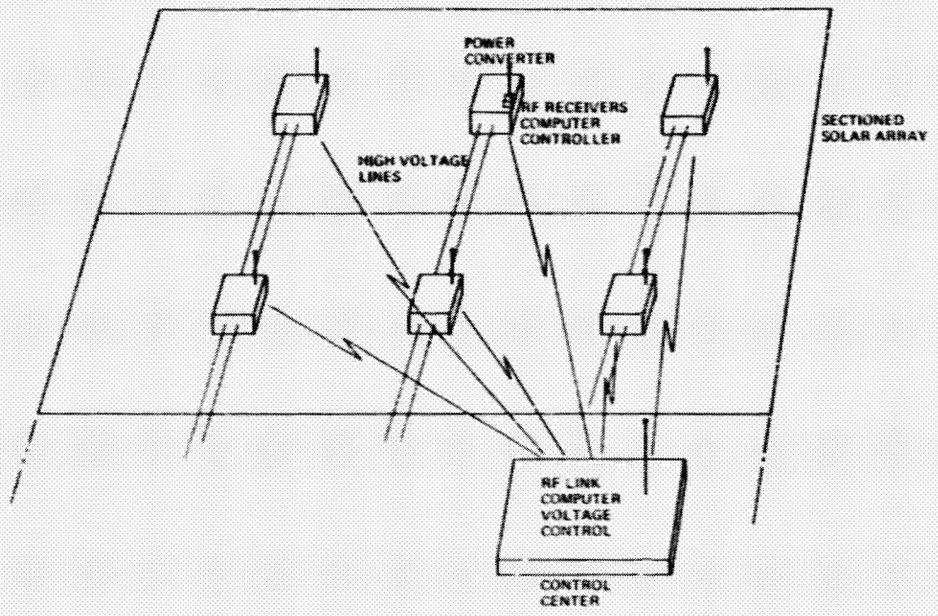

Figure 5.- Spacecraft distribution.

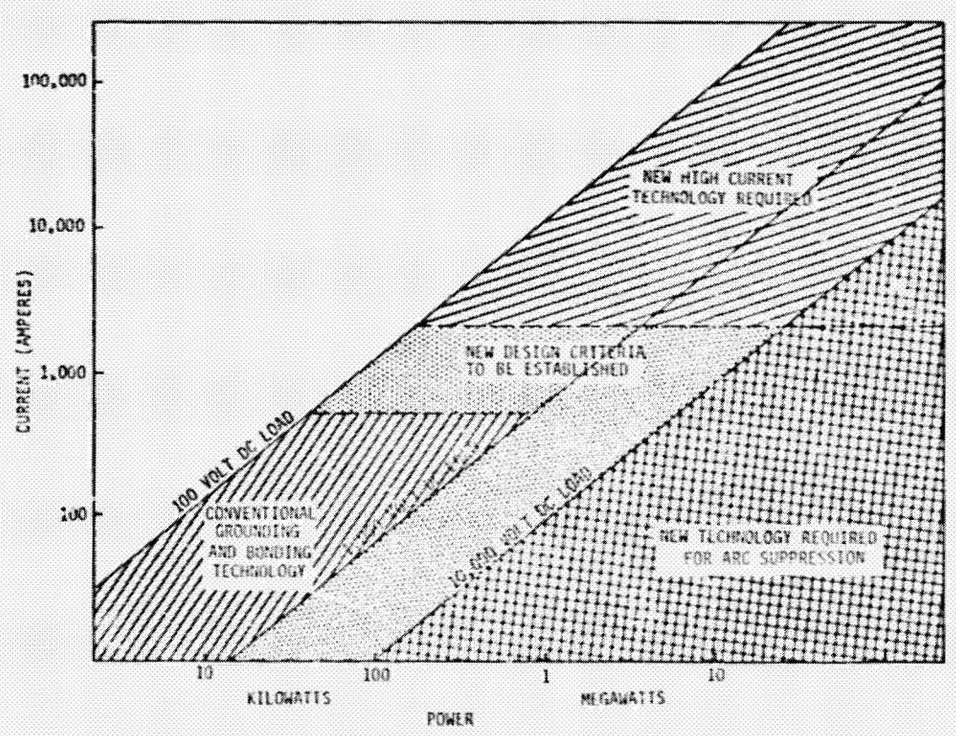

Figure 6.- Bonding and grounding applications for power systems.

POWER LEVEL (MAXIMUM)	VOLTAGE, VOLTS	CURRENT, AMPERES	EQUIPMENT STATUS
25 KW	28 - 200 V	250	• SPECIFICATION AND STANDARDS COMPLETE • USE EXISTING TECHNOLOGY
250 KW	200 - 2,000 V	250	• HIGH VOLTAGE SPECIFICATION REQUIRED • NEW INSULATION AND INSTALLATION REQUIREMENTS • PLASMA, GAS, AND DEBRIS PROBLEMS
2.5 MW	OVER 2,000 VOLTS	1,000	• HIGH VOLTAGE, HIGH CURRENT SPECIFICATION AND EQUIPMENT • NEW CONNECTIONS, BONDING, GROUNDING TECHNOLOGY • PLASMA, GAS, AND DEBRIS PROBLEMS

Figure 7.- Power demand vs. distribution system.

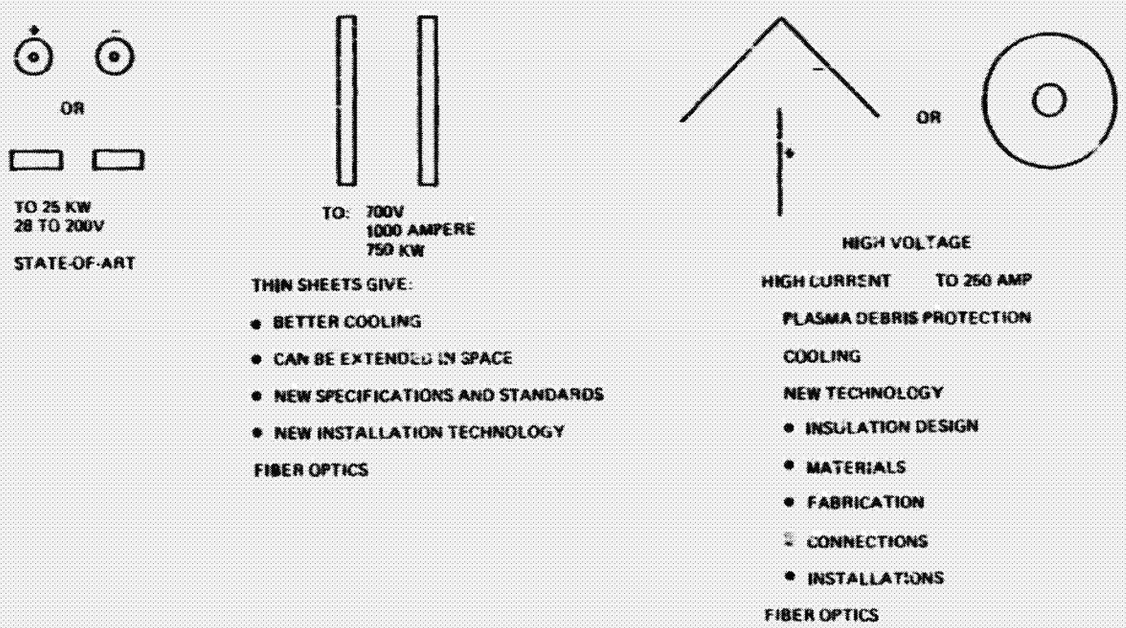

Figure 8.- Conductor configurations.

CONNECTOR CONCEPTS

- ALIGNMENT OF THE MOTHERCRAFT AND DOCKING CHASE CRAFT:
  (FIGURES 9 AND 10) USING RADAR/CAMERA CONTROL WITH ALIGNMENT PINS FOR FINAL ALIGNMENT.

- CONNECTORS FOR COMMUNICATIONS, SENSORS, AND CONTROL CIRCUITS MAY BE MOUNTED ON A PLATE. THE PLATE PROBE ALIGNMENT PINS MATCH THE SPACECRAFT PINS. THE PLATE IS SPRING LOADED TO APPLY A CONSTANT FORCE ON ALL CONNECTORS DURING MATING AND WHEN DOCKED. (FIGURE 11)
- FOUR CONNECTOR CONCEPTS: (FIGURES 12 THROUGH 15)
  - FIGURE 12 - MULTIPIN CIRCULAR CONFIGURATION WITH KEYED INSET
  - FIGURE 13 - SINGLE CONDUCTOR HIGH VOLTAGE CONNECTOR - OVER 250 VOLTS
  - FIGURE 14 - BUS BAR CONNECTION WITH SPRING ALIGNMENT FINGERS
  - FIGURE 15 - SIDE VIEW OF BUS BAR CONFIGURATION SHOWING LATCHING MECHANISM

- A ROUND CONNECTOR LATCHING/UNCOUPLING TOOL:
  (FIGURE 16) TOOL GRIPS THE MATING RING AND TURNS UNTIL THE CONNECTOR IS FULLY MATED BY EITHER THREADS OR LATCHING

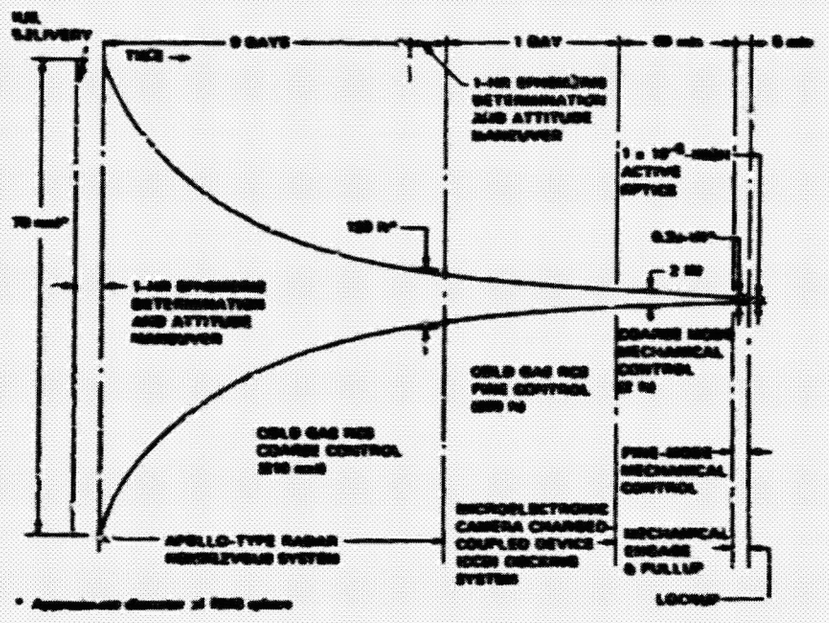

Figure 9.- Docking operation schematic showing use of Apollo-type radar rendezvous system.

ORIGINAL PAGE IS
OF POOR QUALITY

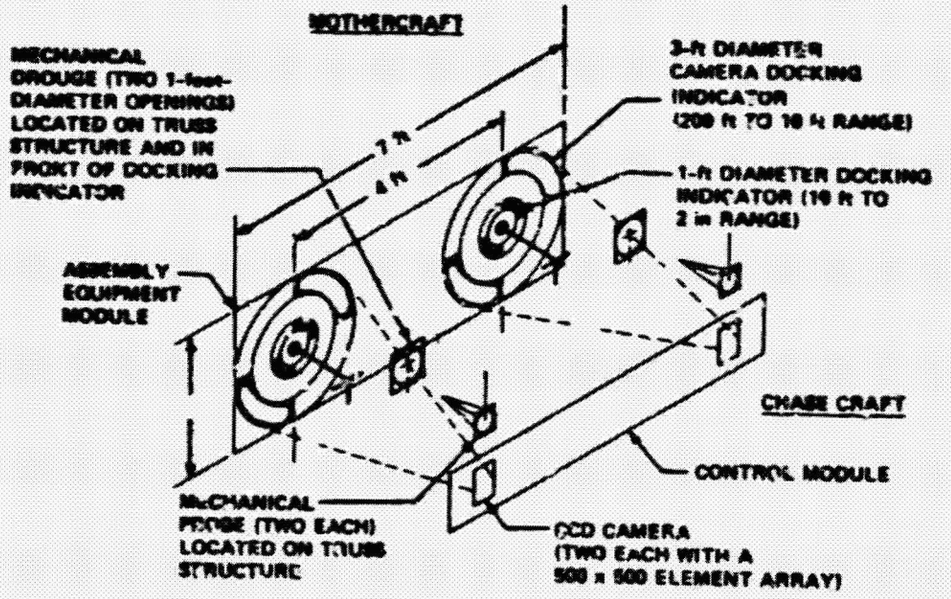

Figure 10.- Microelectronic camera system for mechanical final alignment of drouge to spacecraft during docking.

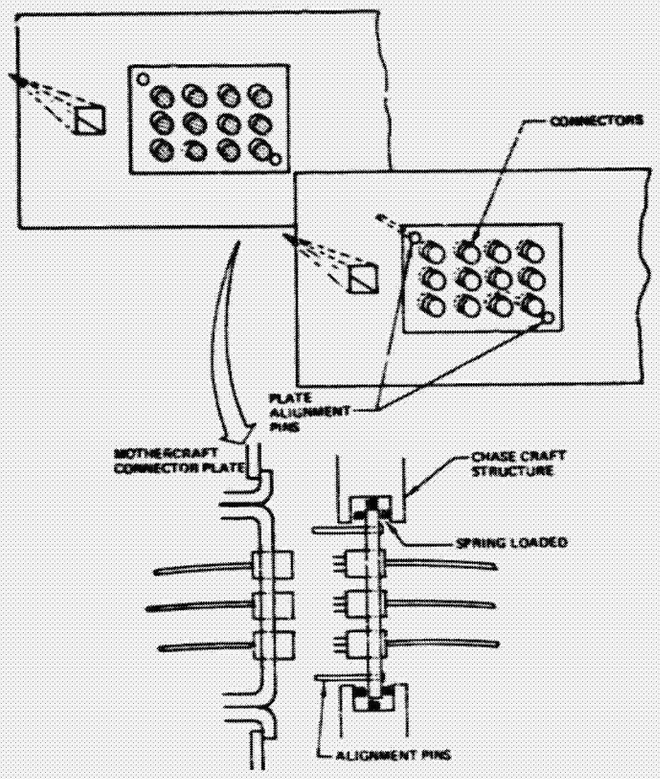

Figure 11.- Connector plate alignment.

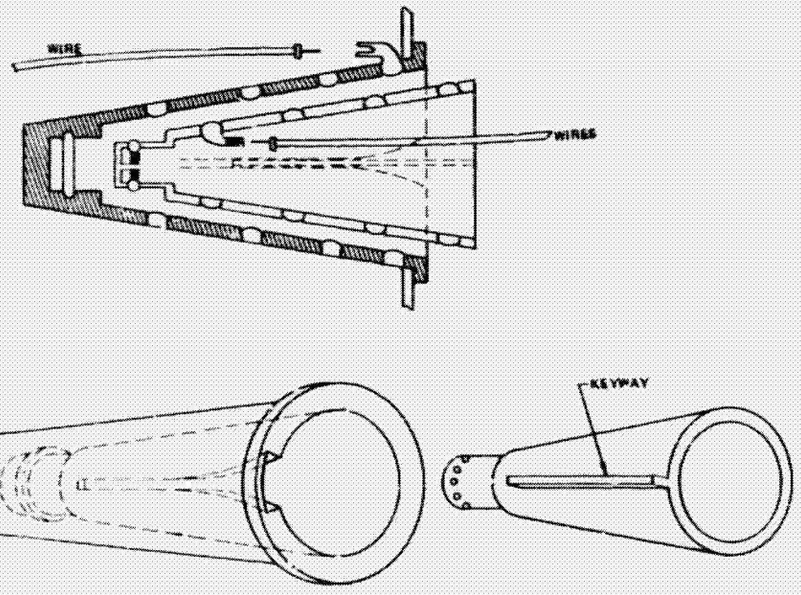

Figure 12.- Cone connector concept.

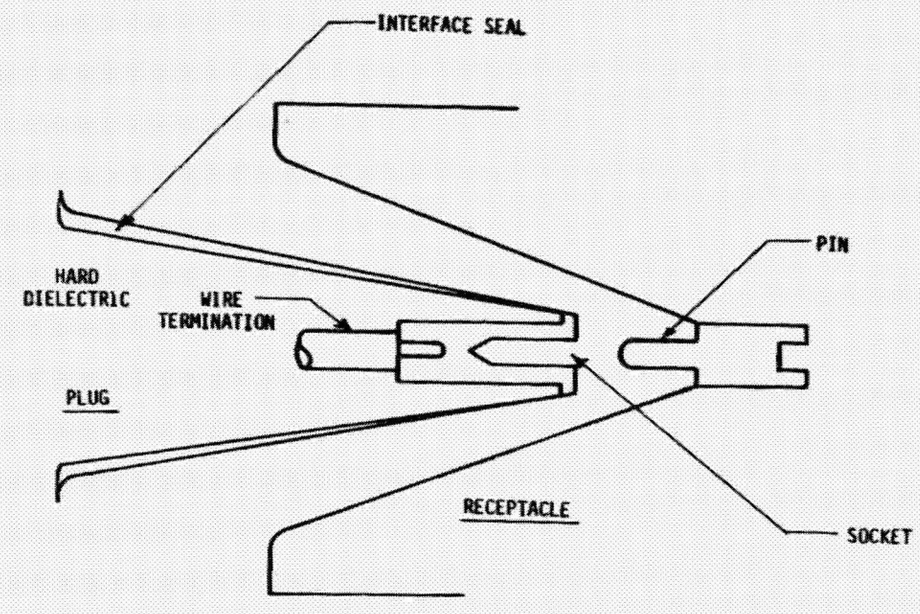

Figure 13.- Cone connector concept.

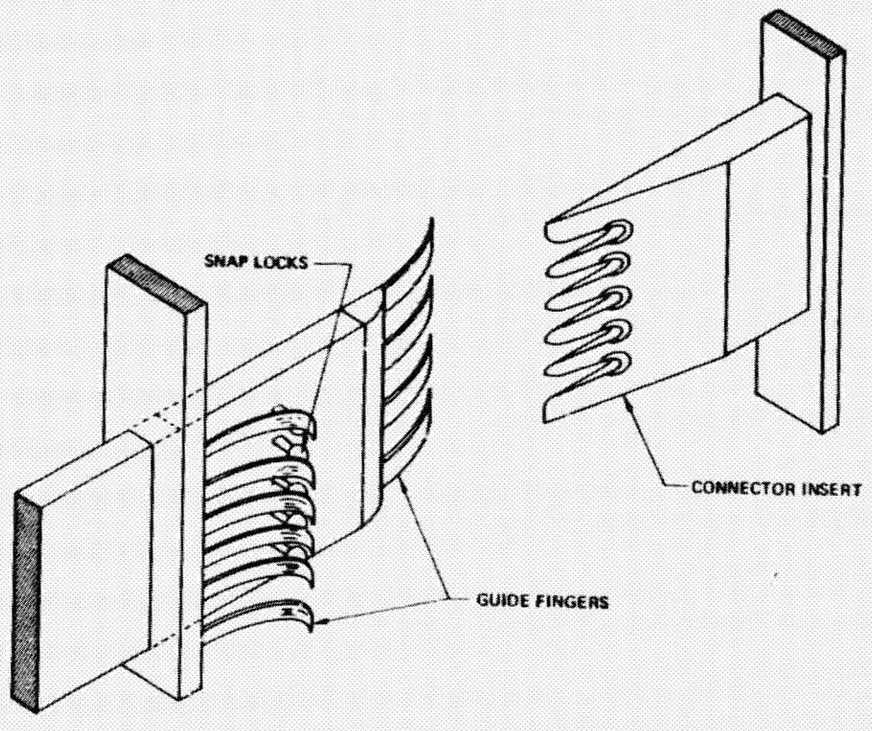

Figure 14.- Rectangular bar connection.

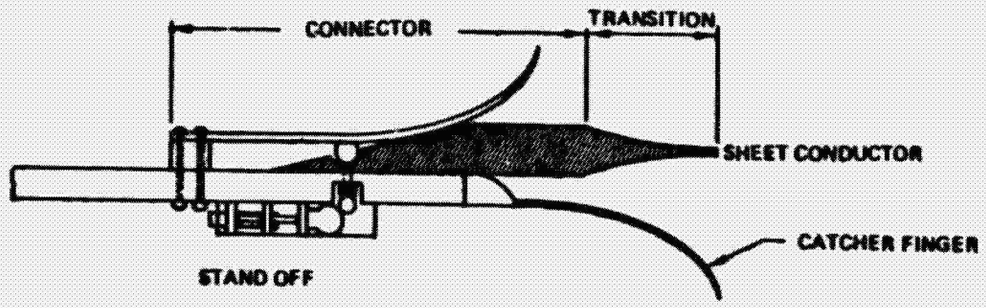

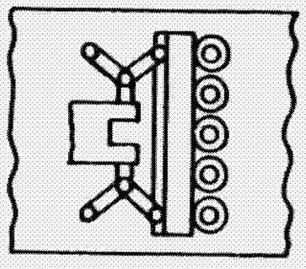

Figure 15.- Sheet metal connector detail.

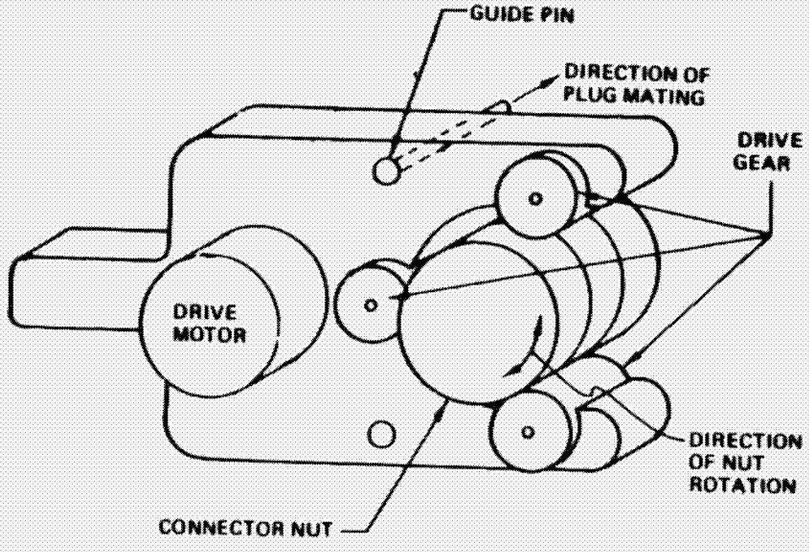

Figure 16.- Connector latching tool.

CONNECTOR STATUS

- LOW VOLTAGE CONNECTORS: 28 TO 250 VOLTS; 1 TO 150 AMPERES
  - 40 M SERIES CONNECTORS -- AVAILABLE
  - MIL-C-38999 CONNECTORS -- AVAILABLE
- HIGH VOLTAGE OVER 250 VOLTS -- NEW TECHNOLOGY
- HIGH CURRENT BUS BAR TYPE -- NEW TECHNOLOGY
- SPECIAL TOOLS AND SHELL DESIGNS REQUIRED FOR COUPLING/UNCOUPLING CONNECTORS IN SPACE
- NEW CONTACT CONFIGURATIONS REQUIRING 5 TO 70% DECREASE IN MATING FORCE ARE AVAILABLE (HYPERTAC). THESE ARE AVAILABLE FOR PRESENT 40 M AND MIL-C-38999 CONNECTORS

GROUNDING DESIGN REQUIREMENT

- GROUND IMPEDANCE SIGNIFICANTLY LOWER THAN THE CIRCUIT COMMON MODE IMPEDANCE
- GROUND PATH VOLTAGE DROP (ENVIRONMENTAL AND CIRCUITS) LOWER THAN CIRCUIT COMMON MODE VOLTAGE SHARING THE SAME GROUND PATH
- GROUNDING TECHNIQUES
  - CUL-DE-SAC -
    - RELIEVES EXTERNAL STRESSES (SHIELD ROOM)
  - GROUNDING WINDOW -
    - SINGLE AREA CONNECTION ALL CABLES AND CONNECTIONS THROUGH A SINGLE PLATE
  - ELECTRONIC SHIELDED COMPARTMENTS -
    - LIMITED TO 15 METER PER LONGEST SIDE. MAY BE SQUARE
  - CUL-DE-SAC CONSTRUCTION OF COPPER OR ALUMINUM
    - ALUMINUM COMPARTMENTS REQUIRE EXTRA HEAVY FASTENER
  - BOND PER MIL-B-5087 OR EQUIVALENT

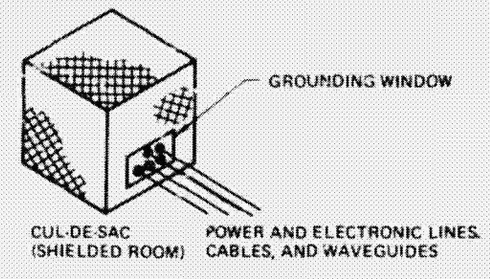

BONDING REQUIREMENTS

- POWER RETURN
- VOLTAGE REFERENCE
- ANTENNA COUNTERPOISE
- STATIC BLEED

GRAPHITE EPOXY STRUCTURE SHOULD NOT BE A POWER RETURN. MAGNESIUM DOES NOT BOND WELL - OFTEN USED.

ANTENNA OPERATION BELOW 50 kHz POWER FLOW IN STRUCTURE IS UNACCEPTABLE.

ANTENNA COUNTERPOISE SHOULD BE MADE OF DEDICATED METAL STRUCTURE MIL-B-5087 CLASS R (2.5 MILLIOHM) JOINTS FOR MULTIPLE FASTENERS.

GRAPHITE - EPOXY

	FIBER	LENGTHWISE	CROSSFIBER
MAX OHMIC VOLTAGE GRADIENT (V/m)	4000	250	4000
MAX OHMIC CURRENT DENSITY ($AMPS/m^2$)	10^8	4×10^5	10^4
CONDUCTIVITY (MHO/m)	20,000 (Holzschuh)	2000	<20 (Scruggs)

- GRAPHITE JOINTS MUST BE TAILORED TO CURRENT RISE (RATE)

  LOW RESISTANCE AT LOW CURRENT LEVELS REQUIRES MORE FIBER CONTACT THAN FOR HIGH CURRENT.

COEFFICIENT OF LINEAR EXPANSION

MATERIAL	PER UNIT EXPANSION
GRAPHITE EPOXY	1.0
ALUMINUM	45
MAGNESIUM	45
STEEL	20
TITANIUM	18

MATERIALS COMPATIBILITY REQUIREMENTS

- THERMAL COEFFICIENTS OF EXPANSION
- GALVANIC POTENTIAL
- SUSCEPTIBILITY TO MOISTURE AND SPACE RADIATION
- VULNERABILITY TO ENVIRONMENTAL ELECTROMAGNETIC HAZARDS

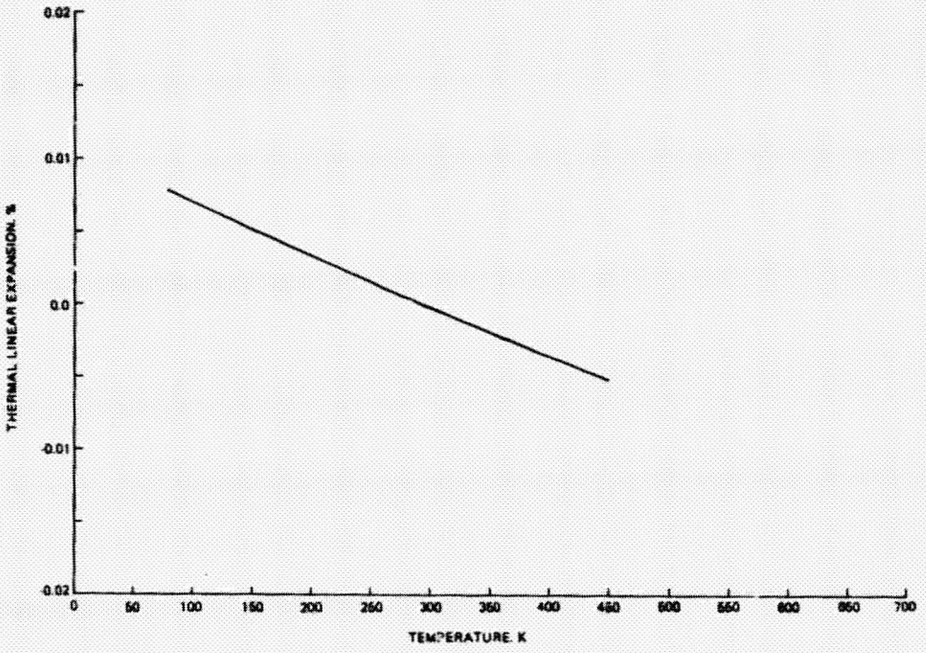

Figure 17.- Longitudinal thermal linear expansion of high strength graphite fiber epoxy composites.

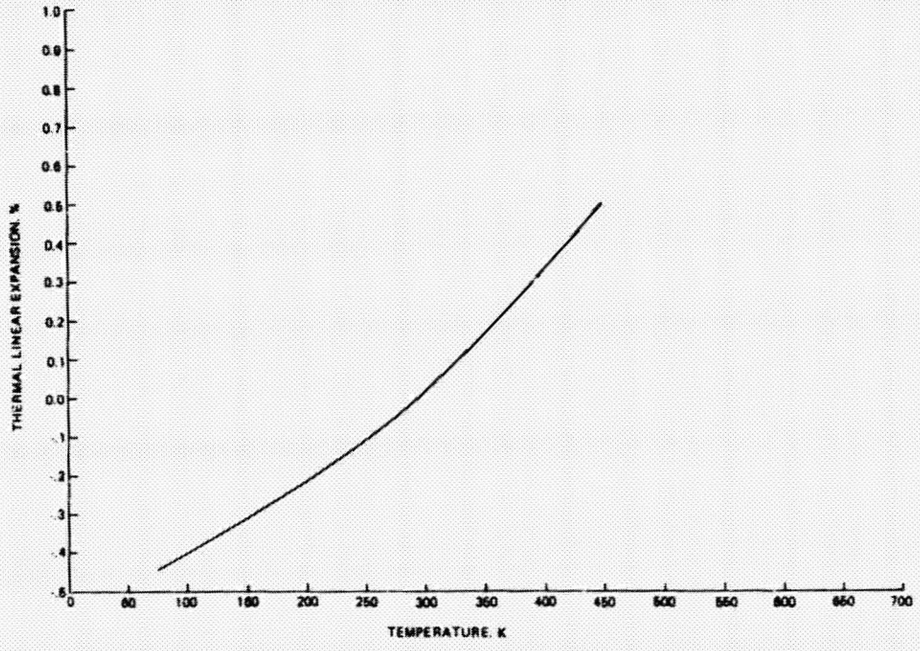

Figure 18.- Transverse thermal linear expansion of high strength graphite fiber epoxy composites.

GALVANIC POTENTIAL

GRAPHITE AND ALUMINUM CAN REACH 2 VOLTS IN MOISTURE. MUST BE SEALED AND MOISTURE-FREE DURING STORAGE OR PAINTED WITH NON-CONDUCTING FINISHES.

MOISTURE AND SPACE RADIATION

- EPOXY HAS A STRONG AFFINITY TO WATER DURING STORAGE.
- COATINGS WILL SEAL IN MOISTURE AND INCREASE OUTGASSING IN SPACE.
- SPACE RADIATION DETERIORATES EXPOSED EPOXY. COATINGS ARE REQUIRED TO PRESERVE STRUCTURAL AND BONDING INTEGRITY OF THE MATERIALS.

RECOMMENDATIONS

IN DESIGNS WHERE GRAPHITE/EPOXY IS COUPLED WITH MATERIALS, FOLLOW THE RULES BELOW:

METAL GROUPING

I	II	III	IV
MAGNESIUM AND MAGNESIUM ALLOYS	ALUMINUM ALLOYS, CADMIUM AND ZINC PLATE	LEAD, TIN, BARE IRON AND CARBON OR LOW ALLOY STEELS	CRES, NICKEL, AND COBALT BASED ALLOYS, TITANIUM, COPPER, BRASS, CHROME PLATE

- DO NOT COUPLE GROUP I, II, OR III METALS DIRECTLY TO GRAPHITE/EPOX .
- WHEN GROUP I, II, OR III METALS ARE WITHIN 3 INCHES OF GRAPHITE/EPOXY AND CONNECTED BY AN ELECTRICALLY CONDUCTIVE PATH THROUGH OTHER STRUCTURES, ISOLATE* THE GRAPHITE/EPOXY SURFACES AND EDGES.
- TITANIUM, CRES (A286 OR 300 SERIES STAINLESS STEEL), NICKEL, AND CORALT-BASED ALLOYS MAY BE COUPLED TO GRAPHITE/EPOXY STRUCTURES. WHEN OTHER GROUP IV METALS ARE COUPLED, ISOLATE* THE GRAPHITE/EPOXY SURFACES AND EDGES.

* ISOLATION SYSTEM:

- ONE LAYER OF TEDLAR; OR TYPE 120 GLASS FABRIC WITH A COMPATIBLE RESIN; OR FINISH.

PARTICULATE PROBLEM

THERE ARE THREE SOURCES OF PARTICULATE DEBRIS CONTAMINATION FOR LARGE STRUCTURE SPACECRAFT. THEY ARE THE EARTH ENVIRONMENT, SPACE ENVIRONMENT AND THE SPACECRAFT ITSELF. PARTICULATES STRIKING THE SPACECRAFT SURFACE, AT HIGH VELOCITY, MAY BREAK LOOSE MUCH MORE MATERIAL TO ADD TO THE PROBLEM.

THE ELECTRIC FIELDS AROUND A HIGH VOLTAGE SURFACE (CONDUCTOR) WILL ACT AS A PRECIPITATOR COLLECTING THE DEBRIS FROM SEVERAL METERS OF SURFACE AREA AS SHOWN IN FIGURE 19. AS THE PARTICULATE ACCUMULATES "BEADS OF PEARLS" WILL FORM TOWARD THE SURFACES OF OPPOSITE POLARITY. IN TIME ARCING WILL TAKE PLACE THROUGH THESE "BEADS OF PEARLS" AS SHOWN IN FIGURE 20.

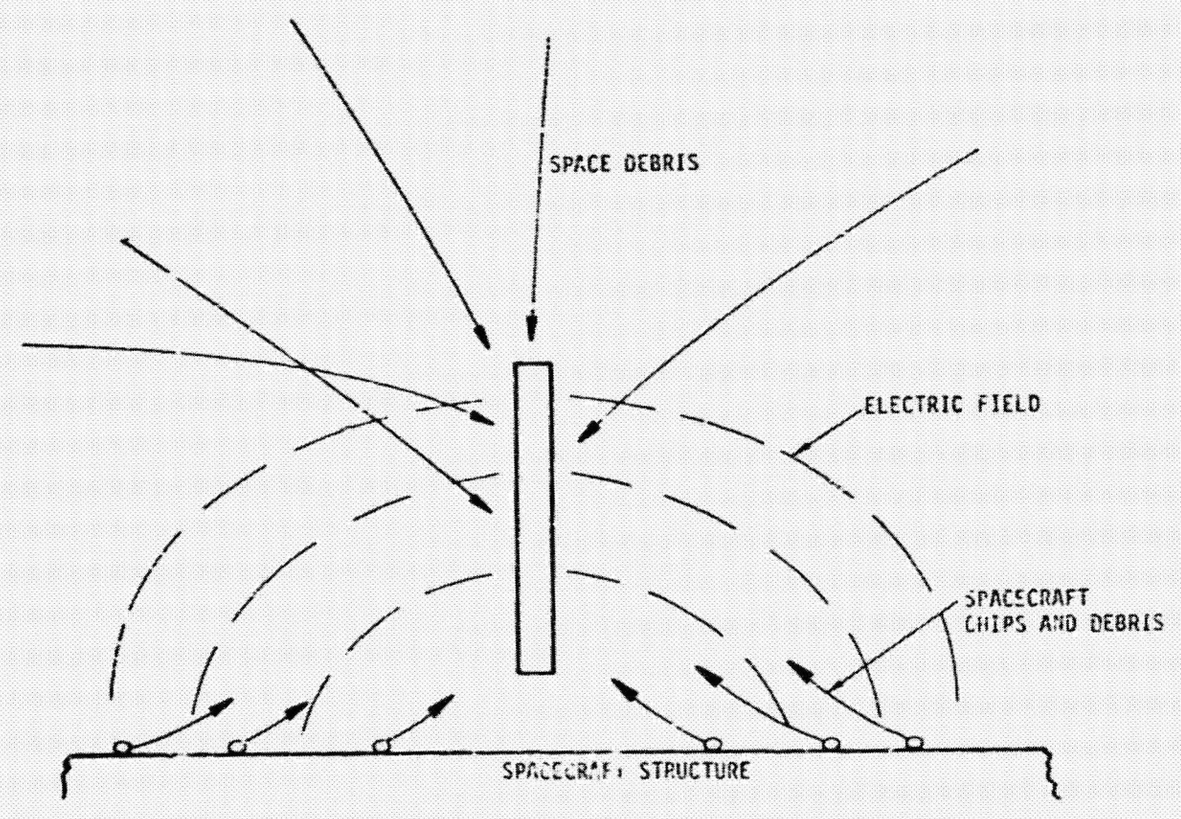

Figure 19.- Particulate damage.

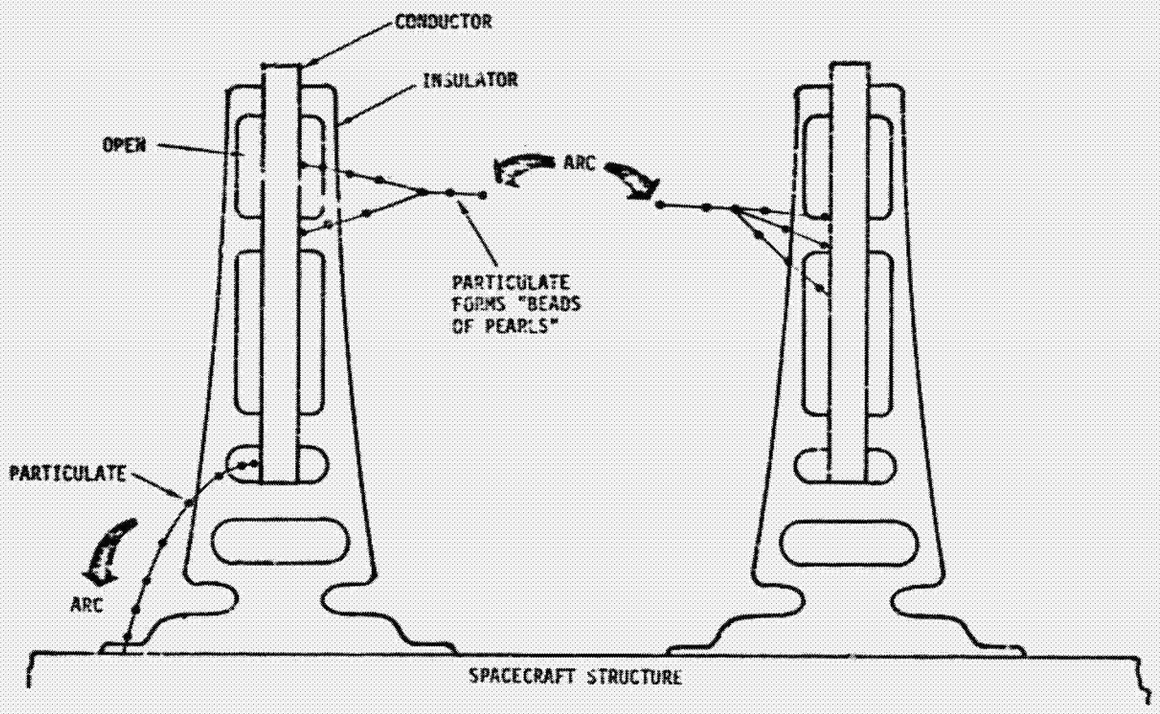

Figure 20.- Particulate damage.

N80-19169

SOLID-STATE SWITCH MODELING

Wilford D. Raburn

The University of Alabama

DISCUSSION

The objective of this work is to predict voltages and currents of passive loads during turn-on and turn-off of remote power controllers (RPC'S). This report will be concerned with two devices built by Westinghouse for NASA, a five ampere device and a twenty ampere device. Both devices can be represented by the general model shown in Figure 1. When the RPC is turned on it will first act as a current source (position 1 of Figure 1) that supplies current to the passive load essentially independent of the elements of the load. This condition will hold until the switch saturates. The switch saturates when the load voltage reaches V_L^1 which is the applied voltage minus the saturated switch drop of about one half volt.

When the load voltage reaches V_L^1, S will switch to position 2 and the load voltage will remain at V_L^1. The load current will be determined by the load parameters and the conditions at switching. The steady state conditions will then be reached according to time constants determined by the load. However if the load current remains above a certain value (approximately 150 percent of rated current) for a period of time (approximately two seconds), a triping mechanism will disconnect the load.

When the RPC is turned off by the controller the load voltage will see an immediate small drop. This is represented in the model of Figure 1 as switching of S from position 2 to position 3. The load voltage will remain at a

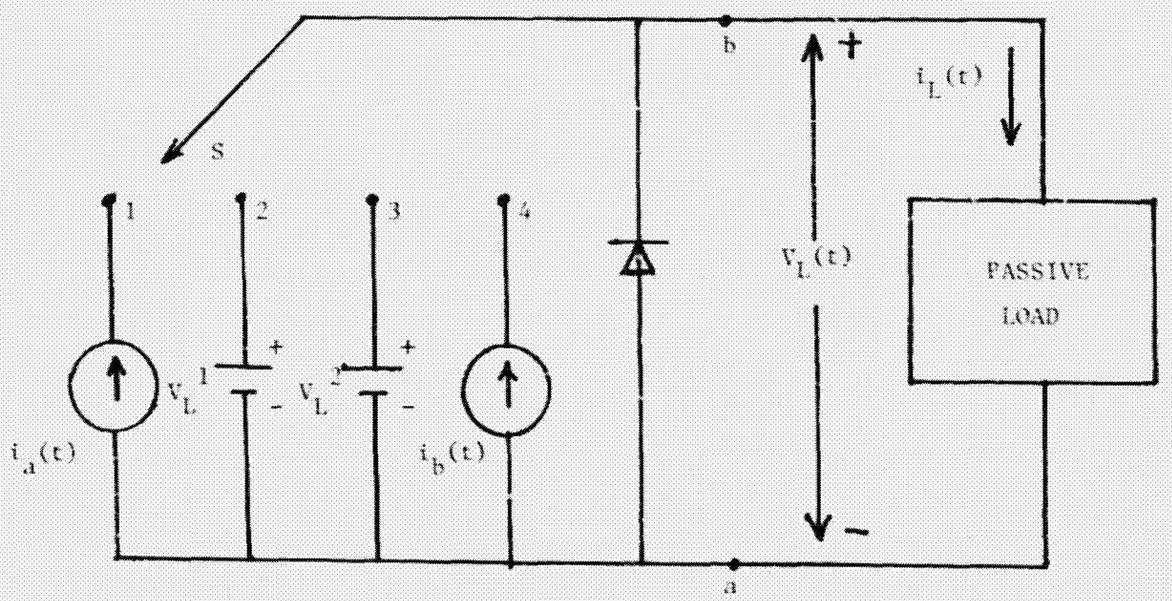

FIGURE 1

constant value V_L^2 for a time, t_s, which is a weak function of the value of load current at switching. After t_s the RPC will again act as a current source. This is represented in Figure 1 with S switching from position 3 to position 4.

The model of Figure 1 contains a diode across the load. Usually this diode is reverse biased and can be ignored. However for certain inductive loads it is possible for the load voltage to go negative. When the load voltage goes negative the diode starts to conduct and the load current is no longer equal i_b of Figure 1. This conduction has been considered in analyzing turn-off of inductive loads. The model will now be used to analyze the turn-on and turn-off of certain loads. Experimental results will be given for comparison. However, the equations of the current and voltages of Figure 1 will first be given. They are:

$$i_a(t) = \frac{I_1}{T_1}\left[t\,U(t) - (t - T_1)\,U(t - T_1)\right] + I_2\left[1 - e^{-\alpha(t - T_1)}\right]U(t - T_1) \tag{1}$$

$$V_L^1 = V_a - V_{ss}^1 \approx V_a - 0.5 \text{ Volts} \tag{2}$$

$$V_L^2 = V_a - V_{ss}^2 \approx V_a - 1.5 \text{ Volts} \tag{3}$$

and

$$i_b(t) = I_3\, e^{-\frac{t - t_s}{\tau}}\, U(t - t_s) \tag{4}$$

R-C Load

The circuit of Figure 2 will be used to analyze a general R-C load. When the RPC is first turned on $i_L(t)$ will equal $i_a(t)$ of Equation 1. Of course $i_L = i_1 + i_2$. The load voltage will be given by

$$V_L = \frac{I_1 R_2}{T_1}\left[\{t - R_2C(1 - e^{-\beta t})\}\,U(t) - \{t - T_1 - R_2C(1 - e^{-\beta(t - T_1)})\}\,U(t - T_1)\right] + R_2 I_2\left[1 + \frac{1}{1 - \alpha/\beta}\{\alpha C R_2\, e^{-\beta(t - T_1)} - (1 - \alpha C R_1)\, e^{-\alpha(t - T_1)}\}\right]U(t - T_1) \tag{5}$$

where $\beta = \frac{1}{C(R_1 + R_2)}$.

The time, T_2, that S switches from position 1 to position 2 is found by the relation

$$V_L(T_2) = V_L^1 \tag{6}$$

After T_2 the voltage, V_L, across the load remains at V_L^1 and the current is given by

$$i_L(t) = \left[\frac{V_L^1}{R_2} + \left(\frac{V_L^1 - V_C(T_2)}{R_1}\right) e^{-\frac{(t - T_2)}{R_1 C}}\right] U(t - T_2) \tag{7}$$

where $V_C(T_2)$ is the capacitor voltage at T_2 and is given by

$$V_C(T_2) = (I_1 + I_2) R_2 + \frac{I_1 R_2 C(R_1 + R_2)}{T_1} \left(e^{-\beta T_2} - e^{-\beta(T_2 - T_1)}\right)$$

$$+ \frac{1}{1 - \alpha/\beta} \left\{\alpha C I_2 R_2 (R_1 + R_2) \left(e^{-\beta(T_2 - T_1)} - e^{-\alpha(T_2 - T_1)}\right)\right\} \tag{8}$$

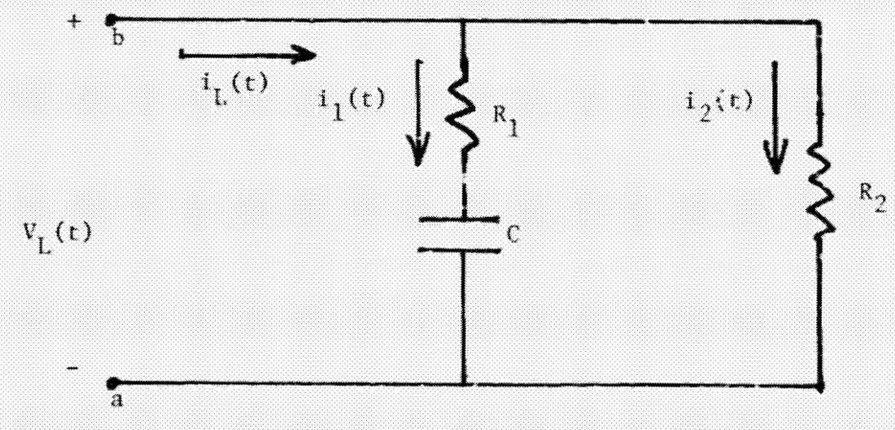

FIGURE 2

For the turn-off assume that a steady state is reached and the RPC is turned off at t = 0. S is then moved from position 2 to position 3. At switching the voltage across the capacitor will be equal to $V_L^1 > V_L^2$ and hence, $i_1(t)$ will at first be negative and the total load current $i_L(t)$ will be less than V_L^2/R_2. The total load current for the range $0 \leq t \leq t_s$ will be given by

$$i_L(t) = \frac{V_L^2}{R_2} - \left(\frac{V_L^1 - V_L^2}{R_1}\right)e^{-t/R_1C} \tag{9}$$

This equation holds until $t = t_s$. Then

$$i_L(t_s) = \frac{V_L^2}{R_2} - \left(\frac{V_L^1 - V_L^2}{R_1}\right) e^{-t_s/R_1C} \cong I_3 \tag{10}$$

At $t = t_s$ the S switches from position 3 to position 4, and

$$i_L(t) = I_3 e^{-(t - t_s)/\tau} U(t - t_s) \tag{11}$$

The load voltage is given by

$$V_L(t) = \left[\frac{R_2 I_3}{C(R_1 + R_2) - \tau}\left\{(R_1C - \tau) e^{-(t - t_s)/\tau} + \frac{2R_2}{R_1 + R_2} e^{-\beta(t - t_s)}\right\}\right.$$

$$\left. + \frac{R_2 V_C(T_3)}{R_1 + R_2} e^{-\beta(t - t_s)}\right] U(t - t_s) \tag{12}$$

Figure 3 shows the turn-on and turn-off characteristics of the R-C load of Figure 2. Traces of the load current versus time are given in Figure 3(a) for two different values of capacitance. The corresponding traces of load voltage versus time are given in 3(b).

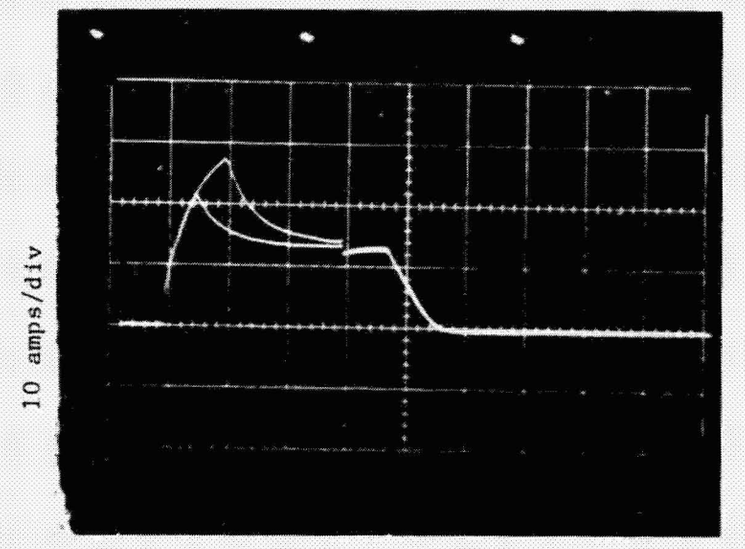

(a)

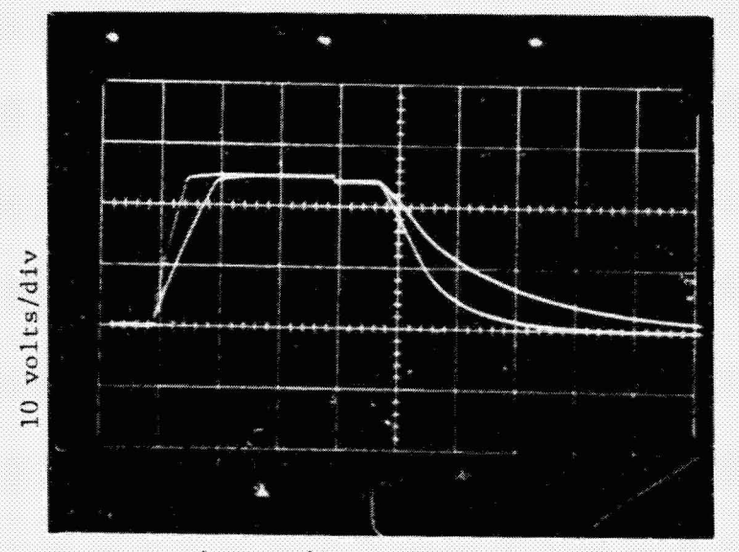

(b)

FIGURE 3

ORIGINAL PAGE IS
OF POOR QUALITY

R-L Load

The R-L load is analyzed the same as the R-C load. For the notation refer to Figure 4. For turn-on, the load current is given by equation (1) for load voltages less than V_L^1. The corresponding load voltage is given by

$$V_L(t) = \frac{I_1}{T_1}\left[\left\{\frac{R_2^2}{\beta(R_1+R_2)}\left(1-e^{-\beta t}\right)+\frac{R_1R_2}{R_1+R_2}\,t\right\}U(t)-\left\{\frac{R_2^2}{\beta(R_1+R_2)}\right.\right.$$

$$\left.\left.\times\left(1-e^{-\beta(t-T_1)}\right)+\frac{R_1R_2}{R_1+R_2}\,(t-T_1)\right\}U(t-T_1)\right]$$

$$+I_2\left[\frac{R_1R_2}{R_1+R_2}-\frac{\alpha R_2^2}{(R_1+R_2)(\beta-\alpha)}\,e^{-\beta(t-T_1)}\right.$$

$$\left.-\frac{1\,R_2(R_1-\alpha L)}{L(\beta-\alpha)}\,e^{-\alpha(t-T_1)}\right]U(t-T_1) \qquad (13)$$

where $\beta = \dfrac{R_1+R_2}{L}$.

Equation (13) is monitored to determine the time T_2 that $V_L(t) = V_L^1$. The load voltage will remain at V_L^1 for $t > T_2$. To determine $i_L(t)$ for $t > T_2$ the value $I_o = i_1(T_2) = i_L(T_2) - V_L^1/R_2$ is first found. It is given by

$$I_o = i_1(T_2) = \frac{I_1}{T_1}\left[\left\{\frac{R_2}{R_1+R_2}\,T_2-\frac{R_2}{\beta(R_1+R_2)}\left(1-e^{-\beta T_2}\right)\right\}\right.$$

$$+\left\{\frac{R_2}{\beta(R_1+R_2)}\left(1-e^{-\beta(T_2-T_1)}\right)-\frac{R_2}{R_1+R_2}\,(T_2-T_1)\right\}\Big]$$

$$+I_2\left[\frac{R_2}{R_1+R_2}-\frac{L\beta-R_1}{L(\beta-\alpha)}\,e^{-\alpha(T_2-T_1)}+\frac{\alpha R_2\,e^{-\beta(T_2-T_1)}}{(R_1+R_2)(\beta-\alpha)}\right. \qquad (14)$$

Then the load current is

$$i_L(t) = \left\{\left(\frac{1}{R_1}+\frac{1}{R_2}\right)V_L^1+\left(I_o-\frac{V_L^1}{R_1}\right)e^{-\frac{R_1}{L}(t-T_2)}\right\}U(t-T_2) \qquad (15)$$

For the turn-off the load voltage will again be V_L^2 for $t < t_s$ and the load current for this time will be

$$i_L(t) = \left(\frac{1}{R_1} + \frac{1}{R_2}\right) V_L^2 + \left[\frac{V_L^1 - V_L^2}{R_1}\right] e^{-\frac{R_1}{L} t} \tag{16}$$

At $t = t_s$ the switch comes out of saturation and the load current is given by Equation (4). To find the value of $i_1(t_s)$, the value of current through the inductor at switching is monitored. It is given by

$$I^o = i_1(t_s) = i_L(t_s) - \frac{V_L^2}{R_2} \tag{17}$$

The load voltage is then given by

$$V_L(t) = \frac{I_3}{\tau(R_1 + R_2) - L} \left\{(\tau R_1 - L)\, e^{-(t - t_s)/\tau} + \tau R_2 e^{-\beta(t - t_s)}\right\} U(t - t_s)$$

$$- R_2 I_o^{\,o}(T_3)\, e^{-\beta(t - t_3)} U(t - t_s) \tag{18}$$

The above analysis is complete except for certain R-L loads that will drive the load voltage negative. If the load voltage goes more negative than the built-in voltage of the diode (few tenths of a volt) the diode will start to conduct and must be included in the analysis. For this analysis assume

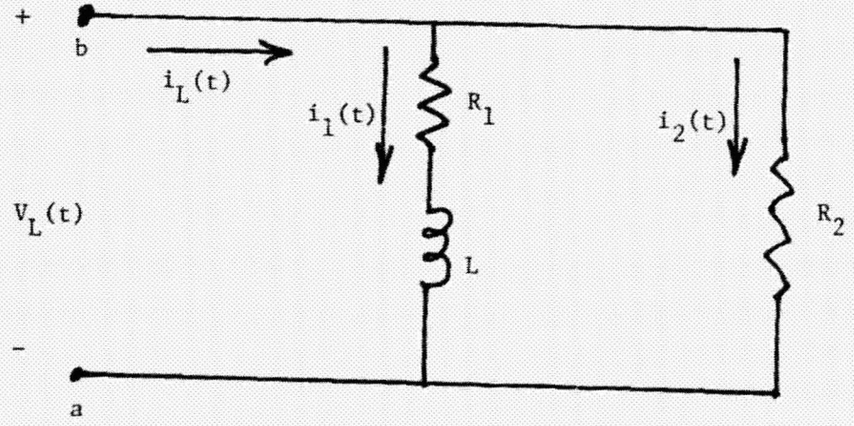

FIGURE 4

$V_L(t) = -V_{bi}$ at $t = T_4$. The value of T_4 can be determined from equation (18). Again the value of current through the inductor at T_4 must be determined. This value is given by

$$I_o^o = i_1(T_4) = i_L(T_4) + \frac{V_{bi}}{R_2} \tag{19}$$

Assuming that the diode can be modeled with a resistance γ_d the load voltage and current for $t > T_4$ are given by

$$V_L(t) = \frac{I_3 R_2}{\tau(R_2 + R_1) - L}\{(\tau R_1 - L)\, e^{-(t - t_s)/\tau} + \tau R_2\, e^{-\beta(t - t_s)}\}\, U(t - t_s)$$

$$- R_2 I_o^o(T_4)\, e^{-\beta(t - T_4)}\, U(t - T_4) \tag{20}$$

and

$$i_L(t) = \frac{R_2 I_o^o(T_4)}{\gamma_d} e^{-\beta(t - T_4)} U(t - T_4) + I_3\left[1 - \frac{R_2(\tau R_1 - L)}{\gamma_d\{\tau(R + R_1) - L\}}\right]$$

$$e^{-(t - t_s)/\tau}\, U(t - T_3) - \frac{I_3 \tau R_2^2}{\gamma_d\{\tau(R + R_1) - L\}} e^{-\beta(t - t_s)}\, U(t - T_s) \tag{21}$$

Figure 5 shows the turn-on and turn-off characteristics for a R-L load. Figure 5(a) is traces of the load currents versus time for two different values of R_1 and L. Figure 5(b) shows the corresponding traces of load voltage versus time. In each case the load configuration of Figure 4 was used.

All the experimental results were obtained using the Westinghouse twenty ampere RPC. Two Sears Die Hard batteries were connected in series and used as the power supply. The control signal was from a Hewlett Packard 214 pulser with a pulse rate low enough so that all transients in the RPC and the load would completely vanish before the next pulse.

The parameters for Equations (1) and (4) were obtained by using pure resistive loads and fitting experimental results to the equations. The values were found to be: $T_1 = 0.1$ m sec, $I_1 = 3.5$ amps, $I_2 = 27.3$ amps, $\alpha = 0.9$ /m sec, $t_s = t_o - K_1 I_3$ (where $t_o = 1.86$ m sec and $K_1 = 0.027$ m sec/amp) and $\tau = \tau_o + K_2 I_3$ (where $\tau_o = 0.39$ m sec and $K_2 = 0.076$ m sec/amp).

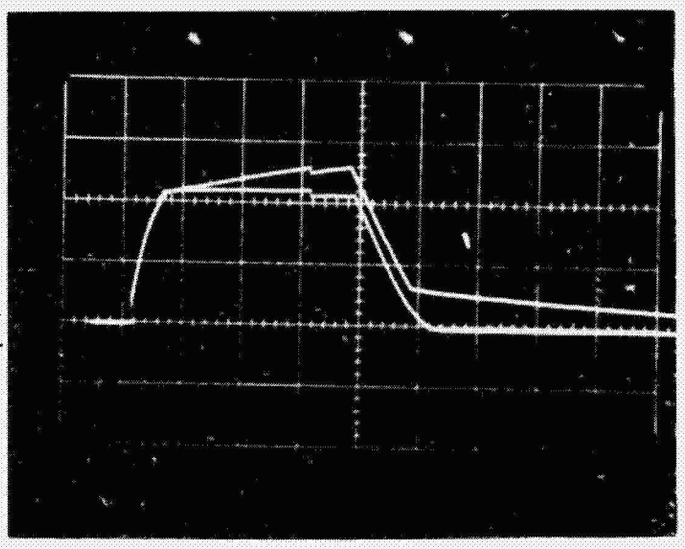

(a)

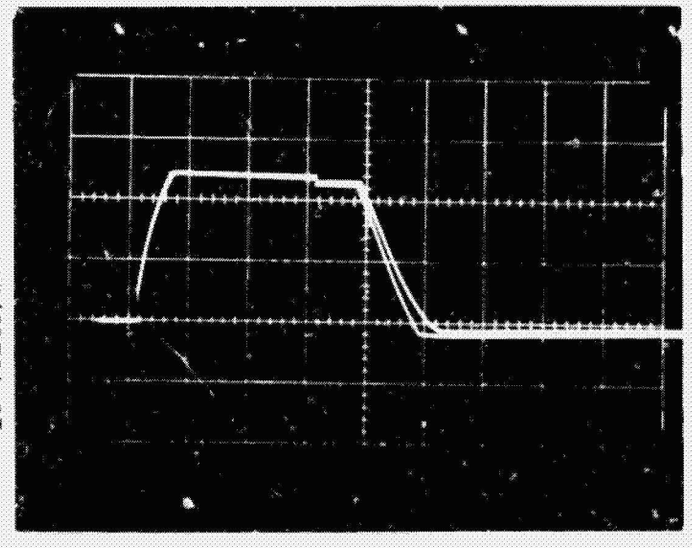

(b)

FIGURE 5

ORIGINAL PAGE IS
OF POOR QUALITY

N80-19170

FY 79 - DEVELOPMENT OF FIBER OPTICS
CONNECTOR TECHNOLOGY FOR LARGE SPACE SYSTEMS

Thomas G. Campbell
Langley Research Center
November 8, 1979

DEVELOPMENT OF FIBER OPTICS
TECHNOLOGY FOR LARGE SPACE STRUCTURES

OBJECTIVE:

TO DEVELOP PHYSICAL CONCEPTS FOR INTEGRATING FIBER OPTIC CONNECTORS AND CABLES WITH STRUCTURAL CONCEPTS PROPOSED FOR LSST. EMPHASIS IS PLACED ON REMOTE CONNECTIONS USING INTEGRATED CABLES.

The inherent advantages in using a fiber optics communications system are listed below

F/O COMMUNICATION SYSTEM QUALITIES

- HIGH DATA RATES
- NO CROSS TALK
- NO EMI
- SECURE COMMUNICATIONS
- LIGHT WEIGHT

The LSST Electronics development plan is shown below. This plan separates the fiber optic activity from the basic connector/cabling activity that is under the management of the Marshall Space Flight Center.

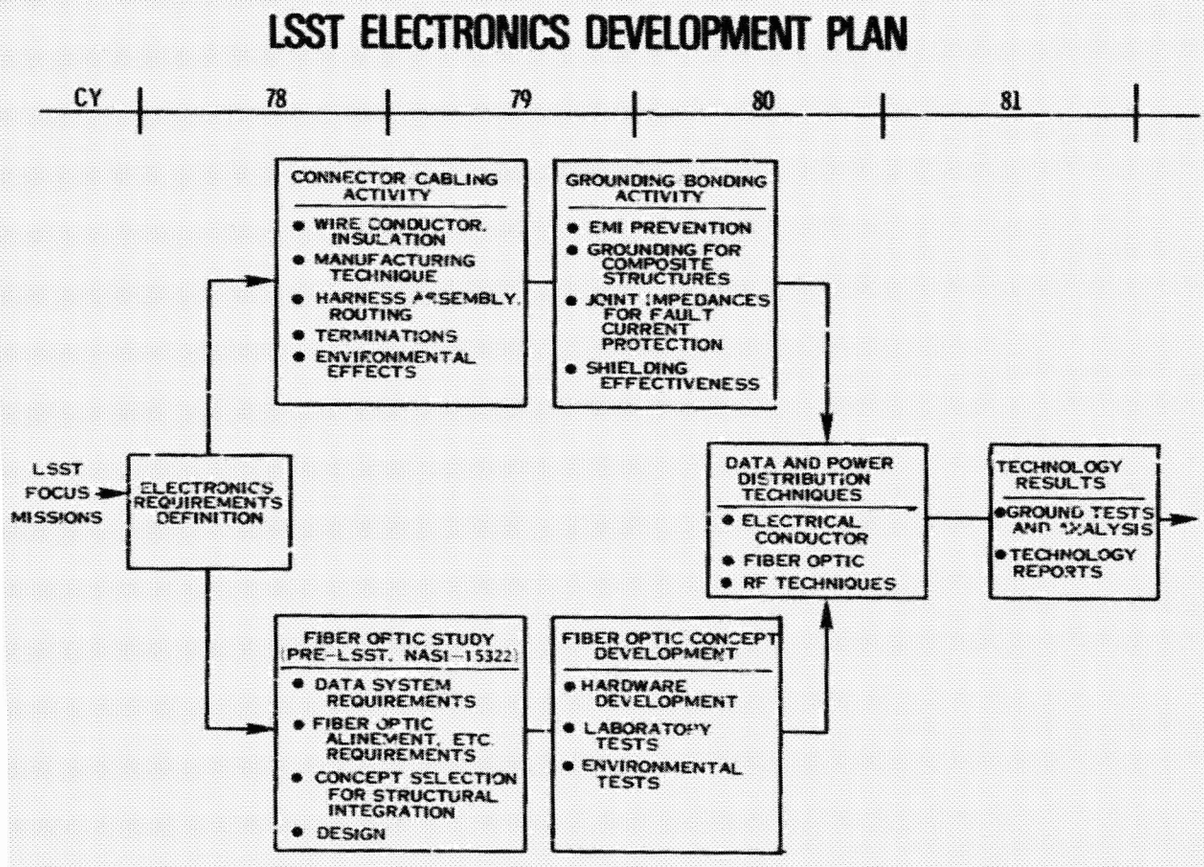

The fiber optics development effort for large space structures was initiated with a specific structured element in mind, specifically, the nestable column as shown below. The F/O connector is being developed to be compatible with the union joint cluster and the assembly concept using the End-Effector of the Shuttle RMS.

NESTABLE COLUMN

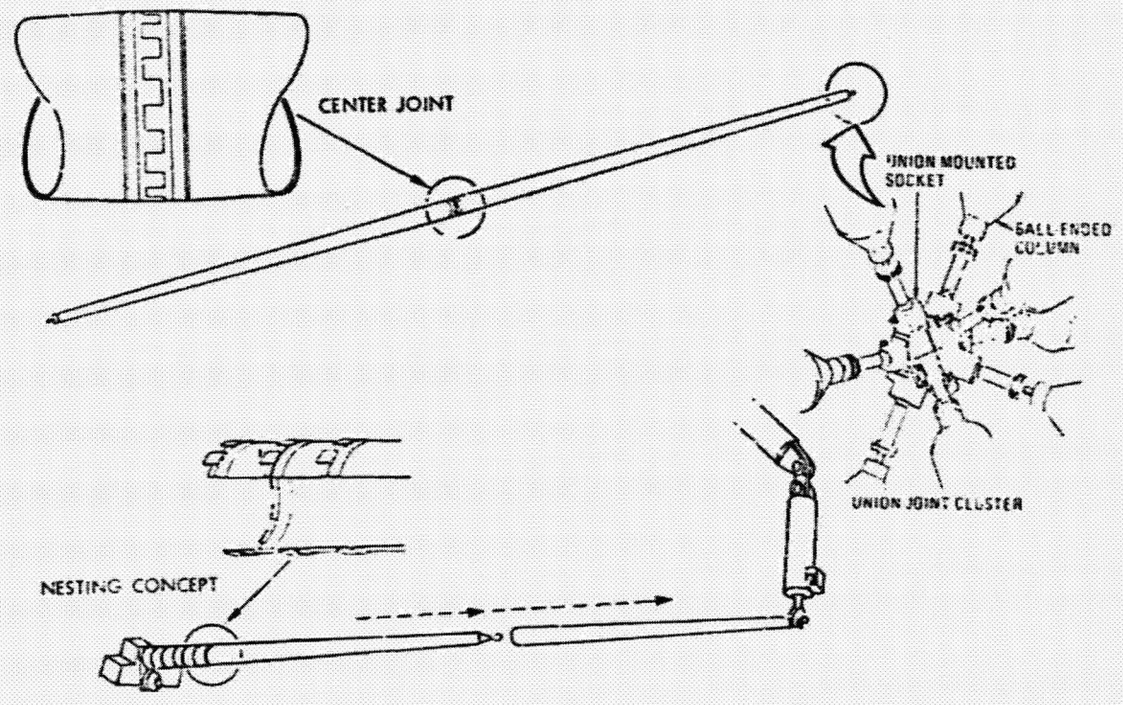

This figure shows the basic concept of integrating the F/O connector into the large space structure.

ANTENNA TO CENTRAL PROCESSOR CABLE PATH

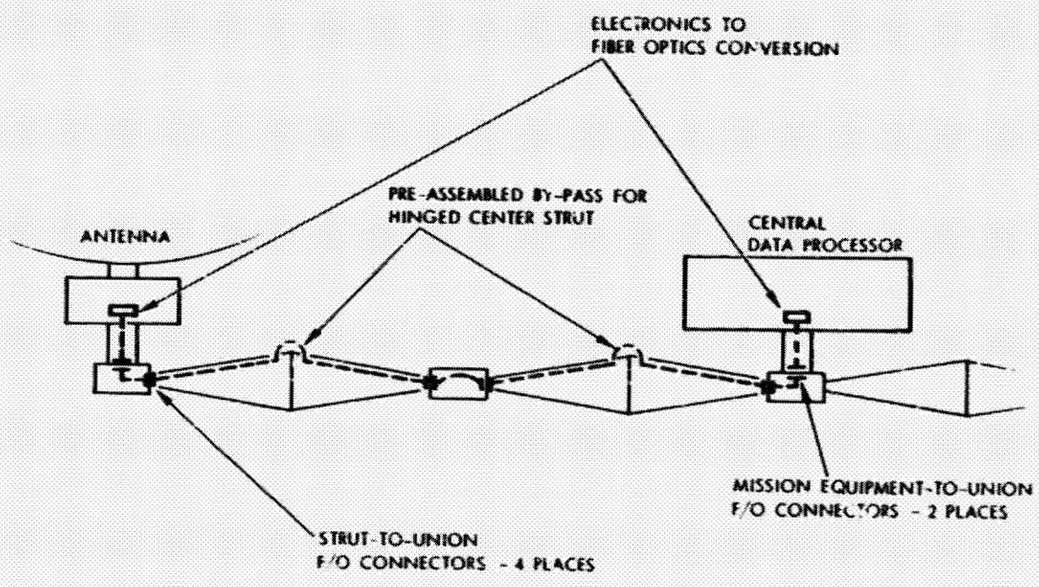

The Electronic Mail Satellite (EMS) concept shown below was used to define the requirements for the fiber optics development effort.

TASK 1 MODEL SYSTEM
ELECTRONIC MAIL SATELLITE

550 POSTAL CENTERS
48 M PAGES MAIL/24 HRS (AV)
5 OPERATING AREAS
5 ACTIVE IN-ORBIT ANTENNAS
+1 SPARE
110 CHANNELS/ANTENNAE

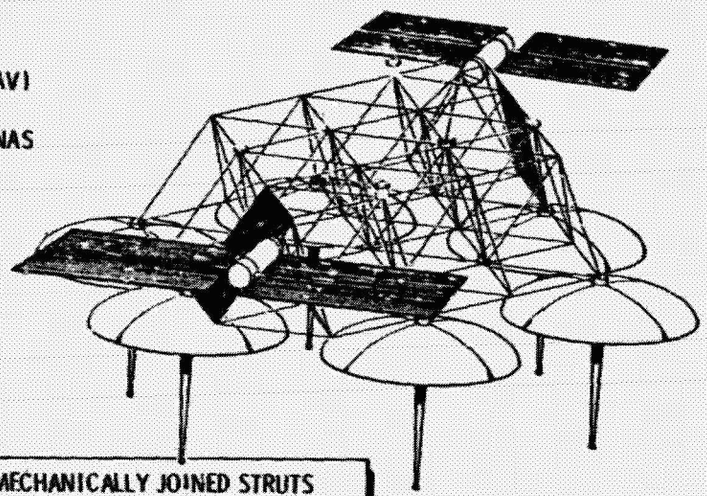

STRUCTURE: MECHANICALLY JOINED STRUTS
129 STRUTS, EA 15M LONG
33 UNIONS, EA 17 CM DIA

DIMENSIONS: LENGTH 96M
WIDTH 61M
HEIGHT 12M

WEIGHT: 37,280 LB (DRY)

A schematic wiring diagram for the conceptual EMS system is shown below.

SCHEMATIC WIRING DIAGRAM, COMMUNICATIONS, FOR EMS MODEL

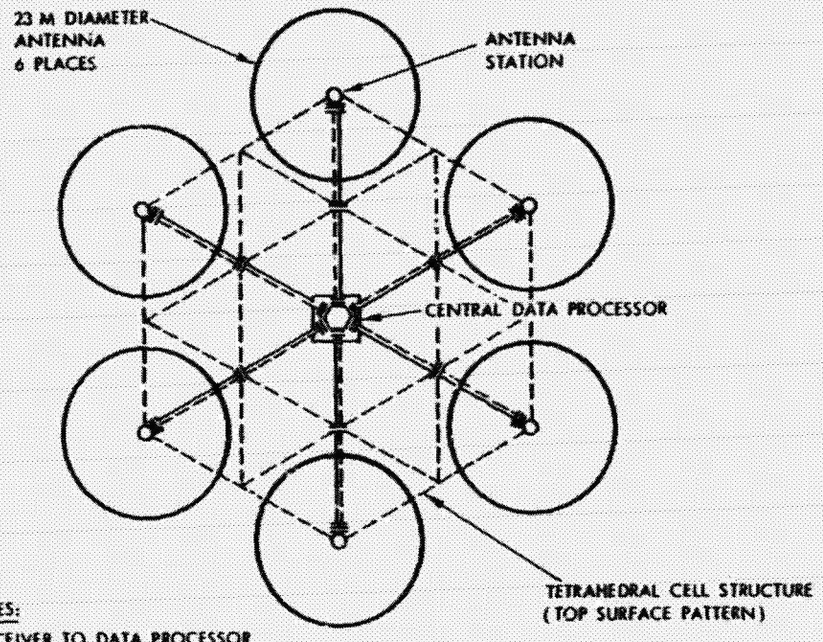

The requirements proposed for the Electronic Mail Satellite mission scenario are presented below. Also presented is a comparison of various cable systems and the weight reduction that a typical F/O system would have over conventional systems.

REQUIREMENTS PROPOSED FOR ELECTRONIC MAIL SATELLITE

- FREQUENCY: 3 GHz
- 110 CHANNELS PER STATION (6 STATIONS)
- 4 DATA LINES PER STATION
- 4 CONTROL LINES PER STATION
- SEGMENT LENGTH: 32.2 METERS
- FIVE REFLECTORS, ONE SPARE
- TOTAL CABLE REQUIRED: 42.5 KM (141,666 FEET)
- DATA RATE = 85 MBPS PER DATA LINE
- BANDWIDTH = 100 MHz
- BER = 10^{-9}
- S/N = 13 DB
- F/O LINES PER BRANCH: 8

CABLE COMPARISON

CABLE	LOSS	WEIGHT
SHIELDED TWISTED PAIR	198 DB/KM	4,014 LB
SEMI-RIGID	92 DB/KM	11,687 LB
COAX	294	944 LB
FIBER OPTIC	20	41 LB

The various power and signal installation options are shown below. Option D is the desired configuration for the F/O distribution system.

POWER AND SIGNAL INSTALLATION OPTIONS

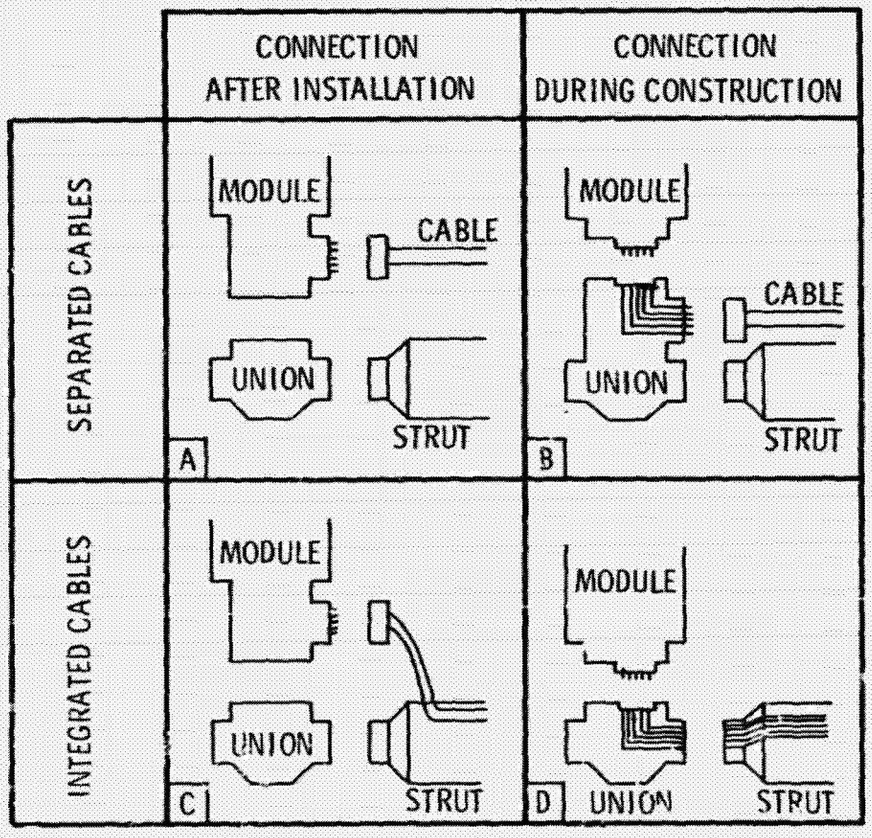

Based on requirements for the EMS system and an assessment of F/O technology, the following critical technologies were identified.

CRITICAL TECHNOLOGY IDENTIFIED

1. F/O CABLE TECHNOLOGY

- A SINGLE FIBER AND/OR MULTI-FIBER BUNDLES ARE REQUIRED THAT CAN WITHSTAND RADIATION EFFECTS (10^7 RADS) AND TEMPERATURE EXTREMES AS WELL AS PROVIDE SUFFICIENT CORE DIAMETER FOR CONNECTOR ALINEMENT.

(NO CABLE EXISTS AT THIS TIME THAT CAN MEET THESE REQUIREMENTS.)

2. CONNECTOR TECHNOLOGY

- A CONNECTOR IS REQUIRED THAT WOULD BE COMPATIBLE WITH CABLE DESCRIBED ABOVE.
- AN ASSEMBLY CONCEPT IS REQUIRED FOR MATING F/O CONNECTORS REMOTELY WITHIN STATE-OF-THE-ART LOSSES.

3. STRUCTURE INTEGRATION TECHNOLOGY

- METHODS MUST BE DEVELOPED FOR INTEGRATING F/O COMPONENTS INTO STRUCTURAL ELEMENTS.

The F/O integrated connector assembly presently being developed by Rockwell International is shown below. This connector assembly shall be used to test two commercially available F/O connectors - (Amphenol and Hughes). These connectors will be assembled and tested so that the various system losses can be determined.

INTEGRATED CONNECTOR ASSEMBLY

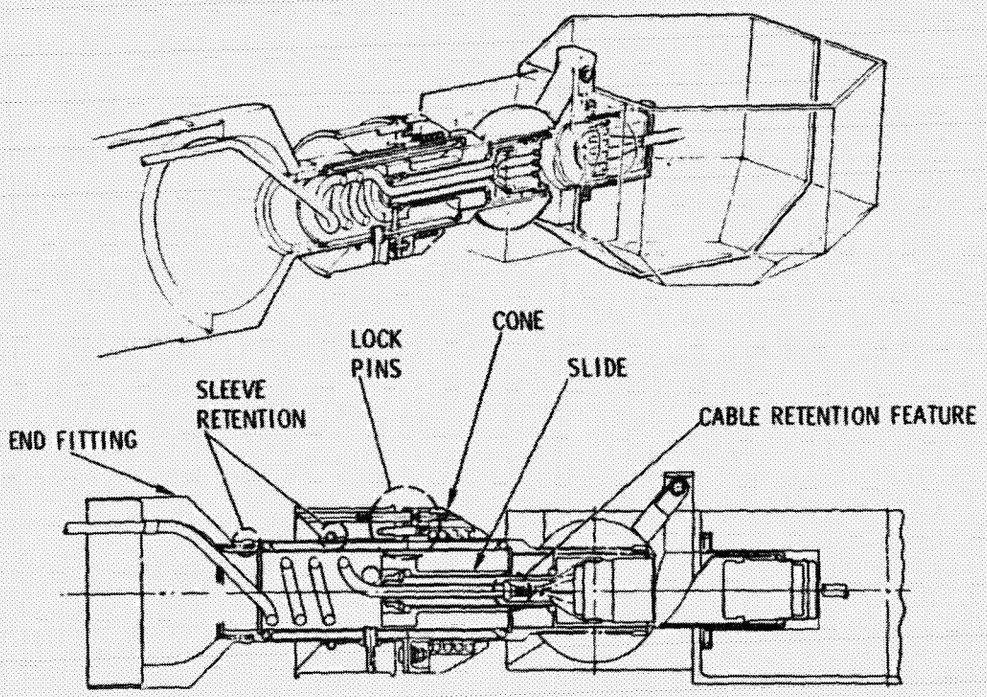

The Amphenol 8-Channel F/O connector is shown below.

AMPHENOL 8-CHANNEL FIBER OPTIC CONNECTOR

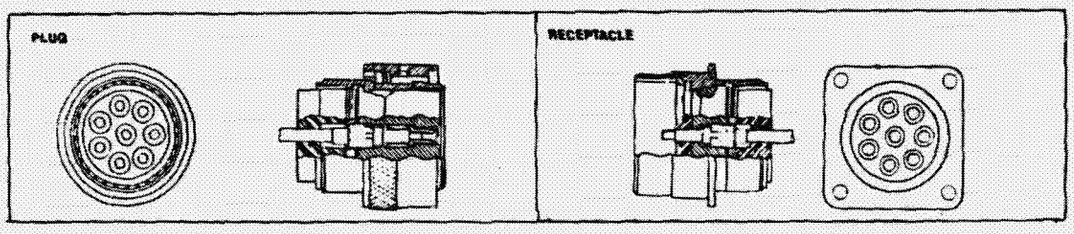

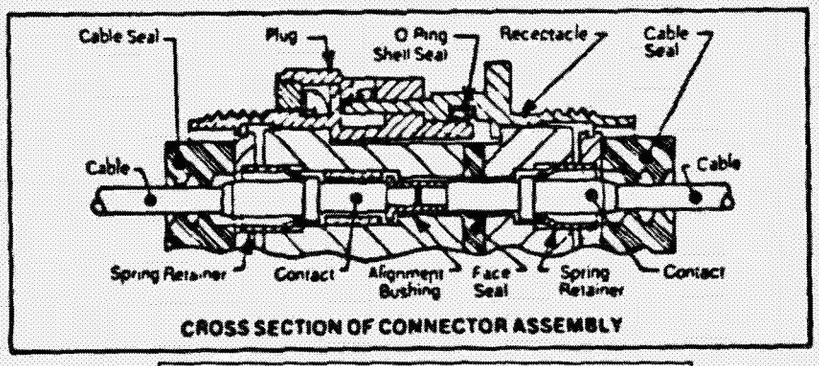

CROSS SECTION OF CONNECTOR ASSEMBLY

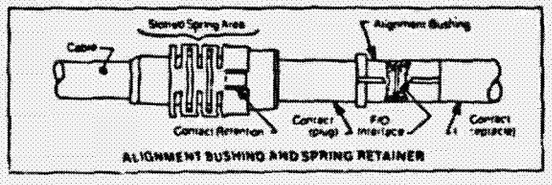

ALIGNMENT BUSHING AND SPRING RETAINER

The Hughes 8-Channel F/O connector is shown below.

HUGHES 8-CHANNEL FIBER OPTIC CONNECTOR

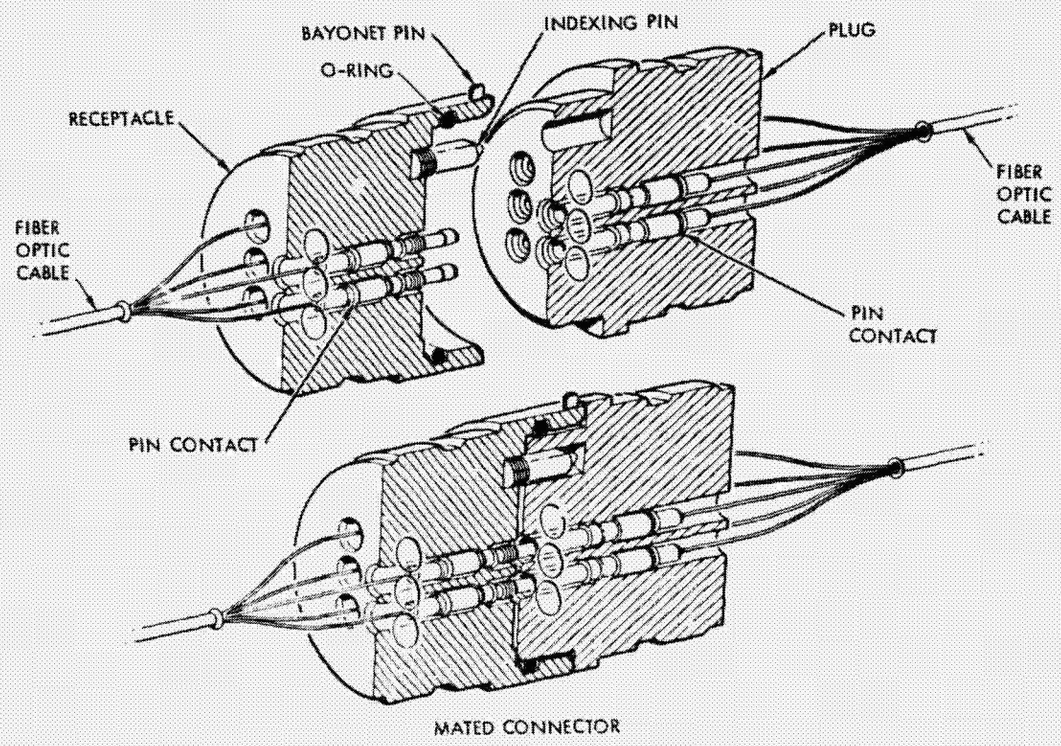

After the F/O Integrated Connector Assembly is fabricated,the following tests shall be conducted.

LARGE SPACE STRUCTURES

PROPOSED CONNECTION TESTS

- MEASURE FIBER OPTICS LIGHT LOSSES OF ASSEMBLY
- PERFORM REPEATED MATE/DEMATE OPERATIONS
- MEASURE LIGHT LOSSES DURING TEST CYCLE
- IDENTIFY LOSS PORTIONS
- MODIFY CONNECTION ASSEMBLY TO REDUCE LIGHT LOSSES
- REPEAT CYCLIC TESTS
- PREPARE TEST REPORT

N80-19171

FLEXIBLE MATERIALS TECHNOLOGY

W. H. Steurer
Jet Propulsion Laboratory
Pasadena, California

LSST 1ST ANNUAL TECHNICAL REVIEW

November 7-8, 1979

OBJECTIVES

The study program was focused at four major objectives as follows:

First, an identification of flexible components -- specific components for Phase II systems and typical components for a wide spectrum of potential large space systems, including Phase I systems.

Second, the definition of the material requirements for the identified flexible components in terms of material types, forms and typical or critical properties, and the generation of applicable materials data for near-term systems.

Third, the assessment of the interrelation between the characteristics of flexible materials and systems performance. This was to be demonstrated in quantitative terms for specific designs and materials of large deployable antennas.

The ultimate objective of the study was the identification of advanced material concepts and the formulation of a plan for the required materials Research and Development.

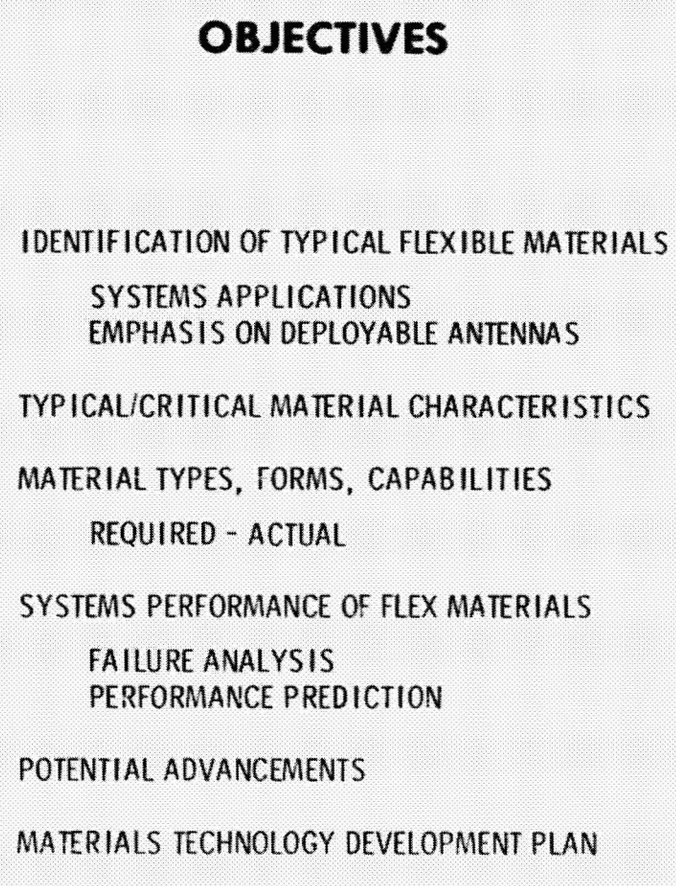

ACCOMPLISHMENTS

A survey of all presently defined or proposed large space systems indicated an ever-increasing demand for flexible components and materials, primarily as a result of the widening disparity between the stowage space of launch vehicles and the size of advanced systems. Typical flexible components and material requirements were identified on the basis of recurrence and/or functional commonality. This was followed by the evaluation of candidate materials and the search for material capabilities which promise to satisfy the postulated requirements. Particular attention was placed on thin films, and on the requirements of deployable antennas. The assessment of the performance of specific materials was based primarily on the failure mode, derived from a detailed failure analysis. In view of extensive ongoing work on thermal and environmental degradation effects, prime emphasis was placed on the assessment of the performance loss by meteoroid damage. Quantitative data were generated for tension members and antenna reflector materials. A methodology was developed for the representation of the overall materials performance as related to systems service life. A number of promising new concepts for flexible materials were identified. Work on a proposed materials R & D plan is still in progress.

ACCOMPLISHMENTS

- TYPICAL FLEXIBLE MATERIALS, APPLICATIONS AND REQUIREMENTS IDENTIFIED
- MATERIALS EVALUATED
  - PROPERTIES
  - THIN FILMS
  - DEPLOYABLE ANTENNAS
- SYSTEMS PERFORMANCE ANALYZED
  - SYSTEMS REQUIREMENTS, ENVIRONMENTS
  - FAILURE MODES
  - PERFORMANCE PREDICTION
  - EMPHASIS ON METEOROID HAZARD
- POTENTIAL ADVANCEMENTS IDENTIFIED
- R&D PLAN IN PREPARATION

FLEXIBLE COMPONENTS OF DEPLOYABLE SPACE ANTENNAS

The purpose of this figure of two deployable antennas is to illustrate the extensive use of flexible materials in large space systems. Flexible components are identified by bold lines and rigid components by dotted lines. Note the predominance of flexible materials.

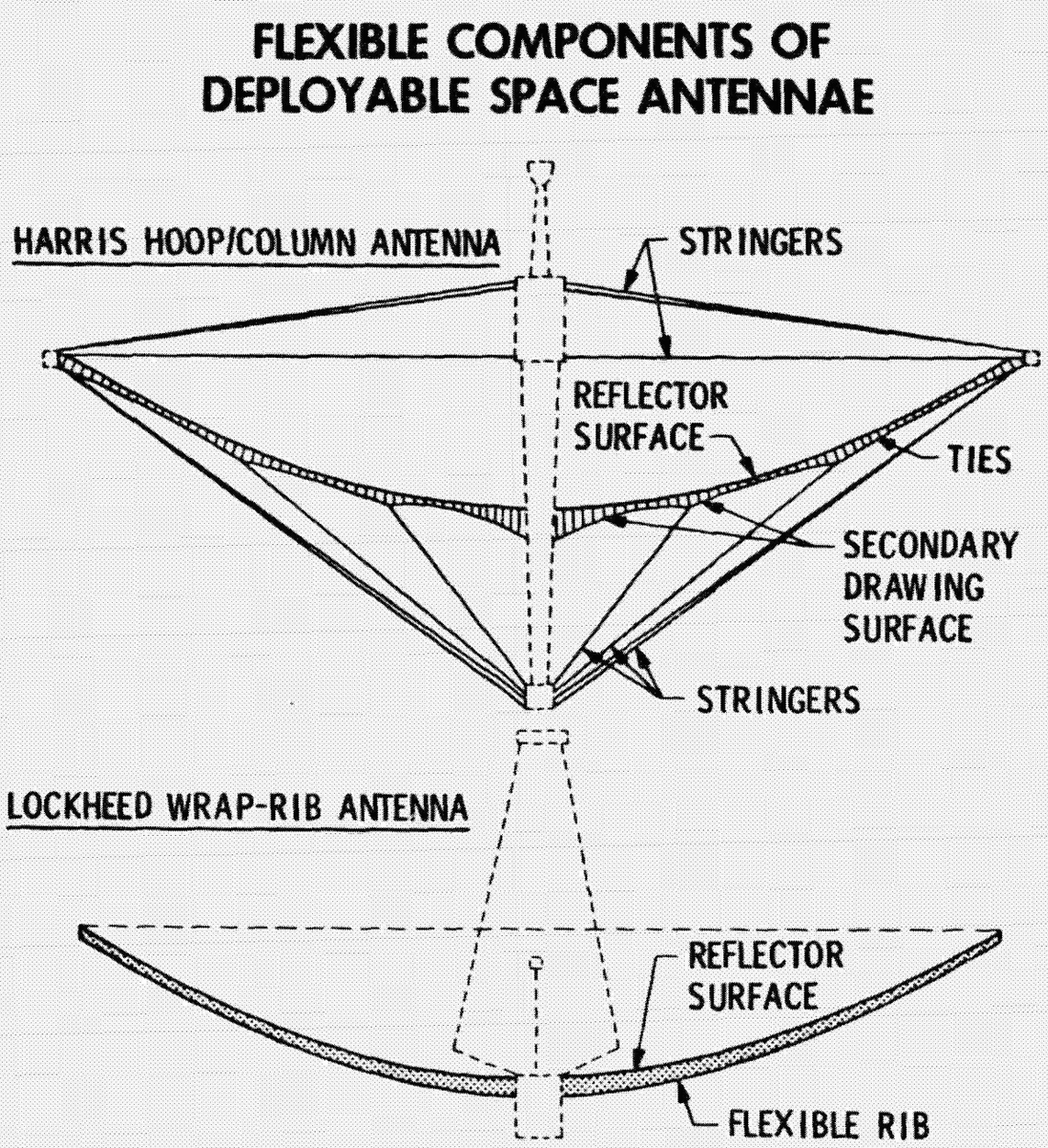

TYPICAL FLEXIBLE COMPONENTS AND MATERIALS

There is a wide variety of flexible components with an equal variety of forms and material types. The fundamental requirement of all flexible components is a purely elastic material deformation in stowed condition. Most widely used are membranes, meshes or fabrics for large reflective surfaces (RF, light etc.) and cables, tapes or single filaments for tension members. Both applications involve thin materials in the form of films or wires (fibers) to preclude any plastic deformation during stowage. The only flexible component with substantial wall thickness is, at least at present, the wrap-rib; it is, however, also only elastically deformed in stowed conditions. In the case of extendible booms and vanes, both the surface material (film, fabric) and the supporting structural elements are stowed elastically. The use of metal foil for deployable drag shields calls for a controlled stowage configuration (wave pattern between ribs) to assure purely elastic deformation.

TYPICAL FLEXIBLE COMPONENTS AND MATERIALS

COMPONENTS	FORMS	MATERIALS
REFLECTOR SURFACES	KNIT MESH WEAVE MESH MEMBRANES	COATED METAL WIRE METALLIZED POLYMER YARN METALLIZED POLYMER FILM
TENSION MEMBERS STAYS STRINGERS TIES	CABLES CORDS TAPES WIRES	DIELECTRIC COMPOSITES SILICA, POLYMERS GRAPHITE FIBER COMPOSITES INVAR WIRE
FLEXIBLE RIBS	LOW CTE LAY-UP COMPOSITES	GRAPHITE/POLYMER GRAPHITE/AL OR MG
FLEXIBLE JOINTS	"CARPENTER TAPE" ELASTIC HINGES	SPRING METAL FOIL
EXTENDIBLE BOOMS	THIN-WALL CYLINDERS	REINFORCED THIN FILMS WIRE GRIDS
STATION KEEPING VANES	TENSIONED MEMBRANES ELASTIC FRAMES	METALLIZED POLYMER FILM GRAPHITE FIBER COMPOSITE
DRAG SHIELDS	METAL FOIL	NI-BASE SUPER ALLOYS

FLEXIBLE MATERIAL PROPERTIES

In the definition of material requirements and capabilities a distinction is made between basic and specific properties. Basic properties are those which apply to flexible materials for space structures in general, such as flexibility for stowage and deployment, or dimensional stability and resistance to space environments in service. Some components call for additional material capabilities, designated as specific properties.

Emphasis was placed on thermal properties (thermal expansion, conductivity, cycling), creep (particularly applicable to polymers), optical surface properties, environmental materials degradation and failure due to meteoroid impact. It was attempted to relate all properties to their individual or collective effect upon systems performance and useful service life.

REQUIRED MATERIAL PROPERTIES

BASIC PROPERTIES

- FLEXIBILITY (ELASTICITY)
  - STOWAGE
  - DEPLOYMENT
- DIMENSIONAL STABILITY
  - LOW THERMAL EXPANSION
  - LOW PLASTIC DEFORMATION
  - NO CREEP
- LOW DENSITY
- OPTICAL SURF. PROPERTIES
- RESISTANCE TO SPACE ENVIRONMENT
  - VACUUM
  - UV AND HIGH ENERGY RADIATION
  - MICROMETEOROID IMPACT

ADDITIONAL SPECIFIC PROPERTIES

REFLECTOR SURFACES
- ADAPTABILITY TO METALLIC COATING (Ag, Au)
- SURFACE INTEGRITY DURING STOWAGE

TENSION MEMBERS
- HIGH STRENGTH
- HIGH MODULUS
- HIGH ELASTIC RANGE

FLEX RIBS
- HIGH STIFFNESS AS DEPLOYED
- ADEQUATE THERMAL CONDUCTIVITY

FLEX JOINTS
- HIGH ELASTIC MODULUS AND RANGE

THIN FILM APPLICATIONS

Thin film applications comprise active functions (RF reflectors, light reflectors, drag shields), primary structural functions (extensible booms, inflatable systems) or structural support functions (solar array substrate). With the exception of the drag shield where high temperatures call for metal foil, all applications involve polymer films, either plain, metallized or reinforced. For antenna reflectors in the GHz regime the usefulness of polymer films is questionable, even with active shape control, due to progressive plastic deformation. Self-rigidizing films appear to have considerable potential; they are, however, completely undeveloped.

THIN FILM APPLICATIONS

APPLICATIONS	SPACE	ENERGY	FILM MATERIAL	R&D	ENGG.
ANTENNA REFLECTORS	●		METALLIZED POLYMER	√	√
SOLAR ARRAY SUBSTRATE	●	●	POLYMERS	√	√
" – CONCENTRATORS	●	●	METALLIZED POLYMER	√	√
SOLAR REFLECTORS - FLAT	●	●	"	√	
SOLAR CONCENTRATORS	●	●	"	√	√
EXTENDABLE BOOMS	●		REINFORCED POLYMERS	√	
SOLAR SAIL / VANES	●		METALLIZED POLYMER	√	√
ENV. SHIELDS, ENCLOSURES	●		"	√	
DRAG SHIELDS (AEROBRAKE)	●		METAL FOIL	√	√
GAS FILLED LENSES	●		POLYMERS	√	
INFLATABLE STRUCTURES	●	(●)	"	√	
" – RIGIDIZED	●	(●)	SELF-RIGIDIZING POLYM.	√	

PROPERTIES OF POLYMER FILMS

The most important property of thin films for space applications is the resistance to high-energy radiation; the materials in the chart are, therefore, arranged in the order of decreasing radiation threshold value (with the exception of parylene placed at the bottom as it is unstable in air, yet stable at synchronous altitude). Some polymers, such as epoxies or polystyrene, are even more resistant, but not available as films.

The effectiveness of a film material depends on the specific application. Most cases call for a combination of low environmental degradation, low thermal expansion, reasonably low density and reasonably high strength and temperature stability. In this combination of requirements, polyimide outranks all other film materials.

PROPERTIES OF POLYMER FILMS

	CTE 10^{-5}	ρ g/cc	F_{tu} ksi	M_T ksi	TEMP. °C	RAD 10^X
POLYIMIDE (KAPTON)	2.5	1.42	25	430	350	8.5-9.5
MYLAR	5.3	1.38	25	550	150	6.5-7.5
POLYCARB. (LEXAN)	3.8	1.20	9	290	135	6.5-7.5
TEFLON FEP	8-10	2.15	3	70	200	5-6
TEFLON PFA	7-11	2.15	7	70	260	5-6
POLYSULFONE	3.1	1.24	12	450	150	5-6
PARYLENE*	3.5	1.12	7		350	9

*NOT STABLE IN AIR

COMPARISON OF ANTENNA MESH MATERIALS

This chart is designed to convey an overview of the merits of typical antenna mesh materials. It compares the two predominantly used materials, molybdenum wire and polymer yarn, with the potential advanced materials, graphite yarn, and with plain silver wire as reference. The significant properties are electrical resistance, thermal expansion and density. As all materials are coated with silver or gold, they exhibit the same electrical surface properties. The added significance of the coefficient of thermal expansion is reflected in the merit function 1/R (silver wire = unity). The superiority of molybdenum wire over polymer yarn is reversed if we also account for mesh weight (merit function $1/R\alpha$).

Even though graphite yarn mesh is not yet available, the extremely high merit values make a strong case for a development effort.

COMPARISON OF ANTENNA MESH MATERIALS

WIRE OR YARN	COATING	RESIST. R $\mu\Omega$cm	CTE $10^{-6}/^{0}C$	DENS. ρ g/cc	MERIT FUNCTIONS $\frac{1}{R}$	$\frac{1}{R\alpha}$	$\frac{1}{R\alpha\rho}$
SILVER WIRE	–	1.47	19.6	10.5	1	1	1
MOLYBDENUM WIRE	SILVER	1.6	6.3	10.2	0.92	2.85	2.94
	GOLD	2.4		10.5	0.62	1.90	1.90
POLYESTER YARN	SILVER	1.6	22	1.6	0.92	0.81	5.3
	GOLD	2.4		1.9	0.62	0.52	2.8
GRAPHITE YARN	SILVER	1.6	1.0	2.4	0.92	18.0	78.5
	GOLD	2.4		3.2	0.62	12.0	39.4

FAILURE MODES

There are essentially two basic modes of material-induced systems failure: (1) loss of systems performance and (2) catastrophic failure.

Loss of systems performance may occur as the result of repetitive transient effects, such as excessive thermally or load-induced deformations; this may be avoided by proper design and accurate materials data. Gradual performance loss due to intrinsic material characteristics and environmental effects, in contrast, is unavoidable and has to be taken in account in the prediction of systems performance over the specified systems life. This places emphasis on the consideration of such time-dependent material characteristics as creep, internal (molecular) changes, environmental degradation and meteoroid damage.

Catastrophic failure may occur by either of two modes: (1) complete environmental material degradation due to high solar activity or unknown long-term effects, or both; (2) unexpected meteoroid rupture of several redundant tension members. Since both effects are unpredictable, they cannot be included in failure analyses and performance predictions. This is acceptable in view of the very low risk.

FAILURE MODES

LOSS OF SYSTEMS PERFORMANCE	SoA
EXCESSIVE STRUCT LOADS/DEFORMATION	●
EXCESSIVE THERMAL EXPANSION	●
CREEP	○
INTERNAL MATERIAL CHANGES	●
ENVIRONMENTAL DEGRADATION	●
PROGRESSIVE METEOROID DAMAGE	(–)
CATASTROPHIC	
ENVIRONMENTAL DEGRADATION	●
METEOROID IMPACT FRACTURE	(–)

MICROMETEOROID FLUX

The meteoroid flux model, below, served as basis for the assessment of the gradual loss of performance due to meteoroid damage. It identifies the number of hits per m^2 and year by particles greater than the "mean particle diameter" for (1) "free" space (solid line) and (2) geosynchronous altitude (dotted line) accounting for the earth body-shielding and de-focusing effects. In this evaluation, the "JPL" data are used with confidence, as they have been derived from satellite measurements and have been successfully used in the design of JPL missions for years. The curve marked "Langley-Rockwell" represents flux data from the "Preliminary Handbook of Near Earth Environments," April 1979 (unpublished) which differ from the JPL data by almost 3 orders of magnitude.

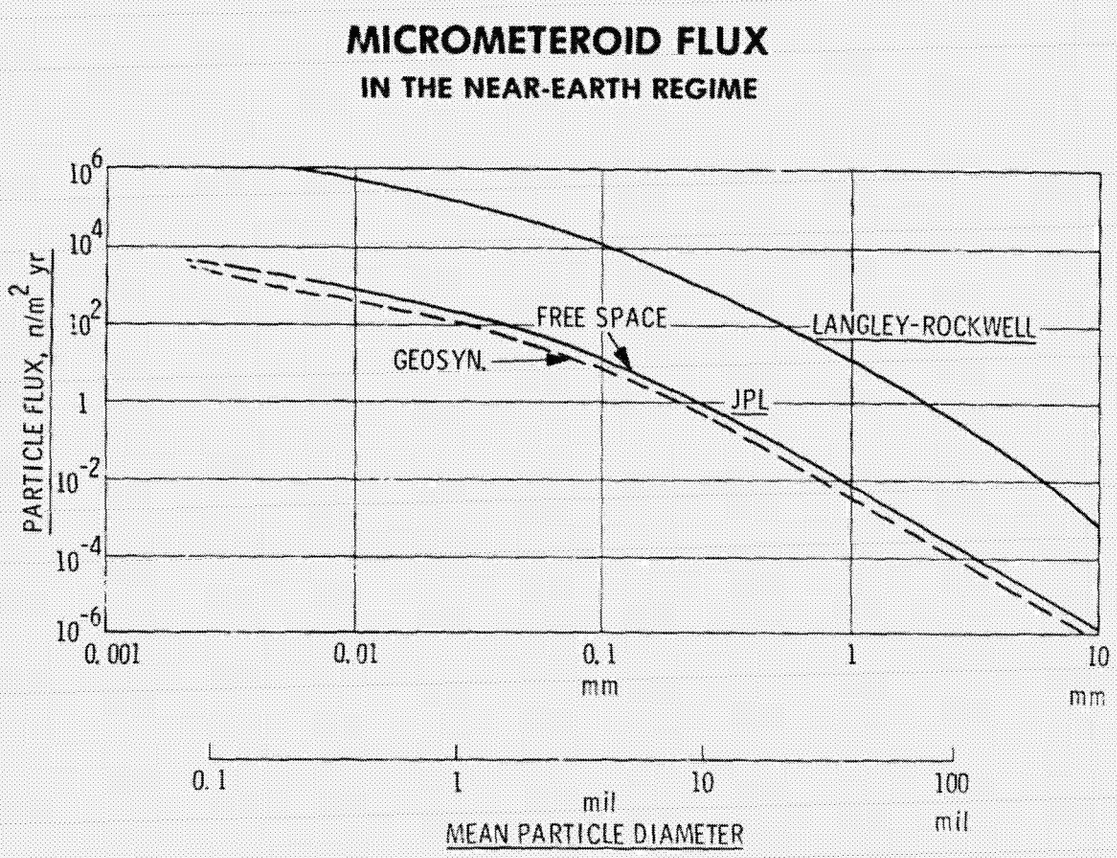

The degree of damage due to exposure to the meteoroid environment is determined by the number of ruptures expected within a given exposure time. For mesh reflector materials, the smallest meteoroid particle which causes rupture is dependent on the filament (wire) diameter and defined by the ratio d_p/d_w of min. particle diameter to filament diameter. For reflector meshes, a conservative value of 0.8 has been adopted, which accounts for some redundancy of the invariably multifilar base materials. The susceptible surface area, further, is determined by the mesh transparency.

The chart below identifies the expected meteoroid damage to mesh reflectors over a 10-year period. For a given filament or wire diameter and a given transparency the diagram permits the determination of the number of cell ruptures per m^2 (in 10 years) and the mean spacing of these ruptures which, in turn, serves as basis for the prediction of the resulting surface deformation.

METEOROID DAMAGE TO MESH REFLECTORS

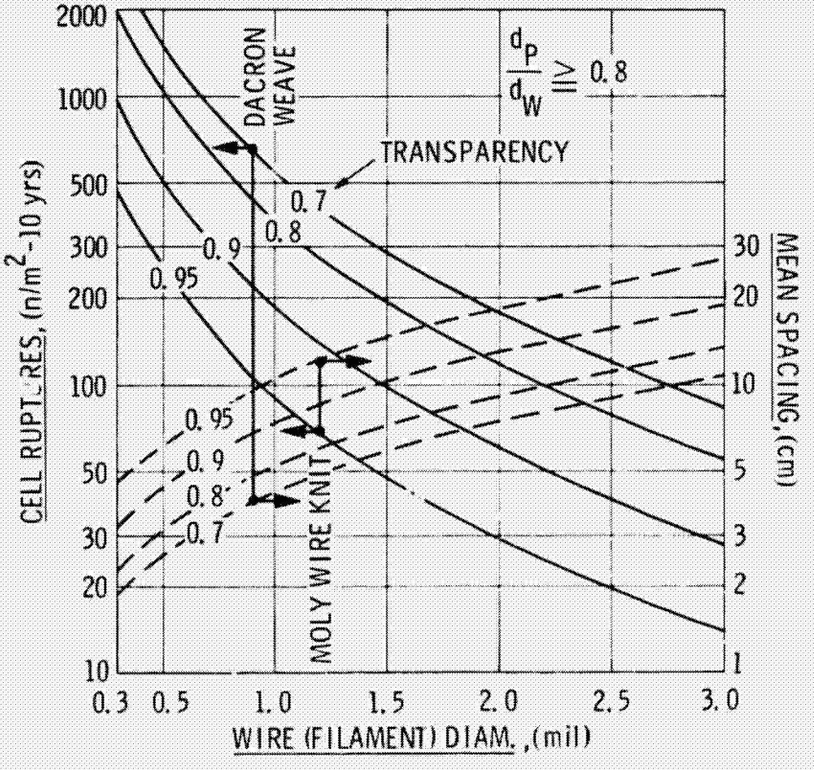

REFLECTOR DEFORMATION DUE TO METEOROID DAMAGE

Progressive deformation ("sagging") of the reflector surface starts as soon as the cumulative local cell deformations (stretching) due to meteoroid-induced ruptures exceed the elastic deformation due to mesh preload tension (Elastic Limit "e"). As illustrated in the diagram below, this point can be expressed in years of service. For the selected example of a molybdenum wire knit with a wire diameter of 1.2 mils and 25 cells per inch (cell size 1 mm) and an elastic preload deformation of 1%, excessive surface deformation starts after 14.7 years of service.

As shown by the relationships, the surface deformation and time to failure are determined by the following terms: (1) mean rupture spacing at time t, derived from the number of ruptures per year and mesh transparency; (2) local rupture deformation as related to cell size; (3) linear elastic preload (lbs/in); (4) linear elastic modulus (lbs/in) and; (5) Poissons ratio of the mesh.

REFLECTOR DEFORMATION DUE TO METEOROID DAMAGE

$$\Delta\epsilon = \frac{\text{LOCAL DEFORMATION}}{\text{RUPTURE SPACING}}$$

$$= c\,\nu\,\sqrt{n \cdot t \cdot (1 - T)} \quad (m/m)$$

- c CELL SIZE (m)
- ν POISSONS RATIO
- n DAMAGING PARTICLES/m^2 yr
- t EXPOSURE TIME (yrs)
- T TRANSPARENCY

$$t_{FAIL} = \frac{e^2}{(c\nu)^2 \cdot n \cdot (1 - T)} \quad (yrs)$$

- e ELASTIC LIMIT (m/m)

OR

$$t_{FAIL} = \frac{\sigma_L^2}{(E_L\, c\,\nu)^2 \cdot n \cdot (1 - T)} \quad (yrs)$$

- σ_L LINEAR TENSION (N/m)
- E_L LINEAR MODULUS (N/m)

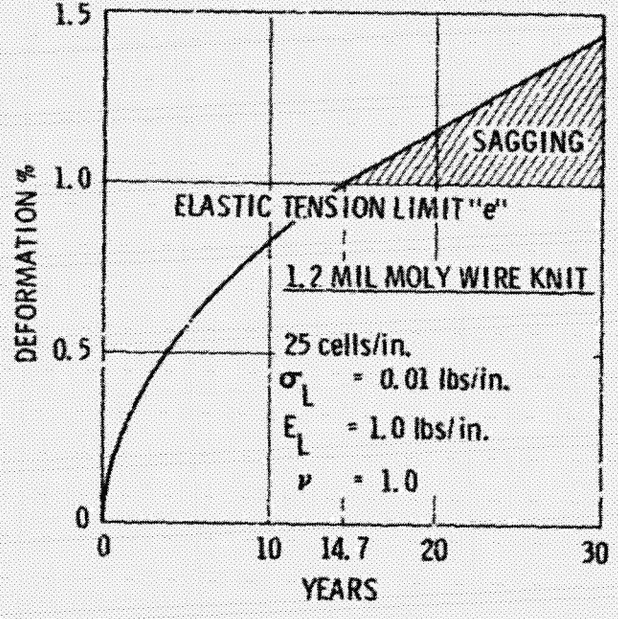

COMPARISON OF REFLECTOR MATERIALS

The table below is designed to convey an overview of the merits and shortcomings of four typical antenna reflector materials by means of approximate data for atmospheric and solar light pressure, deformation resulting from thermal and micrometeoroid environments, total mass and stowability. All data are based on a reflector diameter of 100m and a 10-year service life.

The molybdenum wire knit exhibits the most favorable combination of properties; its only shortcoming is the high sensitivity to meteoroid damage, leading to substantial deformation. While the welded wire mesh is fairly resistant to meteoroid damage and thermal deformation, it exhibits poor stowability. A thin film reflector offers the advantage of meteoroid insensitivity, low weight and unparalleled stowability; this is offset by a poor thermal deformation resistance and an appreciable drag force due to solar light pressure. The Dacron weave mesh exhibits the most unfavorable combination of properties.

Omitted in this comparison is the resistance to degradation (UV, high energy radiation) since it is partially reflected in the thermal deformation properties. It tends to shift the emphasis again toward metallic mesh materials.

COMPARISON OF REFLECTOR MATERIALS

● REFLECTOR DIAM. 100 m ● SERVICE LIFE 10 YEARS		MO KNIT MESH	MO WELDED MESH	DACRON WEAVE MESH	POLY-IMIDE FILM
THICKNESS (WIRE, FILAM., FILM)	mil	1.2	1.8	0.9	0.3
CELL COUNT	n/in.	25 x 50	25 x 25	25 x 25	0
TRANSPARENCY	%	95	90	70	0
MAX. ATMOSPH. PRESS.	q	0.014	0.011	0.036	0.12
SOLAR LIGHT PRESSURE	q	0.84	0.67	2.02	6.75
THERMAL DEFORMATN.	%	0	0.2	0.5	0.8
TOTAL CREEP	%	< 0.1	0.2	1.0	0.5
DAMAGING METEOR. HITS/m^2		68	72	660	4.2
— DEFORMATION	%	0.8	< 0.1	2.1	0
TOTAL SURFACE MASS	kg	289	326	218	96
STOWABILITY		Good	Poor	Good	Excell.

FAILURE OF WIRES/CORDS DUE TO
METEOROID IMPACT

In contrast to reflectors, the highly stressed condition of tension members is more sensitive to meteoroid impact, reflected in a smaller damaging particle size. The diagram identifies the number of expected ruptures per km length and year for tension members with circular cross-section (wires, cords, cables), as related to wire diameter and relative minimum damaging particle size (d_p/d_w).

While meteoroid damage in reflector surfaces produces a graduai loss of dimensional accuracy and performance, the rupture of a tension member may well be catastrophic, particularly at strategic locations. This places emphasis on a high degree of redundancy, either by appropriate material systems or design measures.

FAILURE OF WIRES/CORDS DUE TO METEOROID IMPACT

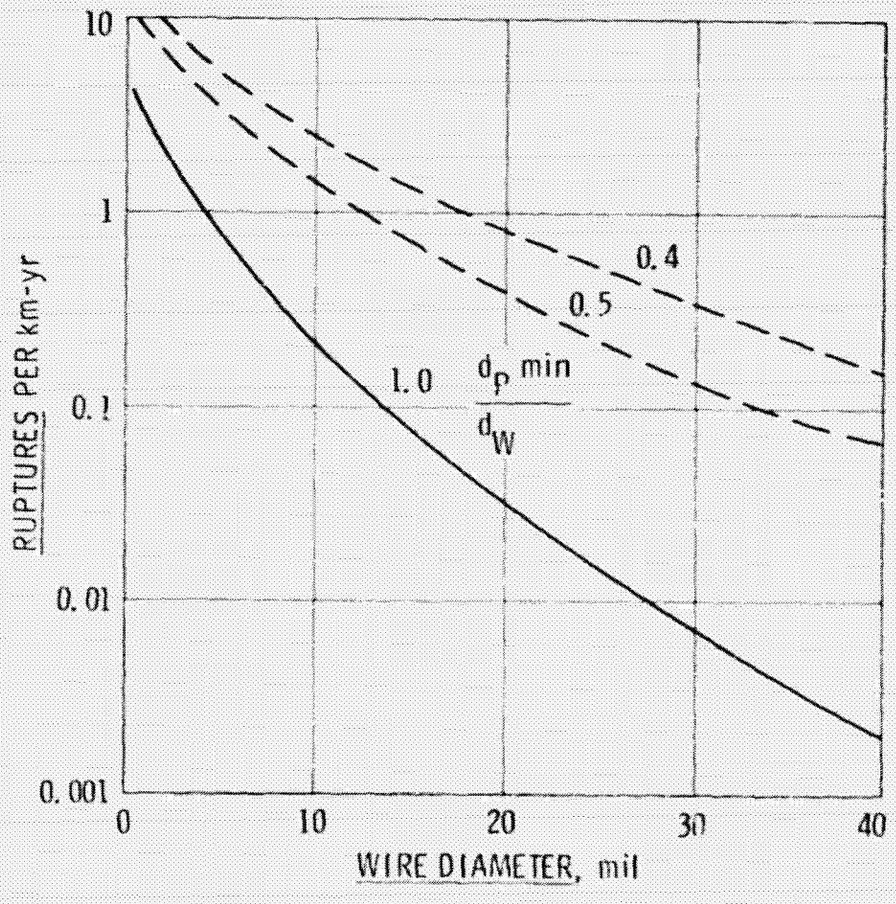

MAXIMUM SAFE LENGTH OF TENSION MEMBERS

Even though tension members in the form of wires or stranded filaments represent only a small surface area, potential meteoroid encounter has quite severe consequences since the fracture of a single tension element in a strategic position may cause substantial deformation over a large part of the reflector surface.

The chart below identifies the maximum length of a tension member which may be considered as "safe", representing an extremely low probability of meteoroid induced fracture. For tension members, a low ratio of critical particle diameter to wire (cord) diameter has been applied ($d_p/d_w = 0.4$) in view of the stressed condition and the absence of redundancy.

MAX SAFE LENGTH OF TENSION MEMBERS
TO PREVENT RUPTURE BY METEOROIDS

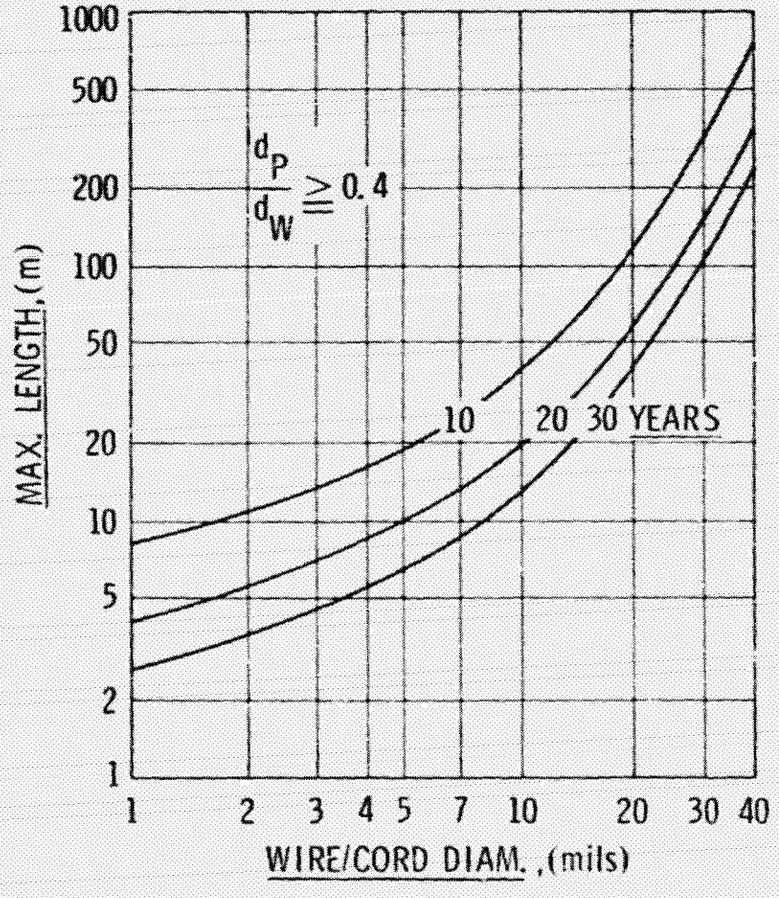

MATERIAL PERFORMANCE PREDICTION

It was attempted to develop a methodology for the prediction and comparison of the overall materials performance in a large space system. The adopted concept is best illustrated by the example of excessive deformation as systems failure criterion, as it applies to high-gain reflectors. For a given material, the total deformation is composed of a constant value due to sustained effects, repetitive maxima due to transient (cyclic) effects, and a steadily increasing deformation value due to time-dependent materials characteristics as outlined in the chart at right. Since the total deformation or sum of these values contains a time-dependent term, it is equally time-related and permits the determination of the time at which it starts to exceed the maximum allowable deformation e_{LIM} postulated by systems performance. A very useful single value for the comparison of materials performance is the ratio of this time limit and the specified systems service life, designated as "Material Confidence Level". This value should in any case be greater than 1.0. Extremely high values indicate the potential of design relaxation.

MATERIAL PERFORMANCE PREDICTION

TIME DEPENDENT EFFECTS

- CREEP
- MOLECULAR CHANGES
- METEOROID IMPACT
- ENVIRONMENTAL DEGRADATION

TRANSIENT EFFECTS

- THERMAL EXPANSION
- CONTROL LOADS
- INDUCED STRUCTURAL LOADS

SUSTAINED EFFECTS

- STRUCTURAL PRE-LOADS
- ATMOSPHERIC DRAG
- SOLAR LIGHT PRESSURE

de/dt

$\Sigma e_{max} + t \frac{de}{dt} \leq e_{LIM.}$

$t_{LIM} = \frac{e_{LIM} - e_{max}}{de/dt}$

e_{max}

MATERIAL CONFIDENCE LEVEL:

$L_C = \frac{t_{LIM}}{t_{SERV}}$

POSTULATED: $L_C > 1.0$

In the course of the study, a number of promising advanced concepts for flexible materials or material systems were identified. Of particular interest are unidirectional composite tapes and multifilar material systems for tension members of high redundancy, polymer film-based graphite mesh for reflectors of high dimensional stability and inflatable/self-rigidizing polymer-base materials for a variety of structural applications (booms, hoops or even reflectors). These advanced material concepts are presently integrated in the proposed R & D plan.

POTENTIAL ADVANCEMENTS

- REDUNDANT TENSION MEMBERS (MULTIFILAR)
- COMPOSITE TAPES IN LIEU OF STRINGS
- GRAPHITE YARN MESH (REFLECTORS)
- THIN FILMS/ELECTROSTATIC SHAPE CONTROL
- MG/GRAPHITE COMPOSITES FOR FLEX RIBS
- FLEX JOINTS IN LIEU OF HINGES
- INFLATABLE SYSTEMS
- SELF-RIGIDIZING FLEXIBLE MATERIALS
  - STRUCTURAL COMPONENTS
  - REFLECTORS
- IMPROVED METHODOLOGY FOR MATERIALS PERFORMANCE PREDICTION

N80-19172

ADVANCED MATERIALS FOR SPACE

Darrel R. Tenney, Wayne S. Slemp,
Edward R. Long, Jr., and George F. Sykes
Langley Research Center

LSST 1ST ANNUAL TECHNICAL REVIEW

November 7-8, 1979

SPACE MATERIALS PROGRAM

The resources for the space materials program at Langley during FY-79 were provided by LSST and by NASA's Base R&T program. Funds from both sources were used to fund two major contracts to assess the radiation stability of current composites. These contractual efforts represent the bulk of the materials program and are directed at the space durability of composites which is considered to be the principal uncertainty associated with the long term (25-30 years) use of composites in thin-gage minimum weight large space structures. In general, the long-term basic issues are being addressed in the Base R&T program while the more near-term systems oriented tasks are being worked as part of the LSST program. The goal of the base R&T program is to determine radiation damage mechanisms of resin matrix composites and formulate new polymer matrices that are inherently more stable in the space environment. New composites will be manufactured with these improved resins to develop a class of composites optimized for long term use in the space environment.

The principal thrust of the LSST program is to develop the materials technology required for confident design of large space systems such as antennas and platforms. Areas of research in the FY-79 program include evaluation of polysulfones, measurement of the coefficient of thermal expansion of low expansion composite laminates, thermal cycling effects, and cable technology. The development of new long life thermal control coatings and adhesives for use in space will be included in the LSST materials program next year.

SPACE MATERIALS PROGRAM

BASE R & T

- RADIATION STABILITY OF COMPOSITES
  - ABSORBED DOSE EFFECTS
  - EQUIVALENCE OF e^-, p^+, γ
  - COMBINED EFFECTS
  - INSITU TEST REQUIREMENTS
  - POLYMER CHEMISTRY
  - DOSE / DEPTH PROFILE ANALYSIS
  - IN-HOUSE RADIATION CAPABILITY
- THERMAL CONTROL COATINGS
  - WHITE PAINT COATINGS
  - VAPOR DEPOSITED METALS
- HIGH DIMENSIONAL STABILITY COMPOSITES
  - Gr / Mg - PROPERTY CHARACTERIZATION
  - Gr / GLASS - MATERIALS DEVELOPMENT
  - SiC / Ti - SELECTIVE REINFORCEMENT
- INDUCTION WELDING OF COMPOSITES

LSST MATERIALS

- CABLES
  - MECHANICAL / PHYSICAL PROPERTIES
  - MECHANICAL CREEP
  - ENVIRONMENTAL EFFECTS
  - PACKAGING AND DEPLOYMENT
- DIMENSIONAL STABILITY
  - CTE MEASUREMENT TECHNIQUES
  - ENVIRONMENTAL EFFECTS
  - PROCESSING VARIABLES
  - LAMINATE ANALYSIS
  - THERMAL FATIGUE OF JOINTS
  - THERMAL CONTROL

Figure 1

LSST MATERIALS PROGRAM

The activities currently included in the LSST materials program at Langley are shown in figure 2. The program began in FY-78 and will be completed during the first quarter of FY-83. The areas being addressed in FY-80 include cables and dimensional stability of composites. These activities are projected to continue through FY-82 yielding the expected results shown on the right hand side of figure 2. The activities associated with the space durability of composites are largely contractual and will be completed during FY-80 and 81. Space durability research will continue past FY-80 but will be funded through Langley's Base R&T program rather than through LSST. Consideration is being given to including research on metal matrix composites and composite joints in the LSST materials program.

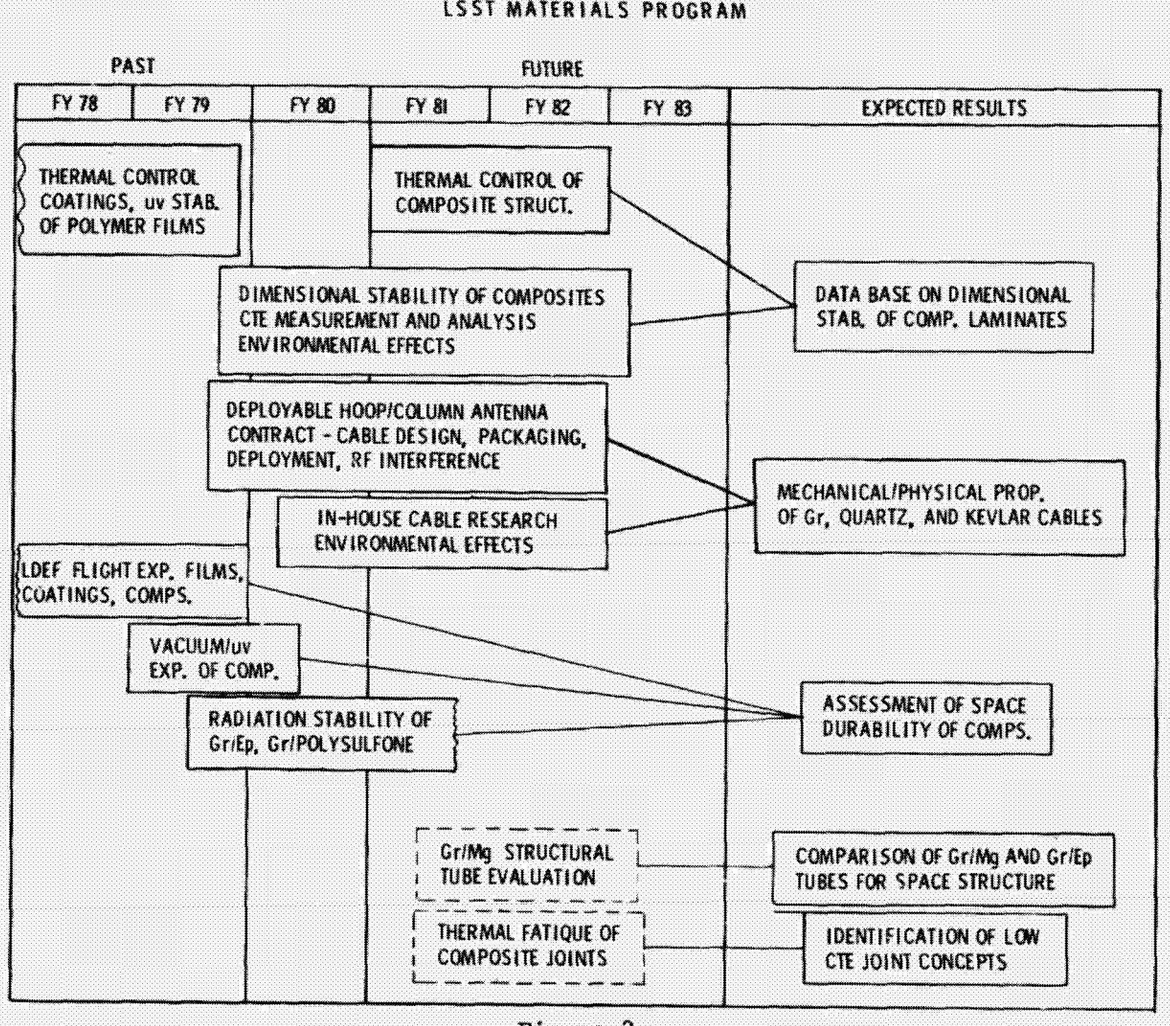

Figure 2

DURABILITY CONCERN FOR STRUCTURAL COMPOSITES IN SPACE

A composite structural member, designed for space use, is actually a system of components consisting of a thermal control coating, structural adhesive for bonded joints and the composite laminate as indicated in figure 3. Each component has specific properties which must be maintained, with little or no degradation, throughout the use-life of the structure. Optical properties of coatings will be designed to maintain spacecraft temperature within acceptable limits. The coatings will absorb UV, much of the proton flux and the low energy electrons. Coatings which undergo optical changes and/or spallation on exposure to the environment could result in exposure of the underlying composite or result in the temperature limits of the structure being exceeded.

Composites must also maintain acceptable properties through the design life of the structure. The radiation environment however, consisting primarily of high energy electrons, is expected to generate changes in the mechanical and physical properties of the polymeric matrix material because of the relatively high radiation dose level which would be absorbed for long term (10-30 years) missions. Crosslinking and degradation of the polymer matrix are expected to occur. Changes in stiffness, strength, or dimensional stability must therefore be considered in the initial design of the system.

Structural adhesives used for bonded joints should be stable in the space environment.

DURABILITY CONCERNS FOR STRUCTURAL COMPOSITES

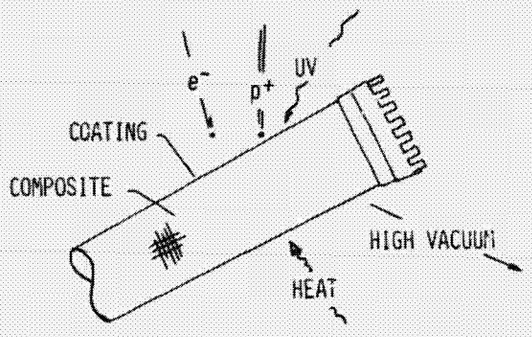

DESIRED PROPERTIES OF THERMAL CONTROL COATINGS

- LOW α / ε
- ABSORB UV, p^+, LOW EN. e^-

DESIRED COMPOSITE PROPERTIES

- HIGH STIFFNESS
- HIGH SPECIFIC STRENGTH (TENSION, COMPRESSION, SHEAR)
- GOOD DIMENSIONAL STABILITY (LOW α / K_T)
- LOW MINIMUM GAGE
- HIGH RESISTANCE TO MICROCREEP
- LOW RATE OF OUTGASSING

ENVIRONMENTAL CONCERNS

- COMPOSITE PROPERTY CHANGES
- OPTICAL CHANGES IN COATINGS
- SPALLING OF COATINGS
- SPACECRAFT CHARGING
- LOSS OF LOW MOL. WT. SPECIES
- LOSS OF SHEAR STRENGTH IN ADHESIVE BOND JOINTS

Figure 3

SUMMARY OF IMPORTANT SPACE ENVIRONMENT PARAMETERS

A major factor affecting the selection and utilization of materials for any space application is understanding the service environment and the interaction of this environment with the materials of interest. The key elements of the space environment that are known to affect organic materials and the principal concerns associated with each of the major elements are given in figure 4. This table shows the major parameters, nominal range and reason for interest in each parameter.

The major environmental parameters in the space environment are low pressure (high vacuum), ultraviolet radiation, ionizing radiation (e^- and p^+) and thermal cycling. Other types of radiation exist in space, but are not considered, at this time, to be significant.

Each phase of the space environment can have significant effects upon polymer matrix structural composites. The constant low pressure for example, may cause dimensional changes due to outgassing and microcracking. UV can cause degradation of coatings. High energy electrons may affect both the surface and bulk properties of the composite. High proton flux may degrade thermal control coating efficiency. The combination of these environmental elements acting together on the structural element may also cause combined or synergistic effects. The combination of high vacuum, ionizing radiation and thermal cycling can be a severe test of the materials' ability to perform.

SUMMARY OF IMPORTANT SPACE ENVIRONMENTAL PARAMETERS
AND MATERIALS UNCERTAINTY ASSOCIATED WITH EACH PARAMETERS

ENVIRONMENTAL PARAMETER	NOMINAL RANGE OF PARAMETER	REASON FOR INTEREST IN PARAMETER
VACUUM	PRESSURE 10^{-5}-10^{-13} mPa	VACUUM OUTGASSING RESULTS IN LOSS OF MOISTURE AND SOLVENTS RESULTING IN DIMENSIONAL CHANGES
ULTRAVIOLET	WAVELENGTH 0.1-0.4 μm INTENSITY 1.4 Kw/m^2	DEGRADATION OF COATINGS
PROTONS	ENERGY 0.1-4 MeV FLUX $10^8 p^+/cm^2$-sec	DEGRADATION OF COATINGS AND SURFACE PLIES OF COMPOSITES
ELECTRONS	ENERGY 0.1-4 MeV FLUX $10^8 e^-/cm^2$-sec	SURFACE AND BULK DAMAGE; SPACECRAFT CHARGING
TEMPERATURE CYCLING	MATERIAL TEMP 80 K TO 420 K	MICROCRACKING, THERMAL WARPING, DETERIORATION OF ANTENNA GAIN DUE TO SURFACE DISTORTIONS

Figure 4

ENERGY DEPOSITION FROM THE SPACE RADIATION ENVIRONMENT

To fully understand the effect of space radiation on the properties of composite materials, it is necessary to know where the radiation is absorbed in the composite. Calculations are being conducted to determine the deposited energy density averaged over macroscopic dimensions and thus determine the dose gradients as a function of orbital parameters. This information is useful for selecting exposure conditions for ground based simulations of GEO. Effort is also being directed at trying to find a LEO orbit which would give an absorbed radiation dose similar to that expected for GEO exposure. A long term materials flight experiment in LEO is preferred to one in GEO because of the possibility of periodic Shuttle rendezvous to remove and replace specimens.

Energy deposition on a microscopic scale is also being examined in search of possible anomalous effects due to the proton track structure. The energy distribution over the molecular unit must be known to fully understand radiation damage mechanisms. The source strength of specific chemical precursors will be estimated along with the density of volatile products formed.

ENERGY DEPOSITION FROM THE SPACE RADIATION ENVIRONMENT

- Macroscopic Energy Density as a Function of Orbital Parameters
    1. Determination of energy density gradient
    2. LEO simulation of GEO
    3. Laboratory simulation of GEO
- Microscopic Energy Density Distribution (Relative Electron-Proton Quality)
- Energy Distribution Over Basic Molecular Unit
- Source Strength of Specific Chemical Precursors
- Calculation of Initial Source of Volatile Products

Figure 5

DOSE FOR TYPICAL TRAPPED RADIATIONS IN THREE GEOMETRIES

The dose for typical electron and proton spectra is shown as a function of depth from the surface in the different geometries. The sphere and slab geometries were chosen to bracket the exposure in any other geometry. The cone was taken as a "typical" geometry. Dose gradients will be calcuated using these techniques as a function of orbit parameters to estimate the absorbed dose for long term exposure in the space environment for specific structural elements.

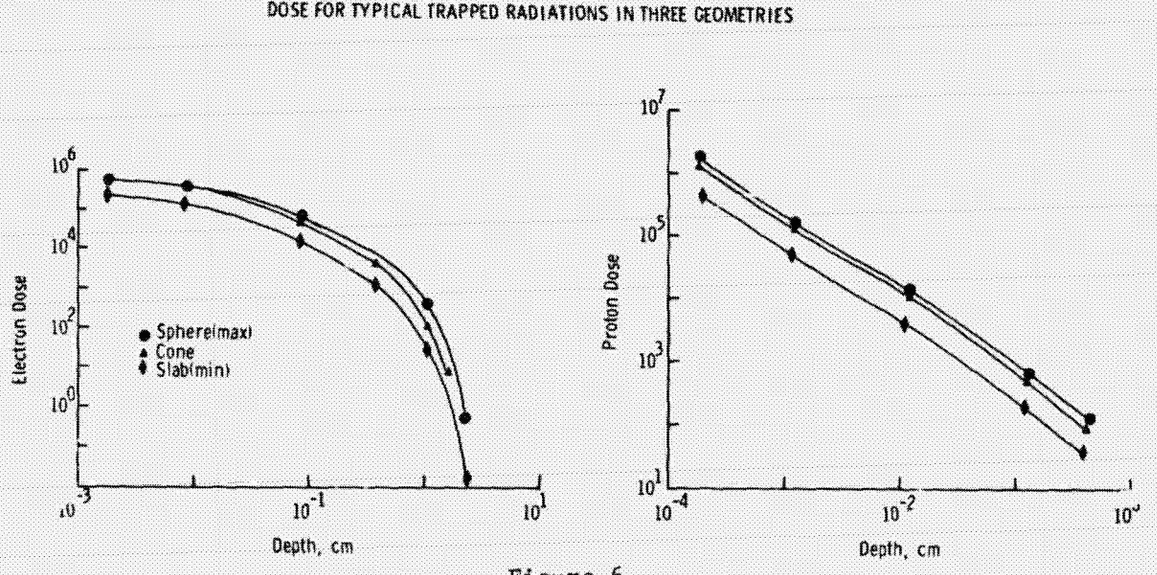

Figure 6

ELECTRON AND PROTON PENETRATION IN CURED NEAT RESIN AND COMPOSITES

Electron and proton penetrations have been determined for a graphite/epoxy composite. The values of penetration were determined from Bethe's stopping power relations for inelastic collisions (excitation and ionization). Figure 7a suggests that the energy absorption profiles for a 4 Mev electron in a composite is not appreciably different from that for a neat resin. Similar conclusions may be made for electrons having different initial energies.

Figure 7b indicates that the penetration of electrons with initial energies between 0.2 and 4.0 Mev is linearly dependent on the energy. The absorption of all the electron's energy, and hence the electron, depends on the electron's initial energy and the material thickness. A resin thickness of 0.05 cm (approximately 4-ply composite) would capture electrons with initial energies less than 0.25 Mev and absorb approximately 0.31 Mev of energy from electrons with initial energies greater than 0.25 Mev. Similarly, resin thickness of 0.25 cm (20 ply composite) would capture electrons with energies less than 0.85 Mev and absorb approximately 0.63 Mev of energy from electrons with energies more than 0.85 Mev. Thus, considerable energy doses would be absorbed by composite materials used in long duration space missions.

Figure 7c is a plot of pathlength of electrons with initial energies between 1 and 2 Kev. Figure 7d is a plot of pathlength of protons with initial energies between 0.5 and 1.75 Mev. Most of the protons in the space environment would be absorbed in a thin layer near the surface.

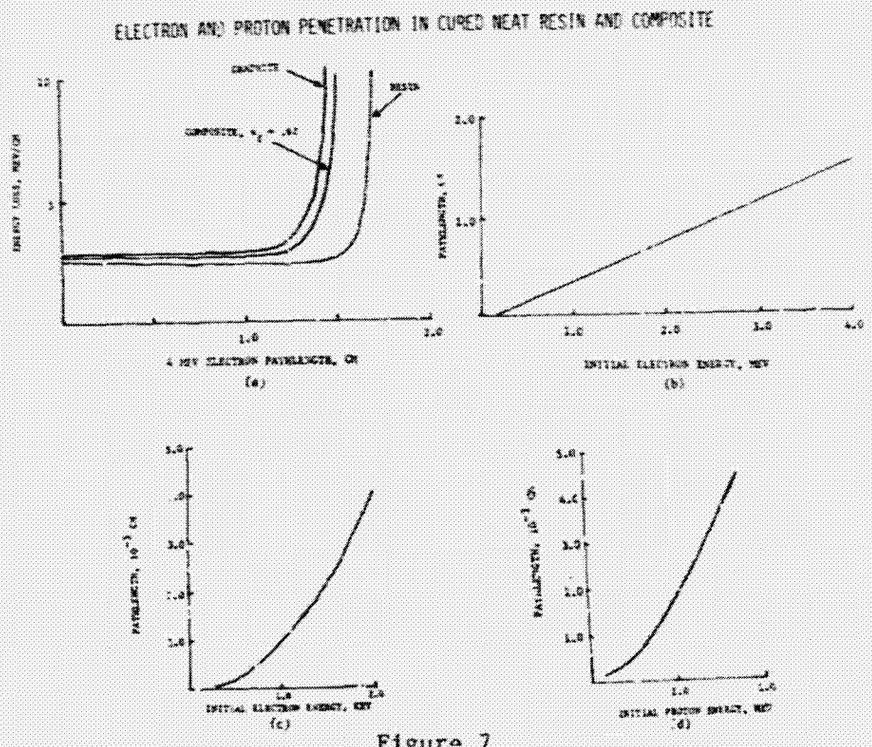

Figure 7

EFFECTS OF ELECTRON AND GAMMA RADIATION ON FLEXURAL PROPERTIES OF COMPOSITES

A study is underway to compare the effects of electron and gamma radiation on the flexural properties of graphite/polymer composites. The electron energy is 0.5 MeV. The gamma source is Cobalt-60. The test specimens are 4-ply unidirectional graphite/polymer composites which measure 2.34 x 1.27 cm. The flexural property measurements are made with a three-point bending fixture. Specimens are predried to remove moisture. For the electron exposures the specimens are inserted in thin-walled metal vacuum bags and remotely inserted into and removed from the electron beam by a conveyer belt system. For the gamma exposures, the fifteen centimeter exposure cell is maintained under vacuum during exposure. The specimens' flexural properties are immediately tested upon completion of exposure. Flexural property testing after electron exposure has been conducted for two composite materials: T300/5208, a graphite/epoxy, and C6000/PMR15, a graphite/polyimide. For graphite/epoxy the strength and modulus increased for total doses up to $2.5(10)^8$ rads. Similar increases for other materials have been attributed to cross coupling. Above $2.5(10)^8$ rads, the increase diminishes possibly due to onset of chain scission. The graphite/polyimide composite showed more radiation resistance. The changes in flexural properties following gamma exposure have the same trend with respect to total dose. However, the peak increase occurs at a lower dose. The study will continue with measurements of changes in flexural properties for larger radiation doses, similar to that expected for 20-30 years of space exposure at GEO.

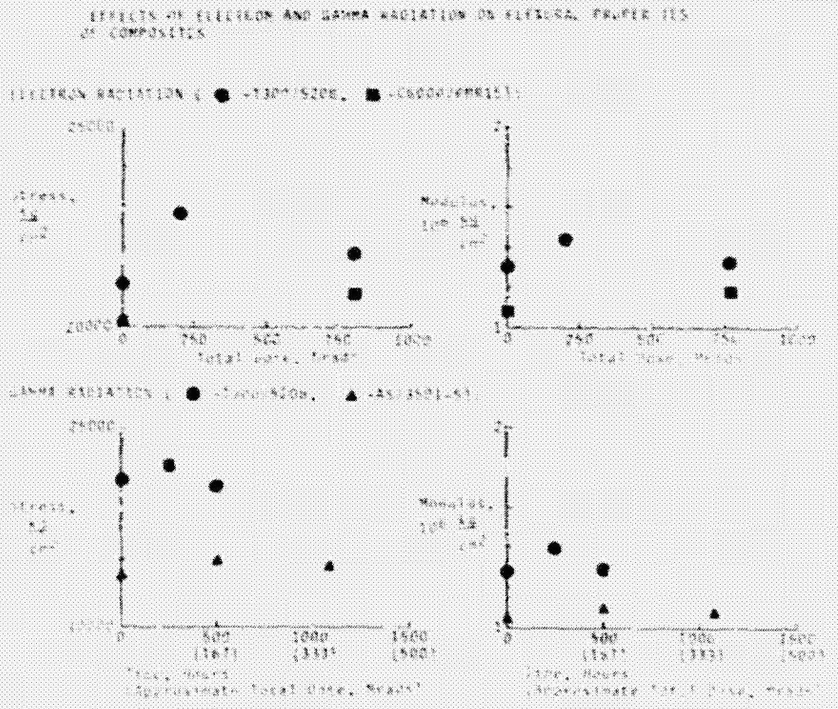

Figure 6

DECREASE IN OPTICAL TRANSMISSION OF H-FILM AFTER AN ABSORBED ELECTRON DOSE OF 10^9 RADS

Measurements of changes in the optical transmission of polymer films due to ionizing radiation is a method for measuring the degradation due to absorbed dose. Measurements are made in the visible region to detect creation of molecular complexes analogous to color-centers in solid state physics. The measurements in the UV region show molecular energy level changes because UV energy excites the electrons in molecular orbitals to higher energy states. Changes in optical transmission due to electron and proton radiation may also indicate differences in the two forms of radiation. Finally the measurements may also be important for detection of combined UV and ionizing radiation synergistic effects. The transmission spectra for electron irradiated H-film were taken on a Cary-14 spectrometer. The spectra show tha_ permanent molecular structure change has occurred because the absorption of UV has almost doubled.

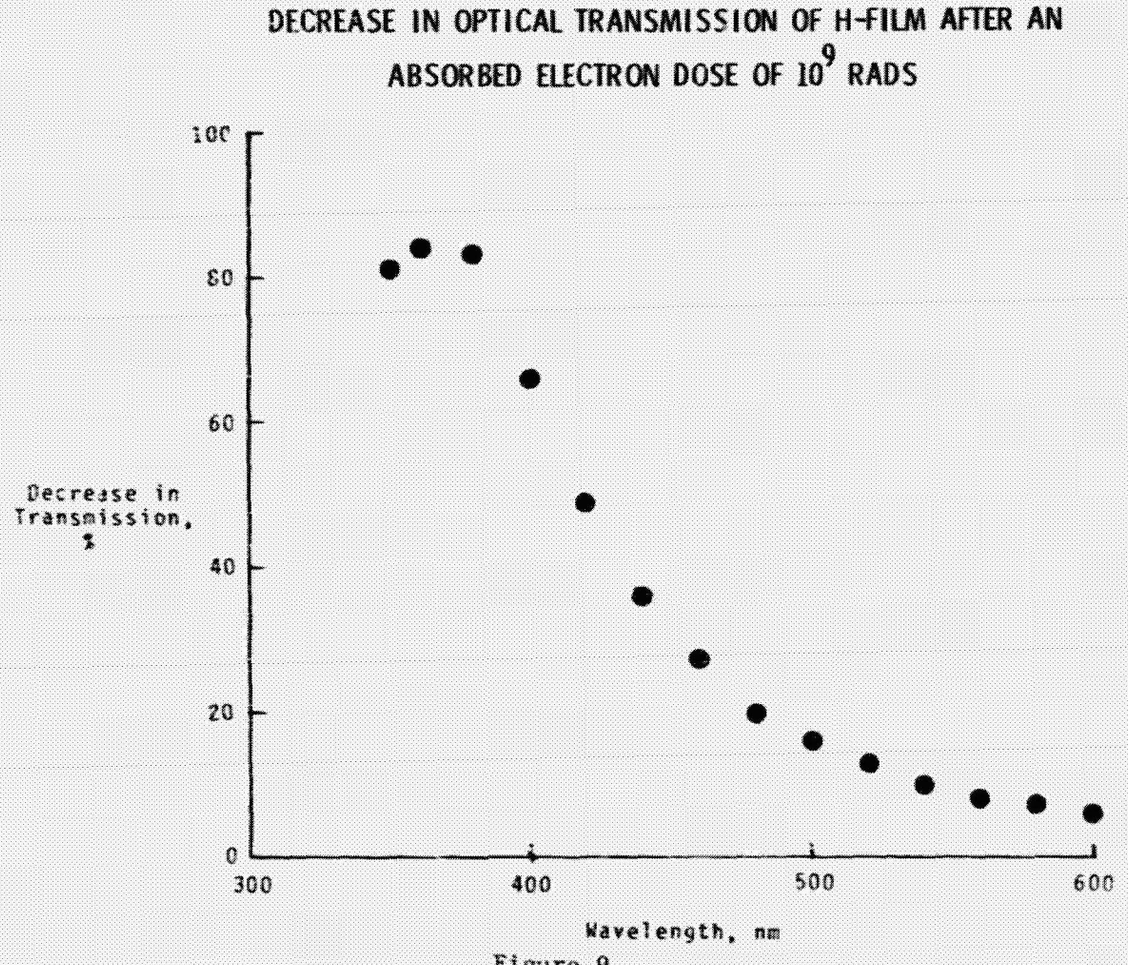

Figure 9

EFFECTS OF ELECTRON RADIATION ON H-FILM AS DETERMINED BY INFRARED SPECTROSCOPY

Infrared (IR) spectroscopy measures a materials transmission or reflection of electromagnetic radiation wavelength from approximately 2 to 25 microns. This range of wavelengths corresponds to the energies required to cause molecular bonds to vibrate. Therefore, the variation in transmission (absorption) of the IR radiation with respect to IR wavelength is a description of the bonds within the molecular structure. The IR spectra shown below are for an H-film. The spectra are shown for before, at the tail end of, and five minutes after a 6 KeV electron dose of 10^{10} rads. The bonds responsible for the spectra are identified. An example molecular structure for H-film is given which shows where such bonds occur. The spectra show that transmission increased when the polymer film was irradiated with electrons and continued to increase after electron radiation. An interpretation of the increase is that the number of bonds have decreased, that is the molecular structure has been damaged. In particular, the number of aromatic ether bonds, C-O-C, is the most affected. Thus this bond may be the weakest link in the backbone of the polymer chain. A portion of spectra is shown in the lower right for a 10^9 rad dose. The spectrum for after radiation appears to have nearly returned to preradiation conditions. Recovery after a 10^9 rad radiation dose has also been observed for mechanical properties of the film. The two forms of observed recovery may correspond to one another. If so, then permanent changes in mechanical properties may occur for doses larger than 10^9 rads where the IR spectra were permanently altered.

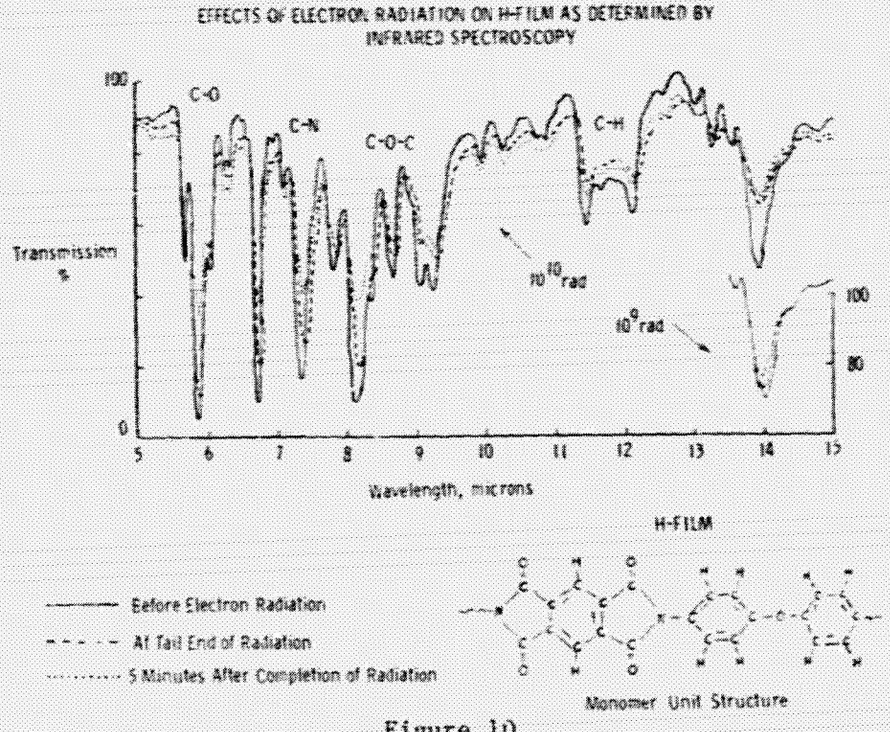

Figure 10

RADIATION EXPOSURE OF COMPOSITE MATERIALS

The objective of this research is to provide simulated space radiation exposure of a variety of laminated graphite fiber reinforced polymeric matrix composites. The effects of radiation on the mechanical, chemical and physical properties will be evaluated to assess the space durability of these materials and to determine if synergistic radiation effects are significant for composites. The radiation exposure program includes both individual, simultaneous and sequential exposure to 300 KeV electrons and/or 2.0 MeV protons with fluences to 2×10^9 rads (absorbed dose) at specimen temperatures of 25°C and 120°C. These data will be used to determine whether radiation damage due to simultaneous electron and proton exposure is greater than due to sequential electron and proton exposure. Synergism has been verified in the optical properties of thermal control coatings but no data could be found in the literature for mechanical and physical properties of composites.

RADIATION EXPOSURE OF COMPOSITE MATERIALS

OBJECTIVE: TO PROVIDE RADIATION EXPOSURES OF COMPOSITE MATERIALS FOR EVALUATION OF SPACE RADIATION EFFECTS ON MECHANICAL, CHEMICAL & PHYSICAL PROPERTIES

CAPABILITIES: 250-300 KeV e^-; 2.2 MeV p^+; e^- + p^+;
p^+ + e^-; e^- + p^+; BEAM AREA - 20 cm. Dia.;
FLUX TO: 5×10^{11} e^-/cm^2-sec or p^+/cm^2-sec

TESTING PROGRAM	MATERIAL SYSTEMS
EFFECTS OF:	T300/934
TYPE OF RADIATION	T300/5208
SINGLE, COMBINED AND SEQUENTIAL EXPOSURES	T300/POLYSULFONE
TOTAL DOSE	CELION 6000/PMR15
DOSE RATE	GY-70/E793
SPECIMEN TEMPERATURE	GY-70/7740 GLASS
LOAD ON SPECIMEN	NEAT RESINS

Figure 11

RADIATION EXPOSURE TEST METHODOLOGY

The objective of this research program is to evaluate the effects of 1.0 MeV electrons on composite materials in-situ, in-air and in-vacuum to determine the effects of post exposure test conditions and to evaluate the effect of continuous versus interrupted radiation exposure on the degradation of composites. A series of approximately 10 exposures of 3 composites (18 specimens/exposure) to 2×10^9 rads of 800 KeV electrons will be conducted with substrate temperatures of 25°C and 120°C. The post irradiation tests will be conducted in-situ (during irradiation), in-vacuum and in dry air to determine if future testing can be conducted in dry air using conventional laboratory mechanical property testing equipment or if these tests will require expensive vacuum test equipment. These data will also evaluate the effects of continuous versus interrupted radiation exposure on the degradation of composites. Part of these exposures will be performed for 8 hours/day over a week and some continuously for 24 hours/day for the same total hours.

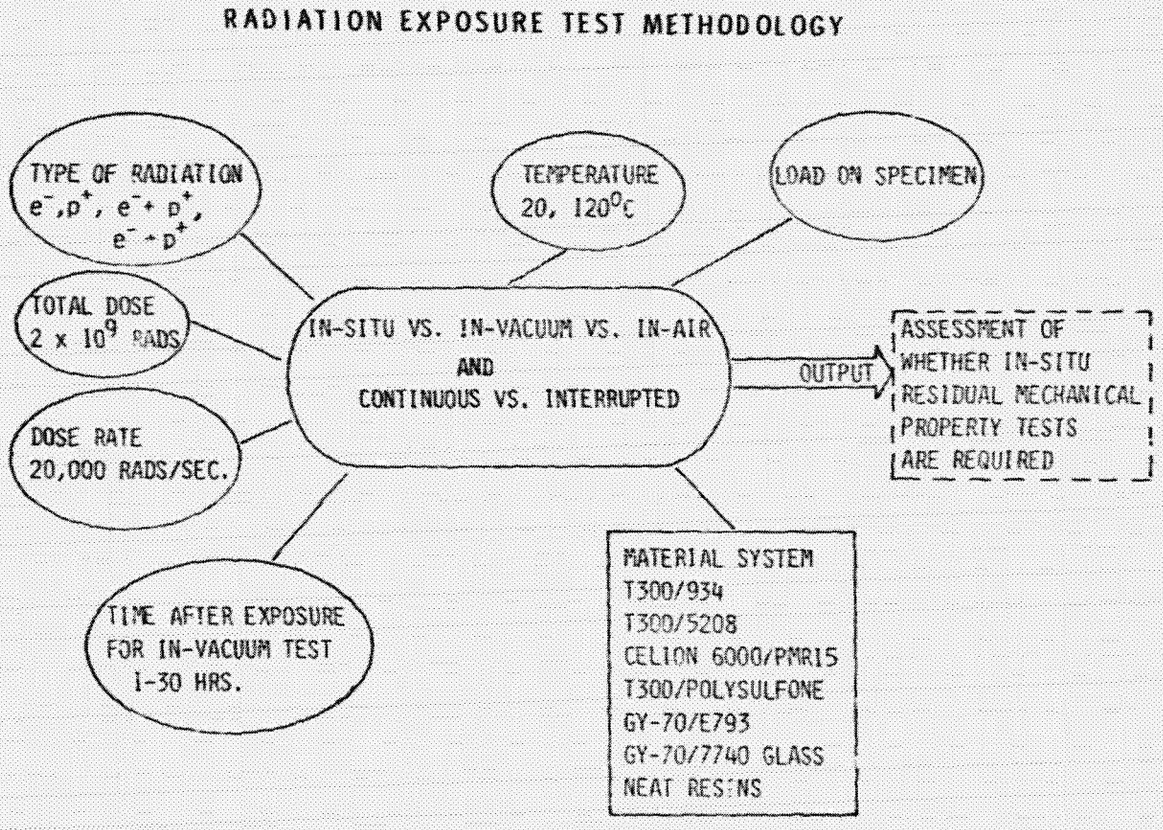

Figure 12

INVESTIGATION OF DEGRADATION MECHANISMS IN COMPOSITE MATRICES

The objectives of this program are: (1) to establish the mechanisms of degradation for composite matrices and to provide data to predict the long-term durability of composites in geosynchronous orbit; (2) to establish the feasibility of using current low α_s/ϵ thermal control paints for UV protection of composites.

One technique used to establish the damage mechanism is to collect the gas given off during irradiation, analyze both the condensible and non-condensible constituents in this gas and relate this to the known polymer compound. This is being performed on films of the composite matrix material and the composites.

Other tests to be conducted include: ultimate flexure, tension and compression strengths; dynamic mechanical analysis (modulus); electron microscopy surface studies, and other tests to determine the extent of crosslinking where applicable.

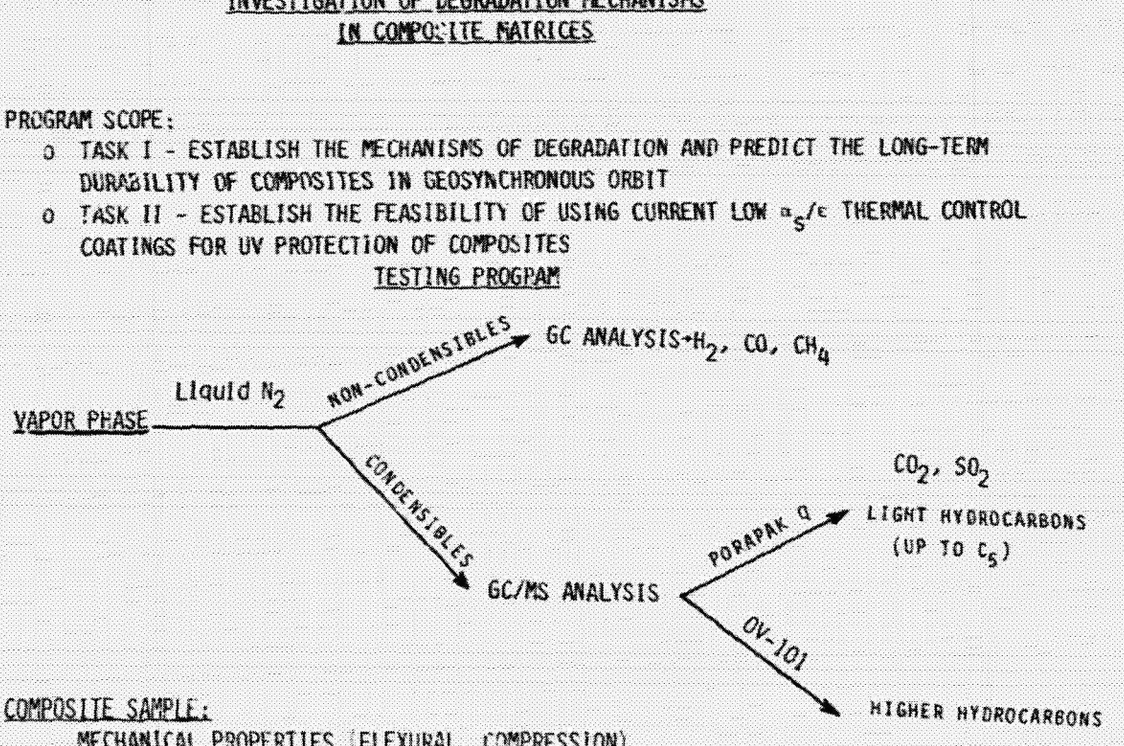

Figure 13

A1100 SILANE PRIMED S13G/LO COATED COMPOSITE ADHESION TEST

Thermal control coatings will be required to minimize the temperature variation in large space structures and thus limit the thermal expansion of these structures. Part of the study of coating application to composites was to evaluate primers which would promote adhesion to composites without requiring abrasion of the composite surface. A group of primers was experimentally evaluated and the A1100 primer proved to be the best for all types of composites. This primer was subsequently evaluated using abraded and non-abraded composites and the results are shown in this figure. The non-abraded surface performed as well as the abraded surface in each adhesion test. This significantly reduces the time and cost of application of white paints to composites.

The effect of coating thickness on solar absorptance was also evaluated for S13G/LO applied to a selected group of graphite reinforced resin matrix composites including epoxy, polysulfone and polyimide resins. As the thickness increased from 3 mils to 10 mils, the solar absorptance decreased from approximately 0.29 to 0.18. This demonstrated that a low solar absorptance can be obtained with typical white paints over graphite reinforced composites.

A1100 SILANE PRIMED S13G/LO COATED COMPOSITE ADHESION TEST

(ABRADED SURFACE VS. NONABRADED SURFACE)

SUBSTRATE*	COATING THICKNESS (IN.)	LIQUID N_2 TEST (72 HR CURE)	KNIFE TEST 72 HR CURE	KNIFE TEST 264 HR CURE
5208/T300	A)0.007	PASS	GOOD	GOOD
	B)0.008	PASS	GOOD	GOOD
3501-6/AS	A)0.008	PASS	GOOD	GOOD
	B)0.007	PASS	GOOD	GOOD
P1700/ CELION 6000	A)0.008	PASS	FAIR	FAIR
	B)0.010	PASS	FAIR	FAIR
PMR-15 CELION 6000	A)0.006	PASS	GOOD	GOOD
	B)0.007	PASS	GOOD	GOOD

*A) ABRADED SURFACE
B) NONABRADED SURFACE

ABRADING SURFACE DOES NOT APPEAR TO ENHANCE COATING ADHESION. SOLVENT CLEANING APPEARS ADEQUATE.

Figure 14

DIMENSIONAL STABILITY OF STRUCTURAL COMPOSITES

The performance characteristics of many of the proposed space communication antennas and space-based laser systems are dependent on the dimensional stability of the supporting structure. For these applications, the thermal properties of the materials should include: high thermal conductivity (K_t), high specific heat (C_p), and low coefficient of thermal expansion. These parameters are important because thermal cycling is one of the principal design considerations in development of good dimensional stability. The cycling results from shadowing of structural elements by other structural elements, from orbital movement from sunlight to earth shadow, and for some applications from electrical power heating.

Thermal cycling must be controlled so that total system deflections and thermal loads can be minimized. From a material point of view, thermal cycling control can be accomplished by two basic methods: (1) selecting a material system with a low or near zero coefficient of thermal expansion (CTE), (2) controlling the delta temperature through application of materials coatings or through careful surface preparation such as polishing.

Langley's program in this area is basically directed at analytical calculation and measurement of coefficients of thermal expansion of resin matrix composite laminates and the effect of thermal cycling on CTE. Thermal cycling is known to affect the CTE of certain composite laminates presumably because of microscopic damage to the composite. Also measurements made on small specimens have not always agreed with measurements made on much longer structural elements. These factors will be investigated in this program.

DIMENSIONAL STABILITY OF STRUCTURAL COMPOSITES

OBJECTIVE: DEVELOP ANALYTICAL AND EXPERIMENTAL TECHNIQUES TO ACCURATELY PREDICT THE DIMENSIONAL STABILITY OF LOW CTE STRUCTURAL COMPOSITES SUBJECTED TO THE SPACE ENVIRONMENT.

APPROACH: RESEARCH PROGRAM WILL BE A JOINT IN-HOUSE AND GRANT ACTIVITY WITH THE PRINCIPAL THRUST DIRECTED AT DETERMINING THE CHANGES IN CTE OF COMPOSITES DUE TO ENVIRONMENT EFFECTS.

- o ENVIRONMENTAL VARIABLES TO BE STUDIED
  - o TEMPERATURE
  - o THERMAL CYCLING
  - o LOAD
  - o PARTICULATE RADIATION
- o MEASUREMENT TECHNIQUES
  - o LASER INTERFEROMETER
  - o SIMULTANEOUS LASER INTERFEROMETER AND STRAIN GAGE MEASUREMENTS TO ASSESS ACCURACY OF LITERATURE DATA
- o CORRELATE ANALYTICAL PREDICTIONS WITH EXPERIMENTAL DATA

Figure 15

PRECISION MEASUREMENT OF THERMAL EXPANSION OF COMPOSITES

Moiré interferometry was selected as the measurement technique for CTE of composites for the reasons listed in figure 16. Moiré interferometry as described here differs from that of classical Moiré strain measurement techniques in that a fringe multiplication technique is employed. This allows a relatively coarse phase grating to be applied to the specimen while utilizing the resolution capabilities of a much finer reference grating. For this study a reference grating with 1200 lines/mm (30,000 lines/in) on a fused silica blank was purchased from Bausch & Lomb. An RTV silicon rubber phase grating is replicated onto the specimen surface using a 600 line/mm (15,000 lines/in) phase grating on a photographic glass plate. The specimen grating is approximately 0.025 mm thick and the ratio of Young's modulus of the grating to that of the composite is 10^{-3} to 10^{-4}; thus any reinforcement effect is considered negligible. The specimen is mounted in an environmental chamber capable of cycling between +180°C and -150°C. A five milliwatt He-Ne laser is used to illuminate the specimen. Measurements are made by counting fringes between two gage marks cast in the grating, giving a strain resolution of five microstrain.

PRECISION MEASUREMENT OF THERMAL EXPANSION OF COMPOSITES

Moiré Interferometry

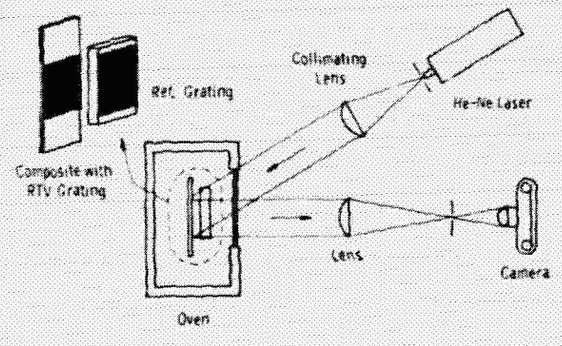

Advantages

- PURELY GEOMETRICAL MEASUREMENT OF SURFACE DISPLACEMENTS
- RESOLUTION IS ADJUSTABLE TO FIT THE REQUIREMENTS (RESOLUTION OF 5×10^{-6} WAS SELECTED)
- ELIMINATION OF SPECIMEN END EFFECTS
- FULL FIELD OBSERVATION INCLUDING FREE EDGE EFFECTS
- EASE OF IMPLEMENTATION INCLUDING TEMPERATURE COMPENSATION
- NEGLIGIBLE REINFORCEMENT
- DIRECTLY APPLICABLE FOR MEASUREMENT OF CTE UNDER LOAD
- LOW COST

Figure 16

ORIGINAL PAGE IS OF POOR QUALITY

COEFFICIENT OF EXPANSION AS A FUNCTION OF LAMINATE CONFIGURATION

Laminate analysis is being used to calculate the effect of fiber misorientation and inhomogeneous fiber volume content on the coefficient of thermal expansion of a number of different composite laminates. The above factors can produce unsymmetric laminate configurations which cause a coupling between bending and extensional behavior. This means that surface strains will not be correctly predicted by only a laminate coefficient of expansion, but that a laminate coefficient of curvature must also be used in the prediction. By using laminate analysis, the above factors may be easily and quickly studied to determine their influence. Another improvement that has been incorporated into the laminate analysis is the temperature dependence of the mechanical and thermal properties. This more closely simulates the real material behavior.

COEFFICIENT OF EXPANSION AS A FUNCTION OF LAMINATE CONFIGURATION

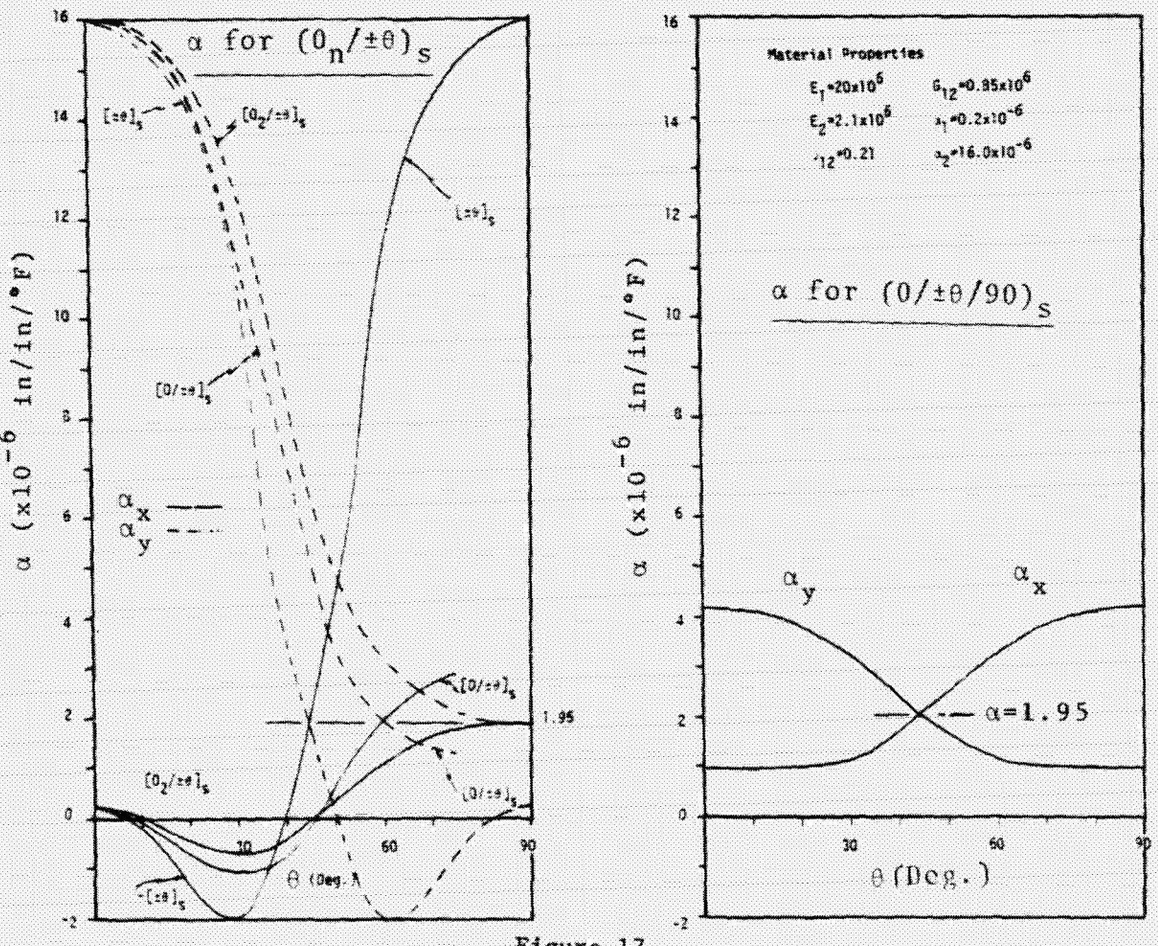

Figure 17

CABLE TECHNOLGOY FOR TENSION STABILIZED STRUCTURES

A common element in many large space structures is the long deployable cable. Many of the advanced concepts for large space antennas are based on tension stabilized structures where the mesh surface of the antenna is maintained to a prescribed shape by tensioning cables. Deployable antenna applications required cables with the following general characteristics: low CTE throughout temperature range; non RF interfering (low loss tangent and dielectric constant); deployable from spool at low temperature extremes; compatible with cable manufacturing equipment; high effective modulus at low prestrains; minimal creep with age and space exposure; high UV resistance; stable upon moisture dry-out, minimal hysteresis; and non self-abrasive. Quartz historically has been the most successful material for deployable antenna applications and will be the prime candidate for new antennas. However, high modulus graphite fibers will be seriously considered for all future applications particularly where RF interference is not a prime requirement.

The objective of this effort is to design and develop cable technology for multiple use requirements in antennas or other tension stabilized structures. A variety of cable fibers, both quartz and graphite, and constructions will be investigated in this study. Cables will be manufactured and tested to determine their mechanical and physical properties, effect of space environment on these cables, and ability of these cables to be spooled and deployed.

CABLE TECHNOLOGY FOR TENSION STABILIZED STRUCTURES

OBJECTIVE: DEVELOP MINIMUM WEIGHT AND SIZE CABLES WITH HIGH STIFFNESS, STRENGTH, AND DIMENSIONAL STABILITY WHICH CAN BE TIGHTLY PACKAGED AND READILY DEPLOYED IN SPACE.

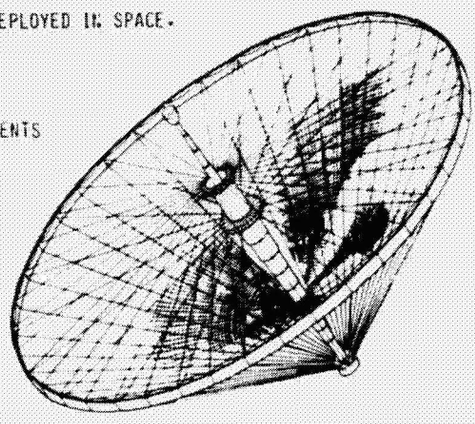

CONTRACTOR MATERIALS ACTIVITIES

- DEFINE ANTENNA CABLE REQUIREMENTS
  - o STRENGTH, STIFFNESS
  - o CTE, CREEP, HYSTERESIS
- PACKAGING AND DEPLOYMENT
  - o SPOOLING, JACKETING
  - o CABLE SELF-ABRASION
- RF INTERFERENCE

IN-HOUSE MATERIALS ACTIVITIES

- COMBINED LOAD/VACUUM/UV RADIATION TESTS ON KEVLAR
- COMBINED VACUUM/THERMAL CYCLING TESTS FOR CABLE STRUCTURAL CREEP
- THERMAL CYCLING AND TESTING OF CABLE FASTENERS

CANDIDATE MATERIALS: QUARTZ, GRAPHITE, KEVLAR

Figure 18

SUMMARY OF FY-79 LSST MATERIALS PROGRAM

NASA has identified numerous concepts for large space systems; communications and power transmission antennas and platforms for scientific experiments are of current interest. Advanced filamentary composite materials have the potential of providing extremely lightweight structures for these applications. There are, however, a number of technology needs associated with the long term use of organic matrix composites in the space environment. During FY-79 the LSST materials program has addressed various aspects of most of the material technology needs identified. Because the long-term durability of composites in the space environment is a particularly long lead time area most of the FY-79 resources were used to initiate programs to obtain an early assessment of the space durability of composites to scope the magnitude of the problem and to assist in the planning of a base R&T program to work this area.

Programs were also undertaken to improve thermal control coating technology for composites, measurement of thermal expansion of composites, and development of high strength lightweight cables for tension stabilized structures. During FY-80 the LSST materials program will be focused to address cable technology and dimensional stability of composites.

SUMMARY OF FY-79 LSST MATERIALS PROGRAM

- RADIATION EXPOSURES OF RESIN MATRIX COMPOSITES UNDERWAY ON CONTRACT AND IN-HOUSE
- DOSE/DEPTH PROFILE CALCULATIONS FOR ELECTRONS AND PROTONS IN COMPOSITES UNDERWAY
- LOW ENERGY e^- AND HIGH ENERGY p+ COMPARATIVE STUDY UNDERWAY
- WHITE PAINT THERMAL CONTROL COATINGS SUCCESSFULLY APPLIED TO COMPOSITES
- MOIRÉ INTERFEROMETER SYSTEM DESIGNED TO MEASURE CTE OF LOW EXPANSION COMPOSITES
- HIGH STRENGTH, DIMENSIONALLY STABLE CABLES UNDER DEVELOPMENT FOR TENSION STABILIZED STRUCTURES

Figure 19